Loughborough University

This item was submitted to Loughborough's Institutional Repository (https://dspace.lboro.ac.uk/) by the author and is made available under the following Creative Commons Licence conditions.

creative commons

COMMONS DEED

**Attribution-NonCommercial-NoDerivs 2.5**

**You are free:**

- to copy, distribute, display, and perform the work

**Under the following conditions:**

**Attribution**. You must attribute the work in the manner specified by the author or licensor.

**Noncommercial**. You may not use this work for commercial purposes.

**No Derivative Works**. You may not alter, transform, or build upon this work.

- For any reuse or distribution, you must make clear to others the license terms of this work.
- Any of these conditions can be waived if you get permission from the copyright holder.

**Your fair use and other rights are in no way affected by the above.**

This is a human-readable summary of the Legal Code (the full license).

Disclaimer

For the full text of this licence, please go to:
http://creativecommons.org/licenses/by-nc-nd/2.5/

Department of Materials

# THE INFLUENCE OF REACTIVE MODIFICATION ON THE COMPATIBILITY OF POLYOLEFINS WITH NON-OLEFINIC THERMOPLASTICS

**By**

**HENRY C.A. LIM**

A DOCTORAL THESIS

Submitted in partial fulfilment of the requirements for the award of Doctor of Philosophy of the Loughborough University

January 2011

© by H.C.A. Lim, 2011

**Confidential Report – not available for consultation without the permission of the Project Supervisors**

# ABSTRACT

Polyethylene (PE) resins being non-polar in nature and having a high degree of crystallinity have limited miscibility and compatibility when blended with polar polymers. The miscibility and compatibility of these blends are generally worsened when they are prepared by direct injection moulding without a pre-compounding process. Such situations are commonly encountered in particular by polymer converters when blending colour and/or additive concentrates, commonly known as masterbatches. Typically, masterbatches are mixtures containing high loading of pigments and/or additives predispersed in a suitable solid vehicle (commonly known as carrier) such as a polyethylene resin. These masterbatches are usually used for the colouration of a wide range of polymers and the carrier used must therefore be compatible with these matrix (host) polymers.

The preliminary stage of this study involved the investigation of the properties of blends based on high density polyethylene (HDPE) and a range of engineering thermoplastics (ABS, PC, PBT, PA6), prepared by injection moulding. Five different types of compatibilisers namely, ethylene-vinyl acetate (EVA) copolymer, ethylene-methyl acrylate (EMA) copolymer, ethylene-glycidyl methacrylate (E-GMA) copolymer, ethylene-methyl acrylate-glycidyl methacrylate (E-MA-GMA) terpolymer and maleic anhydride grafted HDPE (HDPE-g-MAH) copolymer were evaluated with respect to their efficiencies in compatibilising HDPE with the four engineering polymers. The pre-compounded HDPE/compatibiliser binary blends at 2 different blend ratios (1:1 and 3:1) were added at 15 wt% concentration to each engineering thermoplastics and test samples were produced directly by injection moulding. Results of mechanical testing and characterisation of the blends showed that glycidyl methacrylate compatibilisers, E-MA-GMA, in particular have the most universal compatibilising effectiveness for a range of engineering thermoplastics including ABS, PC, PBT, and PA6. Blends compatibilised with E-MA-GMA compatibiliser had the best notched impact performance irrespective of matrix polymer type. The presence of an acrylic ester (methyl acrylate) comonomer in E-MA-GMA resulted in increased polarity of the

compatibiliser leading to improved miscibility with the polar matrix polymers demonstrated by fine blend morphologies, melting point depression and reduction in crystallinity of the HDPE dispersed phase.

The second stage of this study involved the reactive modification of HDPE using a low molecular weight di-functional solid diglycidyl ether of bisphenol A (DGEBA) type epoxy resin compatibilised with HDPE-g-MAH in an attempt to improve its compatibility with ABS, PBT and PA6. The maleic anhydride moieties in HDPE-g-MAH served as reactive sites for anchoring the epoxy moieties while the HDPE backbone was miscible with the HDPE resin. An excessive amount of reactive groups resulted in the formation of crosslinked gels while the addition of EVA co-compatibiliser helped in the reduction of gel content and further improved the dispersion of the epoxy. The effectiveness of epoxy grafted HDPE (with and without EVA co-compatibiliser) in compatibilising ABS/HDPE, PBT/HDPE, and PA6/HDPE was investigated by injection moulding of 5 wt% functionalised HDPE with these matrix polymers into test bars for mechanical testing, and characterisation by differential scanning calorimtery (DSC) and optical microscopy. The reactively functionalised HDPE blends, improved the mechanical properties of ABS and PA6 blends especially with EVA as co-compatibiliser. However, the mechanical properties of PBT blends were unmodified by the functionalised HDPE which was believed to be due to end-capping of the PBT chain-ends by ungrafted epoxy resins.

**Keywords:** Reactive compatibilisation, miscibility, compatibiliser, compatibility, solubility, mechanical properties, high density polyethylene, epoxy, acrylonitrile-butadiene-styrene, polycarbonate, Poly(butylene terephthalate), polyamide 6, ethylene-vinyl acetate, ethylene-methyl acrylate, ethylene-glycidyl methacrylate, ethylene-methyl acrylate-glycidyl methacrylate, maleic anhydride, universal masterbatches.

# ACKNOWLEDGEMENTS

I wish to express my sincere gratitude and appreciation to my supervisor, ***Professor Marianne Gilbert***, for her invaluable guidance, support, continuous encouragements, and inspiration throughout the course of this research.

My very special thanks to my company research supervisor, ***Dr. Frederick Axtell***, for his great help, suggestions, support and encouragement.

I also wish to acknowledge with deep appreciation to ***Mdm Gladys Soh***, Business Unit Manager (Masterbatches) of Clariant Singapore who provided me with the opportunity and space to carry out this research to completion.

Acknowledgement is due to ***Clariant (Singapore) Pte Ltd*** for the support of this research.

I am particularly indebted to my colleagues, ***Yean Thye***, ***Alfie***, ***Chee Keong***, ***Derrick***, ***Chi Wei*** and ***Gaun Joo*** for their great assistance, support, and encouragement.

My special appreciation to ***Dr. Hendrik Kammler*** and ***Dr. Angelica Marson*** of Clariant International, for sharing with me their experiences, encouragement and also great assistance rendered in locating literatures that are not widely attainable.

Finally, a special thanks to my family that encouraged and supported me in this latest effort.

# TABLE OF CONTENTS


| | Page |
|---|---|
| ABSTRACT | i |
| ACKNOWLEDGEMENTS | iii |
| TABLE OF CONTENTS | iv |
| NOMENCLATURE | ix |
| **CHAPTER 1: INTRODUCTION** | 1 |
| 1.1 Masterbatches | 1 |
| 1.2 Carrier considerations for universal masterbatches | 3 |
| 1.2.1 Ethylene vinyl acetate (EVA) copolymer | 4 |
| 1.2.2 Ethylene methyl acrylate (EMA) copolymer | 5 |
| 1.3 Titanium dioxide ($TiO_2$) pigment and masterbatches | 6 |
| 1.4 Aims of the investigation | 8 |
| 1.4.1 Research protocol | 9 |
| **CHAPTER 2: LITERATURE REVIEW** | 10 |
| 2.1 Polymer-polymer miscibility | 12 |
| 2.1.1 Thermodynamics of polymer-polymer miscibility | 16 |
| 2.2 Strategies for compatibilisation of polymer blends | 23 |
| 2.2.1 Addition of pre-made block and graft copolymers | 28 |
| 2.2.2 Reactive compatibilisation | 33 |
| 2.2.2.1 Compatibilisation through addition of maleic anhydride functionalised compatibilisers | 39 |

Page

2.2.2.2 Compatibilisation through addition of glycidyl methacrylate functionalised compatibilisers 44

2.2.2.3 Compatibilisation through addition of epoxy resin compatibilisers 50

2.3 Survey of blends containing polyethylene 54

2.3.1 Polyamide-polyethylene blends 55

2.3.2 Polyester-polyethylene blends 60

2.3.3 Polycarbonate-polyethylene blends 64

2.3.4 Styrene-polyethylene blends 67

2.4 Characterisation and properties of polymer blends 71

2.4.1 Blend characterisation by differential scanning calorimetry 71

2.4.2 Blend characterisation by infrared spectroscopy 75

2.4.3 Blend morphology characterisation by microscopy 78

2.4.3.1 Optical microscopy (OM) 79

2.4.3.2 Electron microscopy 80

2.4.4 Mechanical properties of blends 82

**CHAPTER 3: EXPERIMENTAL** 85

3.1 Materials 85

3.1.1 Raw materials 86

3.2 Processing of polymer blends 90

3.2.1 Compounding 91

3.3.2 Injection moulding 95

Page

3.3 Reactivity studies using extrusion plastometer 98

3.3.1 Stoichiometry considerations 100

3.4 Mechanical properties of blends 103

3.4.1 Izod impact testing 103

3.4.2 Tensile testing 104

3.5 Characterisation of blends 105

3.5.1 Differential scanning calorimetry (DSC) 105

3.5.2 Thermogravimetric analysis (TGA) 108

3.5.3 Fourier transform infrared spectroscopy (FTIR) 109

3.5.4 Scanning electron microscopy (SEM) 110

3.5.5 Optical microscopy (OM) 111

3.6 Characterisation of gels and other soluble components 112

**CHAPTER 4: RESULTS & DISCUSSION**
**EVALUATION OF COMPATIBILISERS AND POLYMER BLENDS** 116

4.1 Thermal analysis of HDPE/compatibiliser blends 116

4.2 Evaluation of ABS/HDPE blends 120

4.2.1 Mechanical properties of blends 120

4.2.2 Thermal analysis of blends 123

4.2.3 Morphology of blends 126

4.2.4 Summary 127

4.3 Evaluation of PC/HDPE blends 130

4.3.1 Mechanical properties of blends 130

4.3.2 Thermal analysis of blends 133

Page

4.3.3 Morphology of blends 135

4.3.4 Summary 139

4.4 Evaluation of PBT/HDPE blends 140

4.4.1 Mechanical properties of blends 140

4.4.2 Thermal analysis of blends 144

4.4.3 Morphology of blends 147

4.4.4 Summary 150

4.5 Evaluation of PA6/HDPE blends 151

4.5.1 Mechanical properties of blends 151

4.5.2 Thermal analysis of blends 155

4.5.3 Morphology of blends 159

4.5.4 Summary 160

4.6 Conclusions 163

**CHAPTER 5: RESULTS & DISCUSSION REACTIVE MODIFICATION OF HDPE** 167

5.1 Characterisation of raw materials 168

5.1.1 The influence of moisture on reactive chemistry of maleic anhydride 169

5.1.2 Structural chemistry of epoxy resin 174

5.2 Functionalisation and characterisation of HDPE blends 177

5.2.1 Reactive studies on maleic anhydride and epoxy functionalities 178

Page

5.2.2 Miscibility and morphological studies of blends 187

5.2.3 Characterisation of gels and other soluble components 191

5.3 Compatibility studies on blends of functionalised HDPE with ABS, PBT and PA6 202

5.3.1 The influence of reactive grafting of HDPE on the mechanical properties of blends 202

5.3.2 Thermal analysis of blends 207

5.3.3 Morphology of blends 212

5.4 Conclusions 217

**CHAPTER 6 : GENERAL DISCUSSION** 219

**CHAPTER 7 : CONCLUSIONS & SUGGESTIONS FOR FUTURE WORK** 226

**REFERENCES** 231

**APPENDIX** 249

# NOMENCLATURE

| Abbreviation | Description |
|---|---|
| AA | Acrylic acid |
| ABS | Acrylonitrile-butadiene-styrene |
| CP | Compatibiliser precursors |
| CPE | Chlorinated polyethylene |
| DGEBA | Diglycidyl ether of bisphenol A |
| DMTA | Dynamic mechanical thermal analysis |
| DSC | Differential scanning calorimtery/calorimeter(s) |
| EA | Ethylene acrylate |
| EAA | Ethylene acrylic acid |
| EBS | Ethylene bis-stearamide |
| EEA | Ethylene-ethyl acrylate |
| EMA | Ethylene-methyl acrylate copolymer |
| EMAA | Ethylene-methacrylic acid copolymer |
| E-MA-GMA | Ethylene-methyl acrylate-glycidyl methacrylate terpolymer |
| EP | Epoxy |
| EPDM | Ethylene propylene diene monomer |
| EPR | Ethylene-propylene rubber |
| EVA | Ethylene-vinyl acetate |
| FTIR | Fourier transform infrared (spectroscopy) |
| GMA | Glycidyl methacrylate |
| HDPE | High density polyethylene |
| HDPE-g-MAH | High density polyethylene grafted with maleic anhydride |
| HIPS | High impact polystyrene |
| LCP | Liquid crystalline polymer |
| LCST | Lower critical solution temperature |
| LDPE | Low density polyethylene |
| LLDPE | Linear low density polyethylene |
| MA | Methyl acrylate |
| MAH | Maleic anhydride |
| MFR | Melt flow rate |
| MMA | Methyl methacrylate |
| NR | Natural rubber |
| OM | Optical microscopy/microscope(s) |
| OPS | Oxazoline functionalized polystyrene |
| PA6 | Polyamide 6 |
| PA66 | Polyamide 66 |
| PBO | Bis-oxazoline |

| Abbreviation | Description |
|---|---|
| PBT | Poly(butylene terephthalate) |
| PC | Polycarbonate |
| PCL | Poly(ϵ-caprolactone) |
| PE | Polyethylene |
| PEI | Poly(ether imide) |
| PEO | Poly(ethylene octene) copolymer |
| PET | Poly(ethylene terephthalate) |
| PMMA | Poly(methyl methacrylate) |
| PP | Polypropylene |
| PPE | Poly(phenylene ether) |
| PS | Polystyrene |
| PVAc | Poly(vinyl acetate) |
| PVC | Poly(vinyl chloride) |
| $PVF_2$ | Poly(vinylidene fluoride) |
| PVME | Poly(vinyl methyl ether) |
| PVPh | Poly(vinyl phenol) |
| SA | Succinic anhydride |
| SAG | Styrene-acrylonitrile-glycidyl methacrylate |
| SAN | Styrene acrylonitrile |
| SBC | Styrene-butadiene-styrene copolymer |
| SBS | Styrene-butadiene-styrene triblock copolymer |
| S-EB | Styrene-ethylene butadiene diblock copolymer |
| SEBS | Styrene-ethylene/butylene-styrene triblock copolymer |
| SEM | Scanning electron microscopy/microscope(s) |
| S-EP | Styrene-ethylene propylene diblock copolymer |
| SGMA | Styrene-co-glycidyl methacrylate |
| TEM | Transmission electron microscopy/microscope(s) |
| Tg | Glass transition temperature |
| TGDDM | Tetraglycidyl ether of diphenyl diaminomethane |
| Tm | Melting temperature |
| UCST | Upper critical solution temperature |

# CHAPTER 1

# INTRODUCTION

Thermoplastic blends and alloys prepared by compounding have received much academic and commercial research interest in the past decades. Blends containing a high density polyethylene (HDPE) dispersed phase have been extensively studied with particular focus on PET/HDPE [1-4] for recycling of mixed polymer scrap and compatibilisation studies. To date, there are no extensive studies conducted on blends that are prepared via injection moulding. So far, literature on blends prepared via direct injection-moulding has not been cited. One important application that involves direct blending of polymer blends via injection moulding is the dosage of masterbatches for the purpose of introducing either additives and/or colourants into matrix polymers. Often the polymer carrier used in these masterbatches is a widely used inexpensive polymer such as polyethylene, irrespective of the polymer to which it is added.

## 1.1 Masterbatches

A masterbatch is a solid concentrate of colourants and / or performance enhancing additives that is added to a matrix polymer to impart aesthetic and or functional attributes.

The typical components of a masterbatch are [5]:

- Polymer as carrier or vehicle (e.g. polyethylene resin)
- Colourant (e.g. titanium dioxide pigment)
- Dispersing agent (e.g. zinc stearate waxes)
- Other additives if necessary (e.g. antistatic agents, UV stabilisers)

The masterbatch is normally blended with a matrix polymer typically at a dosage of 1 to 8 wt%. There are two main types of masterbatches available in the industry:

- Polymer specific masterbatches
- Universal masterbatches

One major problem of using masterbatches is the relative compatibility between the carriers and matrix polymers when they are mismatched with one another. It is therefore a common industrial practice to use the same type of polymer as carrier for the masterbatch and matrix, commonly known as polymer specific masterbatches.

**Table 1.1 Advantages and disadvantages of using colour masterbatches**

| **Advantages** | **Disadvantages** |
|---|---|
| • Dust free handling | • Not universally applicable (incompatibility of polymers) |
| • Little cleaning required when changing colours during production | • More expensive |
| • Optimal utilisation of the tinting strength of the colorants | • Colour inconsistency at lower masterbatch dosages |

Despite some disadvantages as presented in Table 1.1, the advantages of a masterbatch predominate especially with respect to handling and optimal utilisation of the tinting strength of the colorants.

A universal masterbatch employs a carrier resin that is capable of carrying the high quantities of additives necessary to deliver the end use properties required as well as affording the essential compatibility required across a broad range of polymers. This concept is practically not feasible when we consider the chemical differences between different types of polymers.

Another major hindrance to the use of universal masterbatches is the fact that not all colorants can be applied in every type of polymer for many reasons such as heat stability, light fastness, or weather resistance, or in the case of dyes the migration phenomenon in semi-crystalline polymers. Therefore some color hues cannot be made as true “universal masterbatches” but only as “partial universal masterbatches”.

The following factors are to be taken into consideration during designing of masterbatches:

- Compatibility of masterbatch carrier resin
- Pigment strength
- Colour tone
- Dilutability (i.e. quality of masterbatch distribution in matrix polymers)
- Effects on physical and mechanical properties
- Temperature stability

## 1.2 Carrier Considerations For Universal Masterbatches

The carrier of a universal masterbatch, as mentioned, must have excellent compatibility with a broad spectrum of matrix polymers. Ethylene vinyl acetate (EVA) and ethylene methyl acrylate (EMA) are commonly used in the masterbatch industry as carrier resins in universal masterbatches as they are reasonably compatible with a wide array of matrix polymers. Sometimes, waxes such as ethylene bis-stearamide (EBS) are used as carriers for universal masterbatches but this approach may result in problems like screw slippage during processing, plate-out on moulds and poor adhesion of pad printing. Another common industrial practice in making universal masterbatch is by blending polystyrene and colophony ester which is a rosin derivative that functions as a compatibiliser [6].

### 1.2.1 Ethylene Vinyl Acetate (EVA) Copolymer

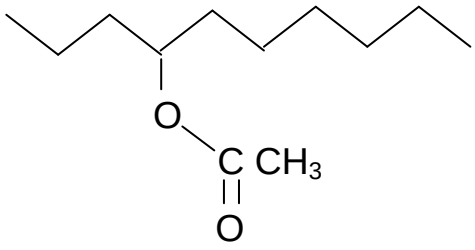


**Figure 1.1 Typical structure of an EVA copolymer**

Ethylene vinyl acetate (EVA) copolymer, is commonly used in the masterbatch industry as a carrier polymer in universal masterbatches [7] as the polarity of vinyl acetate enables good compatibility of EVA with various thermoplastics. It has been reported by Teo [8] that EVA improved dispersion quality and interfacial adhesion between antimony trioxide and ABS when an EVA based antimony trioxide masterbatch was letdown in ABS resins. However, this copolymer has limited thermal stability and releases acetic acid above 200$^{o}$C. This limits the use of EVA based masterbatches in engineering polymers as they are commonly processed at temperatures that are much higher than 200$^{o}$C. The acetic acid by-product could catalyse degradation of the matrix polymers [9], cause corrosion of machinery and odour problems during manufacturing processes.

On the other hand, the low melting and Vicat softening point of EVA resin (typically 82℃/47℃ respectively for a copolymer c ontaining approximately 20 wt% vinyl acetate co-monomer) has also restricted its use in universal masterbatch carriers for high temperature matrix engineering polymers as the EVA will be melted in the hopper during the drying process which typically exceeds 100℃.

### 1.2.2 Ethylene Methyl Acrylate (EMA) Copolymer

The concept of using this non reactive polar copolymer (EMA) is to reduce interfacial tension and increase the adhesion by creation of a specific interaction like hydrogen bonding or Van der Waals forces.

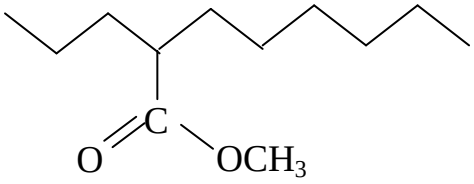


**Figure 1.2 Typical structure of a EMA copolymer**

An increased in the comonomer content of EMA would results in higher level of polarity that makes these polymers compatible with a variety of different engineering polymers [10]. Such characteristic properties not only enable them to function well as compatibilisers or impact modifiers but also as carrier resins for universal masterbatches [11] due to their high filler acceptance capability.

EMA copolymers are used as polymer modifiers in high performance engineering thermoplastics like polyamide (PA), polyethylene terephthalate (PET) and polybutylene terephthalate (PBT), and they are also suitable for use in non-polar polyolefins such as polypropylene (PP) and polyethylene (PE) or in polar, nonreactive polymers such as acrylonitrile butadiene styrene (ABS).

A typical property profile of EMAs is as follows:

- Polarity and compatibility
- Low temperature flexibility
- Higher thermal stability than conventional EVA copolymers

As with EVA copolymers, EMA copolymers exhibit a low melting and Vicat softening point (typically 80℃ / 48℃ respectively for a copolymer containing approximately 20 wt% acrylate co-monomer) which has also restricted their use in universal masterbatch carriers for high temperature matrix engineering polymers as the EMA would be melted in the hopper during the drying process which typically exceeds 100℃.

## 1.3 Titanium Dioxide ($TiO_2$) Pigment And Masterbatches

Titanium dioxide ($TiO_2$) is, today, the most important white pigment used in the plastic industry. It is a totally synthetic inorganic colourant that is insoluble in water and resin and effectively scatters visible light better than any other commercially available white pigment [12]. It is chemically inert, and heat stable under the harshest of processing conditions. $TiO_2$ is commercially available in two crystal forms – anatase and rutile. Rutile $TiO_2$ pigments are preferred because they scatter light more efficiently as shown in Table 1.2. They are more stable and less photo-reactive than anatase pigments.

Most commercial grades of $TiO_2$ have inorganic and in some cases organic treatments deposited on the surface of the $TiO_2$ particles by precipitation or by mechanical blending. Inorganic surface treatment such as alumina and/or silica provide improvements in one or more important performance properties of the pigment such as hiding power efficiency, ease of dispersion, weatherability and discoloration resistance. Organic coatings are generally utilised to improve dispersability and flow characteristics of $TiO_2$.

**Table 1.2 Refractive Indices of Several White Powders [13]**

| White Powder | Refractive Index |
|---|---|
| Titanium Dioxide - Rutile | 2.70 |
| Titanium Dioxide - Anatase | 2.55 |
| Zirconium Oxide | 2.40 |
| Zinc Sulphide | 2.30 |
| Antimony Oxide | 2.30 |
| Zinc Oxide | 2.02 |
| Lithopone (30% ZnS) | 1.84 |
| Barium Sulphate | 1.64 |
| Calcium Carbonate | 1.57 |
| Low Density Polyethylene | 1.50 |

One of the largest applications of $TiO_2$ by the plastic industry is for the production of colour masterbatches [14]. Typically, colour masterbatches have a $TiO_2$ loading range from 50 to 70wt%, with polyethylene being the most popular carrier; a common letdown ratio is 25:1.

Good dispersion of the pigment in masterbatch is essential for the production of homogenous pigmented end products. The degree of dispersion is dependent on the type and concentration of the $TiO_2$ used, the wetting power of the polymer and the compression and shear forces generated during the incorporation process [15].

## 1.4 Aims Of The Investigation

In the injection moulding industry, the vast majority of the colour and other functional properties are introduced to the matrix polymers through direct blending with colour and / or additive masterbatches at the injection moulding stage without going through compounding steps. The greatest challenge in performing this task will be the limited mixing capacities of the injection moulding machine and also compatibility issues of the carrier polymers used in these masterbatches with the matrix resins. The effects, if any, brought about by the addition of the masterbatches on mechanical properties of the final products are often neglected or assumed to be insignificant.

The preliminary stage of this research aims to:

- investigate the feasibility of producing compatibilised blends through direct injection moulding of pre-compounded HDPE/compatibiliser binary blends with several types of matrix polymers follow by investigation of their mechanical, thermal and morphological properties.
- study the compatibilisation efficiency of five commercially available polar/non-reactive and polar/reactive compatibilisers in compatibilisation of ABS/HDPE, PC/HDPE, PBT/HDPE and PA6/HDPE blends.

The second stage of this research aims to:

- improve the compatibility of high density polyethylene (HDPE) with various non-olefinic matrix resins, through reactive modification. The use of maleic anhydride grafted HDPE (HDPE-g-MAH) as a compatibiliser which provides sites for reacting with a low molecular weight epoxy resin will be assessed.
- study the reaction mechanisms between HDPE-g-MAH and epoxy molecules and develop analytical methods for characterisation of the reactive blends.
- investigate the compatibilisation efficiency of selected functionalised HDPEs with ABS, PBT and PA6.

### 1.4.1 Research Protocol

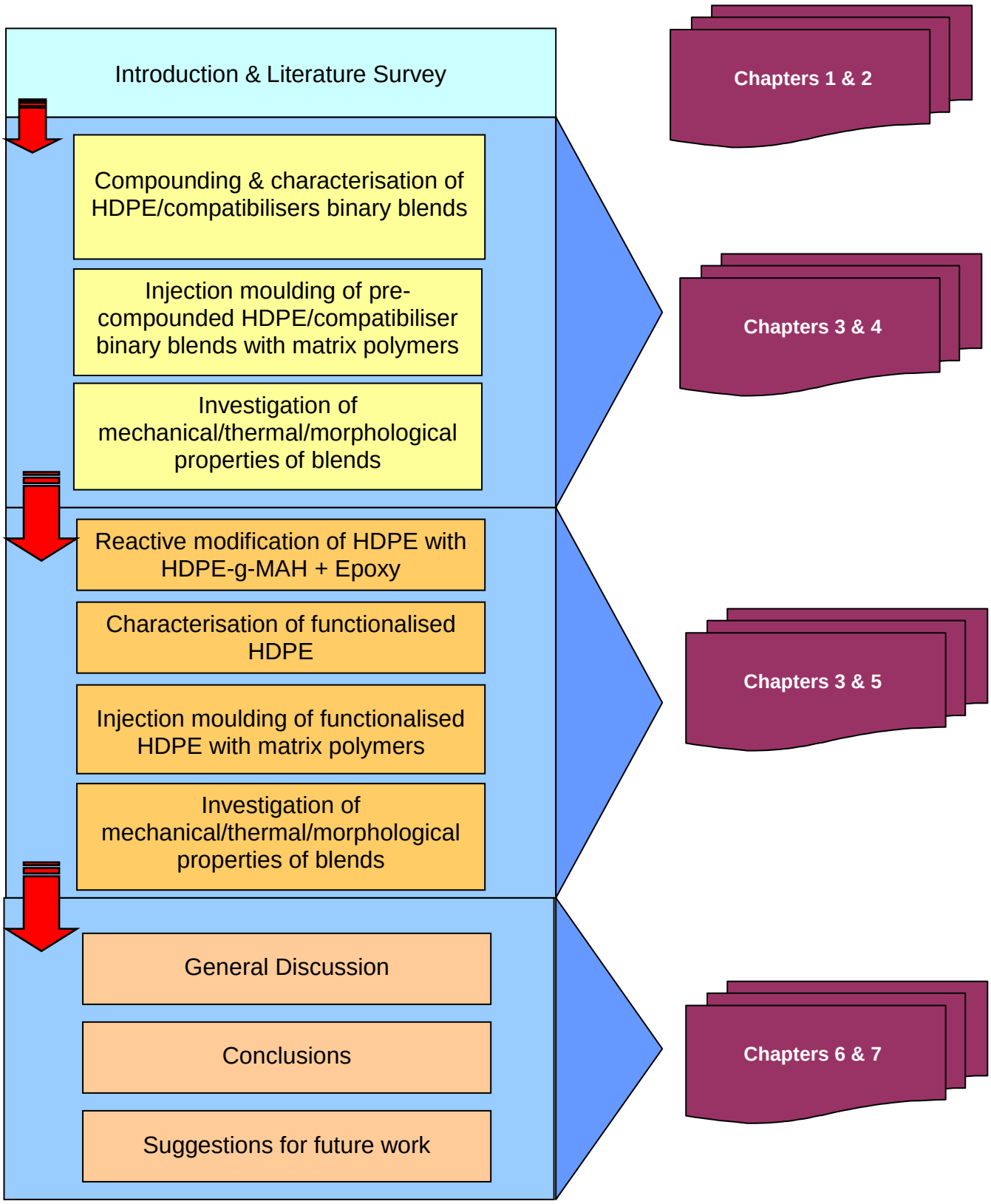

# CHAPTER 2

# LITERATURE REVIEW

Polymer blends are macroscopically homogenous mixtures of two or more different species of polymer [16]. For practical reasons, the name blend is given to a system only when the minor component content exceeds 2 wt% [17]. A polymer alloy in turn is defined as an immiscible polymer blend having modified interface and / or morphology [18]. Therefore all polymer alloys can be considered as polymer blends, but not all polymer blends are alloys as illustrated in Figure 2.1. For this reason, the use of the term “polymer alloy” for “polymer blend” is strongly discouraged.

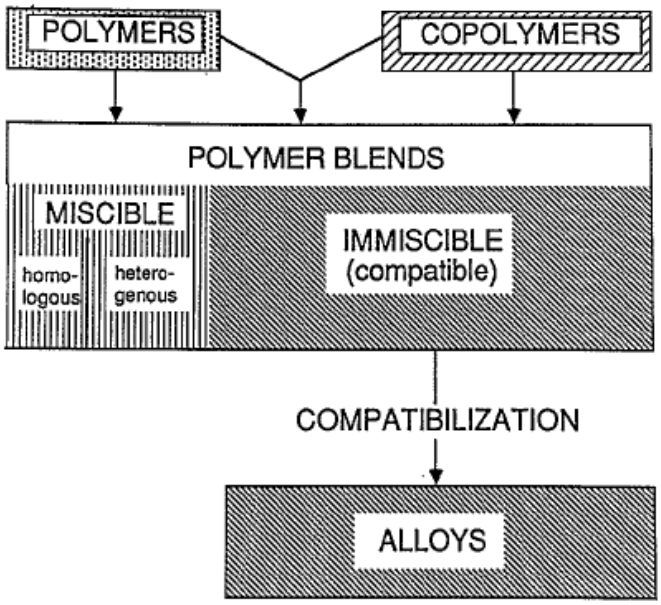


**Figure 2.1 Interrelations in polymer blend nomenclature [20]**

In 1846, Alexander Parkes, filed the first patent for polymer blends based on mixtures of two polyisoprene isomers, natural rubber and gutta purcha [19]. Utracki [20] has summarised the polymer blend patent literature in Table 2.1 which indicated that impact strength improvement and processability enhancement dominate the field of thermoplastic blends.

**Table 2.1 Principal properties claimed in polymer blend patents [20]**

| Property | Frequency (%) |
|---|---|
| **High impact strength** | 38 |
| **Processability (including weld line)** | 18 |
| **Tensile Strength** | 11 |
| **Rigidity/modulus** | 8 |
| **Heat Deflection Temperature** | 8 |
| **Flammability** | 4 |
| **Solvent resistance** | 4 |
| **Thermal stability** | 3 |
| **Dimension stability** | 3 |
| **Elongation** | 2 |
| **Gloss** | 2 |
| **Others** | 4 |

Over the past decades, extensive research works have been conducted on polymer blends and alloys by researchers leading to the publications of many useful text books, patents and research papers [1-3, 17-25, 28, 29, 35-41, 49, 97, 145, 189 etc]**.**

Polymer blending can bring about completely new materials with properties superior to the original components. In many cases, the materials produced have optimal cost/performance behaviour. They fill the gap between high cost engineering resins and low cost commodity polymers. Several advantages of blending can be identified as follows:

a.) blends with unique properties, morphologies and processabilities can be tailor made rapidly as compared to the synthesis of a new polymer,
b.) blending involves low capital investment in equipment whereby most of the blends can be processed using conventional extruders for thermoplastic compounding,

c.) cost reduction can be achieved by blending expensive engineering polymers with less expensive commodity polymers while retaining 90% of their original properties,
d.) blending provides a route for recycling industrial and post-consumer scraps.

In this research work, the main reason for blending is the addition of colour masterbatches into matrix engineering thermoplastics for colouration purposes. The presence of polymeric masterbatch carriers which are incompatible with the matrix polymers are detrimental to the mechanical properties of the final colored products. Therefore, compatibility between the carrier and matrix polymers has to be achieved during the blending process.

## 2.1 Polymer-Polymer Miscibility

The term *miscibility* has been described by Olabisi et al [21] as polymer-polymer blends with behaviour similar to that expected of a single-phase system. On the other hand, the term *compatibility* is generally used to describe the adhesion properties between the constituents of polymer-polymer blends.

Polymer blends fall into three main categories, miscible, immiscible, and partially miscible. Miscibility refers to mixing in the amorphous phase and does not preclude crystallisation of blend components. In the absence of crystallinity, miscible blends mix completely at all ratios, forming a single homogenous, molecularly mixed amorphous phase. In most instances the critical property will be the glass transition temperature. Figure 2.2 (a) shows that a pair of polymers exhibiting a single glass transition temperature with very fine morphology can be classified as miscible. Because of the lack of structure, miscible amorphous blends are transparent and therefore transparency is often being used as evidence of miscibility. However, this is not always true as immiscible blends can also be transparent if the refractive index of the dispersed phase matches that of the matrix. Relatively few

polymers form truly miscible blends characterized by a single Tg and homogeneity at a 5-10 nm scale [22].

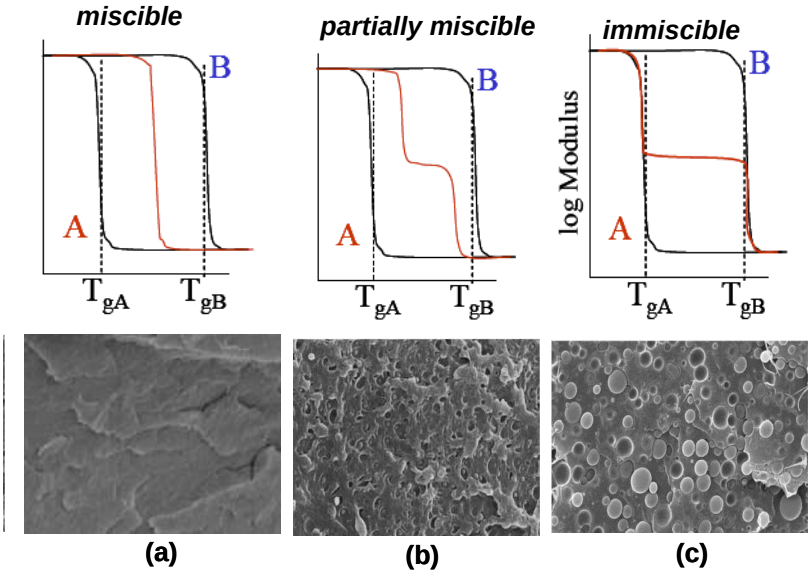


**Figure 2.2 Schematic of the dependence of glass transition temperature on the morphology of the blend; (a) miscible blend, (b) partially miscible blend, and (c) immiscible blend**

The first fully miscible blends were patented in 1968 by Cizek [23]. He discovered that polyphenylene ether (PPE) and polystyrene (PS) were completely miscible as indicated by a single Tg and a relationship between the concentration and glass transition of the blends as shown in Figure 2.3. PPE/PS blends have been commercialized by GE Plastics under the trade name Noryl [24].

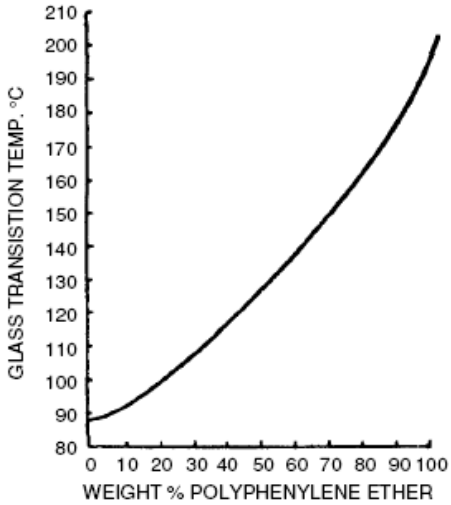


**Figure 2.3 Tg of PPE/PS blends [23]**

Immiscible blends result from mixing two materials with little affinity for each other. The polymer present in the largest volume fraction is usually the continuous phase. The minor component is usually a dispersed second phase forming a distinct interfacial boundary with the matrix polymer as shown in Figure 2.2 (c). The glass transition temperatures of individual components remained relatively unchanged indicating minimum or no interaction between the two phases. With little adhesion between the phases, blends of immiscible polymers frequently exhibit inferior mechanical properties which preclude their use for most commercial purposes.

Compatibilisation of immiscible polymers through the action of block or graft copolymers improves dispersion and phase adhesion giving blends with useful engineering properties. In successfully compatibilised blends, the best properties of each material can often be combined.

Lindsey and co-workers [25] demonstrated that a styrene-ethylene butadiene-styrene (SEBS) triblock copolymer greatly improved the ductility of the immiscible HDPE/PS blend but with an accompanying loss in yield strength and modulus as shown in Figure 2.4.

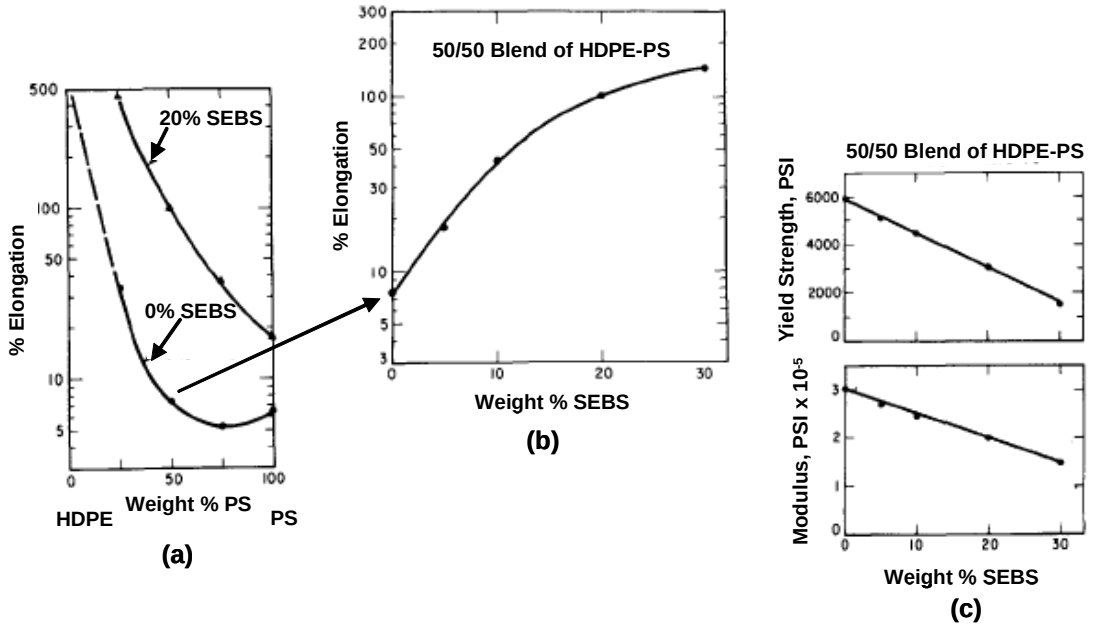


**Figure 2.4 (a) Percent elongation at break for binary blends and ternary blends containing 20% SEBS, effects of SEBS level on (b) percent elongation at break, (c) yield strength and modulus of blends containing equal parts of HDPE and PS [25]**

Some blends are neither completely miscible nor immiscible. These partially miscible blends show limited mutual affinity and the interactions are insufficient to generate completely soluble systems. Nishi [26] et al investigated the thermally induced phase separation behaviour of polystyrene/poly(vinyl methyl ether), (PS/PVME), mixture and postulated that the phase separation of this partially miscible blend was dependent on composition and temperature as shown in Figure 2.5.

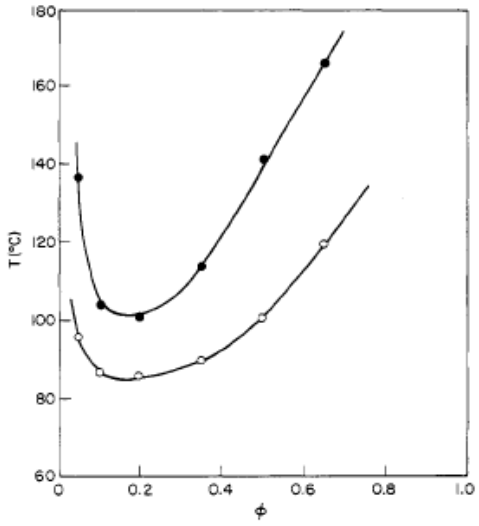


**Figure 2.5 Plot of the initial temperatures (o) and apparent completion temperatures (●) of phase separation for several PS concentrations, Ø, of PS/PVME mixtures at a heating rate of 0.2$^{o}$C/min [26]**

Chun et al [27] studied the thermal properties and morphology of poly(ether imide)/polycarbonate (PEI/PC) blends. They found that the glass transition temperature of the PEI-rich phase decreased at the higher PEI weight fraction and a maximum 6 $^{o}$C decrease occurred at 90wt% PEI as observed in Figure 2.6, indicating that the blends were partially miscible.

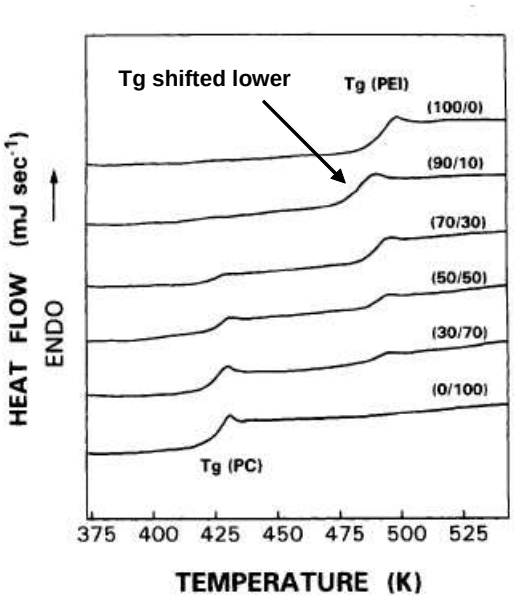


**Figure 2.6 DSC traces showing the glass transition temperature (Tg) of various composition of PEI/PC blends [27]**

## 2.1.1 Thermodynamics of Polymer-Polymer Miscibility

The state of miscibility of any mixture is governed by the free energy of mixing, $\Delta G_{mix}$, which is defined as:

$$\Delta G_{mix} = \Delta H_{mix} - T\,\Delta S_{mix} \qquad (1.0)$$

Where $\Delta H_{mix}$ is the enthalpy of mixing, T is the absolute temperature, and $\Delta S_{mix}$ is the entropy of mixing.

The thermodynamic driving force for mixing is minimisation of $\Delta G_{mix}$. Thus if the free energy is positive, the system is immiscible. While for small molecules the entropy is high enough to ensure miscibility, for polymers the entropy is almost zero, causing enthalpy to be decisive in determining miscibility. For spontaneous mixing, $\Delta G_{mix}$ must be negative, and so

$$\Delta H_{mix} - T\,\Delta S_{mix} < 0 \qquad (1.1)$$

For complete miscibility to occur, a negative free energy of mixing is necessary but not sufficient. Figure 2.7 shows that $\Delta G_{mix}$ for a binary mixture can vary with composition in several ways [28]:

a.) Complete immiscibility (Curve A) exists if $\Delta G_{mix}$ is positive
b.) Complete miscibility (Curve B) exists only if

$$\Delta Gmix < 0 \tag{1.2}$$

and that the second derivative of $\Delta G_{mix}$ with respect to the volume fraction of either component must be greater than zero over the whole composition range.

Curve B meets both requirements and the curve is convex downwards over the whole range of Ø, so that for all points

$$\left(\frac{\partial^2 \Delta G_m}{\partial \phi^2}\right)_{T,P} > 0 \tag{1.3}$$

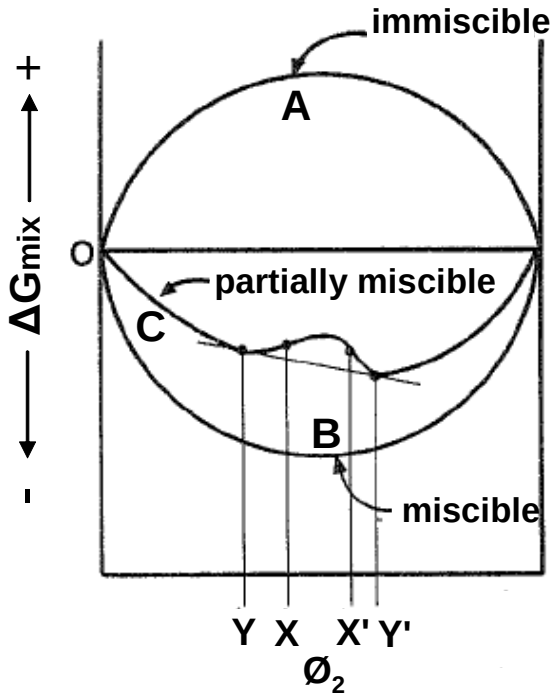


**Figure 2.7 Possible free energy of mixing diagram for binary mixtures [28]**

c.) Curve C represents a system that is partially miscible as it only satisfies equation (1.2) but not the derivative criterion expressed by equation (1.3) at all points along the ΔGmix-composition curve since it passes through points of inflexion defined by

$$\left(\frac{\partial^2 \Delta G_m}{\partial \phi^2}\right)_{T,P} = 0 \qquad (1.4)$$

at points X and X' in Figure 2.7. Between these spinodal points the system will phase separate spontaneously into bimodal compositions Y and Y', with a decrease in free energy.

For two-component blends it is possible to construct a phase diagram, which may exhibit upper or lower critical solution temperature (UCST or LCST) as shown in Figure 2.8.

Generally, UCST behaviour is characteristic of systems which mix endothermically while LCST behaviour is a characteristic of exothermic mixing (which could arise from specific chemical interactions) and associated with entropy effects.

For low molecular weight materials, increasing temperature generally leads to increasing miscibility as the $T\Delta S_{mix}$ term increase, thus driving $\Delta G_{mix}$ to more negative values. Thus liquid-liquid and polymer-solvent mixtures usually exhibit UCST.

LCST behaviour is more commonly observed in polymer blends as phase separation occurs when temperature increases because the intermolecular attractive forces responsible for the miscibility behaviour tend to disappear as the internal energy of the molecules becomes high enough to overcome them.

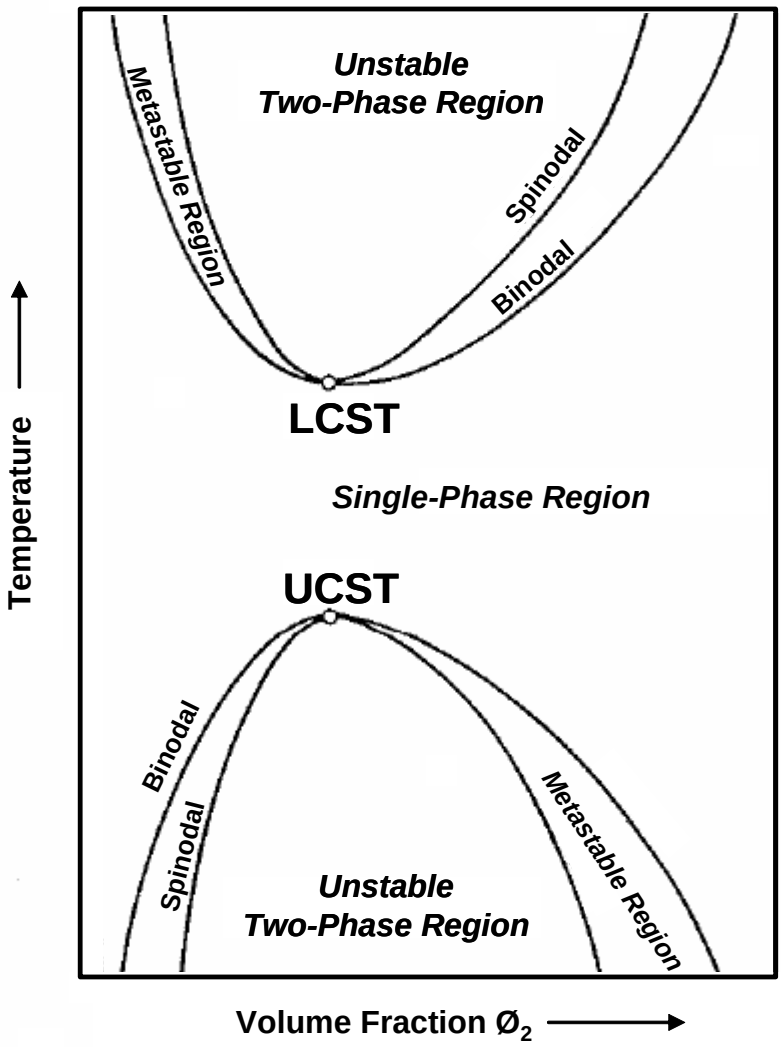


**Figure 2.8 Schematic phase diagram for a system exhibiting both UCST and LCST behaviour [29]**

Mathematical models of polymer solutions like Flory-Huggins model [30] are useful for understanding how various factors can affect polymer solubility. The Flory-Huggins model uses combinatorial analysis to estimate the increase in configurations available to the system when a flexible polymer in a disordered state is mixed with solvent.

The entropy of mixing, $\Delta S_{mix}$, arising from the increased number of ways of arranging the polymer and solvent molecules in the solution is given by

$$\Delta S_{mix} = -R(n_1 \ln \phi_1 + n_2 \ln \phi_2) \quad (1.5)$$

where $n_1$ and $n_2$ are mole fractions of solvent and solute; $\phi_1$ and $\phi_2$ are their volume fractions; and R is the gas constant. In almost all polymer solutions the increase in entropy is the driving force for the mixing process.

An expression for the enthalpy of mixing, $\Delta H_{mix}$, can be obtained by considering the change in adjacent neighbour (molecules or segments) interactions on the lattice upon mixing:

$$\Delta H_{mix} = RT\chi_{12} n_1 \phi_2 \quad (1.6)$$

where $\chi_{12}$ is the Flory-Huggins interaction parameter.

Thermodynamically, $\chi_{12}$ is one of the key parameters to determine the miscibility of polymer blends and it may be shown that the Flory-Huggins parameter and solubility parameters are related by

$$\chi_{12} = \frac{V_r (\delta_1 - \delta_2)^2}{RT} \quad (1.7)$$

where $\delta_i$ are the solubility parameters of two homopolymers or copolymers, R is the gas constant, T is the absolute temperature, and $V_r$ is a reference volume, taken as 100 $cm^3$ for polymers.

The interaction parameter $\chi_{12}$ is a useful measure of the solvent power [31]. It has been shown both theoretically and experimentally that a $\chi_{12}$ value of about 0.55 is the dividing line between poor solvents and non-solvents [32]. The region of poor solvency extends from about 0.31 to 0.55. Values of $\chi_{12}$ less than 0.30 indicate good solvents. In general, the smaller the $\chi_{12}$, the

stronger the polymer-diluent interaction and consequently the better the solvent.

The Hildebrand solubility parameters of homopolymers can be calculated using

$$\delta = \frac{\rho \sum Fi}{M} \tag{1.8}$$

where $\delta$ is the solubility parameter of the polymer, ΣFi is the sum of the molar attraction constants of all the groups in the repeat group of the polymer, M is the molecular weight of the repeat group, and ρ is the density of the polymer at the temperature of interest.

The solubility parameters of random copolymers can be calculated using

$$\delta_c = \sum \delta_i \phi_i \tag{1.9}$$

where $\delta_c$ is the solubility parameter of the copolymer, $\delta_i$ is the solubility parameter of the homopolymer corresponding to repeat group *i*, and $\phi_i$ is the volume fraction of repeat group i in the copolymer.

Substitution of the expression for entropy in equation (1.5) and enthalpy in equation (1.6) into the expression for free energy of mixing in equation (1.0) yields the well-known Flory Huggins expression for the Gibbs free energy of mixing

$$\Delta G_{mix} = RT\left(n_1 \ln \phi_1 + n_2 \ln \phi_2 + \chi_{12} n_1 \phi_2\right) \tag{2.0}$$

From equation (2.0), the smaller that $\chi_{12}$ is, the more stable is the solution relative to the pure components and the more likely that the system is miscible over a wide range of concentrations. For most systems $\chi_{12}$ decreases with increasing temperature and increases with increasing concentration of

polymer. In dilute solutions, the polymer molecules are isolated from each other by regions of pure solvent, i.e., the polymer segments are not uniformly distributed in the lattice. In view of this, the Flory-Huggins theory is least satisfactory for dilute polymer solutions and only applies to concentrated solutions or mixtures.

The majority of polymer pairs exhibit an endothermic heat of mixing when blended together, which does not favour the formation of a single amorphous phase. Values of $\Delta H_{mix}$ which indicate whether pairs may be miscible, can be estimated for nonpolar components by using the Hildebrand approach to regular solutions which introduces the concept of the solubility parameter $\delta$. Demixing of liquids is attributed to the tendency of molecules to attract their own species more strongly than a dissimilar species. This idea is expressed quantitatively in the equation

$$\Delta H_{mix} = V_{mix}\, \phi_1 \phi_2 \left(\delta_1 - \delta_2\right)^2 \qquad (2.1)$$

where $V_{mix}$ is the molar volume of the mixture.

Chemically similar molecules are in most cases found to have similar solubility parameters, and thus a reduced tendency to demix. Therefore, miscibility or solubility will be predicted if the absolute value of the ($\delta_1$ - $\delta_2$) difference is zero or small (less than 2 $MPa^{1/2}$). Specific effects such as hydrogen bonding and charge transfer interactions can lead to negative $\Delta H_{mix}$ but these are not taken into account by equation (2.1) since the right hand side of the equation cannot be negative, the solubility parameter method does not comprehend exothermic mixing. Therefore, to improve the prediction of polymer miscibility, a three-dimensional solubility parameter which gives individual contributions for dispersive (i.e. van der Waals), polar, and hydrogen bonding interactions as proposed by Hansen is sometimes used.

The overall solubility parameter is then the sum of the various contributions [31],

$$\delta = \sqrt{\delta_d{}^2 + \delta_p{}^2 + \delta_h{}^2} \tag{2.2}$$

where $\delta_d$ is the dispersion component of $\delta$, $\delta_p$ is the polar component of $\delta$, and $\delta_h$ is the hydrogen bonding component of $\delta$.

The degree of similarity in the structure of two polymers (a criterion for miscibility) is the distance between the two components of the blend in three-dimensional space using the three components of the solubility parameter as coordinates. Mathematically, it is represented by $\delta_m$ and is defined as

$$\delta_m = \sqrt{\left(\delta_{d,1} - \delta_{d,2}\right)^2 + \left(\delta_{p,1} - \delta_{p,2}\right)^2 + \left(\delta_{h,1} - \delta_{h,2}\right)^2} \tag{2.3}$$

Huang et al [33] applied the three-dimensional solubility parameter method to predict the miscibility trend of PVC/homopolymer and PVC/copolymer blends. A homopolymer system was reported to be miscible when $\delta_m$ was 11 but for copolymers the miscibility turned semi-miscible when $\delta_m$ was 5.8. They concluded that the smaller distance between the solubility parameter of copolymer and that of PVC indicate better chances of miscibility due to the ability to adjust the solubility parameter through the copolymer composition.

## 2.2 Strategies for Compatibilisation of Polymer Blends

In recent years, new commercial polymers have been introduced via blending of older well established polymers which produces polymer blends with unique properties that are generally not attainable from either of the individual components. Compatibilisation can be defined as the process of modification of the interfacial properties in an immiscible polymer blend that results in formation of the interphases and stabilisation of the morphology, leading to the creation of a polymer alloy [16].

In an immiscible blend, the situation at the blend interface is critical, i.e., a high interfacial tension and poor adhesion between the phases are observed. The high interfacial tension results in poor dispersion during mixing and the subsequent lack of stability during later processing or use. Often such blends show poor mechanical properties, due to weak interfacial interaction in these blends leading to premature failure under stress.

Therefore, in order to ascertain high performance of immiscible blends, usually compatibilisation is required. There are three aspects of compatibilisation [17]:

1.) Reduction of the interfacial tension that facilitates fine dispersion;
2.) Stabilisation of the morphology against changes during subsequent high stress and strain processing (e.g. during injection moulding); and
3.) Enhancement of adhesion between the phases in the solid state, facilitating the stress transfer, hence improving the mechanical properties of the product.

When two immiscible polymers are brought together in the melt, a distinct two-phase blend is formed. It is well known that the properties of such a blend are closely related to the state of dispersion or morphology (particle shape, size, size distribution, spatial arrangement and orientation of the particles). Therefore, in order to produce blends with improved properties, the control of phase morphology during the blending process is critical. Figure 2.9 summarises the processes that occur when two immiscible polymers are melt blended. The morphology development starts from the transformation of solid pellets to the corresponding polymer melt, followed by the stretching/deformation of the molten polymer to slender threads. If the local radius of the thread becomes sufficiently small, interfacial (“Rayleigh”) disturbances grow on the thread and result in the breakup of these liquid threads into small dispersed droplets.

In regions of low shear rate in the mixing equipment, coalescence of non-stabilised dispersed droplets occurs and results in the coarsening of the

phase morphology. The dispersed phase may also coalesce into large domains when the blend is subjected to further thermal processing such as moulding or heat aging. Such phase agglomeration in moulded parts may result in gross phase segregation and delamination on a macroscopic scale and/or brittleness or poor surface appearance.

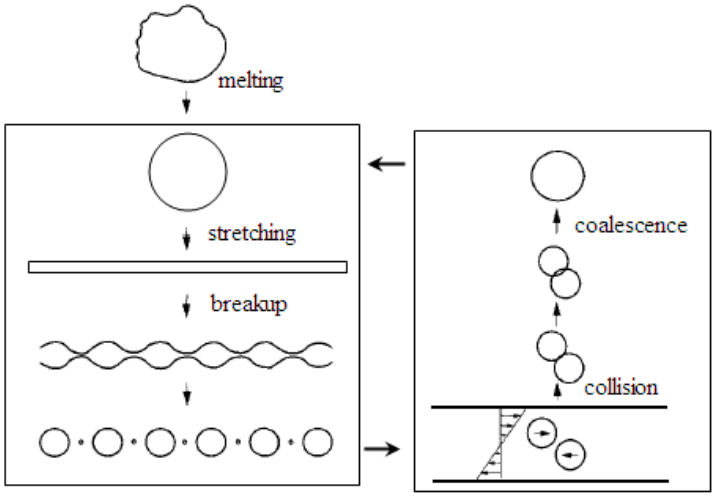


**Figure 2.9 Schematic representation of the processes occurring during the melt blending of two polymers** [**34**]

Compounds acting as interfacial agents are commonly known as "compatibilisers" in polymer blends [35]. A compatibiliser is a polymer or copolymer that, when added to an immiscible polymer blend, modifies its interfacial character and stabilises its morphology [16]. Compatibilisers are classified into two major categories: non-reactive and reactive [22].

**Table 2.2 Classification of compatibilisers [22]**

| Non-reactive | Reactive |
|---|---|
| A-co-B | A-X |
| A-co-D | C-X |
| C-co-D | A-B |
| C | Ionomer |

A, B, components of the blend; A-B, reaction products from interchange reaction between A and B; C, polymer is miscible or nearly miscible with A; D, polymer is miscible or nearly miscible with B; X, reactive group.

Based on the nature of the chemical structure and the respective compatibilising mechanisms, these two major groups could be further subdivided into several subgroups as shown in Table 2.2. Examples of blends compatibilised using these classes of compatibilisers are summarised in Table 2.3.

**Table 2.3 Compatibilisation of blends through various types of compatibilisers [22]**

| Compatibiliser type | Blends | Compatibilisers |
|---|---|---|
| ***A-co-B*** | PS/PE | PS-g-PE |
| ***A-co-D*** | PS/PC | PS-b-PCL |
| ***C-co-D*** | PPE/PET | PS-b-PC |
| ***C*** | PC/SAN | PCL |
| ***A-X*** | PA/PP | PP-g-MAH |
| ***C-X*** | PET/PPE | SGMA |
| ***A-B*** | PET/PA | PET-co-PA |
| ***Ionomer*** | PET/PE | Sodium ionomer of poly(ethylene-co-methacrylic acid) |

Co-crystallisation and co-crosslinking can often result in stable morphologies that are resistant to coalescence [36]. However, Datta and Lohse [37] pointed out that a compatibiliser is not a process and thus suggested that while curing or crosslinking can fix a blend at a certain degree and size of phase separation, as can crystallisation, these processes can only be viewed as preserving a certain degree of compatibility.

The presence of compatibilisers in compatibilised blends will retard the formation of the Rayleigh disturbances on the threads as a result of a reduced interfacial tension during the blending process. The lower the interfacial tension, the longer the deformation tension exceeds the interfacial tension, the longer the stretching of the thread will proceed, the smaller the diameter of the resulting thread will become, and, consequently, the smaller the size of the dispersed droplets. Therefore compatibilised blends are characterised by the presence of a finely dispersed phase and resistance to gross phase segregation as shown in Figure 2.10.

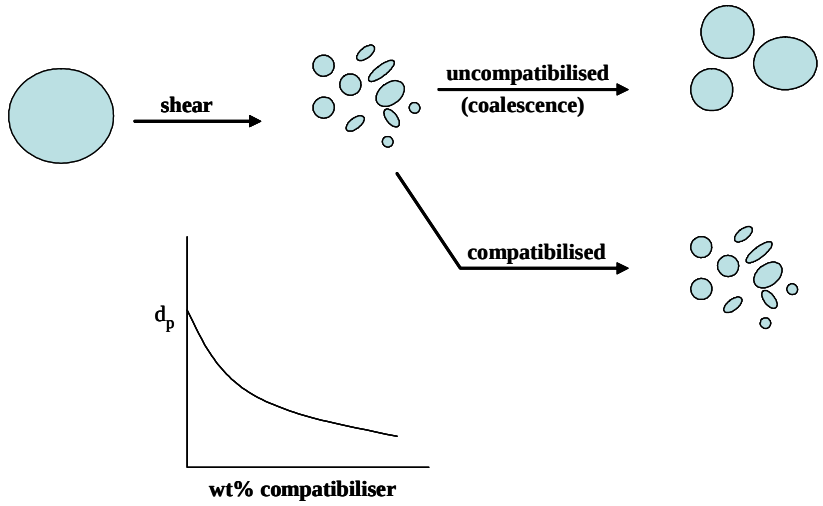


**Figure 2.10 Generalised illustration of effect of compatibiliser methods on particle size ($d_p$) [38]**

Two polymers form a compatible mixture when they possess one or more of the following characteristics [39]:

a.) Segmental structural identity.
*Example: a graft or block copolymer of butadiene and styrene is compatible with either polybutadiene or polystyrene.*

b.) Solubility parameter (δ) differences less than 2.0 $MPa^{1/2}$, generally less than 0.4 $MPa^{1/2}$.

*Example: polyvinyl chloride, polyethyl acrylate, and polymethyl methacrylate have solubility parameters in the 18.8 $MPa^{1/2}$ to 19.0 $MPa^{1/2}$ range and form compatible mixtures.*

c.) Functional groups capable of interactions.
*Example: functional groups capable of generating covalent, ionic, donor-acceptor, or hydrogen bonds between the polymers.*

There are two basic strategies for improving compatibility of immiscible polymer blends [35]:

a.) By addition of a third component (compatibiliser) capable of specific interactions and/or chemical reactions with the blend components. Block and graft copolymers (non-reactive and reactive functionalised types) and a variety of low molecular weight reactive chemicals fall under this category. The main criterion for selection of block or graft copolymers as compatibiliser is on the basis of miscibility or reactivity of its segments with at least one of the blend components.

b.) By blending suitably functionalised polymers capable of enhanced specific interactions and/or chemical reactions. The in situ formed compatibilisers have segments that are chemically identical to those in the respective unreacted homopolymers and are thought to be located preferentially at the interface. They may therefore be considered to be equivalent to the block or graft copolymers that are added separately as described in (a).

### 2.2.1 Addition of Pre-made Block and Graft Copolymers

For the immiscible blend of polymers A and B, copolymers such as A-co-B, A-co-D, and C-co-D type described in Table 2.2 can be used as compatibilisers. This is provided that C is miscible or nearly miscible with A; and D is miscible or nearly miscible with B.

For the block or graft copolymer to be effective it must locate preferentially at the blend interface [40]. Figure 2.11 illustrates the schematic diagram of the possible locations of a A-co-B block copolymer (the circle denotes the junction between segments A and B) in the A/B blend. The entropy part of the free energy favours location of this junction at random rather than in a well defined interface plane. However, the thermodynamic driving force tends to orient the junction at the interface plane. Consequently, a diffuse interfacial zone as shown by the shaded area of Figure 2.11 may be formed.

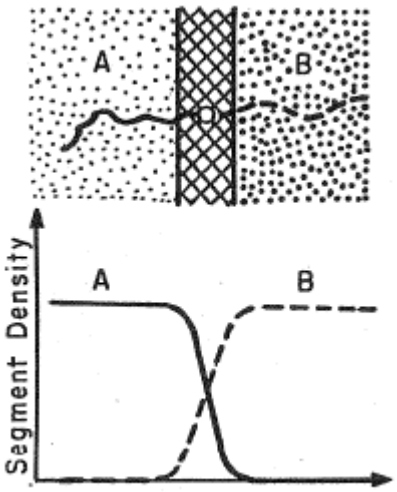


**Figure 2.11 Schematic diagram showing possible locations of A-co-B block copolymer in the A/B blend** [40]

In order to act effectively as a compatibiliser, A-co-B type copolymer should have segmental blocks with molecular weights of at least equal or higher than the molecular weights of the respective homopolymers. Good interfacial adhesion is only possible if the segments of the A-co-B copolymer penetrate into the parent phases A and B to be entangled with the constitutive chains. This is one setback of A-co-B copolymer compared to A-co-D and C-co-D systems where C and D components are thermodynamically miscible with A and B, respectively [22].

Figure 2.12 presents a schematic diagram of the supposed conformation of some compatibiliser molecules at the interface of a heterogeneous polymer

blend. Shown are diblock, triblock, multi-grafted and single-grafted copolymers.

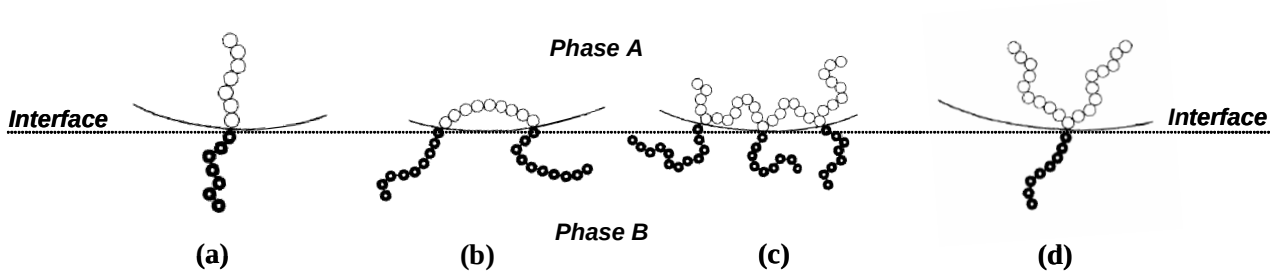


**Figure 2.12 Schematic diagram showing conformations of (a) diblock, (b) triblock, (c) multi-graft and (d) single-graft copolymers at the interface of a heterogeneous polymer blend** [**34**]

Block copolymers are generally more effective than graft copolymers as compatibilising agents, particularly when branches are located on a single backbone in the latter and restrict the opportunities for the backbone to penetrate its homopolymer phase [39-41]. For the same reasons, diblock copolymers might be more effective than triblocks.

The disadvantage of adding copolymer as a separate species to immiscible polymer blends is that diffusion to the interface may not be effective within the residence time of a typical extrusion blending process which is usually around 2 to 5 minutes. In addition, there is a tendency to form micelles as a third distinct phase that do not contribute to compatibilisation when high concentrations of copolymers are added [18].

The addition of block or graft copolymers represents one of the most extensively researched approach to compatibilisation of immiscible polymer blends. Many works [25, 97, 98, 132-141] have been carried out on compatibilisation of polystyrene-polyethylene blends using copolymer type compatibilisers. These will be discussed in greater detail later in Section 2.3.4 of this review.

Styrene block copolymer compatibilisers particularly triblock type copolymers like SEBS have been found to produce improvements in the mechanical

behaviour of a wide range of polyolefin/engineering thermoplastics blends by Gergen and Davison [42]. They suggested that the block copolymer acts to stabilise the blend morphology and to prevent the formation of grossly heterogeneous structures that would otherwise result. They observed the formation of an interlocking, or interpenetrating network of phases by the addition of the block copolymers which is an ideal morphology for an immiscible blend as it allows more equal sharing of imposed stresses by the blend components.

Traugott et al [1] compared the compatibilisation effectiveness of SEBS and an a ethylene-propylene elastomer in HDPE/PET blends. They observed that the triblock compatibiliser adhered better to both PET and HDPE than this pair does to each other. They claimed that the adhesion of the triblock to HDPE was due to similarity of the polyolefin mid-block to polyethylene whereas the aromatic character of the end block contributed to its adhesion properties with PET. On the other hand, the ethylene-propylene elastomer only adhered very well to HDPE but very poorly to PET leading to poor compatibility as compared to the SEBS triblock copolymer.

The compatibilisation of poly(2,6 dimethyl 1,4-phenylene ether) (PPE) and PP using SEBS triblock and S-EP diblock copolymers has been carried out by Akkapeddi and VanBuskirk [43]. They observed that low molecular weight SEBS triblock copolymer was more efficient in compatibilising the PPE-PP blends than a higher molecular weight type due to slower diffusion rate of the latter and hence less efficient absorption at the interface. They found that the diblock copolymer acted as a good emulsifier to the blend which contributed to good impact performance of the resultant blends. However, the blends showed brittle failure mode and lower tensile elongation due to poor interfacial adhesion of the phases. On the other hand, the blends that were compatibilised using SEBS triblock showed better impact performance and tensile elongation due to better interfacial adhesion. This was claimed to be due to the entanglement (anchoring) of the middle EB block of the SEBS with the PP chains of the matrix while the polystyrene end blocks remained solubilised in the PPE phase due to strong segmental interaction. Through the

application of electron microscopy, they observed that only a fraction of both the diblock and triblock copolymers were located at the interface of the blends with significant amount of the copolymers appearing as dispersions (micelles formation) in the PP matrix. Other factors like melt viscosity ratio between the dispersed phase and the matrix, and also the sequence of blending of the components was postulated to have great influence on the final blend properties.

Halimatudahliana and co-workers [44, 45] adopted a similar concept of using triblock SEBS copolymer for the compatibilisation of polystyrene-polypropylene (PS-PP) blends. Similarly, they observed improvements in toughness and ductility of the blends compatibilised with SEBS in comparison with uncompatibilised ones. It has been proposed that the compatibilising effect was contributed by the affinity between the ethylene-butylene mid-block with the polypropylene and also the interaction of the styrene end blocks with the polystyrene phase. SEM micrographs in their studies [45] showed that SEBS was able to reduce the particle size of the PS dispersed phase and also improved adhesion between the PP-PS phases of the blends. However, they observed that the addition of SEBS to PS-PP blends reduced the tensile strength for all blend compositions. This is a common observation as the addition of thermoplastic elastomers tends to reduce tensile strength and modulus of the blends as proposed by Lindsey et al [25].

Srinivasan and Gupta [46] attempted to improve the tensile and flexural properties of a PP-SEBS binary blend by blending with a rigid polycarbonate (PC) with this binary system. They found that a good combination of flexural and tensile properties could be achieved when the PP-SEBS-PC ternary blends contain not too low PC content and not too high SEBS content. They observed through SEM analysis that the PC dispersed droplets were surrounded by a layer of the SEBS triblock copolymer. The average PC droplet size decreased on increasing the SEBS level of the blend. On the other hand, increasing the amount of PC increased the average PC droplet size. These bigger droplets of PC may or may not be entirely covered by an SEBS envelop, depending upon the ratio of SEBS to PC present in the

ternary blend. Therefore the morphology of the PP-SEBS-PC ternary blend was proposed to be governed by the ratio of SEBS to PC present in the blend. The authors claimed that PP-SEBS content of 95/5 or 90/10 and PC content of about 10 wt% produces blends with good combination of flexural and tensile properties.

Adewole and co-workers [47] postulated that PP-g-PS graft copolymer was more effective in compatibilising polypropylene-polystyrene blends than SEBS triblock copolymer. They observed that the morphology of the blends compatibilised by the graft copolymer had finer dispersed domains and also much lower motion induced particle coalescence i.e. the graft copolymer is more effective with respect to both particle break-up and phase stabilisation.

Macosko et al [48] investigated the compatibilising effects of P(S-b-MMA) diblock copolymers in immiscible melt blended poly(methyl methacrylate) (PMMA) and polystyrene (PS). They observed that the diblock copolymers were effective in reducing the particle size of dispersed PMMA phase even at a low dosage level of 1%. They also claimed that low molecular weight diblocks had faster diffusion rate to the blend interface which reduced the interfacial tension and also prevented dynamic coalescence. On the other hand, higher molecular weight diblocks were not effective as their critical micelle concentration was very low and the segments of the diblocks tended to get caught in the micelles.

### 2.2.2 Reactive Compatibilisation

One of the most economical and efficient processes for adding a copolymer to a blend of immiscible polymers is to form the copolymer in situ by a chemical reaction during the extrusion process during establishment of the immiscible phase morphology. The process is known as *Reactive Compatibilisation* [18].

Reactive processing is an integration of polymer chemistry with polymer processing. During the reactive blending process, copolymer may be formed

through an interchain reaction. Interchain copolymer formation may be defined as reaction of two (or more) polymers to form a copolymer. The five basic chemical processes by which interchain copolymer formation has been achieved in an extruder are summarised in Table 2.4 [49]. The types of copolymers formed are illustrated through the reaction of two polymers, AAAAA and BBBBB.

The reactive compatibilisation method is not universally applicable to all polymer pairs. It is applicable to those pairs in which at least one of the blend constituents possess certain functional groups, at the chain ends or within the main chains, which could react with the reactive compatibiliser.

**Table 2.4 Chemical processes for interchain copolymer formation in extruder reactors [49]**

| Type | Chemical Reaction | Type of Copolymer Obtained |
|---|---|---|
| 1 | chain cleavage / recombination | block and random copolymers: AAAAABBBBB + AABBBBBAAA + AABBAAABBB etc. |
| 2 | end-group of 1st polymer reacting with end-group of 2nd polymer | block copolymer: AAAAABBBBB |
| 3 | end-group of 1st polymer reacting with pendant functionality of 2nd polymer | graft copolymer:<br>A<br>A — BBBBB<br>A<br>A — BBBBB<br>A |
| 4 | covalent crosslinking: reaction either between pendant groups or main chains of the two polymers | graft copolymer or crosslinked network |
| 5 | Ionic bond formation | Usually graft, frequently crosslinked system |

Brown [49] stated 5 basic requirements for efficient reactive compatibilisation:

- Sufficient mixing to achieve the desired morphology of one polymer in another.
- Presence of suitable reactive functionality for covalent or ionic bond formation.
- Functionalities are of suitable reactivity to react across the melt phase boundary.
- Reaction must take place within the residence time of the extruder.
- The formed covalent (or ionic) bonds must remain stable in subsequent processing steps.

The majority of commercial polymers that are utilised to form interchain copolymers have nucleophilic end groups such as carboxylic acid, amine or hydroxyl. These nucleophilic end groups can react with suitable electrophilic functionalities like cyclic anhydride, epoxide, oxazoline, isocyanate and carbodiimide that are attached to a second polymer to form covalent bonding. Since the probability of two end groups reacting within the residence time in an extruder is low, highly reactive functionality is necessary and sometimes lower molecular weight polymers.

Orr et al [50] measured the rates of nine melt coupling reactions by reacting terminally functionalised polymer chains. The rate of reaction was monitored by determining the amount of coupled chains using gel permeation chromatography. The authors [50] observed that of the functional group pairs studied, only the acid/epoxy and amine/anhydride pairs have significant conversion within 2 minutes. These also happen to be the main coupling reactions used commercially.

Ferrari and Baker [51] observed that during melt blending, the reaction rate of a reactive compatibilisation process can possibly be reduced by the restricted access of the reactive sites as compared to those in low viscosity solution systems. The authors [51] suggested that steric hindrance of the polymer backbones and also the limited ability of the chains with reactive sites to

reorient themselves for greater exposure of functional groups due to entanglements of these chains with diluent macromolecules (non reactive chains), could lead to the reduction in the reaction rate. On the other hand, polymer chains in low viscosity systems could easily re-orientate themselves for greater exposure of the reactive sites and also the expanded state of these chains allows easier diffusion of the other reactive moieties to the reactive sites.

Jeon and co-workers [52] investigated the effect of functional group location on coupling kinetics by comparing reactions of an end-functional polymer versus a mid-functional polymer. They found that coupling with the mid-functional polymer was slower than with the end-functional polymer even in a homogeneous melt. They attributed this finding to the shielding of the mid-functional group by a steric hindrance effect of the polymer chain.

To achieve reactive compatibilisation, two main routes which generate in situ formed copolymers are commonly employed, namely, reactive blending of suitably functionalised blend components, and the incorporation of a third component reactive compatibiliser.

**a.) In situ Formed Copolymers by Reactive Blending**

Graft or block copolymers acting as compatibilisers for immiscible polymer blends can be formed in situ through covalent or ionic bonding during melt blending of suitably functionalised polymers as shown in Figure 2.13.

This method is different from other compatibilising routes in that the blend components are either chosen or modified so that reaction can occur during melt blending, with no addition of a separate compatibiliser. The in situ formed compatibilisers have segments that are chemically identical to those in the respective unreacted homopolymers and are thought to be located preferentially at the interface of the binary blends; thus, they lower interfacial tension and promote mechanical interlocking through interpenetration and entanglements.

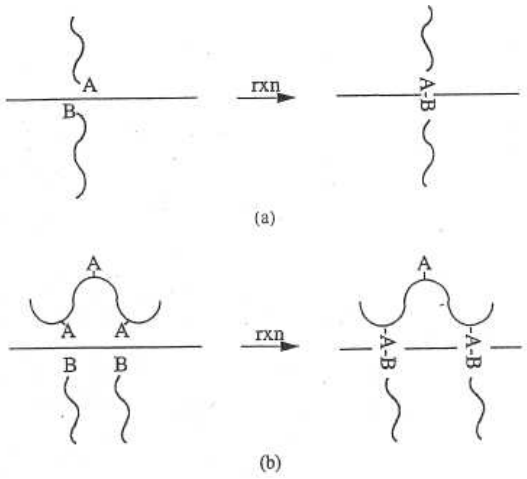


**Figure 2.13 Reaction of polymer-bound functional groups A and B to form (a) a block copolymer and (b) a graft copolymer at the interface between two immiscible polymer phases [53]**

The in situ compatibilisation of immiscible blends is normally carried out in 2 separate reactive processing steps. The functionalisation of a chemically inert polymer is first carried out by reactive processing and is then blended with another functionalised polymer in a second reactive processing step. Liu and co-workers [54] grafted maleic anhydride onto low density polyethylene (LDPE) and then melt blend the grafted LDPE with polystyrene containing oxazoline functional groups (OPS) in a Haake internal mixer. An increase in torque during mixing was observed in the reactive blends against corresponding nonreactive blends without functional groups suggested possibility of interpolymer coupling reactions between the maleic anhydride and oxazoline functional groups. The detection of new strong peak at 1734 $cm^{-1}$ from the resultant blends using Fourier Transform Infrared spectroscopy (FTIR) justified the formation of ester linkage due to interpolymer reactions between the functional groups. The interpolymer reactions also resulted in fine morphology as observed using a scanning electron microscope.

Sun et al [55] investigated the possibilities of conducting the in situ compatibilisation of PP/PBT blends in a one-step reactive process i.e. both functionalisation and reactive blending steps were executed in the same extrusion process. Three reactive functional groups, namely, acrylic acid (AA), maleic anhydride (MAH), and glycidyl methacrylate (GMA) were melt grafted onto the PP chain by free radical reactions for comparative studies of their

compatibilising efficiencies on the PP/PBT blends. They claimed that GMA was most effective in compatibilising PP/PBT blends, demonstrating a fifteen to twenty fold improvement in elongation at break and impact strength over uncompatibilised PP/PBT blends. They also concluded that the one-step reactive extrusion process was comparable to, if not better than, those of the blend obtained by a two-step process.

**b.) In situ Formed Copolymers by Addition of Reactive Compatibilisers**

The addition of a reactive compatibiliser, miscible with one blend component and reactive towards functional groups attached to the second blend component results in the in situ formation of block or grafted copolymers. Typically a C-X reactive copolymer could be a compatibiliser for polymer blend A/B, where C is structurally identical or miscible with A, and X can react with B component (mostly at chain ends) to form an in situ C-X-B graft or block copolymer as shown in Figure 2.14.

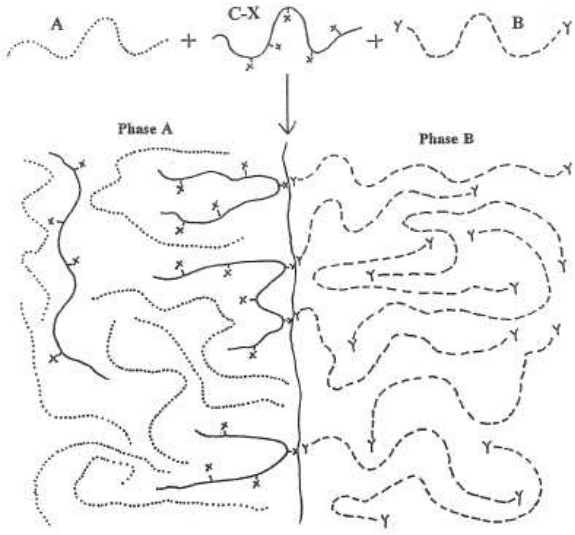


**Figure 2.14 Schematic diagram shows the formation of C-X-B grafted copolymers at interface of a ternary A/C-X/B blend [22]**

The majority of the reactions that take place in such ternary blends are actually similar to those that occur during reactive blending of binary blends discussed above. For example, the reaction that takes place in binary blends

of polyamide/maleated PP is the same as those observed in ternary blends of polyamide/maleated PP/PP.

A variety of reactive polymers have been utilized for compatibilising polymer blends. They can be classified into six major categories [56] with each category having one type of functional group, namely, maleic anhydride, carboxylic acid, carboxylic derivatives, primary and secondary amines, hydroxyl and epoxide, and groups capable of ionic interactions. Reactive compatibilisation involves a variety of chemical reactions during the melt blending process, including addition and substitution reactions such as amidation, imidation, esterification, and concerted addition; interchange reactions such as aminolysis, transesterification, and amide-ester exchange; and ring-opening reactions involving epoxide, oxazoline, and lactam; as well as ionic bonding.

The following section of this review will focus on 2 major functionalities, maleic anhydride and epoxide, that are widely utilised in reactive compatibilisation of immiscible polymer blends.

#### 2.2.2.1 Compatibilisation through addition of maleic anhydride functionalised compatibilisers

In recent decades maleic anhydride (MAH) grafted polyolefins and elastomers have been extensively investigated as precursors for the reactive compatibilisation of various polyamide/polyolefin blends. As shown in Figure 2.15 (a), maleic anhydride possesses a double reactivity: free radical reactivity (unsaturation of the C=C double bonds) and functional reactivity (cyclic anhydride). Once grafted onto the polymer backbone in the form of a substituted succinic anhydride (SA) (See Figure 2.15 (b)), it provides the polymer substrate with high reactivity towards various nucleophilic groups (amines, alcohols, thiols, etc.) or electrophilic groups (epoxies) in the presence of a catalyst [57].

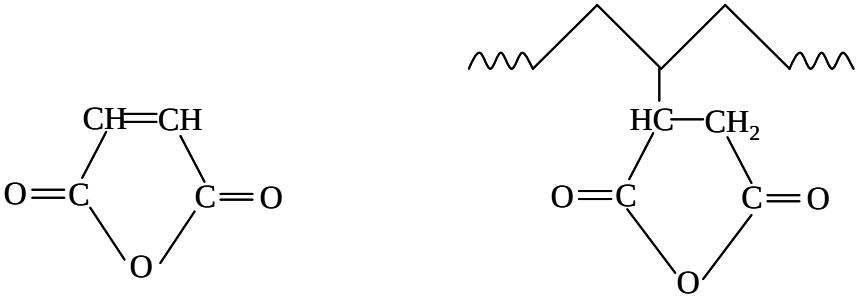


(a) (b)

**Figure 2.15 Chemical structures of (a) maleic anhydride (MAH), (b) grafted succinic anhydride**

The grafted succinic moieties may exist in either the acid or the anhydride form as five-membered cyclic anhydride shown in Figure 2.16. The cyclic anhydride can undergo hydrolysis in the presence of moisture to form carboxylic dimmer acids while these dicarboxylic acids can be converted back to the cyclic anhydride form through heating (dehydration process). The conversion of dicarboxylic acids to cyclic anhydrides can be monitored using infrared spectroscopy through the variation of the absorbances at 1713 $cm^{-1}$ and 1790 $cm^{-1}$, characteristics of the acid carbonyls and anhydride carbonyls, respectively. Bettini and Agnelli [58] observed an increase in the cyclic anhydride carbonyl band at 1790 $cm^{-1}$, when samples of maleic anhydride functionalised PP were subjected to heat treatment at 130℃ for 96 hours.

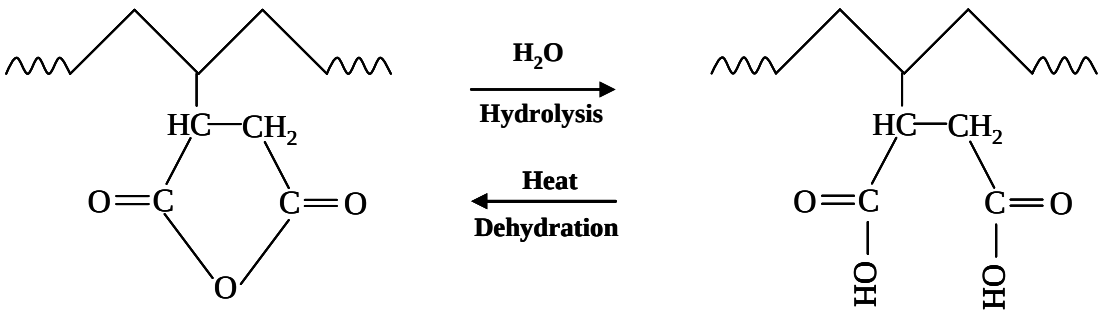


**Figure 2.16 Reversible reactions of succinic anhydride under the influence of water (hydrolysis reaction) and heat (dehydration)**

MAH grafted polyolefin and rubbers are important classes of reactive functionalised polymers for application as compatibilisers in polymer blends (particularly in impact modification of polyamides), as adhesion promoters for polymer and composites and as bonding agents for polymer and metal.

During the early 1970s, Ide and Hasegawa [59] attempted to compatibilise immiscible blends of isotactic PP and polyamide 6 in the presence of a maleic anhydride grafted PP compatibiliser. They observed marked improvements in the dispersion quality of the blends which they claimed to be due to the formation of PP-graft-PA6 copolymer. They proposed that during the melt blending process, the PA6 amine end groups reacted with the succinic anhydride of the functionalised PP to form PP-graft-PA6 copolymer as shown in Figure 2.17. The presence of PP-graft-PA6 copolymer at the interface of the PP and PA6 blends improved both dispersion quality and interfacial adhesion of the phases.

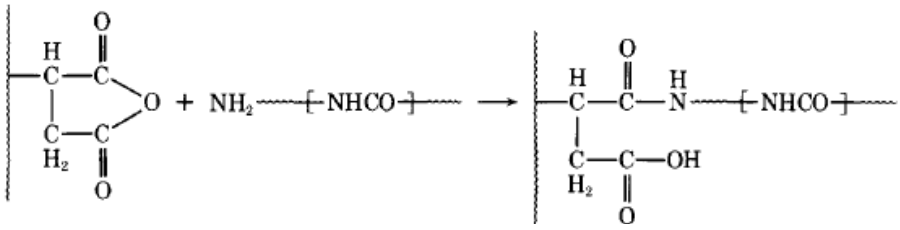

**Figure 2.17 Formation of PP-g-PA6 copolymer through amine-anhydride reaction [59]**

In their studies conducted on PA6/PP blends, González-Montiel and co-workers [60] found that maleated rubbers such as ethylene-propylene random copolymer (EPR-g-MAH) and styrene-ethylene/butylene-styrene triblock copolymer (SEBS-g-MAH) were effective in functioning as impact modifiers as well as compatibilisers in the ternary blends. The authors proposed that the maleic anhydride moieties of the maleated rubbers reacted with the amine end-groups of the polyamide which formed rubber-PA6 graft copolymers that locate at the interface between PA6 and PP acting as compatibilisers. EPR-g-MAH was claimed to impart lower ductile-brittle transition temperatures to the blends than SEBS-g-MAH due to the inherent lower glass transition

temperature of the EPR-g-MAH (Tg approx. -45℃) rubber as compared to SEBS-g-MAH (Tg approx. -38℃). On the other hand, SEBS-g-MAH was postulated to have better compatibilising effects as the authors observed better dispersion quality of the polypropylene and rubber phases in the blends.

Valenza and Acierno [61] investigated the effectiveness of maleic anhydride and acrylic acid grafted PP as a compatibiliser in blends of polyamide 12 and PP. They observed that the mechanical properties of the blends were improved by the presence of either compatibiliser, while the maleic anhydride functionalised PP showed a better compatibilising effect, imparting better tensile strength and elongation than blends compatibilised by the acrylic acid functionalised PP as shown in Figure 2.18.

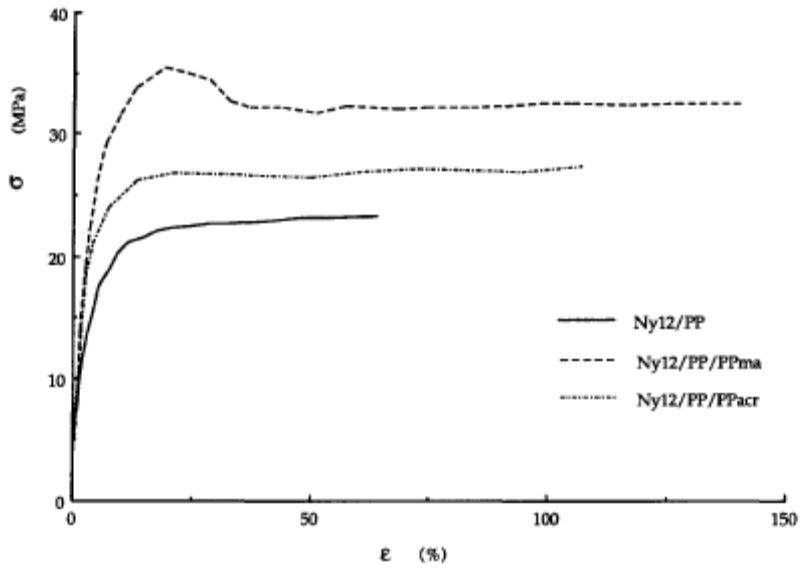


**Figure 2.18 Stress-strain curves of uncompatibilised and compatibilised polyamide 12/polypropylene blends [61]**

The functionalities of polyamides play an important role during their compatibilisation with maleic anhydride functionalised polymers. Oshinski and co-workers [62, 63] studied the impact modifications of polyamide 6 (PA6) and polyamide 66 (PA66) with maleated styrene/ethylene/butylene/styrene block copolymers (SEBS-g-MAH). They observed that PA66 could be made super-tough by blending with SEBS-g-MAH alone, whereas for PA6, such

toughness levels could be achieved only by blending with a combination of SEBS-g-MAH and SEBS. Melt blending of SEBS-g-MAH alone with PA6 resulted in rubber particles that were too small (approximately 0.05 µm) for effective toughening, but dilution of the rubber with the non-reactive SEBS increases the particle size to within the optimal range (just less than 1 µm). On the other hand, melt blending of SEBS-g-MAH with PA66 resulted in particles that were already within the optimal range for toughening. The authors [63] proposed that chemical differences between the two polyamides contributed to this difference in morphology of the blends. It appears that the basic difference between the two nylons is that PA6 is monofunctional whereas the PA66 is difunctional in terms of their reactions with anhydrides [64]. PA6 has amide linkages that are unidirectional and each chain typically has one amine and one acid group at either end as made by lactam ring-opening polymerisation.

For PA66, the orientation of amide linkages is alternating and individual chains may have all amine or all acid groups or one of each and are therefore difunctional in nature. Since an amine end reacts with an anhydride unit to form an imide linkage as shown in Figure 2.17, PA6 can only undergo simple grafting reactions that involve one point of attachment per polyamide chain as shown in Figure 2.19. Such interaction leads to a decrease in interfacial tension and some stabilisation against coalescence.

On the other hand PA66 can have up to two particle attachments per chain due to its difunctionality to anhydride. Figure 2.19 shows that PA66 may form loops or bridges between particles when they approach each other in near proximity. It was claimed that such chain connections could act to prevent particle break-up, encourage coalescence and provide a mechanism for occlusion of matrix material into the rubber particles.

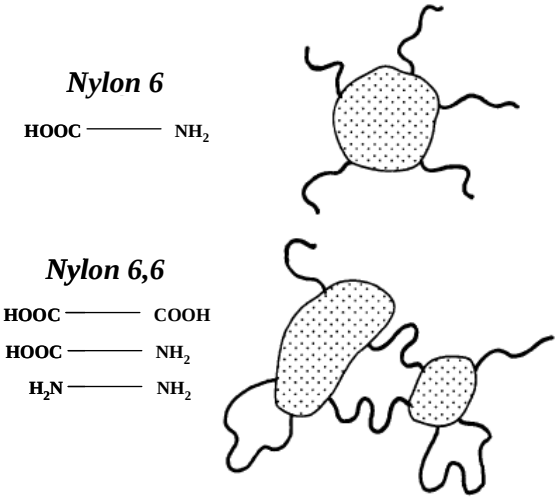


**Figure 2.19 Schematic representation of modes of attachment of PA6 and PA66 to maleated elastomers [63]**

Kriengchieocharn, Axtell and co-workers [65, 66] attempted to compatibilise PA6 with natural rubber (NR) using maleated NR (NR-g-MAH) as compatibiliser. The maleic anhydride was grafted onto the NR backbone via a free radical reaction which was initiated by heating and shearing the NR, generating free radicals due to the chain scission of the NR molecules without the use of peroxide initiators. They found that the addition of NR-g-MAH resulted in fine dispersions of NR in PA6 which improved the toughness and other mechanical properties compared with uncompatibilised blends. Through the results of the Molau test and infra-red analysis, the authors suggested that the reaction between the maleic anhydride of the NR-g-MAH rubber and amide/amine groups of the PA6 resulted in the formation of chemical compatibilising copolymers which improved the adhesion of the two phases.

### 2.2.2.2 Compatibilisation through addition of glycidyl methacrylate functionalised compatibilisers

Glycidyl methacrylate (GMA) is a dual functional monomer that contains both acrylic and epoxy groups as shown in Figure 2.20. The dual functionality of GMA brings together its ability to react with an extremely wide range of

monomers and functionalised molecules, thus providing greater flexibility and freedom in the design of functionalised polymers.

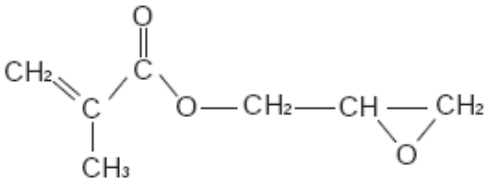

**Figure 2.20 Glycidyl Methacrylate (GMA) chemical Structure [67]**

Figure 2.21 demonstrates three examples of GMA functionalised polymers obtained through grafting the methacrylate groups of the GMA and the backbone of these polymers. The epoxy group of the GMA possess reactivity towards various functional groups such as —COOH, —OH, and —$NH_2$ thus rendering GMA functionalised polymers ideal compatibilisers in reactive blending.

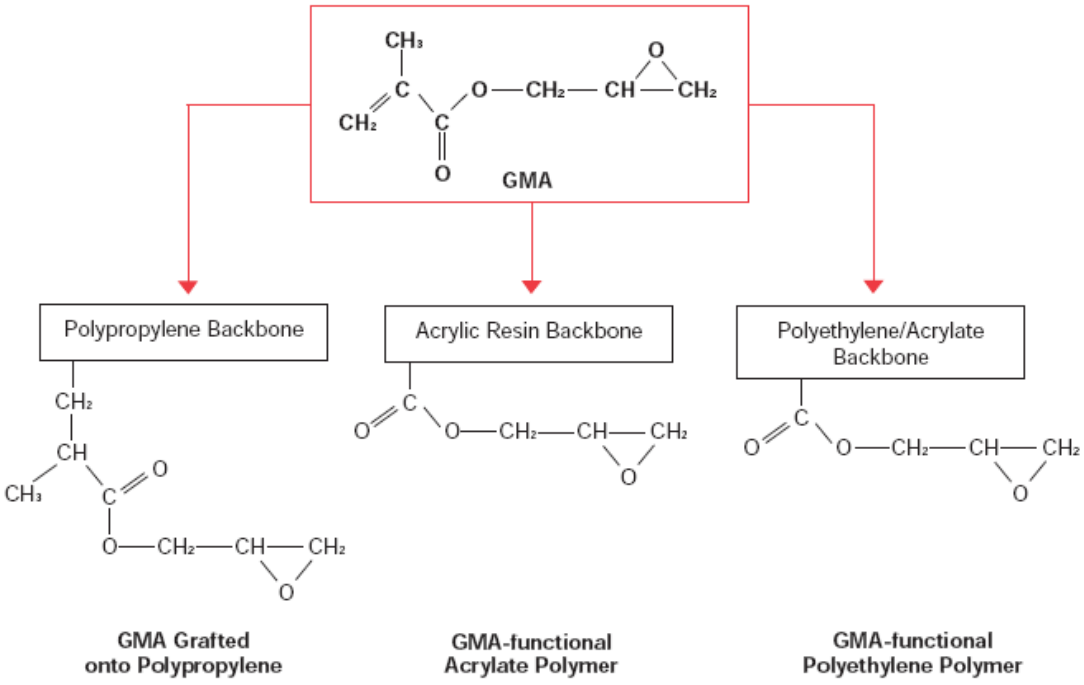


**Figure 2.21 Typical grafting reactions through methacrylate group of GMA [67]**

GMA functionalised polyolefins have been extensively studied as compatibilisers in polyester/polyolefin blends (polyester/polyethylene blends will be discussed in detail later in section 2.3.2 of this review). Compatibilisers containing GMA functionality are well suited for compatibilising polyester related blends as inherently most polyesters contain carboxylic acid and/or hydroxyl end-groups that are reactive towards the epoxy moiety of the GMA.

Holsti-Miettinen and co-workers [68] attempted to compatibilise PP/PBT and PP/LCP blends using ethylene/ethyl acrylate/glycidyl methacrylate (E-EA-GMA) terpolymer as compatibiliser. They first justified the possible interactions between the polyesters and compatibiliser through binary blends of PBT/E-EA-GMA and LCP/E-EA-GMA. The results of FTIR analysis coupled with the increase in torque of the binary blends with time and development of fine morphology indicated possible reactions between the carboxyl end groups of the polyesters and the epoxy group of the compatibiliser. They observed that the notched Charpy impact strength of blends of PP/PBT at compositions of 80/20 and 20/80 were significantly improved by the presence of 5 wt% of E-EA-GMA compatibiliser due to fine dispersion of the minor phase in the matrix. The compatibiliser was most effective in improving unnotched Charpy impact strength of PP/LCP using a composition of 80/20.

On the other hand, Chiou et al [69] studied the compatibilisation of PP/LCP blends using ethylene-co-glycidyl methacrylate (E-GMA) as compatibiliser. At 2.5 parts per hundred of the PP/LCP blends (ranging from 5 wt% to 20 wt% of LCP content), the E-GMA was effective in improving the unnotched toughness across the blends indicating improved interfacial adhesion of the phases. The presence of ethyl triphenylphosphonium bromide as catalyst in these blends was found to further enhance the toughness of the blends which indicated improvements in compatibilisation. The authors also reported that the formation of E-GMA-g-LCP copolymers at the blend interface caused a reduction in the crystallinity of PP component as reflected by the substantial reduction in stiffness of the blends.

The effectiveness of ethylene-co-glycidyl methacrylate (E-GMA) in compatibilising PBT/PP blends was evaluated by Tsai and Chang [70]. They postulated the possibility of a ring opening reaction of the epoxy moiety from the E-GMA during the melt blending process by the observation of disappearing FTIR peaks at 909 $cm^{-1}$ and 995 $cm^{-1}$. The authors also proposed the possibility of E-GMA-g-PBT copolymer formation at the interface of the blends but without any evidence from FTIR analysis. However, the effectiveness of E-GMA as compatibiliser was demonstrated by the improvements in the unnotched impact toughness and elongation at break of the blends due to better interfacial adhesion of the phases. The compatibilising effect was claimed to be further enhanced by increasing the content of GMA in E-GMA and also by the addition of 50 ppm ethyltriphenyl phosphonium bromide as catalyst in the compatibilised blends. Champagne et al [71] on the other hand reported that a lower GMA content in their PP-g-GMA compatibiliser was more efficient in emulsifying PP/PET blends. They attributed this observation to the possibility of higher non-grafted GMA content present in the high GMA content PP-g-GMA compatibiliser. The unbound GMA species was claimed to compete with the GMA-grafted PP chains for the PET end-groups. The deactivation of the PET end-groups by unbounded GMA could decrease availability of reactive sites for reaction with PP-g-GMA.

It has been reported by Maa [72], Lee [73], and Chang [74] that lightly grafted copolymers have better compatibilising efficiency than excessively grafted copolymers. Excessive grafting may result in a highly branched comb-like structure or even crosslinked network. Maa and Chang [72] studied the compatibilisation of PET/PS blends using styrene-glycidyl methacrylate (SG) as compatibiliser. They demonstrated that excessive grafting of PET onto SG resulted in highly branched SG-g-PET copolymer as shown in Figure 2.22 (A). The excessively branched SG-g-PET copolymer has PET chains shielding the styrene segments of the SG copolymer thus minimising its possible contact with the polystyrene component of the PET/PS blends. On the other hand, lightly grafted copolymer as shown in Figure 2.22 (B) with one or a few grafts per chain has been proposed to have a better compatibilising effect.

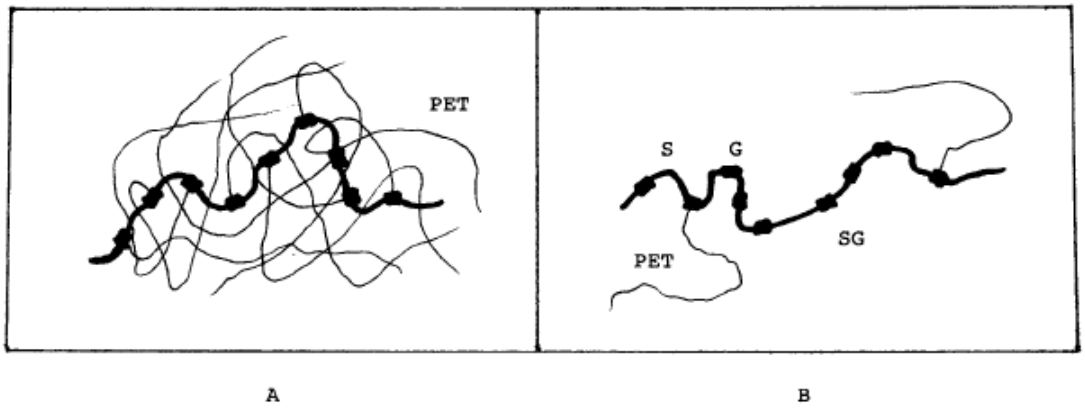


**Figure 2.22 Schematic representation of the excessively and lightly grafted SG-g-PET copolymers: (A) excessively grafted copolymer, (B) lightly grafted copolymer [72].**

Similar claims of lower efficiencies of excessively grafted copolymers have been reported by Lee and co-workers [73] on styrene-acrylonitrile-glycidyl methacrylate (SAG) copolymer compatibilised PBT/ABS blends and also Change et al [74] for SAG compatibilised ABS/PA 66 blends.

Sun and colleagues [55] utilised a one-step reactive extrusion process which enabled the functionalisation of PP with reactive monomers like acrylic acid (AA), maleic anhydride (MAH), and GMA and then subsequent interfacial reaction of the functionalised PP with the PBT in one single extrusion process. Of the three reactive monomers, GMA was reported to have the best compatibilising effect shown by its substantial improvements in impact toughness and elongation at break compared with the uncompatibilised PP/PBT blend and the other blends containing AA and MAH monomers. The poor compatibilising effects of AA and MAH were also reflected in the coarse morphological properties of the resultant blends. The authors [55] pointed out that the use of acrylic acid functionality of a compatibiliser has the disadvantage of being kinetically slower than the other 2 monomers when esterified with the terminal OH groups of the polyester, whereas at high processing temperatures of 240℃, the condition is unfavourable for the reaction of MAH with the hydroxyl group of the PBT to form the desirable PP-g-PBT copolymers.

Heino et al [75] compared the effectiveness of unfunctionalised SEBS and two functionalised SEBS compatibilisers containing either maleic anhydride (SEBS-g-MAH) or glycidyl methacrylate (SEBS-g-GMA) in incompatible blends of PET/PP. They reported finer morphology and better mechanical properties observed for blends compatibilised with either functionalised SEBS. However, the authors also observed greater compatibilisation effects for SEBS-g-GMA in blends with PET rich compositions thus indicating greater reactivity of the GMA functionality towards the end groups of PET than the MAH moieties.

Tedesco and co-workers [76] evaluated the effectiveness of maleic anhydride (PP-g-MAH) and glycidyl methacrylate (PP-g-GMA) functionalised polypropylene in compatibilisation of polypropylene/polyamide 6 blends. The PP-g-MAH was found to be more effective in compatibilising PP/PA6 than PP-g-GMA. The blend compatibilised by PP-g-MAH was found to exhibit very fine morphology and also better mechanical properties. The authors suggested that the modification of crystallisation behaviour of the PP and PA6 components indicated the formation of PP-g-PA6 copolymers at the blend interface.

PP-g-GMA was also successfully utilised by Yin and co-workers [77] in the compatibilisation of polypropylene/polycarbonate (PP/PC) blends. The reaction between PP-g-GMA and terminal hydroxyl groups of PC contributed to the reduction of the interfacial tension and also promoted adhesion of the two phases which resulted in improved mechanical properties.

### 2.2.2.3 Compatibilisation through addition of epoxy resin compatibilisers

In recent years, there is an increasing trend in studies conducted on the blending of epoxy resins with various thermoplastics for various reasons:

a.) chain extension of polyesters resins [78-80],
b.) impact modification of epoxy resins [81-82],
c.) dynamic vulcanisation process [83-85]
d.) compatibilisation of polymer blends [87-96]

Other than GMA functionalised polymers that were discussed in the last section of this review, there are two classes of epoxy resins that have been commonly studied as compatibilisers in polymer blends. They are low molecular weight bifunctional diglycidyl ether of bisphenol-A (DGEBA) and multifunctional tetraglycidyl ether of diphenyl diaminomethane (TGDDM) resins as shown in Figure 2.23.

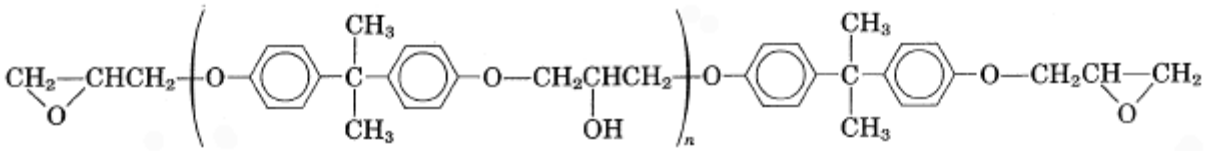

**(a)**

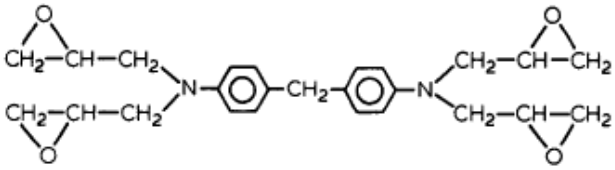

**(b)**

**Figure 2.23 The molecular structure of (a) diglycidyl ether of bisphenol-A (DGEBA), and (b) tetraglycidyl ether of diphenyl diaminomethane (TGDDM)**

Based on the literature cited, it seems that there is less research work conducted on compatibilisation using epoxy resin compared with MAH and GMA type compatibilisers. Low molecular weight compatibilisers are usually added at relatively low concentrations (typically 0.1% to 3% by weight) and thus they may offer economic advantages versus polymeric compatibilisers that are usually effective at higher concentrations [86].

In most of the immiscible blends, epoxy resins are neither identical nor miscible with either of the blend components thus forcing them to reside preferentially at the blend interface during melt blending. Such preferential residence behaviour provides the epoxy moieties greater opportunities for reaction with both components of the blends to produce in situ formed copolymers which are effective compatibilisers.

Due to the presence of chain-end functional groups for possible reactions with epoxy moieties, polyesters (—COOH and/or —OH), polyamides (—$NH_2$), and polyphenylene ethers (phenolic—OH) are particularly suitable for in situ reactive compatibilisation. If one of the blend components is non-reactive, it can be prefunctionalised with certain reactive groups for further reactions. This concept has been applied by Shieh and co-workers [87] using dual compatibilisers composed of a maleic anhydride grafted polypropylene (PP-g-MAH) and TGDDM multifunctional epoxy resin for the compatibilisation of polypropylene and polybutylene terephthalate (PP/PBT) blends. The strategy of their compatibilisation work was to react the maleic anhydride group of PP-g-MAH (which is miscible with the polypropylene component) with the epoxy group of TGDDM to form a PP-MAH-co-epoxy copolymer intermediate which will then react with the end-group of PBT to form PP-MAH-co-epoxy-co-PBT copolymers at the interface of the blends as compatibilisers. They observed from unnotched impact testing that with PBT rich blends, excessive inclusion of the epoxy compatibilising agent at 0.5 phr of the blend, produced a dramatic reduction in the toughness of the blends. They attributed this observation to the reaction of the epoxy resin with the PBT which resulted in lightly crosslinked PBT phases and lack of a compatibilising effect. The best compatibilising effect was observed to be at 0.3 phr of epoxy in PBT rich

blends. However, in PP rich blends, the toughness of the blends improved with increasing epoxy content from 0.3 phr to 0.5 phr. The authors also concluded that the epoxy is ineffective as a compatibiliser without the presence of PP-g-MAH co-compatibiliser across the blends.

The same strategy of using a dual compatibiliser system was applied by Tjong and Meng [88] in their attempt to improve the mechanical properties of polycarbonate/polyacrylonitrile-butadiene-styrene (PC/ABS) blends. First they melt blended the PP-g-MAH compatibiliser with ABS followed by blending them with PC and a difunctional DGEBA resin. It was claimed that the epoxy resin offered an optimum compatibilising effect at 2 phr level for blends containing less than 40 wt% of ABS disperse phase. The presence of both compatibilisers resulted in significant improvement in tensile ductility and impact toughness. They also observed dramatic reduction in the ABS dispersed phase due to the presence of both compatibilisers, implying an effective compatibilisation mechanism.

The effectiveness of using difunctional DGEBA resin for compatibilisation of PBT/PPE blends was justified by Jana and colleagues [89]. A mechanism of compatibilisation was proposed based on their FTIR findings. The reduction in the epoxy peak observed from PBT-epoxy mixtures with prolonged reaction time was postulated to be due to the conversion of the epoxy group during the reaction with PBT. However, from the FTIR analysis of PPE-epoxy mixtures they claimed that negligible reaction had occurred between PPE and the epoxy resin. The authors concluded that the mechanism of compatibilisation could be due to hydrogen bonding interactions between the phenolic —OH groups of the PPE and the epoxy group of the in situ formed PBT-epoxy copolymers as shown in Figure 2.24.

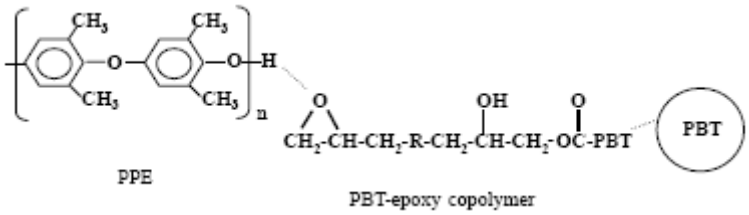


**Figure 2.24 Possible compatibilisation route between PBT and PPE by PBT-epoxy copolymer [89]**

Aróstegui and Nazábal, [90, 91] investigated the effectiveness of a difunctional epoxy resin in the compatibilisation of PBT/polyethylene octene copolymer blends (PBT/PEO). In these blends, the epoxy resin, at 1% concentration, was found to be effective in reducing the interfacial tension of the blends even though it only reacted with the PBT component of the blends. The authors observed that the Izod impact toughness of the blends was improved due to a finely dispersed PEO phase in the PBT matrix with the inter-particle distance as the main controlling factor over the toughness of the blends (the transition to super-toughness took place at an inter-particle distance of 0.48 μm). They also observed that the ductility of the blends behaved in the opposite direction to the Izod impact toughness which led to their conclusion that the level of interfacial adhesion required for high ductility is higher than that necessary for super-toughness of the blends.

Solid difunctional DGEBA resin has been demonstrated by Chin and co-workers [92] to be an effective compatibiliser for PET/LCP blends. The epoxy compatibiliser was able to react with PET and LCP simultaneously to produce in situ formed epoxy-b-PET-b-LCP copolymer which is highly effective in compatibilising the PET/LCP blends. They claimed that such compatibilising effects actually enhanced the LCP fibril formation which resulted in substantial improvements on both stiffness and toughness of the blends. However, in their subsequent research work [93] they discovered that the mechanical properties of these blends could be improved more by using multifunctional TGDDM as compatibiliser and it required less than one-tenth of the original DGEBA level to achieve similar properties. Their FTIR analysis indicated

reduction in epoxy functional groups after the melt blending process but was unable to prove if this was due to reactions with the end-groups of PET and LCP. Multifunctional TGDDM resins have also been reported to have shown positive compatibilisation efficiencies in PA6/PPE [94], PBT/PA66 [95], and PA6/PBT [96] blends.

## 2.3 Survey of Blends Containing Polyethylene

Polyethylene (PE) being economical and having broad range of physical properties, has found itself in many applications like packaging, agriculture, constructions, toys etc. In recent decades, blends containing polyethylene have been extensive investigated for the following reasons:

a. re-use of plastic scraps
b. impact modification
c. reduction of moisture absorption behaviour of hygroscopic polymers
d. increase chemical resistance of amorphous polymers
e. improve processability
f. reduction in notch sensitivity of some polymers like PA, PC
g. addition of colour masterbatches containing polyethylene carriers

Due to the non-polar nature of polyethylene resins, they have limited miscibility and compatibility with other polymers especially polymers that are polar in nature. To overcome the incompatibility of polyethylene resins with other polymers during blending, the resins are normally functionalised with reactive groups for potential interactions and/or reactions with other polymers or by the addition of a suitable compatibiliser into blends. The approaches on compatibilisation of blends containing polyethylene with various polymer types have been generally reviewed by Bonner and Hope [97], Datta [37], and Hope [98].

An overview of various strategies in compatibilising polyethylene resins with other non-olefinic thermoplastics will be discussed in the following sections, 2.3.1 to 2.3.4, of this review.

### 2.3.1 Polyamide-Polyethylene Blends

Polyamide (PA) is a large volume commercial polymer as it possesses good mechanical properties, exceptional chemical and solvent resistance. However, polyamides tend to absorb moisture from the environment which reduce the mechanical properties and affect the dimensional stability of the moulded parts [99]. Gaymans et al [100] studied the influence of water on the mechanical properties of PA6 and PA6/EPDM blends. They reported that the blends absorbed lower amount of water than PA6 and thus the dimensional stability of the blends was expected to improve with the volume fraction of the rubber. However, the addition of rubbery modifiers caused significant reduction in modulus and strength of the PA which is undesirable in engineering applications.

Blends of PE with PA have attracted much academic and commercial attention in the past decades as the resultant blends possess potential synergistic combinations of typical properties of the individual polymers. PE has the typical characteristics of toughness, ductility, insensitive to moisture and ease of processing. PA on the other hand possesses good mechanical properties, thermal stability and barrier properties to oxygen and solvents. However, the blending of PA with PE leads to a thermodynamically immiscible two-phase system which requires the introduction of appropriate compatibilisers for property enhancement.

Based on results obtained from optical microscopy and thermal analysis on blends of PA66 with various compositions of polyethylene, Orofino and McNeely [101] reported that polyethylene, irrespective of type and molecular weight, is incompatible with PA66 even at concentrations as low as 1 wt%. Precursors like maleic anhydride grafted polyethylene (or elastomers), ethylene acrylic acid (EAA), and ethylene-glycidylmethacrylate copolymers (E-GMA) have been popularly selected for investigation as compatibilisers for the compatibilisation of PA/PE blends as shown in Table 2.5.

Armat and Moet [102] studied the effect of compatibilising PA6 (75 wt%) and LDPE (25 wt%) with maleic anhydride functionalised styrene-ethylene-co-butylene-styrene block copolymer (SEBS-g-MAH). They observed that the SEBS-g-MAH was capable in reducing the interfacial tension of the blends and also improving the interfacial adhesion through the observation of reduction in LDPE dispersed phase and also formation of micro-bridges between the PA6 matrix and the PE phase in the presence of SEBS-g-MAH compatibiliser. The authors also demonstrated that excessive incorporation of SEBS-g-MAH (>10 phr) resulted in flow instabilities leading to moulding defects based on results of ultimate elongation.

**Table 2.5 Reactive compatibilisation of PA/PE blends**

| Compatibilisers | Blends | Ref |
|---|---|---|
| SEBS-g-MAH | PA6/LDPE | [102, 103] |
| SEP-g-MAH | PA6/LDPE | [103] |
| HDPE-g-MAH | PA6/LDPE | [103,105] |
| | PA6/HDPE | [104] |
| | PA66/HDPE | [107] |
| LDPE-g-MAH | PA6/LDPE | [105] |
| LLDPE-g-MAH | PA6/LLDPE | [106] |
| EAA | PA6/EAA | [108] |
| EEA, Ionomer | PA6/LDPE | [109] |
| EEA, PBO* | PA6/LDPE | [110] |
| PE-g-GMA | PA6, 11, 12, 6,10 6,12/PE-g-GMA | [111] |

* Bis-oxazoline

During compatibilisation of PA/PE blends, the compatibility efficiency of a compatibiliser precursor is dependent on the matrix polymer. It has been found that better compatibilising efficiencies are normally more pronounced in

PE-rich blends [103, 104]. Filippi et al [103] conducted a comparative study on compatibiliser effectiveness of three different maleic anhydride grafted compatibiliser precursors (CP) namely, SEP-g-MAH (maleic anhydride grafted styrene-b-ethylene-co-propylene copolymer), SEBS-g-MAH, and HDPE-g-MAH (maleic anhydride functionalised HDPE), on LDPE/PA6 blends. A better compatibilising effect was observed when LDPE was the matrix phase as the migration of the PA-g-CP copolymers formed to the blend interface were easier than when PA6 was the matrix, as partial inclusion of the formed copolymers into the PA6 matrix hindered compatibilisation of the blends. All three compatibilisers demonstrated almost similar compatibilisation efficiency when LDPE was the matrix. However, the size of the dispersed phase became much larger and HDPE-g-MAH became less efficient than the other two compatibilisers when PA6 was the matrix. Kim and co-workers [104] made similar observations when they attempted to compatibilise HDPE/PA6 blends with HDPE-g-MAH. They found that the compatibilisation efficiency of HDPE-g-MAH was more pronounced in PE-rich compositions through the evidence of blend morphologies.

Another important factor that influences the compatibilisation efficiency of a compatibiliser precursor in ternary blends is the degree of miscibility between the precursor and matrix polymer of the blends. Jiang et al [105] noted that HDPE-g-MAH showed better compatibilisation efficiency as compared to LDPE-g-MAH in LDPE/PA6 blends. The HDPE-g-MAH which is not miscible with the LDPE matrix was able to migrate easily to the LDPE/PA6 interface for compatibilisation reaction. On the other hand, LDPE-g-MAH which was dissolved in the LDPE matrix due to good miscibility, had lower chance of interaction with the PA dispersed phase.

Kudva and co-workers [106] described the influence of PA6 matrix molecular weight and concentration of LLDPE-g-MAH compatibiliser on the impact toughness of ternary blends of PA6, LLDPE and LLDPE-g-MAH. Low molecular PA6 matrix was claimed to be insensitive to the composition of the polyethylene phase which exhibited brittle failure at all compositions. However, increasing the molecular weight of the PA6 matrix and the ratio of

maleated to non-maleated polyethylene resulted in marked improvement in impact strength due to the presence of very finely dispersed polyethylene particles of <0.1 μm.

Chen et al [107] investigated the compatibilisation effectiveness of HDPE-g-MAH on PA66/HDPE blends. They observed a very fine dispersion of HDPE in PA66 matrix and improved mechanical properties particularly impact toughness with increased concentrations of HDPE-g-MAH indicating improvements in miscibility and interfacial adhesion between the phases.

Another popular approach in the compatibilisation of PA/PE blends is the use of ethylene acrylic acid copolymers (EAA). The interaction between carboxyl containing polyethylene and the PA can result in the formation of hydrogen bonding (interaction between amide group and acrylic acid) and covalent bonding (reaction between acrylic acid and terminal amine group of PA) as shown in Figure 2.25 [39, 41].

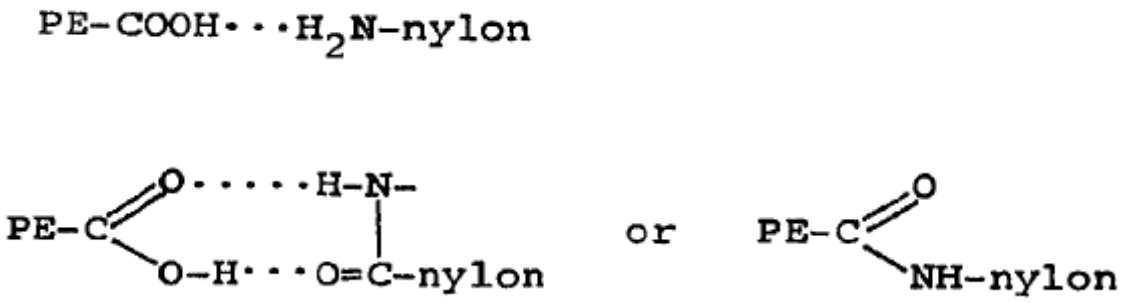


**Figure 2.25 Possible interactions between carboxyl containing polyethylene and polyamide [39]**

Based on the results of FTIR analysis of PA6/EAA blends, Valenza et al [108] suggested that hydrogen bonding interaction between the NH group of the polyamide phase and the C=O group in EAA is more significant than that of the hydrogen bonding between the hydroxyl group of the acrylic acid and the carbonyl group of the polyamide. Since stronger interaction was found in PA6 blends having higher concentration of $NH_2$ end groups with no detectable condensation reaction and new phase formation, the authors [108] concluded

that the compatibilisation mechanism of the blends studied involved the hydrogen bonding between the amine end groups of the polyamide and the carboxylic group of the acrylic acid. During the compatibilisation of PA6/LDPE blends, the efficiency of EAA as compatibiliser is dependent on the concentration of the acrylic acid present in the precursors [109]. However, the EAA reacts with PA much more slowly than PE-g-MAH [105]. Further enhancement of compatibilisation efficiency could be achieved through partial neutralisation of the carboxyl groups of EAA with zinc (EEA zinc ionomer) which could accelerate the acidolysis reaction that is responsible for the formation of CP-g-PA copolymers as described by Filippi and co-workers [109].

Scaffaro et al [110] attempted to increase the compatibilisation efficiency of EAA in blends of PA6/LDPE by incorporation of a low molecular weight bis-oxazoline (PBO) as a fourth component to the ternary blends. The PBO was found to function well as a promoter for the formation of PA-g-EAA copolymers in the blends as shown in Figure 2.26. At a concentration as low as 0.2 phr, the PBO was able to improve the mechanical properties particularly the impact toughness of the PA/LDPE/EAA blends through its reaction with carboxyl groups of EAA and amine (or carboxyl) end groups of PA forming a chemical link between the two.

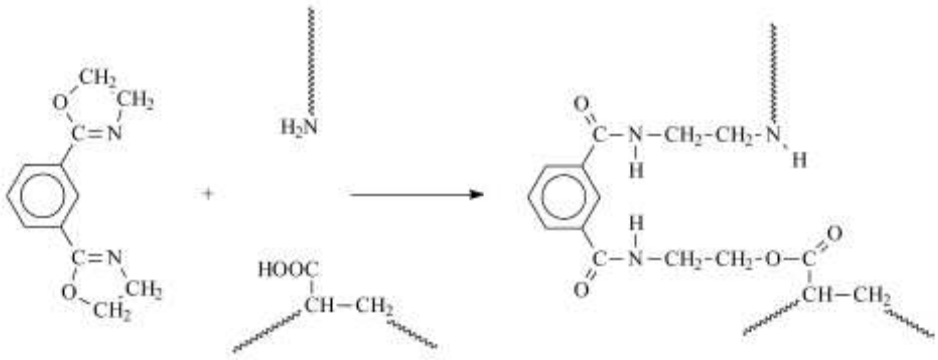

**Figure 2.26 Bridging reaction between PA6 and EAA by bis-oxazoline for the formation of PA-g-EAA [110]**

Polyethylene containing glycidyl methacrylate (PE-g-GMA) had been used by Koulouri et al [111] in binary blends with various polyamides. They observed

that the most efficient reaction of polyamide end groups with the epoxy rings of the PE-g-GMA occurred with polyamide 11/PE-g-GMA blends.

### 2.3.2 Polyester-Polyethylene Blends

Of the polyester-polyethylene blends, PET/HDPE blends have attracted considerable research activity due to the fact that both PET and HDPE have been widely used in packaging applications and thus constitute a large portion of post-consumer waste. Recycling offers an alternative solution for handling plastic wastes, however the immiscibility and lack of compatibility between PET and HDPE leads to poor interfacial adhesion and mechanical properties [1-4, 113-115].

In an earlier research conducted by Chen and Lai [4], EVA was incorporated as compatibiliser for HDPE/PET blends. Based on torque rheometer tests, they found that the addition of EVA at concentrations up to 5 wt% of the blends caused an increase in equilibrium torque suggesting the possibility of specific interactions between the polymers. However, at 10 wt% EVA concentration, the torque decreased probably due to a plasticising effect. The addition of EVA did not improve the miscibility between HDPE and PET as the glass transition temperature of the PET phase remained relatively unchanged. However, increasing the EVA content in the blend led to decrease in degree of crystallinity of HDPE and PET which indicates that interaction was created by the EVA copolymer.

In recent years, glycidyl methacrylate (GMA) functionalised polyolefin compatibilisers have been extensively studied in the compatibilisation of polyester-polyolefin blends. In contrast with maleic anhydride (MAH) functionality the GMA could react with both carboxyl and hydroxyl terminal groups of the polyester whereas the MAH could only react with the hydroxyl moieties and partly so because of the reversibility of the esterification reaction at high melt processing temperatures.

The efficiency of GMA over those of MAH functionalities on the toughening of PBT and compatibilisation of PET/HDPE blends were studied by Hert [112] and Kalfoglou et al [3] respectively. Hert [112] investigated the toughening efficiency of ethylene/ethyl acrylate/glycidyl methacrylate (E-EA-GMA) and ethylene/ethyl acrylate/maleic anhydride (E-EA-MAH) modifiers on PBT. The E-EA-MAH could only improve the notched Charpy impact strength of PBT by a factor of 3.5, which the author considered as poor toughening efficiency. The E-EA-GMA terpolymer on the other hand was able to improve the toughness enormously by a factor of 10. The reaction of GMA with acidic and hydroxyl chain ends of PBT accounted for the increase in melt viscosity of the blends containing E-EA-GMA and the observation of a finely dispersed (0.4 μm) E-EA-GMA phase.

Kalfoglou et al [3] investigated the efficiency of four different compatibilisers by melt mixing PET/HDPE/compatibiliser at the composition of 70/20/10. The compatibilisers studied were an ethylene/glycidyl methacrylate copolymer (E-GMA), ethylene/ethyl acrylate/glycidyl methacrylate (E-EA-GMA), a hydrogenated styrene/butadiene/styrene copolymer grafted with maleic anhydride (SEBS-g-MAH), and a maleic anhydride grafted ethylene/methyl acrylate copolymer (E-MA-g-MAH). Based on morphological evidence and tensile testing, the best compatibilising effect was obtained with copolymers containing GMA functionality.

Dagli and Kamdar [2] investigated the effects of component addition protocol on the reactive compatibilisation of HDPE/PET blends in a co-rotating intermeshing twin screw extruder. A small amount of E-GMA copolymer was found to be sufficient in achieving an adequate level of compatibilisation. The compatibilisation effectiveness was postulated to be dependent on the different sequences and modes of component addition. A two step process which involved the pre-blending E-GMA and HDPE followed by blending the precursor with PET resulted in best compatibilisation effectiveness. This protocol of component addition enabled the GMA moieties to orient themselves in a way that favoured the copolymer formation right at the interface when the E-GMA/HDPE co-melted during the melt blending process

with PET, whereas direct blending of E-GMA with PET resulted in a coarser morphology and inferior mechanical properties which could be a consequence of the entrapment of the E-GMA/PET copolymer molecules in the PET phase rending GMA moieties unavailable at the blend interface for compatibilisation.

Pawlak and co-workers [113] studied blends of post-consumer PET and HDPE in weight compositions of 75/25 and 25/75. The efficiency of three compatibilisers, E-GMA, SEBS-g-MAH, and HDPE-g-MAH, with variable contents were investigated. The best results for mechanical and morphological properties were obtained for 75/25 PET/HDPE blends compatibilised with 4 parts per hundred of E-GMA, and 25/75 PET/HDPE blends compatibilised with 10 parts per hundred of SEBS-g-MAH. The HDPE-g-MAH was claimed to be much less effective in compatibilising blends with PET as major component, probably due to entrapment of the MAH moieties in the HDPE phase, but it was more effective as compatibiliser for HDPE- rich blends.

Fasce et al [114] compatibilised blends of equal composition of virgin PET and HDPE with 1 and 7 wt% of ethylene/methacrylic acid copolymer (EMAA) as compatibiliser. A significant improvement of the mechanical properties, in particular the elongation at break and fracture toughness, was achieved in blends containing 7 wt% of EMAA compatibiliser indicating an improved degree of adhesion at the blend interface, possibly contributed by the interaction between the EMAA and the hydroxyl PET chain ends. The sample preparation method was found to have significant influence on the mechanical properties of the blends. PET adopted a globular morphology in the compression moulded samples but it took the form of microfibers in extruded samples which functioned like reinforced composites.

A handful of publications dealing with the use of ionomeric compounds to enhance the compatibility of PET/PE blends has been cited. Guerrero and co-workers [115] reported the effect of a copolymer of ethylene and methacrylic acid partially neutralized with zinc (zinc ionomer) on the compatibilisation of PET/HDPE blends. Blends compatibilised with this ionomer exhibit melting

point depression of both PET and HDPE components by 3℃ and 2.8℃ respectively suggesting possible PET-ionomer and HDPE-ionomer interactions. The broadening of the FTIR carbonyl band of PET indicated strong hydrogen bonding between this functional group and the carboxylic acid group of the ionomer. Interfacial adhesion was evident when 7.5 wt% of ionomer was added to PET/HDPE (75/25 wt%) blends by the improvement of elongation at break from 2.6 to 41.5% and Izod impact strength of 27.2 to 49.3 J/m.

Kalfoglou et al [116] studied the effectiveness of the sodium ionomer of ethylene methacrylic acid copolymer as compatibiliser for PET/LLDPE at various blending ratios and ionomer contents. The PET/LLDPE ratio was found to influence the degree of compatibilisation obtained. With moderate amounts of sodium ionomer (about 10 wt%), the best properties were obtained at high PET levels. It was proposed that the compatibilising effectiveness of the sodium ionomer was due to its strong interaction to PET which is the result of intermolecular chemical reactions (transesterification by acidolysis) occurring at their interface when blending at high temperatures.

Mascia and Bellahdeb [117] used graft copolymers and coionomeric mixtures as compatibilisers for binary blends of HDPE/PET. The compatibilisers were produced by mixing a phenoxy polymer (polyhydroxyether of bisphenol A) respectively with ethylene-propylene copolymers, containing grafted maleic anhydride groups (EP-g-MAH), and the sodium ionomers of the terpolymers of ethylene, an alkyl acrylate and a carboxylic acid, the ionomeric character of which was enhanced by the addition of either sodium benzoate (weak base) or sodium ethoxide (strong base). Both graft copolymers of EP-g-MAH and phenoxy, and sodium coionomeric mixtures of ethylene methacrylic acid copolymers with phenoxy, exhibited surfactant actions in the blends of HDPE and PET, giving rise to an appreciable reduction in particle size of the dispersed phase. The authors [117] postulated that coionomeric mixtures were able to promote stronger interfacial adhesion between the two phases in the blends and to nucleate the PET phase which contributed to larger

improvements in both tensile and elongation at break of the blends over a wide composition range.

In contrast with objectives for PET/PE blends, PBT being brittle and with poor notched impact strength is normally blended with polyethylene for the improvement of toughness. A series of works relating to toughening of PBT by blending with metallocenic polyethylene-octene (PEO) copolymers and different compatibilisers has been carried out by Aróstegui and co-workers [90, 118-119]. Maleic anhydride grafted PEO [118], difunctional epoxy resin [90], and E-GMA copolymer [119] were used as compatibilisers. The maximum impact strength of PBT/PEO (20 wt% PEO) blends compatibilised with maleic anhydride, epoxy resin, and E-GMA were 645 J/m, 575 J/m, and 710 J/m respectively. It can be seen that like the PET/HDPE blends, the GMA functionality is more effective than maleic anhydride functionality in compatibilisation of PBT/PEO blends. The epoxy resin was able to reduce the interfacial tension between the PBT and PEO resulting in a finer PEO dispersed phase which indicates a compatibilisation effect. The inter-particle distance (τ) appeared to be the main parameter that controlled the toughness in these PBT/PEO blends.

### 2.3.3 Polycarbonate-Polyethylene Blends

Being one the most widely used engineering thermoplastics, polycarbonate (PC) possesses several excellent properties which include excellent toughness, high transparency, very good dimensional stability, good thermal stability and electrical properties [120]. However, PC is known to be notch sensitive, has poor processability due to high melt viscosity, and also a tendency of PC to craze and crack when in contact with organic solvents. Dobrescu and Cobzabru [121] demonstrated that the addition of a very small amount of polyethylene (<1 wt%) to PC could cause dramatic reduction in its viscosity which could lead to better processability. Yang et al [122] studied the rheological behaviour of compatibilised and uncompatibilised HDPE/PC blends whereby they observed lower apparent viscosity of both blend types

compared with that of the neat HDPE and PC over a range of shear rates. However blends that were compatibilised with low density polyethylene grafted diallyl bisphenol A ether (LDPE-g-DBAE) possessed a higher apparent viscosity than the uncompatibilised ones indicating the efficiency of the LDPE-g-DBAE in setting up interactions between the HDPE and PC at their interfaces.

Kunori and Geil [123, 124] studied the mechanical properties and morphologies of PC/HDPE and PC/LDPE blends. From morphological and dynamic mechanical data, they observed no adhesion at the PC/HDPE and PC/LDPE boundaries and that the HDPE and LDPE inclusions were loosely sitting in holes in the PC matrix. This was suggested to be due to the volume contraction of the spherical dispersed PE phase which caused cavitation that reduced the possibility of interfacial adhesion when the PE content was lower than 15 wt%. Similar observations were reported by Leclair and Favis [125]. A substantial level of cavitation was observed in the morphology of blends with HDPE dispersed in a PC matrix (80% PC / 20% HDPE) compared to blends with PC dispersed in an HDPE matrix (20% PC / 80% HDPE). During slow cooling of the HDPE rich blends, the PC dispersed phase solidifies well before the crystallisation of the HDPE matrix. When the HDPE matrix crystallises, it contracts onto the already solidified dispersed PC thereby concentrating the stresses at the interface. Such contraction was postulated by the authors [125] to be responsible for the increase in mechanical properties of the blends as it promoted effective stress transfer at the blend interface.

Sue and co-workers [126] investigated the degree of interfacial adhesion and toughening mechanism of PC/LDPE alloys. They found that the interfacial bonding between the PC and PE was exceptionally strong (~ 30 MPa) and suggested that such bonding could be due to the oxidation of the PE chains which created reactive sites for interaction with the PC matrix. They also suggested that the toughening mechanism of PC/PE was due to the debonding of the PE particles from the PC matrix (a late cavitational process) which relieved the triaxial tension in front of the crack tip, followed by extensive shear yielding of the PC matrix.

From the literature cited in this survey [127-130], ionomeric copolymers appeared to be the most extensively studied and effective compatibiliser for PC/PE blends. These ethylene-functionalised copolymers consist of a hydrocarbon backbone and pendant acid groups, which are partially neutralized with metals or quaternary ammonium ions. Polycarbonate contains main chain carbonate groups which are susceptible to transesterification reactions with the carboxylic acid or carboxylate moieties of the copolymers.

The interaction between polycarbonate and ethylene-methacrylic acid copolymer either in the acid form or partially neutralised with sodium or zinc was investigated by Dias and Fernandes [127]. They reported increase in torque during melt blending of these copolymers with PC compared with the neat PC, suggesting possible grafting of the PC onto the copolymer backbone. This hypothesis was justified by the evidence of new chemical species with ester groups and carbonate side chain structures containing hydroxyl end groups that were detected by FTIR analysis.

Mekhilef et al [128] studied the effectiveness of a styrene-butadiene-styrene copolymer (SBC) and an ionomer (ethylene-methacrylic acid copolymer partially neutralised with sodium) in compatibilising PC/HDPE blends at compatibiliser concentration levels of 1% to 5% by weight. They found that the SBC was ineffective in compatibilisation of the blend as there was no significant difference between the mechanical properties of SBC compatibilised blends and those which were uncompatibilised. On the other hand, the ionomer was found to be effective in improving the Young's modulus and tensile strength of the blend at an addition rate of 1 wt%. A compatibilisation effect was evident, as shown by the significant reduction in the size of the PE dispersed phase which was claimed to be due to the compatibility of the ethylene group of the ionomer with the PE dispersed phase, and the reaction between the acid group of the ionomer and the carbonate group of the PC via transestrification reaction. However, excessive addition of ionomer was found to impart poorer mechanical properties and morphology coarsening of the blends.

Mascia and Valenza [129] utilised ionomeric mixtures (1:1) of phenoxy and the sodium ionomer of a ethylene-methacrylic acid copolymer at two different levels of neutralization for the compatibilisation of PC/HDPE blends at 5 wt% addition level of the dual-component compatibilisers. Both components of the compatibiliser were capable of reacting with the PC phase to produce branched polymer chains which imparted positive compatibilisation effects to the PC/HDPE blends. However, severe embrittlement of the blends was observed when higher levels of sodium in the compatibiliser induced crosslinking reactions of the PC phase.

The effectiveness of sodium ionomer in compatibilising PC/ethylene-1-octylene copolymer (PC/POE) blends at low concentrations was reported by Li et al [130]. They observed improvements in tensile strength and elongation at break but insignificant effects on impact strength of PC/POE (80/20) blends when 0.25 and 0.5 phr of ionomer were added. The addition of 0.5 phr of ionomer was found to induce a finer dispersed phase morphology indicating effective compatibilisation of the blends. However, as with the work carried out by Mekhilef et al [128], the authors [130] observed negative effects on the mechanical properties of the blends when more than 1 phr of the ionomer was added.

### 2.3.4 Styrene-Polyethylene Blends

Polystyrene (PS) being a glassy polymer at ambient temperature exhibits high strength, high modulus, and excellent dimensional stability, but extremely poor ductility. Therefore, significant efforts have been made to improve the toughness of this polymer over the past decades. Classic examples of impact modification of PS is through the inclusion of a rubber phase in the glassy matrix leading to toughened polymer blends like high impact polystyrene (HIPS) and acrylonitrile-butadiene-styrene (ABS) copolymer. However, the inclusion of a low modulus rubbery phase generally leads to sharp reduction in stiffness and strength of the blends.

In recent years, attempts have been made to toughen PS using non-rubbery polymers. Due to its excellent ductility and superior impact performance, polyethylene (PE) is one of the frequently studied polymers in PS blends. Since PS and PE are immiscible and incompatible with each other, mixing the two polymers leads to blends with very poor mechanical properties, and this opens up opportunities in research on compatibilisation of PS/PE blends.

The most conventional and popular approach in the compatibilisation of PS/PE blends is by the addition of a third component compatibiliser which is mainly a graft or block copolymer. Carrick [131] described the preparation of graft copolymers of polyethylene with polystyrene (PS-g-PE) via Friedel-Crafts alkylation of the aromatic rings in PS with the olefinic groups of polyethylene in cyclohexane solution using $AlCl_3$ as the catalyst. Barentsen and co-workers [132, 133] prepared PS-g-LDPE copolymers with almost equal fractions of ethylene and styrene according to the method reported by Carrick [131] for the compatibilisation of PS/LDPE blends. The graft copolymer was first melt blended at 5 and 30 wt% with the polymer forming a dispersed phase before being added to the matrix polymer. The morphologies observed using a scanning electron microscope indicated that the graft copolymer was concentrated at the interface between the PS and LDPE phases, and strongly adhered to both phases. Compared with unmodified PS/LDPE blends, the blends containing the graft copolymer exhibited higher yield strength, elongation and significantly better impact strength.

The compatibilisation of PS/PE blends using styrene-ethylene butadiene (S-EB) diblock polymers has been studied by Fayt and co-workers [134-136]. In their earlier work [134], the addition of 9 wt% S-EB diblock copolymer resulted in fine dispersions of PS particles (< 1 μm) in the LDPE matrix for LDPE-rich blends, whereas PS-rich blends exhibited semicontinuous to continuous two-phase structure. The addition of S-EB diblock copolymer also resulted in significant enhancement of the ultimate tensile strength, and elongation at break of the blends was significantly improved. The same authors also evaluated the effectiveness of S-EB diblock copolymers as compatibilisers in HDPE/PS blends [135]. The addition of copolymer resulted in size reduction

and stabilisation of the dispersed phase. Remarkably large increases in mechanical strength together with high elongation were achieved in PS-rich blends and were postulated to be due to improved interfacial adhesion and to the interlocked-phase morphology which is possibly the formation of interpenetrating polymer networks.

Fayt et al [136] also compared the efficiency of the S-EB diblock copolymer with that of a tapered diblock copolymer with the same composition and molecular weight for the compatibilisation of LDPE/PS blends. A finer dispersion of PS particles was observed in the LDPE matrix of PE-rich blends modified with the tapered diblock copolymer than with the pure diblock copolymer. The tapered diblock copolymer was also found to be able to impart much superior mechanical properties to both PS- and PE-rich blends. The results of morphological and mechanical studies indicated lower interfacial activity of the pure diblock compared to that of the tapered copolymer. The authors related the lower interfacial activity of pure diblock copolymer to the possibility that the larger part of this pure diblock copolymer was either solubilised or formed its own domains in one or other homopolymer phase which caused limited mixing of the two blocks. As such, the driving force for domain formation limited the emulsifying activity of this copolymer. On the other hand, the tapered copolymer with reduced “blockiness” enhanced the mixing of the two blocks thus reducing its tendency to form domains in the melt phase.

In comparison to triblock copolymers, diblock copolymers generally exhibit higher efficiency in reducing the dispersed phase size of PS/PE blends while the former may be more efficient in improving the mechanical properties of the blends [137-138]. Guo et al [138] suggested that high interfacial activity of diblock copolymers alone is insufficient for improving the mechanical properties of blends, and relies on the ability of triblock copolymers to form stronger entanglements at the interface region of the blends. Appleby and co-workers [139] reported that low molecular weight SEBS triblock copolymer was more effective than tapered diblock copolymer in improving the impact strength of equal composition LDPE/PS blends. The impact strength of the

LDPE/PS blends compatibilised with 5 wt% of the triblock copolymer was found to be close to that of a high impact polystyrene.

Tjong and Xu [140] utilised the same low molecular weight SEBS triblock copolymer, for the compatibilisation of PS/HDPE blends. Both the elongation at break and Charpy impact strength of PS/HDPE/10%SEBS blends were observed to increase dramatically with increasing HDPE content. The authors suggested that the improvement in ductility of the HDPE matrix by the incorporation of minor PS phase in the presence of SEBS copolymer could be related to extensive fibrillation of the HDPE matrix associated with debonding of the PS particles from the matrix. In HIPS-rich blends, the stress-strain curve exhibited the typical behaviour of toughened plastics like high impact PS. The SEBS was claimed to act partially as an emulsifier as well as a dispersed rubber toughening agent in the PS matrix.

The compatibilisation of PS/HDPE with styrene-butadiene-styrene (SBS) block copolymer was reported by Wu and co-workers [141]. The addition of 10 wt% of SBS in PS-rich blends resulted in the formation of a string-and-bead structure of the HDPE dispersed phase. Many of the elliptical HDPE particles were linked together by very thin HDPE fibrils. Morphology of the blend observed using a transmission electron microscope (TEM) revealed that the SBS formed a thin interfacial between the HDPE phase and the PS matrix as the styrene block of the SBS is highly miscible with the PS matrix while the butadiene block is compatible with HDPE. The presence of 5 to 15 wt% of SBS in the PS/HDPE ternary blends resulted in dramatic improvements in impact toughness as well as tensile ductility.

Since neither PS nor PE possess reactive functionalities, PS/PE blends are difficult to compatibilise using in situ reactive compatibilisation techniques. Graft copolymers of OPS-g-CPE were produced by Baker and Saleem [142] via an in situ coupling reaction between polystyrene having oxazoline (OPS) groups and polyethylene having carboxyl (CPE) groups by melt blending. The interaction was confirmed by the detection of amido-ester linkages by FTIR. The same authors [143] also reported that fine morphology and significant

improvements in elongation were observed in PE-rich blends. However, no significant improvements in tensile and impact toughness were observed in PS-rich blends indicating that interfacial adhesion is not the only factor that governs the toughening of polymer blends.

Saleem and Baker [144] investigated the effects of addition of pre-made OPS-g-CPE graft copolymer [142, 143] compared with in situ blending of OPS and CPE on the compatibilisation of PS/PE blends. The authors [144] reported that the pre-made OPS-g-CPE graft copolymer was able to impart compatibility to the PS/PE blends but was not as effective as direct blending of the PS and PE with OPS and CPE. The in situ grafting reaction during melt blending was postulated to impart better distribution of the in situ formed graft polymer at the blend interface.

## 2.4 Characterisation and Properties of Polymer Blends

The final properties of polymer blends are dependent on the blends' miscibility, compatibility, morphology, and crystallinity etc. Details of such characteristics can be obtained by various characterisation techniques such as mechanical testing, thermal analysis, electron and optical microscopy, and spectroscopic methods.

This section reviews various techniques that are commonly utilised in the characterisation of polymer blends with an emphasis on differential scanning calorimetry, electron and optical microscopy, infrared spectroscopy and mechanical testing.

### 2.4.1 Blend Characterisation by Differential Scanning Calorimetry

Differential Scanning Calorimetry (DSC) has been widely used for the determination of a polymer's melting temperature, glass transition temperature, specific heat, heats of fusion or crystallisation, rate of

crystallisation, onset of thermal degradation and degree of cure. DSC provides the advantage of rapid measurement and requires only minor amounts of specimen (5 – 20 mg). Shanks and Amarasinghe [145] made a comprehensive review of the application of DSC in the analysis of polymer blends. Blends of amorphous polymers are usually characterised by the glass transition (Tg) inflections in the DSC thermograms. The shift of Tg measured by DSC is a good measure of the miscibility of the blends. The blending of 2 completely miscible amorphous polymers will result in the observation of a single Tg between the Tgs of the components. In cases where the two polymers are only partially miscible, two Tgs will be observed, but they will be shifted towards each other. When the polymers are immiscible, the individual polymer's Tg will remain unchanged. Figure 2.27 presents a general scheme for the classification of polymer blends as a function of DSC response [145].

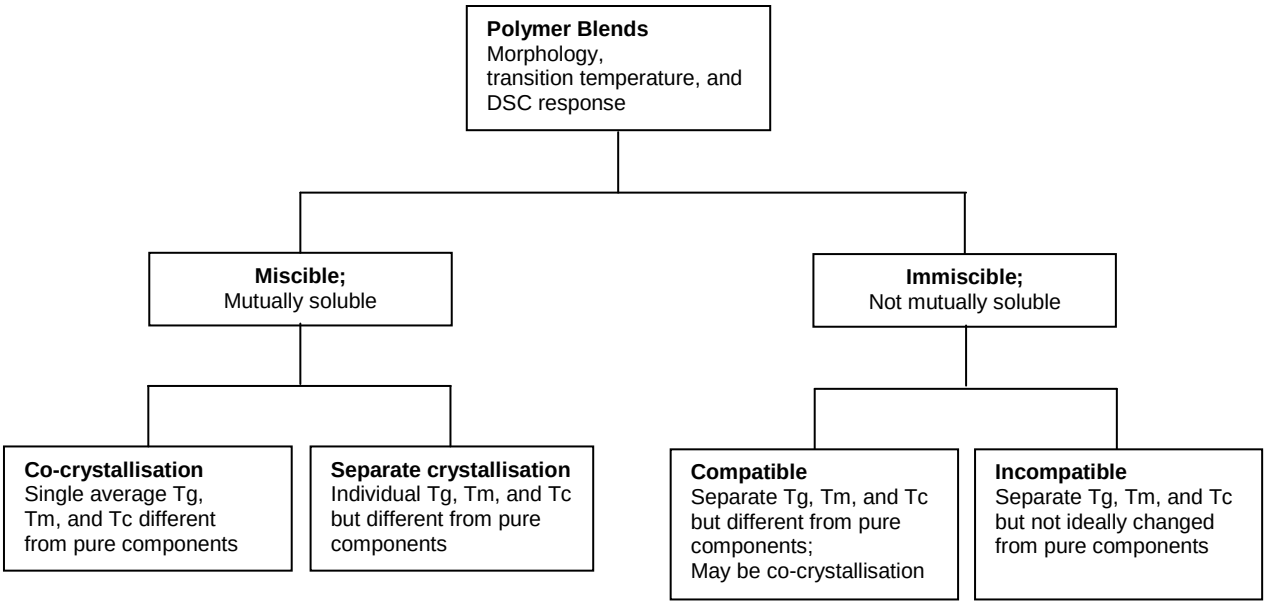


**Figure 2.27 Classification chart for polymer blends as a function of DSC response [145]**

In their studies conducted on miscibility in blends of poly(methyl methacrylate) (PMMA) with poly(vinyl acetate) (PVAc), Song and Long [146] observed good miscibility of PMMA with PVAc at all compositions as only single Tg was observed from DSC thermograms of these blends.

In general, DSC is not well suited to Tg measurement since it lacks sensitivity for many polymers particularly in the case of semi-crystalline polymers. With highly crystalline polymers, the Tg inflection is not usually detected by DSC [145]. The closeness of blend component Tgs may be an even more severe problem for detection by DSC and thus the detection of Tgs separated by less than about 30℃ involves high degree of uncertainty [147]. In order to obtain precise measurements of Tg, other characterisation techniques such as dynamic mechanical thermal analysis (DMTA) are preferred. As this technique has not been used in this work, the application of DMTA in the characterisation of polymer blends is beyond the scope of this review.

In polymer blends where at least one component is crystallisable, the presence of the other non-crystallisable component can have significant influence on crystallisation behaviour. When a crystalline polymer is dispersed in an amorphous polymer matrix, the crystallinity of the crystalline polymer tends to decrease, and in some cases disappears. Several researchers [148-152] reported the observation of the “fractionated crystallisation” phenomenon by DSC when crystallisable polymers were finely dispersed in an immiscible amorphous matrix. Fractional crystallisation is manifested by the observation of multiple crystallisation behaviour of the dispersed crystalline phase when DSC is performed on immiscible blends. This is due to changes in the nucleation mechanism of the crystallisable component whereby the nucleation changes from preferentially heterogeneous to preferentially homogeneous as the size of the dispersed phase decreases.

Ghijsels et al [148] investigated the crystallisation behaviour in blends of polypropylene and styrene-butadiene-styrene (SBS) triblock copolymer using DSC. A single crystallisation peak was observed at 106℃ and 108℃ for unblended PP and blends of PP/SBS at 75/25 blend ratio respectively. A slight increment in crystallisation of the PP/SBS blend was due to the weak nucleating effects of the SBS dispersed phase. However, at PP/SBS blend ratios of 50/50 and 25/75 the crystallisation behaviour was altered dramatically. At 50/50 PP/SBS blend shows three distinct crystallisation exotherms at 108℃, 74℃ and 46℃ instead of a sing le one. In the 25/75

PP/SBS blend, the crystallisation exotherm at 108℃ was no longer present but the exotherm at 43℃ was more intense. The authors attributed the observation of crystallisation at 74℃ to homogeneous nucleation rather than heterogeneous nucleation of the PP dispersed phase. The homogeneous nucleation occurred when the number of isolated PP domains (dispersed phase) was greater than the number of heterogeneous nuclei (some domains were free from heterogeneous nuclei). Therefore those PP domains that are free from heterogeneous nuclei did not crystallise at the normal PP crystallisation temperature (106℃), but at lower temperatures via a homogeneous nucleation mechanism. The authors concluded that fractionated crystallisation could be utilised in assessing the degree of dispersion of the PP phase using DSC.

A thorough review on fractionated crystallisation has been conducted by Frensch et al [153]. They concluded that the following important effects could be observed when crystallisable polymers are finely dispersed into immiscible matrices:

a.) subdivision of the crystallisation into several distinct steps, the temperature of which can differ by several ten degrees;
b.) inhibition of the crystallisation at the usual temperature;
c.) coincidence of the crystallisation of both components (in the case of immiscible blends containing two crystallisable components) at that temperature at which one of them usually crystallises, or at another temperature;
d.) occasionally homogeneously nucleated crystallisation.

Fractionated crystallisation phenomenon has also been reported in the following amorphous/crystalline blends: PS/PP blends [149], PS/Linear Low Density Polyethylene (LLDPE) blends [150], PC/PET blends [151], and PC/PP blends [152].

DSC is also particularly useful in the investigation of miscibility between crystalline/crystalline polymer blends. Datta and Birley [154] observed single melting peak from DSC thermograms of LLDPE/HDPE blends containing 30,

50, and 70 wt% of LLDPE, indicating the existence of only one type of crystal species at these compositions. They attributed this observation to the co-crystallisation of the high melting point constituent of LLDPE and HDPE, i.e. LLDPE and HDPE are compatible in the crystalline phase.

The depression of the melting point (Tm) of a crystalline polymer in a polymer blend provides important information about its miscibility and its associated polymer-polymer interaction parameter $\chi_{12}$. The temperature reduction is caused by thermodynamic depression arising from reduction in the chemical potential due to the presence of the polymeric solvent. When two polymers are miscible in the melt, the chemical potential of the crystallisable polymer is decreased due to the addition of the second component. This leads to a reduction in the equilibrium melting temperature with increasing amorphous polymer content, especially in blends containing specific interactions between the components. Nishi and Wang [155] observed significant depression in the melting and crystallisation temperatures of poly(vinylidene fluoride) ($PVF_2$) in solution cast mixtures of $PVF_2$/PMMA. The $\chi_{12}$ between $PVF_2$ and PMMA was determined to be -0.295 at 160℃ indicating the pol ymer pair is miscible in the molten state. Li et al [156] postulated that LLDPE was partially miscible with EVA in LLDPE/EVA blends through the observation of gradual reduction of the Tm of LLDPE with the increase of EVA component. On the other hand, through the results obtained from DSC analysis, Haghighat [157] suggested that blends of EVA/LDPE were immiscible as there was no detectable shift in melting point of LDPE which indicated no interaction between EVA and LDPE.

### 2.4.2 Blend Characterisation by Infrared Spectroscopy

The application of Fourier Transform Infrared Spectroscopy (FTIR) for the characterisation of polymer blends is extensive. FTIR is ideal for studies of the phase behaviour of polymer blends as it is able to detect molecular vibrations, and thus the size scale is generally that of the chemical group, of the order of a few angstroms i.e. nanometer scale [158]. Hydrogen bonding interactions can be detected by the shift in frequency of the absorption peak for the

hydrogen bonded units. Specific groups that are capable of hydrogen bonding include the O-H stretching transition around 3600 $cm^{-1}$; the carbonyl group C=O (in acid or ester units) with specific absorbance in the range of about 1730 $cm^{-1}$; and amide groups, which exhibit both N-H and C=O stretching modes in the range of 3300 $cm^{-1}$ and 1640 $cm^{-1}$, respectively [38]. Therefore infrared measurements of polymer blends allow the characterization of the nature and strength of relatively strong intermolecular interactions, which are often the driving force for mixing in polymer blends.

FTIR spectroscopy was employed by Coleman and co-workers [159] to follow changes in relative strength of intermolecular interactions occurring in blends of EVA with PVC and chlorinated PE (CPE) as a function of temperature. Figure 2.28 shows a plot of temperature versus the carbonyl peak position for an 80:20 wt% CPE-EVA blend as a function of temperature. At 30℃, the carbonyl band of the blend was shifted about 5 $cm^{-1}$ from that of the pure EVA band indicating the presence of hydrogen bonding. However, upon heating this difference became progressively smaller implying weaker interactions. The point where shift of the carbonyl has almost disappeared was observed to coincide with lower critical solution temperature (LCST) of the blend. Similar observations were reported on a 80:20 wt% PVC-EVA blend by the same authors [159].

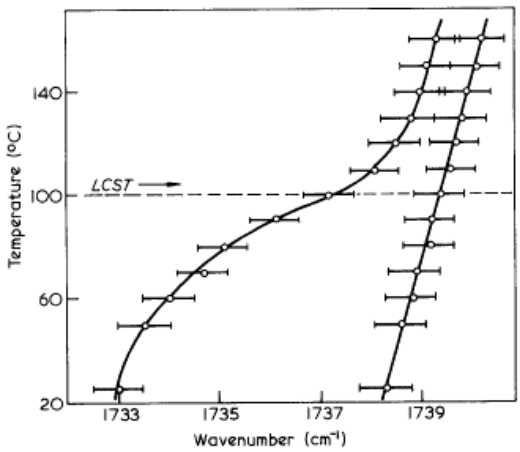


**Figure 2.28 Plot of temperature versus the carbonyl peak position for an 80:20 wt% CPE-EVA blend [159]**

Another typical example is the application of FTIR in the analysis of mixtures of poly(vinyl phenol) (PVPh) with an EVA copolymer. Figure 2.29 shows the FTIR spectra obtained from films of miscible PVPh/EVA blends of varying composition acquired at 120℃ [160]. Hydrogen bonding is evident when the absorption peak of the EVA carbonyl group at 1737 $cm^{-1}$ shifted to 1708 $cm^{-1}$ as this acetoxy group interacted with the phenolic moiety of the PVPh.

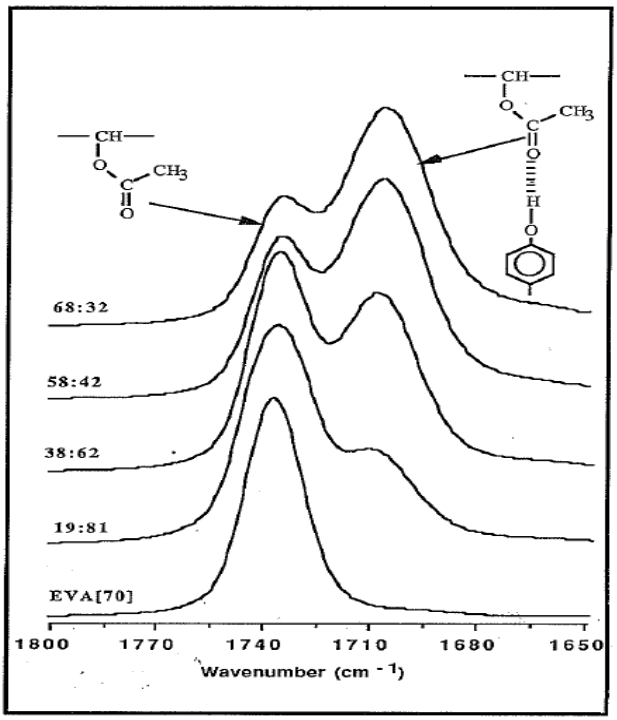


**Figure 2.29 FTIR spectra of PVPh/EVA blends at 120°C showing evidence of hydrogen bonding [160]**

Apart from being utilised extensively for the study of hydrogen bonding in polymer blends such as PVPh/poly(vinyl acetate) (PVAc) [161], PVPh and poly(ε-caprolactone) (PCL) [162], FTIR spectroscopy also finds applications in the identification of the mechanisms of other specific interactions in blends such as the esterification reaction between polypropylene-g-maleic anhydride/poly(ethylene-co-vinyl alcohol) [163], transesterification in PC/PBT blends [164], and the oxazoline-succinic anhydride reaction in maleated PE/oxazoline functionalised PS [54].

## 2.4.3 Blend Morphology Characterisation By Microscopy

When two immiscible polymers are brought together by melt blending, a distinct two-phase blend is formed. The size, shape and distribution of one phase into the other depends on material parameters (i.e., blend composition, viscosity ratio, elasticity ratio, and surface tension) as well as processing conditions (i.e., temperature, time, and intensity of mixing, and the nature of the flow). It is well known that the properties of such a blend (e.g., mechanical, rheological, optical, barrier, and dielectrical properties) are closely related to the state of dispersion or blend morphology which describes the size, shape, and spatial distribution of the component phases with respect to each other. Therefore, characterisation of the morphology of phase separated blends is the key to understanding structure-property relationships.

Figure 2.30 [165] shows schematically various useful polymer blend morphologies for different end properties such as high strength and toughness, toughness coupled with stiffness, good barrier and high flow properties that can be produced by polymer-polymer melt blending processes.

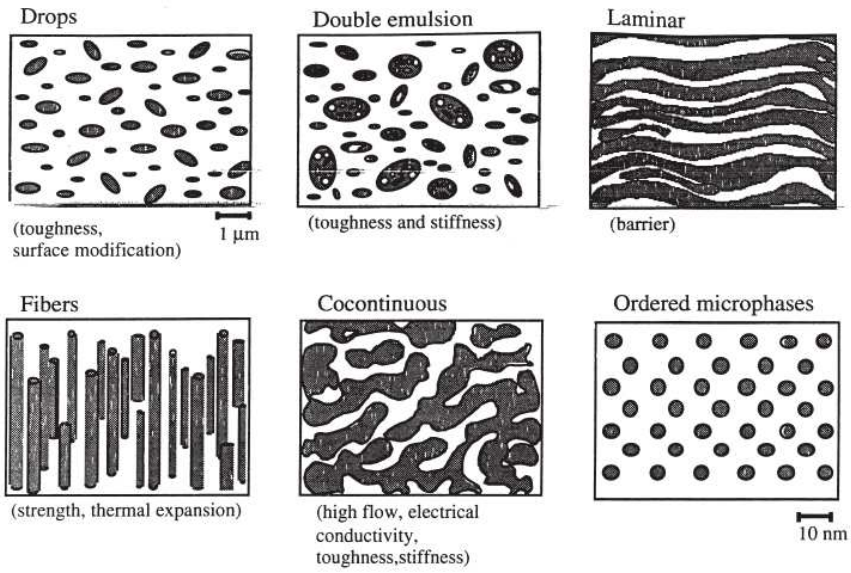


**Figure 2.30 Schematic of useful morphologies of polymer blends [165]**

In polymer blends the main application of microscopy is not so much to determine miscibility but rather to study their morphology [20]. As shown in Table 2.6, the microscopic methods can be divided into three categories: optical or light microscopy (OM), scanning electron microscopy (SEM), and transmission electron microscopy (TEM) [20].

**Table 2.6 Microscopic Methods [20]**

| No. | Parameter | Units | Optical Microscopy (OM) | Scanning Microscopy (SEM) | Transmission Microscopy (TEM) |
|---|---|---|---|---|---|
| 1 | Magnification | (times) x | 1 to 500 | 10 to $10^5$ | $10^2$ to $5.10^6$ |
| 2 | Resolution | nm | 500 to 1000 | 5 to 10 | 0.1 to 0.2 |
| 3 | Dimensionality | - | 2 to 3 | 3 | 2 |
| 4 | Field depth | µm | ~ 1 (at high magn.) | 10 to 100 | ~ 1 |
| 5 | Field size | µm | $10^3$ to $10^5$ | 1 to $10^4$ | 0.1 to 100 |
| 6 | Specimen | - | Solid or liquid | solid | solid |

Notes: No. 1 total range of available magnification within each category;

No. 2 finest detail the microscope can resolve;

No. 3 nearly planar vision (2 dimensions) in TEM and at high resolution OM;

No. 4 ability to discern details perpendicular to the field direction;

No. 5 the diagonal size of field under observation;

No. 6 only OM allows observation of liquid/liquid phase changes.

### 2.4.3.1 Optical Microscopy (OM)

Optical microscopy is readily available, low cost and generally offers the starting point for morphological characterization of polymer blends [38]. However, the classical light microcopy is limited by diffraction to domains larger than 500nm. In OM, the necessary contrast for detecting different phases might arise from a number of different sources such as colour, opacity, refractive index, orientation, absorption, or dichroic differences [166]. OM is typically used for the characterisation of heterophases, such as fillers [167], or pigments and additives [168], which are commonly added to blends. These features are normally visible in reflected or transmitted light using polished or microtomed samples.

For polymer blends a minimum domain size of 500 nm can be examined in the optical microscope using one or more of the imaging methods like phase contrast, polarised light, bright-dark field, and interference microscopy, [169, 170].

Polarised light optical microscopy constitutes a very useful technique to obtain qualitative and quantitative features of the microstructure and crystallisation kinetics of polymer blends [171]. Qualitative studies, such as those of morphology of the phases, miscibility, phase separation, and compatibilisation, can easily be performed; quantitative studies regarding crystallisation kinetics of the components, size and size distribution of the dispersed phase, and orientation can also be done if accessories like a hot stage and a video camera coupled to a computer with digital image processing are used. Optical microscopy applied to polymer blends has been reviewed in [170-175]. Examples of the application of polarising microscopy for the investigation of spherulitic structures have been reported by Lovinger and Williams [176] on polyethylene/polypropylene blends, Martuscelli and co-workers [177] on poly(ethylene oxide)/poly(methyl methacrylate) blends, and Bulakh et al [178] on poly(phenylene sulphide)/amorphous polyamide blends.

The use of OM in the analysis of polymer blends is often limited by the small size of typical dispersions. As a result, many researchers routinely defer to higher magnification techniques like scanning electron microscopy (SEM) and transmission electron microscopy (TEM).

### 2.4.3.2 Electron Microscopy

Compared with optical microscopes, electron microscopes like the SEM and TEM are capable of much higher resolution. SEM is normally employed for the analysis of surfaces and is of lower resolution than TEM. This method focuses an electron beam onto a surface, and the emission of electrons from the specimen is detected and amplified to obtain an image. The accelerating voltage is typically in the range of 1-40 kV; much lower than TEM. As SEM

exhibits a relatively large depth of field, it can show topological features better than other microscopy methods (except perhaps atomic force microscopy). Samples require surface conductivity, thus a thin layer (~10 nm) of a conductive metal (gold or platinum) is normally sputtered onto the surface of samples before analysis. Staining and etching process are commonly employed to provide improved contrast. To obtain information of morphology in the bulk of the material, it is necessary to remove the surface layer. Only when adhesion between the phases is poor, a new surface that reflects the bulk morphology can be created by fracturing the sample. Cryogenic fracture is usually employed to prevent plastic deformation and provide surfaces with better defined topological features than possible with higher temperature fracture. Particles, such as fillers or impact modifiers, will often be exposed and debonded during cryogenic fracture revealing the desired contrast.

On the other hand, TEM is analogous to transmission optical microscopy except that an electron beam instead of a light beam is employed. The electron beam is formed with high accelerating voltage (100-400 kV) and viewed on a fluorescent screen. The wavelength of electrons allows for higher resolution and thus much smaller dimensional resolution than optical methods. TEM samples have to be sufficiently thin (usually microtomed into thin slices of less than 100 nm) to allow electron beam penetration [170]. Since polymers are mainly composed of C, H, N and O atoms, the electron density difference between polymers is not large enough to achieve sufficient contrast in heterogeneous materials. Thus the key to success employing TEM involves developing phase contrast of the components. Osmium tetraoxide, $OsO_4$, is the most common staining material employed and is particularly useful for polymers with unsaturation, because it reacts with the double bond to yield an osmate ester providing excellent contrast.

The application of SEM and TEM in the characterisation of polymer blends has been reviewed in references [170, 173-175, 179]. Microscopic methods are frequently used in parallel, the SEM/TEM pair being the most frequent. Lee and Han investigated the evolution of polymer blend morphology of

various blend systems during compounding in an internal mixer [180] and a twin screw extruder [181] using SEM and TEM.

### 2.4.4 Mechanical Properties of Blends

As discussed in section 2.2 of this literature review, uncompatibilised blends of immiscible polymers exhibit a coarse and unstable phase morphology with poor interfacial adhesion. The mechanical properties of these blends are often poorer than those of either component. The poor mechanical properties can be improved with the addition of a small amount of interfacial agent that lowers the interfacial tension in the melt and enhances interfacial adhesion in the solid.

Mechanical testing is frequently employed to evaluate the compatibility of the polymer blends by comparison of the mechanical property profile with and without compatibilisation [29, 38, 40, 182-184]. Two types of mechanical tests have been used: the low rate of deformation (in a tensile, compressive, or bending mode), and the high speed impact tests.

The low speed mechanical properties of polymer blends have been frequently used to discriminate between different formulations or methods of preparation [183]. Of these, the tensile elongation at break is very sensitive to blend component adhesion strength and is routinely used to evaluate the degree of compatibilisation in polymer alloys [3, 185-187]. Figure 2.31 shows the stress-strain curves for polyethylene-PVC blends with and without chlorinated polyethylene (CPE) compatibiliser [185]. The addition of 20% CPE transformed the brittle nature of unmodified HDPE/PVC and LDPE/PVC into very ductile blends.

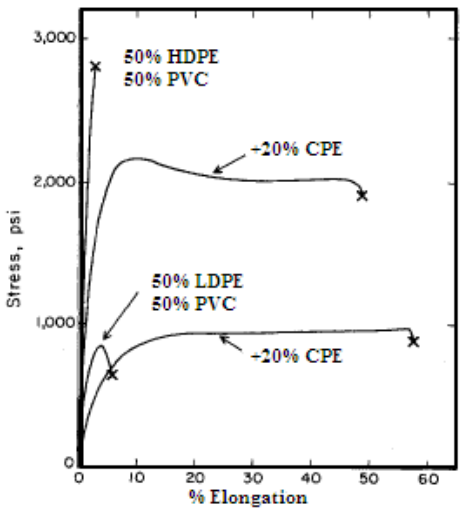


**Figure 2.31 Effect of chlorinated polyethylene (CPE) on stress-strain curves for polyethylene-PVC blends [185]**

One of the most important mechanical properties of polymer blends is the achievement of enhanced impact strength [38]. Toughness is defined as the total area under the stress-strain curve, thus abruptly ending curves without a yield point are characteristic of brittle materials. High impact strength and toughness are generally characterised by yielding accompanied by a high elongation to break and a large area under the stress-strain curve. However, a polymer that has a yield point using slow speed testing may fracture in a brittle manner at high speeds. Also, many polymers that are ductile under normal testing conditions may appear to be brittle if the test specimen contains a notch or a crack [184].

Various testing methods have been developed to quantify the toughness of polymers. These usually involve the delivery of a sharp blow by either a hammer or by a projectile propelled at the polymer or dropped on it [188]. Commonly used impact test methods include Izod impact tests, Charpy impact tests, tensile impact tests and falling weight impact tests. A comprehensive survey on these test methods has been conducted by Perkins [188].

Polymeric systems are roughly classified as [189]:

- *Type I polymers*: Brittle, having low crack initiation as well as low propagation energy in impact. They fail by crazing as the main fracture mechanism. Therefore they exhibit low unnotched and notched impact strengths. Examples: polystyrene, SAN and poly(methyl methacrylate);
- *Type II polymers*: Ductile, have high crack initiation energy, but low crack propagation energy on impact. They fail by yielding as the main fracture mechanism. Therefore they normally do not fail when unnotched, but show much lower impact strength when notched. Example: polyamide, poly(ethylene terephthalate) and polycarbonate.

For blends that are brittle under standard notched Izod impact testing, the impact behaviour of both uncompatibilised and compatibilised blends will be brittle with nearly identical impact strength. Therefore unnotched impact strength will be a more appropriate way to differentiate the toughness change of the notch-sensitive blends through compatibilisation as demonstrated by Tsai [70] and Shieh [87] et al.

When used alone or in combination, both slow speed tensile testing and high speed Izod impact testing have been proven to be useful tools in evaluating the efficiency of blend compatibilisation and mechanism of rubber toughening by many researchers.

# CHAPTER 3

# EXPERIMENTAL

This research was carried out in two separate studies. The preliminary stage involved the evaluation of the effectiveness of five reactive and non-reactive polar compatibilisers namely, EVA, EMA, E-GMA, E-MA-GMA and HDPE-g-MAH, in compatibilising HDPE with four different types of engineering polymers namely, ABS, PC, PBT and PA6. A laboratory co-rotating twin screw extruder was used for the preparation of HDPE/compatibiliser binary blends. The compounded binary blends were then blended with the matrix polymers and injection moulded into test bars for mechanical testing and characterisation of the resultant ternary blends.

The second stage of work consisted of reactive grafting of a low molecular weight epoxy onto maleic anhydride functionalised HDPE (HDPE-g-MAH), characterisation of these grafted blends, and investigation of the compatibilisation effectiveness of these reactive grafted blends with ABS, PBT and PA6 matrix polymers. An extrusion plastometer was initially utilised for screening the reactive formulations whereby the most promising formulations were selected for scaling-up using a twin screw extruder. These compounded reactive blends were subsequently injection moulded for evaluation of their compatibility with the three matrix polymers.

This chapter covers the details of raw materials used, approaches in processing of the blends, and also discusses the experimental techniques employed in characterisation of the blends.

## 3.1 Materials

This section of the thesis covers detailed information of raw materials used in the studies and also discusses the reasons for material selection.

### 3.1.1 Raw Materials

The raw materials used in this research are categorised into the following main groups:

- Non reactive polar compatibilisers
- Reactive compatibilisers
- Non reactive and non polar carrier polymer
- Matrix polymers
- Catalyst

**a.) Non Reactive Polar Compatibilisers:**

Two commonly used polar non reactive compatibilisers namely Ethylene-vinyl acetate (EVA) and ethylene-methyl acrylate (EMA) copolymers were selected to compare their effectiveness in compatibilising HDPE with four matrix polymers (ABS, PC, PBT and PA6). Details of these two compatibilisers are as follows:

| | |
|---|---|
| **Compatibiliser Type** | : **Ethylene-vinyl acetate copolymer (EVA)** |
| **Trade Name** | : ***NUC-3460*** |
| **Characteristics / Properties** | : Melt flow rate 20 g/10min (190℃/2.16kg), vinyl acetate content 20 wt% |
| **Manufacturer** | : Nippon Unicar Company Limited |

| | |
|---|---|
| **Compatibiliser Type** | : **Ethylene-methyl acrylate copolymer (EMA)** |
| **Trade Name** | : ***Lotryl 20MA08*** |
| **Characteristics / Properties** | : Melt flow rate 8 g/10min (190℃/2.16kg), methyl acrylate content 20 wt% |
| **Manufacturer** | : Arkema |

**b.) Reactive Compatibilisers :**

Maleic anhydride (MAH) and glycidyl methacrylate (GMA) are the two most studied reactive functionalities in compatibilising polyamide and polyester based blends respectively. In this work, their effectiveness in compatibilising HDPE with ABS, PC, PBT and PA6 was investigated by using commercially available MAH and GMA functionalised copolymers and terpolymer. A high density polyethylene grafted with maleic anhydride (HDPE-g-MAH), a ethylene-glycidyl methacrylate (E-GMA) copolymer and a ethylene-methyl acrylate-glycidyl methacrylate (E-MA-GMA) terpolymer were selected for this study. Details of these three compatibilisers are as follows:

| | |
|---|---|
| **Compatibiliser Type** | : **High density polyethylene grafted with maleic anhydride (HDPE-g-MAH)** |
| **Trade Name** | : ***Polybond 3009*** |
| **Characteristics / Properties** | : Melt flow rate 6 g/10min (190℃/2.16kg), maleic anhydride content 1.0 wt% |
| **Manufacturer** | : Chemtura |

| | |
|---|---|
| **Compatibiliser Type** | : **Ethylene-glycidyl methacrylate copolymer (E-GMA)** |
| **Trade Name** | : ***Lotader AX8840*** |
| **Characteristics / Properties** | : Melt flow rate 5 g/10min (190℃/2.16kg), glycidyl methacrylate content 8 wt% |
| **Manufacturer** | : Arkema |

| | |
|---|---|
| **Compatibiliser Type** | : **Ethylene-methly acrylate-glycidyl methacrylate terpolymer (E-MA-GMA)** |
| **Trade Name** | : ***Lotader: AX8900*** |
| **Characteristics / Properties** | : Melt flow rate 6 g/10min (190℃/2.16kg), methyl acrylate content 25 wt%, glycidyl methacrylate content 8 wt% |
| **Manufacturer** | : Arkema |

Apart from evaluating the effectiveness of commercially available reactive compatibilisers, a low molecular weight digylcidyl ether bisphenol A (DGEBA) epoxy resin was selected for evaluation as a potential compatibiliser for compatibilising HDPE and the four matrix polymers. In contrast with commercial copolymers/terpolymers, the use of low molecular weight epoxy would allow greater flexibility in customising the level of the reactivity and also require much lower dosage than using pre-made compatibilisers. Details of this DGEBA are as follows:

**Chemical structure of DGEBA:**

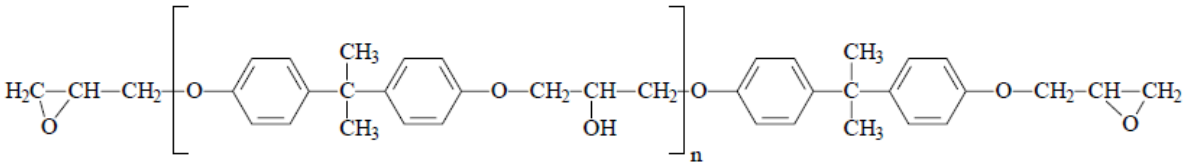

| | |
|---|---|
| **Compatibiliser Type** | : **<u>Diglycidyl ether of bisphenol A (DGEBA) epoxy resin</u>** |
| **Trade Name** | : ***Araldite GT 7072*** |
| **Characteristics / Properties** | : Epoxy equivalent 595 g/Eq, hydroxyl content 2.5 Eq/kg, 'n' value (degree of polymerisation) approximately 3 |
| **Manufacturer** | : Huntsman Advanced Materials |

**c.) <u>Non Reactive and Non Polar Carrier Polymer</u> :**

In this research HDPE is the base polymer used for evaluating the effectiveness of compatibilisers. Compared with other polyethylenes, its high melting point of about 130℃ allows the pre-drying of its modified blends to be carried out in the same hopper drier without softening as other engineering polymers that are typically dried at around 120℃ b efore processing. Details of this HDPE are as follows:

| | |
|---|---|
| **Polymer Type** | : **<u>High density polyethylene (HDPE)</u>** |
| **Trade Name** | : ***Escorene HMA-016*** |
| **Characteristics / Properties** | : Melt flow rate 20 g/10min (190℃/2.16kg), density 0.956 g/cm$^3$ |
| **Manufacturer** | : ExxonMobil Chemical |

**d.) <u>Matrix Polymers for Evaluation with Carrier Polymers :</u>**

Four matrix polymers, namely acrylonitrile-butadiene-styrene (ABS), polycarbonate (PC), poly(butylene terephthalate) (PBT), and polyamide 6 (PA6), were selected for this study to represent polymers with a broad range of properties in terms of differences in morphology (amorphous or semi-crystalline), polarity, and reactivity (different end groups of condensation polymers). Since HDPE has very limited miscibility and compatibility with these matrix polymers, preparing blends with different compatibilities provides evidence of their effectiveness in compatibilisation. Details of the four matrix polymers are as follows:

| | |
|---|---|
| **Polymer Type** | : **<u>Acrylonitrile-butadiene-styrene (ABS)</u>** |
| **Trade Name** | : ***Terluran GP-35*** |
| **Characteristics / Properties** | : Melt volume rate 34 cm$^3$/10min (220℃/10kg) |
| **Manufacturer** | : BASF |

| | |
|---|---|
| **Polymer Type** | : **<u>Polycarbonate (PC)</u>** |
| **Trade Name** | : ***Calibre 201-22*** |
| **Characteristics / Properties** | : Melt flow rate 22 g/10min (300℃/1.2kg) |
| **Manufacturer** | : LG-Dow Polycarbonate Ltd. |

| | |
|---|---|
| **Polymer Type** | : **Poly(butylene terephthalate) (PBT)** |
| **Trade Name** | : ***PBT 1200-211M*** |
| **Characteristics / Properties** | : Intrinsic viscosity 0.83 dl/g, melting point 225 ℃ |
| **Manufacturer** | : Chang Chun Plastics Co., Ltd. |

| | |
|---|---|
| **Polymer Type** | : **Polyamide 6 (PA6 )** |
| **Trade Name** | : ***Ultramid B3S*** |
| **Characteristics / Properties** | : Melt volume rate 175 $cm^3$/10min (275℃/5kg), melting point 220℃ |
| **Manufacturer** | : BASF |

**e.) Catalyst Used for Reactive Grafting :**

Hydrated zinc acetate was chosen as a potential catalyst for catalysing esterification reactions between epoxy and maleic anhydride functionalities of blends due to its ability to release water molecules during processing. Details of this catalyst is as follows:

| | |
|---|---|
| **Catalyst Type** | : **Hydrated zinc acetate** |
| **Trade Name** | : ***Zinc acetate dehydrate (catalogue no.: 108802)*** |
| **Characteristics / Properties** | : $(CH_3COO)_2Zn$ * 2H2O, molar mass 219.49 g/mol |
| **Manufacturer** | : Merck |

## 3.2 Processing of Polymer Blends

This section covers the extrusion (compounding) and injection moulding processes used for preparation of blends for this study. The sample compositions of these blends are listed according to the compounding or injection moulding processes used during sample preparation.

### 3.2.1 Compounding

The compounding of polyethylene/compatibiliser blends was carried out using a laboratory scale 27mm diameter co-rotating twin screw extruder, Leistritz ZSE27HP, with a length to diameter (L/D) ratio of 44:1 as shown schematically in Figure 3.1, which includes its detailed screw configuration. The melt strands were pulled from a 3-hole die head into a water bath for cooling and subsequently passing through an air blower for drying and into a pelletiser which converts the strands into cylindrical shaped pellets.

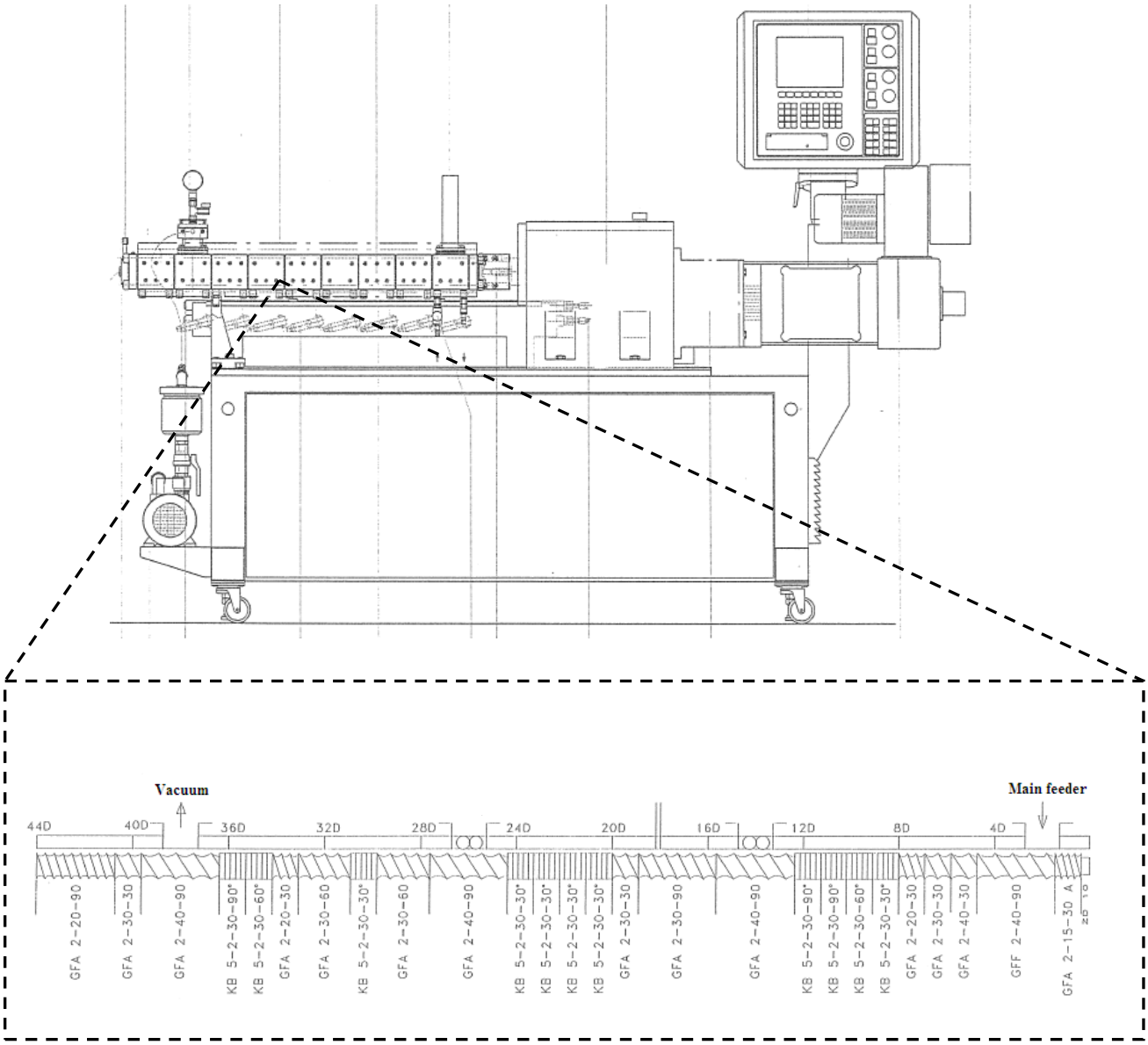


**Figure 3.1 Schematic representation of Leistritz ZSE27HP laboratory twin screw extruder with detailed screw configuration**

The formulations presented in Tables 3.1 were used for initial investigations in this project. HDPE was melt blended with EVA, EMA, E-GMA, E-MA-GMA and HDPE-g-MAH at 2 different HDPE/compatibiliser ratios of 1:1 and 3:1.

**Table 3.1 Binary blends of HDPE/compatibilisers**

| Sample Code | Sample Composition | Binary blend Compositions | |
|---|---|---|---|
| | | HDPE (wt%) | Compatibiliser (wt%) |
| EV1 | HDPE/EVA | 50 | 50 |
| EV2 | HDPE/EVA | 75 | 25 |
| EM1 | HDPE/EMA | 50 | 50 |
| EM2 | HDPE/EMA | 75 | 25 |
| EG1 | HDPE/E-GMA | 50 | 50 |
| EG2 | HDPE/E-GMA | 75 | 25 |
| MG1 | HDPE/E-MA-GMA | 50 | 50 |
| MG2 | HDPE/E-MA-GMA | 75 | 25 |
| HM1 | HDPE/HDPE-g-MAH | 50 | 50 |
| HM2 | HDPE/HDPE-g-MAH | 75 | 25 |

The processing conditions applied for the compounding of formulations in Table 3.1 are presented in Tables 3.2 and 3.3.

**Table 3.2 Compounding conditions for binary blends of HDPE with EVA, EMA and E-GMA**

| Operating Parameters | | Formulations | | | | | |
|---|---|---|---|---|---|---|---|
| | | EV1 | EV2 | EM1 | EM2 | EG1 | EG2 |
| **Zone 1 (Feed Zone)** | **Extruder Temperature Profile (℃)** | 50 | 50 | 50 | 50 | 50 | 50 |
| **Zone 2** | | 130 | 130 | 130 | 130 | 130 | 130 |
| **Zone 3** | | 130 | 130 | 130 | 130 | 130 | 130 |
| **Zone 4** | | 130 | 130 | 130 | 130 | 130 | 130 |
| **Zone 5** | | 140 | 140 | 140 | 140 | 140 | 140 |
| **Zone 6** | | 140 | 140 | 140 | 140 | 140 | 140 |
| **Zone 7** | | 140 | 140 | 140 | 140 | 140 | 140 |
| **Zone 8** | | 140 | 140 | 140 | 140 | 140 | 140 |
| **Zone 9** | | 140 | 140 | 140 | 140 | 140 | 140 |
| **Zone 10** | | 150 | 150 | 150 | 150 | 150 | 150 |
| **Flange** | | 150 | 150 | 150 | 150 | 150 | 150 |
| **Die Head 1** | | 150 | 150 | 150 | 150 | 150 | 150 |
| **Die Head 2** | | 150 | 150 | 150 | 150 | 150 | 150 |
| **Melt Temperature** | | 156 | 155 | 159 | 157 | 156 | 154 |
| | | | | | | | |
| **Screw Speed** | **rpm** | 300 | 300 | 300 | 300 | 300 | 300 |
| **Torque** | **%** | 39 | 52 | 42 | 51 | 48 | 55 |

The temperature profile and screw speed of the extruder were constant for all the formulations so that all the blends were subjected to similar processing history. All the raw components in pellet form were pre-blended in a plastic bag by hand in sample batch sizes of 5kg before dosing into the hopper of the extruder.

**Table 3.3 Compounding conditions for binary blends of HDPE with E-MA-GMA and HDPE-g-MAH**

| Operating Parameters | | Formulations | | | |
|---|---|---|---|---|---|
| | | MG1 | MG2 | HM1 | HM2 |
| Zone 1 (Feed Zone) | Extruder Temperature Profile (°C) | 50 | 50 | 50 | 50 |
| Zone 2 | | 130 | 130 | 130 | 130 |
| Zone 3 | | 130 | 130 | 130 | 130 |
| Zone 4 | | 130 | 130 | 130 | 130 |
| Zone 5 | | 140 | 140 | 140 | 140 |
| Zone 6 | | 140 | 140 | 140 | 140 |
| Zone 7 | | 140 | 140 | 140 | 140 |
| Zone 8 | | 140 | 140 | 140 | 140 |
| Zone 9 | | 140 | 140 | 140 | 140 |
| Zone 10 | | 150 | 150 | 150 | 150 |
| Flange | | 150 | 150 | 150 | 150 |
| Die Head 1 | | 150 | 150 | 150 | 150 |
| Die Head 2 | | 150 | 150 | 150 | 150 |
| Melt Temperature | | 155 | 158 | 160 | 156 |
| | | | | | |
| Screw Speed | rpm | 300 | 300 | 300 | 300 |
| Torque | % | 40 | 44 | 67 | 67 |

Reactive formulations that were selected from the screening process in Section 3.3 are presented in Table 3.4. For sample HDPE-ME5Ca, the epoxy and EVA components were pre-compounded separately as a masterbatch (epoxy-EVA MB) so that the two components were homogenously mixed before compounding with the rest of the components.

The processing conditions applied for the compounding of formulations in Table 3.4 are presented in Table 3.5. Due to the inherently low melting point and viscosity of the epoxy resin, the epoxy-EVA MB was compounded at a lower temperature setting especially at the feed zone to prevent bridging problems and also provide better melt strength for the stranding process.

**Table 3.4 Scaled-up selected reactive HDPE blends and compatibiliser masterbatch**

| Sample Code | Sample Composition | Active Components in Blends (wt%) | | | |
|---|---|---|---|---|---|
| | | HDPE-g-MAH | Epoxy | EVA | Catalyst* |
| HDPE-ME3Ca | HDPE/HDPE-g-MAH/epoxy | 10 (0.1) | 3.0 | - | 0.11 |
| HDPE-ME5Ca | HDPE/HDPE-g-MAH/epoxy/EVA | 10 (0.1) | 3.0[#] | 3.0[#] | 0.11 |
| | | | | | |
| Epoxy-EVA MB | Epoxy/EVA | - | 50 | 50 | - |

*For samples HDPE-ME3Ca and HDPE-ME5Ca, HDPE content = 100% – (total components in Table)*

*Figures in parenthesis denote active content (wt%) of maleic anhydride*

**Hydrated zinc acetate catalyst*

[#] *The epoxy and EVA were pre-compounded as a masterbatch, Epoxy/EVA MB (ratio1:1), followed by the second stage compounding with HDPE, HDPE-g-MAH, and catalyst in HDPE-ME5Ca*

**Table 3.5 Compounding conditions for selected reactive HDPE blends and compatibiliser masterbatch.**

| Operating Parameters | | Formulations | | |
|---|---|---|---|---|
| | | HDPE-ME3Ca | epoxy-EVA MB | HDPE-ME5Ca |
| Zone 1 (Feed Zone) | Extruder Temperature Profile (°C) | 50 | 10 | 50 |
| Zone 2 | | 50 | 10 | 50 |
| Zone 3 | | 100 | 50 | 100 |
| Zone 4 | | 120 | 120 | 120 |
| Zone 5 | | 150 | 120 | 150 |
| Zone 6 | | 180 | 120 | 180 |
| Zone 7 | | 180 | 130 | 180 |
| Zone 8 | | 180 | 130 | 180 |
| Zone 9 | | 180 | 130 | 180 |
| Zone 10 | | 180 | 150 | 180 |
| Flange | | 180 | 150 | 180 |
| Die Head 1 | | 180 | 150 | 180 |
| Die Head 2 | | 180 | 150 | 180 |
| Melt Temperature | | 209 | 168 | 196 |
| | | | | |
| Screw Speed | rpm | 300 | 300 | 300 |
| Torque | % | 69 | 26 | 65 |

### 3.2.2 Injection Moulding

All tensile and Izod impact test bars were moulded using a 60 ton Nissei PS-60E9A injection moulding machine shown schematically in Figure 3.2. Compositions of blends are presented in Tables 3.6 and 3.7 for stage 1 (Chapter 4) and 2 (Chapter 5) studies respectively.

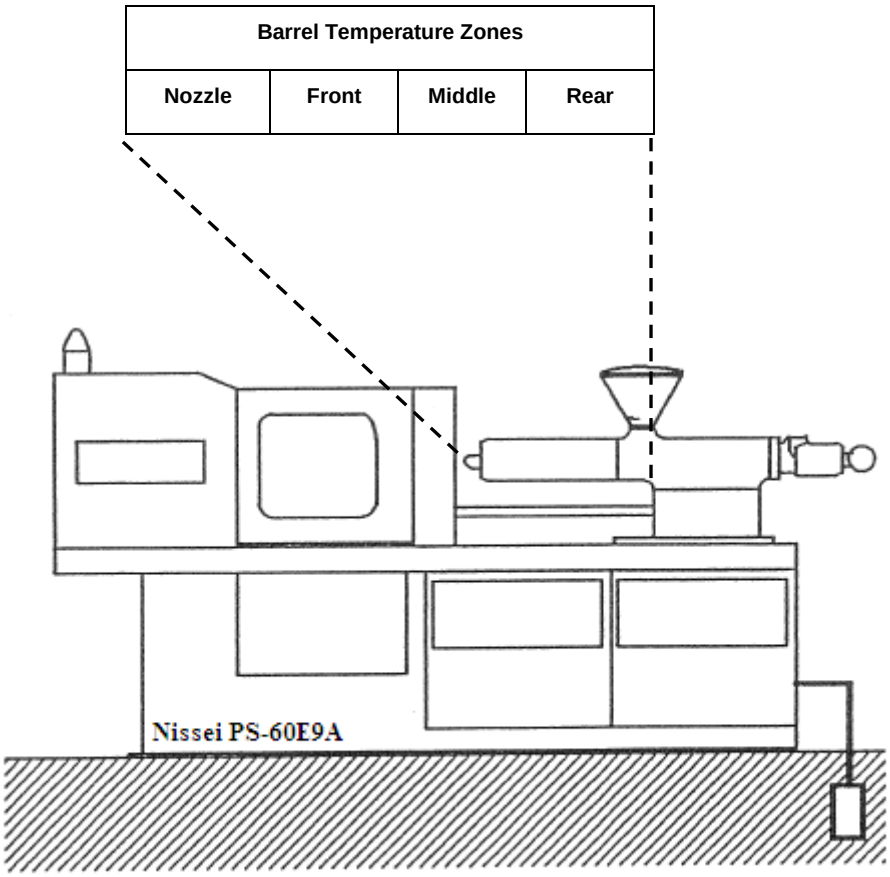


**Figure 3.2 Schematic representation of Nissei PS-60E9A injection moulding machine**

Pellets of compounded samples were dry blended homogeneously with individual matrix polymers in a plastic bag by hand before pouring into the hopper of the injection moulding machine.

**Table 3.6 Blends of matrix polymers with compatibilised and uncompatibilised HDPE for injection moulding**

| Sample Code | Sample Composition | Matrix Polymer (wt%) | HDPE/Compatibiliser binary blends (Pre-compounded) | |
|---|---|---|---|---|
| | | | HDPE (wt%) | Compatibiliser (wt%) |
| ABS-H15 | ABS/HDPE | 85 | 15 | - |
| ABS-EV1 | ABS/[HDPE/EVA] | 85 | 7.5 | 7.5 |
| ABS-EV2 | ABS/[HDPE/EVA] | 85 | 11.25 | 3.75 |
| ABS-EM1 | ABS/[HDPE/EMA] | 85 | 7.5 | 7.5 |
| ABS-EM2 | ABS/[HDPE/EMA] | 85 | 11.25 | 3.75 |
| ABS-EG1 | ABS/[HDPE/E-GMA] | 85 | 7.5 | 7.5 |
| ABS-EG2 | ABS/[HDPE/E-GMA] | 85 | 11.25 | 3.75 |
| ABS-MG1 | ABS/[HDPE/E-MA-GMA] | 85 | 7.5 | 7.5 |
| ABS-MG2 | ABS/[HDPE/E-MA-GMA] | 85 | 11.25 | 3.75 |
| ABS-HM1 | ABS/[HDPE/HDPE-g-MAH] | 85 | 7.5 | 7.5 |
| ABS-HM2 | ABS/[HDPE/HDPE-g-MAH] | 85 | 11.25 | 3.75 |
| PC-H15 | PC/HDPE | 85 | 15 | - |
| PC-EV1 | PC/[HDPE/EVA] | 85 | 7.5 | 7.5 |
| PC-EV2 | PC/[HDPE/EVA] | 85 | 11.25 | 3.75 |
| PC-EM1 | PC/[HDPE/EMA] | 85 | 7.5 | 7.5 |
| PC-EM2 | PC/[HDPE/EMA] | 85 | 11.25 | 3.75 |
| PC-EG1 | PC/[HDPE/E-GMA] | 85 | 7.5 | 7.5 |
| PC-EG2 | PC/[HDPE/E-GMA] | 85 | 11.25 | 3.75 |
| PC-MG1 | PC/[HDPE/E-MA-GMA] | 85 | 7.5 | 7.5 |
| PC-MG2 | PC/[HDPE/E-MA-GMA] | 85 | 11.25 | 3.75 |
| PC-HM1 | PC/[HDPE/HDPE-g-MAH] | 85 | 7.5 | 7.5 |
| PC-HM2 | PC/[HDPE/HDPE-g-MAH] | 85 | 11.25 | 3.75 |
| PBT-H15 | PBT-HDPE | 85 | 15 | - |
| PBT-EV1 | PBT/[HDPE/EVA] | 85 | 7.5 | 7.5 |
| PBT-EV2 | PBT/[HDPE/EVA] | 85 | 11.25 | 3.75 |
| PBT-EM1 | PBT/[HDPE/EMA] | 85 | 7.5 | 7.5 |
| PBT-EM2 | PBT/[HDPE/EMA] | 85 | 11.25 | 3.75 |
| PBT-EG1 | PBT/[HDPE/E-GMA] | 85 | 7.5 | 7.5 |
| PBT-EG2 | PBT/[HDPE/E-GMA] | 85 | 11.25 | 3.75 |
| PBT-MG1 | PBT/[HDPE/E-MA-GMA] | 85 | 7.5 | 7.5 |
| PBT-MG2 | PBT/[HDPE/E-MA-GMA] | 85 | 11.25 | 3.75 |
| PBT-HM1 | PBT/[HDPE/HDPE-g-MAH] | 85 | 7.5 | 7.5 |
| PBT-HM2 | PBT/[HDPE/HDPE-g-MAH] | 85 | 11.25 | 3.75 |
| PA6-H15 | PA6/HDPE | 85 | 15 | - |
| PA6-EV1 | PA6/[HDPE/EVA] | 85 | 7.5 | 7.5 |
| PA6-EV2 | PA6/[HDPE/EVA] | 85 | 11.25 | 3.75 |
| PA6-EM1 | PA6/[HDPE/EMA] | 85 | 7.5 | 7.5 |
| PA6-EM2 | PA6/[HDPE/EMA] | 85 | 11.25 | 3.75 |
| PA6-EG1 | PA6/[HDPE/E-GMA] | 85 | 7.5 | 7.5 |
| PA6-EG2 | PA6/[HDPE/E-GMA] | 85 | 11.25 | 3.75 |
| PA6-MG1 | PA6/[HDPE/E-MA-GMA] | 85 | 7.5 | 7.5 |
| PA6-MG2 | PA6/[HDPE/E-MA-GMA] | 85 | 11.25 | 3.75 |
| PA6-HM1 | PA6/[HDPE/HDPE-g-MAH] | 85 | 7.5 | 7.5 |
| PA6-HM2 | PA6/[HDPE/HDPE-g-MAH] | 85 | 11.25 | 3.75 |

**Table 3.7 Blends of matrix polymers with reactively compatibilised and uncompatibilised HDPE for injection moulding**

| Sample Code | Sample Composition | Matrix Polymer (wt%) | HDPE (wt%) | ME3Ca (wt%) | ME5Ca (wt%) |
|---|---|---|---|---|---|
| ABS-H5 | ABS/HDPE | 95 | 5 | - | - |
| ABS-ME3Ca | ABS/**[HDPE/HDPE-g-MAH/epoxy]** | 95 | - | 5 | - |
| ABS-ME5Ca | ABS/**[HDPE/HDPE-g-MAH/epoxy/EVA]** | 95 | - | - | 5 |
| PBT-H5 | PBT/HDPE | 95 | 5 | - | - |
| PBT-ME3Ca | PBT/**[HDPE/HDPE-g-MAH/epoxy]** | 95 | - | 5 | - |
| PBT-ME5Ca | PBT/**[HDPE/HDPE-g-MAH/epoxy/EVA]** | 95 | - | - | 5 |
| PA6-H5 | PA6/HDPE | 95 | 5 | - | - |
| PA6-ME3Ca | PA6/**[HDPE/HDPE-g-MAH/epoxy]** | 95 | - | 5 | - |
| PA6-ME5Ca | PA6/**[HDPE/HDPE-g-MAH/epoxy/EVA]** | 95 | - | - | 5 |

Table 3.8 shows the injection moulding conditions based on matrix polymer type for blends presented in Tables 3.6 and 3.7.

**Table 3.8 Injection moulding conditions for blends of compatibilised and uncompatibilised HDPE with matrix polymers**

| Operating Parameters | | Polymer Type | | | |
|---|---|---|---|---|---|
| | | ABS | PC | PBT | PA6 |
| **Rear Zone (feed)** | **Barrel Temp. Profile (℃)** | 200 | 260 | 230 | 230 |
| **Middle Zone** | | 210 | 270 | 240 | 240 |
| **Front Zone** | | 220 | 280 | 250 | 250 |
| **Nozzle** | | 220 | 280 | 250 | 250 |
| | | | | | |
| **Shot size** | mm | 29-32 | 27-33 | 28-35 | 32-36 |
| **Screw back after dosing** | mm | 3 | 3 | 3 | 3 |
| **Cushion** | mm | 3.9-4.7 | 3.6-4.9 | 3.1-3.9 | 3.4-4.7 |
| **Injection speed** | % | 30 | 30 | 30 | 30 |
| **Plasticising speed** | % | 80 | 60 | 80 | 80 |
| **Injection pressure** | % | 30 | 30 | 20 | 20 |
| **Holding pressure** | % | 30 | 30 | 20 | 20 |
| **Back pressure** | $Kgf/cm^2$ | 30 | 30 | 30 | 30 |
| **Injection time** | Sec | 5 | 5 | 5 | 5 |
| **Holding time** | Sec | 2 | 2 | 2 | 2 |
| **Cooling time** | Sec | 15-18 | 15-20 | 15-18 | 15-18 |
| | | | | | |
| **Mould temperature** | ℃ | 30 | 80 | 80 | 80 |
| **Drying temperature** | ℃ | 100 | 120 | 120 | 80 |
| **Drying time** | Hours | 2 | 2 | 2 | 4 |

## 3.3 Reactivity Studies Using Extrusion Plastometer

The second stage of this research covers the evaluation of reactivity between functional groups of the compatibilisers using a Tinius Olsen MP987 extrusion plastometer (also known as melt indexer). Figure 3.3 shows a schematic representation of a typical extrusion plastometer which consists of a heated barrel, an orifice at the bottom of the barrel, a piston and a dead weight for pushing the melt out of the heated barrel through the orifice.

In this study, the extrusion plastometer was used as a “reactor” since it allows a fixed amount of polymer mixture to reside in a uniformly heated barrel for a fixed residence time, temperature and load. Any reactions that took place in the barrel could result in a change in viscosity of the melt leading to changes in the melt flow rate of the sample under constant test conditions.

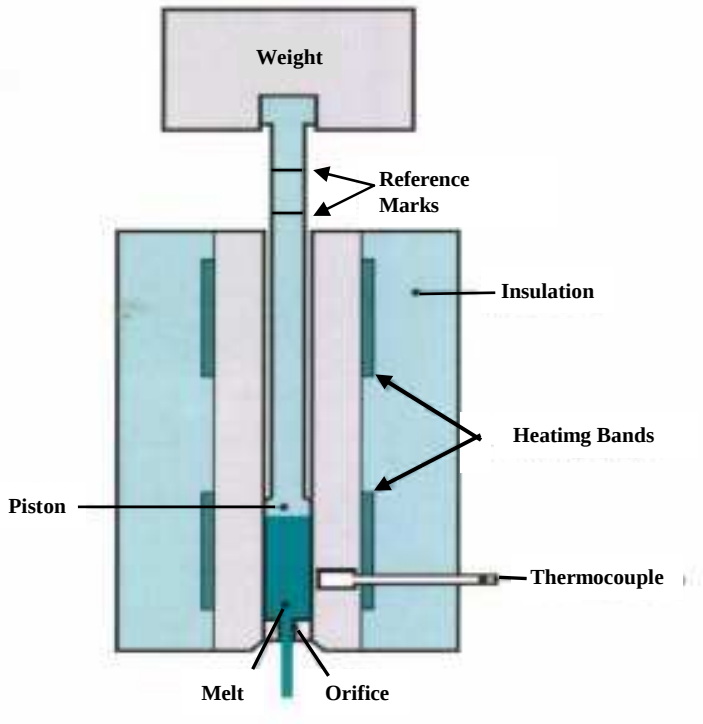


**Figure 3.3 Schematic representation of an extrusion plastometer (melt indexer)**

In order to ensure that the mixtures were homogenously mixed in the heated barrel, all HDPE and HDPE-g-MAH pellets were pulverised using a Retsch

ultra centrigual mill ZM 200 to grain size of about 1 mm. The epoxy flakes which are brittle under room conditions were physically ground into powder using mortar and pestle. The powder mixtures were weighed and hand mixed in a plastic bag in a sample batch size of 100 g.

During the melt flow rate tests, 6 g of each homogenous powder mixture was loaded into the barrel and heated at 190℃ with pre-heating dwell times of 5 and 15 minutes under a standard load of 2.16 kg. The extrudates obtained after the pre-heating time were weighed and melt flow rates expressed in grams per 10 minutes were obtained by dividing the mass of the extrudate by the time interval (in seconds) used in obtaining the extrudate and then multiplied by 600. All melt flow rates reported in this study are average of 3 determinations (see Appendices B3-1 to B3-3). Extrudates collected from the extrusion plastometer were used for further characterisation such as DSC, FTIR, optical microscopy and solvent extraction.

Blends of varying ratios of HDPE with HDPE-g-MAH in Table 3.9 were evaluated for the possible influence of pre-heating time in the extrusion plastometer on the flow behaviour of the blends. They also served as basis for detecting any reaction when epoxy was added.

**Table 3.9 Powder dry blends of HDPE/HDPE-g-MAH**

| Sample Code | Sample Composition | HDPE (wt%) | HDPE-g-MAH (wt%) |
|---|---|---|---|
| HDPE-M1 | HDPE/HDPE-g-MAH | 50 | 50 (0.5) |
| HDPE-M2 | HDPE/HDPE-g-MAH | 75 | 25 (0.25) |
| HDPE-M3 | HDPE/HDPE-g-MAH | 90 | 10 (0.1) |
| HDPE-M4 | HDPE/HDPE-g-MAH | 95 | 5 (0.05) |

*Figures in parenthesis denote active content (wt%) of maleic anhydride*

Similarly, blends of HDPE with varying amounts of epoxy resin as shown in Table 3.10 was evaluated for possible influences of the epoxy on the flow rate of the HDPE without interaction (before the addition of HDPE-g-MAH).

**Table 3.10 Powder dry blends of HDPE/epoxy**

| Sample Code | Sample Composition | HDPE (wt%) | Epoxy (wt%) |
|---|---|---|---|
| HDPE-E1 | HDPE/epoxy | 94 | 6.0 |
| HDPE-E2 | HDPE/epoxy | 97 | 3.0 |
| HDPE-E3 | HDPE/epoxy | 98.8 | 1.2 |
| HDPE-E4 | HDPE/epoxy | 99.4 | 0.6 |

## 3.3.1 Stoichiometry Considerations

The components used in the reactive formulations were calculated stoichiometrically as follows:

**a.) Determination of MAH concentration:**

The commercial grade of HDPE-g-MAH used in this study contains 1 wt% of grafted MAH. Thus if 10 grams of this HDPE-g-MAH is used in a formulation based on 100 grams sample, it should contain 0.1 gram of active grafted MAH. Therefore the number of moles of grafted MAH present in 10 gram of the HDPE-g-MAH is, (0.1 g / 99 $gmol^{-1}$) = 0.00101 mole, where 99 $gmol^{-1}$ is the molecular weight of the grafted MAH moiety based on the chemical structure of MAH as follows:

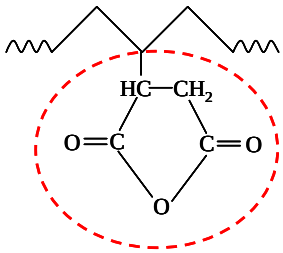

**b.) <u>Determination of catalyst (hydrated zinc acetate) concentration:</u>**

In order for maleic anhydride to react with the epoxy, it has to be first converted into carboxylic acid through a hydrolysis reaction with water. This can be achieved by the addition of hydrated zinc acetate as a catalyst which releases the required amount of water during processing.

Basic information:

- Molecular weight of hydrated zinc acetate $(CH_3COO)_2Zn * 2H2O$): **219.49 $gmol^{-1}$**
- Molecular weight of $H_2O$ = **18 $gmol^{-1}$**
- Percentage of $H_2O$ present in hydrated zinc acetate: [(2 x 18 $gmol^{-1}$) / 219.49 $gmol^{-1}$] x 100% = **16.4 wt%**

To obtain 0.00101 mole of $H_2O$, (0.00101 mole x 18 $gmol^{-1}$) = 0.01818 gram is needed.

Since the hydrated zinc acetate contains 16.4 wt% of water, [(0.01818 g x 100 wt%) / 16.4 wt%] = 0.11 gram of hydrated zinc acetate is required to produce 0.00101 mole of water.

Therefore in 100 grams of sample formulation that contains 10 grams of HDPE-g-MAH i.e. 0.00101 moles of grafted MAH moieties, 0.11 gram of hydrated zinc acetate catalyst is required to achieve an equimolar reaction. An example of a formulation having equimolar concentration of MAH and catalyst is HDPE-ME3C in Table 3.11.

**c.) <u>Determination of DGEBA concentration:</u>**

The equivalent weight of DGEBA epoxy resin used in this study is approximately 595 $gEq^{-1}$ and since the functionality of the linear epoxy resin is 2, the molecular weight is thus approximately equal to, (595 $gEq^{-1}$ x 2) = 1190 $gmol^{-1}$. This also corresponds to the n value (degree of polymerisation) of 3 for the DGEBA provided by the supplier.

Based on 100 grams of sample, in order to obtain the same molar concentration of MAH (0.00101 moles), the amount of DGEBA needed will be (0.00101 mole x 1190 $gmol^{-1}$) = 1.2 grams. Therefore, for every 0.1 gram of MAH moiety present in the formulation, 1.2 grams of DGEBA will be needed for an equimolar reaction. An example of formulation having an equimolar concentration of MAH and epoxy moieties is HDPE-ME3 in Table 3.11.

After obtaining the stoichiometric ratios of the MAH, epoxy and catalyst components, the various formulations presented in Table 3.11 were evaluated for the effect of molar ratio of MAH:epoxy, and also the influence of catalyst on the esterification of the MAH and epoxy.

**Table 3.11 Powder dry blends of catalysed and uncatalysed HDPE/HDPE-g-MAH/epoxy**

| Sample Code | Sample Composition | Active Components in Blends (wt%) | | |
|---|---|---|---|---|
| | | HDPE-g-MAH | Epoxy | Catalyst* |
| HDPE-ME1 | HDPE/HDPE-g-MAH/epoxy | 50 (0.5) | 6.0 | - |
| HDPE-ME1C | HDPE/HDPE-g-MAH/epoxy/cat. | 50 (0.5) | 6.0 | 0.55 |
| HDPE-ME2 | HDPE/HDPE-g-MAH/epoxy | 25 (0.25) | 3.0 | - |
| HDPE-ME2C | HDPE/HDPE-g-MAH/epoxy/cat. | 25 (0.25) | 3.0 | 0.28 |
| HDPE-ME3 | HDPE/HDPE-g-MAH/epoxy | 10 (0.1) | 1.2 | - |
| HDPE-ME3C | HDPE/HDPE-g-MAH/epoxy/cat. | 10 (0.1) | 1.2 | 0.11 |
| HDPE-ME3Ca | HDPE/HDPE-g-MAH/epoxy/cat. | 10 (0.1) | 3.0 | 0.11 |
| HDPE-ME4 | HDPE/HDPE-g-MAH/epoxy | 5 (0.05) | 0.6 | - |
| HDPE-ME4C | HDPE/HDPE-g-MAH/epoxy/cat. | 5 (0.05) | 0.6 | 0.06 |
| HDPE-ME4Ca | HDPE/HDPE-g-MAH/epoxy/cat. | 5 (0.05) | 3.0 | 0.06 |

*Figures in parenthesis denote active content (wt%) of maleic anhydride*

**Hydrated zinc acetate catalyst*

From the results of evaluation on the extrudates of these blends, the most promising blend was selected for scaling up and further modification on the twin screw extruder. The short-listed formulations from this section of work for scaling up were presented earlier in Table 3.4.

## 3.4 Mechanical Properties of Blends

### 3.4.1 Izod Impact Testing

Izod Impact testing was performed in accordance with ASTM D256, methods A (notched) and E (reversed notch), on a Ceast Resil Impactor. All Izod impact test specimens were moulded according to conditions stated in Table 3.8. The moulded specimens were notched using a Ceast motorised Notchvis machine with notch depth of 2.54 mm and radius of 0.25 mm. The overall dimensions of the impact test specimen are shown in Figure 3.4.

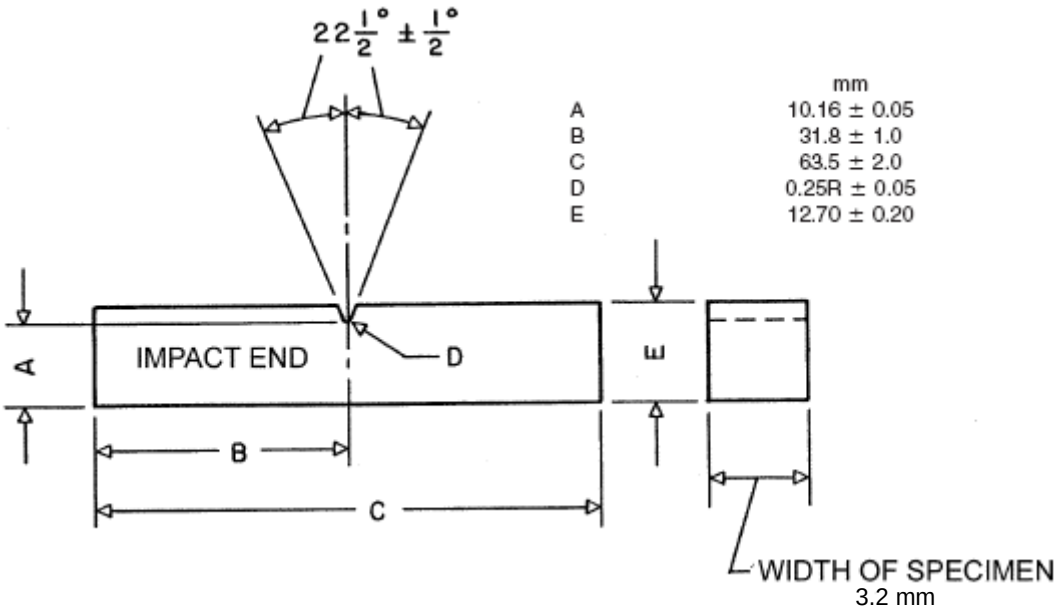


**Figure 3.4 Dimensions of a notched Izod test specimen [ASTM D256]**

The purpose of conducting reversed notch impact is that most of the brittle materials exhibit brittle failure under notched impact tests for both compatibilised and uncompatibilised blends. Thus the reversed notch impact test is a more appropriate approach in differentiating the toughness change of the notch-sensitive blends through compatibilisation. A total of 21 impact specimens were tested for each reported value after conditioned at 23 ± 2℃ and relative humidity of 50 ± 5% for 48 hours (see Appendices B2-1 to B2-7). The Izod impact tests were conducted under laboratory conditions of 23 ± 2℃ and relative humidity of 50 ± 5%.

## 3.4.2 Tensile Testing

All type IV tensile test bars (ASTM D638 type) were moulded according to conditions stated in Table 3.8. The overall dimensions of the tensile bar are shown in Figure 3.5. Tensile properties of the moulded bars were evaluated using a Zwick universal testing machine, Model BZ020, in accordance with ASTM D638. A 10 KN load cell was used at a grip separation speed of 5 mm/minute and a gauge length of 25 mm. An average of five specimens were tested for each type of sample after the test bars were conditioned at 23 ± 2℃ and relative humidity of 50 ± 5% for 48 hours. The tensile tests were conducted under laboratory conditions of 23 ± 2℃ a nd relative humidity of 50 ± 5%. The tensile results reported include tensile strengths at yield and break, and elongations at yield and break. Figure 3.6 illustrates the typical stress-strain curves from which values of tensile strengths at yield and break, and elongations at yield and break were derived. Examples of tensile stress-strain curves can be found in Appendices B1-1 to B1-11.

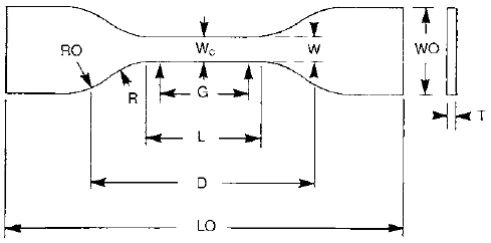


**Figure 3.5 Dimensions of a type IV tensile test specimen [ASTM D638]**

where:

- Width of narrow section: W = Wc = 6 mm
- Length of narrow section: L = 33 mm
- Gage length: G = 25 mm
- Radius of fillet: R = 14 mm
- Thickness: T = 3.2 mm
- Overall width: WO = 19 mm
- Overall length: LO = 115 mm
- Distance between grips: D = 65 mm
- Outer radius: RO = 25 mm

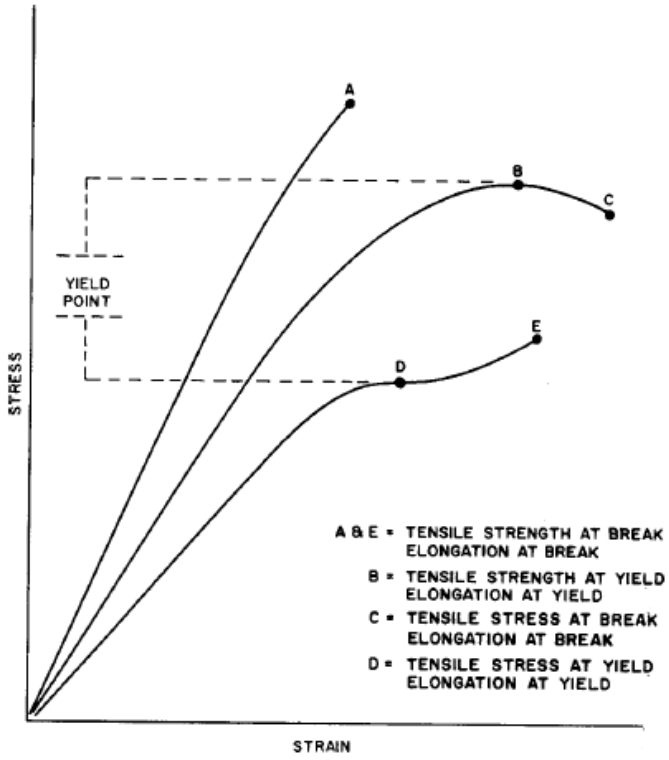


**Figure 3.6 Typical stress-stain curves [ASTM D638]**

## 3.5 Characterisation of Blends

### 3.5.1 Differential Scanning Calorimetry (DSC)

A Mettler Toledo DSC822$^e$ differential scanning calorimeter (DSC) equipped with a STAR$^e$ version 8.10 software was employed to study the changes in transition temperatures and crystallisation behaviour of the polymer blends. All details of transitions and crystallisation behaviour were obtained from re-heat and cooling traces respectively as shown in schematically in Figure 3.7.

Sample sizes between 5 to 6 mg were cut from the centre of injection moulded Izod impact bars and measurements were done on three samples of each blend composition to ascertain the reproducibility of the results. All scanning was conducted under a nitrogen environment at heating and cooling rates of 10$^o$C/min.

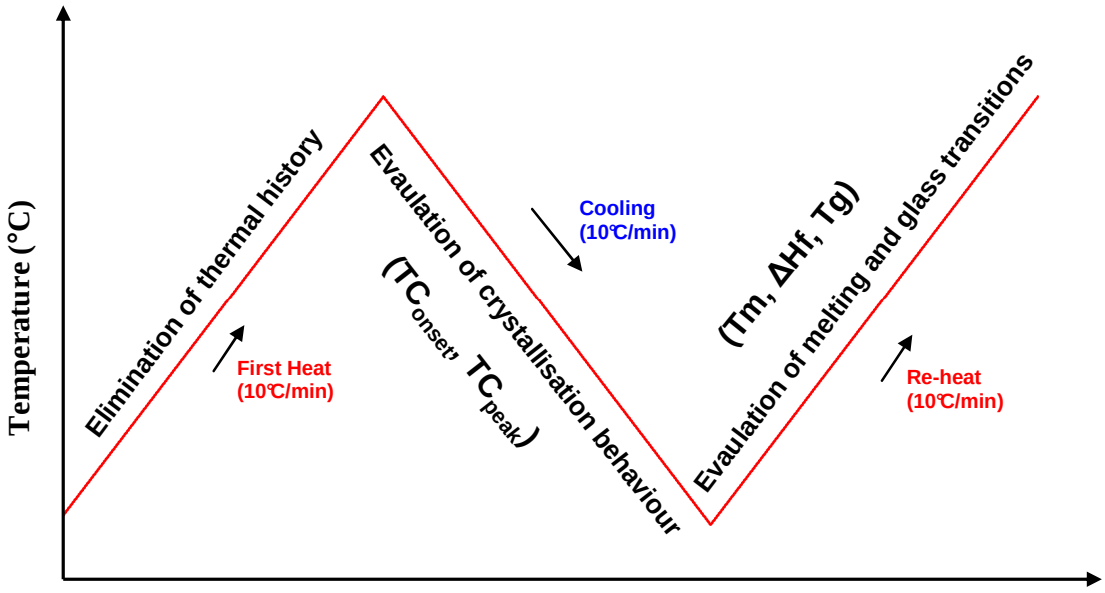


**Figure 3.7 DSC heating/cooling cycles applied to samples**

As shown in Figure 3.8, the melting temperature (Tm) and melting enthalpy (ΔHf ) were determine from the DSC endothermic peaks of the re-heat traces. Glass transition temperatures, Tg, were estimated as onset temperatures. The crystallisation temperatures, $TC_{peak}$ and $TC_{onset}$, were obtained from the exothermic peaks of the cooling traces. Evaluation of these parameters were carried out on the DSC traces using STAR$^{e}$ software.

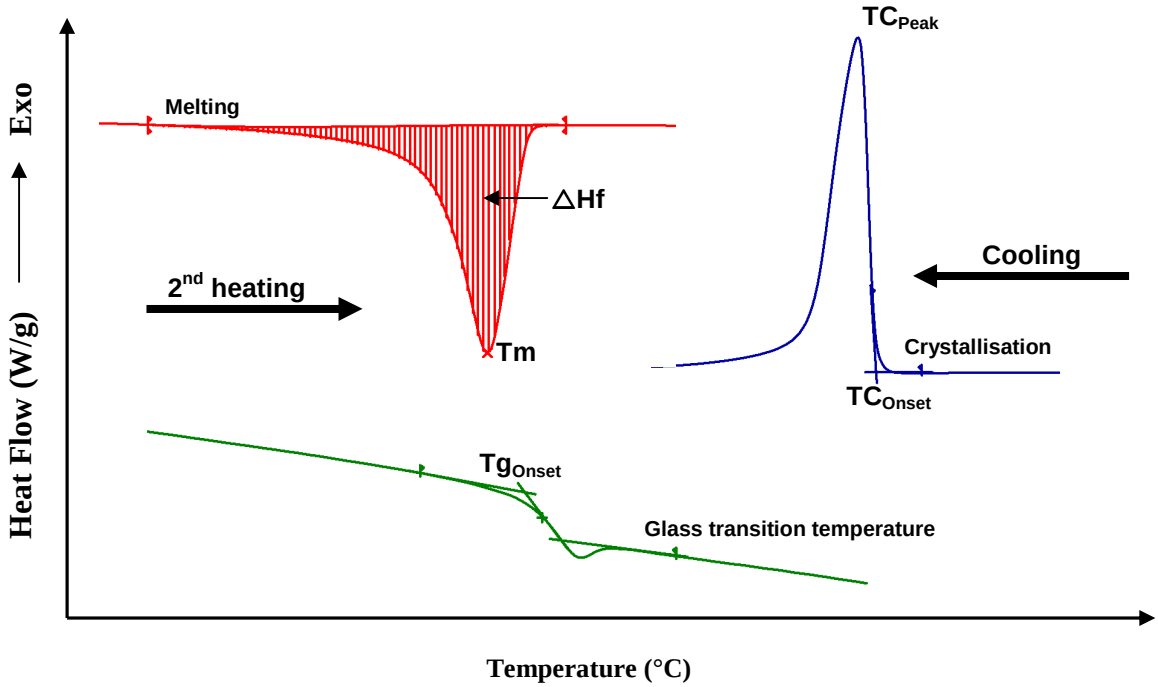


**Figure 3.8 Schematic representation of the method of determination of characteristic temperature, enthalpy, and glass transition temperature**

In order to obtain information on the degree of crystallinity of individual semi-crystalline blend components (i.e. HDPE, PBT and PA6), the individual ΔHf values of these component were normalised to the amount of the phase under consideration and degree of crystallinity calculated using the following equation :

$$X_C\ (\%) = \frac{\Delta Hf}{\Delta Hf_{100}\phi_n} \times 100$$

where $X_C$ is the percentage crystallinity of the blend component of interest, ΔHf is its measured heat of fusion, $\Delta Hf_{100}$ is the heat of fusion of a theoretical 100% crystalline polymer, and $\varnothing_n$ is its weight fraction in the blend.

The $\Delta Hf_{100}$ values used in the above calculations were obtained from reference [190] as follows:

PE : 293 J/g
PBT : 145 J/g
PA6 : 230 J/g

ΔHf values normalised to the overall amount of the sample were used, e.g. in Table 5.5, whenever the exact concentration of the relevant component was unknown and also for all neat semi-crystalline resin samples. For the ABS matrix polymer, a melting peak observed at around 144℃ with a ΔHf value of about 5.9 J/g belonged to an ethylene bis-stearamide (EBS) lubricating wax, and this peak overlapped partially with the melting endotherm of HDPE phase in blends containing HDPE. As such, during the evaluation of HDPE peak in all ABS/HDPE blends, the ΔHf value that belonged to EBS was subtracted from the total peak area, e.g. in Table 4.2, 5.0 J/g was subtracted from the ΔHf values of all HDPE phases before normalising as the blends contained 85 wt% of ABS.

The overall rate of crystallisation represented by ΔTC, was obtained by subtracting the values of crystallisation peak from the values of crystallisation onset, i.e. $\Delta TC = TC_{Onset} - TC_{Peak}$. The smaller the value of ΔTC, the greater the rate of crystallisation. Examples of DSC traces can be found in Appendices A1-1 to A1-44.

### 3.5.2 Thermogravimetric Analysis (TGA)

Thermogravimetry (TG) is commonly used to measure changes in mass of a sample as a function of temperature or time. Changes of mass occur during evaporation, decomposition, sublimation, and chemical reactions. A schematic representation of a typical TG thermogram is presented in Figure 3.9.

In this work, a Mettler Toledo TGA/SDTA852$^e$ thermogravimetric analyser equipped with STAR$^e$ version 8.10 software was employed for the determination of the water content in the hydrated zinc acetate sample in accordance with ASTM E1131. A sample mass of 23 mg was scanned from 30℃ to 1000℃ at a heating rate of 10 ℃/min with a nitrogen flow rate of 50 ml/min.

The content of water in hydrated zinc acetate sample (content marked “V” in Figure 3.9) was obtained by evaluating the TG thermogram for percentage mass loss from 30℃ to 130℃ corresponding to ‘0’ t o X respectively marked on the x-axis in Figure 3.9.

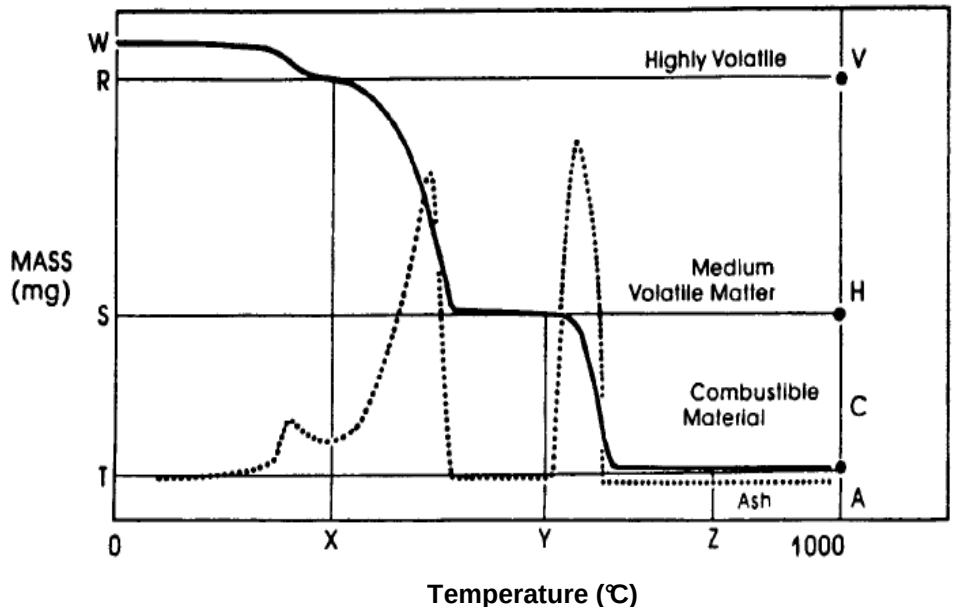


**Figure 3.9 A typical thermogravimetric curve (reconstructed from ref. [ASTM E1131])**

### 3.5.3 Fourier Transform Infrared Spectroscopy (FTIR)

Fourier transform infrared spectroscopy (FTIR) was employed for analysis of potential reactions between reactive polymer blends. A Perkin Elmer System 2000 Infrared Spectrophotometer was used in this work. Sample preparations were carried out using hot pressed film method, KBr pressed pellet technique, and also Attenuated Total Reflectance (ATR) technique using a MKII Golden Gate single reflection ATR system as appropriate. Examples of FTIR spectra can be found in Appendices A2-1 to A2-8.

**a.) Analysis of polymer resins and reactive blends**

Films of all neat polymer resins (except epoxy) and reactive blends obtained from the extrusion plastometer or by compounding were prepared by hot pressing at 200℃ for 2 minutes into films about 25 μm thick. As the epoxy resin was too brittle to be prepared as a hot pressed film, the sample was ground with KBr powder using a mortar and pestle at a ratio of quantity of sample to KBr powder of 1/50. The KBr mixture was then placed in a special die and compressed into a small disk with a thickness of about 0.3 mm. Each

spectrum was obtained by performing 32 scans from 4000 to 400 $cm^{-1}$ at a resolution of 4 $cm^{-1}$ on the pressed films or KBr disks.

**b.) Analysis of gels from solvent extraction**

Rubbery gel samples recovered from solvent extraction could not to be pressed into thin film or ground with KBr powder and therefore the samples were examined directly using the ATR technique. Each spectrum was obtained by performing 32 scans from 4000 to 650 $cm^{-1}$ at a resolution of 4 $cm^{-1}$ directly on the samples.

**c.) Analysis of soluble components from solvent extraction**

For the analysis of soluble components, about 2 ml of solution were transferred onto a mortar and allowed to dry in a hot air oven at 110℃ for 30 minutes. The dried residues were examined directly using ATR and each spectrum was obtained by performing 32 scans from 4000 to 650 $cm^{-1}$ at a resolution of 4 $cm^{-1}$ directly on the samples.

**d.) Analysis of precipitated components from solvent extraction**

For the analysis of precipitated components, the precipitates were rinsed with about 50 ml of xylene/methanol mixture (1:1 ratio) followed by drying in an oven at 100℃ for 1 hour. The dried residues were also examined directly using ATR and each spectrum was obtained by performing 32 scans from 4000 to 650 $cm^{-1}$ at a resolution of 4 $cm^{-1}$ directly on the samples.

## 3.5.4 Scanning Electron Microscopy (SEM)

Scanning electron microscopy (SEM) was employed for the study of blend morphologies using a low vacuum scanning electron microscope, JEOL JSM-5600LV, or an ultra high resolution field emission scanning electron microscope (FESEM), Zeiss SUPRA 40, operated at an accelerating voltage of 10 to 20 kV. Fractured surfaces of the Izod impact test bars were sputter coated with gold to render the surface conductive prior to examination to prevent charging up the surfaces of the specimens. Micrographs of the blend morphologies were taken at 3 000 X, 6 000 X and 10 000 X magnifications

depending on the size of the phases of blends under observation. Table 3.12 summarises the list of samples examined using Jeol JSM-5600LV and Zeiss SUPRA 40 electron microscopes.

**Table 3.12 Samples examined using SEM**

| Blend Type | Acc. Volt (kV) | JEOL JSM-5600LV | | | | | |
|---|---|---|---|---|---|---|---|
| **ABS** | 20 | ABS-H15 | ABS-EV1 | ABS-EV2 | ABS-EG1 | ABS-EG2 | |
| **PC** | 20 | PC-H15 | PC-EV1 | PC-EV2 | PC-EG1 | PC-EG2 | |
| **PBT** | 10 | PBT-H15 | PBT-EV1 | PBT-EV2 | PBT-EG1 | PBT-EG2 | |
| **PA6** | 20 | PA6-H15 | PA6-EV1 | PA6-EV2 | PA6-EG1 | PA6-EG2 | |
| **Blend Type** | **Acc. Volt (kV)** | **Zeiss SUPRA 40** | | | | | |
| **ABS** | 20 | ABS-EM1 | ABS-EM2 | ABS-MG1 | ABS-MG2 | ABS-HM1 | ABS-HM2 |
| **PC** | 20 | PC-EM1 | PC-EM2 | PC-MG1 | PC-MG2 | PC-HM1 | PC-HM2 |
| **PBT** | 20 | PBT-EM1 | PBT-EM2 | PBT-MG1 | PBT-MG2 | PBT-HM1 | PBT-HM2 |
| **PA6** | 20 | PA6-EM1 | PA6-EM2 | PA6-MG1 | PA6-MG2 | PA6-HM1 | PA6-HM2 |

### 3.5.5 Optical Microscopy (OM)

Optical microscopy (OM) studies were carried out with a Leica DM EP polarising microscope in conjunction with a Leica DC 180 digital camera.

Two microscopic slides were placed on a hot plate set at 200℃ for HDPE blends, 250℃ for ABS blends, and 280℃ for PBT and PA6 blends. After thermal equilibrium has been reached, a small piece of specimen about 0.4 to 0.6 mg was introduced between the two slides and kept on the hotplate at the above pre-set temperatures for 30 seconds with a 10 kg load placed on top of the slides. The specimen was cooled to about 23℃ and conditioned for 10 minutes before observation under the microscope. Transmitted light was used when blends were examined for their phases and dispersion quality. Spherulitic structures of these blends were studied under polarised light. Micrographs of the blend morphologies were taken at 400 X, and 630 X magnifications depending on the size of the phases of blends under observation.

## 3.6 Characterisation of Gels and Other Soluble Components

In this work, sol-gel analysis by a solvent extraction method was performed on the reactive blends to determine the content and characterise the insoluble fraction (gel) of the blends. The solution (sol) of the extract which corresponded to the soluble fraction of the reactive blends, considered as non-crosslinked fractions were also subjected to further characterisation. The extraction apparatus used for this study was set up in accordance with ASTM D2765 as shown in Figure 3.10.

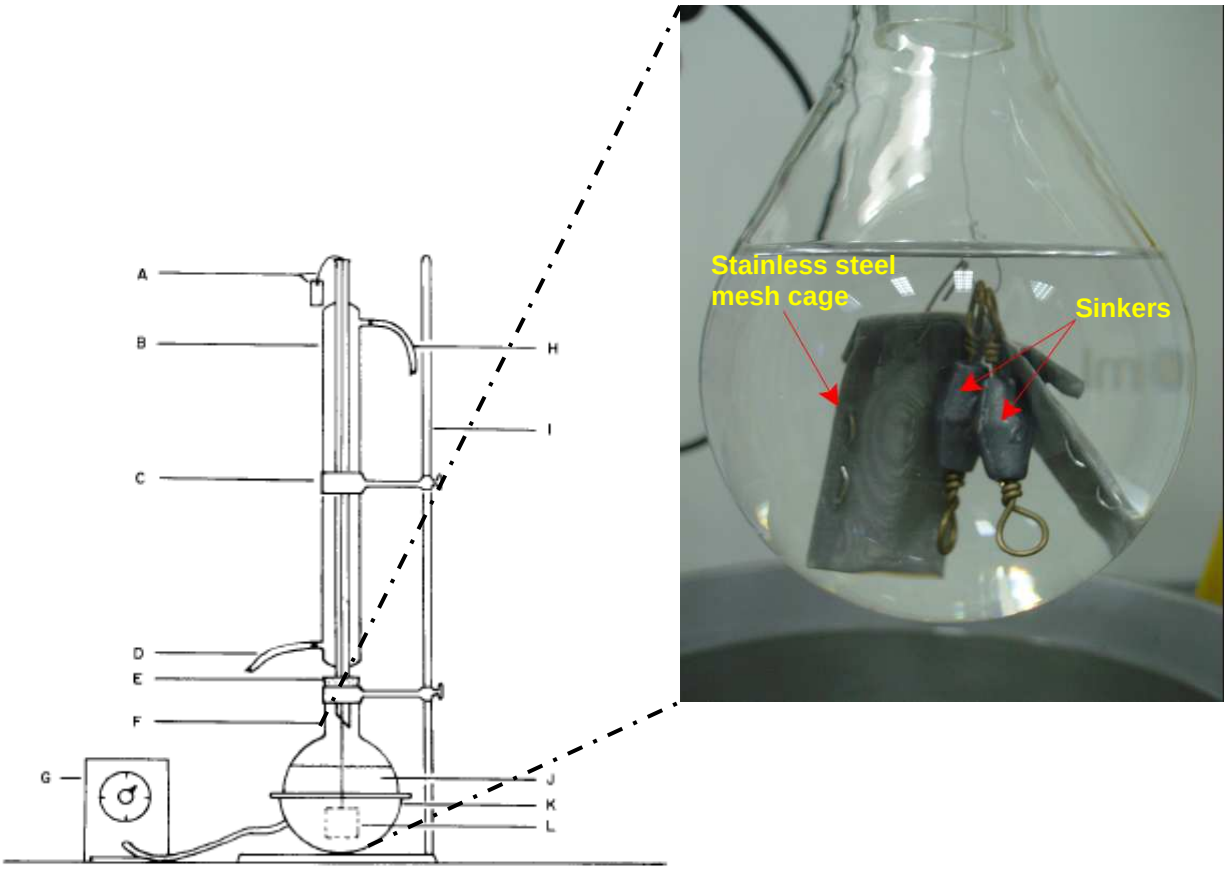


**Figure 3.10 Extraction apparatus [ASTM D2765]**

**a.) <u>Gel Analysis</u>**

The specimen holder in the form of a stainless steel mesh cage shown in Figure 3.10 was prepared by cutting a piece of 120-mesh stainless steel cloth to dimensions of approximately 80 by 30 mm. It was then folded by half of original length into approximate dimension of 40 x 30 mm. The two sides were then folded and stapled to form an open pouch as shown in Figure 3.11. The weight of the pouch was taken as ***W1***.

Specimens of 0.300 ± 0.015 grams were cut from samples of reactive blends in the form of extrudates from the extrusion plastometer or pellets from compounding. The specimens were then placed in the pouch through the top open end of the pouch. The weight of pouch with specimen was taken as ***W2***.

The open side of the pouch was then folded with the edge stapled to form a cage. The weight of the cage and specimen was taken as ***W3***.

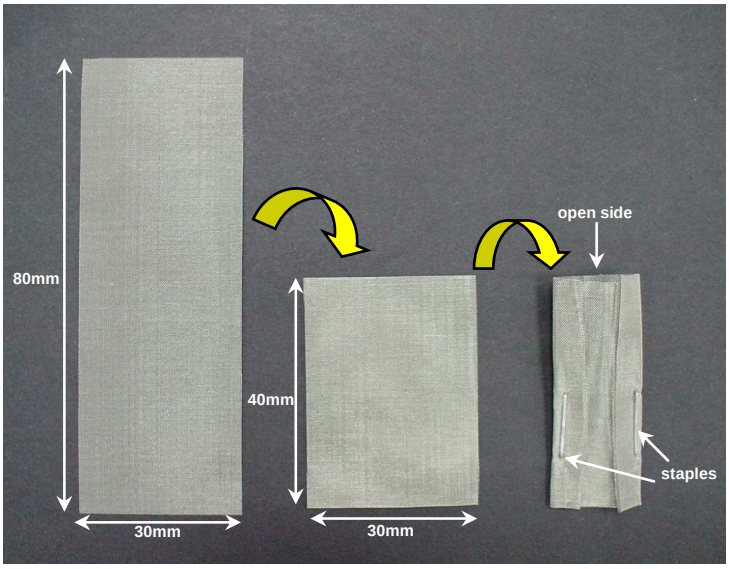


**Figure 3.11 Preparation of a stainless steel mesh cage**

A 250 ml round-bottomed flask was filled with 200 ml (172 gram) of xylene which was sufficient to submerge two stainless steel mesh cages completely. About 1 wt% (1.72 gram) of a phenolic antioxidant (Irganox 1010 from Ciba

Chemicals) was added into the xylene to inhibit further crosslinking of the specimen.

The cages containing the specimens were kept suspended in the solvent so that the bottom edge of each cage was almost touching the bottom of the flask by attaching the cage to a piece of small wire which was extended through the reflux condenser, and tying sinkers to the cages as shown in Figure 3.10.

The extraction process was carried out by boiling the xylene at 160℃ for 12 hours under reflux conditions. After the first extraction process, the cages were removed and a fresh batch of xylene with antioxidant was prepared. The cages were re-introduced into the refluxing unit and further refluxed for 2 hours. The solution obtained from the first extraction was retained for subsequent sol analysis. After the second extraction, the cages were placed in an oven immediately and dried at 150℃ until a consistent weight (***W4***) was reached.

The gel fraction was calculated as follows:

$$Extract,(\%) = \frac{(Weight\ lost\ during\ extraction)}{(Weight\ of\ original\ specimen)}$$

$$Extract,(\%) = \frac{(W3 - W4)}{(W2 - W1)} \times 100$$

$$Gel\ Content,(\%) = 100 - percent\ extract$$

where:

*W1* = weight of the pouch (sealed on three sides, one side open),

*W2* = weight of the specimen and the pouch (sealed on three sides, one side open),

*W3* = weight of the specimen and the cage, after being stapled shut, and

*W4* = weight of the specimen and the cage after extraction and drying.

The average results obtained from the two cages were taken as the gel content of the blends (see Appendix A3-1). The insoluble gels were recovered

from the stainless steel mesh cage for further characterisation by DSC and FTIR as described in Sections 3.5.1 and 3.5.3 respectively.

**b.) Sol Analysis**

After the first extraction process, 100 ml of the solution was transferred to a new round bottomed flask. 100 ml of methanol was added to the solution for precipitation of the dissolved PE. The solution with precipitate was filtered and rinsed thoroughly with another 50 ml of xylene:methanol (1:1) mixture. The recovered precipitates and solution were further characterised using FTIR as described in Section 3.5.3.

# CHAPTER 4

# RESULTS AND DISCUSSION

# EVALUATION OF COMPATIBILISERS AND BLENDS

In this chapter the properties of blends based on HDPE and a range of engineering thermoplastics (ABS, PC, PBT, PA6), prepared by injection moulding, were investigated. Five different types of compatibilisers namely, EVA, EMA, E-GMA, E-MA-GMA and HDPE-g-MAH, were evaluated with respect to their efficiencies in compatibilising HDPE with the four engineering polymers. The pre-compounded HDPE/compatibiliser binary blends of 2 different blend ratios (1:1 and 3:1) were first investigated for their blend miscibility by thermal analysis. These binary blends were then injection moulded at 15 wt% with the engineering polymers for the characterisation of mechanical, thermal and morphological properties.

## 4.1 Thermal Analysis of HDPE/Compatibiliser Blends

The DSC results of HDPE blends with EVA, EMA, E-GMA, E-MA-GMA and HDPE-g-MAH at blending ratios of 1:1 and 3:1 are summarised in Table 4.1. All DSC traces are presented in Figure 4.1 and Appendices A1-1 to A1-6.

It is evident from Table 4.1 and the DSC traces of Figure 4.1 that the melting point of compatibiliser and HDPE phases remained relatively unchanged across the blends indicating the lack of miscibility between the crystalline phases of the HDPE and the compatibilisers (except for the HDPE/HDPE-g-MAH blends whereby both components have similar melting points and are considered to be miscible). Similarly, Haghighat [157] observed no detectable shift in melting point of LDPE phase in EVA/LDPE blends which he suggested to be due to the lack of interaction between the EVA and LDPE.

However, the lack of miscibility between the crystalline phases does not necessarily imply total immiscibility and or incompatibility between the blends. Since all the compatibiliser copolymers contained ethylene segments,

miscibility of the blends may have occurred in the amorphous regions which are normally manifested by changes in Tg of the blend components. Ray and Khastgir [191] reported the co-existence of miscibility in amorphous regions of LDPE and EVA blends with the presence of individual immiscible crystalline zones. Through the use of DMA, the authors observed changes in Tg of the blends with composition according to the Fox and Gordon-Taylor relations which indicate miscibility and were supported by evidence of co-continuous morphology.

**Table 4.1 Thermal analysis of HDPE phase in HDPE/EVA, HDPE/EMA, HDPE/E-GMA, HDPE/E-MA-GMA, and HDPE/HDPE-g-MAH blends**

| Sample Code | HDPE Phase | | | | | |
|---|---|---|---|---|---|---|
| | Tm (℃) | ΔHf (J/g) | $X_c$ (%) | $TC_{Onset}$ (℃) | $TC_{Peak}$ (℃) | ΔTC (℃) |
| **HDPE** | **130** *(1)* | **189.8**[a]*(0.4)* | **65** *(0)* | **118** *(0)* | **116** *(0)* | **2** |
| **EV1** | **129** *(0)* | **199.7**[b]*(3.4)* | **68** *(1)* | **118** *(0)* | **116** *(0)* | **2** |
| **EV2** | **130** *(1)* | **198.2**[b]*(2.7)* | **68** *(1)* | **118** *(1)* | **116** *(0)* | **2** |
| **EM1** | **129** *(0)* | **192.8**[b]*(0.8)* | **66** *(0)* | **118** *(0)* | **116** *(0)* | **2** |
| **EM2** | **130** *(0)* | **191.3**[b]*(3.0)* | **65** *(1)* | **118** *(0)* | **116** *(0)* | **2** |
| **EG1** | **130** *(0)* | **181.8**[b]*(1.4)* | **62** *(0)* | **118** *(0)* | **116** *(0)* | **2** |
| **EG2** | **130** *(0)* | **189.4**[b]*(2.1)* | **65** *(1)* | **118** *(0)* | **117** *(0)* | **1** |
| **MG1** | **130** *(1)* | **194.2**[b]*(3.5)* | **66** *(2)* | **118** *(0)* | **116** *(1)* | **2** |
| **MG2** | **130** *(0)* | **196.0**[b]*(3.4)* | **67** *(1)* | **118** *(0)* | **116** *(0)* | **2** |
| **HM1** | **129** *(0)* | **186.6**[a]*(1.8)* | **64** *(1)* | **119** *(0)* | **117** *(1)* | **2** |
| **HM2** | **130** *(0)* | **197.8**[a]*(1.4)* | **68** *(1)* | **119** *(0)* | **118** *(1)* | **1** |

*Values in parentheses denote standard deviations*
[a] *Values normalised to the total amount of the blend or resin*
[b] *Values normalised to the amount of the relevant phase*

Since DSC is not a suitable technique for measurement of Tg [147] and also due to the lack of cooling capability to below -100℃ of the current DSC instrument used in this study, the degree of miscibility/compatibility at the amorphous regions of the HDPE/compatibiliser blends could not be verified.

Other than EV1, EV2 and EG1 blends, the presence of compatibilisers in the HDPE/compatibiliser binary blends did not cause significant changes to the degree of crystallinity of the HDPE phases. The degree of crystallinity of the HDPE phases in the blends of EV1 and EV2, were increased by the addition of EVA compatibiliser. It is believed that in blends of crystallisable component (HDPE) with miscible amorphous polymer (of EVA), the inter-lamellar region (which contains the amorphous fraction) will be obviously increased which yield additional mobility to the crystallisable species and thus allow for a higher fraction of this species in the crystalline phase [192]. In comparison with other compatibilisers, the E-GMA compatibiliser caused disruption to the crystallinity of the HDPE phase at high compatibiliser dosage (sample EG1) which may imply slightly better miscibility of this compatibiliser with HDPE in the crystalline phase.

The crystallisation behaviours of the binary blends obtained from non-isothermal DSC crystallisation traces are presented in Table 4.1. The overall rate of cystallisation of the HDPE phase of the all binary blends represented by the parameter ($TC_{onset}$ – $TC_{peak}$) [193] were relatively unchanged in the presence of compatibilisers irrespective of the type and quantity. This further justifies the lack of miscibility between the crystalline phase of the HDPE and the EVA, EMA, E-GMA and E-MA-GMA compatibilisers. However, the presence of MAH moiety in HM1 and HM2 blends seems to have slight nucleating effect on the HDPE phase as indicated by the increased in onset and peak of crystallisation.

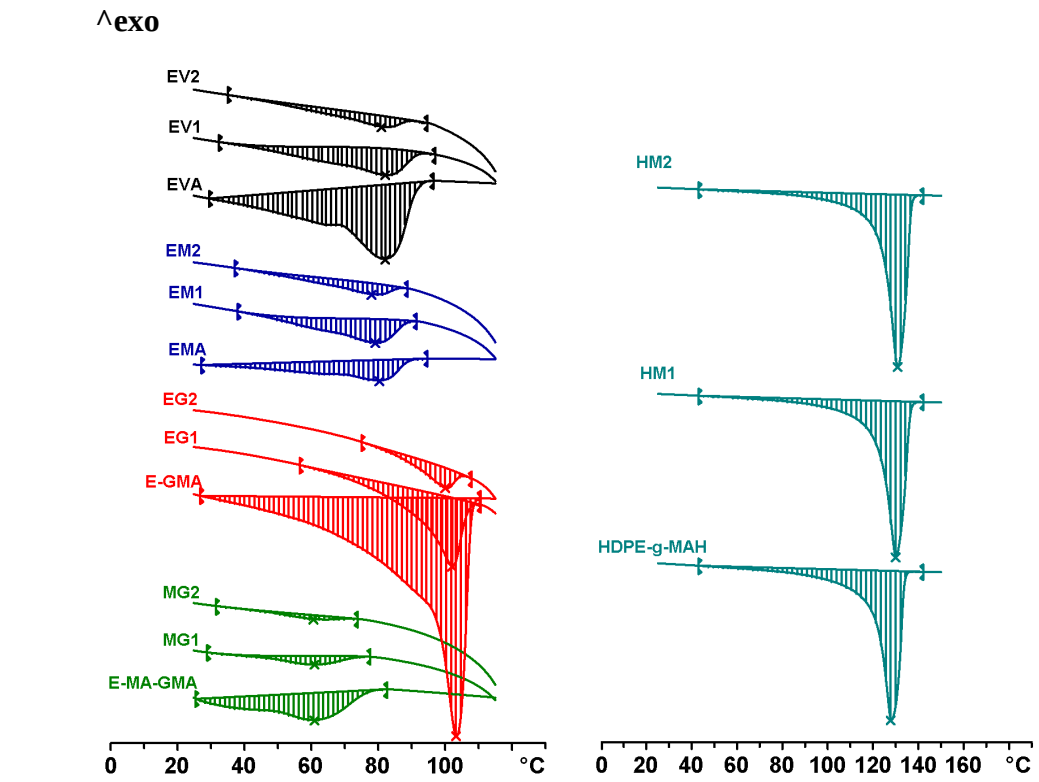


(a)

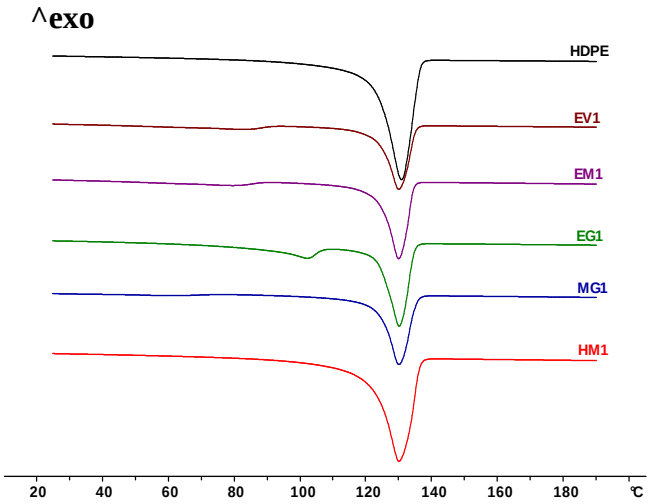


(b)

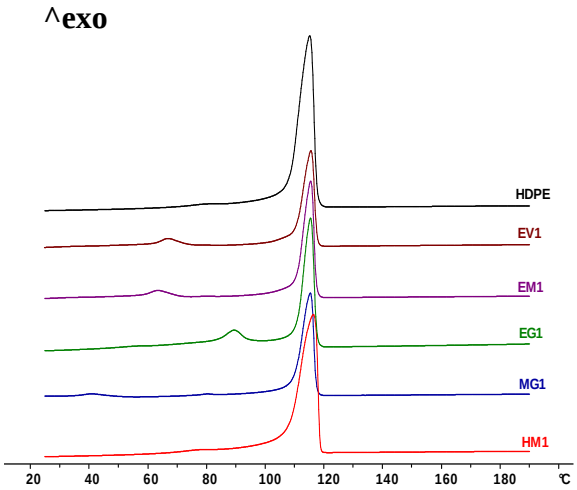


(c)

**Figure 4.1 DSC traces of (a) re-heat endotherms of compatibilisers before and after blending with HDPE, (b) re-heat endotherms of HDPE before and after blending at 1:1 ratio with compatibilisers, and (c) cooling of HDPE/compabiliser blends at 1:1 blend ratio**

## 4.2 Evaluation of ABS/HDPE Blends

### 4.2.1 Mechanical Properties of Blends

The mechanical properties of ABS, HDPE, binary blend of ABS/HDPE and ternary blends of ABS/(HDPE/compatibiliser) blends are presented in Table 4.2. Examples of stress-strain curves of the blends are presented in Appendices B1-1 to B1-2. The results show that the presence of HDPE at 15 wt% resulted in dramatic reduction in the ductility of the ABS which is demonstrated by the reduction in elongation at break and impact strengths (notched and reversed notch) of the blends which indicate poor interfacial adhesion between the ABS/HDPE phases.

The yield strength of the neat ABS was reduced by the addition of HDPE in ABS-H15 blend due to poor interfacial bonding. The HDPE phase which has lower yield strength than the neat ABS polymer could have also contributed to the lower yield strength of the uncompatibilised blend. It is also observed from Table 4.2 that the presence of compatibilisers irrespective of their chemical structure did not have significant influence of the yield strength of the blends. Therefore it will be difficult to discriminate between poor interfacial adhesion and the inherent weakness of the second component of a ABS/HDPE blends by the use of tensile yield strength. The elongation at yield of the uncompatibilised ABS/HDPE blend remained relatively unchanged from the neat ABS polymer indicating that it is not sensitive to blend component adhesion strength. Slight increased in elongation at yield of some compatibilised blends are likely due to the contribution of the elastomeric nature of the various compatibilisers. On the other hand, the elongation at break was dramatically reduced in the same blends.

In order to have a clearer overview of the effectiveness of the compatibilisers in the ABS/HDPE blends, the Izod impact strength (notched and reversed notch) and elongation at break of these blends are normalised to 100% based on data of neat ABS as shown in Figure 4.2. For uncompatibilised ABS/HDPE blend, the notched, and reversed notch impact strength and elongation at

break were reduced to 20%, 7% and 11% respectively of the neat ABS polymer. All the compatibilisers studied except E-MA-GMA, were ineffective in improving these properties significantly at either high or low compatibiliser concentration levels. This could be due to the disruption of the original rubber toughening mechanism of the neat ABS polymer by the presence of a much larger HDPE dispersed phase. The toughness of polymer blends are strongly influenced by the size of the dispersed phase domains. Blends will normally become brittle if the sizes of the dispersed domains are larger than the critical diameter [189].

**Table 4.2 Mechanical properties of ABS, HDPE, binary ABS/HDPE and ternary ABS/(HDPE/compatibiliser) blends**

| Sample Code | *Izod Impact Strength* | | *Tensile Properties* | | |
|---|---|---|---|---|---|
| | **Notched (J/m)** | **Reversed notch (J/m)** | **Elongation @ Break (%)** | **Elongation @ Yield (%)** | **Strength @ Yield (MPa)** |
| **ABS** | **231** *(6)* | **1628** *(271)* | **28** *(2)* | **3** *(0)* | **38** *(0)* |
| **HDPE** | **29** *(1)* | **-** | **191** *(6)* | **11** *(0)* | **23** *(0)* |
| **ABS-H15** | **47** *(5)* | **113** *(7)* | **3** *(0)* | **3** *(0)* | **29** *(0)* |
| **ABS -EV1** | **72** *(5)* | **214** *(11)* | **3** *(0)* | **3** *(0)* | **27** *(0)* |
| **ABS -EV2** | **64** *(5)* | **179** *(16)* | **3** *(0)* | **3** *(0)* | **31** *(0)* |
| **ABS -EM1** | **81** *(4)* | **251** *(11)* | **4** *(0)* | **3** *(0)* | **29** *(1)* |
| **ABS -EM2** | **66** *(5)* | **187** *(12)* | **3** *(0)* | **3** *(0)* | **30** *(0)* |
| **ABS -EG1** | **70** *(3)* | **248** *(30)* | **3** *(0)* | **3** *(0)* | **33** *(1)* |
| **ABS -EG2** | **59** *(5)* | **184** *(26)* | **4** *(0)* | **3** *(0)* | **32** *(0)* |
| **ABS -MG1** | **119** *(8)* | **1105** *(276)* | **6** *(1)* | **3** *(0)* | **28** *(0)* |
| **ABS -MG2** | **66** *(3)* | **218** *(14)* | **4** *(0)* | **3** *(0)* | **30** *(0)* |
| **ABS -HM1** | **62** *(6)* | **167** *(9)* | **4** *(0)* | **3** *(0)* | **35** *(0)* |
| **ABS -HM2** | **56** *(8)* | **132** *(6)* | **3** *(0)* | **3** *(0)* | **31** *(0)* |

*Values in parentheses denote standard deviations*

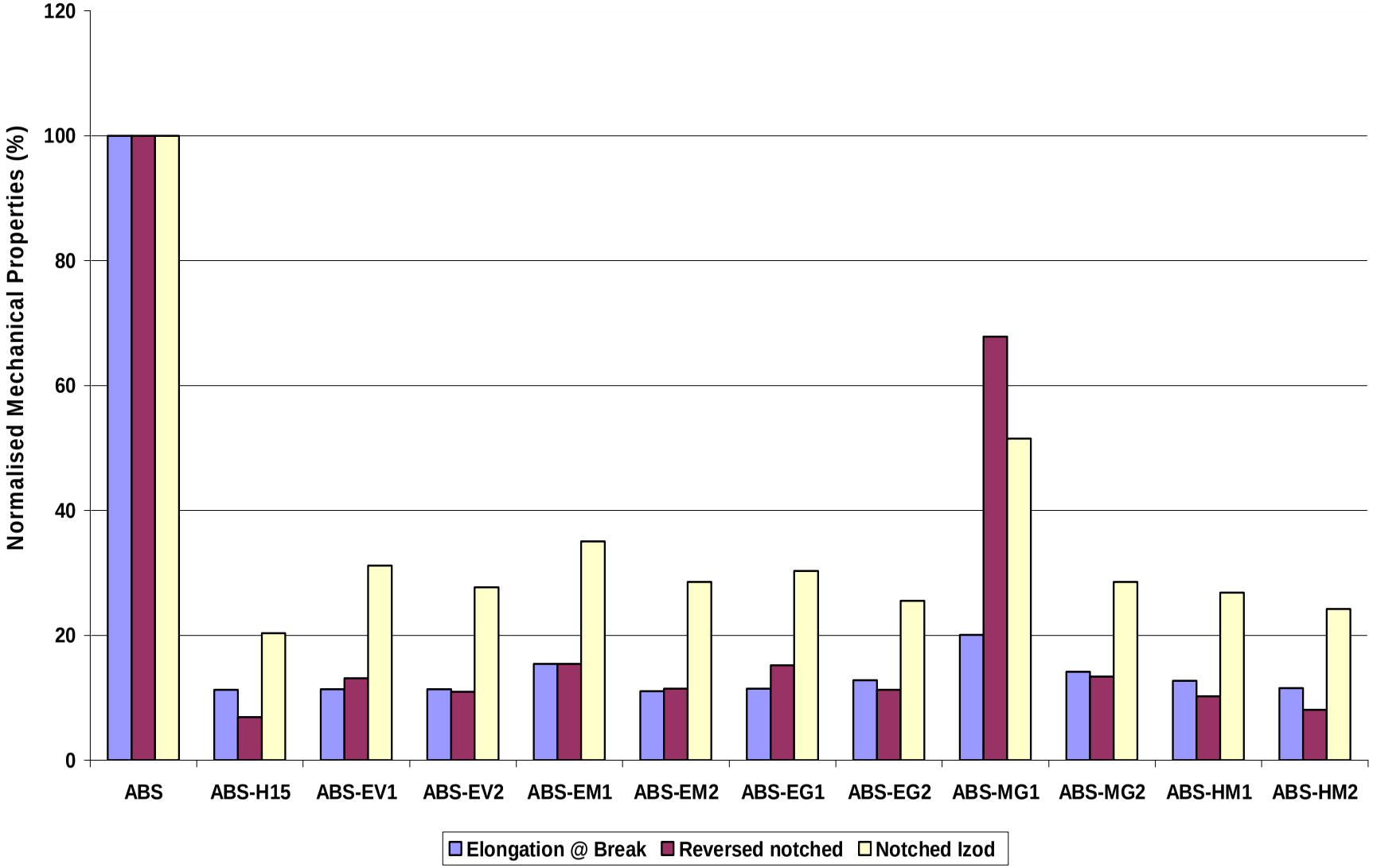


**Figure 4.2 Mechanical properties of uncompatibilised and compatibilised ABS/HDPE blends**

Figure 4.2 shows that E-MA-GMA has the best overall performance with notched, and reversed notch impact strength and elongation at break of ABS-MG1 blend at 52%, 68%, and 20% of ABS respectively at high compatibiliser concentration. The presence of methyl acrylate (MA) and glycidyl methacrylate (GMA) in E-MA-GMA has probably reduced the miscibility of the E-MA-GMA with the HDPE rendering it more efficient in diffusing to the ABS/HDPE interphases as compared with EMA and E-GMA when used alone. Improvement in interfacial adhesion is evident by the improvement of elongation at break of the ABS-MG1 blend. The mechanism of compatibilisation could possibly be due to the reaction of epoxides from the GMA with the nitrile moiety of the SAN in ABS to form oxazoline linkage as follows [194]:

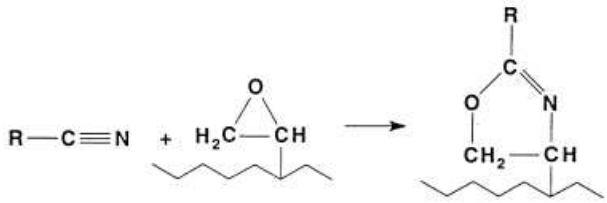


### 4.2.2 Thermal Analysis of Blends

Table 4.3 summarises the thermal properties of ABS/HDPE blends obtained from non-isothermal DSC experiments and representative DSC traces of these blends are presented in Figure 4.3 and Appendices A1-7 to A1-10. The presence of a melting peak at around 144℃ of the ABS sample in Figure 4.3 is contributed by ethylene bis stearamide (EBS) wax which is commonly added as lubricant during the production of ABS resin (see Appendix C1-1). Since a portion of this EBS melting peak overlapped those of HDPE, the heat of fusion which is contributed by the EBS was subtracted from the total heat of fusion of the combined peaks of ABS/HDPE blends.

From Table 4.3, a significant reduction in the degree of crystallinity of the HDPE dispersed phase is observed in all compatibilised and uncompatibilised blends. As the crystallisation of dispersed HDPE phases took place in the presence of solidified ABS matrix, the decrease in crystallinity could be resulted from the limitations on the growth process of the polyethylene due to the presence of the solidified ABS. In most polymer blends, the degree of

crystallinity of the crystallising polymer component is generally reduced because of the presence of a second component [195]. Aref-Azar et al [196] reported a decrease in the degree of crystallinity of polyethylene with increasing polystyrene contents in PE/PS blends. The authors postulated that the crystallisation behaviour of the PE dispersed phase is dependent on the size and number of dispersed particles and in particular on the nucleation density. When the number of dispersed particles exceeded that of heterogeneous nuclei, larger supercoolings likely to be due to homogenous nucleation are required for crystallisation to develop further i.e. the phenomenon of "fractionated crystallisation" is occurring [148-152].

**Table 4.3 Thermal analysis of ABS, HDPE, binary ABS/HDPE and ternary ABS/(HDPE/compatibiliser) blends**

| Sample Code | ABS | HDPE Phase | | |
|---|---|---|---|---|
| | Tg (℃) | Tm (℃) | ∆Hf (J/g) | $X_c$ (%) |
| **ABS** | **101** *(1)* | - | - | - |
| **HDPE** | - | **130** *(1)* | **189.8**[a] *(0.4)* | **65** *(0)* |
| **ABS-H15** | **100** *(1)* | **131** *(0)* | **162.7**[b] *(4.5)* | **56** *(2)* |
| **ABS-EV1** | **100** *(1)* | **130** *(0)* | **152.5**[b] *(10.1)* | **52** *(3)* |
| **ABS-EV2** | **102** *(1)* | **129** *(0)* | **121.9**[b] *(6.9)* | **42** *(2)* |
| **ABS-EM1** | **101** *(0)* | **129** *(0)* | **131.7**[b] *(2.1)* | **45** *(1)* |
| **ABS-EM2** | **101** *(1)* | **130** *(0)* | **145.6**[b] *(5.7)* | **50** *(2)* |
| **ABS-EG1** | **105** *(1)* | **130** *(0)* | **132.0**[b] *(9.2)* | **45** *(3)* |
| **ABS-EG2** | **104** *(0)* | **130** *(0)* | **135.8**[b] *(2.6)* | **46** *(1)* |
| **ABS-MG1** | **102** *(1)* | **129** *(0)* | **120.8**[b] *(1.7)* | **41** *(1)* |
| **ABS-MG2** | **101** *(1)* | **130** *(0)* | **124.7**[b] *(1.8)* | **43** *(1)* |
| **ABS-HM1** | **100** *(1)* | **130** *(0)* | **126.4**[b] *(3.5)* | **43** *(1)* |
| **ABS-HM2** | **101** *(1)* | **131** *(0)* | **152.7**[b] *(3.7)* | **52** *(1)* |

*Values in parentheses denote standard deviations*
[a] *Values normalised to the total amount of the blend or resin*
[b] *Values normalised to the amount of the relevant phase*

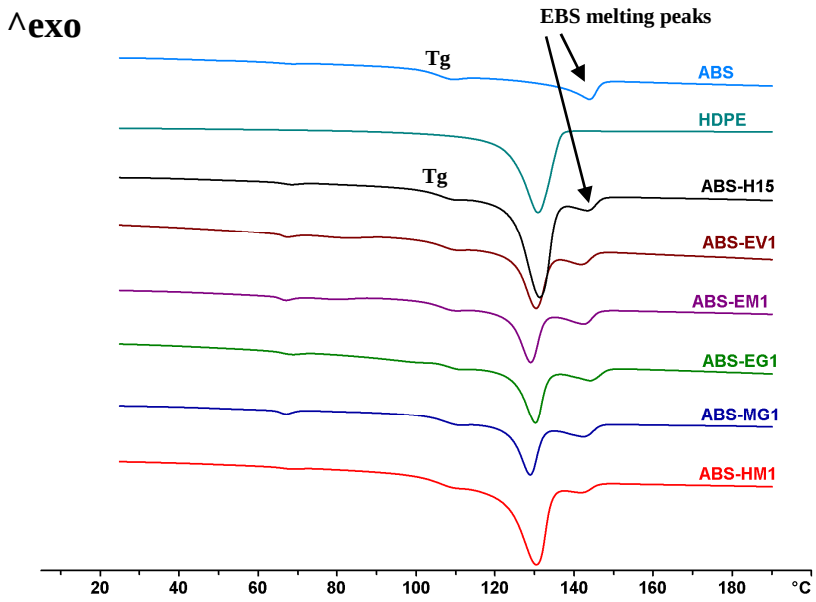


(a)

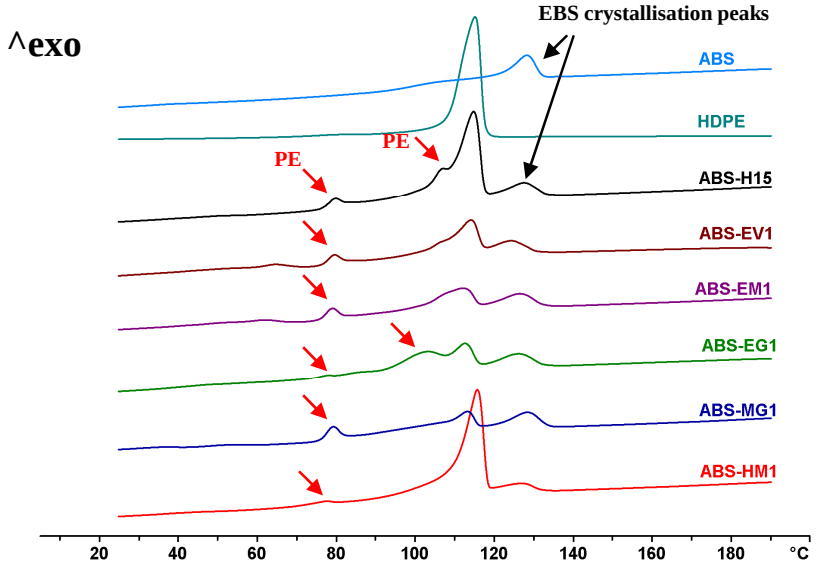


(b)

**Figure 4.3 DSC traces of ABS, HDPE, uncompatibilised and compatibilised ABS/HDPE blends (a) second heating and (b) cooling**

The observation of multiple crystallisation peaks during non-isothermal cooling of both compatibilised and uncompatibilised ABS/HDPE blends in Figure 4.3 (b) support the occurrence of fractionated crystallisation of the HDPE dispersed phases in the ABS matrix.

Of all the blends, only ABS-EM1 and ABS-MG1 are observed to have greater melting point depression of the HDPE phase indicating possible interactions with the ABS matrix. This is supported by earlier observation of improvements in toughness and interfacial adhesion of these blends as seen from Izod impact strength and elongation at break respectively. On the other hand, the Tg of ABS in all (except ABS-EG1 and ABS-EG2) blends remain relatively unchanged. The slight increase in Tg of ABS-EG1 and ABS-EG2 may imply possible interactions between the phases.

### 4.2.3 Morphology of Blends

The micrographs of uncompatibilised and compatibilised ABS/HDPE blends are presented in Figures 4.4 and 4.5. As shown in Figure 4.4, the uncompatibilised ABS-H15 blend exhibits two distinct phases with clear boundaries between the two phases. Many extremely small and intermediate sized dispersed phases are also observed. This observation justifies the occurrence of fractionated crystallisation whereby the small dispersed particles are crystallised via homogenous nucleation.

With the presence of EVA and EMA compatibilisers, the dispersed phase remained distinct but appear to have a rougher surface which is accompanied by the reduction in particle size implying possible interactions between the phases. The interfacial boundary of blends containing E-GMA at high concentration (ABS-EG1) become less distinct with further reduction in dispersed particle sizes suggesting some interactions between the phases. The presence of this interaction is supported by an increased in the Tg of the ABS and a small improvement in notched impact strength.

On the other hand, the blend containing a high concentration of E-MA-GMA (ABS-MG1) appears to have very fine morphology with blurred interphases

and ductile failure surface. This observation is supported by the improvement in ductility of the blend and melting point depression of the PE domains discussed earlier. However, coarsening of morphology with more distinctive phases occurred when the E-MA-GMA in the blend was reduced.

Blends compatibilised with HDPE-g-MAH have sharp interfacial morphology with irregularly shaped HDPE domains sitting loosely in the cavities of the ABS matrix. This could be due to considerable volume contraction of the HDPE domains after crystallisation has occurred. This lack of interfacial adhesion contributed to the poor mechanical properties of the blends.

### 4.2.4 Summary

Based on mechanical testing performed on the blends, the compatibilising effectiveness of the blends are ranked in descending order of values for notched and reversed notch Izod impact strengths, and elongation at break as follows:

| **Notched Izod impact Strength:** | **Reverse notched Izod impact Strength:** |
|---|---|
| 1. ABS-**MG1** (119 J/m) | 1. ABS-**MG1** (1105 J/m) |
| 2. ABS-**EM1** (81 J/m) | 2. ABS-**EM1** (251 J/m) |
| 3. ABS-**EV1** (72 J/m) | 3. ABS-**EG1** (248 J/m) |

**Elongation at break:**

1. ABS-**MG1** (5.5 %)
2. ABS-**EM1** (4.3 %)
3. ABS-**MG2** (3.9 %)

The results show that ABS/HDPE blends are best compatibilised with E-MA-GMA which has the best overall performance in terms of mechanical properties. This is further justified by observation of fine blend morphology from SEM and also evidences of melting point depression and reduction in degree of crystallinity in the HDPE components of the blends from DSC.

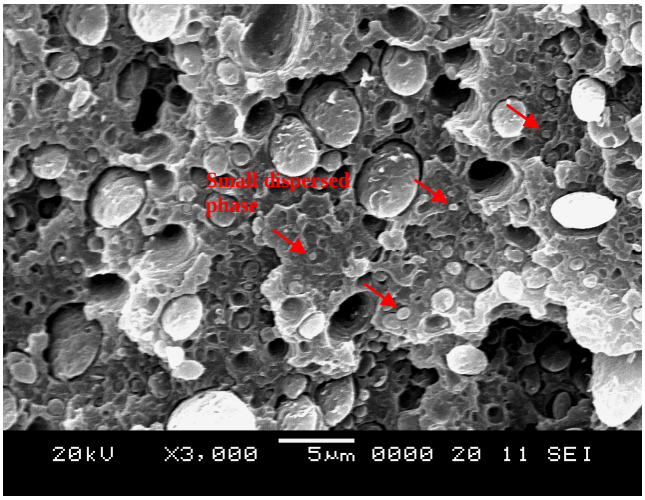


**ABS-H15**

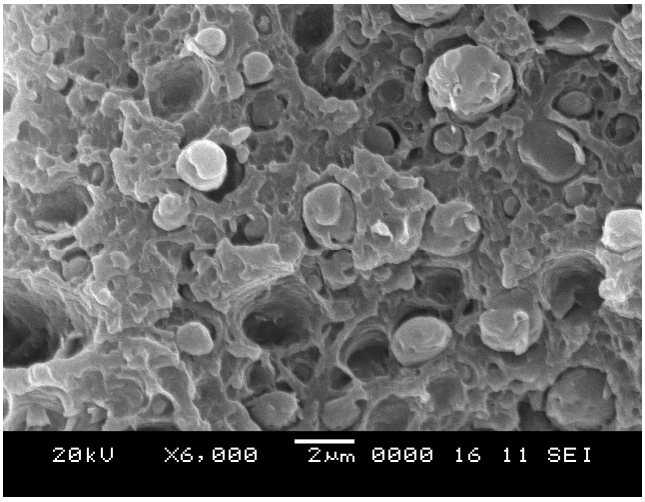


**ABS-EV1**

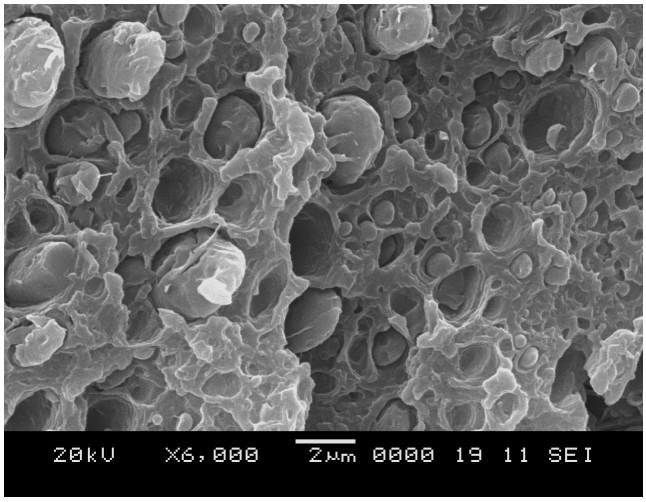


**ABS-EV2**

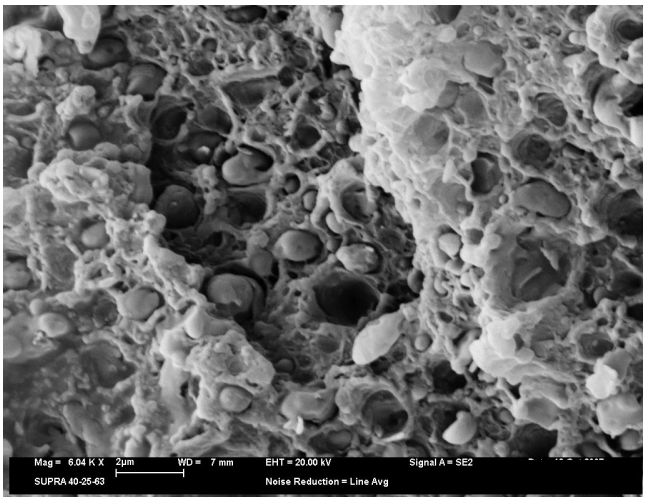


**ABS-EM1**

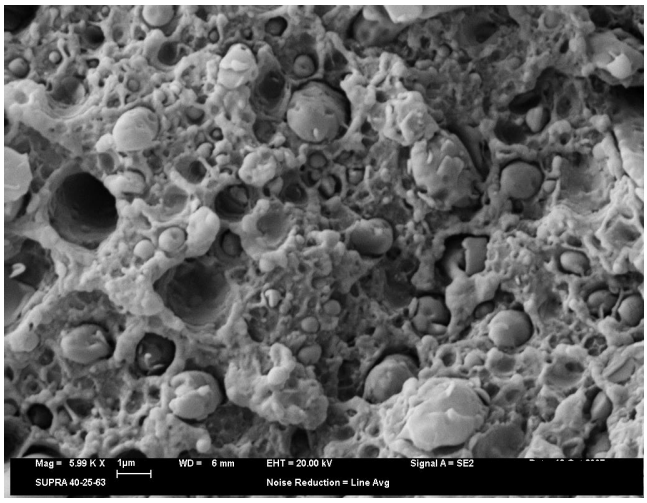


**ABS-EM2**

**Figure 4.4 SEM morphology of uncompatibilised, EVA and EMA compatibilised ABS/HDPE blends**

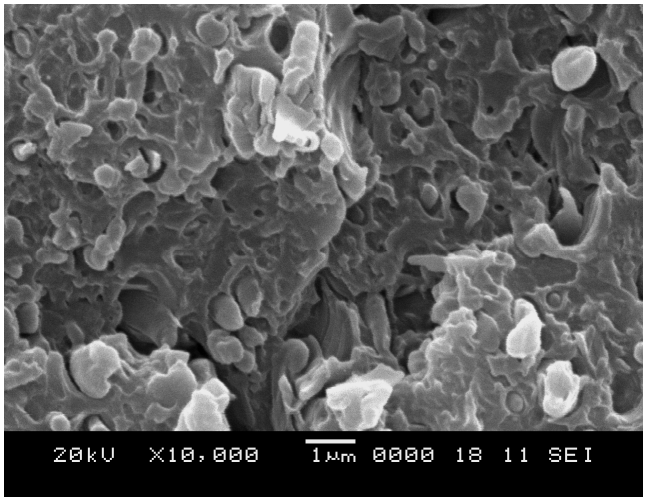


ABS-EG1

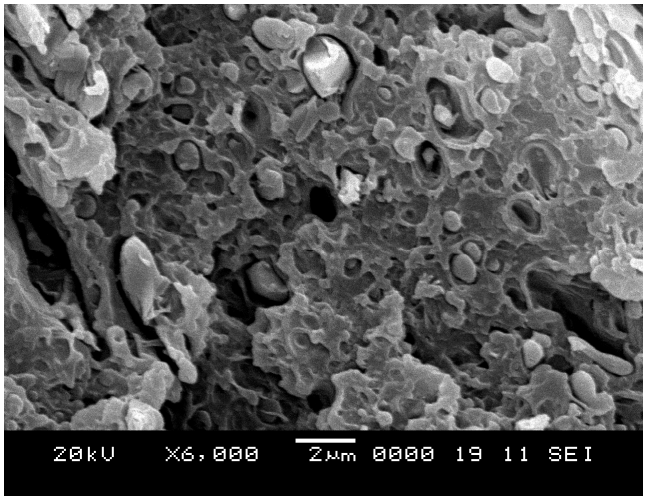


ABS-EG2

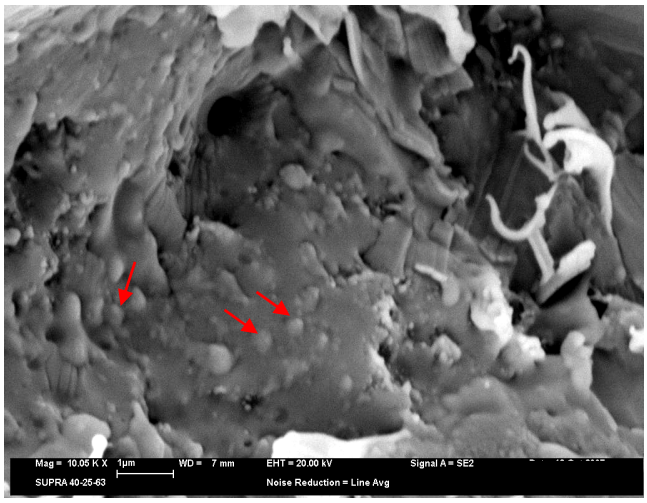


ABS-MG1

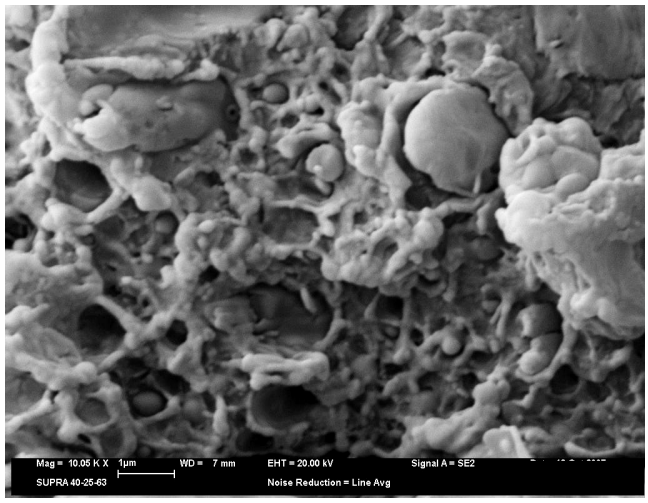


ABS-MG2

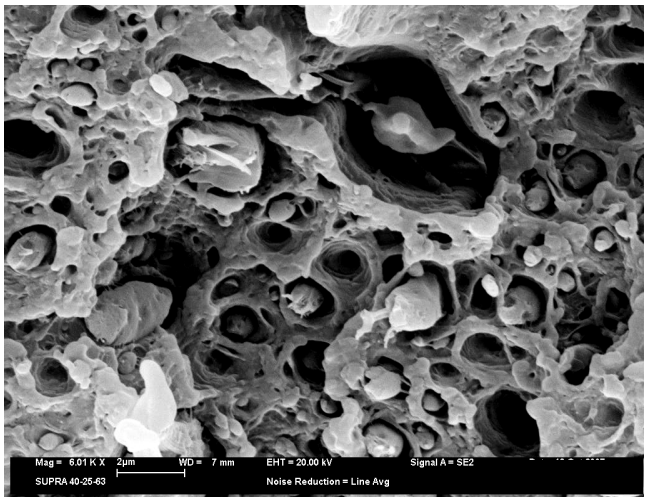


ABS-HM1

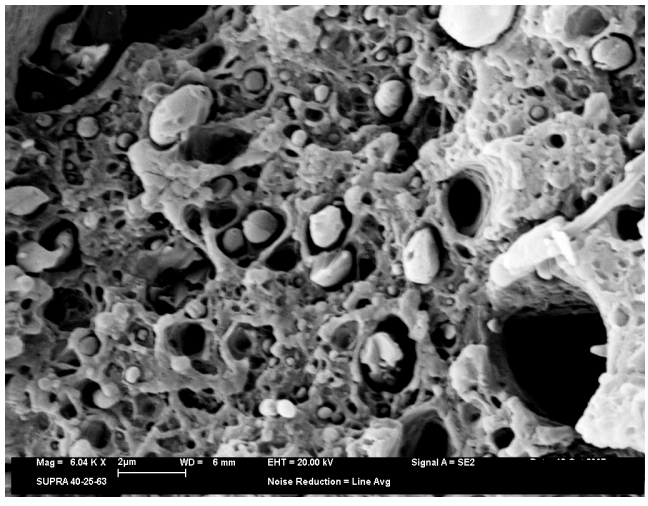


ABS-HM2

**Figure 4.5 SEM morphology of E-GMA, E-MA-GMA and HDPE-g-MAH compatibilised ABS/HDPE blends**

## 4.3 Evaluation of PC/HDPE Blends

### 4.3.1 Mechanical Properties of Blends

The mechanical properties of uncompatibilised and compatibilised PC/HDPE blends are summarised in Table 4.4 and examples of stress-strain curves of the blends are presented in Appendices B1-3 to B1-4. The Izod impact strength (notched and reversed notch) and elongation at break of these blends are normalised to 100% based on data of neat PC as presented in Figure 4.6 The addition of HDPE dramatically reduces the elongation at break and notched/reversed notch impact strength of the neat PC suggesting no interfacial adhesion at the PC/HDPE boundaries [123]. The elongation at yield of both uncompatibilised and compatibilised blends PC/HDPE remained relatively unchanged from the neat PC polymer indicating its insensitivity in detecting interfacial changes of the blends. The tensile strength at yield of the uncompatibilised blend, PC-H15, was reduced with the addition of HDPE and show no improvement even with the addition of compatibilisers. This is presumably due to the vast difference between the yield strength of neat PC and HDPE whereby the presence of interfacial adhesion is not sufficient to bring about dramatic improvement in the yield strength of the blends.

Figure 4.6 shows that all compatibilisers evaluated are efficient in improving the interfacial bonding between the PC and HDPE interface as indicated by the increase in elongation at break of the compatibilised blends. All compatibilisers except HDPE-g-MAH (PC-HM1), were able to impart substantial interfacial adhesion to the phases rendering the elongation at break of these compatibilised blends greater than that of the neat PC polymer. PC-EG2 has the greatest improvement in elongation at break but has surprisingly lower notched Izod impact strength than the uncompatibilised blend which suggest that good interfacial adhesion alone is not sufficient in improving the the Izod impact strength of the blends. On the other hand, all compatibilisers have insignificant influence on both notched and reversed notch impact toughness of the blends. In their work Kunori and Geil [123, 124] observed that in blends of PC/HDPE, the uncompatibilised HDPE dispersed

phase crystallised after the solidification of PC matrix creating gaps between the phase boundaries of the blends due to substantial volume contraction of the HDPE phase. They postulated that such morphologies are mechanically equivalent to a foamed matrix. In this study, the addition of HDPE in the PC matrix resulted in the transformation of ductile failure of the neat PC to brittle failure of the blends. The brittle behaviour remained consistent even with the addition of compatibilised HDPE as they are possibly having similar foam morphology due to the fact that interfacial adhesion at the phase boundaries were unable to prevent huge volume contractions of the compatibilised HDPE phases.

**Table 4.4 Mechanical properties of PC, binary PC/HDPE and ternary PC/(HDPE/compatibiliser) blends**

| Sample Code | *Izod Impact Strength* | | *Tensile Properties* | | |
|---|---|---|---|---|---|
| | **Notched (J/m)** | **Reversed notch (J/m)** | **Elongation @ Break (%)** | **Elongation @ Yield (%)** | **Strength @ Yield (MPa)** |
| **PC** | **728** *(33)* | **3036** *(186)* | **123** *(4)* | **7** *(0)* | **59** *(0)* |
| **HDPE** | **29** *(1)* | **-** | **191** *(6)* | **11** *(0)* | **23** *(0)* |
| **PC -H15** | **535** *(22)* | **2411** *(108)* | **56** *(16)* | **7** *(0)* | **49** *(1)* |
| **PC -EV1** | **553** *(12)* | **2356** *(165)* | **141** *(6)* | **7** *(0)* | **44** *(0)* |
| **PC -EV2** | **489** *(11)* | **2361** *(178)* | **136** *(9)* | **7** *(0)* | **46** *(0)* |
| **PC -EM1** | **584** *(21)* | **2341** *(82)* | **168** *(12)* | **7** *(0)* | **46** *(0)* |
| **PC -EM2** | **506** *(8)* | **2456** *(115)* | **88** *(23)* | **7** *(0)* | **45** *(0)* |
| **PC -EG1** | **524** *(13)* | **2558** *(199)* | **150** *(17)* | **7** *(0)* | **44** *(0)* |
| **PC -EG2** | **493** *(17)* | **2527** *(154)* | **213** *(19)* | **7** *(0)* | **46** *(1)* |
| **PC -MG1** | **611** *(16)* | **2394** *(149)* | **152** *(8)* | **7** *(0)* | **43** *(0)* |
| **PC -MG2** | **549** *(14)* | **2380** *(140)* | **140** *(14)* | **7** *(0)* | **44** *(1)* |
| **PC -HM1** | **478** *(26)* | **2467** *(135)* | **53** *(4)* | **7** *(0)* | **48** *(0)* |
| **PC -HM2** | **502** *(24)* | **2359** *(92)* | **102** *(1)* | **7** *(0)* | **48** *(0)* |

*Values in parentheses denote standard deviations*

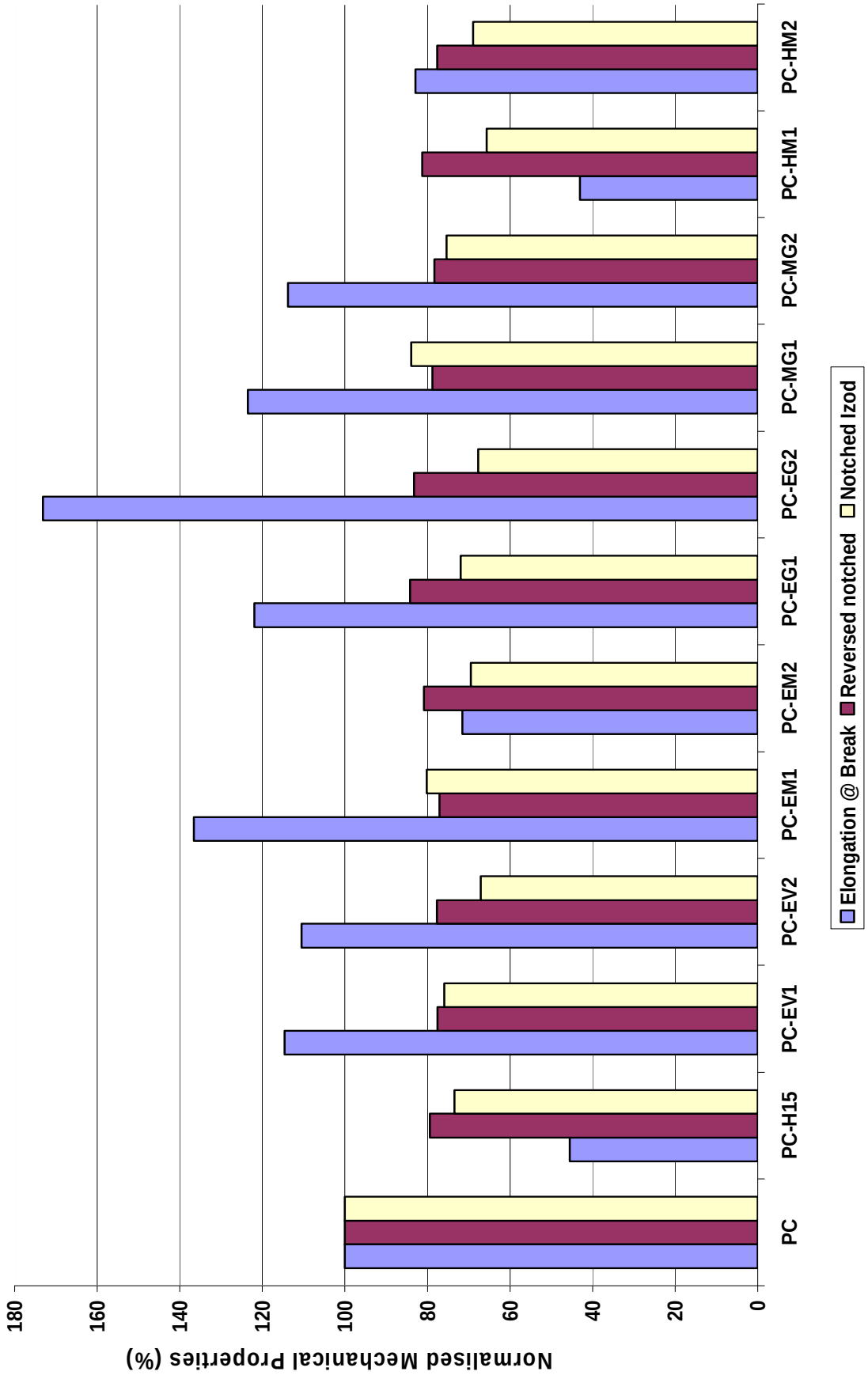


Figure 4.6 Mechanical properties of uncompatibilised and compatibilised PC/HDPE blends

### 4.3.2 Thermal Analysis of Blends

Table 4.5 summarises the thermal properties of PC/HDPE blends obtained from non-isothermal DSC experiments and representative DSC traces of these blends are presented in Figure 4.7 and Appendices A1-11 to A1-14.

**Table 4.5 Thermal analysis of PC, HDPE, binary PC/HDPE and ternary PC/(HDPE/compatibiliser) blends**

| Sample Code | PC | HDPE Phase | | |
|---|---|---|---|---|
| | Tg (℃) | Tm (℃) | ∆Hf (J/g) | $X_c$ (%) |
| **PC** | **143** *(1)* | - | - | - |
| **HDPE** | - | **130** *(1)* | **189.8**[a] *(0.4)* | **65** *(0)* |
| **PC-H15** | **145** *(1)* | **130** *(0)* | **158.9**[b] *(1.6)* | **54** *(1)* |
| **PC-EV1** | **144** *(0)* | **129** *(1)* | **156.0**[b] *(4.7)* | **53** *(2)* |
| **PC-EV2** | **145** *(1)* | **130** *(0)* | **160.6**[b] *(10.0)* | **55** *(3)* |
| **PC-EM1** | **145** *(1)* | **128** *(0)* | **129.8**[b] *(2.2)* | **44** *(1)* |
| **PC-EM2** | **145** *(1)* | **128** *(0)* | **168.3**[b] *(3.0)* | **57** *(1)* |
| **PC-EG1** | **145** *(1)* | **128** *(0)* | **156.8**[b] *(8.7)* | **54** *(3)* |
| **PC-EG2** | **145** *(1)* | **129** *(1)* | **184.2**[b]*(6.2)* | **63** *(2)* |
| **PC-MG1** | **144** *(1)* | **128** *(1)* | **154.4**[b] *(7.0)* | **53** *(2)* |
| **PC-MG2** | **145** *(1)* | **128** *(0)* | **155.6**[b] *(2.7)* | **53** *(1)* |
| **PC-HM1** | **145** *(1)* | **128** *(0)* | **164.8**[b] *(2.7)* | **56** *(1)* |
| **PC-HM2** | **144** *(1)* | **129** *(0)* | **167.5**[b] *(4.2)* | **57** *(1)* |

*Values in parentheses denote standard deviations*
[a] *Values normalised to the total amount of the blend or resin*
[b] *Values normalised to the amount of the relevant phase*

Similar to the ABS/HDPE blends, the degree of crystallinity of the HDPE phase is observed to be lowered when blended into the PC matrix. Similarly Yang and co-workers [122] observed that the crystallinity of HDPE in blends

of PC/HDPE decreased especially for blends with added compatibiliser, which they attributed to the interaction between the compatibiliser and the PC. However, in this study most of the compatibilisers have insignificant influence on the degree of crystallinity of the HDPE phase except for EMA (PC-EM1) and E-GMA (PC-EG2) compatibilised blends.

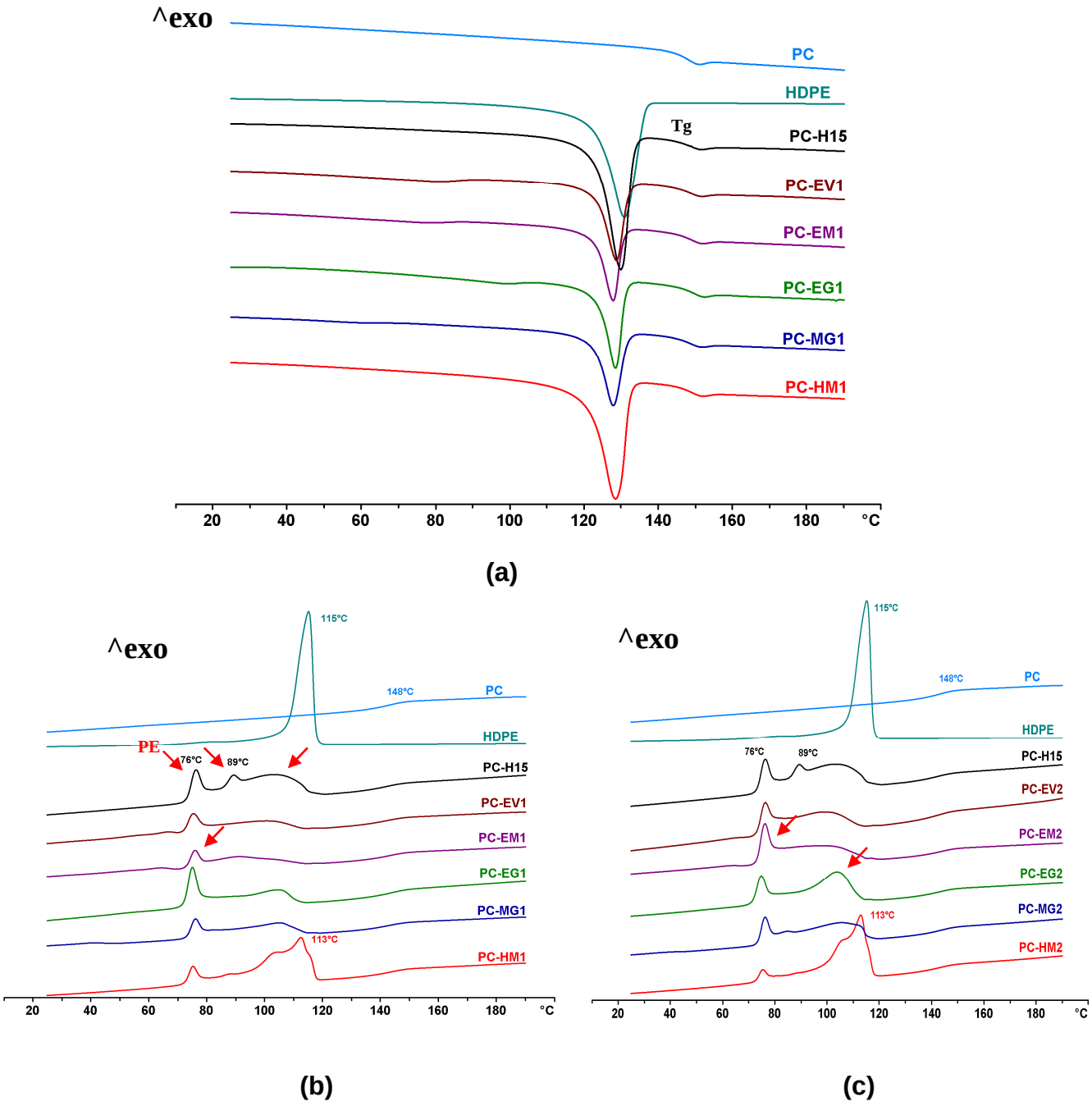


**Figure 4.7 DSC traces of PC, HDPE, uncompatibilised and compatibilised PC/HDPE blends (a) second heating and (b), (c) cooling**

The observation of multiple crystallisation peaks during non-isothermal cooling of both compatibilised and uncompatibilised PC/HDPE blends in Figure 4.7 (b) and (c) again suggests fractionated crystallisation of the HDPE dispersed phase in the PC matrix. Figure 4.7 (b) shows that PC-EM1 has a low enthalpy of crystallisation which mainly occurs after a large supercooling suggesting the crystallisation has occurred via homogenous nucleation. This explains the lower degree of crystallinity of PC-EM1 observed in Table 4.5. For PC-EG2 blends, a higher enthalpy of crystallisation was observed at smaller supercooling as shown in Figure 4.7 (c) indicating that crystallisation of HDPE occurred mainly via heterogeneous nucleation which contributed to the higher degree of crystallinity obtained.

Therefore, from the DSC non-isothermal crystallisation traces, it is believed that the reduction of crystallisation in both uncompatibilised and compatibilised blends is mainly due to the occurrence of fractionated crystallisation when the HDPE melt crystallises in the environment of a solidified PC matrix. Table 4.5 shows that the Tg of PC is slightly increased in the presence of HDPE phase for both uncompatibilised and compatibilised blends which is possibly due to a “filler effect” imparted by the HDPE domains that restricted some molecular motion. In general, a slight reduction in the melting point of the HDPE is observed in all blends. This could possibly be due to the presence of less perfect crystals during fractionated crystallisation of the HDPE domains of the blends.

### 4.3.3 Morphology of Blends

The micrographs of both uncompatibilised and compatibilised PC/HDPE blends are presented in Figures 4.8 and 4.9. Two distinct phases are again observed in uncompatibilised blends. The HDPE domains appeared to be located loosely in voids of PC matrix with no evidence of adhesion [123].

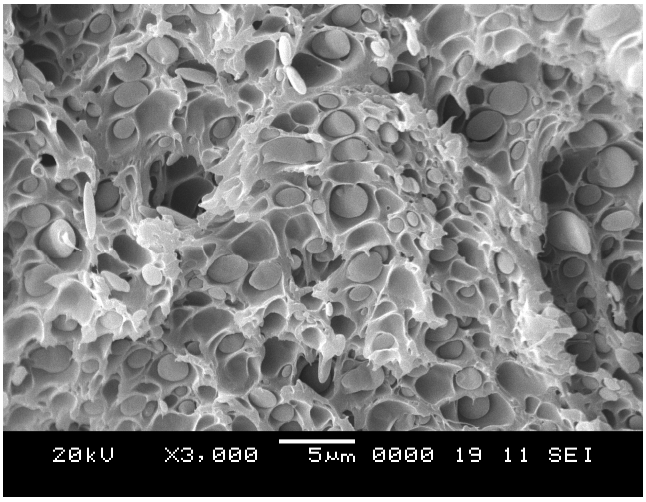


**PC-H15**

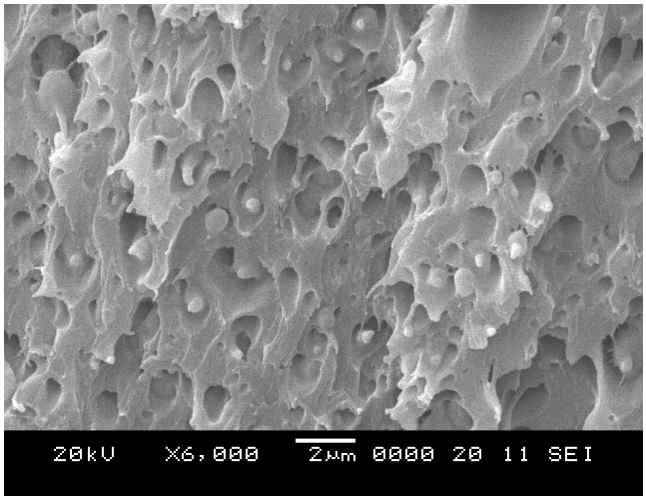


**PC-EV1**

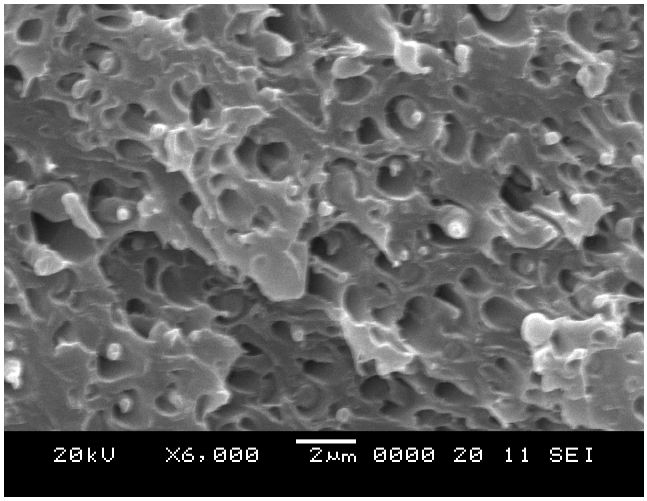


**PC-EV2**

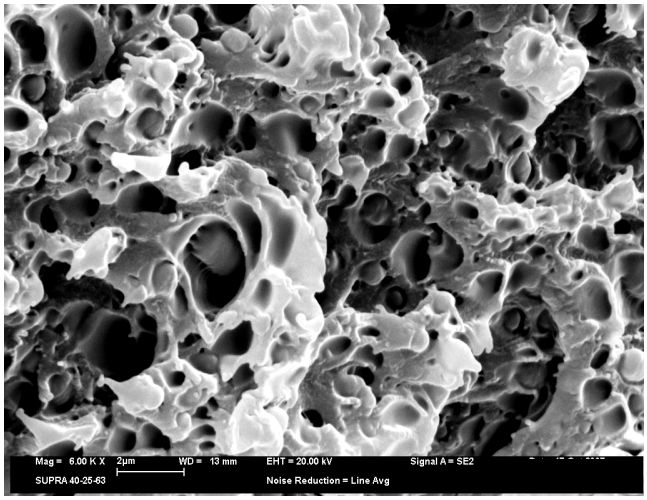


**PC-EM1**

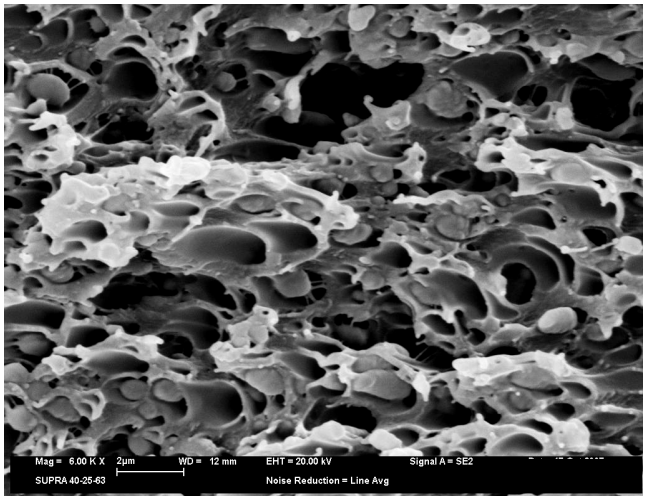


**PC-EM2**

**Figure 4.8 SEM morphology of uncompatibilised, EVA and EMA compatibilised PC/HDPE blends**

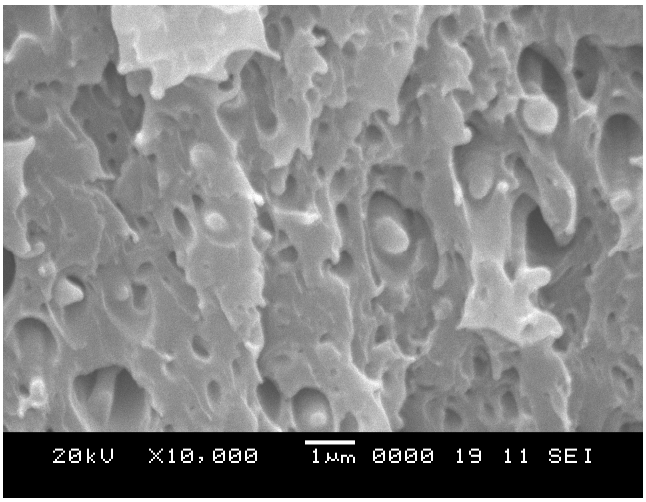


PC-EG1

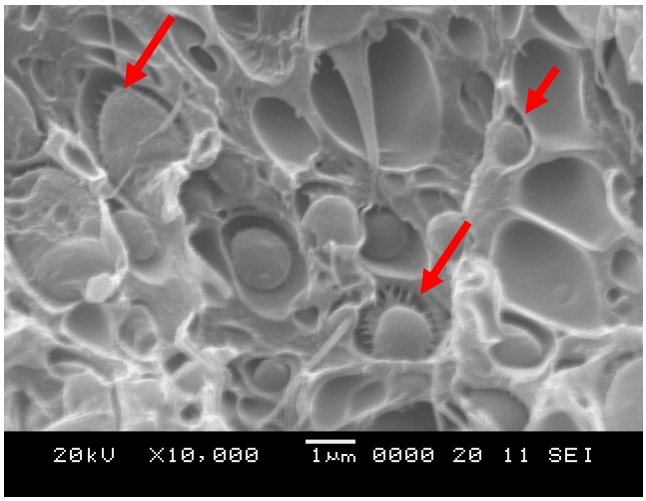


PC-EG2

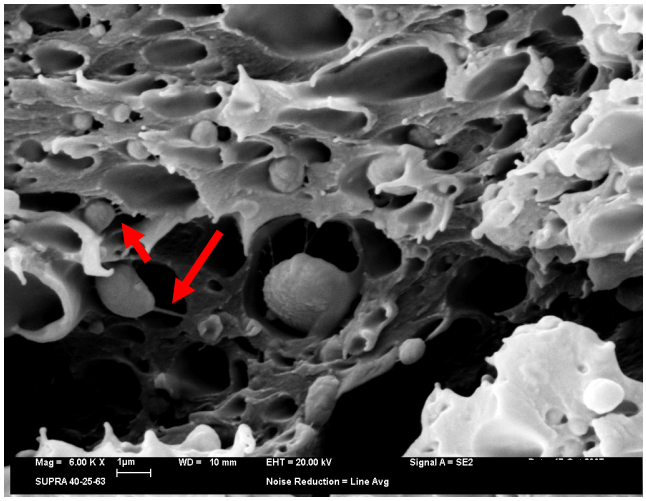


PC-MG1

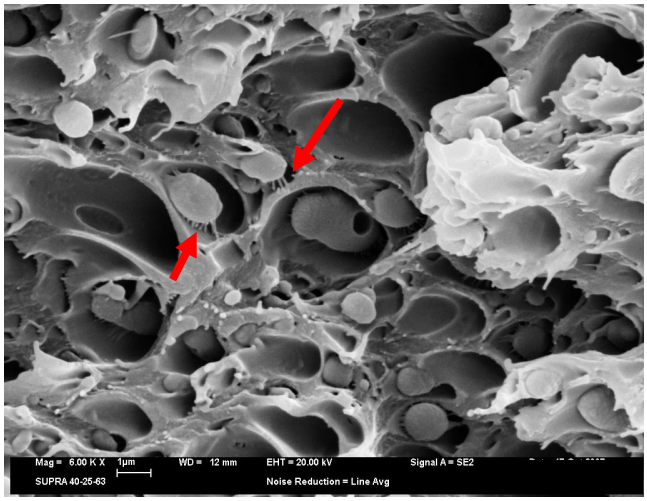


PC-MG2

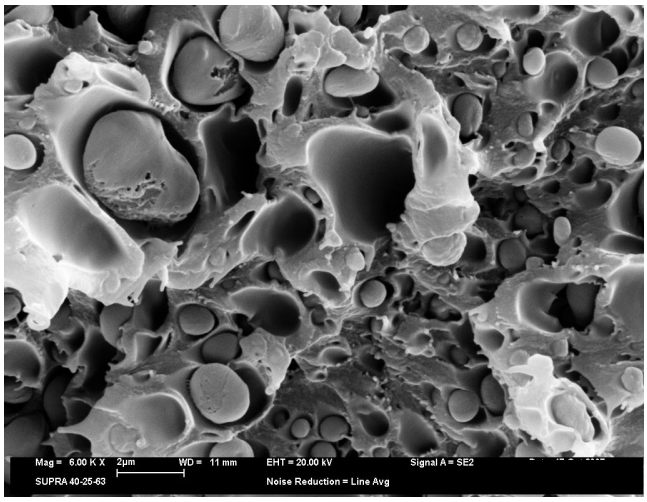


PC-HM1

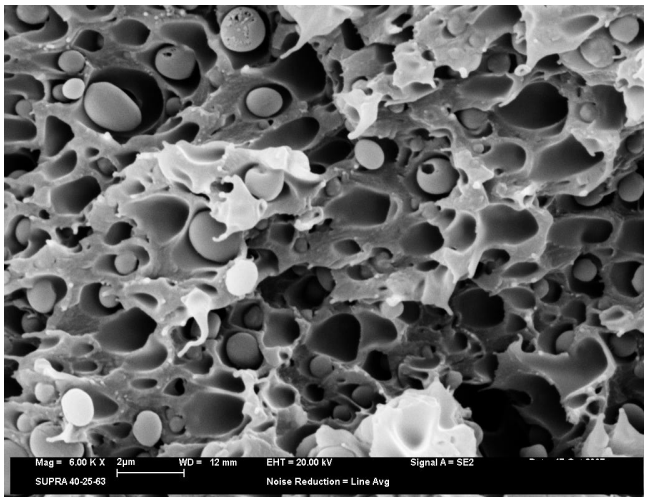


PC-HM2

**Figure 4.9 SEM morphology of E-GMA, E-MA-GMA and HDPE-g-MAH compatibilised PC/HDPE blends**

As shown in DSC traces of Figures 4.7 (b) and 4.7 (c), the vitrification of PC during the cooling process occurred before the crystallisation of HDPE. When HDPE crystallises on the solidified PC matrix, large changes in the specific volume as shown in Figure 4.10 caused the HDPE to contract inwards creating voids between the HDPE domain and the PC matrix.

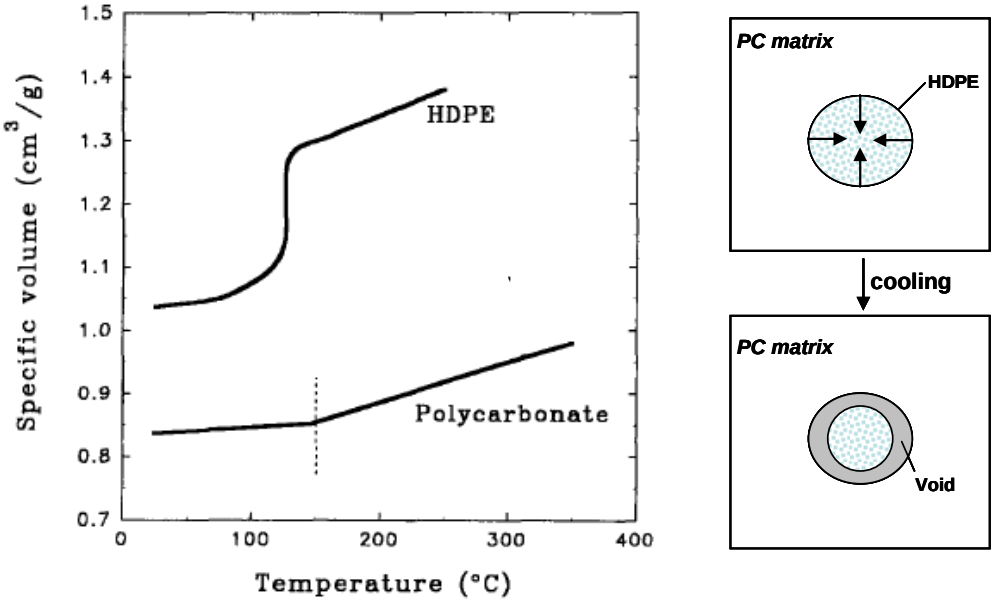


**Figure 4.10 Dependence of specific volume of PC and HDPE on temperature and its influence on morphology (reconstructed from ref. [125])**

The addition of EVA compatibilisers caused a dramatic reduction in the size of the HDPE phase from about 3 µm to less than 0.5 µm suggesting improved miscibility and compatibility of the phases. It is believed that good miscibility between the amorphous phase of the HDPE and EVA as discussed earlier has improved the miscibility between the amorphous phase of the HDPE and the PC matrix.

In general, all compatibilisers caused reduction in size of HDPE domains indicating their efficiency in improving the compatibility of the blends. Fibrils that interconnect PC and the HDPE phases are observed in blends compatibilised using EMA, E-GMA and E-MA-GMA suggesting good interfacial adhesion (examples of fibrils are indicated by the red arrows in Figure 4.9). A similar observation of fibrils was reported by Kunori and Geil

[124] who suggested that the fibrils were HDPE. The micrograph of PC-EG2 shows the most fibrillation of the dispersed phase which is supported by the exceptionally large elongation at break as discussed earlier.

The morphology of PC-HM1 reveals two distinct phases with large voids between the HDPE particles and the PC matrix. The lack of interfacial adhesion is supported by the evidence of lower elongation at break than other compatibilised blends.

It has been shown in this study that the morphology of blends in particular those containing an amorphous matrix with crystalline dispersed phases are not only dependent on the miscibility and compatibility between the blend components but also the crystallisation behaviour of the dispersed phase. The crystallisation of the dispersed phase occurring after the vitrification of the matrix could lead to formation of voids or gaps between the two phases leading to poor mechanical properties, especially the impact strengths of the resultant blends.

### 4.3.4 Summary

Based on mechanical testing performed on the blends, the compatibilising effectiveness of the blends are ranked in descending order of values for notched and reversed notch Izod impact strengths, and elongation at break as follows:

| **Notched Izod impact Strength:** | **Reverse notched Izod impact Strength:** |
|---|---|
| 1. PC-**MG1** (611 J/m) | 1. PC-**EG1** (2558 J/m) |
| 2. PC-**EM1** (584 J/m) | 2. PC-**EG2** (2527 J/m) |
| 3. PC-**EV1** (553 J/m) | 3. PC-**HM1** (2467 J/m) |

**Elongation at break:**

1. PC-**EG2** (213 %)
2. PC-**EM1** (168 %)
3. PC-**MG1** (152%)

The outstanding elongation at break of PC/HDPE blends compatibilised with E-GMA compatibiliser suggests strong interfacial adhesion and is manifested by the presence of HDPE fibrils that interconnect the PC and HDPE domains from SEM. On the other hand, notched Izod impact strength of PC/HDPE blends are best improved with E-MA-GMA compatibiliser which exhibit ductile morphology and evidences of interconnected HDPE fibrils with the PC matrix from SEM.

## 4.4 Evaluation of PBT/HDPE Blends

### 4.4.1 Mechanical Properties of Blends

PBT is a ductile polymer having elongation at break of 384% when tested under slow speed tensile test as shown in Table 4.6 and stress-strain curves in Appendices B1-5 to B1-6. However, its notched impact strength is very low and it is observed that the addition of HDPE without compatibiliser does not have any significant influence on the notched impact strength of the blend [70, 87]. Data of Izod impact tests are presented in Appendices B2-1 to B2-7.

On the other hand, as shown in Figure 4.11, dramatic reduction in the reversed notch impact and elongation at break are observed suggesting a transformation of ductile to brittle failure. Reason for the observed differences in notched and reversed behaviour of the two blends is that impact tests conducted on notched specimens tend to measure resistance to crack propagation, whereas tests conducted on reversed notch specimens place a greater emphasis upon ductility prior to crack initiation. The addition of HDPE in PBT caused a reduction in ductility due to poor compatibility between the two polymers but does not have significant influence on the resistance to crack propagation. As such the changes in ductility due to compatibilisation of blends are best followed using reversed notch impact and also elongation at break of the blends.

**Table 4.6 Mechanical properties of PBT, binary PBT/HDPE and ternary PBT/(HDPE/compatibiliser) blends**

| Sample Code | *Izod Impact Strength* | | *Tensile Properties* | | |
|---|---|---|---|---|---|
| | **Notched (J/m)** | **Reversed notch (J/m)** | **Elongation @ Break (%)** | **Elongation @ Yield (%)** | **Strength @ Yield (MPa)** |
| **PBT** | **29** *(2)* | **1060** *(129)* | **384** *(16)* | **14** *(0)* | **53** *(0)* |
| **HDPE** | **29** *(1)* | **-** | **191** *(6)* | **11** *(0)* | **23** *(0)* |
| **PBT-H15** | **25** *(2)* | **396** *(24)* | **13** *(1)* | **5** *(0)* | **41** *(0)* |
| **PBT-EV1** | **39** *(3)* | **761** *(20)* | **25** *(2)* | **11** *(1)* | **40** *(0)* |
| **PBT-EV2** | **29** *(2)* | **596** *(24)* | **18** *(1)* | **11** *(0)* | **41** *(0)* |
| **PBT-EM1** | **31** *(2)* | **728** *(41)* | **17** *(1)* | **8** *(0)* | **39** *(0)* |
| **PBT-EM2** | **27** *(3)* | **564** *(21)* | **15** *(0)* | **9** *(0)* | **40** *(0)* |
| **PBT-EG1** | **62** *(3)* | **1339** *(24)* | **49** *(7)* | **13** *(0)* | **44** *(0)* |
| **PBT-EG2** | **55** *(3)* | **1306** *(24)* | **53** *(2)* | **14** *(0)* | **45** *(0)* |
| **PBT-MG1** | **79** *(4)* | **1345** *(52)* | **24** *(2)* | **9** *(0)* | **39** *(1)* |
| **PBT-MG2** | **54** *(4)* | **1170** *(31)* | **19** *(3)* | **10** *(0)* | **43** *(0)* |
| **PBT -HM1** | **32** *(1)* | **867** *(31)* | **26** *(1)* | **13** *(0)* | **46** *(0)* |
| **PBT-HM2** | **30** *(2)* | **656** *(28)* | **19** *(1)* | **11** *(0)* | **45** *(0)* |

*Values in parentheses denote standard deviations*

Figure 4.11 shows that compatibilisers containing GMA functionality (E-GMA and E-MA-GMA) are the most efficient in improving both types of impact toughness with impact strengths exceeding those of the neat PBT. This is a strong indication of improvement in compatibilisation between the phases due to reaction of the epoxy moieties in both compatibilisers with the carboxylic end-groups of the PBT molecules contributed to formation of strong covalent bonds at the blend interface. On the other hand, the HDPE-g-MAH functionality seems to have positive interaction with the PBT end-groups which also lead to significant improvements in both impact properties. Both polar non-reactive EVA and EMA compatibilisers were effective in improving the impact strengths particularly the notched impact.

The elongation at break of all compatibilised blends remained low irrespective of compatibiliser types. The PBT matrix seems to be sensitive to the inclusion of a dispersed phase as it acts as a stress concentration point in the matrix material. The broadening of the elongation at yield of the compatibilised blends in similar manner as the impact toughness as shown in Table 4.6 suggests that the compatibilisers improved the shear yielding mechanism of the blends. There was no significant influence of the compatibilisers on the tensile yield strength of all the blends indicating the yield strength is not sensitive in detecting compatibilisation in this series of blends.

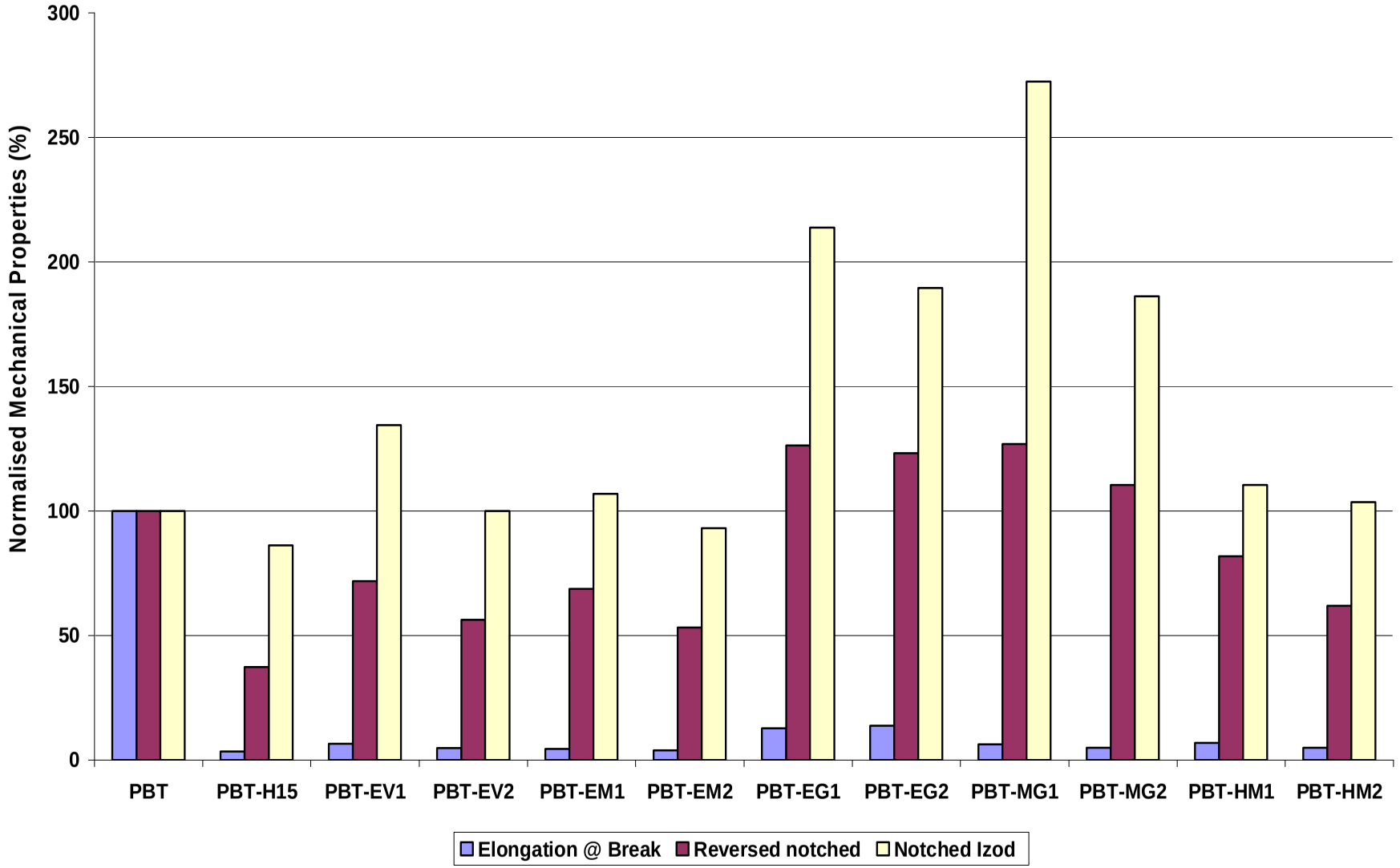


**Figure 4.11 Mechanical properties of uncompatibilised and compatibilised PBT/HDPE blends**

### 4.4.2 Thermal Analysis of Blends

Table 4.7 summarises the thermal properties of PBT/HDPE blends obtained from non-isothermal DSC experiments and representative DSC traces of these blends are presented in Figure 4.12 and Appendices A1-15 to A1-18. A small melting endotherm is observed before the main melting peak of PBT which is associated with the crystallisation conditions. Crystals that are formed at high cooling rate are inherently unstable and will anneal on heating which leads to a single endotherm centred at 220℃ [197]. Thus the high temperature peak develops as a result of reorganisation processes during heating. Crystals that are formed by slow cooling are more perfect and resistant to reorganisation which can be identified as crystals formed during the original cooling. In the study, both peaks are taken into consideration during the calculation of percent crystallinity of the blends.

During the crystallisation process of the blends as shown in Figure 4.12 (b), the PBT phase crystallises earlier and thus the HDPE domains are expected to crystallise in the solidified matrix of the PBT. Table 4.7 shows that changes in the melting point and the degree of crystallinity of the HDPE domain in the uncompatibilised blend (PBT-H15) were insignificant which indicates immiscibility of both polymers in their crystalline regions. The non-isothermal DSC traces in Figure 4.12 (b) also shows that fractionated crystallisation did not occur in the uncompatibilised blend.

Table 4.7 shows that all PBT melting peaks remained relatively unmodified by the presence of HDPE and compatibilisers. However, dramatic reduction in degree of crystallinity and depression in the melting point of HDPE components in all compatibilised blends in particular, PBT-MG1 and PBT-MG2 are observed. This suggests possible interactions between the amorphous phase of the PBT and crystalline phase of the HDPE in the compatibilised blends which also caused a delay in crystallisation of HDPE. This is in good agreement with earlier findings that both the E-GMA and E-MA-GMA having better compatibilisation efficiencies resulted in better Izod impact properties of the blends.

**Table 4.7 Thermal analysis of PBT, HDPE, binary PBT/HDPE and ternary PBT/(HDPE/compatibiliser) blends**

| Sample Code | PBT Phase | | | | | | HDPE Phase | | |
|---|---|---|---|---|---|---|---|---|---|
| | Tm (℃) | ΔHf (J/g) | $X_c$ (%) | $TC_{Onset}$ (℃) | $TC_{Peak}$ (℃) | ΔTC (℃) | Tm (℃) | ΔHf (J/g) | $X_c$ (%) |
| **PBT** | **224** *(0)* | **47.1**[a] *(1.0)* | **32** *(1)* | **194** *(0)* | **189** *(0)* | **5** | - | - | - |
| **HDPE** | - | - | - | - | - | - | **130** *(1)* | **189.8**[a] *(0.4)* | **65** *(0)* |
| **PBT-H15** | **224** *(0)* | **45.8**[b] *(1.5)* | **32** *(1)* | **193** *(0)* | **188** *(0)* | **5** | **130** *(0)* | **198.4**[b] *(6.7)* | **68** *(2)* |
| **PBT-EV1** | **223** *(0)* | **43.8**[b] *(1.1)* | **30** *(1)* | **195** *(0)* | **191** *(0)* | **4** | **127** *(0)* | **150.0**[b] *(3.1)* | **51** *(1)* |
| **PBT-EV2** | **224** *(0)* | **40.7**[b] *(1.1)* | **28** *(1)* | **195** *(0)* | **190** *(0)* | **5** | **127** *(0)* | **164.0**[b] *(3.3)* | **56** *(1)* |
| **PBT-EM1** | **223** *(0)* | **46.4**[b] *(2.3)* | **32** *(1.5)* | **195** *(0)* | **191** *(0)* | **4** | **127** *(0)* | **180.7**[b] *(7.1)* | **61** *(2.3)* |
| **PBT-EM2** | **223** *(0)* | **43.9**[b] *(4.9)* | **30** *(1)* | **195** *(0)* | **190** *(1)* | **5** | **127** *(0)* | **167.8**[b] *(2.7)* | **57** *(1)* |
| **PBT-EG1** | **224** *(0)* | **42.7**[b] *(3.9)* | **29** *(3)* | **192** *(1)* | **187** *(1)* | **5** | **128** *(1)* | **152.8**[b] *(3.0)* | **52** *(1)* |
| **PBT-EG2** | **224** *(0)* | **44.6**[b] *(1.4)* | **31** *(1)* | **193** *(0)* | **188** *(0)* | **5** | **128** *(1)* | **159.1**[b] *(6.4)* | **54** *(2)* |
| **PBT-MG1** | **224** *(0)* | **45.0**[b] *(1.8)* | **31** *(1)* | **194** *(0)* | **190** *(0)* | **4** | **127** *(0)* | **142.8**[b] *(3.9)* | **49** *(2)* |
| **PBT-MG2** | **223** *(0)* | **44.2**[b] *(1.7)* | **30** *(2)* | **194** *(0)* | **189** *(0)* | **5** | **127** *(0)* | **145.0**[b] *(7.0)* | **49** *(2)* |
| **PBT-HM1** | **223** *(0)* | **45.4**[b] *(1.1)* | **31** *(1)* | **195** *(0)* | **190** *(0)* | **5** | **127** *(0)* | **150.7**[b] *(4.6)* | **51** *(1)* |
| **PBT-HM2** | **223** *(0)* | **45.6**[b] *(1.1)* | **31** *(1)* | **195** *(0)* | **190** *(0)* | **5** | **128** *(0)* | **154.6**[b] *(3.9)* | **53** *(1)* |

*Values in parentheses denote standard deviations*
[a] *Values normalised to the total amount of the blend or resin*
[b] *Values normalised to the amount of the relevant phase*

Blends compatibilised with EVA have somewhat similar crystallisation behaviour to the EMA. The addition of these compatibilisers caused

nucleating effect in the PBT matrix with increased in overall rate of crystallisation as shown by the increased in onset and peak crystallisation temperatures and reduction in ΔTC respectively. On the other hand, fractionated crystallisation seems to have occurred in the HDPE phase as the main crystallisation peaks shifted lower with very small exotherms appearing at a lower temperature in the cooling curves. This presumably accounts for the observed reduction in the degree of crystallinity of the HDPE domains.

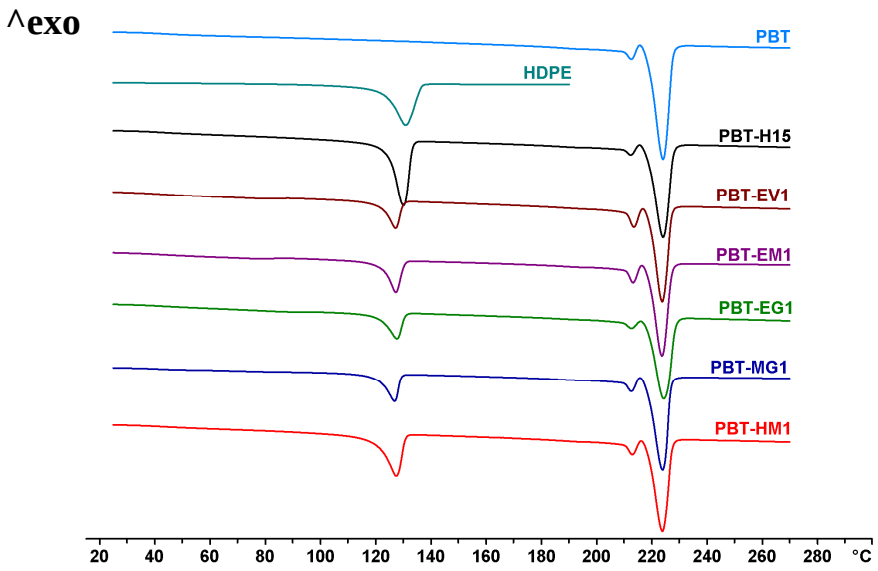


**(a)**

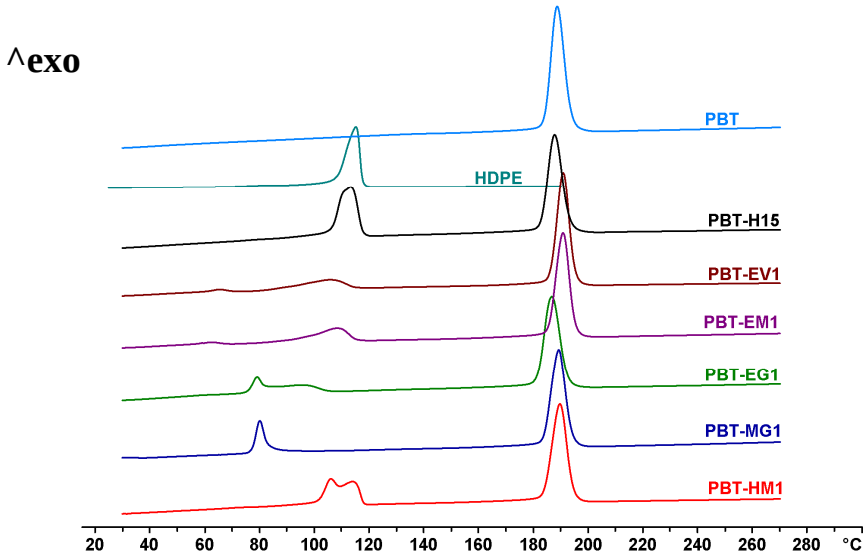


**(b)**

**Figure 4.12 DSC traces of PBT, HDPE, uncompatibilised and compatibilised PBT/HDPE blends (a) second heating and (b) cooling**

### 4.4.3 Morphology of Blends

The micrographs of both uncompatibilised and compatibilised PBT/HDPE blends are presented in Figures 4.13 and 4.14. Two distinct phases are again observed in uncompatibilised blends with large HDPE domains and very well defined cavities. The presence of EVA causes some reduction in the size of the dispersed phase and also improvements in dispersion. However, the boundaries between the phases are still distinct but less than in the EMA compatibilised blends. The EMA seems to have slightly altered the interfacial tension of the blends as some elongated dispersed HDPE phase are observed in the micrographs. Very fine morphologies are observed for the blend containing the higher concentration of E-GMA compatibiliser. Very small HDPE particles can be seen embedded in the PBT matrix with very blurred interfaces as indicated by the red arrows in micrograph of PBT-EG1 in Figure 4.14. The dispersed particles become more distinct with less E-GMA but typical particle sizes are lower than 0.3 µm. On the other hand, the blend compatibilised with higher concentration of E-MA-GMA appeared to have a larger dispersed phase (< 0.7 µm) than the E-GMA but were interconnected by fibrils as indicated by the red arrows in mircrograph of PBT-MG1 in Figure 4.14. This observed larger dispersed phase might have improved the resistance to crack propagation of the blend and is in good agreement with the excellent notched Izod impact strength of the blend noted earlier. The interfacial boundaries become more distinct and fractured surface appeared less ductile with lower dosage of the compatibiliser in PBT-MG2 of Figure 4.14. The superior notched impact strength of blend with high E-MA-GMA (PBT-MG1) emphasises the fact that critical particle size and inter-particle distance [118] are essential parameters for toughening of polymer blends. A too big or too small dispersed phase even with good interfacial adhesion will disrupt the toughening mechanisms.

The observation of fibrils interconnecting the dispersed phase of HDPE-g-MAH compatibilised blend indicated by red arrow in sample PBT-HM1 suggests the evidence of interfacial adhesion. However the dispersed phase domains became more irregular with sharper interfaces when the concentration of the compatibiliser was reduced.

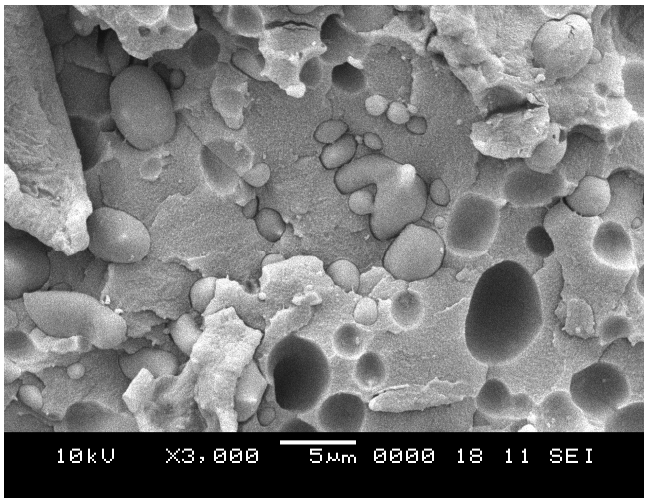


**PBT-H15**

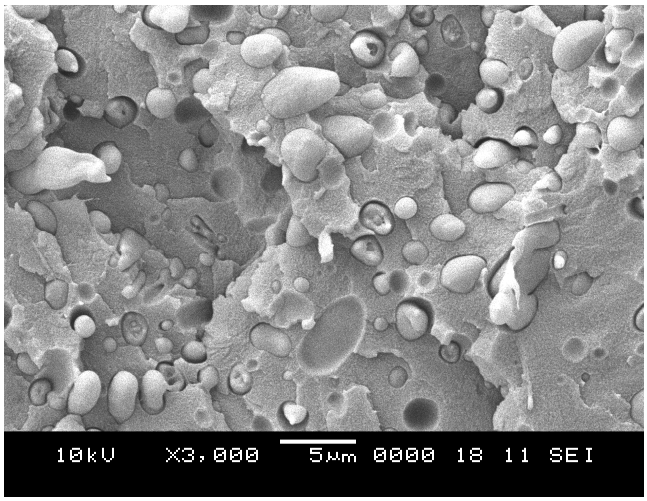


**PBT-EV1**

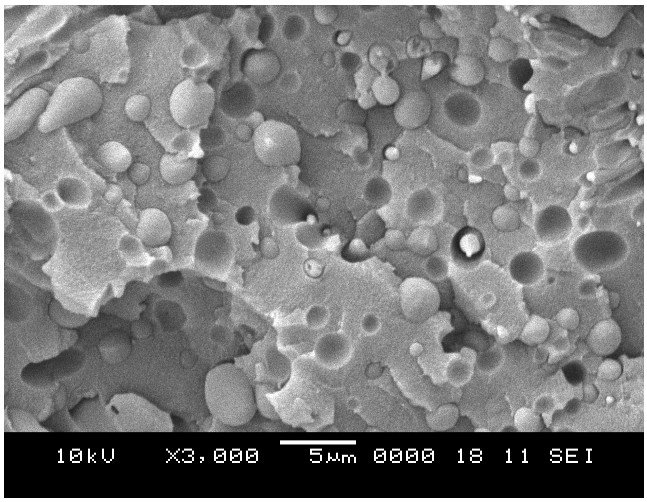


**PBT-EV2**

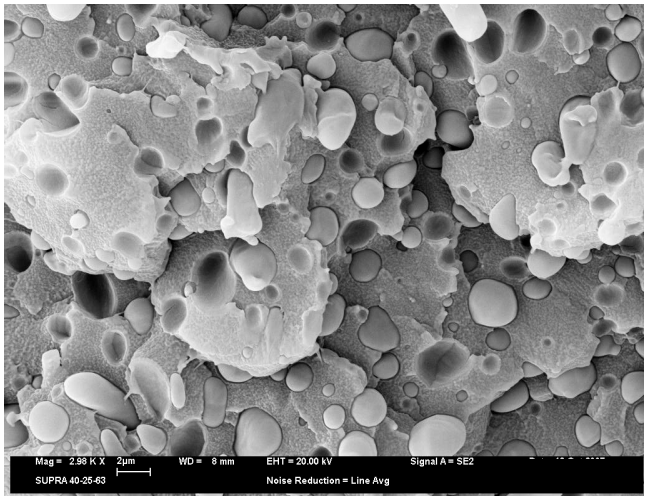


**PBT-EM1**

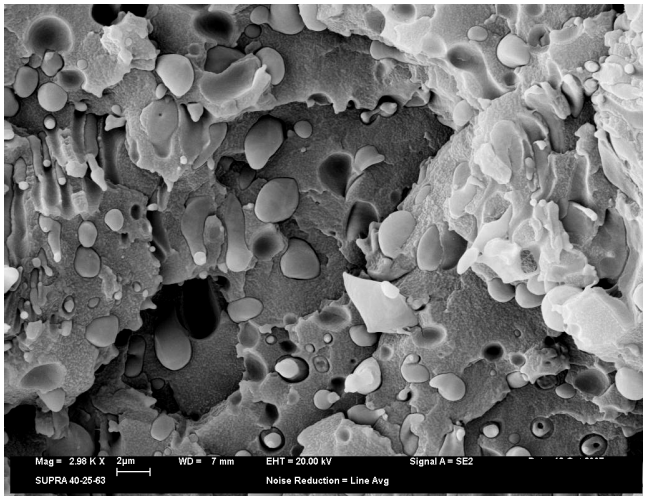


**PBT-EM2**

**Figure 4.13 SEM morphology of uncompatibilised, EVA and EMA compatibilised PBT/HDPE blends**

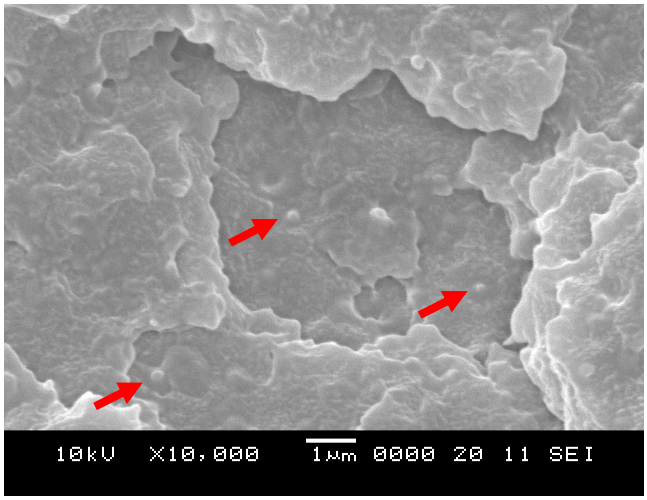


PBT-EG1

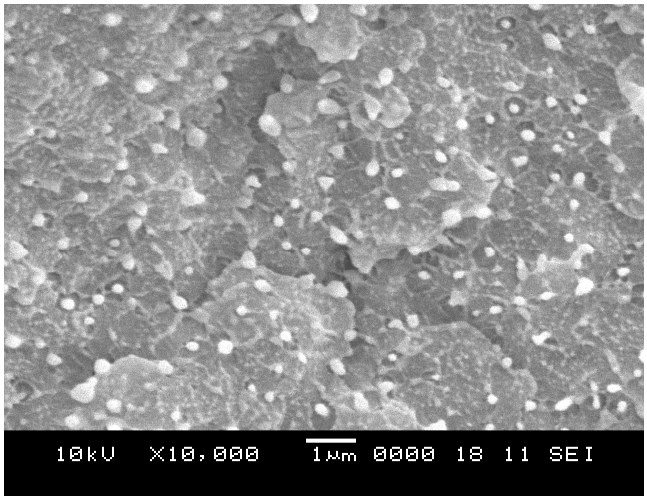


PBT-EG2

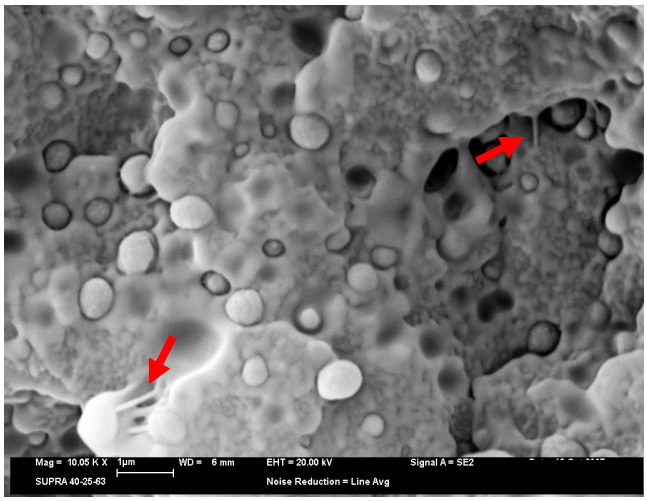


PBT-MG1

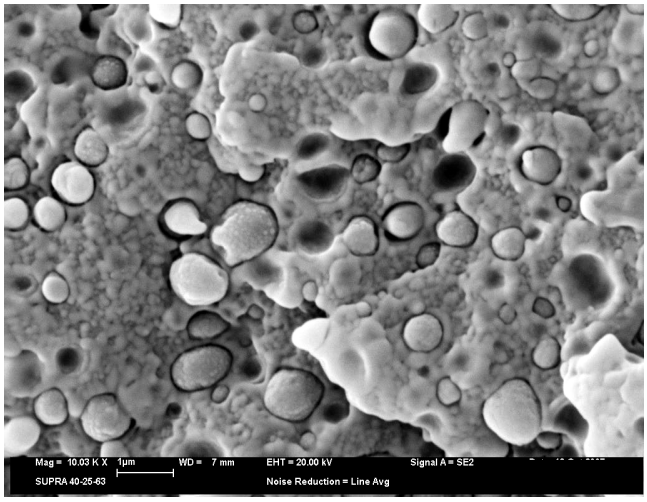


PBT-MG2

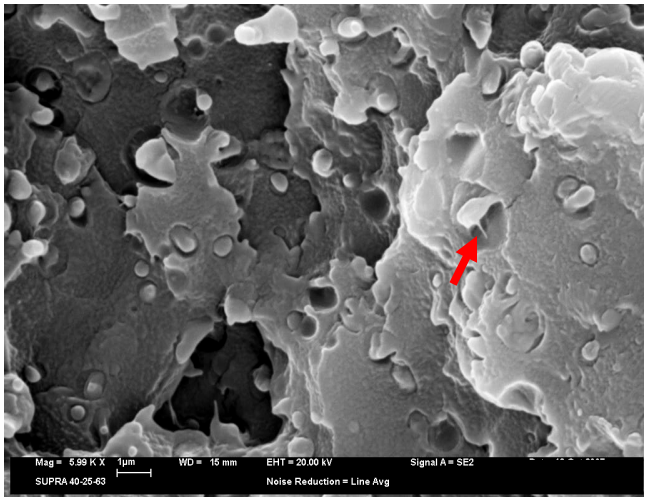


PBT-HM1

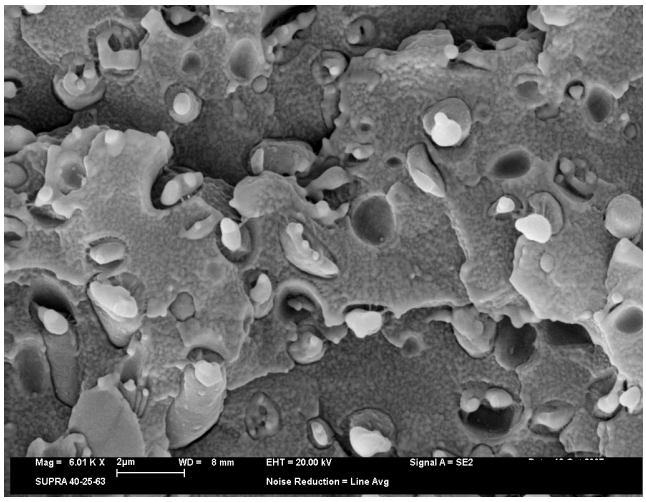


PBT-HM2

**Figure 4.14 SEM morphology of E-GMA, E-MA-GMA and HDPE-g-MAH compatibilised PBT/HDPE blends**

### 4.4.4 Summary

Based on mechanical testing performed on the blends, the compatibilising effectiveness of the blends are ranked in descending order of values for notched and reversed notch Izod impact strengths, and elongation at break as follows:

| **Notched Izod impact Strength:** | **Reverse notched Izod impact Strength:** |
|---|---|
| 1. PBT-**MG1** (79 J/m) | 1. PBT-**MG1** (1345 J/m) |
| 2. PBT-**EG1** (62 J/m) | 2. PBT-**EG1** (1339 J/m) |
| 3. PBT-**EG2** (55 J/m) | 3. PBT-**EG2** (1306 J/m) |

**Elongation at break:**

1. PBT-**EG2** (53 %)
2. PBT-**EG1** (49 %)
3. PBT-**HM1** (26 %)

Both glycidyl methacrylate type of compatibilisers (E-MA-GMA and E-GMA) showed excellent efficiency in improving the notched and reversed notch impact toughening of the PBT/HDPE blends exceeding the toughness of the neat PBT resin. However, none of the compatibilisers evaluated in this study was able to impart significant improvement in elongation at break of the blends. Blends compatibilised with E-GMA exhibited very fine morphology from SEM indicating improved miscibility and compatibility between the HDPE and PBT matrix. Even though E-MA-GMA imparted larger dispersed phase than E-GMA, it exhibited greater notched and reversed notch toughness. The observation of melting point depression and reduction in degree of crystallinity in the HDPE components of the blends further justify the existence interaction between the dispersed HDPE and PBT matrix.

## 4.5 Evaluation of PA6/HDPE Blends

### 4.5.1 Mechanical Properties of Blends

Similar to PBT, PA6 is a ductile polymer when tested using a slow speed tensile test as shown in Table 4.8. It has a similar low notched Izod impact strength to the PBT, which is not significantly changed by the presence of an uncompatibilised HDPE phase. The elongation at yield of all the blends are also relatively unchanged from the neat PA6 polymer in both uncompatibilised and compatibilised blends. Again, the elongation at yield is seen to be insensitive in detecting changes at interfacial regions of the blends. Reduction in tensile yield strength of uncompatibilised blend is observed but shows no significant improvement with the addition of compatibilisers.

From their studies conducted on blends of 75 wt% PA6 with 25 wt% low-density polyethylene (LDPE) compatibilised with a maleic anhydride functionalised styrene-ethylene/butylenes-styrene triblock copolymer (SEBS), Armat and Moet [102] also observed that the elongation at break of these blends are more sensitive to compatibilisation than the yield stress. Surprisingly, EVA and HDPE-g-MAH have similar effects in improving the Izod impact strength but elongation at break of blends compatibilised by EVA are much higher than the rest of the compatibilisers. It seems that the EVA has strong plasticising effect on PA6 supported by relatively strong interactions between the carbonyl group of EVA and the amide and/or end-groups of the PA6 leading to much better ductility than the well known maleic anhydride-polyamide interactions. As the efficiency of compatibilisers is determined by their preferential location on the blend interface which is dependent on diffusion rate of the compatibilisers [17], it could also well be that the lower miscibility between the HDPE/EVA blends as compared with HDPE/HDPE-g-MAH binary blends allow easier and more rapid diffusion of the EVA functionality to the interfacial region of the blends. Similarly, Jiang et al [105] reported that maleic anhydride functionalised low density polyethylene (LDPE-g-MAH) was less effective in compatibilising LDPE/PA6 blends than a HDPE-g-MAH compatibiliser. The authors postulated that the HDPE-g-MAH which is

not miscible with the LDPE was able to migrate to the LDPE/PA6 interface while the LDPE-g-MAH were entrapped within the LDPE component due good miscibility of the LDPE/LDPE-g-MAH blends.

In this study, since the blends were prepared via direct injection moulding of the HDPE binary blends with the PA6, which results in a short residence time for melt blending, rapid diffusion of the compatibilisers to the interface is of utmost importance.

EMA on the other hand is not as effective in improving the Izod impact strength and elongation at break at either concentration levels thus suggesting lower compatibilisation efficiency compared with EVA. The tensile stress-strain curves (Appendices B1-7 and B1-8) shows that all but EMA compatibilised blends have a second yielding at strain levels of between 200 to 300%. The observation of secondary yielding suggests that these compatibilisers impart strong interfacial bonding between the dispersed phase and the matrix and also indicate that EMA did not provide good interfacial bonding between PA6 and HDPE.

The E-GMA is observed to be more effective in improving the Izod toughness of the blends than EVA, EMA and HDPE-g-MAH but more inferior in elongation at break than EVA and HDPE-g-MAH. This may suggest that the blends compatibilised by E-GMA are possibly having lower interfacial adhesion than EVA and HDPE-g-MAH as indicated by their poorer ultimate elongation but more effective in modification of the blend morphology for better impact toughness.

At high compatibiliser concentration, the E-MA-GMA compatibiliser performed the best in improving the notched Izod impact of the PA6/HDPE blend indicating the possibility of improved morphological properties for toughness enhancement. However, the elongation at break of the blends were lower than those compatibilised using E-GMA suggesting poorer interfacial adhesion due to the presence of methyl acrylate which could have hindered the access of the glycidyl moieties towards the end-groups of the PA6.

**Table 4.8 Mechanical properties of PA6, binary PA6/HDPE and ternary PA6/(HDPE/compatibiliser) blends**

| Sample Code | *Izod Impact Strength* | | *Tensile Properties* | | |
|---|---|---|---|---|---|
| | **Notched (J/m)** | **Reversed notch (J/m)** | **Elongation @ Break (%)** | **Elongation @ Yield (%)** | **Strength @ Yield (MPa)** |
| **PA6** | **33** *(4)* | **2902** *(81)* | **265** *(8)* | **5** *(0)* | **72** *(1)* |
| **HDPE** | **29** *(1)* | **-** | **191** *(6)* | **11** *(0)* | **23** *(0)* |
| **PA6-H15** | **36** *(2)* | **1102** *(81)* | **65** *(3)* | **6** *(1)* | **55** *(0)* |
| **PA6-EV1** | **65** *(5)* | **2889** *(129)* | **478** *(31)* | **5** *(0)* | **50** *(1)* |
| **PA6-EV2** | **54** *(5)* | **2941** *(156)* | **484** *(23)* | **5** *(0)* | **50** *(0)* |
| **PA6-EM1** | **37** *(2)* | **1798** *(107)* | **235** *(30)* | **5** *(0)* | **54** *(0)* |
| **PA6-EM2** | **39** *(3)* | **1412** *(89)* | **123** *(11)* | **5** *(0)* | **55** *(0)* |
| **PA6-EG1** | **85** *(6)* | **3021** *(132)* | **371** *(32)* | **6** *(0)* | **55** *(1)* |
| **PA6-EG2** | **73** *(5)* | **3298** *(165)* | **419** *(24)* | **6** *(0)* | **55** *(1)* |
| **PA6-MG1** | **133** *(4)* | **3019** *(125)* | **316** *(24)* | **5** *(0)* | **50** *(1)* |
| **PA6-MG2** | **63** *(5)* | **2865** *(247)* | **344** *(19)* | **5** *(0)* | **52** *(0)* |
| **PA6-HM1** | **64** *(2)* | **2811** *(142)* | **437** *(27)* | **5** *(0)* | **56** *(0)* |
| **PA6-HM2** | **63** *(2)* | **3127** *(135)* | **463** *(17)* | **5** *(0)* | **57** *(1)* |

*Values in parentheses denote standard deviations*

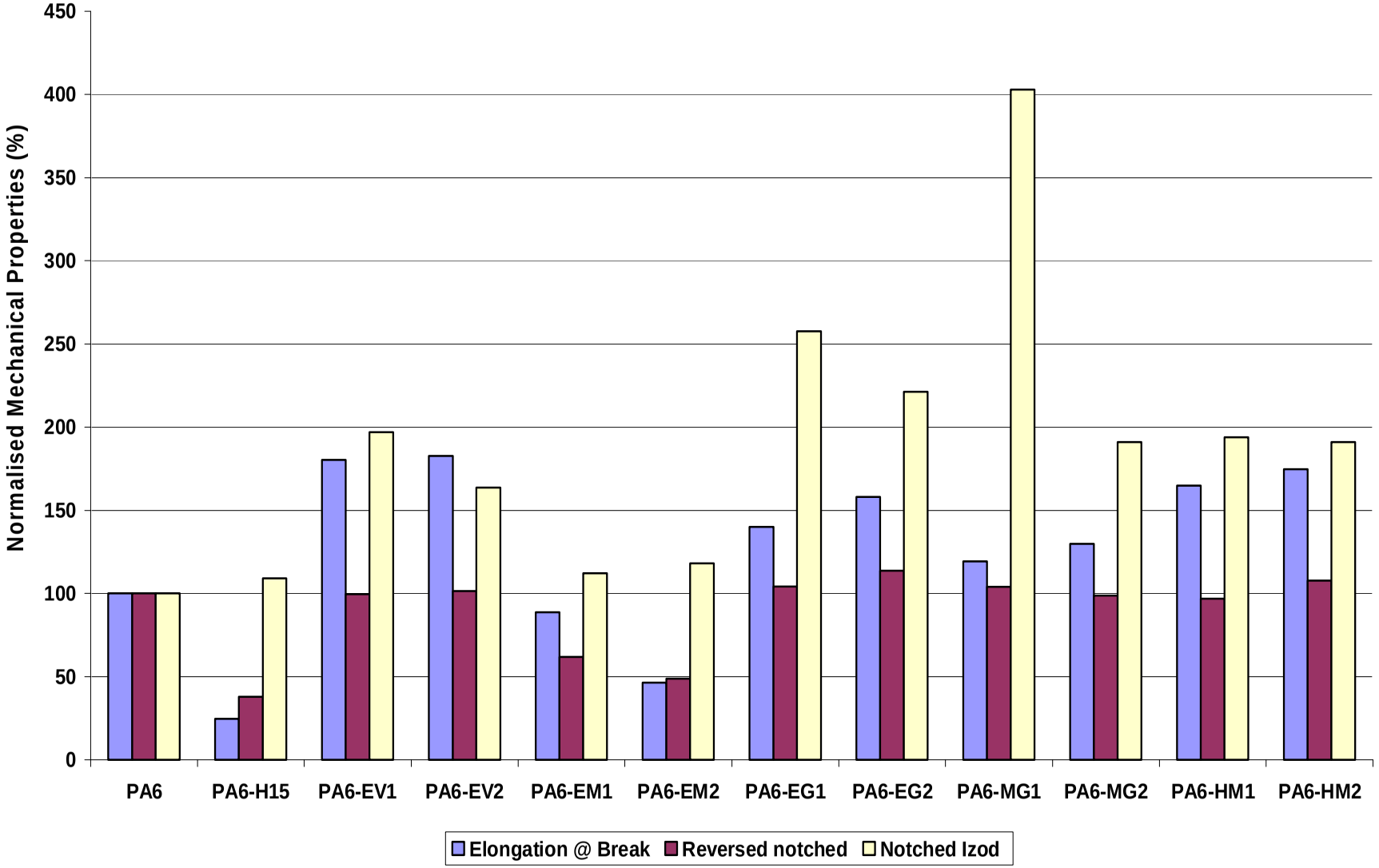


**Figure 4.15 Mechanical properties of uncompatibilised and compatibilised PA6/HDPE blends**

### 4.5.2 Thermal Analysis of Blends

As shown in Table 4.9, the melting point of PA6 and degree of crystallinity for both uncompatibilised and compatibilised blends remain relatively unchanged suggesting that the presence of HDPE and compatibilisers have insignificant effects on the crystalline phase of the PA6 (see Appendices A1-19 to A1-22). However, significant delays in onset and peak of crystallisation are observed on blends that were compatibilised with E-MA-GMA. On the other hand, only the crystallisation peaks were delayed in blends compatibilised with E-GMA.

The delays in crystallisation peaks as observed in E-MA-GMA and E-GMA compatibilised blends could be attributable to the interactions of the compatbilised HDPE with the amorphous phase of the PA6 which affected its crystallisation behaviour. However, as these interactions did not occur in the crystalline region of the PA6, the melting point and degree of crystallinity of the PA6 matrices remained relatively unmodified. The rest of the compatibilisers are observed to have insignificant influence on the crystallisation peaks of PA6.

The non-isothermal DSC traces in Figure 4.16 (b) show that during the crystallisation of the blends, the PA6 phase crystallises ahead of the HDPE and thus leaving the HDPE phase to crystallise within the solidified matrix of the PA6 like the PBT/HDPE blends. From Table 4.9, it is observed that there is an increased in the degree of crystallinity of the HDPE phase of the uncompatibilised blend. This could possibly be due to the migration of nucleating species from the PA6 matrix to the HDPE dispersed phase as the crystallisation peak of the HDPE phase in PA-H15 is observed to have shifted slightly higher which is indicated by the red arrow in Figure 4.16 (b). The transferring of heterogeneities from a styrene-butadiene-styrene (SBS) copolymer to the PP component of a PP/PS/SBS (18/80/2) blend was reported by Santana et al [149].

**Table 4.9 Thermal properties of PA6, HDPE, binary PA6/HDPE and ternary PA6/(HDPE/compatibiliser) blends**

| Sample Code | PA6 Phase | | | | | | HDPE Phase | | |
|---|---|---|---|---|---|---|---|---|---|
| | Tm (℃) | ΔHf (J/g) | $X_c$ (%) | $TC_{Onset}$ (℃) | $TC_{Peak}$ (℃) | ΔTC (℃) | Tm (℃) | ΔHf (J/g) | $X_c$ (%) |
| **PA6** | **220** *(0)* | **80.4**[a] *(0.4)* | **35** *(1)* | **198** *(0)* | **193** *(0)* | **5** | - | - | - |
| **HDPE** | - | - | - | - | - | - | **130** *(1)* | **189.8**[a] *(0.4)* | **65** *(0)* |
| **PA6-H15** | **221** *(0)* | **75.2**[b] *(1.7)* | **33** *(1)* | **197** *(0)* | **193** *(0)* | **4** | **132** *(0)* | **218.9**[b] *(4.2)* | **75** *(2)* |
| **PA6-EV1** | **221** *(1)* | **75.5**[b] *(0.8)* | **33** *(1)* | **197** *(0)* | **193** *(0)* | **4** | **130** *(1)* | **180.9**[b] *(4.2)* | **62** *(2)* |
| **PA6-EV2** | **221** *(0)* | **77.5**[b] *(2.1)* | **34** *(1)* | **196** *(0)* | **193** *(0)* | **3** | **130** *(1)* | **186.5**[b] *(8.2)* | **64** *(4)* |
| **PA6-EM1** | **221** *(0)* | **74.7**[b] *(6.0)* | **32** *(2.5)* | **197** *(0)* | **192** *(0)* | **5** | **129** *(0)* | **168.6**[b] *(3.7)* | **58** *(1.5)* |
| **PA6-EM2** | **221** *(0)* | **78.8**[b] *(3.9)* | **34** *(2)* | **197** *(0)* | **192** *(0)* | **5** | **130** *(0)* | **178.8**[b] *(5.4)* | **61** *(2)* |
| **PA6-EG1** | **221** *(0)* | **72.1**[b] *(3.2)* | **31** *(1)* | **196** *(0)* | **192** *(0)* | **4** | **127** *(1)* | **145.2**[b] *(7.0)* | **50** *(3)* |
| **PA6-EG2** | **221** *(0)* | **76.2**[b] *(4.7)* | **33** *(2)* | **196** *(0)* | **192** *(0)* | **4** | **128** *(1)* | **171.7**[b] *(6.5)* | **59** *(3)* |
| **PA6-MG1** | **220** *(0)* | **73.3**[b] *(4.9)* | **32** *(2)* | **195** *(0)* | **191** *(0)* | **4** | **127** *(0)* | **132.3**[b] *(0.9)* | **45** *(1)* |
| **PA6-MG2** | **220** *(0)* | **74.4**[b] *(3.3)* | **32** *(2)* | **196** *(0)* | **192** *(0)* | **4** | **127** *(0)* | **161.7**[b] *(1.4)* | **55** *(1)* |
| **PA6-HM1** | **220** *(0)* | **76.6**[b] *(1.8)* | **33** *(1)* | **196** *(0)* | **192** *(0)* | **4** | **127** *(0)* | **157.4**[b] *(5.4)* | **54** *(3)* |
| **PA6-HM2** | **220** *(0)* | **74.3**[b] *(0.7)* | **32** *(1)* | **196** *(0)* | **192** *(0)* | **4** | **127** *(0)* | **155.4**[b] *(3.7)* | **53** *(2)* |

*Values in parentheses denote standard deviations*

[a] *Values normalised to the total amount of the blend or resin*

[b] *Values normalised to the amount of the relevant phase*

Table 4.9 and Figure 4.16 (a) show reduction in degree of crystallinity and depression of melting point in HDPE phases of all compatibilised blends. Since there is no obvious fractionated crystallisation observed in Figure 4.16 (b), the melting point depression and reduction in crystallinity of the HDPE could presumably be due to interactions of the amorphous region of the PA6 matrix with the HDPE-rich phase in the compatibilised blends. From Table 4.9, more significant melting point depression of the HDPE components are observed in blends compatibilised with reactive compatibilisers i.e. E-GMA, E-MA-GMA and HDPE-g-MAH which suggests better miscibility and compatibility and of these blends.

Armat and co-work [102] reported the reduction in crystallinity of both components in PA6/LDPE blends as the amount of maleic anhydride grafted Styrene-ethylene/butylene-styrene triblock copolymer (SEBS-g-MAH) compatibiliser was increased indicating improved compatibility.

As shown in Figure 4.16 (b) the crystallisation peaks of the HDPE components in blends compatibilised with EVA, EMA, and HDPE-g-MAH were not significantly modified by the presence of these compatibilisers while those with E-GMA and E-MA-GMA show delays and less intense crystallisation as indicated by the red arrows. This is in good agreement with the observed lower degree of crystallinity of the HDPE components of these two blends in Table 4.9.

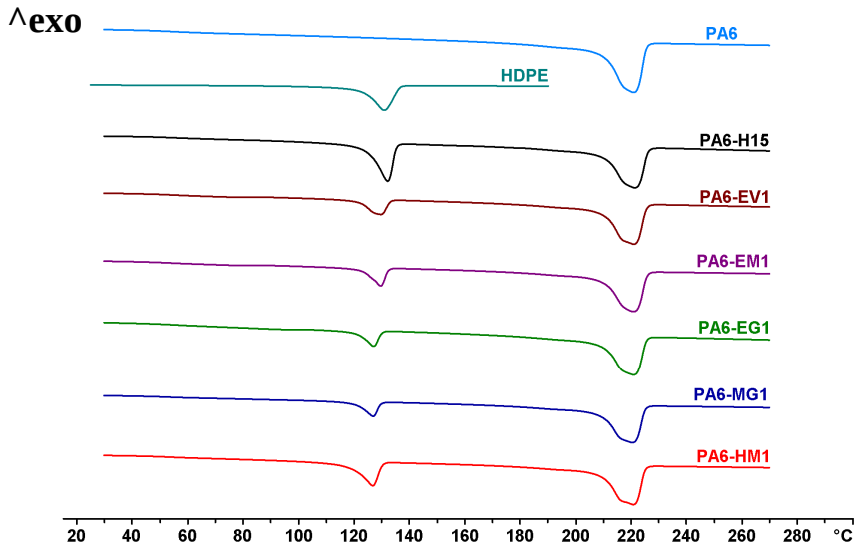


(a)

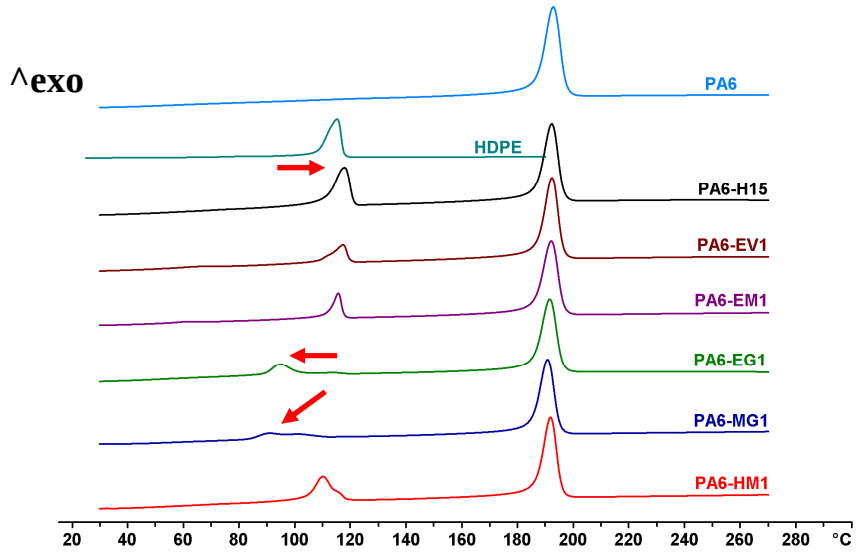


(b)

**Figure 4.16 DSC traces of PA6, HDPE, uncompatibilised and compatibilised PA6/HDPE blends (a) second heating and (b) cooling**

### 4.5.3 Morphology of Blends

A distinct spherical HDPE dispersed phase with well defined boundaries with the PA6 matrix is observed in the micrograph of uncompatibilised PA6/HDPE blends in Figure 4.17 suggesting poor miscibility and compatibility. In comparison with EMA, the EVA compatibilised blends are observed to have slightly smaller well dispersed HDPE domains with less defined boundaries. This is in good agreement with the finding of EVA compatibilised blends having better mechanical properties than the EMA type.

Very fine morphology is observed for blends compatibilised with E-GMA which has typical domain size of <0.25 µm which is very similar to the PBT/HDPE blends compatibilised with the same compatibiliser. The blend that is compatibilised with a higher concentration of E-MA-GMA has a larger dispersed phase (<1 µm) than the E-GMA which could be a critical particle size for the observed higher notched impact strength [111].

Blend compatibilised with a higher level of HDPE-g-MAH has a well dispersed HDPE phase with good interfacial bonding. At lower compatibiliser dosage, the shape of the dispersed phase becomes more irregular but this does not have significant changes in mechanical properties.

### 4.5.4 Summary

Based on mechanical testing performed on the blends, the compatibilising effectiveness of the blends are ranked in descending order of values for notched and reversed notch Izod impact strengths, and elongation at break as follows:

| **Notched Izod impact Strength:** | **Reverse notched Izod impact Strength:** |
|---|---|
| 1. PA6-**MG1** (133 J/m) | 1. PA6-**EG2** (3298 J/m) |
| 2. PA6-**EG1** (85 J/m) | 2. PA6-**HM2** (3127 J/m) |
| 3. PA6-**EG2** (73 J/m) | 3. PA6-**EG1** (3019 J/m) |

**Elongation at break:**

1. PA6-**EV2** (484 %)
2. PA6-**EV1** (478 %)
3. PA6-**HM2** (463 %)

HDPE-g-MAH compatibiliser was outperformed by E-MA-GMA and E-GMA compatibilisers in improving the notched and reversed notch Izod impact strengths respectively. Very fine morphology are observed in blend compatibilised with E-GMA which resulted in better performance in reversed notch Izod impact property. Blend compatibilised with E-MA-GMA has larger dispersed phase which resulted in better notched Izod impact strength. More surprising, the elongation at break was also outlasted unexpectedly by EVA compatibiliser. The dispersed HDPE phase is much bigger than blends of E-MA-GMA and E-GMA but appeared to be less distinct and well bonded on the PA6 matrix

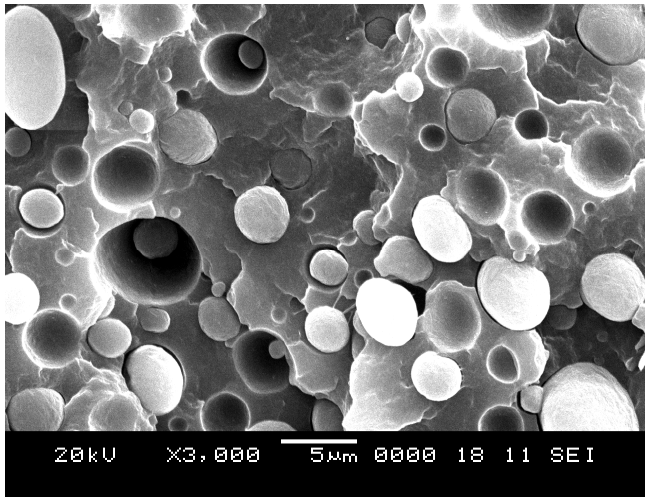


**PA6-H15**

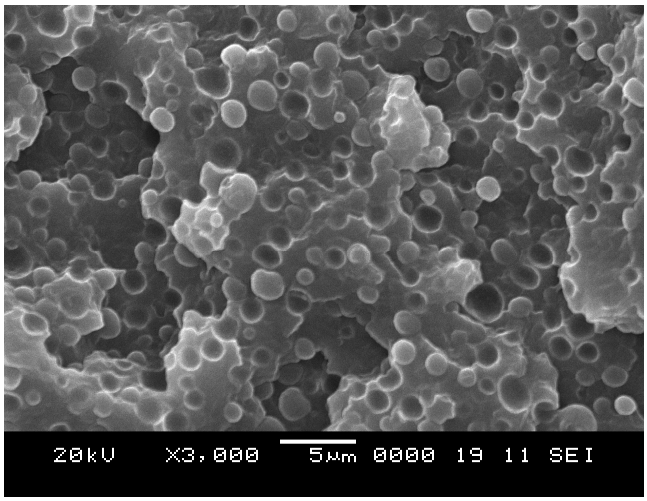


**PA6-EV1**

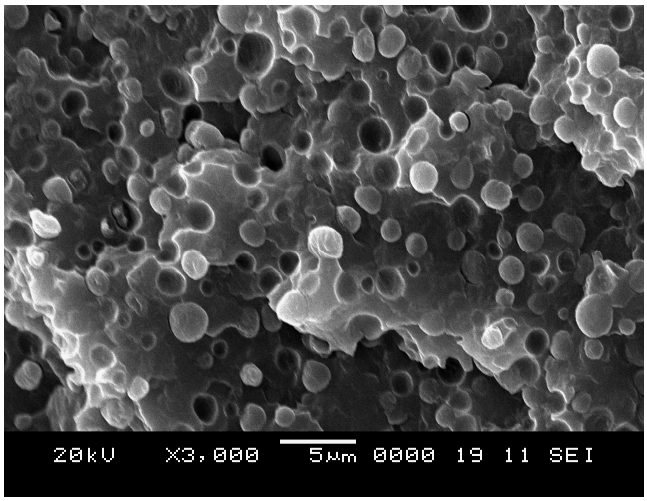


**PA6-EV2**

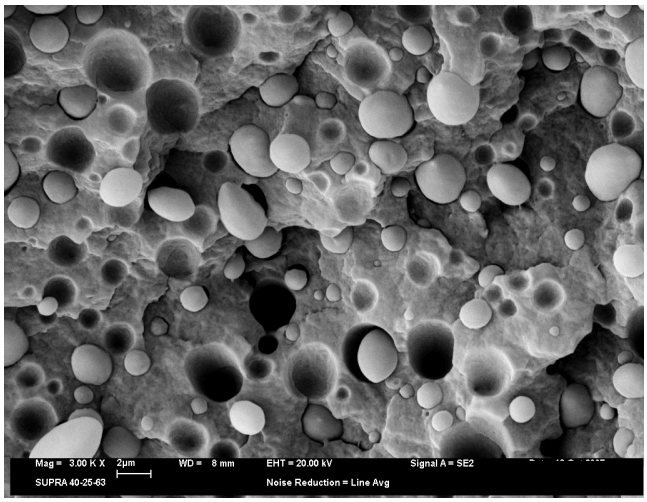


**PA6-EM1**

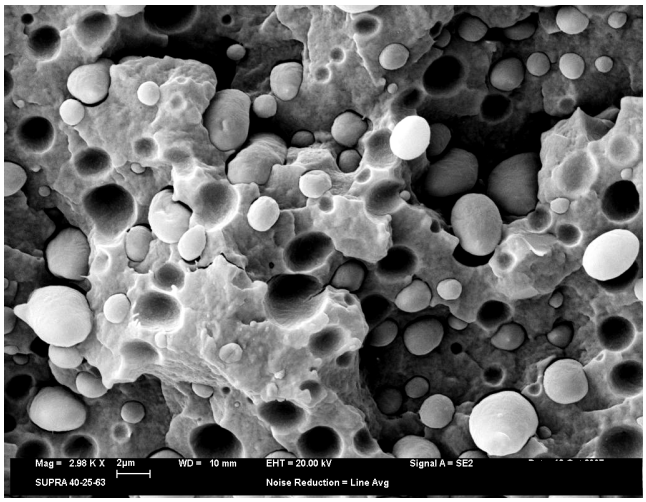


**PA6-EM2**

**Figure 4.17 SEM morphology of uncompatibilised, EVA and EMA compatibilised PA6/HDPE blends**

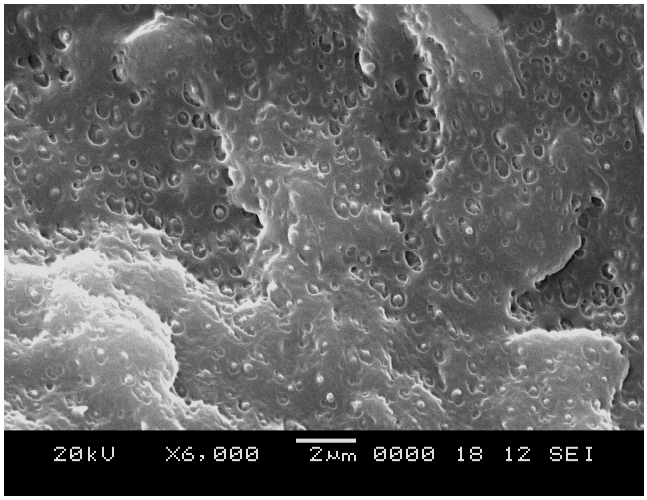


PA6-EG1

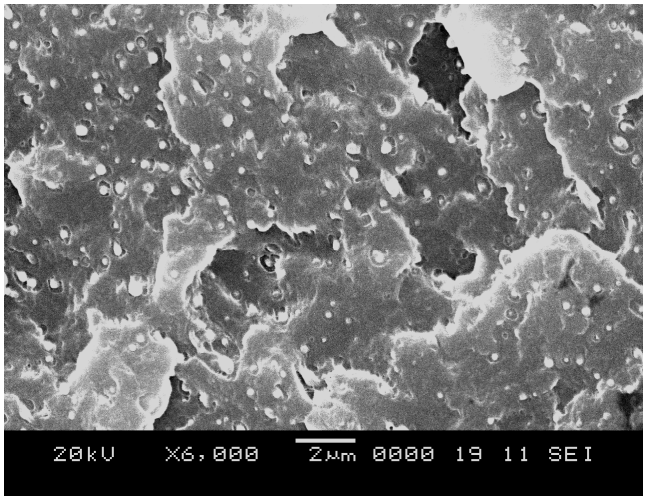


PA6-EG2

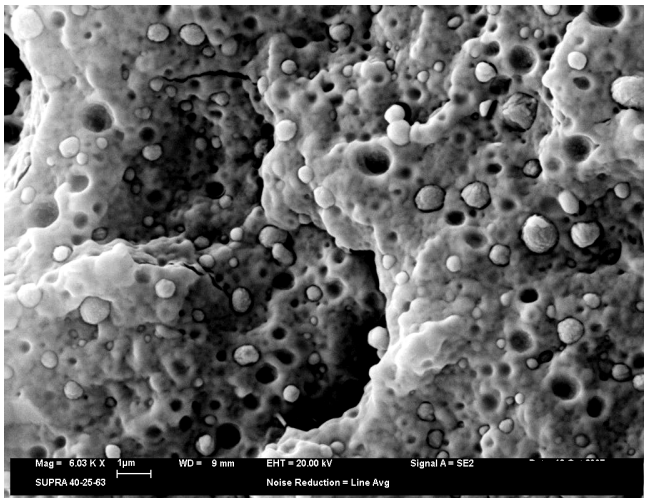


PA6-MG1

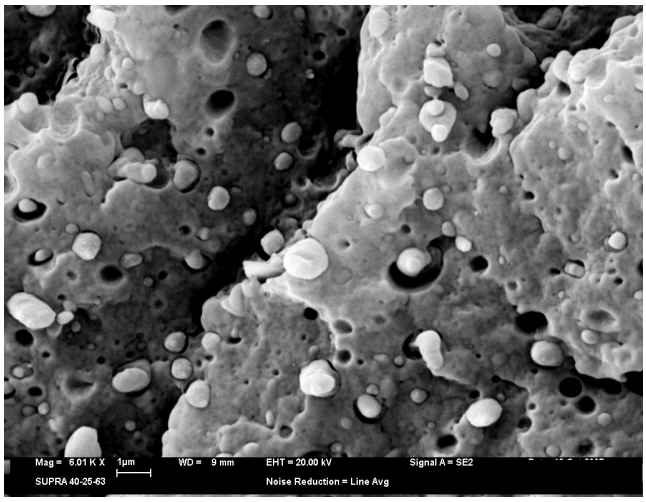


PA6-MG2

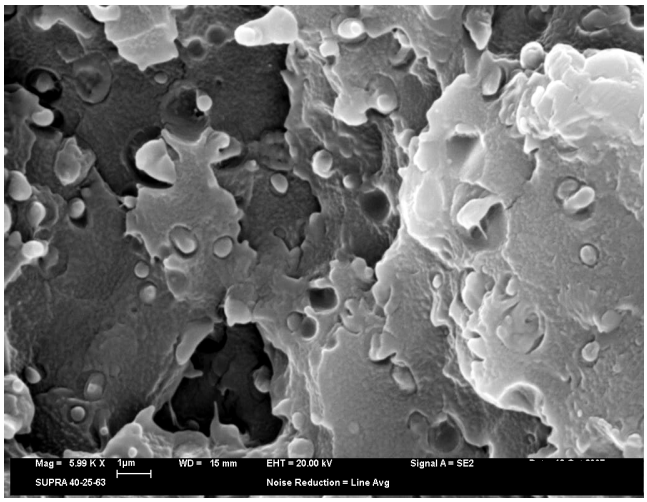


PA6-HM1

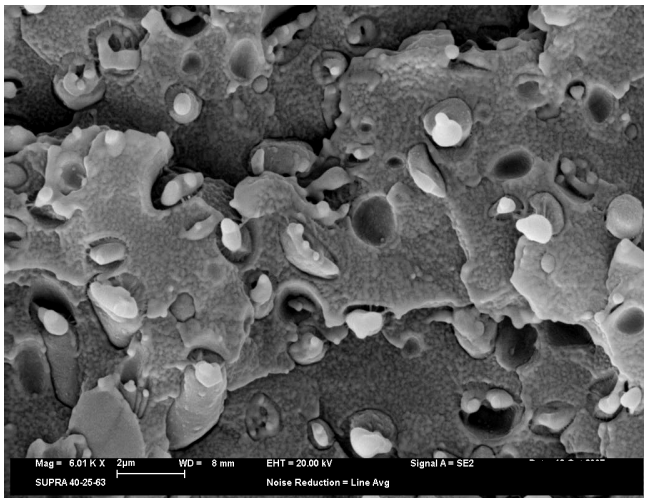


PA6-HM2

**Figure 4.18 SEM morphology of E-GMA, E-MA-GMA and HDPE-g-MAH compatibilised PA6/HDPE blends**

## 4.6 Conclusions

**HDPE/Compatibiliser Binary Blends:**

The crystalline phase of HDPE in binary blends of HDPE with compatibilisers is unmodified by the presence of the compatibilisers. However, miscibility and compatibility occur in the amorphous regions.

**Overall Performance of Compatibilisers:**

In this study, compatibilisers containing reactive epoxy moieties, in particular E-MA-GMA, are observed to have the most universal compatibilising effectiveness across the range of engineering thermoplastics studied (ABS, PC, PBT, and PA6) compared with EVA, EMA, and HDPE-g-MAH. As neither yield stress nor strain showed sensitivity towards blend compatibilisation, the comparison of overall performances of these compatibilisers is based on elongation at break, notched and reversed notch Izod impact strengths as presented in Table 4.10. It is observed that only E-MA-GMA is effective for at least one of these properties across all matrix resins.

**Table 4.10 Summary of blends with best performance in elongation at break, notched and reversed notch Izod Impact strengths**

| Matrix Polymer | Izod Impact | | Elongation @ Break |
|---|---|---|---|
| | Notched | Reversed Notch | |
| **ABS** | ABS-**MG1** | ABS-**MG1** | ABS-**MG1** |
| **PC** | PC-**MG1** | PC-**EG1** | PC-**EG2** |
| **PBT** | PBT-**MG1** | PBT-**MG1** | PBT-**EG2** |
| **PA6** | PA6-**MG1** | PA6-**EG2** | PA6-**EV2** |

Blends compatibilised with E-MA-GMA compatibiliser represented by the suffix “MG1” in Table 4.10 have the best notched impact performance irrespective of matrix polymer type. The presence of acrylic ester (methyl acrylate) comonomer in E-MA-GMA resulted in increased polarity of the compatibiliser leading to improved miscibility with the polar matrix polymers as demonstrated by fine blend morphologies, melting point depression and

reduction in crystallinity. ABS/HDPE blends are seen to be best compatibilised with E-MA-GMA possibly due to improved miscibility between E-MA-GMA and the SAN matrix of the ABS [194]. On the other hand, the acrylic ester could have restricted the diffusion of the E-MA-GMA compatibiliser towards the end-groups of the polyesters and polyamide due to its polar interaction with their carbonyl and amide groups in the main chain respectively. As such E-GMA compatibiliser, without the presence of an acrylic comonomer, has noticeably better performance for elongation at break of PC and PBT and reversed notch ductility in PC and PA6 blends due to easier access of the epoxy moiety to the end-groups of these polymers.

Surprisingly, EVA was the only non-reactive compatibiliser that imparted exceptionally good tensile ductility in PA6/HDPE blends. It could well be that the EVA has greater plasticising effect on the PA6 than other compatibilisers and therefore ductility may not necessarily be solely due to good interfacial adhesion of the phases.

**ABS/HDPE Blends:**

- Mechanical properties of ABS were dramatically reduced by the presence of an incompatible HDPE phase. None of the compatibilisers evaluated in this study was able to bring the mechanical properties back to the level of neat ABS polymer.
- Fractionated crystallisation of the HDPE phases was observed in all uncompatibilised and compatibilised blends.
- Very fine morphology imparted by a high concentration of E-MA-GMA (ABS-MG1 sample) contributed to high Izod impact toughness of the blends.
- Blends with the best notched and reversed notch Izod impact strength, and tensile elongation at break were compatibilised using E-MA-GMA as compatibiliser.

**PC/HDPE Blends:**

- The impact toughness of PC is very sensitive to the inclusion of HDPE phase. None of the compatibilisers evaluated in this study was able to bring the Izod impact properties back to the level of neat PC polymer. However, most of the compatibilisers were able to improve the ductility of the blends as shown by increase in elongation at break.
- Fractionated crystallisation of the HDPE phase was observed in all uncompatibilised and compatibilised blends.
- E-GMA imparted a very fine morphology with interconnected fibrils of the phases contributing to high Izod impact toughness of the blends.
- Blends with the best notched Izod impact strength are compatibilised with E-MA-GMA as compatibiliser while blends with the best reversed notch Izod impact strength and elongation at break were compatibilised with E-GMA.

**PBT/HDPE Blends:**

- The ductility, in terms of tensile elongation at break, of PBT is very sensitive to the inclusion of HDPE. None of the compatibilisers evaluated in this study was able to bring the elongation at break back to the level of the neat PBT polymer. However, most of the compatibilisers were able to improve the Izod impact strength of the blends significantly.
- Fractionated crystallisation of the HDPE phases was observed in all compatibilised blends.
- The crystalline phase of PBT remained unmodified by the presence of HDPE and compatibilisers. Interactions occurred mainly in the amorphous region of the PBT.
- E-GMA imparted a very fine morphology but high Izod impact toughness of the blends is dependent on critical particle size which is <0.7 µm.
- Blends with the best notched and reversed notch Izod impact strength were compatibilised with E-MA-GMA while blends with best elongation at break were compatibilised with E-GMA.

**PA6/HDPE Blends:**

- The ductility in terms of tensile elongation at break of PA6 is very sensitive to inclusion of the HDPE. Most of the compatibilisers evaluated in this study except EMA were able to bring the elongation at break to a higher level than the neat PA6 polymer.
- The crystalline phase of PA6 remained unmodified by the presence of HDPE and compatibilisers. Interactions occurred mainly in the amorphous region of the PA6.
- Fractionated crystallisation of the HDPE was not observed in any of the blends.
- E-GMA imparted a very fine morphology but high Izod impact toughness of the blends is dependent on critical particle size which is <1 µm.
- Blends with the best notched Izod impact strength were compatibilised with E-MA-GMA compatibiliser while blends with best reversed notch Izod impact strength were compatibilised with E-GMA. Blends with exceptionally high elongation at break were compatibilised with EVA.

# CHAPTER 5

# RESULTS AND DISCUSSION

# REACTIVE MODIFICATION OF HDPE

Studies conducted in Chapter 4 of this thesis show that epoxy functionality has the best compatibilisation efficiency in ABS/HDPE, PC/HDPE, PBT/HDPE and PA6/HDPE blends. This chapter of the research investigates the possibilities of utilising HDPE-g-MAH to form reactive sites for the grafting of a low molecular weight epoxy resin in ternary blends of HDPE/HDPE-g-MAH/epoxy. As there is limited miscibility and compatibility between HDPE and epoxy resins, the HDPE-g-MAH is expected to serve as compatibiliser for the ternary blends through the reaction between the maleic anhydride moiety of the HDPE-g-MAH and the oxirane ring of the epoxy resin and the miscibility between HDPE-g-MAH and HDPE resin. The resultant ternary blends with grafted epoxy functionality are expected to have good compatibility with a series of thermoplastic resins through reaction with end-groups of the polymer chains or polar interaction between the oxirane ring or hydroxyl groups of the grafted epoxy and the matrix resin.

The initial reactivity studies between the two reactive polymers were carried out in an extrusion plastometer (commonly utilised for the measurement of melt flow rates (MFR) of thermoplastic resins) with varying dwell time of the blends in its heated barrel. Analytical techniques such as FTIR, DSC, and optical microscopy were employed for the characterisation of the reactive ternary blends. The selected formulations were then scaled-up in a laboratory twin screw extruder and the compounded blends subjected to further characterisation.

The compounded HDPE/HDPE-g-MAH/epoxy ternary blends were subsequently investigated for compatibility with ABS, PBT and PA6 resins by injection moulding of these resins into test bars with the reactive ternary blends at 5 wt% dosage level. Notched and reversed notch Izod impact tests,

tensile tests, thermal analysis, and optical microscopy were conducted to assess the level of compatibility of the injection moulded blends.

## 5.1 Characterisation of Raw Materials

In this work, the selection of reactive components for the blends is vital in controlling the degree of grafting reactions. As highlighted by Chang [22], excessive grafting may result in a highly branched comb-like structure or even a crosslinked network and thus a lightly grafted copolymer is believed to be a more efficient compatibiliser than an excessively grafted one.

For the above reasons, a HDPE-g-MAH with a low level of grafted MAH (1 wt%) and a low molecular weight di-functional solid DGEBA type epoxy resin were selected for this investigation. Being solid at room temperature enables good physical mixing characteristics of the epoxy resin with other thermoplastic resins and additives in both pellets and powder forms before the extrusion (compounding) process. Because of the low molecular weight nature of the epoxy resin, effective diffusion of its functional groups to the blend interfaces for reaction can be expected.

As the reactive grafting process could cause a reduction in flow rates of HDPE resin due to possibilities of extensive chain branching and gelation as discussed earlier, a high flow rate injection moulding grade HDPE resin was selected for this study to ensure sufficient flowability of the final ternary blends.

### 5.1.1 The Influence of Moisture on Reactive Chemistry of Maleic Anhydride

It is known that cyclic maleic anhydride undergoes hydrolysis in the presence of water producing dicarboxylic acids while heating reverts these dicarboxylic acids back to the five-membered cyclic anhydride form [198]. These reversible reactions can be represented by Reaction Scheme 1. The dicarboxylic acids and five-membered cyclic anhydride can be identified through FTIR analysis and are represented by peaks located around 1714 $cm^{-1}$ (due to C=O stretching of carboxylic acid) and 1866 $cm^{-1}$ / 1790$cm^{-1}$ (due to asymmetric / symmetric C=O stretching of cyclic anhydride) respectively [58, 198]. The presence of another characteristic band around 916 $cm^{-1}$ is due to the symmetric COC stretching of the cyclic ethers.

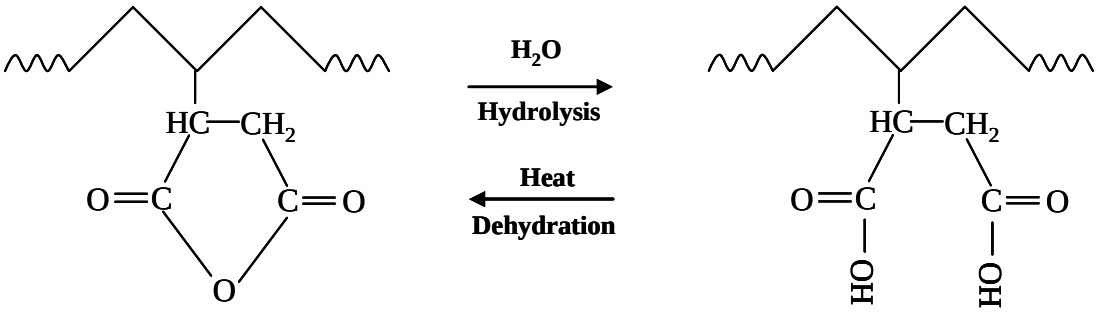


**Reaction Scheme 1: Hydrolysis and dehydration of maleic anhydride moiety of HDPE-g-MAH**

The HDPE-g-MAH used in this work contains both dicarboxylic acids and cyclic anhydride as shown in the FTIR spectrum in Figure 5.1. Some of the cyclic maleic anhydride moieties appeared to be hydrolysed by the atmospheric moisture during storage and also possibly by moisture that was picked up during the manufacturing (grafting) process. The sharp doublet at around 730 / 719 $cm^{-1}$ is a characteristic of the methylene rocking mode vibration of a partially crystalline or highly ordered long chain aliphatic hydrocarbon of the HDPE.

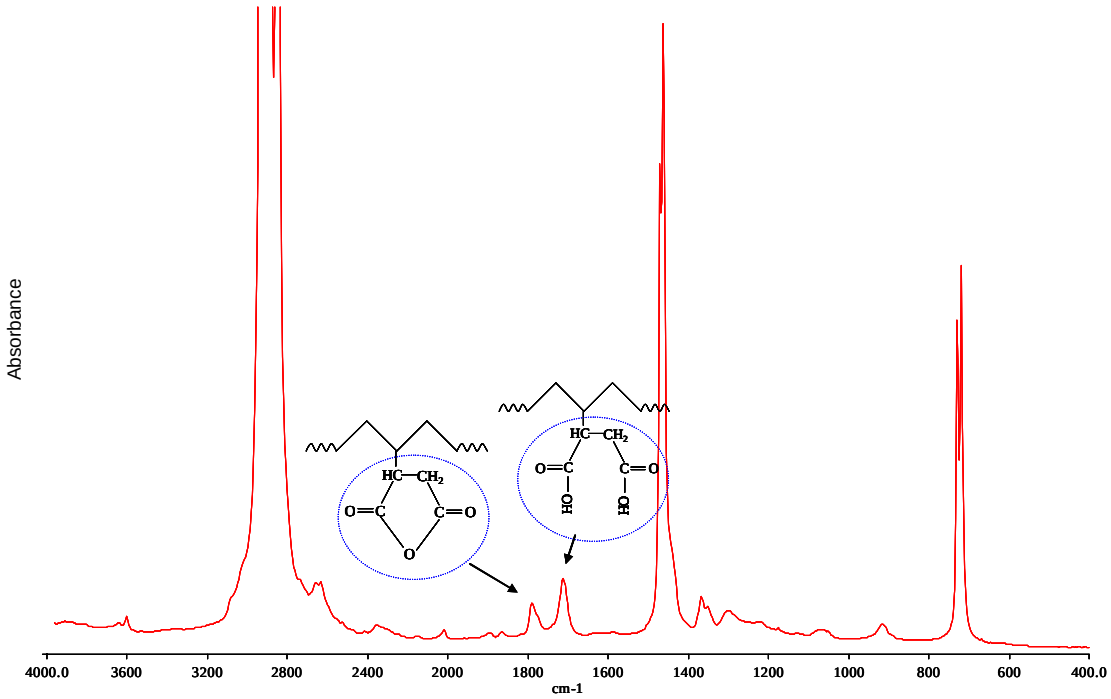


**Figure 5.1 FTIR spectrum of HDPE-g-MAH**

Heating the HDPE-g-MAH pellets in an oven at 110℃ converts the dicarboxylic acid back to their cyclic anhydride form as shown in Figure 5.2. The FTIR spectra indicate that it is possible to convert almost all dicarboxylic acid into its cyclic form after a prolonged heating time (above 40 hours).

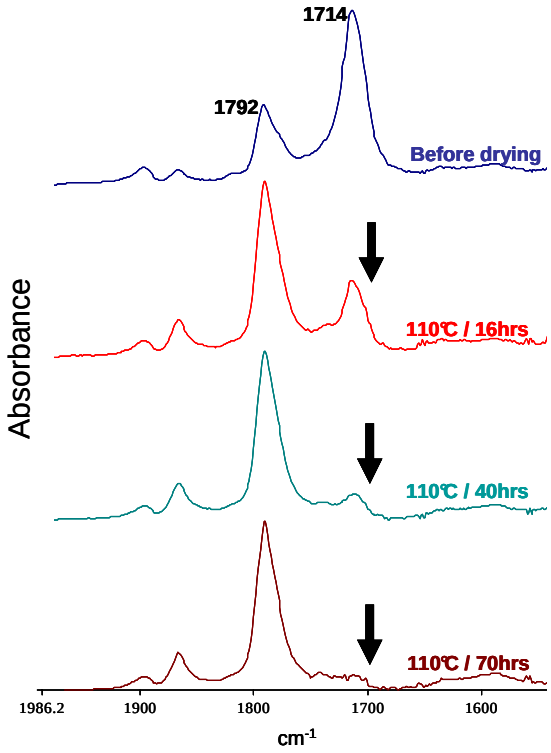


**Figure 5.2 FTIR spectra of HDPE-g-MAH with various drying time**

In this work, the HDPE-g-MAH functions as a compatibiliser between HDPE and epoxy through reaction between maleic anhydride and epoxy moieties. However, as shown in Reaction Scheme 2, it is known that the cyclic anhydride groups do not react directly with epoxy groups [199].

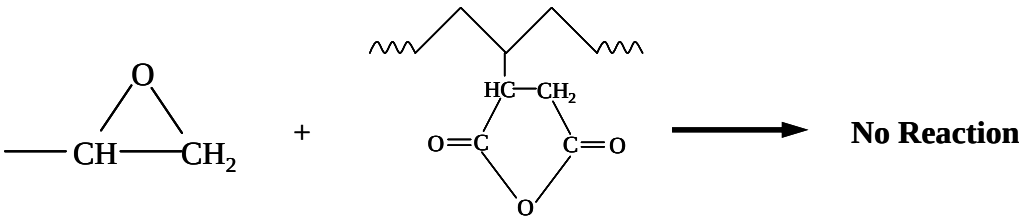


**Reaction Scheme 2: Reaction between epoxy and cyclic anhydride moieties**

Thus it is essential to convert the anhydride rings to dicarboxylic acid through the hydrolysis reaction shown in Reaction Scheme 1 before esterification with epoxy ring of the DGEBA can take place as illustrated in Reaction Scheme 3.

One of the carboxylic acid groups reacts with the epoxy ring to form a half-ester and a hydroxyl group. This is followed by another reaction of the remaining carboxylic acid moiety of the half-ester with another epoxy moiety to form an ester linkage and another hydroxyl group. Therefore as illustrated in Reaction Scheme 3, the DGEBA can be anchored onto the backbone of the HDPE molecule through esterification between the carboxylic acids and the epoxy ring.

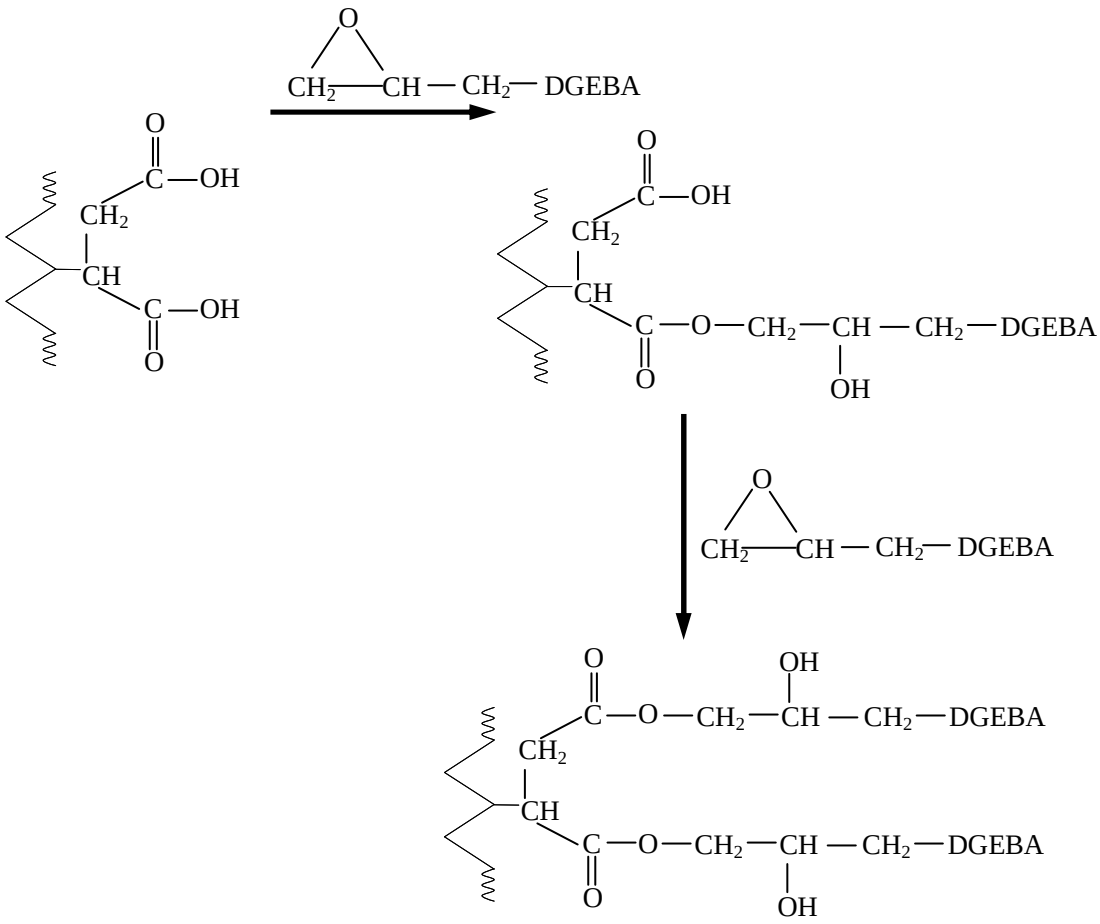


**Reaction Scheme 3: Expected esterification reaction between anhydride and epoxy group catalysed by hydrated zinc acetate**

Bayram and his co-workers [200, 201] reported the effectiveness of using hydrated zinc acetate as an esterification catalyst in reactions involving styrene maleic anhydride/GMA [200] and styrene maleic anhydride/polyol [201] blends. Hydrated zinc acetate has been selected in this study as a potential catalyst for catalysing the esterification reaction between the anhydride and epoxy groups as it is expected to be able to liberate water molecules during processing via dehydration as shown in Reaction Scheme 4 [202].

$$Zn(CH_3COO)_2 \cdot 2H_2O \longrightarrow Zn(CH_3COO)_2 + 2H_2O$$

**Reaction Scheme 4: Dehydration of zinc acetate dihydrate** [202]

Thermogravimetric analysis (TGA) performed on the hydrated zinc acetate as shown in Figure 5.3 indicates that the dehydration process started at around 72℃ and ends at around 114℃. About 16wt% of water was librated during the dehydration process and this is in good agreement with the molecular formula of the zinc dihydrate. Thus the liberation of water molecules from the hydrated zinc acetate can be expected during the compounding processes.

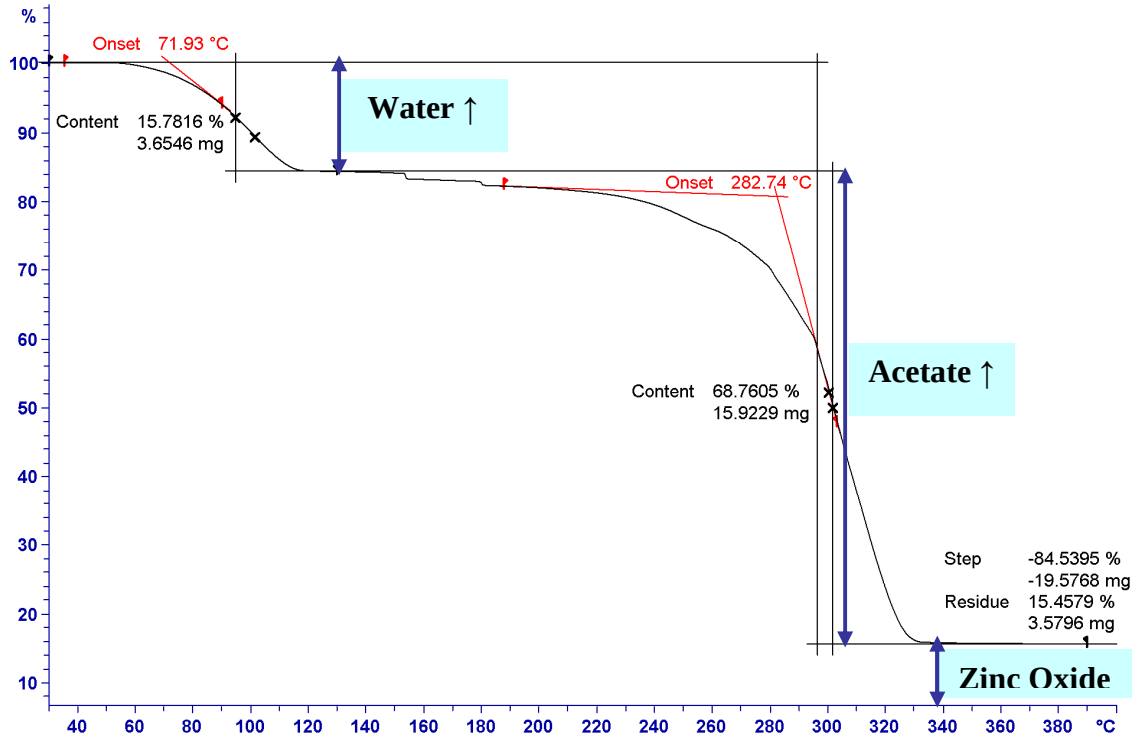


**Figure 5.3 TGA thermogram of zinc acetate dihydrate**

## 5.1.2 Structural Chemistry of Epoxy Resin

The FTIR spectrum of the DGEBA resin used in this study is presented in Figure 5.4. The spectrum reveals the presence of characteristic absorption bands of the para disubstituted aromatic ring at 829 $cm^{-1}$, epoxy group at 915 $cm^{-1}$, the geminal dimethyl groups of bisphenol A as a doublet at 1384 $cm^{-1}$ and 1362 $cm^{-1}$, the aromatic ether group at 1039 $cm^{-1}$ and 1245 $cm^{-1}$, and the hydroxyl group can be seen at 3446 $cm^{-1}$. The detailed peak assignments of this unreacted epoxy resin are listed in Table 5.1.

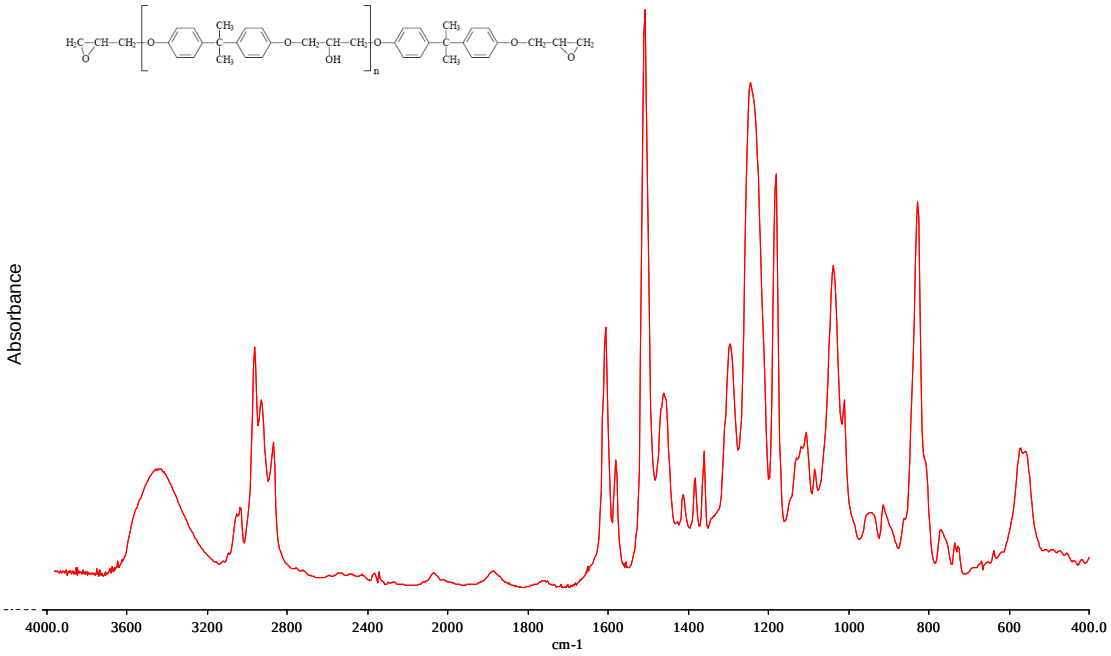


**Figure 5.4 FTIR spectrum of epoxy resin**

**Table 5.1 DGEBA Infrared Spectral Peak Assignments [203-205]**

| Wavenumber, $cm^{-1}$ | Assignment |
|---|---|
| 3446 | O-H stretching |
| 3055 | -CH-(O-$CH_2$) epoxy stretching |
| 3037 | Aromatic C-H stretching |
| 2966, 2931, 2872 | Aliphatic C-H stretching |
| 2070, 1887 | Disubstituted aromatic rings |
| 1607, 1582, 1509 | Aromatic C=C stretching |
| 1462 | Methylene C-H bend |
| 1413 | (C-H ) epoxy deformation |
| 1384 & 1362 (doublet band) | $CH_3$ bending of the geminal dimethly groups of bisphenol A |
| 1245 | Phenyl-oxygen stretching |
| 1183, 1085 | In-plane aromatic C-H bending |
| 1039 | Aromatic ether alkyl C-O stretching |
| 1012 | In-plane aromatic C-H bending |
| 945 | Out-of-plane aromatic C-H bending |
| 915 | Epoxy ring (CH-O-$CH_2$) deformation |
| 830, 573, 559 | Out-of-plane bending of 2 adjacent H of para-disubstituted aromatic rings |

Other than the 915 $cm^{-1}$ band, there are a total of three absorption bands which appear at 1253, 911 and 839 $cm^{-1}$ respectively and have been proposed to be the characteristic bands for the epoxide group [203]. As mentioned by Nishikida and Coates [203], for bisphenol A type epoxides, the first of these bands is expected to occur at around 1233 $cm^{-1}$. The overlapping of this band with the aromatic ether absorption band at 1245 $cm^{-1}$, leaves the 915 $cm^{-1}$ absorption of the terminal epoxy group,

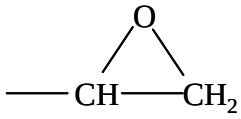


as the main band for characterization, and for monitoring the kinetics of curing and the determination of unreacted epoxide groups. However in this study, the 915 $cm^{-1}$ region of the epoxy spectrum cannot be utilised for the monitoring of epoxy reaction as it is overlapped by components of the HDPE and HDPE-g-MAH as illustrated in Figure 5.5. The 908 $cm^{-1}$ region of the HDPE spectrum is due to the presence of vinyl unsaturation (−CH = $CH_2$) while the 916 $cm^{-1}$ of the HDPE-g-MAH as discussed earlier is due to the symmetric COC stretching of the cyclic ether. Due to the overlapping of major FTIR absorption peaks of the terminal epoxy groups of the DGEBA, the carbonyl region of the blends were evaluated for possible reactions through monitoring of the maleic anhydride / dicarboxylic acid content and also formation of new ester groups due to esterification reactions.

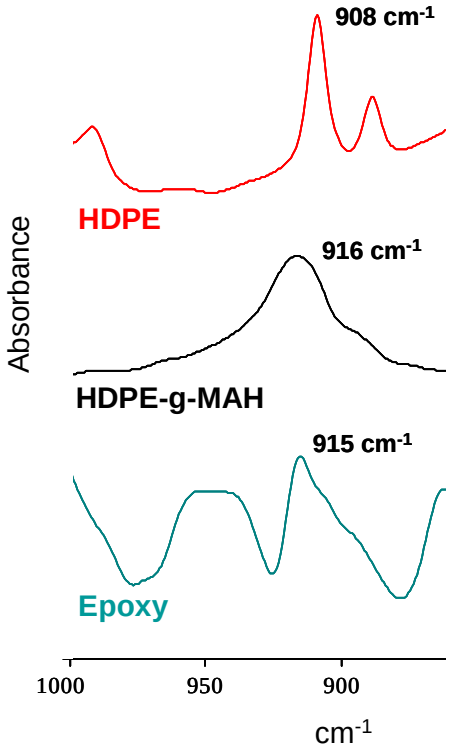


**Figure 5.5 FTIR spectra of HDPE, HDPE-g-MAH and Epoxy**

## 5.2 Functionalisation and Characterisation of HDPE Blends

In this section, the extrusion plastometer was used as a rheological, sample preparation, and formulation screening tool for studying the reactivity of various formulations with varying MAH, epoxy and catalyst concentrations. In order to improve the homogeneity of the blends in the barrel of the plastometer, all raw materials in pellet form were pulverised before the blending process. The extrudates obtained after 5 and 15 minutes preheating dwell time in the plastometer were subjected to further characterisation. The final formulation was selected for compounding in a twin screw extruder on the basis of a balance of melt flow behaviour, gel content, and evidence of reaction between the functional groups. An ethylene (vinyl actetate) (EVA) copolymer was selected for evaluation as a potential co-compatibiliser for improvement of miscibility and compatibility between the epoxy and

HDPE/HDPE-g-MAH blends on basis of good miscibility between poly(vinyl acetate) (PVAc) with uncured epoxy resins [206].

### 5.2.1 Reactive Studies on Maleic Anhydride and Epoxy Functionalities

Torque rheometers have been effectively utilised by many workers [2, 54, 70, 83, 85] in following compatibilisation reactions whereby an increase in mixing torque is commonly postulated to be associated with coupling reactions between reactive functional groups that result in increase in molecular weight and viscosity. Another simple and yet sensitive method for detecting changes in melt viscosity is melt flow rate (MFR) measurement. The MFR of reactive blends can be affected by factors such as chain extension(branching) and crosslinking. These reactions in the blends are normally manifested by reduction in MFRs which are related to increase in melt viscosity [54, 70, 87]. These MFR measurements are normally conducted with fixed dwell time but with varying concentrations of reactive functional groups for evidence of reaction and also for comparing the degree of reaction.

In this research, MFR was conducted using dwell times of 5 and 15 minutes. In this way, it also simulates the residence time of the blends in the extruder barrel which allows comparison in terms of degree of reaction of various reactive formulations. Table 5.2 summarises the MFR tests on various dry blends and compounded blends conducted at 190℃/2.1 6 kg with preheating dwell times of 5 and 15 minutes.

**Table 5.2 Melt flow rate of powder dry blends and compounded pellets samples**

| Sample Code | Active Components in Blends (wt%) | | | Melt Flow Rate Test at 190℃/2.16 kg (g/10 min) | |
|---|---|---|---|---|---|
| | MAH | Epoxy | Catalyst* | Dwell Time 5 min | Dwell Time 15 min |
| **HDPE** | - | - | - | **17.3** *(0.1)* | **17.3** *(0.0)* |
| **HDPE-g-MAH** | 1.0 | - | - | **3.7** *(0.2)* | **3.2** *(0.1)* |
| **HDPE-M1** | 0.5 | - | - | **9.3** *(0.3)* | **8.8** *(0.3)* |
| **HDPE-M2** | 0.25 | - | - | **12.9** *(0.2)* | **12.6** *(0.2)* |
| **HDPE-M3** | 0.1 | - | - | **15.4** *(0.0)* | **15.4** *(0.1)* |
| **HDPE-M4** | 0.05 | - | - | **16.4** *(0.1)* | **16.4** *(0.2)* |
| **HDPE-E1** | - | 6.0 | - | **28.1** *(0.5)* | **27.2** *(0.0)* |
| **HDPE-E2** | - | 3.0 | - | **21.0** *(0.9)* | **21.0** *(0.1)* |
| **HDPE-E3** | - | 1.2 | - | **19.0** *(0.6)* | **18.8** *(0.3)* |
| **HDPE-E4** | - | 0.6 | - | **18.0** *(0.2)* | **18.1** *(0.2)* |
| **HDPE-ME1** | 0.5 | 6.0 | - | **No Flow** | **No Flow** |
| **HDPE-ME1C** | 0.5 | 6.0 | 0.55 | **No Flow** | **No Flow** |
| **HDPE-ME2** | 0.25 | 3.0 | - | **3.2** *(0.1)* | **3.0** *(0.2)* |
| **HDPE-ME2C** | 0.25 | 3.0 | 0.28 | **3.6** *(0.3)* | **3.2** *(0.4)* |
| **HDPE-ME3** | 0.1 | 1.2 | - | **11.4** *(0.4)* | **9.5** *(0.1)* |
| **HDPE-ME3C** | 0.1 | 1.2 | 0.11 | **10.4** *(0.3)* | **10.3** *(0.3)* |
| **HDPE-ME3Ca** | 0.1 | 3.0 | 0.11 | **10.8** *(0.3)* | **10.6** *(0.1)* |
| **HDPE-ME3Ca$^{C}$** | 0.1 | 3.0 | 0.11 | **8.1** *(0.2)* | **8.1** *(0.1)* |
| **HDPE-ME4** | 0.05 | 0.6 | - | **15.1** *(0.4)* | **14.3** *(0.1)* |
| **HDPE-ME4C** | 0.05 | 0.6 | 0.06 | **15.1** *(0.2)* | **14.2** *(0.3)* |
| **HDPE-ME4Ca** | 0.05 | 3.0 | 0.06 | **14.9** *(0.2)* | **14.7** *(0.3)* |
| **HDPE-ME5Ca$^{\#C}$** | 0.1 | 3.0 | 0.11 | **7.4** *(0.1)* | **7.0** *(0.1)* |

***** *Hydrated zinc acetate catalyst,* $^{\#}$ *Formulation contains 3wt% EVA compatibiliser*

$^{C}$ *Compounded pellets samples, Values in parentheses denote standard deviations*

Results of samples HDPE-M1 to HDPE-M4 with varying maleic anhydride concentrations presented in Table 5.2 show that MFRs of HDPE were reduced when blended with low flow HDPE-g-MAH compatibiliser and were not significantly affected by MFR dwell time. Based on the simplest rule of mixture [207], the addition of low flow rate HDPE-g-MAH is expected to reduce the flow rate of the original HDPE resin and more reduction could be expected as the amount of HDPE-g-MAH is increased. Figure 5.6 illustrates

that the MFR of blends of HDPE/HDPE-g-MAH followed the trend in rule of mixtures but were consistently lower than the theoretically calculated values. Results also showed that the deviation became larger as the contents of HDPE-g-MAH were increased. This is likely to be due to inhomogenity in melt mixing between HDPE and HDPE-g-MAH phases.

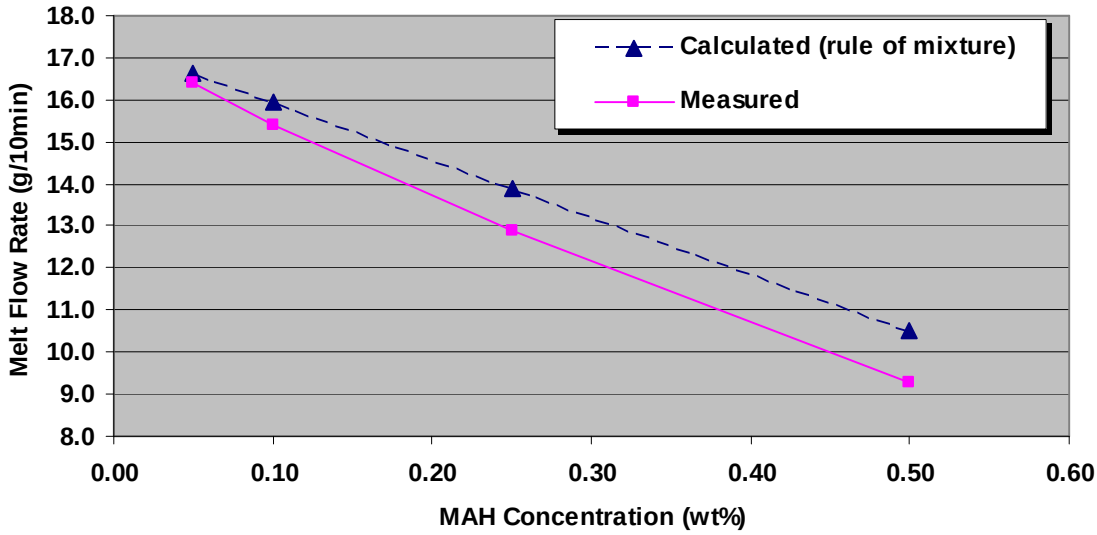


**Figure 5.6 Plots of theoretical against measured MFR values (5 minutes dwell time) of HDPE/HDPE-g-MAH blends**

On the other hand, the addition of epoxy improved the flow of HDPE as shown in samples HDPE-E1 to HDPE-E4 (Table 5.2) which are also not affected by dwell time. Table 5.2 shows that the addition of 6 wt% of epoxy into blends containing 0.5 wt% of MAH (HDPE-ME1, HDPE-ME1C) resulted in a no flow phenomenon which indicated extensive reaction of the blends has taken place in the barrel of the plastometer.

Figure 5.7 summarises results from Table 5.2 showing the influence of epoxy on blends with various concentrations of MAH. At the same epoxy concentration of 3 wt%, the reduction in MFR of the blends became less significant as the MAH concentration were reduced indicating less extent in reaction. At the same MAH and epoxy concentrations, the sample compounded with a twin screw extruder (HDPE-ME3Ca$^{C}$) exhibited a lower MFR than its respective dry blend sample prepared in a plastometer (HDPE-ME3Ca). This is likely to be due to longer heat history and higher shear stress

experienced by the blends during the extrusion process which resulted in higher degree of reaction as compared with blends prepared in a plastometer which exerts much lower shear and heat history.

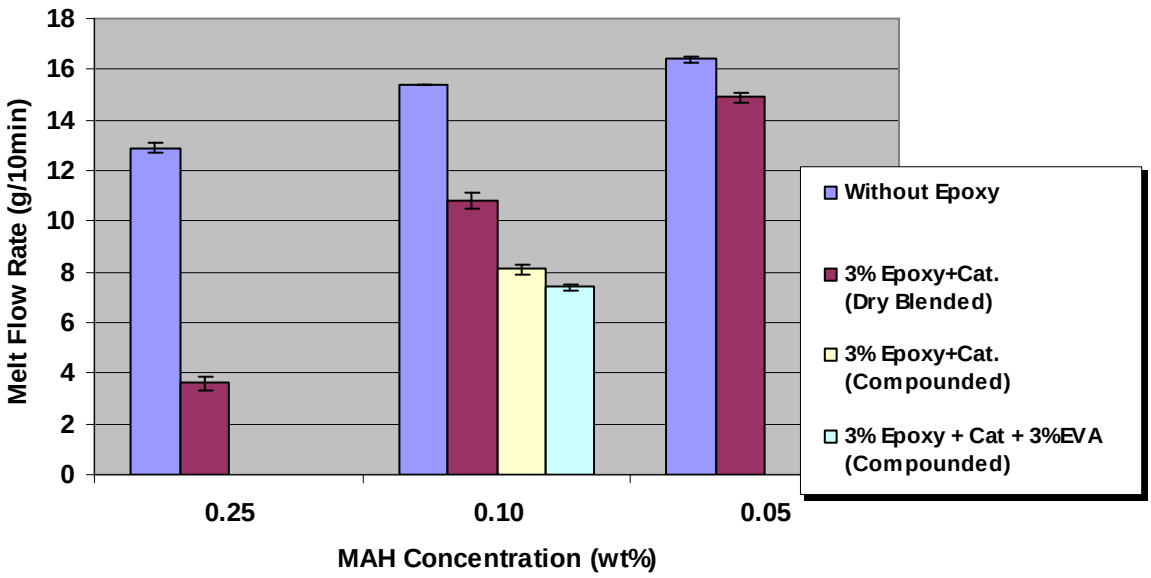


**Figure 5.7 Effect of epoxy, EVA, and compounding on the melt flow rate (5 minutes dwell time) of HDPE/HDPE-g-MAH blends**

Significant increases in MFR of samples HDPE-ME2 and HDPE-ME2C compared with HDPE-ME1 and HDPE-ME1C were observed even though the concentrations of functional groups in these samples were only half of HDPE-ME1 samples. The presence of EVA in the compounded sample, HDPE-ME5Ca, resulted in slight MFR reduction compared with sample HDPE-ME3Ca having same concentration of functionality but without EVA. Since the generic MFR of EVA is about 19.7 g/10 mins, its flow is even higher than the HDPE resin. Thus the reduction of MFR in the presence of EVA could possibly be due to the enhanced dispersibility of the epoxy resin in the blends rendering a higher chance of interaction with the MAH.

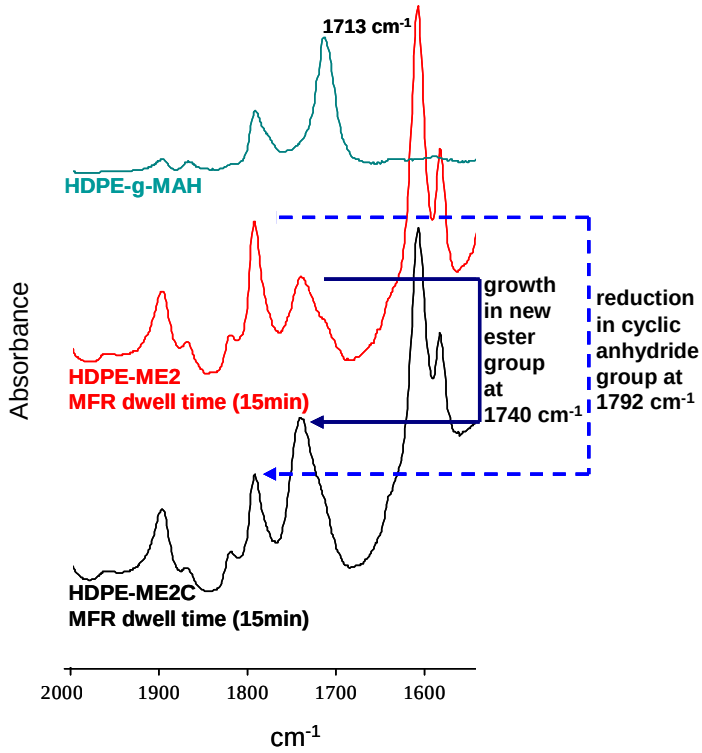


**Figure 5.8 FTIR spectra of HDPE-g-MAH, uncatalysed (HDPE-ME2) and catalysed (HDPE-ME2C) HDPE/HDPE-g-MAH/epoxy blends.**

Results in Table 5.2 also show that the presence of hydrated zinc acetate catalyst has a relatively insignificant effect on the flow rates of the blends. However, FTIR analysis of catalysed and uncatalysed blends in Figure 5.8 shows more intense growth of the new ester peak at 1740 $cm^{-1}$ for the catalysed blend indicating that an esterification reaction had taken place between maleic anhydride and epoxy moieties [208]. The reduction of the absorbance peak at 1792 $cm^{-1}$ provides further evidence that more anhydride is disappearing due to the esterification reaction with epoxy catalysed by the hydrated zinc acetate. FTIR spectra of blends with various concentrations of maleic anhydride and epoxy are presented in Figure 5.9 (a). It can be observed from the spectra that a new ester carbonyl group at about 1740$cm^{-1}$ was generated by the reaction between maleic anhydride groups and the epoxy groups catalysed by hydrated zinc acetate at 190$^{o}$C for 15 minutes.

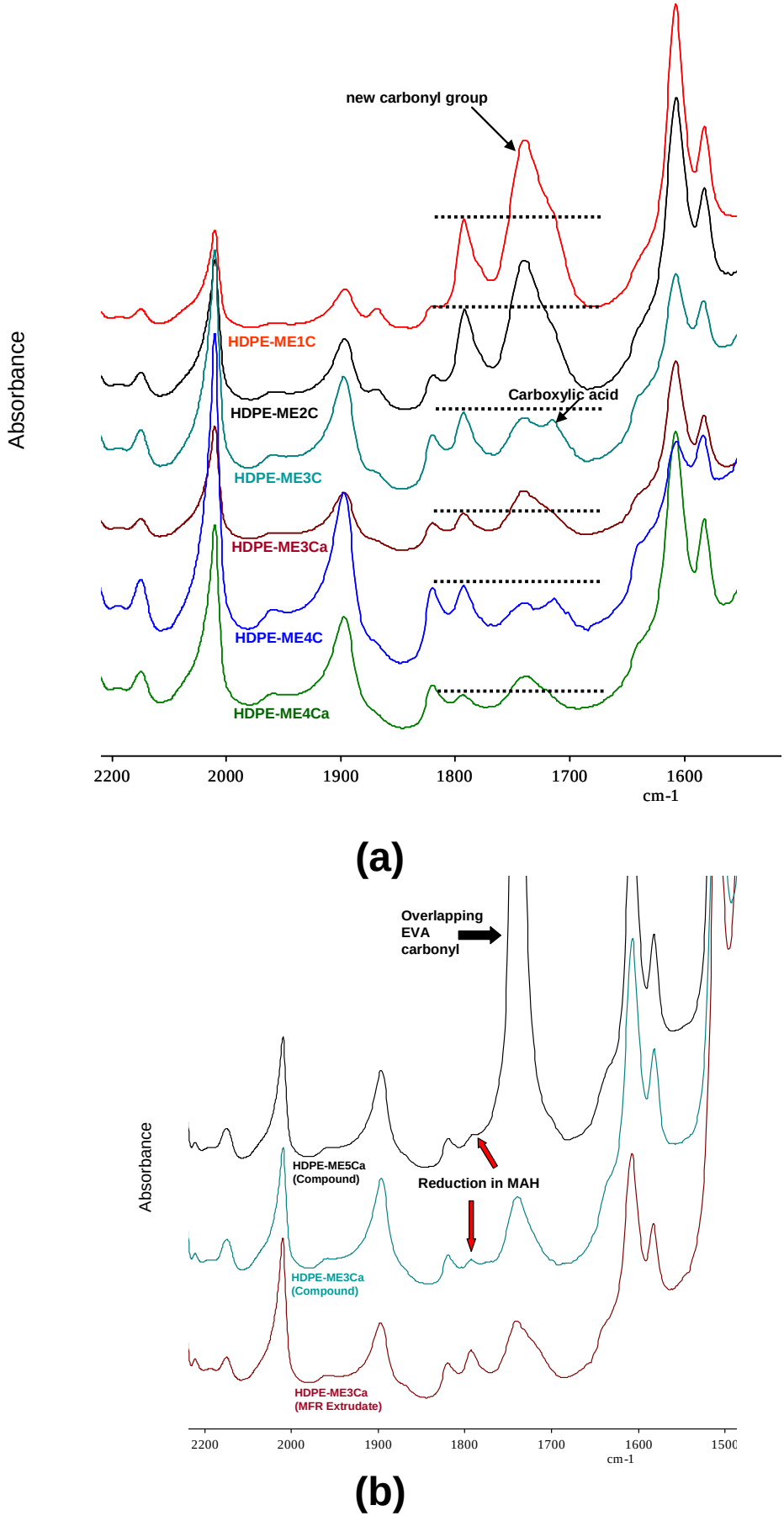


**Figure 5.9 FTIR spectra of HDPE/HDPE-g-MAH/Epoxy blends from (a) extrudates of MFR tests with 15 minutes dwell time (b) compounding**

Figure 5.9 shows that at low maleic anhydride and epoxy contents, HDPE-ME3C and HDPE-ME4C, the carbonyl groups at 1740 $cm^{-1}$ is less pronounced and the carboxylic acid peak is present at about 1713 $cm^{-1}$ indicating incomplete reaction between the epoxy and dicarboxylic acid moieties. This is possibly the result of poor miscibility of the epoxy at low maleic anhydride concentrations restricted the chances of interactions between the functional groups. However, the carboxylic acid peaks disappeared as the epoxy content was increased as shown in samples HDPE-ME3Ca and HDPE-ME4Ca. Both blends are observed to have a more pronounced carbonyl peak at 1740 $cm^{-1}$ which was greater than that of the maleic anhydride carbonyl peak at about 1790 $cm^{-1}$. HDPE-ME4Ca having less maleic anhydride than HDPE-ME3Ca is observed to have a less intense 1740 $cm^{-1}$ peak.

The new ester peak at 1740 $cm^{-1}$ is the most pronounced for sample, HDPE-ME1C, which contains very high concentrations of epoxy (at 6 wt%) and maleic anhydride (at 0.5 wt%). This observation is in good agreement with the earlier observation of no flow phenomenon during the MFR test which indicates extensive reaction has taken place. Such extensive reaction could possibly result in chain branching and or crosslinking leading to a dramatic reduction in MFR.

The FTIR spectra in Figure 5.9 (b) show the influence of compounding on the reactivity of the blends with same MAH and epoxy components and also with EVA as co-compatibiliser. As discussed earlier, the sample that is compounded using a twin screw extruder had a lower MFR than that prepared from a extrusion plastometer. The blue spectrum in Figure 5.9 (b) which belongs to compounded blend HDPE-ME3Ca has a less pronounced peak at 1790 $cm^{-1}$ as compared with blend that is prepared by the extrusion plastometer which is represented by the red FTIR spectrum. This indicates that more maleic anhydride moieties have been consumed in the reaction with epoxy rings during compounding in a twin screw extruder and thus a more intense reaction has taken place. The sample containing EVA co-compatibiliser also shows less pronounced peak at 1790 $cm^{-1}$. The strong

absorbance peak at 1740 $cm^{-1}$ is due to the overlapping of the EVA carbonyl groups and thus the formation of new carbonyl group at 1740 $cm^{-1}$ due to reaction of maleic anhydride and epoxy cannot be distinguished from the spectrum.

The thermal analysis results of the reactive HDPE blends of extrudates obtained from MFR tests with 5 minutes and 15 minutes dwell time as well as compounded blends are summarised in Table 5.3. Examples of DSC traces can be found in Appendices A1-23 to A1-32.

It is evident from the results that both the melting and crystallisation behaviour of the HDPE phase are modified due to reactive blending. In general, the reactive blends are observed to have higher melting point, higher onset of crystallisation, lower degree of crystallinity, and slower rate of crystallisation. The observed changes are possibly related to the reactions between the maleic anhydride and epoxy moieties of the blends.

At high maleic anhydride and epoxy contents (HDPE-ME1 and HDPE-ME1C samples), the degree of HDPE crystallinity were dramatically reduced even though the onset of crystallisation temperatures were higher than the unmodified HDPE resin indicating the possibility of a nucleating effect. The observed nucleating effect is likely to be influenced by the presence of the epoxy phase of the blends. The nucleation of PP by the presence of epoxy resin has been reported by Jiang and co-workers [83-85]. Similarly, despite the nucleating effect of the epoxy, they observed a reduction in degree of crystallinity of the PP phase. However, in their study [84] the nucleating effect resulted in higher overall rate of crystallisation of the PP which was reflected by the reduction in of the difference between the onset and peak crystallisation temperatures ($\Delta$TC). In this study, the opposite trend in terms of rate of crystallisation is observed. The increased in $\Delta$TC observed in this study could possibly be due to the occurrence of gelation which hindered the rate of crystallisation.

**Table 5.3 Thermal analysis of MFR extrudates and compounded pellets samples**

| Sample Code | HDPE Phase | | | | | |
|---|---|---|---|---|---|---|
| | Tm (℃) | ΔHf [a] (J/g) | $X_c$ (%) | $TC_{Onset}$ (℃) | $TC_{Peak}$ (℃) | ΔTC (℃) |
| **HDPE*** | **130** *(1)* | **189.8** *(0.4)* | **65** *(0)* | **118** *(0)* | **116** *(0)* | **2** |
| **HDPE-ME1^** | **131** *(0)* | **168.0** *(2.9)* | **57** *(1)* | **119** *(0)* | **115** *(1)* | **4** |
| **HDPE-ME1^^** | **131** *(1)* | **161.7** *(3.3)* | **55** *(1)* | **119** *(0)* | **114** *(1)* | **5** |
| **HDPE-ME1C^** | **131** *(0)* | **161.2** *(3.5)* | **55** *(1)* | **119** *(0)* | **114** *(1)* | **5** |
| **HDPE-ME1C^^** | **131** *(0)* | **158.8** *(1.3)* | **54** *(0)* | **119** *(0)* | **114** *(0)* | **5** |
| **HDPE-ME2^** | **132** *(0)* | **170.4** *(0.8)* | **58** *(0)* | **119** *(0)* | **117** *(0)* | **2** |
| **HDPE-ME2^^** | **132** *(0)* | **169.1** *(0.3)* | **58** *(0)* | **119** *(0)* | **116** *(0)* | **3** |
| **HDPE-ME2C^** | **132** *(0)* | **164.7** *(1.1)* | **56** *(0)* | **119** *(0)* | **116** *(1)* | **3** |
| **HDPE-ME2C^^** | **132** *(0)* | **168.7** *(0.4)* | **58** *(0)* | **119** *(0)* | **116** *(1)* | **3** |
| **HDPE-ME3^** | **132** *(0)* | **173.9** *(1.5)* | **59** *(1)* | **119** *(0)* | **117** *(0)* | **2** |
| **HDPE-ME3^^** | **132** *(0)* | **172.2** *(1.3)* | **59** *(1)* | **119** *(0)* | **117** *(0)* | **2** |
| **HDPE-ME3C^** | **132** *(0)* | **172.1** *(2.0)* | **59** *(1)* | **119** *(0)* | **117** *(0)* | **2** |
| **HDPE-ME3C^^** | **132** *(0)* | **172.2** *(1.2)* | **59** *(0)* | **119** *(0)* | **117** *(0)* | **2** |
| **HDPE-ME3Ca^** | **132** *(0)* | **174.7** *(1.6)* | **60** *(1)* | **119** *(0)* | **117** *(0)* | **2** |
| **HDPE-ME3Ca^^** | **132** *(0)* | **174.5** *(2.5)* | **60** *(1)* | **119** *(0)* | **117** *(0)* | **2** |
| **HDPE-ME3Ca[C]** | **133** *(0)* | **177.1** *(1.5)* | **60** *(1)* | **121** *(0)* | **118** *(0)* | **3** |
| **HDPE-ME4^** | **132** *(1)* | **173.2** *(1.1)* | **59** *(0)* | **119** *(0)* | **117** *(0)* | **2** |
| **HDPE-ME4^^** | **132** *(0)* | **173.4** *(3.6)* | **59** *(1)* | **119** *(0)* | **117** *(0)* | **2** |
| **HDPE-ME4C^** | **132** *(0)* | **173.3** *(2.7)* | **59** *(1)* | **119** *(0)* | **117** *(0)* | **2** |
| **HDPE-ME4C^^** | **132** *(0)* | **173.7** *(2.1)* | **59** *(1)* | **119** *(0)* | **117** *(0)* | **2** |
| **HDPE-ME4Ca^** | **133** *(0)* | **176.7** *(0.5)* | **60** *(0)* | **119** *(0)* | **117** *(0)* | **2** |
| **HDPE-ME4Ca^^** | **132** *(0)* | **175.8** *(3.4)* | **60** *(1)* | **119** *(0)* | **117** *(0)* | **2** |
| **HDPE-ME5Ca[#C]** | **133** *(0)* | **176.0** *(0.4)* | **60** *(0)* | **121** *(0)* | **118** *(1)* | **3** |

*Values in parentheses denote standard deviations*
***** *Data from Table 4.1 for comparison purposes*
**^** *Extrudates with 5 minutes dwell time in extrusion plastometer*
**^^** *Extrudates with 15 minutes dwell time in extrusion plastometer*
[a] *Values normalised to the amount of the relevant phase*
[C] *Compounded Samples in pellets form*
[#] *Formulation contains 3 wt% EVA compatibiliser*

In general, the melting temperatures of HDPE phases in all blends were higher than the unmodified HDPE resin indicating of the presence of larger HDPE crystals in the reactive blends.

The sample of HDPE-ME3Ca[c] which was prepared by the twin screw compounding exhibited more intense nucleation as both the onset and peak of crystallisation exotherm were higher than blends prepared via the extrusion

plastometer. The more intense shearing in the compounding process may have produced blends with much finer epoxy dispersed phase and thus a more nucleated HDPE phases. On the other hand, the dwell time of the MFR test did not appear to have a significant influence on the melting and crystallisation behaviour of the extrudates.

### 5.2.2 Miscibility and Morphological Studies of Blends

Optical microscopy is a powerful technique commonly employed for investigation of miscibility [81] and crystalline morphology [83, 84] of polymer blends. In this study, a polarising optical microscope was employed to study the dispersibility of epoxy phases and their influences on spherulitic textures of HDPE in HDPE/HDPE-g-MAH/epoxy blends.

Figure 5.10 shows the influence of the epoxy dispersed phase on the spherulitic textures of HDPE. In Figure 5.10 (a) the spherulitic structures of unmodified HDPE resin are large and well defined. However, the addition of 3 wt% epoxy resin in Figure 5.10 (b) results in a decrease in the size of the HDPE spherulites with less defined spherulitic texture.

The reduction in spherulite size suggests that the epoxy resin acts as a nucleating agent and is in good agreement with the shifts in onset of crystallisation temperature observed earlier during DSC analysis of the blends. When observed under transmitted light in Figure 5.10 (c), both large and small epoxy dispersed phases of about 18 to 28 µm and < 4 µm respectively, can be seen located on the HDPE matrix indicating poor dispersion and miscibility of epoxy with HDPE. The dispersed phase appeared as dark spots under polarised light.

(a)

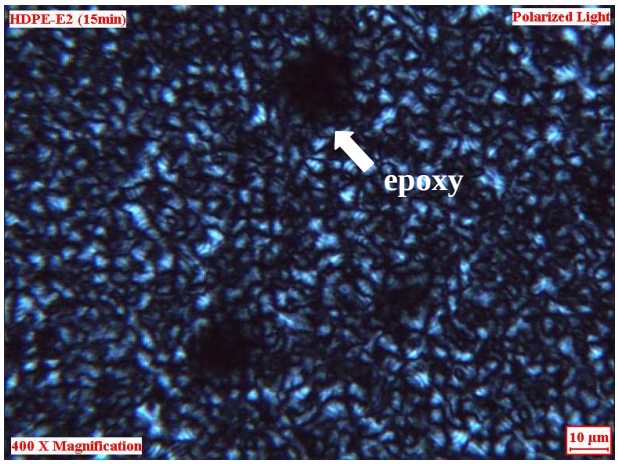


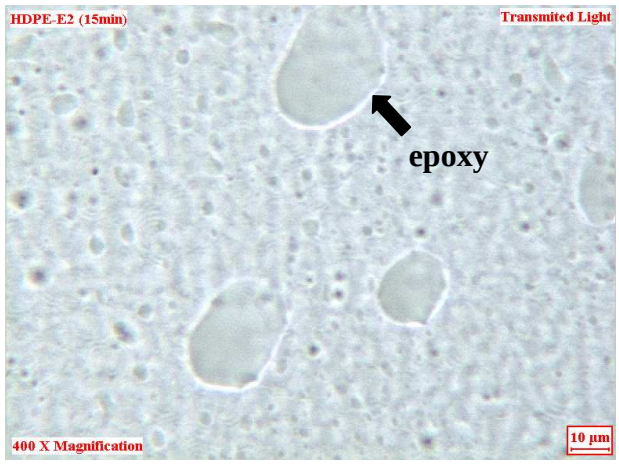


(b) (c)

**Figure 5.10 Optical micrographs (400 x magnification) of (a) HDPE under polarised light and uncompatibilised HDPE/3%epoxy extrudates (with 15 minutes dwell time) under (b) polarised light and (c) transmitted light**

Figure 5.11 shows that the miscibility of epoxy with HDPE can be improved with the addition of HDPE-g-MAH. Increasing MAH concentrations reduce the size of epoxy dispersed phases observed under transmitted light. Faint streaks are also observed in these micrographs which appeared as bright streaks when observed under polarised light. According to Scheirs [209] polymeric gels will appear as bright spots when observed under polarised light which suggests that the bright streaks observed in Figure 5.11 are likely to be crosslinked gels of the blends. The bright streaks become less distinct when MAH concentration in the blends was reduced.

**Polarised Light** **Transmitted Light**

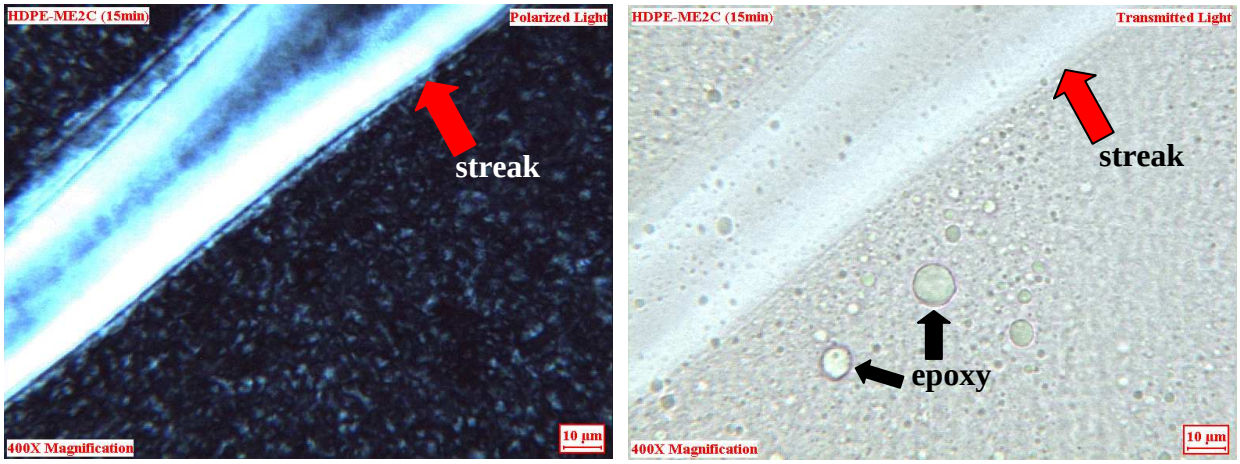


**(a) HDPE-ME2C**

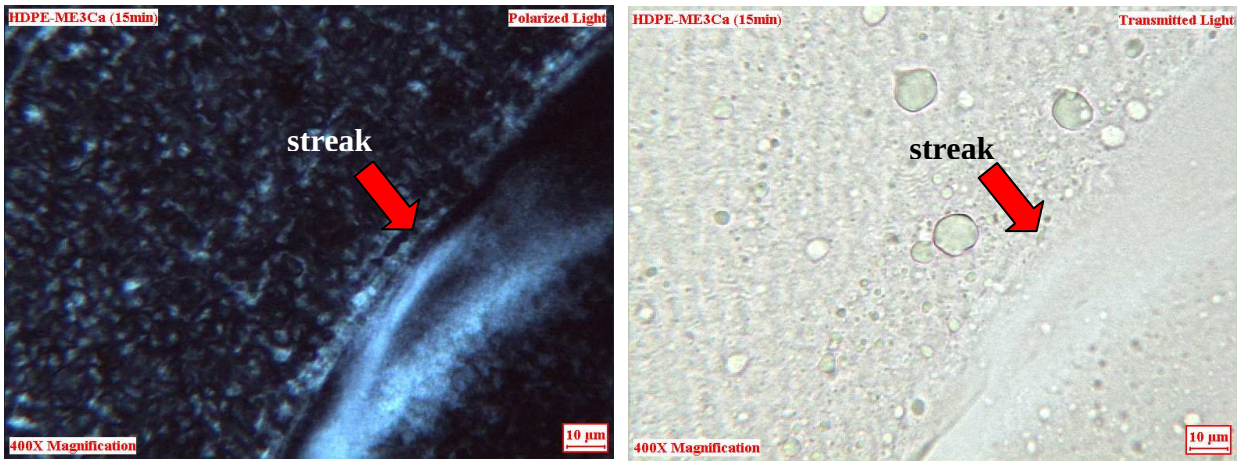


**(b) HDPE-ME3Ca**

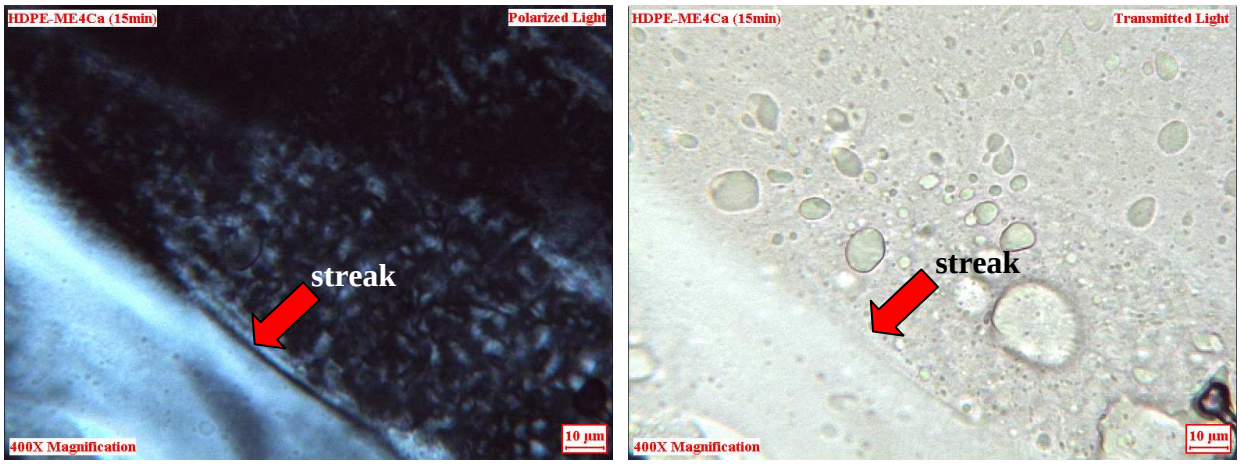


**(c) HDPE-ME4Ca**

**Figure 5.11 Optical micrographs (400 x magnification) of extrudates (with 15 minutes dwell time) of compatibilised HDPE/HDPE-g-MAH/Epoxy blends (a) 0.25%MAH/3%epoxy (b) 0.10%MAH/3%epoxy (c) 0.05%MAH/3%epoxy**

The dispersion quality of the epoxy can be improved when the blends are produced using a twin screw extruder. Figure 5.12 (a) shows that the size of the epoxy dispersed phase of the blend containing 0.1 wt% MAH / 3 wt% epoxy can be reduced to less than 4 µm after compounding. Bright specks were observed when the blend was viewed under polarised light suggesting presence of gels in the matrix. The finer spherulitic texture observed indicates a higher degree of nucleation than for the uncompounded blends which was confirmed earlier by DSC crystallisation data of the blend.

On the other hand, Figure 5.12 (b) shows the addition of 3 wt% EVA in the same blend resulted in a dramatic reduction of the size of the epoxy phase to less than 1 µm. This confirms that EVA serves as a good co-compatibiliser for the blend as the ethylene segment is miscible with the HDPE matrix while the vinyl acetate can be solubilised in the epoxy phases [206] thus reducing the interfacial tension of the blend. The presence of EVA also resulted in finer spherulitic texture and reduced gel content (reduced bright specks) when viewed under polarised light.

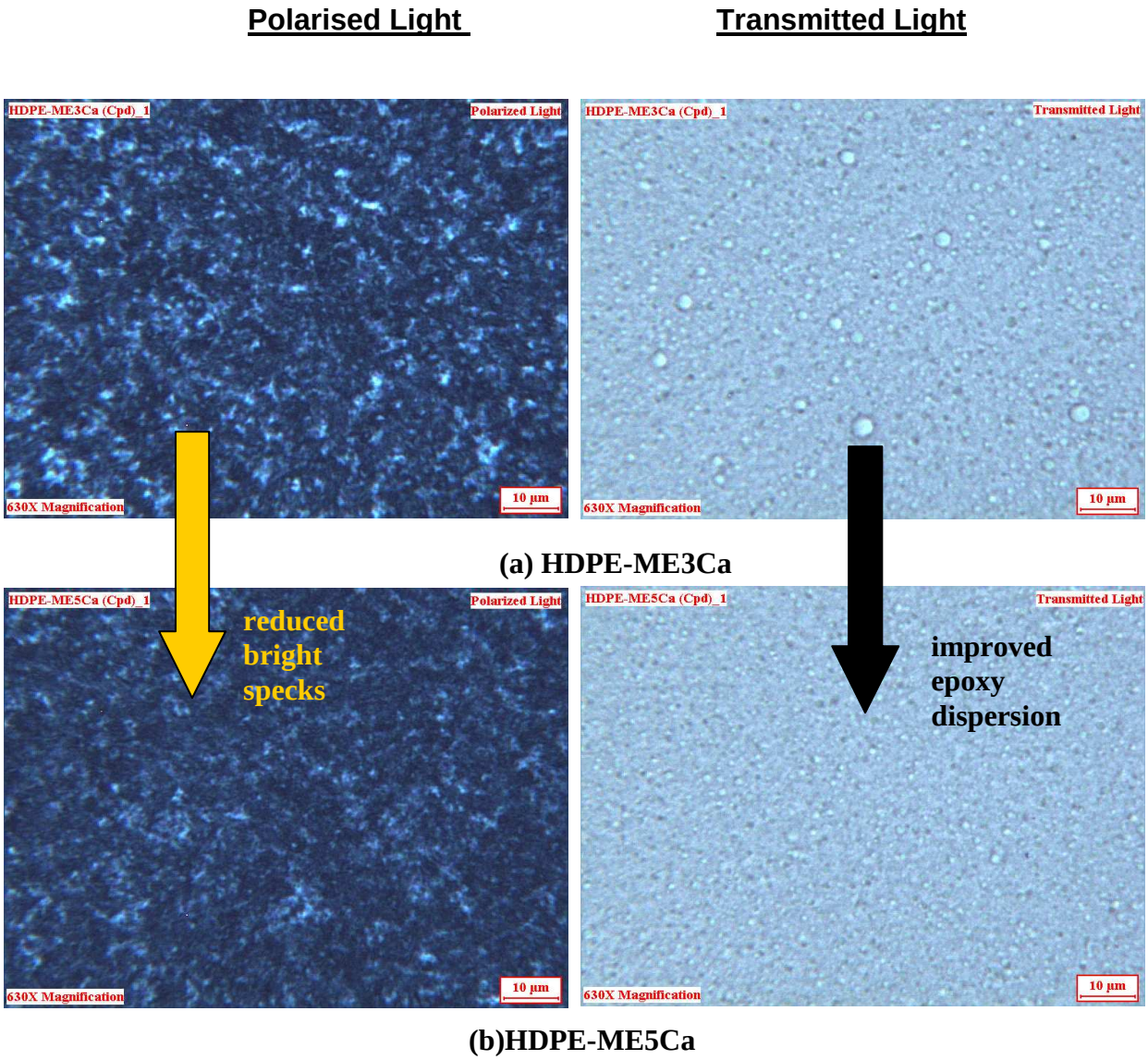


**Figure 5.12 Optical micrographs (630 x magnification) of compounded blends (a) 0.1%MAH/3%epoxy (b) 0.1%MAH/3%epoxy/3%EVA**

### 5.2.3 Characterisation of Gels and Other Soluble Components

In order to verify whether chain branching or crosslinking has taken place in the reactive blends, the extrudates obtained from both extrusion plastometer and twin screw extrusion (samples in pellets form) were subjected to extraction with xylene at 160℃ for 14 hours. The amount of insoluble fractions of residues retained in the stainless steel mesh cage after the extraction processes were considered as a measure of gel content. In this study, the gels obtained after solvent extraction processes were recovered

and characterised using DSC and FTIR-ATR (attenuated total reflectance) methods as these gels exhibited rubbery behaviour with very high viscosity when subject to heating and could not therefore be melt pressed into films.

As shown in Figure 5.13 the solutions obtained after the extraction of samples HDPE-ME3Ca (compounded) and HDPE-ME5Ca (compounded) appeared to have precipitated during cooling as HDPE is insoluble in xylene at room temperature. The round bottom flask containing sample HDPE-ME3Ca has a clearer solution compared with that of sample HDPE-ME5Ca which appears cloudy. Both solutions and precipitates were sampled for further analysis using the FTIR-ATR method.

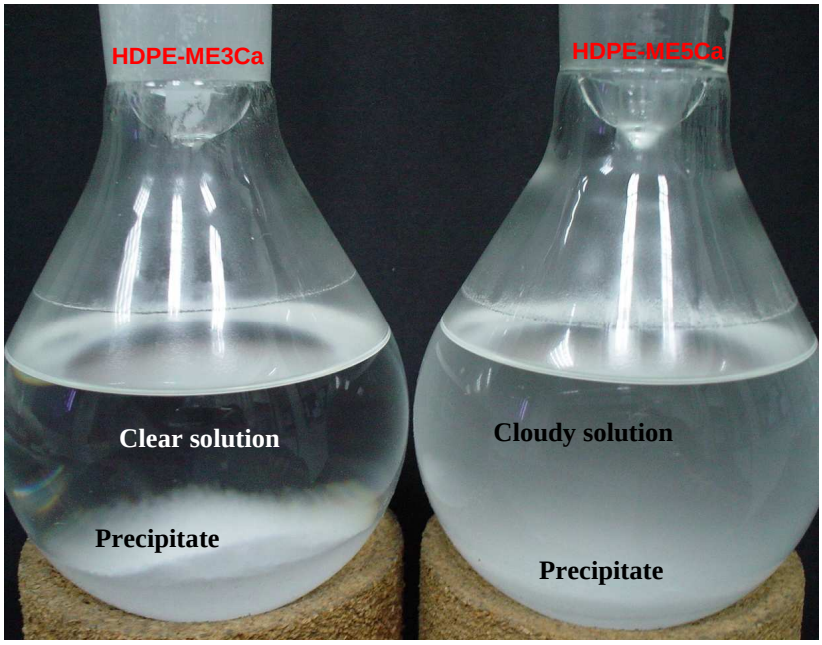


**Figure 5.13 Solutions of samples HDPE-ME3Ca and HDPE-ME5Ca after extraction**

Results of gel content analysis are presented in Table 5.4. The gel contents correlate well with the MFR results discussed earlier in Section 5.2.1. The lower the MFR of the blends, the higher the gel content as the gels hinder the flow of the blends. In general, the presence of catalyst resulted in higher gel content of the blends which is in good agreement with FTIR spectra of Figure 5.8.

**Table 5.4 Gel content of compounded pellets samples and extrudates with 15 minutes dwell time in extrusion plastometer**

| Sample Code | Gel Content (wt%) |
|---|---|
| **HDPE** | **0.8** *(0.1)* |
| **HDPE-ME1** | **21.8** *(0.1)* |
| **HDPE-ME1C** | **26.2** *(0.2)* |
| **HDPE-ME2** | **9.8** *(0.8)* |
| **HDPE-ME2C** | **12.9** *(0.2)* |
| **HDPE-ME3** | **2.9** *(0.8)* |
| **HDPE-ME3C** | **4.3** *(0.3)* |
| **HDPE-ME3Ca** | **5.1** *(0.4)* |
| **HDPE-ME3Ca**[C] | **9.9** *(0.4)* |
| **HDPE-ME4** | **1.2** *(0.2)* |
| **HDPE-ME4C** | **1.7** *(0.1)* |
| **HDPE-ME4Ca** | **2.6** *(0.1)* |
| **HDPE-ME5Ca**[#C] | **7.2** *(0.3)* |

*Values in parentheses denote standard deviations*
[C] *Compounded pellets samples*
[#] *Formulation contains 3wt% EVA compatibiliser*

Figure 5.14 summarises the influence of epoxy-MAH ratio, presence of EVA and compounding process on the gel contents of the blends from Table 5.4. It shows that by keeping the epoxy content at constant concentration of 3 wt%, the gel content of the blends were reduced by the reduction in HDPE-g-MAH concentrations as shown in samples HDPE-ME2C, HDPE-ME3Ca, and HDPE-ME4Ca.

Compounding in the twin screw extruder resulted in blends with higher gel content than those obtained from the extrusion plastometer due to more intense heat history and shear stress of the compounding process leading to more reaction. A similar trend was observed earlier in MFR tests on HDPE-ME3Ca samples (see Table 5.2) whereby compounding resulted in lower MFR of the blends. With 15 minutes dwell time in the extrusion plastometer, the MFR was reduced from 10.6 g/10min to 8.1 g/10min. In Table 5.4, the gel content was increased from 5.1 wt% to 9.9 wt% respectively.

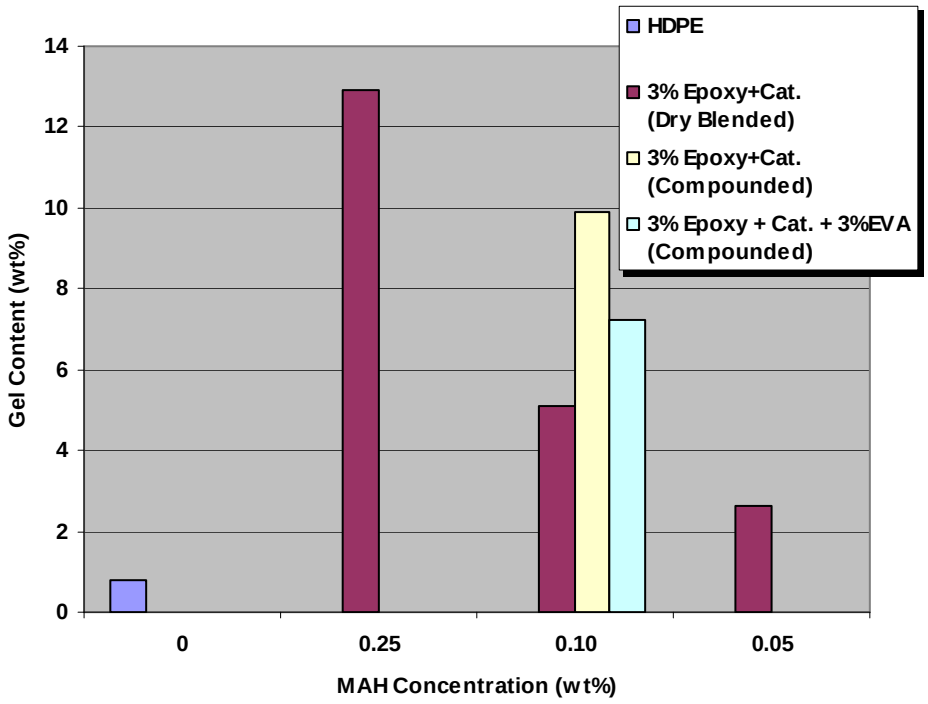


**Figure 5.14 The influence of epoxy-MAH ratio, presence of EVA, and compounding process on the gel content of blends**

The addition of 3 wt% EVA (HDPE-ME5Ca) during compounding resulted in a blend with a lower gel content than the same blend (HDPE-ME3Ca) without the EVA co-compatibiliser. This is possibly due to improvement in dispersion of the epoxy phase in the HDPE/HDPE-g-MAH matrix by the EVA compatibiliser as seen in optical micrographs of Figure 5.12 earlier. Spacing out the epoxy phases in the blend through better dispersion may have lowered the chance of a grafted epoxy to react with a carboxylic moiety of a neighbouring molecule to form a cross-linked network. Thus the smaller droplets of epoxy dispersed phases are likely to experience less intensive crosslinking than blends with poorly dispersed epoxy phases. This also indicates that EVA has improved the miscibility and compatibility between the epoxy and HDPE/HDPE-g-MAH phases by lowering the interfacial tension between the phases leading to a finer epoxy phase. The gel contents of blends are thus dependent on factors such as presence of catalyst, ratio of reactive MAH/epoxy components, and degree of dispersion of the epoxy in the HDPE/HDPE-g-MAH matrices.

The FTIR spectra of these insoluble gel fractions are presented in Figure 5.15. The presence of $CH_2$ asymmetric stretching band at 2915 $cm^{-1}$, $CH_2$ symmetric stretching band at 2849 $cm^{-1}$, $CH_2$ deformation bands at about 1463 $cm^{-1}$, and $CH_2$ rocking bands at about 720 $cm^{-1}$ provide the evidences of the presence of polyethylene segments in the gel. The detection of a peak at 720 $cm^{-1}$ implies the presence of molecules with 4 or more $–(CH_2)_n–$ groups ($n \geq 4$ ) in a row [210]. On the other hand, the absence of a doublet at 730 and 720 $cm^{-1}$ originally present in HDPE which is associated with the crystalline fraction indicates a limited degree of crystallinity in the crosslinked gels (see inserted spectra of Figure 5.15).

The detection of carbonyl peaks at 1740 $cm^{-1}$ and characteristic bands of DGEBA at around 829 $cm^{-1}$, 1042 $cm^{-1}$, 1362 $cm^{-1}$, and 1510 $cm^{-1}$ (see Figure 5.15**)** in all gel samples suggests that the gels contained polyethylene segments that are linked by ring opened DGEBA segments formed through interactions between carboxylic acid moieties of HDPE-g-MAH and oxirane rings of the DGEBA.

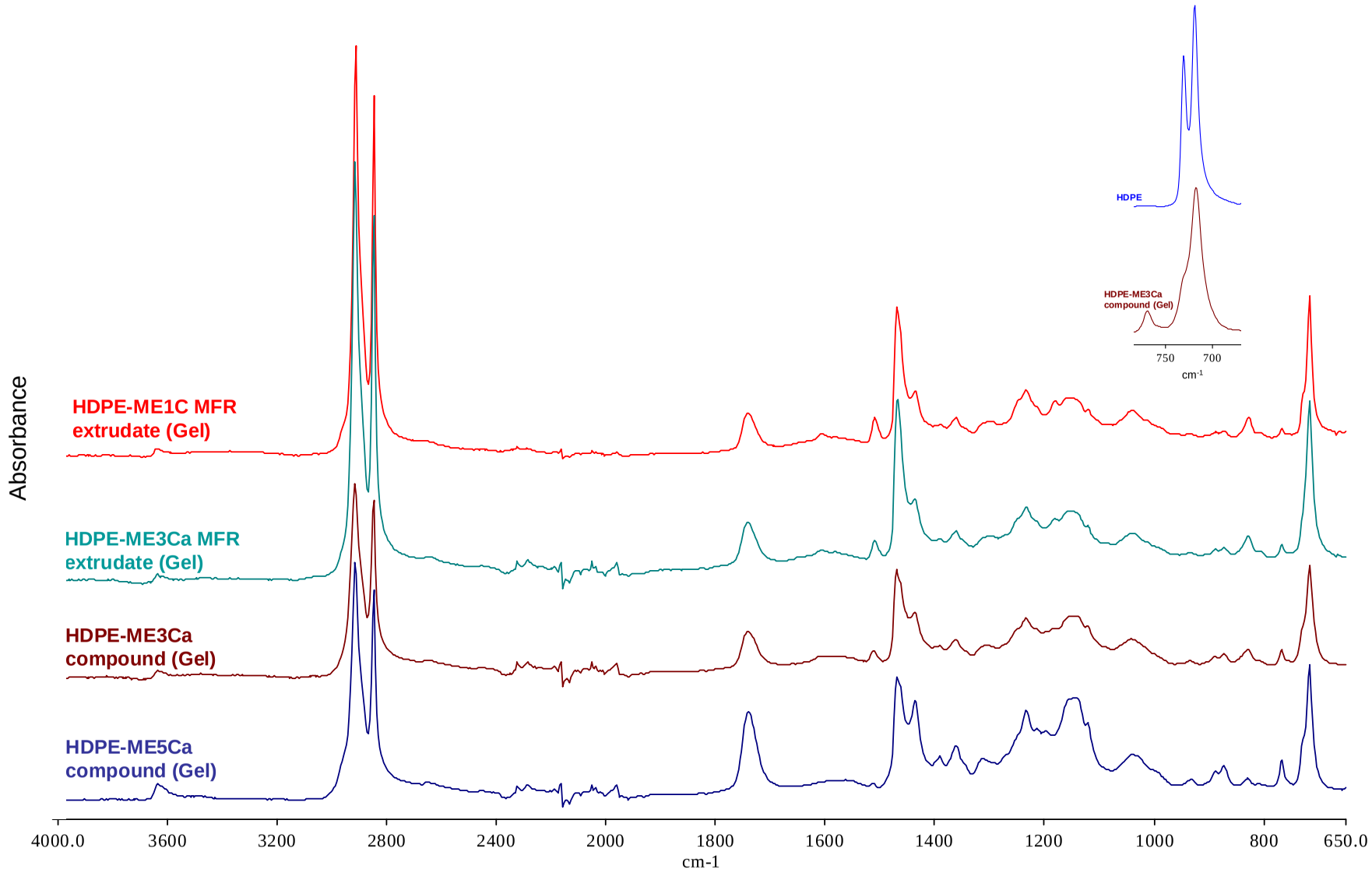


**Figure 5.15 FTIR spectra of gels recovered from solvent extraction**

Table 5.5 provides a summary of melting and crystallisation behaviour of the insoluble residues (gel fractions) obtained after solvent extraction of the extrudates prepared from the extrusion plastometer with a 15 minute dwell time. Examples of DSC traces can be found in Appendices A1-33 to A1-38. The percent crystallinity of the polyethylene phases could not be calculated because the exact amount of polyethylene present in the gels was unknown as these gels contained DGEBA components observed from earlier FTIR analysis. Thus the overall heat of fusion obtained from the gel fractions are being used for comparing the degree of crystallinity in the gels.

**Table 5.5 Thermal analysis of gels that were extracted from compounded pellets samples and extrudates with 15 minutes dwell time in extrusion plastometer**

| Sample Code | Gel | | | | |
|---|---|---|---|---|---|
| | Tm (℃) | ∆Hf [a] (J/g) | $TC_{Onset}$ (℃) | $TC_{Peak}$ (℃) | ∆TC (℃) |
| **HDPE*** | **130** *(1)* | **189.8** *(0.4)* | **118** *(0)* | **116** *(0)* | **2** |
| **HDPE-ME1^^** | **126** *(2)* | **104.7** *(2.5)* | **116** *(2)* | **109** *(2)* | **7** |
| **HDPE-ME1C^^** | **125** *(1)* | **108.3** *(1.5)* | **114** *(0)* | **106** *(1)* | **8** |
| **HDPE-ME2^^** | **124** *(1)* | **95.2** *(3.7)* | **115** *(1)* | **110** *(1)* | **5** |
| **HDPE-ME2C^^** | **125** *(1)* | **106.8** *(2.8)* | **113** *(0)* | **106** *(1)* | **7** |
| **HDPE-ME3^^** | **122** *(1)* | **102.9** *(4.3)* | **115** *(1)* | **113** *(0)* | **2** |
| **HDPE-ME3C^^** | **121** *(1)* | **96.3** *(1.9)* | **115** *(1)* | **110** *(1)* | **5** |
| **HDPE-ME3Ca^^** | **123** *(0)* | **103.5** *(2.9)* | **113** *(0)* | **107** *(0)* | **6** |
| **HDPE-ME3Ca [C]** | **122** *(0)* | **98.9** *(2.5)* | **118** *(0)* | **112** *(1)* | **6** |
| **HDPE-ME4^^** | **121** *(1)* | **97.3** *(3.0)* | **116** *(0)* | **112** *(0)* | **4** |
| **HDPE-ME4C^^** | **121** *(0)* | **98.3** *(3.0)* | **115** *(0)* | **111***(0)* | **4** |
| **HDPE-ME4Ca^^** | **123** *(0)* | **101.7** *(2.7)* | **114** *(0)* | **109** *(1)* | **5** |
| **HDPE-ME5Ca [C#]** | **122** *(1)* | **105.5** *(3.7)* | **118** *(1)* | **114** *(1)* | **4** |

*Values in parentheses denote standard deviations*
***** *Data from Table 4.1 for comparison purposes*
**^^** *Extrudates with 15 minutes dwell time in extrusion plastometer*
**C** *Compounded pellets Samples*
[#] *Formulation contains 3 wt% EVA compatibiliser*
**a** *Values normalised to the total amount of the blend or resin*

Melting endotherms for the gel samples were at lower melting points compared with the HDPE resin. This indicates that the distances of PE chain segments between the crosslinks were long enough for the formation of smaller imperfect crystallites and hence lower melting points are observed.

This is in good agreement with the FTIR findings whereby a single absorbance peak was detected at around 720 $cm^{-1}$.

The presence of crosslinks restricts the crystallisation of the PE segments and is manifested by delay in crystallisation (lower onset and peak of crystallisation), slower rate of crystallisation (larger $\Delta$TC values) and lower degree of crystallinity (lower heat of fusion). As mentioned earlier, the presence of EVA in the compounded HDPE-ME5Ca sample helped to disperse the epoxy in the blend leading to lower levels of gelation. The results in Table 5.5 also indicate that HDPE-ME5Ca is likely to have a lower degree of crosslinking compared with HDPE-ME3Ca (compounded) by the observation of more rapid rate of crystallisation, less delay in crystallisation and possibly a higher degree of crystallinity.

The solutions of extracts obtained after the solvent extraction processes of HDPE-ME3Ca and HDPE-ME5Ca were dried on a mortar and FTIR-ATR analysis was carried out on the recovered residues of the solutions. The precipitates recovered from the solutions were rinsed thoroughly with xylene and dried before being subjected to FTIR-ATR analysis. The FTIR spectra of dissolved and precipitated components of HDPE-ME3Ca and HDPE-ME5Ca are presented in Figure 5.16 and Figure 5.17 respectively.

Figure 5.16 shows that the FTIR spectrum of the dissolved components is very similar to the fingerprint region of epoxy resin with unreacted oxirane rings detected at around 915 $cm^{-1}$. Since epoxies are soluble in xylene, it is possible that the excess unreacted epoxy resins are being dissolved in the xylene solvent during extraction. On the other hand, the detection of absorbance peaks at around 2921 $cm^{-1}$, 2851 $cm^{-1}$, 1473 $cm^{-1}$, 734 $cm^{-1}$, and 719 $cm^{-1}$, indicate the presence of PE segments. The observation of a new carbonyl group at around 1737 $cm^{-1}$, indicates the possibility of grafted epoxy on PE formed from the reaction of carboxylic acid moieties of the HDPE-g-MAH and oxirane rings of the epoxy resin. The FTIR spectrum of the precipitates shows that the precipitates are mainly PE. However, the low peak absorbance value at 730 $cm^{-1}$ compared with 720 $cm^{-1}$, indicates a limited

degree of crystallinity which is in good agreement with the DSC findings in Table 5.5.

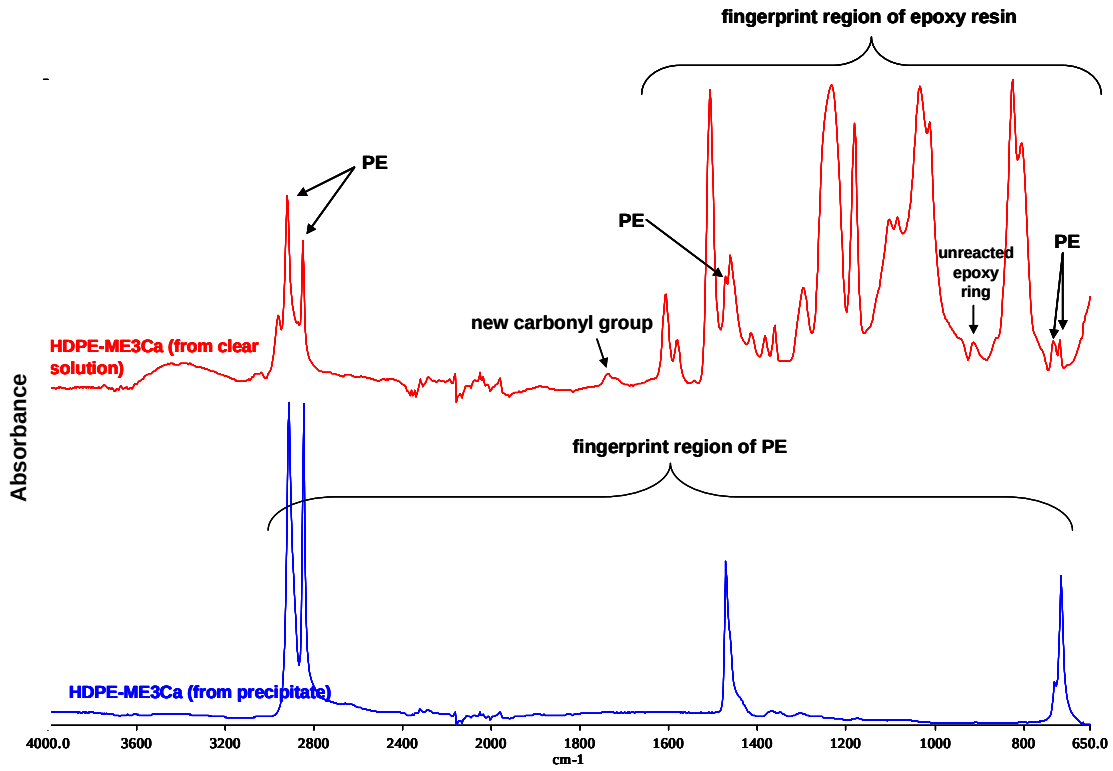


**Figure 5.16 FTIR spectra of dissolved and precipitated components of HDPE-ME3Ca**

Compared with HDPE-ME3Ca, the FTIR spectra of HDPE-ME5Ca in Figure 5.17 also shows that the dissolved components consist of epoxy resin. The sharp carbonyl peak detected at around 1738 $cm^{-1}$ indicates the possible presence of EVA polymer. The presence of EVA in the solution could be the reason for the observation of cloudiness of the solution after the solvent extraction process. There are also evidence of the presence of PE from the observation of peaks at around the regions of 2915 $cm^{-1}$, 2849 $cm^{-1}$, 732 $cm^{-1}$, and 717 $cm^{-1}$. It is possible that these PE segments are part of the EVA copolymer and also from grafted epoxy. However, due to chance of overlapping carbonyl peaks at 1738 $cm^{-1}$, the grafting of epoxy cannot be confirmed.

On the other hand, the FTIR spectrum of the precipitate in Figure 5.17 shows the presence of absorbance peaks at around 2915 $cm^{-1}$, 2849 $cm^{-1}$, 1471$cm^{-1}$, 734 $cm^{-1}$, 731 $cm^{-1}$ and 716 $cm^{-1}$, indicating the presence of PE segments. Since the peak at 731 $cm^{-1}$, is slightly more prominent than that of HDPE-ME3Ca, this confirms the DSC findings in Table 5.5 that the HDPE-ME5Ca has higher overall heat of fusion indicating a higher degree of crystallinity. Absorbance peaks at 1741 $cm^{-1}$, 1369 $cm^{-1}$, and 1241 $cm^{-1}$, indicate the presence of EVA in the precipitate which also suggests miscibility of the two polymers.

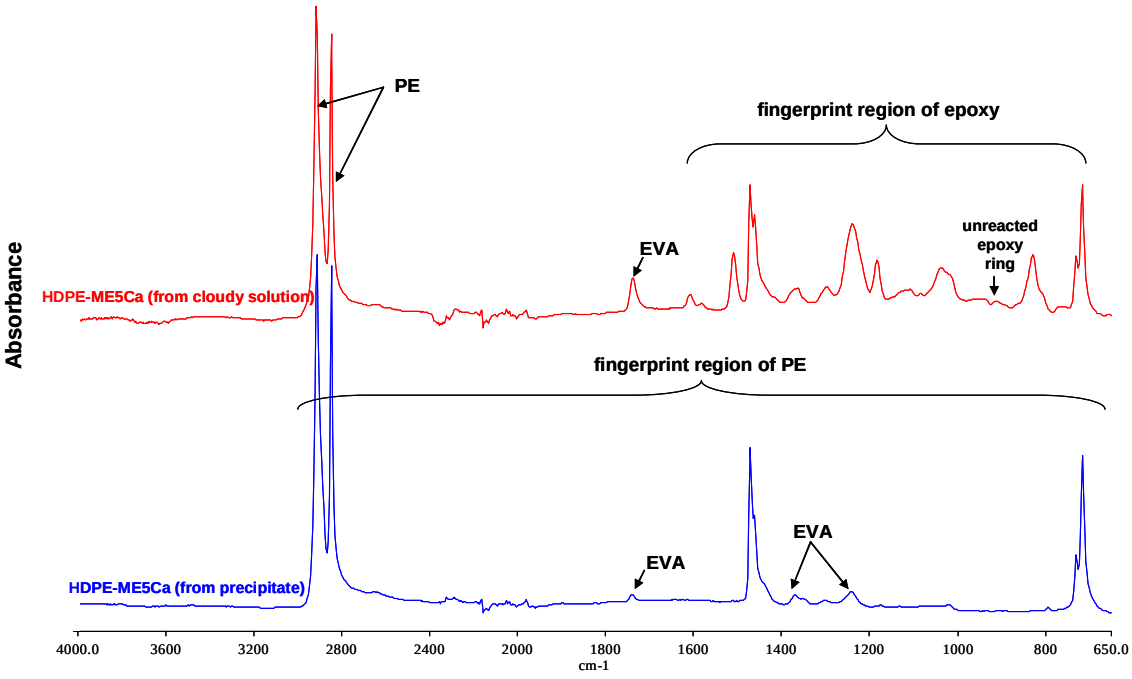


**Figure 5.17 FTIR spectra of dissolved and precipitated components of HDPE-ME5Ca**

Based on results obtained from the above analysis of the gels, dissolved components (in solution), and precipitates, the following conclusions could be drawn:

- All reactive blends contained gels in a quantity dependent on the concentrations of the reactive functionality present, presence of catalyst, the degree of epoxy dispersion and also type of processing method.

- The gels contained PE segments that were long enough for crystallisation to occur.
- The crosslinks were formed through the bridging of the PE segments by the epoxy molecule.
- The blends contained both epoxy grafted PE segments and also excess unreacted epoxy resin which are soluble in xylene.
- A schematic representation of a gel structure based on the above findings is proposed as follows:

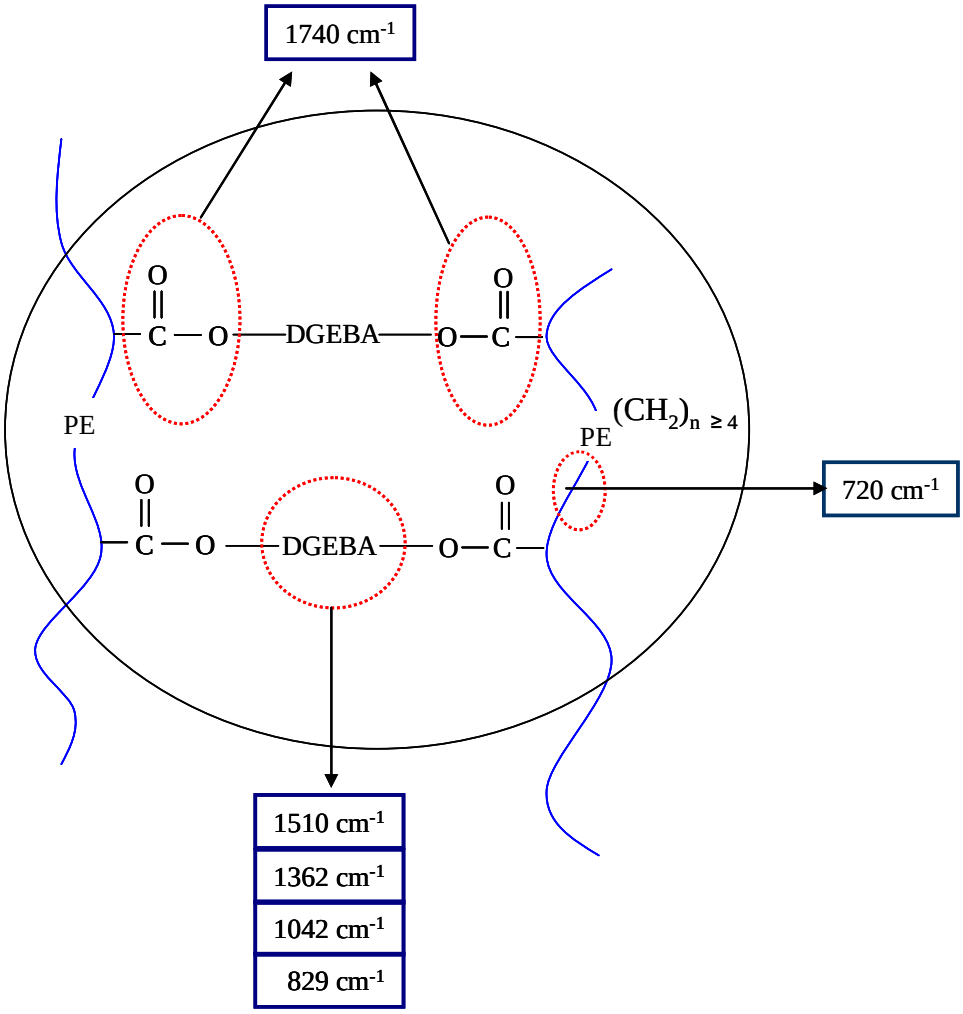


**Figure 5.18 Proposed schematic structure of gels obtained from solvent extraction**

## 5.3 Compatibility Studies on Blends of Functionalised HDPE with ABS, PBT and PA6

This section of the research covers the evaluation of compatibilisation effectiveness of the compounded reactive blends, HDPE-ME3Ca and HDPE-ME5Ca, with three matrix polymers namely, ABS, PBT and PA6. Mechanical properties including notched and reversed notch Izod impact and tensile elongation at break were carried out on these blends to judge the compatibility by evidence of interfacial adhesion. DSC was employed to study the phases of the blends in terms of possible changes in transition temperatures, and crystallisation behaviour. The morphological behaviour of the blends was characterised using optical microscopy.

### 5.3.1 The Influence of Reactive Grafting of HDPE on the Mechanical Properties of Blends

HDPE-ME3Ca, HDPE-ME5Ca and a HDPE resin were blended at 5 wt% with 95 wt% of ABS, PBT and PA6 matrix polymers by injection moulding. Izod impact and tensile tests were conducted on injection moulded bars. Table 5.6 summarises the Izod impact and tensile properties of the blends.

Blending HDPE at 5 wt% with ABS matrix polymer without a compatibiliser, resulted in substantial reduction in both notched and reversed notched Izod impact strength, tensile elongation at break and tensile strength at break. However both tensile strength and elongation at yield were relatively unaffected by the inclusion of the HDPE phases.

**Table 5.6 Mechanical properties of uncompatibilised and compatibilised HDPE blends with ABS, PBT and PA6**

| Sample Code | *Izod Impact Strength* | | *Tensile Properties* | | | |
|---|---|---|---|---|---|---|
| | Notched (J/m) | Reversed notch (J/m) | Elongation @ Break (%) | Strength @ Break (MPa) | Elongation @ Yield (%) | Strength @ Yield (MPa) |
| **ABS**[*] | **231** *(6)* | **1628** *(271)* | **28** *(2)* | **28** *(1)* | **3** *(0)* | **38** *(0)* |
| **ABS-H5** | **162** *(12)* | **678** *(206)* | **11** *(2)* | **23** *(1)* | **3** *(0)* | **38** *(0)* |
| **ABS –ME3Ca** | **182** *(8)* | **894** *(167)* | **44** *(3)* | **27** *(1)* | **3** *(0)* | **38** *(0)* |
| **ABS –ME5Ca** | **177** *(11)* | **876** *(253)* | **59** *(7)* | **26** *(2)* | **3** *(0)* | **38** *(0)* |
| **PBT**[#] | **29** *(2)* | **1060** *(129)* | **384** *(16)* | **31** *(3)* | **14** *(0)* | **53** *(0)* |
| **PBT-H5** | **30** *(3)* | **712** *(25)* | **22** *(1)* | **39** *(2)* | **11** *(1)* | **48** *(1)* |
| **PBT –ME3Ca** | **28** *(4)* | **734** *(43)* | **23** *(2)* | **38** *(2)* | **11** *(0)* | **49** *(0)* |
| **PBT –ME5Ca** | **28** *(4)* | **721** *(28)* | **22** *(1)* | **38** *(1)* | **10** *(0)* | **48** *(0)* |
| **PA6^** | **33** *(4)* | **2902** *(81)* | **265** *(8)* | **52** *(0)* | **5** *(0)* | **72** *(1)* |
| **PA6-H5** | **37** *(2)* | **1909** *(111)* | **217** *(5)* | **55** *(2)* | **5** *(0)* | **65** *(1)* |
| **PA6 –ME3Ca** | **38** *(2)* | **2632** *(112)* | **215** *(21)* | **56** *(2)* | **4** *(0)* | **66** *(1)* |
| **PA6–ME5Ca** | **45** *(2)* | **2695** *(110)* | **426** *(41)* | **64** *(3)* | **4** *(0)* | **64** *(2)* |

*Values in parentheses denote standard deviations.*
[*] *Data from Table 4.2 for comparison purposes*
[#] *Data from Table 4.6 for comparison purposes*
**^** *Data from Table 4.8 for comparison purposes*

On the other hand, blending HDPE-ME3Ca and HDPE-ME5Ca at 5 wt% with ABS also resulted in relatively unchanged tensile strength and elongation at yield. However, dramatic improvements in elongation at break were observed for both blends thus suggesting interfacial adhesion of the blends was improved due to compatilisation effects in particular when EVA was present in sample ABS-ME5Ca (see Appendix B1-9). The Izod impact strengths (notched and reversed notch) of both blends were also somewhat improved.

For PBT blends, the addition of HDPE without a compatibiliser has no significant influence on the notched Izod impact strength of the PBT but dramatically reduces its reversed notch impact strength and elongation at break (see Appendix B1-10). This observation is consistent with Section 4.4.1 and confirms the fact that the tensile elongation which represents the tensile toughness of the PBT is very similar to reversed notch impact behaviour [70, 87].

On the other hand, when PBT was blended with 5 wt% of HDPE-ME3Ca and HDPE-ME5Ca, other than the very slight improvement observed on the reversed notch impact strength, all other properties remained somewhat unchanged in comparison with the uncompatibilised PBT/HDPE blend. This is a surprising observation as the epoxy functionality in both HDPE-ME3Ca and HDPE-ME5Ca was expected to improve the compatibility between HDPE and PBT through reactions with the carboxyl end-groups of PBT.

The likely reason for this observation is because of ungrafted epoxy resin, which was detected in solutions of extracts in Section 5.2.3, with the end-groups of PBT rendering them unavailable for interaction with the grafted epoxy moieties. Since the ungrafted epoxy is a much smaller molecule compared with the grafted epoxy, its expected to have greater mobility and thus enable quicker diffusion towards the PBT chain-ends.

Like the PBT/HDPE blend, the notched Izod impact test did not detect the incompatibility of the PA6/HDPE blend as shown in Table 5.6. The reversed notch and elongation at break demonstrated a more dramatic effect than the incompatible PA6/HDPE blend. On the other hand, significant improvements in reversed notch impact strength were observed when PA6 was blended with 5 wt% of HDPE-ME3Ca and HDPE-ME5Ca suggesting compatibilisation effects in the blends. The HDPE-ME5Ca which contained EVA showed the most significant improvement in the notched/reversed notch Izod impact strength, and tensile elongation/strength at break of the blend.

This is in good agreement with the findings of Chapter 4 where both EVA and HDPE-g-MAH exhibited excellent compatibilising effects in PA6/HDPE blends. As shown in the tensile stress-strain curve of PA6-ME5Ca in Appendix B1-11, excellent interfacial adhesion was demonstrated by the presence of a 'secondary' yield peak located at a strain level of around 168 % due to the higher level of stress needed for de-bonding the phases when the failure reached the interface region of the blend. Such a 'secondary' yield peak was not observed in other blends.

For better overview on the effectiveness of the compatibilisers in ABS/HDPE, PBT/HDPE and PA6/HDPE blends, the Izod impact strength (notched and reversed notch) and elongation at break of these blends are normalised to 100% based on data of neat matrix polymers as shown in Figure 5.19.

From Figure 5.19, the following conclusions on mechanical properties of the blends could be drawn:

- Neither ABS-ME3Ca nor ABS-ME5Ca cause a significant improvement in the notched Izod impact strength but cause moderate improvements in the reversed notch impact strength of the blend. However, both blends exhibited exceptionally high elongation at break which exceeded more than 150% for ABS-ME3Ca blend, and more than 200% for ABS-ME5Ca blend of the neat ABS matrix polymer.
- Neither PBT-ME3Ca nor PBT-ME5Ca has produce significant differences in mechanical properties comparing to uncompatibilised PBT/HDPE blends.
- Neither PA6-ME3Ca nor PA6-ME5Ca produces significant improvements in reversed notch impact strength of the blends. PA6-ME3Ca produces no significant improvement in notched Izod impact strength while PA6-ME5Ca has more than 100% improvement in elongation at break as compared with the uncompatibilised blend.

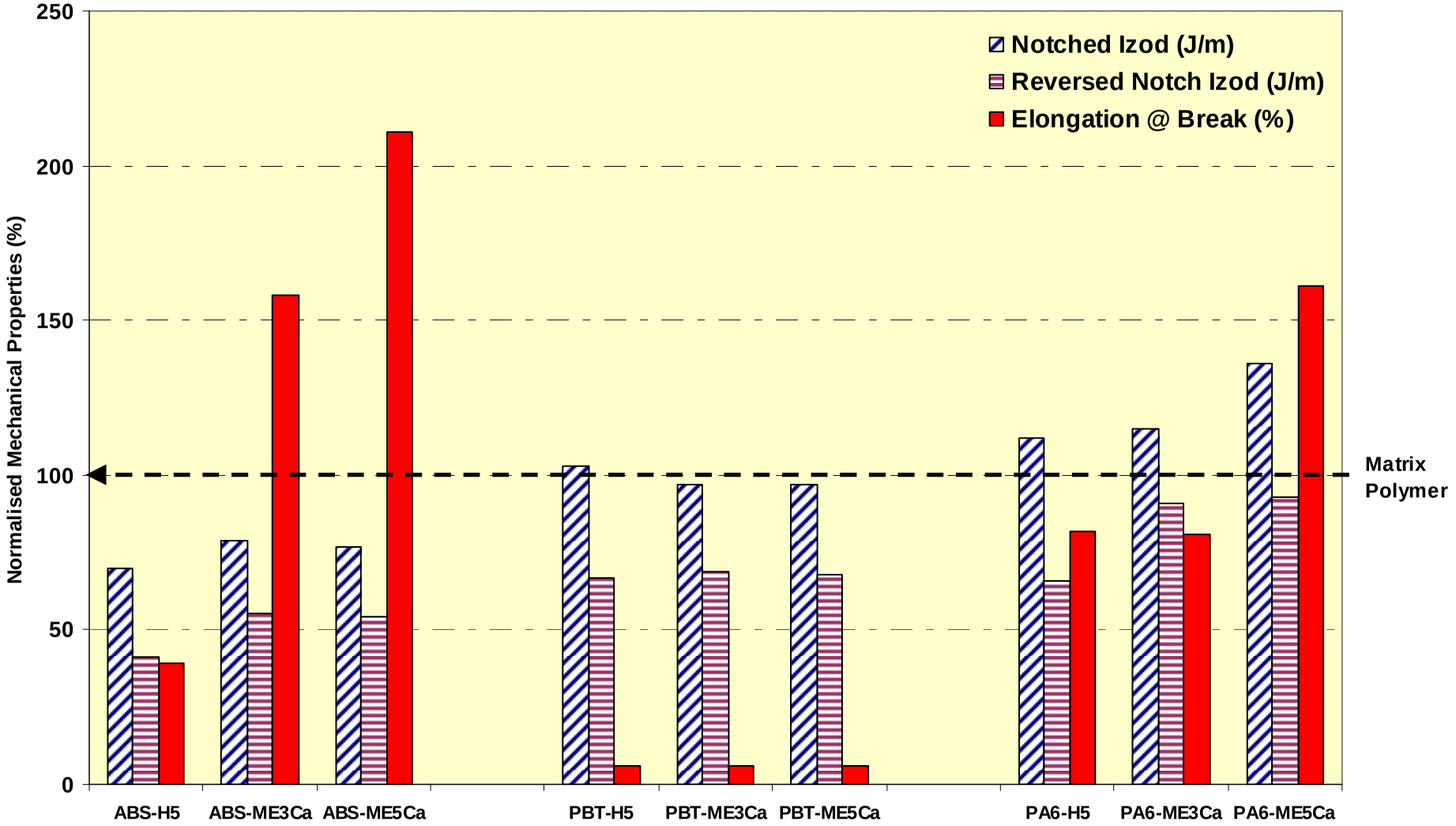


**Figure 5.19 Normalised mechanical properties of uncompatibilised and compatibilised ABS/HDPE, PBT/HDPE and PA6/HDPE blends**

### 5.3.2 Thermal Analysis of Blends

Tables 5.7 and 5.8 summarise the thermal properties of uncompatibilised and compatibilised blends of ABS/HDPE, PBT/HDPE and PA6/HDPE produced via injection moulding. The DSC cooling traces of these blends are presented in Figure 5.20.

From Table 5.7, it can be seen that the glass transition temperatures of the ABS matrices in all blends remained unchanged in all uncompatibilised and compatibilised blends thereby suggesting that the styrene acrylonitrile (SAN) of the ABS in the blends was unmodified. However, it is observed that the degree of crystallinity of the HDPE phase were dramatically reduced in all the blends. For the uncompatibilised blend containing 5 wt% HDPE (sample ABS-H5), the reduction in crystallinity was significantly lower than that of a 15 wt% HDPE observed in Table 4.3 of earlier study. This is again due to the occurrence of fractionated crystallisation of the HDPE phase in the ABS matrix as shown in Figure 5.20. Homogenous nucleation is observed to be more important than the heterogeneous nucleation which is manifested by the higher exotherm peak at larger supercooling than the main exotherm of the HDPE crystallisation peak which was somewhat shifted to a lower temperature as compared with the neat HDPE resin as shown in Figure 5.20.

On the other hand, the blend containing 15 wt% HDPE shown in Figure 4.3 has a higher main exotherm of HDPE crystallisation than the homogeneous nucleation peak. The likely reason for such an observation is that when there are higher concentrations of nucleating agents in the blend containing 15 wt% of HDPE, thus increases the possibility of the presence of nucleating agents in the dispersed HDPE droplets compared with blends containing 5 wt% HDPE. The more intense homogeneous nucleation in combination with poor compatibility between the phases of the blend could have contributed to poor mechanical properties of the uncompatibilised ASB/HDPE blend as discussed in Section 5.3.1.

The presence of epoxy and HDPE-g-MAH in sample ABS-ME3Ca caused a further reduction in the degree of crystallinity compared with ABS-H5. The presence of gels in the HDPE-ME3Ca may have caused hindrance to the crystallisation. Evidence of a slower rate of crystallisation (higher ΔTC) for gels belonging to compounded samples of HDPE-ME3Ca can be observed in Table 5.5.

On the other hand, the presence of EVA in ABS-ME5Ca helped to increase the degree of crystallinity nearer to the uncompatibilised blend in Table 5.7 which correlates well with higher rate of crystallisation of HDPE-ME5Ca (see Table 5.5) used in blending of ABS-ME5Ca. This hypothesis is further justified by the observation of lower gel content in HDPE-ME5Ca as shown in Table 5.4 thus reinforcing that the fact that EVA helped to lower the gel content of the reactive blend, HDPE-ME5Ca, leading to an increase in its degree of crystallinity when dispersed in the ABS matrix.

**Table 5.7 Thermal analysis of uncompatibilised and compatibilised ABS/HDPE blends**

| Sample Code | ABS | HDPE Phase | | |
|---|---|---|---|---|
| | **Tg (℃)** | **Tm (℃)** | **ΔHf (J/g)** | **$X_c$ (%)** |
| **HDPE*** | - | **130** *(1)* | **189.8**[a] *(0.4)* | **65** *(0)* |
| **ABS**[#] | **101** *(1)* | - | - | - |
| **ABS-H15** | **101** *(0)* | **129** *(0)* | **83.6**[b] *(12.4)* | **29** *(4)* |
| **ABS-ME3Ca** | **101** *(0)* | **129** *(0)* | **64.9**[b] *(17.1)* | **22** *(6)* |
| **ABS-ME5Ca** | **100** *(0)* | **129** *(0)* | **79.0**[b] *(18.3)* | **27** *(6)* |

*Values in parentheses denotes standard deviations*
***** *Data from Table 4.1 for comparison purposes*
[#] *Data from Table 4.3 for comparison purposes*
[a] *Values normalised to the total amount of the blend or resin*
[b] *Values normalised to the amount of the relevant phase*

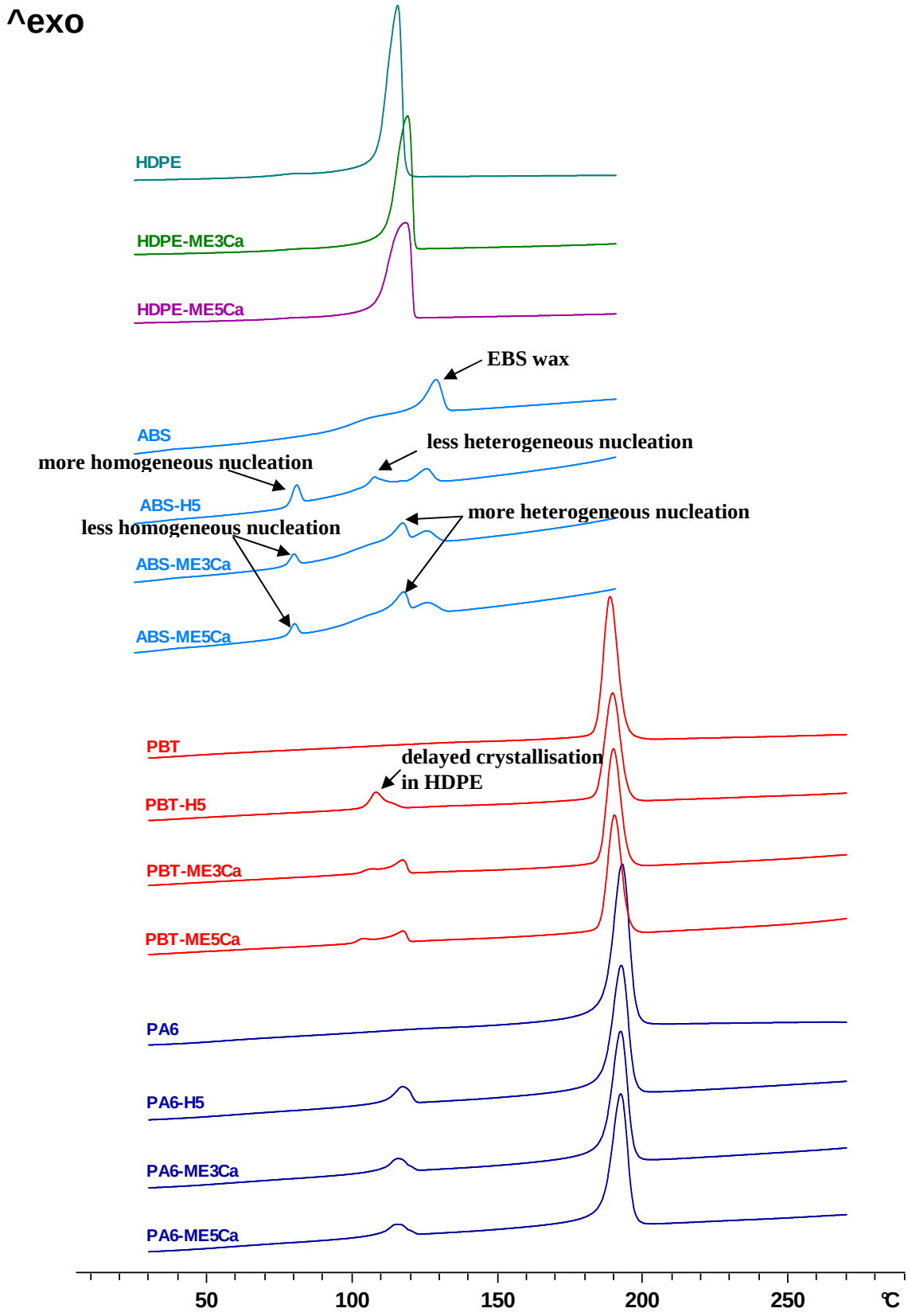


**Figure 5.20 DSC cooling traces of uncompatibilised and compatibilised ABS/HDPE, PBT/HDPE, and PA6/HDPE blends**

Table 5.8 presents the melting and crystalllisation behaviour of PBT and PA6 blends and their respective HDPE phases. In PBT blends, insignificant changes in melting transitions for both PBT and HDPE phases are observed for all uncompatibilised and compatibilised blends indicating lack of miscibility in their crystalline regions. The presence of HDPE in the PBT matrix without a compatibiliser caused restrictions in crystallisation to both phases leading to lower degree of crystallinity compared to their respective neat polymers.

Figure 5.20 shows that the crystallisation of HDPE phase was much delayed comparing to its neat polymer. Since HDPE crystallises in a cooled hardened matrix of the PBT, this delay in crystallisation of HDPE may have lead to the reduction in degree of crystallinity in its dispersed phase as the surrounding matrix quenches the HDPE melt. On the other hand, the crystallisation peaks of the HDPE phase of both reactive blends, PBT-ME3Ca and PBT-ME5Ca, were closer to that of their neat HDPE polymer. This could be the consequence of more nucleated behaviour for both HDPE-ME3Ca and HDPE-ME5Ca leading to earlier crystallisation of the HDPE phase in a warmer PBT matrix which encourages a higher degree of crystallinity.

In conclusion for PBT blends, the lack of changes in melting transition irrespective of compatibilisation indicate poor miscibility in the crystalline regions between the phases and this was reflected in the relatively unmodified mechanical properties of the compatibilised blends compared with the uncompatibilised compound. The degree of crystallinity of the HDPE dispersed phases or PBT matrix polymer has no significant influence on the final mechanical properties of the blends as demonstrated in Figure 5.19.

**Table 5.8 Thermal analysis of uncompatibilised and compatibilised PBT/HDPE and PA6/HDPE blends**

| Sample Code | *PBT Phase* | | | | | | *HDPE Phase* | | |
|---|---|---|---|---|---|---|---|---|---|
| | **Tm (℃)** | **∆Hf (J/g)** | **$X_c$ (%)** | **$TC_{Onset}$ (℃)** | **$TC_{Peak}$ (℃)** | **∆TC (℃)** | **Tm (℃)** | **∆Hf (J/g)** | **$X_c$ (%)** |
| **HDPE*** | - | - | - | - | - | - | **130** *(1)* | **189.8** [a] *(0.4)* | **65** *(0)* |
| **PBT**[#] | **224** *(0)* | **47.1**[a] *(1.0)* | **33** *(1)* | **194** *(0)* | **189** *(0)* | **5** | - | - | - |
| **PBT-H5** | **224** *(0)* | **37.8**[b] *(1.3)* | **26** *(1)* | **194** *(1)* | **189** *(1)* | **5** | **128** *(0)* | **162.3** [b] *(20.7)* | **55** *(7)* |
| **PBT-ME3Ca** | **224** *(0)* | **39.9**[b] *(0.9)* | **28** *(1)* | **195** *(0)* | **190** *(0)* | **5** | **130** *(0)* | **194.9** [b] *(12.9)* | **67** *(4)* |
| **PBT-ME5Ca** | **224** *(0)* | **37.2**[b] *(0.6)* | **26** *(0)* | **195** *(0)* | **190** *(0)* | **5** | **129** *(0)* | **189.2** [b] *(21.7)* | **65** *(7)* |
| **Sample Code** | *PA6 Phase* | | | | | | *HDPE Phase* | | |
| | **Tm (℃)** | **∆Hf (J/g)** | **$X_c$ (%)** | **$TC_{Onset}$ (℃)** | **$TC_{Peak}$ (℃)** | **∆TC (℃)** | **Tm (℃)** | **∆Hf (J/g)** | **$X_c$ (%)** |
| **PA6^** | **220** *(0)* | **80.4**[a] *(0.4)* | **35** *(0.6)* | **198** *(0)* | **193** *(0)* | **5** | - | - | - |
| **PA6-H5** | **221** *(0)* | **69.7** [b] *(0.8)* | **30** *(0)* | **197** *(0)* | **193** *(0)* | **4** | **131** *(0)* | **213.5** [b] *(11.8)* | **73** *(4)* |
| **PA6-ME3Ca** | **221** *(0)* | **67.2** [b] *(0.6)* | **29** *(0)* | **197** *(0)* | **192** *(0)* | **5** | **130** *(0)* | **177.9** [b] *(3.3)* | **61** *(1)* |
| **PA6-ME5Ca** | **221** *(0)* | **70.0** [b] *(0.3)* | **30** *(0)* | **197** *(0)* | **192** *(0)* | **5** | **129** *(0)* | **195.0** [b] *(12.1)* | **67** *(4)* |

*Values in parentheses denote standard deviations*
***** *Data from Table 4.1 for comparison purposes*
[#] *Data from Table 4.7 for comparison purposes*
**^** *Data from Table 4.9 for comparison purposes*
[a] *Values normalised to the total amount of the blend or resin*
[b] *Values normalised to the amount of the relevant phase*

As for the PBT blends, no significant changes in melting transitions of PA6 blends were observed in Table 5.8 for either uncompatibilised or compatibilised blends suggesting lack of miscibility of the crystalline regions of both polymers. The degree of crystallinity of the PA6 matrices were about 4 to

5% lower than the neat PA6 resin for all the blends. The presence of HDPE phases seems to have caused restriction in the crystallisation of the PA6 matrices. As for the degree of crystallinity of HDPE dispersed phases, the uncompatibilised HDPE exhibited exceptionally high crystallinity compared to the neat HDPE resin. This observation is consistent with Section 4.5.2 whereby a similar increment in crystalllinity of PA6 with 15 wt% HDPE was reported. Such a phenomenon could be attributed to the transfer of nucleating particles between polymers as reported by Santana and Müller [149]. For the case of PA6/HDPE blends, it has been observed that only the uncompatibilised blends are observed to have increased crystallinity. Thus it is very likely that the nucleating particles have preference to be transferred from the polar PA6 to the non-polar HDPE.

This section of the research work shows that the melting transitions of blend components are not significantly affected during reactive blending of PA6 blends. Thus possible reactions between the epoxy/MAH reactive groups of the modified HDPE phases and the PA6 matrices are probably happening mainly at the chain-ends of the PA6 molecules.

### 5.3.3 Morphology of Blends

The optical micrographs of uncompatibilised and compatibilised ABS/HDPE, PBT/HDPE, and PA6/HDPE blends observed under polarised light are presented in Figures 5.21, 5.22 and 5.23 respectively. In Figure 5.21, neat ABS matrix appeared only as dark background in micrograph (a) since it is an amorphous polymer. With the inclusion of an HDPE phase in micrograph (b) of Figure 5.21, single spherulitic structures of about 7 to 10 µm sizes as indicated by yellow arrows in the micrograph were seen dispersed on the dark ABS matrix. The observation of single spherulitic structures was attributed to the fractionated crystallisation of the HDPE phases in the ABS matrix as suggested by the DSC results of Figure 5.20. Homogeneous nucleation of the HDPE melt leads to the growth of single HDPE spherulitic structures without any foreign nucleating particles. On the same micrograph, much finer bright

spots are also seen to be dispersed on the same matrix. These finer bright spots are possibly nucleated HDPE spherulites that are grown from foreign nucleating particles via heterogeneous nucleation. Therefore the observed single spherulitic structures and also finely nucleated spherulites justify the proposed DSC findings on fractionated crystallisation of the blend. Finely dispersed bright spots of around 1.5 µm and below are observed in blends that contained epoxy and also EVA in micrographs (c) and (d) respectively of Figure 5.21. This is likely to be due to the nucleating effects of the epoxy and EVA on the HDPE dispersed phase leading to the formation of finely dispersed HDPE spherulites on the ABS matrices. This again is in good agreement with DSC results in Figure 5.20 where by these blends exhibited more heterogeneous nucleation than the uncompatibilised ABS/HDPE blend. The presence of such finely dispersed spherulitic structures may have contributed to better mechanical properties of the compatilised blends as observed in Section 5.3.1.

Presented in Figure 5.22 are optical mircrographs of PBT and its blends with uncompatibilised and compatibilised HDPE. Neat PBT exhibits a large well-defined spherulitic morphology as shown in micrograph (a). However, tiny black spots of around 1 µm and below are observed to be uniformly dispersed in the PBT spherulites when HDPE was blended at 5wt% with the PBT as shown in micrograph (b) of Figure 5.22. The observation of dispersed black spots of an amorphous polymer in the spherulitc structure of the crystalline matrix polymer using an optical microscope has been reported by Bulakh and Jog [178]. In this work, the black spots which are likely to be the HDPE phase and probably appeared black due to mismatch in refractive indices of the two phases and also probably due to immiscibility and incompatibility of the phases. These back spots are observed to become less distinct and fewer in number when epoxy and EVA are present in the blends as shown in micrographs (c) and (d) of Figure 2.22 respectively. This could be an indication of improved miscibility and compatibility between the phases.

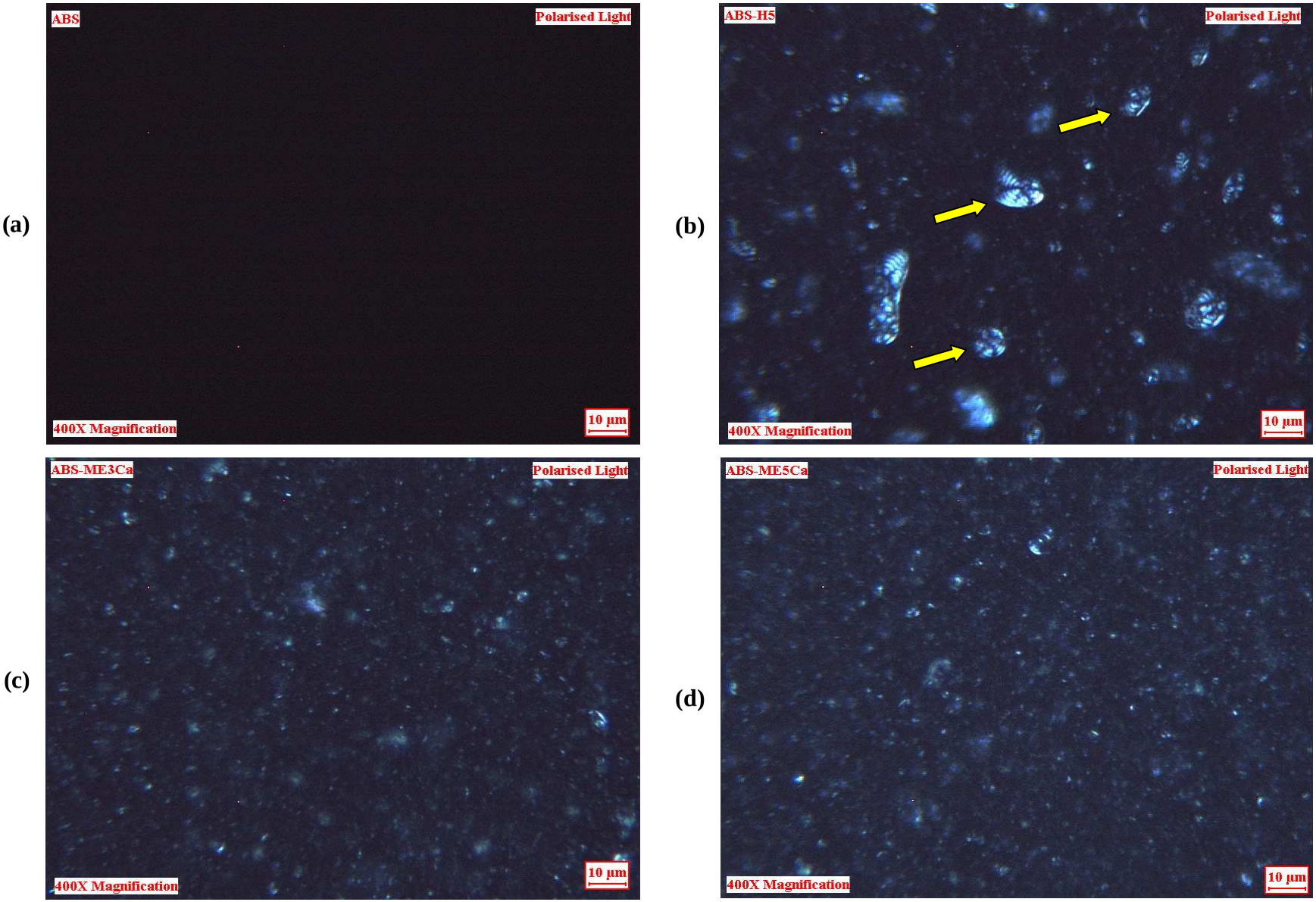


**Figure 5.21 Optical micrographs of (a) ABS, (b) ABS-H5, (c) ABS-ME3Ca, (d) ABS-ME5Ca**

(a)

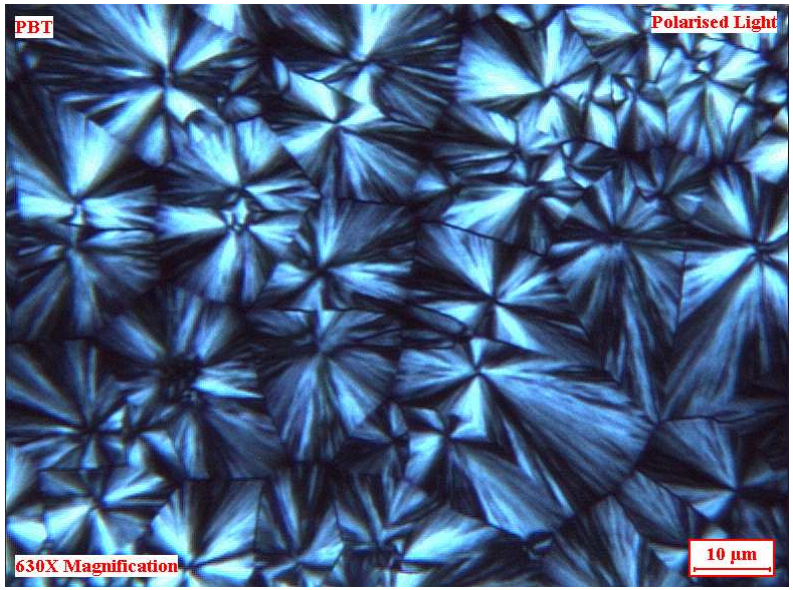


(b)

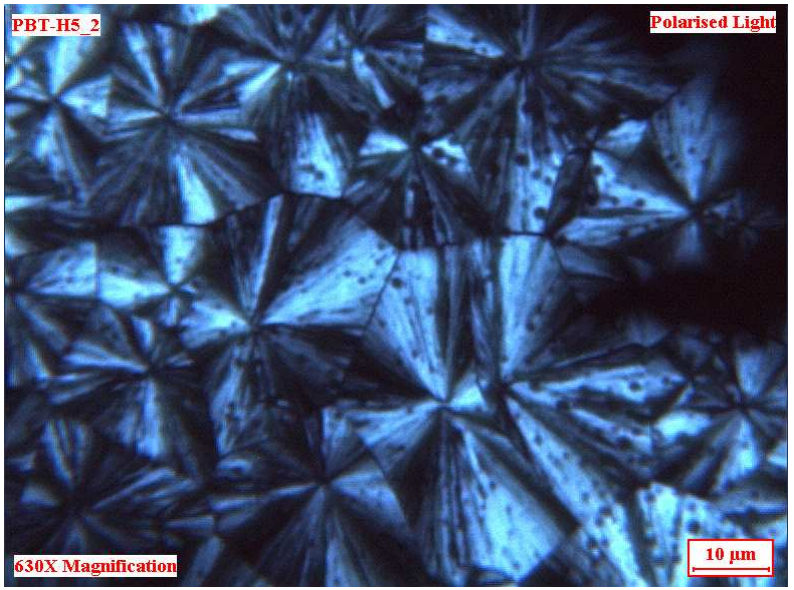


(c)

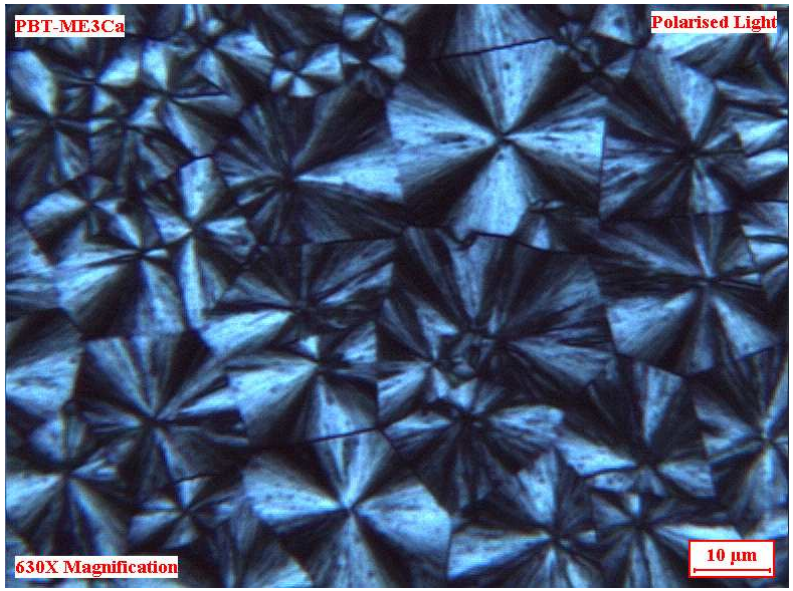


(d)

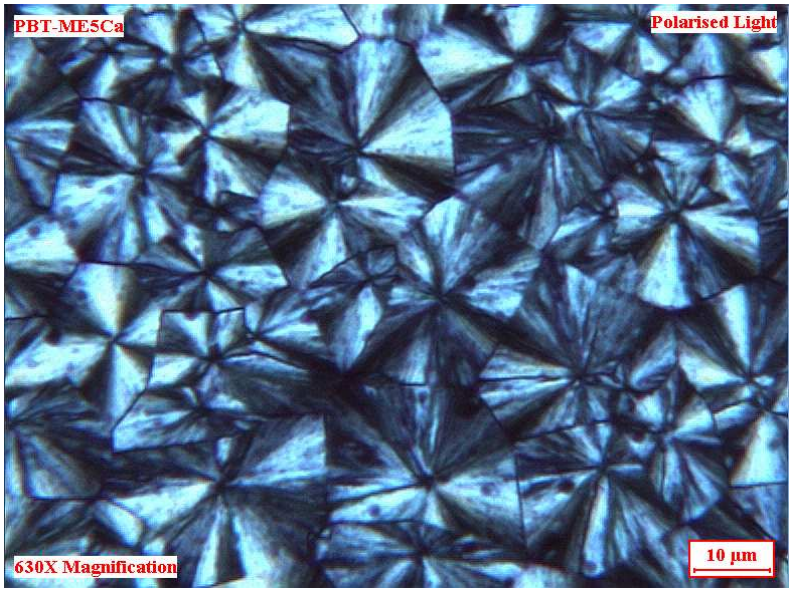


**Figure 5.22 Optical micrographs of (a) PBT, (b) PBT-H5, (c) PBT-ME3Ca, (d) PBT-ME5Ca**

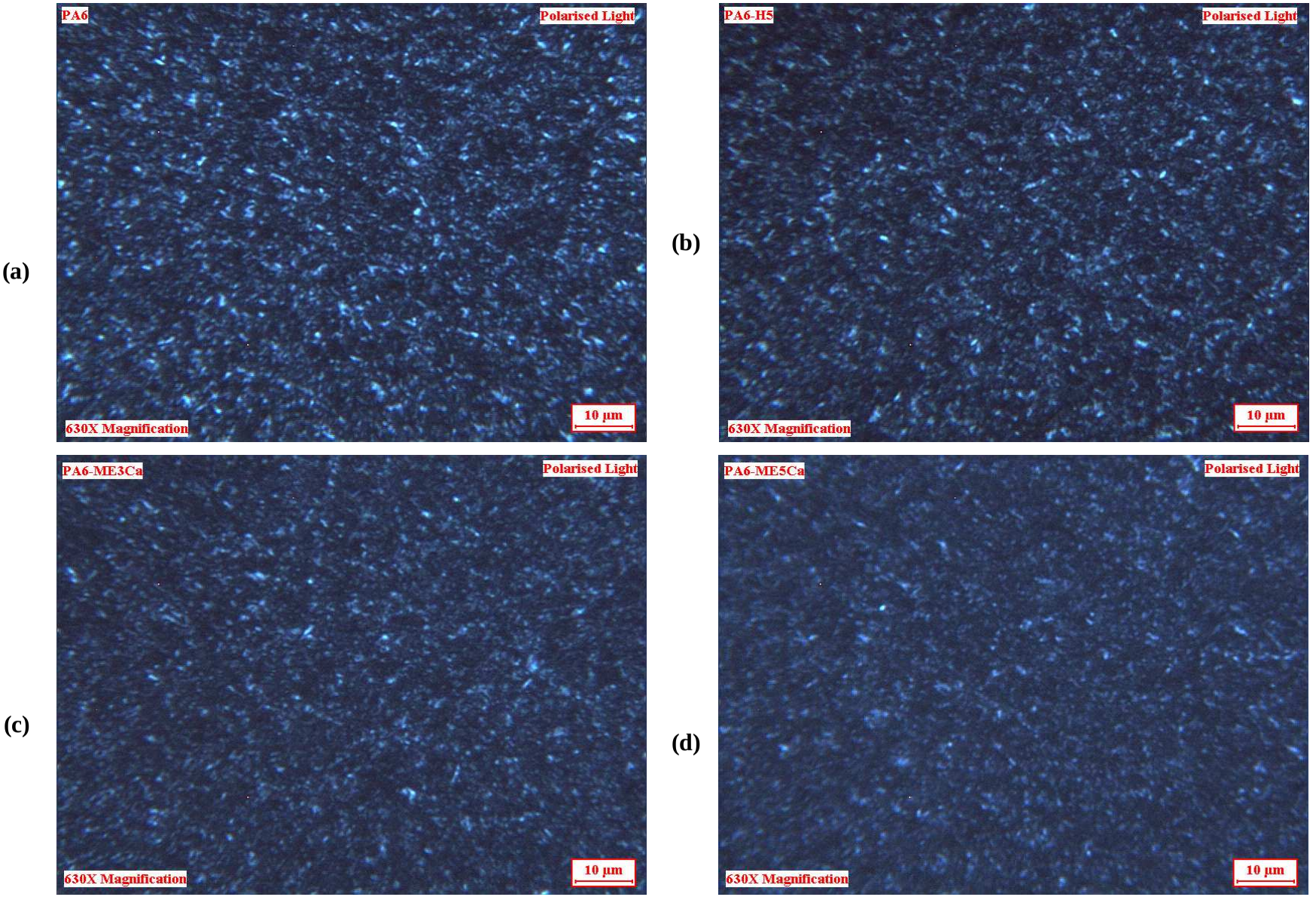


**Figure 5.23 Optical micrographs of (a) PA6, (b) PA6-H5, (c) PA6-ME3Ca, (d) PA6-ME5Ca**

The spherulitic morphologies of PA6 and its blends with uncompatibilised and compatibilised HDPE are shown in optical micrographs of Figure 5.23. The neat PA6 exhibited a very fine spherulitic morphology suggesting that this grade of PA6 has been pre-nucleated during the manufacture of the resin. A non-nucleated PA6 should exhibit well-defined spherulitic structures as shown in Appendix C2-1. Due to the nucleating effects of the PA6 matrix polymer, all blends irrespective of compatibilisation exhibited uniformly dispersed fine spherulitic morphology as shown in micrographs (b), (c) and (d) of Figure 5.23. However, the compatibilised blends in micrographs (c) and (d) appeared to have less distinct dispersed spots which suggests improved miscibility and compatibility of both compatibilised blends.

## 5.4 Conclusions

Blending highly polar amorphous epoxy with non-polar highly crystalline HDPE resulted in phase separation due to gross immiscibility and incompatibility of the two polymers. The addition of HDPE-g-MAH helped in improving the miscibility and compatibility of the blends and was further improved in the presence of EVA copolymer which acted as a secondary compatibiliser. In general, the presence of epoxy in HDPE resulted in changes to its crystallisation behaviour leading to slower rate of crystallisation, higher onset of crystallisation and lower degree of crystallinity.

Melt flow rates of the reactive blends were observed to be influenced by the extent of reaction between the blend components. Lower melt flow rates were observed for blends that had undergone more intensified reaction leading to higher gel content in the blends. The gels contain segments of crystallisable polyethylene chain linked by ring-opened DGEBA molecules.

The compounded blend of HDPE/HDPE-g-MAH/epoxy (HDPE-ME3Ca) exhibited good compatibility in ABS, and PA6 but showed little effect on PBT. On the other hand, the blend containing EVA (HDPE-ME5Ca) showed further improvements in its compatibility with ABS and PA6 but again had

insignificant influence on the compatibility with PBT. Excess epoxy resin used in the reactive formulations resulted in free ungrafted epoxy molecules which have undesirable interaction with the chain-ends of PBT resin rendering the compatilisation ineffective. Both reversed notch Izod impact and elongation at break were sensitive in detecting compatibility between phases of blends while notched Izod and tensile yield strength and break were insensitive to the changes in compatibility of these blends.

# CHAPTER 6
# GENERAL DISCUSSION

The present research consists of two separate studies; the first is a screening experiment examining the efficiency of commercially available compatibilisers for ABS/HDPE, PC/HDPE, PBT/HDPE and PA6/HDPE blends and the second involves reactive modification of HDPE in an attempt to improve its compatibility with ABS, PBT and PA6.

In Chapter 4 of this thesis, formulations containing uncompatibilised and compatibilised ABS/HDPE, PC/HDPE, PBT/HDPE and PA6/HDPE were physically blended and injection moulded into test bars for the investigation of blend compatibility. The uncompatibilised blends consisted of binary blends of 15 wt% of HDPE with ABS, PC, PBT, and PA6, whereas ternary compatibilised blends were prepared by blending pre-compounded binary blends of HDPE with E-MA-GMA, E-GMA, EVA, EMA and HDPE-g-MAH at HDPE/compatibiliser blend ratios of 1:1 and 3:1 at 15 wt% level in the matrix polymers.

HDPE being non-polar in nature and having a solubility parameter value of about 18.0 $(MPa)^{1/2}$ [211] is expected to have limited miscibility and compatibility with polar polymers like ABS, PC, PBT and PA6 which have solubility parameter values of 21.0 $(MPa)^{1/2}$ [211], 21.7 $(MPa)^{1/2}$ [212], 21.9 $(MPa)^{1/2}$ [213], and 24.3 $(MPa)^{1/2}$ [211] respectively. The immiscibility and incompatibility of these blends are manifested by the existence of blend morphologies having two very distinct phases with very little or no adhesion when examined by SEM. Except for PBT and PA6, all blends show a dramatic reduction in their notched and reversed notch Izod impact strength and also tensile elongation at break suggesting the lack of interfacial adhesion. Neat PBT and PA6 resins which are brittle under notched impact conditions were not affected by the inclusion of HDPE. However, like the rest of the blends discussed, they too exhibited low reversed notch Izod

impact strengths and tensile elongation at break. The Izod impact tests conducted on notched specimens tend to measure resistance to crack propagation, whereas tests conducted on reversed notch specimens place a greater emphasis upon ductility prior to crack initiation. The addition of HDPE in PBT and PA6 caused a reduction in ductility due to poor compatibility between the two polymers but did not have a significant influence on the resistance to crack propagation.

On the other hand, both the reversed notch Izod impact strengths and tensile elongation at break of blends showed great sensitivity towards the degree of compatibilisation of the blends. In general, the reversed notch impact follows the trend of elongation at break thus providing useful evidence on the detection of changes in ductility due to variation in compatibilisation at the interfaces of the blends.

On the basis of morphological evidence, and mechanical properties (reversed notch Izod and tensile elongation) the epoxy-containing compatibilisers, in particular, E-MA-GMA exhibited the best overall efficiency in compatibilising HDPE with ABS, PC, PBT and PA6 amongst the five compatibilisers evaluated. This justifies the fact that glycidyl methacrylate compatibilisers which have epoxy functional groups can react with far more chemical groups than MAH as shown in Reaction Scheme 5, have seen increased usage as reactive compatibilisers for vastly different types of polymer blends [22]. This study also justifies why reaction between MAH-grafted polymers and the carboxyl or hydroxyl group from polyesters has not been positively identified [22].

The presence of methyl acrylate comonomer in E-MA-GMA terpolymers resulted in higher polarity that further improved their miscibility with polar matrix polymers. The high polarity of E-MA-GMA would however reduce the degree of miscibility with the HDPE in the binary blends of HDPE/E-MA-GMA leading to better compatibilisation effects due to quicker diffusion of the compatibiliser towards the

interfacial region of the blends for interaction. However, the setback observed in this study was that the methyl acrylate could possibly induce polar-polar interactions with the ester and amide groups of PBT and PA6 respectively hindering the access of epoxy moieties of the compatibiliser towards the chain end-groups of PBT and PA6.

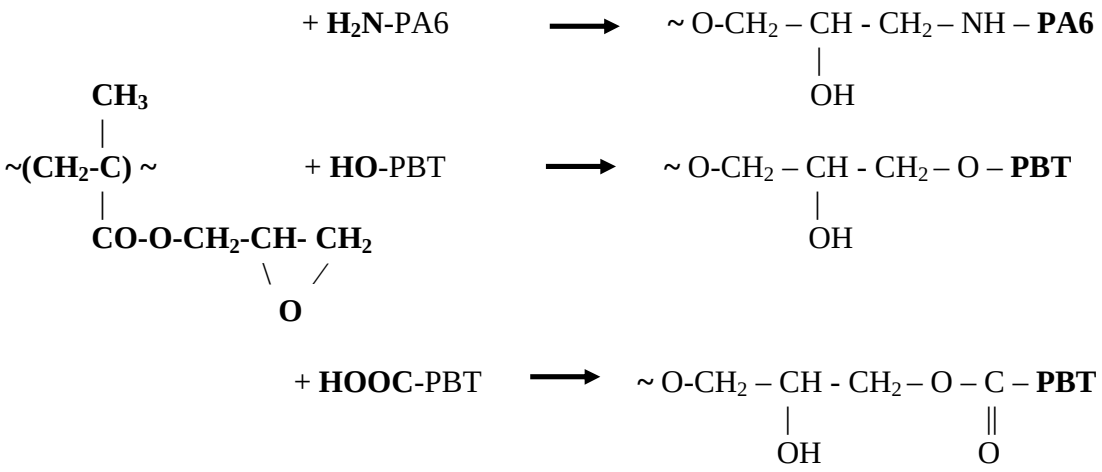


**Reaction Scheme 5: Chemical reactions of GMA with polymer end-groups [68, 70, 111]**

On the other hand, surprisingly HDPE-g-MAH seems to have only moderate compatibilising efficiency in PA6 blends and does not function well as a compatibiliser for ABS, PC and PBT blends due to limited reactivity with the functional groups of these polymers.

The EMA compatibiliser performed reasonably well in amorphous ABS and PC blends but not the crystalline polymer blends. The lack of reactive sites for reaction with chain end-groups of the PBT and PA6 could possibly limit the performance of EMA compared with reactive E-MA-GMA and E-GMA. However, EVA is believed to impart a large plasticisation effect on PA6 blends resulting in dramatic improvement in the tensile ductility of the blends.

In Chapter 5 of this thesis reactive modification of HDPE was carried out using a low molecular weight di-functional solid DGEBA type epoxy resin compatibilised with HDPE-g-MAH. Due to their great differences in polarity, epoxy is highly immiscible and incompatible with HDPE and the addition of HDPE-g-MAH in the blends resulted in noticeable improvements in miscibility of the two polymers. The maleic anhydride moieties in HDPE-g-MAH served as reactive sites for anchoring the epoxy moieties while the HDPE backbone is miscible with the HDPE resin. This resulted in the formation of a grafted copolymer with pedant epoxy groups as shown schematically in Figure 6.1.

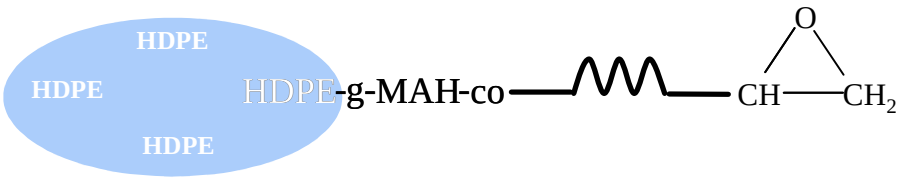


**Figure 6.1 Schematic representation of a HDPE/HDPE-g-MAH/epoxy grafted copolymer**

However, as the maleic anhydride moiety in its five-membered ring form has limited reaction with the epoxy ring, hydrated zinc acetate was used as catalyst to hydrolyse the five-membered ring into dicarboxylic acid. Evidence of esterification between dicarboxylic acid and epoxy was established by FTIR analysis of the blends. The detection of a new carbonyl peak at around 1740 $cm^{-1}$ and reduction in the dicarboxylic acid peak at 1713 $cm^{-1}$ observed by FTIR suggests the occurrence of an esterification reaction.

Optical micrographs of the reactive blends demonstrate that the presence of HDPE-g-MAH improved the dispersion of the epoxy in the blends. Further improvement in dispersability of the epoxy was noted when EVA was added as co-compatibiliser in the blends (sample HDPE-ME5Ca).

An extrusion plastometer was utilised to follow the compatibilisation reactions of the blends through changes in melt viscosity with different dwell times of the blends in the barrel of the plastometer. Extensive reactions in the barrel prevented flow when an excessive amount of functional groups was present in the blends. The observation of bright streaks in these blends when examined under a polarised light microscope suggested the presence of crosslinked gels.

Sol-gel analysis was performed on the blends for further characterisation of the sol (solution) and the gel (insoluble fraction). Insoluble fractions that were retained in the stainless steel mesh cage were reported as the gel content of the blends. FTIR analysis confirmed the presence of epoxy grafted PE segments and unreacted epoxy resins in the soluble fraction of both HDPE-ME3Ca and HDPE-ME5Ca blends. EVA was detected in the solution from HDPE-ME5Ca indicating that the compatibiliser did not participate in the esterification of the blend. However, a lower gel content for HDPE-ME5Ca suggested that better dispersability of the epoxy imparted by EVA helped in minimising the chances of gelation of the epoxy due to reaction with dicarboxylic acid of a neighbouring chain. On the other hand, the DSC and FTIR results of insoluble fractions suggests that the gels are segments of crystallisable polyethylene having more than four methylene ($CH_2$) units linked by ring opened DGEBA.

Quantitative analysis of gel was in good agreement with the results from melt flow rate measurements. Crosslinking resulted in restriction of molecular motion and thus reduction in the flowability of the blends.

The effectiveness of epoxy grafted HDPE (HDPE-ME3Ca and HDPE-ME5Ca) in compatibilising ABS/HDPE, PBT/HDPE, and PA6/HDPE was investigated by blending 5 wt% of the functionalised HDPE with these matrix polymers by injection moulding and mechanical testing and characterisation of the moulded bars.

During melt blending of the epoxy functionalised HDPE with matrix polymers like PBT and PA6, it is expected that the pendant epoxy moieties would react with the end-groups of these condensation polymers thus forming a new copolymer at the blend interphase as shown in Figure 6.2.

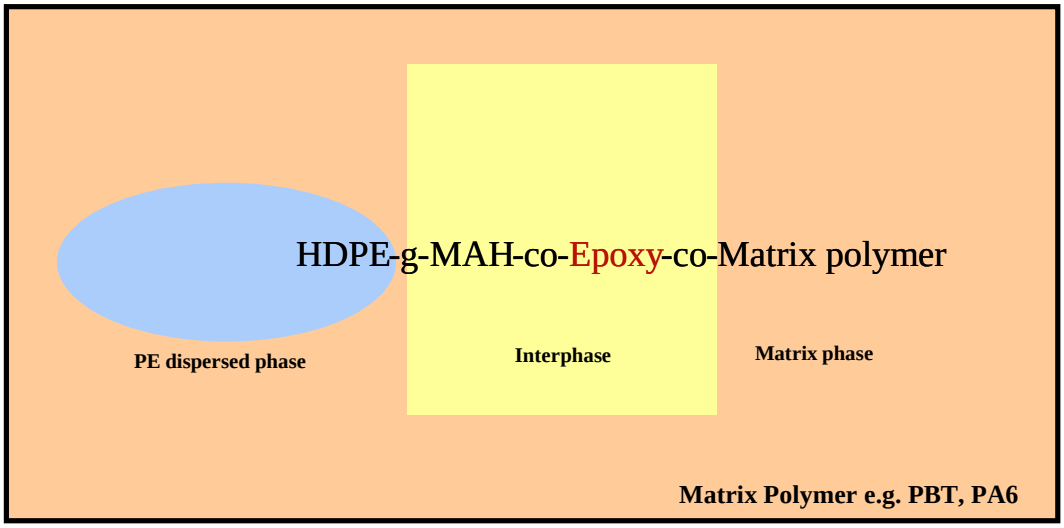


**Figure 6.2 Schematic representation of possible reaction between epoxy functionalised HDPE and matrix polymers**

Reactively functionalised HDPE blends, showed improvement in mechanical properties of ABS and PA6 blends especially with HDPE-ME5Ca which contained EVA as co-compatibiliser. This suggests the possibility of interactions between the epoxy moieties and the acrylonitrile groups and amine groups of the ABS and PA6 respectively.

However, surprisingly the mechanical properties of PBT blends were unaffected by the functionalised HDPE. As shown in Figure 6.3, the excessive unreacted epoxy present in the functionalised HDPE could have reacted with chain-ends of PBT rendering compatibilisation of the blends ineffective.

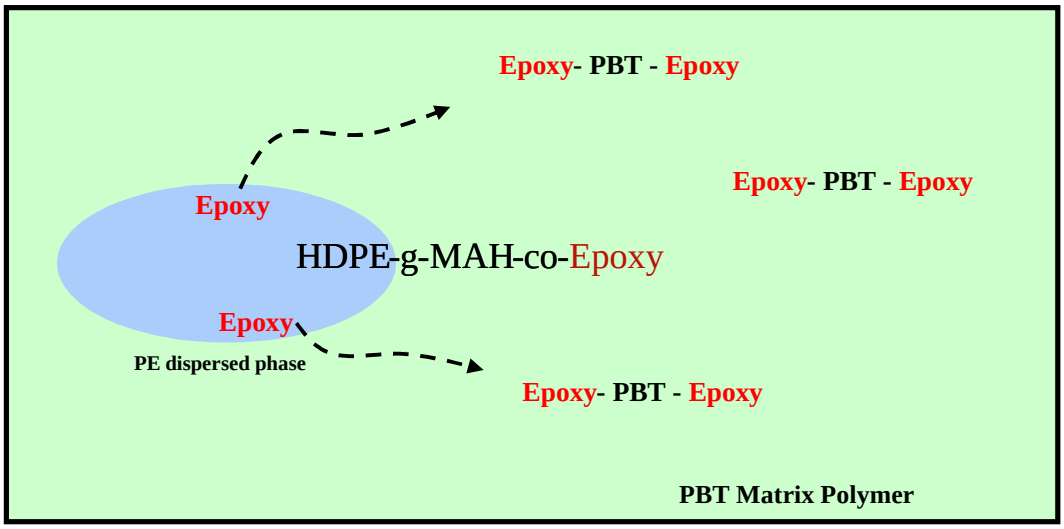


**Figure 6.3 Schematic representation of possible reaction between unreacted epoxy and chain-ends of PBT resin**

The observation of both large single HDPE spherulites and finely nucleated structures in a blend of uncompatibilised ABS/HDPE when examined under a polarised optical microscope confirmed the occurrence of fractionated crystallisation in the blend.

# CHAPTER 7

# CONCLUSIONS AND SUGGESTIONS FOR FUTURE WORK

Universal masterbatches are of great importance to the moulding industry due to the requirements for rapid change over in polymers for different applications while maintaining the same colour and/or additive functions. Keeping inventories of different masterbatches for different polymers of the same colour series causes lead time and inventory issues. On the other hand, using the same masterbatch for different types of polymer could result in detrimental effects on mechanical properties of the end moulded parts due to compatibility issues.

The present work has dealt with the compatibilisation of a high density polyethylene with various matrix polymers and based on results obtained from this study, following conclusions can be drawn:

1. Uncompatibilised ABS/HDPE, PC/HDPE, PBT/HDPE and PA6/HDPE blends clearly exhibited immiscible and incompatible characteristics even at low HDPE content of 5 wt%. Of the five commercial polar reactive and non-reactive compatibilisers evaluated, ethylene-methyl acrylate-glycidyl methacrylate terpolymer exhibited the most universal compatibilising efficiency on ABS/HDPE, PC/HDPE, PBT/HDPE and PA6/HDPE blends.

2. Compatibilisation of blends can be achieved via injection moulding by blending pre-compounded HDPE/compatibiliser binary or ternary blends with the matrix polymers.

3. Mechanical properties such as reversed notch Izod Impact and tensile elongation at break tend to provide more consistent indications on blend compatibilisation than notched Izod impact and tensile yield strain. Both PBT and PA6 exhibited very brittle fracture under notched Izod impact tests and remained

relatively unchanged even when these polymers were blended with incompatible HDPE. However, such incompatibility in blends was clearly evident when the Izod impact tests were carried out under reversed notch conditions and in slow speed tensile test, exhibiting low tensile ductility.

4. Blending HDPE with matrix polymers irrespective of compatibilisation, resulted in the occurrence of fractionated crystallisation in HDPE dispersed phases. The presence of multiple crystallisation peaks from DSC scans and also the observation of coexistence of single spherulitic structures and finely nucleated spherulites using a polarised light optical microscope provided evidence of fractionated crystallisation. The observation of fractionated crystallisation suggests inhomogeneity of the dispersed phase with respect to its nucleation density and also phase morphology.

5. Morphologies of blends are dependent on the type of compatibilisers and their concentration levels in the blends. Very fine morphology was observed in overly compatibilised blends which generally resulted in better interfacial bonding shown by improved elongation at break. However, it is noted that strong interfacial adhesion alone is not sufficient for toughness improvement which is also dependent on the particle sizes of the dispersed phase of the blends.

6. The results obtained from melt flow rate tests are in good agreement with gel content analysis thus indicating the feasibility of utilising an extrusion plastometer to follow blend reactions.

7. The grafting of epoxy onto HDPE can be achieved through the use of HDPE-g-MAH as compatibiliser. The dispersion of epoxy in the HDPE blend can be further improved through the use of an EVA copolymer as co-compatibiliser. It is believed that the improved dispersion of epoxy helped in minimising the chances of crosslinking.

8. ABS/HDPE blends are observed to have the most dramatic reduction in mechanical properties even when compatibilised with high levels of commercial compatibilisers. Reactive blends containing 0.1 wt% of MAH, and 3.0 wt% epoxy, catalysed with 0.11 wt% hydrated zinc acetate (sample HDPE-ME3Ca) are effective in compatibilising ABS/HDPE and PA6/HDPE blends. Further improvement in compatibilisation was achieved through the addition of 3 wt% EVA in the formulation (sample HDPE-ME5Ca).

9. The presence of excess ungrafted epoxy in the functionalised HDPE blends resulted in an adverse effect on compatibilisation of PBT/HDPE blends. It is believed that the free bound epoxy molecules have a faster diffusion rate than the grafted ones towards the chain end-groups of PBT rendering them inactive for reaction with the grafted epoxy moieties by end-capping reactions. Sol-gel analysis of the functionalised HDPE blends suggested the presence of epoxy grafted polyethylene segments, unbounded epoxy, EVA (for sample HDPE-ME5Ca) and crosslinked gels.

10. It was observed that blends compatibilised using reactively modified HDPE produced in this work, had more balanced mechanical properties across different matrix polymers as compared with commercial compatibilisers. Since the major usage of universal masterbatches are in styrenic polymers (particularly ABS) and polyamides, the observed significant improvements in mechanical properties of ABS/HDPE and PA6/HDPE blends signify the potential applications of these reactively modified polymers as carriers for universal masterbatches without compromising mechanical properties of the end moulded parts.

## Suggestions for Future Work

The present study has shown that functionalised HDPE containing excessive epoxy resin not only resulted in the formation of high level of gels but also affected its compatibilisation efficiency with the PBT matrix polymer. It is

therefore recommended to conduct further investigation on blends with a lower concentration of epoxy relative to the HDPE-g-MAH compatibiliser. Further reduction in the concentration of HDPE-g-MAH may also help in the reduction of gel content.

The substitution of HDPE-g-MAH by maleated styrene-ethylene/butylenes-styrene triblock copolymer (SEBS-g-MAH) is also recommended for further improvement in mechanical properties of the blends. The SEBS triblock segment is expected to have good compatibility with HDPE whereas the MAH moieties could serve as reactive sites for anchoring of the epoxy functionality. The SEBS is known to have good compatibility with a broad range of polymers ranging from olefinic, styrenics, polyesters and polyamide as noted in the literature survey, should aid further compatibilisation of the HDPE with these polymers.

The limited residence time of the blends in the barrel of an injection moulding machine, often results in inadequate melt mixing leading to poor distributive mixing of the dispersed phases and the matrix polymers. Apart from poor mechanical properties of end moulded parts, poor distributive mixing could also manifest as flow streaks when colour masterbatches are blended with matrix polymers which affects aesthetic appeal. It is therefore recommended that modification in the direction of flow improvement of the masterbatch carrier resins should be investigated using polar/reactive and more universal processing lubricants like ethylene bis-stearamide (EBS) or low molecular weight ionomer waxes. Apart from flow improvements for better distributive mixing of the dispersed phase, these waxes are also expected to impart better dispersion quality of the colorants and/or additives in the carrier system of the masterbatches.

For justification of the above recommendation, it is thus suggested to further investigate the carrier resins with the incorporation of a suitable universal pigment like titanium dioxide ($TiO_2$) which is intended for application as universal

white masterbatches by twin screw compounding process. Subsequent evaluation of these white universal masterbatches on targeted matrix polymers should produce useful findings for the continuous search of a universal carrier that works for a broad range of matrix polymers.

# REFERENCES


1. Traugott, T.D., Barlow, J.W. and Paul, D.R., "Mechanical Compatibilization of High Density Polyethylene-Poly(ethylene Terephthalate) Blends", J. Appl. Polym. Sci., 28, 2947-2959, (1983)

2. Dagli, S.S. and Kamdar, K.M., "Effects of Component Addition Protocol on the Reactive Compatibilization of HDPE/PET Blends", Polym. Eng. Sci. 34, 1709-1719, (1994)

3. Kalfoglou, N.K., Skafidas, D.S., Kallitsis, J.K., Lambert, J.C. and Stappen, L.V., "Comparison of Compatibilizer Effectiveness for PET/HDPE Blends", Polymer, 36, 4453-4462, (1995)

4. Chen, C., and Lai, F.S., "Processability and Thermal Properties of Blends of High Density Polyethylene, Poly(Ethylene Terephthalate), and Ethyl Vinyl Acetate Compatibilizer", Polym. Eng. Sci. 34, 472-476, (1994)

5. Müller, A.; Chapter 4, "Coloring of Plastics: Fundamentals-Colorants-Preparations", Carl Hanser Verlag, Munich, (2003)

6. Cameron, J.M., Chapter 19, "Dry Color Concentrate Manufacture", in: "Coloring of Plastics: Fundamentals", Charvat, R.A., Ed., Wiley-Interscience, Hoboken, New Jersey, 2nd edition, (2003)

7. Petiniot, N. and Rasquin, P., "Universal Masterbatch", US Patent No. 6,713,545 B2, (2004)

8. Teo, A.S.H., "Improving the Mechanical Properties of Antimony Trioxide Flame Retarded ABS", MSc. Thesis, Loughborough University, UK, (1996)

9. Sepe, M., "Beware the Universal Color Carrier", The Plastics Web, http://www.ides.com/articles/design/2007/sepe_01.asp (Accessed on 15th July 2007)

10. Hausmann, K. and Chou, R., "Additives with Dual Function – Acrylate Ester Copolymers as Modifiers for Engineering Polymers and as Carrier Resin for Masterbatches", Polym. & Polym Comp., 11, 91-100, (2003)

11. "DuPont Modifiers can Serve as Broad-use Masterbatch Carrier Resins for Pigments and Other Additives", http://www.dupont.com/industrial-polymers/plastics/functions/ masterbatch/.html (Accessed on 3rd May 2003)

12. Dean, W., Chapter 67, "Titanium Dioxide", in: "Plastics Additives and Modifiers Handbook", Edenbaum, J. Ed., Van Nostrand Reinhold, New York, (1992)

13. Spriet, C., Paper 2, “Which $TiO_2$ Pigment for Which Plastics Application?”, Conference Proceedings, Enhancing Polymers Using Additives and Modifiers II Symposium, UK, 1-9, (1996)

14. Haber, A. and Audet, R., “Factors Affecting Titanium Dioxide Dispersion in Color Concentrates”, Proceedings of ANTEC 1990, Society of Plastics Engineers, Dallas, 20-24, (1990)

15. Watson, C.L. and Decelles, G., “The Performance of Titanium Dioxide Pigments in Masterbatch Applications”, Proceedings of ANTEC 1994, Society of Plastics Engineers, San Francisco, 2514-2517, (1994)

16. Work, W.J., Horie, K., Hess, M. and Stepto, R.F.T., “Definitions of Terms Related to Polymer Blends, Composites, and Multiphase Polymeric Materials”, Pure Appl. Chem., 76, 1985-2007, (2004)

17. Ajji, A. and Utracki, L.A., “Compatibilisation of Polymer Blends”, Prog. Rub. Plast. Tech., 13, 153-187, (1997)

18. Brown, S.B., Chapter 5, “Reactive Compatibilization of Polymer Blends”, in: “Polymer Blends Handbook Vol. 1”, Utracki, L.A. Ed., Kluwer Academic Publishers, (2002)

19. Utracki, L.A., “History of Commercial Polymer Alloys and Blends (from a Perspective of the Patent Literature)”, Polym. Eng. Sci. 35, 2-17, (1995)

20. Utracki, L.A., “Polymer Alloys and Blends: Thermodynamics and Rheology”, Carl Hanser Verlag, Munich, Vienna, New York, (1990).

21. Olabisis, O., Robeson, L.M., and Shaw, M.T., “Polymer-Polymer Miscibility”, Academic Press, Inc., New York, (1979)

22. Chang, F.C., Chapter 21, “Compatibilized Thermoplastic Blends”, in: “Handbook of Thermoplastics”, Olabisi, O. Ed., Marcel Dekker, Inc., New York, 491-521, (1997)

23. Cizek, E.P., “Blend of a Polyphenylene ether and a Styrene Resin”, US Patent No. 3,383,435, (1968)

24. Utracki, L.A., “Commercial Polymer Blends”, Chapman & Hall, London, (1998)

25. Lindsey, C.R., Paul, D.R., and Barlow, J.W., “Mechanical Properties of HDPE-PS-SEBS Blends”, J. Appl. Polym. Sci., 26, 1-8, (1981)

26. Nishi, T., Wang, T.T., and Kwei, T.K., “Thermally Induced Phase Separation Behavior of Compatible Polymer Mixtures”, Macromolecules, 8, 227-234, (1975)

27. Chun, Y.S., Lee, H.S., and Kim, W.N., “Thermal Properties and Morphology of Blends of Poly(Ether Imide) and Polycarbonate”, Polym. Eng. Sci. 36, 2694-2702, (1994)

28. Barlow, J.W., and Paul, D.R., “Polymer Blends and Alloys-A Review of Selection Considerations”, Polym. Eng. Sci. 21, 985-996, (1981)

29. Bucknall, C.B., “Toughened Plastics”, Applied Science Publishers, London, (1977)

30. Flory, P.J., “Principles of Polymer Chemistry”, Cornell University Press, (1953)

31. Cowie, J.M.G., “Polymers: Chemistry and Physics of Modern Materials”, Blackie Academic & Professional, 2nd edition, (1991)

32. Anagnostopoulos, C.E., Coran, A.Y., and Gamrath, H.R., “Polymer-Diluent Interactions. I. A New Micromethod for Determining Polyvinyl Chloride-Diluent Interactions”, J. Appl. Polym. Sci., 4, 181-192, (1960)

33. Huang, J.C., Chang, D.C., and Deanin, R.D., “Analysis of PVC Blends by Three-Dimensional Solubility Parameters”, Adv. Polym. Tech. 12, 81-90, (1993)

34. Koning, C., van Duin, M., Pagnoulle, C., and Jerome, R., “Strategies for Compatibilization of Polymer Blends”, Prog. Polym. Sci. 23, 707-757, (1998)

35. Xanthos, M., “Interfacial Agents for Multiphase Polymer Systems: Recent Advances”, Polym. Eng. Sci. 28, 1392-1400, (1988)

36. Xanthos, M., and Dagli, S.S., “Compatibilisation of Polymer Blends by Reactive Processing”, Polym. Eng. Sci. 31, 929-935, (1991)

37. Datta, S., and Lohse, D.J., “Polymeric Compatibilizers: Uses and Benefits in Polymer Blends”, Carl Hanser Verlag, Munich, (1996)

38. Robeson, L.M., “Polymer Blends: A Comprehensive Review”, Carl Hanser Verlag, Munich, (2007)

39. Gaylord, N.G., “Compatibilizing Agents: Structure and Function in Polyblends”, J. Macromol. Sci. Chem., A26, 1211-1229, (1989)

40. Paul, D.R., Chapter 12, “Interfacial Agents (“Compatibilizers”) for Polymer Blends”, in: “Polymer Blends, vol. 2”, Paul, D.R., and Newman, S., Eds., Academic Press, New York, 35-62, (1978)

41. Gaylord, N.G., “Use Surfactants to Blend Polymers”, Chemtech (July), 435-440, (1989)

42. Gergen, W.P., and Davison, S., “Multicomponent Polyolefin-Block Copolymer-Polymer Blends”, US Patent No. 4,107,130, (1978)

43. Akkapeddi, M.K., and VanBuskirk, B., “Compatibilization and Toughening of PPE-PP Blends with Hydrogenated, Styrene-Diene Block Copoylmers”, Adv. Polym. Tech. 11, 263-275, (1992)

44. Halimatudahliana, Ismail, H., and Nasir, M., “The Effect of Various Compatibilizers on Mechanical Properties of Polystyrene/Polypropylene Blend”, Polym. Test. 21, 163-170, (2002)

45. Halimatudahliana, Ismail, H., and Nasir, M., “Morphological Studies of uncompatibilized and Compatibilized Polystyrene/Polypropylene blend”, Polym. Test., 21, 263-167, (2002)

46. Srinivasan, K.R., and Gupta, A.K., “Mechanical Properties and Morphology of PP/SEBS/PC Blends”, J. Appl. Polym. Sci., 53, 1-7, (1994)

47. Adewole, A.A., DeNicola, A., Gogos, C.G., and Mascia, L., “Compatibilisation of polypropylene-polystyrene blends Part 1 – Effect of Mixing Intensity on Morphology and Rheological Properties”, Plast. Rubber Compos., 29, 70-79, (2000)

48. Macosko, C.W., Guegan, P., and Khandpur, A.K., “Compatibilizers for Melt Blending: Premade Block Copolymers”, Macromolecules, 29, 5590-5598, (1996)

49. Brown, S.B., Chapter 4, “Reactive Extrusion: A Survey of Chemical Reactions of Monomers and Polymers During Extrusion Processing”, in: “Reactive Extrusion: Principles and Practice”, Xanthos, M. Ed., Hanser Publishers, Munich, (1992)

50. Orr, C.A., Cernohous, J.J., Guegan, P., Hirao, A., Jeon, H.K., and Macosko, C.W., “Homogeneous Reactive Coupling of Terminally Functional Polymers”, Polymer, 42, 8171-8178, (2001)

51. Ferrari, D.F., and Baker, W.E., “Aminolysis Kinetics of Model and Polymer-Bound Anhydride Moieties in Low- and High- Viscosity Media”, J. Polym. Sci., Part A: Polym. Chem., 36, 1573-1582, (1998)

52. Jeon, H.K., Macosko, C.W., Moon, B., Hoye, T.R., and Yin, Z., “Coupling Reactions of End- vs Mid-Functional Polymers”, Macromolecules, 37, 2563-2571, (2004)

53. Majumdar, B., and Paul, D.R., Chapter 17, “Reactive Compatibilization”, in: “Polymer Blends volume 1: Formulation”, Paul, D.R., and Bucknall, C.B., Eds., Wiley, New York, (2000)

54. Liu, N.C., Baker, W.E., and Russell, K.E., “Functionalization of Polyethylenes and Their Use in Reactive Blending”, J. Appl. Polym. Sci., 41, 2285-2300, (1990)

55. Sun, Y.J., Hu, G.H., Lambla, M., Kotlar, H.K., “In Situ Compatibilization of Polypropylene and Poly(butylenes terephthalate) Polymer Blends by One-Step Reactive Extrusion”, Polymer, 37, 4119-4127, (1996)

56. Liu, N.C., and Baker, W.E., “Reactive Polymers for Blend Compatibilization”, Adv. Polym. Tech. 11, 249-262, (1992)

57. Hu, G.H., Flat, J.J., and Lambla, M., Chapter 1, “Free-radical Grafting of Monomers onto Polymers by Reactive Extrusion: Principles and Applications”, in “Reactive Modifiers for Polymers”, Al-Malaika, S. Ed., Chapman & Hall, London; (1997)

58. Bettini, S.H.P., and Agnelli, J.A.M., “Evaluation of Methods Used for Analysing Maleic Anhydride Grafted onto Polypropylene by Reactive Processing”, Polym. Test., 19, 3-15, (2000)

59. Ide, F., and Hasegawa, A., “Studies on Polymer Blend of Nylon 6 and Polypropylene or Nylon 6 and Polystyrene Using the Reaction of Polymer”, J. Appl. Polym. Sci., 18, 963-974, (1974)

60. González-Montiel, A., Keskkula, H., and Paul, D.R., “Impact-modified Nylon 6/Polypropylene Blends: 1. Morphology-property Relationships”, Polymer, 36, 4587-4603, (1995)

61. Valenza, A., and Acierno, D., “Ternary Blends of Nylon 12/Polypropylene/Modified Polypropylene: Influence of Functional Groups on the Modified Polypropylene”, Eur. Polym. J., 30, 1121-1126, (1994)

62. Oshinski, A.J., Keskkula, H., and Paul, D.R., “Rubber Toughening of Polyamides with Functionalised Block Copolymers: 1. Nylon-6”, Polymer, 33, 268-283, (1992)

63. Oshinski, A.J., Keskkula, H., and Paul, D.R., “Rubber Toughening of Polyamides with Functionalised Block Copolymers: 2. Nylon-6,6”, Polymer, 33, 284-293, (1992)

64. Keskkula, H., and Paul, D.R., Chapter 11.6 “Toughened Nylons”, in: “Nylon Plastics Handbook”, Kohan, M.I., Ed., Carl Hanser Verlag, Munich, (1995)

65. Kriengchieocharn, P., “A Study of the Influence of Modified Natural Rubber on Polyamide 6 / Natural Rubber Blends”, MSc. Thesis, Mahidol University, Thailand, (1993)

66. Axtell, F.H., Phinyocheep, P., and Kriengchieocharn, P., “The Effect of Modified Natural Rubber Compatibilisers on Polyamide 6 / Natural Rubber Blends”, J. Sci. Soc. Thailand, 22, 201-216, (1996)

67. Dow Plastics, “Glycidyl Methacrylate (GMA): A High Purity, Dual Functionality Monomer for Coatings and Resins”, Technical Brochure, USA, (1998)

68. Holsti-Miettinen, R.M., Heino, M.T., and Seppälä, J.V., “Use of Epoxy Reactivity for Compatibilization of PP/PBT and PP/LCP Blends”, J. Appl. Polym. Sci., 57, 573-586, (1995)

69. Chiou, Y.P., Chiou, K.C., and Chang, F.C., “In situ Compatibilized Polypropylene/Liquid Crystalline Polymer Blends”, Polymer, 37, 4099-4106, (1996)

70. Tsai, C.H., and Chang, F.C., “Polymer Blends of PBT and PP Compatibilized by Ethylene-co-glycidyl Methacrylate Copolymers”, J. Appl. Polym. Sci., 61, 321-332, (1996)

71. Champagne, M.F., Huneault, M.A., and Roux, C., “Reactive Compatibilization of Polypropylene/Polyethylene Terephthalate Blends”, Polym. Eng. Sci. 39, 976-984, (1999)

72. Maa, C.T., and Chang, F.C., “In Situ Compatibilization of PET/PS Blends through Reactive Copolymers”, J. Appl. Polym. Sci., 49, 913-924, (1993)

73. Lee. P.C., Kuo, W.F., and Chang, F.C., “In Situ Compatibilization of PBT/ABS Blends Through Reactive Copolymers”, Polymer, 35, 5641-5650, (1994)

74. Chang, H.H., Wu, J.S., and Chang, F.C., “Reactive Compatibilization of ABS/Nylon 6,6 Blends: Effects of Reactive Group Concentration and Blending Sequence”, J. Polym. Res., 1, 235-245, (1994)

75. Heino, M., Kirjava, J., Hietaoja, P., and Seppälä, J., “Compatibilization of Polyethylene Terephthalate/Polypropylene Blends with Styrene-Ethylene/Butylene-Styrene (SEBS) Block Copolymers”, J. Appl. Polym. Sci., 65, 241-249, (1997)

76. Tedesco, A., Barbosa, R.V., Nachtigall, S.M.B., and Mauler, R.S., “Comparative Study of PP-MA and PP-GMA as Compatibilizing agents on polypropylene/nylon 6 blends”, Polym. Test., 21, 11-15, (2002)

77. Yin, Z.H., Zhang, Y.J., Zhang, X.M., and Yin, J.H., “Effects of the Compatibilizer PP-g-GMA on Morphology and Mechanical Properties of PP/PC blends”, Polymer, 39, 547-551, (1998)

78. Bikiaris, D.N., and Karayannidis, G.P., “Chain Extension of Polyesters PET and PBT with N,N’-Bis(glycidyl ester) Pyromellitimides. I”, J. Polym. Sci., Part A: Polym. Chem., 33, 1705-1714, (1995)

79. Bikiaris, D.N., and Karayannidis, G.P., “Chain Extension of Polyesters PET and PBT with Two New Diimidodiepoxides. II”, J. Polym. Sci., Part A: Polym. Chem., 34, 1337-1342, (1996)

80. Xanthos, M., and Young, M.W., “Reactive Modification of Polyethylene Terephthalate with Polyepoxides”, Polym. Eng. Sci. 41, 643-655, (2001)

81. Frigione, M., Acierno, D., and Mascia L., “Miscibilization of Low Molecular Weight Functionalized Polyethylenes in Epoxy Resins. I. Effects of Composition and Modifications Chemistry”, J. Appl. Polym. Sci., 73, 1457-1470, (1999)

82. Frigione, M., Acierno, D., and Mascia L., “Miscibilization of Low Molecular Weight Functionalized Polyethylenes in Epoxy Resins. Part 2. Effects of Curing on Morphological Features and Mechanical Properties”, Adv. Polym. Tech. 18, 237-253, (1999)

83. Jiang, X.L., Huang, H., Zhang, Y., and Zhang, Y.X., “Dynamically Cured Polypropylene/Epoxy Blends”, J. Appl. Polym. Sci., 92, 1437-1448, (2004)

84. Jiang, X.L., Zhang, Y., and Zhang Y.X., “Crystallization Behavior of Dynamically Cured Polypropylene/Epoxy Blends”, J. Polym. Sci., Part B: Polym. Phys., 42, 1181-1191, (2004)

85. Jiang, X.L., Zhang, Y., and Zhang Y.X., “Study of Dynamically Cured PP/MAH-g-EPDM/Epoxy Blends”, Polym. Test., 23, 259-266, (2004)

86. Mascia, L., and Xanthos, M., “An Overview of Additives and Modifiers for Polymer Blends: Facts, Deductions, and Uncertainties”, Adv. Polym. Tech. 11, 237-248, (1992)

87. Shieh, Y.T., Liao, T.N., and Chang, F.C., “Reactive Compatibilization of PP/PBT Blends by Mixture of PP-g-MA and Epoxy Resin”, J. Appl. Polym. Sci., 79, 2272-2285, (2001)

88. Tjong, S.C., and Meng, Y.Z., “Effect of Reactive Compatibilizers on the Mechanical Properties of Polycarbonate/Poly(acrylonitrile-butadiene-styrene) blends”, Eur. Polym. J., 36, 123-129, (2000)

89. Jana, S., Patel, N., and Dharaiya, D., “Compatibilization of PBT-PPE Blends Using Low Molecular Weight Epoxy”, Polymer, 42, 8681-8693, (2001)

90. Aróstegui, A., and Nazábal, J., “Super-Toughness in Compatibilized Poly(Butylene Terephthalate)/Poly(Ethylene-Octene) Copolymer Blends”, Polym. Eng. Sci., 43, 1691-1701, (2003)

91. Aróstegui, A., and Nazábal, J., “Compatibilization of a Poly(Butylene Terephthalate)/Poly(Ethylene octene) Copolymer Blends with Different Amounts of An Epoxy Resin”, J. Appl. Polym. Sci., 91, 260-269, (2004)

92. Chin, H.C., Chiou, K.C., and Chang, F.C., “Reactive Compatibilization of the Poly(Ethylene Terephthalate)/Liquid Crystalline Polymer Blends by Solid Epoxy Resin as a Coupling Agent”, J. Appl. Polym. Sci., 60, 2503-2516, (1996)

93. Chin, H.C., and Chang, F.C., “Reactive Compatibilization of the PET/LCP Blends by Multifunctional Epoxy Coupler”, Polymer, 38, 2947-2956, (1997)

94. Chiang, C.R., and Chang, F.C., “Polymer Blends of Polyamide-6 (PA6) and Poly (phenylene ether) (PPE) Compatibilized by Multifunctional Epoxy Coupler”, J. Polym. Sci., Part B: Polym. Phys., 36, 1805-1819, (1998)

95. Huang, C.C., and Chang, F.C., “Reactive Compatibilization of Polymer Blends of Poly(butylene terephthalate) (PBT) and Polyamide-6,6 (PA66): 1. Rheological and Thermal Properties”, Polymer, 38, 2135-2141, (1997)

96. Chiou, K.C., and Chang, F.C., “Reactive Compatibilization of Polyamide-6 (PA6)/Polybutylene Terephthalate (PBT) Blends by a Multifunctional Epoxy Resin”, J. Polym. Sci., Part B: Polym. Phys., 38, 23-33, (2000)

97. Bonner, J.G., and Hope, P.S., Chapter 3, “Compatibilisation and Reactive Blending”, in: “Polymer Blends and Alloys”, Folkes, M.J., and Hope, P.S., Eds., Chapman and Hall, (1993)

98. Hope, P.S., “Compatibilizers for Recycled Polyethylene”, in: “Plastics Additives: An A-Z Reference”, Pritchard G., Ed., Chapman and Hall, (1998)

99. Chapman, R.D., and Chruma, J.L., Chapter 4, “Nylon Plastics”, in: “Engineering Thermoplastics: Properties and Applications”, Margolis, J.M., Ed., Marcel Dekker, New York, (1985)

100. Gaymans, R.J., Borggreve, R.J.M., and Spoelstra, A.B., “Ductile Transition in Nylon-Rubber Blends: Influence of Water”, J. Appl. Polym. Sci., 37, 479-486, (1989)

101. Orofino, T.A., and McNeely, R.L., “Observations on Compatibility of Nylon 66/Polyethylene Mixtures”, J. Macromol. Sci. Phys., B27, 31-39, (1988)

102. Armat, R., and Moet, A., “Morphological Origin of Toughness in Polyethylene-Nylon-6 Blends”, Polymer, 34, 977-985, (1993)

103. Filippi, S., Minkova, L., Dintcheva, N., Narducci, P., and Magagnini, P., “Comparative Study of Different Maleic Anhydride Grafted Compatibilizer Precursors Towards LDPE/PA6 Blends: Morphology and Mechanical properties”, Polymer, 46, 8054-8061, (2005)

104. Kim, B.K., Park, S.Y., and Park, S.J., “Morphological, Thermal and Rheological Properties of Blends: Polyethylene/Nylon-6, Polyethylene/Nylon-6/(Maleic Anhydride-g-Polyethylene) and (Maleic Anhydride-g-Polyethylene)/Nylon-6”, Eur. Polym. J., 27, 349-354, (1991)

105. Jiang, C.H., Filippi, S., and Magagnini, “Reactive Compatibilizer Precursors for LDPE/PA6 Blends. II: Maleic Anhydride Grafted Polyethylenes” Polymer, 44, 2411-2422, (2003)

106. Kudva, R.A., Keskkula, H., and Paul, D.R., “Morphology and Mechanical Properties of Compatibilized Nylon 6/Polyethylene Blends”, Polymer, 40, 6003-6021, (1999)

107. Chen, Z.B., Li, T.S., Yang, Y.L., Zhang, Y., and Lai, S.Q., “The Effect of Phase Structure on the Tribological Properties of PA66/HDPE Blends”, Macromol. Mater. Eng., 289, 662-671, (2004)

108. Valenza, A., Visco, A.M., and Acierno, D., “Characterization of Blends with Polyamide 6 and Ethylene Acrylic Acid Copolymers at Different Acrylic Acid Content”, Polym. Test., 21, 101-109, (2002)

109. Filippi, S., Chiono, V., Polacco, G., Paci, M., Minkova, L., and Magagnini, P., “Reactive Compatibilizer Precursors for LDPE/PA6 Blends, 1: Ethylene/Acrylic Acid Copolymers”, Macromol. Chem. Phys., 203, 1512-1525, (2002).

110. Scaffaro, R., La Mantia, F.P., Canfora, L., Polacco, G., Filippi, S., and Magagnini, P., “Reactive Compatibilization of PA6/LDPE Blends with an Ethylene-Acrylic Acid Copolymer and a Low Molar Mass Bis-oxazoline”, Polymer, 44, 6951-6957, (2003)

111. Koulouri, E.G., Georgaki, A.X., and Kallitsis, J.K., “Reactive Compatibilization of Aliphatic Polyamides with Functionalized Polyethylenes”, Polymer, 38, 4185-4192, (1997)

112. Hert, M., “Tough Thermoplastic Polyesters by Reactive Extrusion with Epoxy-Containing Copolymers”, Angew. Makromol. Chem., 196, 89-99, (1992)

113. Pawlak, A., Morawiec, J., Pazzagli, F., Pracella, M., and Galeski, A., “Recycling of Postconsumer Poly(ethylene terephthalate) and High-Density Polyethylene by Compatibilized Blending”, J. Appl. Polym. Sci., 86, 1473-1485, (2002)

114. Fasce, L., Seltzer, R., Frontini, P., Rodriguez Pita, V.J., Pacheco, E.B.A.V., and Dias, M.L., “Mechanical and Fracture Characterization of 50:50 HDPE/PET Blends Presenting Different Phase Morphologies”, Polym. Eng. Sci., 45, 354-363, (2005)

115. Guerrero, C., Lozano, T., Conzalez, V., and Arroyo, E., “Properties and Morphology of Poly(ethylene terephthalate) and High-Density Polyethylene Blends”, J. Appl. Polym. Sci., 82, 1382-1390, (2001)

116. Kalfoglou, N.K., Skafidas D.S., and Sotiropoulou D.D., “Compatibilization of Blends of Poly(ethylene terephthalate) and Linear Low Density Polyethylene with the Ionomer of Poly(ethylene-co-methacrylic acid)”, Polymer, 35, 3624-3630, (1994)

117. Mascia, L., and Bellahdeb, F., “Graft Copolymers and Ionomeric Associations from Mixtures of Phenoxy with Acid Functionalized Polyolefins- Part II: Compatibilizers for HDPE/PET Blends”, Adv. Polym. Techn., 13, 99-109, (1994)

118. Aróstegui, A., Gaztelumendi, M., and Nazábal, J., “Toughened Poly(butylene terephthalate) by Blending with a Metallocenic Poly(ethylene-octene) Copolymer”, Polymer, 42, 9565-9574, (2001)

119. Aróstegui, A., and Nazábal, J., “New Super-Tough Poly(butylene terephthalate) Materials Based on Compatibilized Blends with Metallocenic Poly(ethylene-octene) Copolymer”, Polym. Adv. Technol., 14, 400-408, (2003)

120. Grigo, U., Kircher, K., and Müller, P.R., Chapter 3, “Polycarbonates”, in: “Engineering Thermoplastics: Polycarbonates Polyacetals Polyesters Cellulose Esters”, Bottenbruch, L., Ed., Hanser/Gardner Publications, Cincinnati, (1996)

121. Dobrescu, V., and Cobzaru, V., “Some Rheological Properties of Polycarbonate Blends”, J. Polym. Sci. Polym. Symp., 64, 27-42, (1978)

122. Yang, M.B., Li, Z.M., and Feng, J.M., “Studies on High Density Polyethylene/Polycarbonate Blend System Compatibilized With Low Density Polyethylene Grafted Diallyl Bisphenol A Ether”, Polym. Eng. Sci., 38, 879-883, (1998)

123. Kunori, T., and Geil, P.H., “Morphology-Property Relationships in Polycarbonate-Based Blends. I. Modulus”, J. Macromol. Sci. Phys., B18, 93-134, (1980)

124. Kunori, T., and Geil, P.H., “Morphology-Property Relationships in Polycarbonate-Based Blends. II. Tensile and Impact Strength”, J. Macromol. Sci. Phys., B18, 135-175, (1980)

125. Leclair, B., and Favis, B.D., “The Role of Interfacial Contact in Immiscible Binary Polymer Blends and Its Influence on Mechanical Properties”, Polymer, 37, 4723-4728, (1996)

126. Sue, H.J., Huang, J., and Yee, A.F., “Interfacial Adhesion and Toughening Mechanisms in An Alloy of Polycarbonate/Polyethylene”, Polymer, 33, 4868-4871, (1992)

127. Dias, M.L., and Fernandes, M.J.A., “Processing Behaviour of Polycarbonate/Functionalized-Ethylene Copolymer Blends”, Polym. Eng. Sci., 40, 2482-2488, (2000)

128. Mekhilef, N., Kadi, A.A., and Ajji, A., “Blends of Modified Polycarbonate and High Density Polyethylene”, Polym. Eng. Sci., 32, 894-902, (1992)

129. Mascia, L., and Valenza, A., “Reactive Dual-Component Compatibilizers for Polycarbonate/High-Density Polyethylene Blends”, Adv. Polym. Tech., 14, 327-335, (1995)

130. Li, C.Q., Zhang, Y., Zhang, Y.X., and Zhang, C.M., “Blends of Polycarbonate and Ethylene-1-Octylene Copolymer”, Eur. Polym. J., 39, 305-311, (2003)

131. Carrick, W.L., “Reactions of Polyolefins with Strong Lewis Acids”, J. Polym. Sci., Part A-1, 8, 215-223, (1970)

132. Barentsen, W.M., and Heikens, D., “Mechanical Properties of Polystyrene/Low Density Polyethylene Blends”, Polymer, 14, 579-583, (1973)

133. Barentsen, W.M., Heikens, D., and Piet, P., “Effect of Addition of Graft Copolymer on the Microstructure and Impact Strength of PS/LDPE Blends”, Polymer, 15, 119-122, (1974)

134. Fayt, R., Jérôme R., and Teyssié, Ph., “Molecular Design of Multicomponent Polymer Systems. I. Emulsifying Effect of Poly(Hydrogenated Butadiene-b-Styrene) Copolymers in LDPE/PS Blends”, J. Polym. Sci., Polym. Lett. Edn, 19, 79-84, (1981)

135. Fayt, R., Jérôme R., and Teyssié, Ph., “Molecular Design of Multicomponent Polymer Systems. II. Emulsifying Effect of Poly(Hydrogenated Butadiene-b-Styrene) Copolymers in High-Density

Polyethylene/Polystyrene Blends", J. Polym. Sci., Polym. Lett. Edn, 19, 1269-1272, (1981)

136. Fayt, R., Jérôme R., and Teyssié, Ph., "Molecular Design of Multicomponent Polymer Systems. III. Comparative Behavior of Pure and Tapered Block Copolymers in Emulsification of Blends of Low-Density Polyethylene and Polystyrene", J. Polym. Sci., Polym. Lett. Edn, 20, 2209-2217, (1982)

137. Taha, M., and Frerejean, V., "Morphology Development of LDPE-PS Blend Compatibilisation", J. Appl. Polym. Sci., 61, 969-979, (1996)

138. Guo, H.F., Packirisamy, S., Mani, R.S., Aronson, C.L., Gvozdic, N.V., and Meier, D.J., "Compatibilizing Effects of Block Copolymers in Low-Density Polyethylene/Polystyrene Blends", Polymer, 39, 2495-2505, (1998)

139. Appleby, T., Cser, F., Moad, G., Rizzardo, E., and Stavropoulos, C., "Compatibilisation of Polystyrene-Polyolefin Blends", Polym. Bull., 32, 479-485, (1994)

140. Tjong, S.C., and Xu, S.A., "Impact and Tensile Properties of SEBS Copolymer Compatibilized PS/HDPE Blends", J. App. Polym. Sci., 68, 1099-1108, (1998)

141. Wu, J.S., Guo, B.H., Chan, C.M., Li, J.X., and Tang, H.S., "Synergistic Toughening Effect of SBS and HDPE on the Fracture of PS/HDPE/SBS Blends", Polymer, 42, 8857-8865, (2001)

142. Baker, W.E., and Saleem, M., "Coupling of Reactive Polystyrene and Polyethylene in Melts", Polymer, 28, 2057-2062, (1987)

143. Baker, W.E., and Saleem, M., "Polystyrene-Polyethylene Melt Blends Obtained Through Reactive Mixing Process", Polym. Eng. Sci., 27, 1634-1641, (1987)

144. Saleem, M., and Baker, W.E., "In Situ Reactive Compatibilization in Polymer Blends: Effects of Functional Group Concentrations" J. App. Polym. Sci., 39, 655-678, (1990)

145. Shanks, R.A., and Amarasinghe, G., Chapter 2 "Applications of Differential Scanning Calorimetry to Analysis of Polymer Blends", in: "Polymer Characterization Techniques and Their Application to Blends", Simon, G.P., Ed., Oxford University Press, New York, (2003)

146. Song, M., and Long, F., "Miscibility in Blends of Poly(Vinyl Acetate) with Poly(Methyl Methacrylate) studied by FTIR and DSC", Eur. Polym. J., 9, 983-986, (1991)

147. MacKnight, W.J., and Karasz, F.E., Chapter 5, “Solid State Transition behaviour of Blends”, in: “Polymer Blends, vol. 1”, Paul, D.R., and Newman, S., Eds., Academic Press, New York, (1978)

148. Ghijsels, A., Groesbeek, N., and Yip, C.W., “Multiple Crystallisation Behaviour of Polypropylene/Thermoplastic Rubber Blends and Its Use in Assessing Blend Morphology”, Polymer, 23, 1913-1916, (1982)

149. Santana, O.O., and Müller, A.J., “Homogeneous Nucleation of the Dispersed Crystallisable Component of Immiscible Polymer Blends”, Polym. Bull., 32, 471-477, (1994)

150. Morales, R.A., Arnal, M.L., and Müller, A.J., “The Evaluation of the State of Dispersion in Immiscible Blends Where the Minor Phase Exhibits Fractionated Crystallisation”, Polym. Bull., 35, 379-386, (1995)

151. Molinuevo, C.H., Mendez, G.A., and Müller, A.J., “Nucleation and Crystallization of PET Droplets Dispersed in An Amorphous PC Matrix”, J. App. Polym. Sci., 70, 1725-1735, (1998)

152. Li, C.Q., Tian, G.H., Zhang, Y., and Zhang, Y.X., “Crystallization Behavior of Polypropylene/Polycarbonate Blends”, Polym. Test., 21, 919-926, (2002)

153. Frensch, H., Harnischfeger, P., and Jungnickel B.J., “Fractionated Crystallization in Incompatible Polymer Blends”, in: “Multiphase Polymers: Blends and Ionomers”, Utracki, L.A., and Weiss, R.A., Eds., ACS Sym. Series, 395, 101-125, (1989)

154. Datta, N.K., and Birley, A.w., “Thermal Analysis of Polyethylene Blends”, Plast. Rubber Process. Appl., 2, 237-245, (1982)

155. Nishi T., and Wang, T.T, “Melting Point Depression and Kinetic Effects of Cooling on Crystallisation in Poly(vinylidene fluoride)-Poly(methyl methacrylate) Mixtures”, Macromolecules, 8, 909-915, (1975)

156. Li, C.X., Kong, Q.S., Zhao, J., Zhao, D., Fan, Q.R., and Xia, Y.Z., “Crystallization of Partially Miscible Linear Low-Density Polyethylene/Poly(Ethylene-co-Vinylacetate) Blends”, Mater. Lett., 58, 3613-3617, (2004)

157. Haghighat, S., “Melt and Solid State Behaviour of Polyolefin Blends”, PhD. Thesis, Loughborough University, UK, (1990)

158. Coleman M.M., and Painter, P.C., Chapter 6 “Infrared Analysis”, in: “Polymer Characterization Techniques and Their Application to Blends”, Simon, G.P., Ed., Oxford University Press, New York, (2003)

159. Coleman, M.M., Moskala E.J., Painter, P.C., Walsh, D.J., and Rostami, S., “A Fourier Transform Infra-red Study of the Phase Behaviour of

Polymer Blends. Ethylene-Vinyl Acetate Copolymer Blends With Poly(vinyl chloride) and Chlorinated Polyethylene", Polymer, 24, 1410-1414, (1983)

160. Coleman, M.M., Graf, J.F., and Painter, P.C., "Specific Interactions and the Miscibility of Polymer Blends", Technomic, Pennsylvannia, (1991)

161. Moskala, E.J., Howe, S.E., Painter, P.C., and Coleman, M.M., "On the Role of Intermolecular Hydrogen Bonding in Miscible Polymer Blends", Macromolecules, 17, 1671-1678, (1984)

162. Moskala, E.J., Varnell, D.F., and Coleman, M.M., "Concerning the Miscibility of Poly(vinylphenol) Blends – FTIR Study", Polymer, 26, 228-234, (1985)

163. Tselios, Ch., Bikiaris, D., Maslis, V., and Panayiotou, C., "In situ Compatibilization of Polypropylene-Polyethylene Blends: a Thermomechanical and Spectroscopic Study", Polymer, 26, 6807-6817, (1998)

164. Hopfe, I., Pompe, G., and Eichhorn, K.J., "Ordered Structures and Progressive Transesterification in PC/PBT melt Blends Studied by FTIR Spectroscopy Combined With DSC and NMR", Polymer, 38, 2321-2327, (1997)

165. Macosko, C.W., "Morphology Development and Control in Immiscible Polymer Blends", Macromol. Symp., 149, 171-184, (2000)

166. Shaw, M.T., Chapter 3 "Microscopy and Other Methods of Studying Blends", in: "Polymer Blends and Mixtures", Walsh, D.J., Higgins, J.S., and Maconnachie, A., Eds., Martinus Nijhoff Publishers, Dordrecht, (1985)

167. Cheremisinoff, N.P., "Polymer Characterization: Laboratory Techniques and Analysis", Noyes Publications, New Jersey, (1996)

168. Ogbobe, O., "Study of the Dispersion of Low-Density Polyethylene Additive Masterbatches in Polyolefins", J. App. Polym. Sci., 49, 381-389, (1993)

169. Hemsley, D., Chapter 33 "Optical Microscopy", in: "Comprehensive Polymer Science, Vol. 1: Polymer Characterization", Booth, C., and Price, C., Eds., Pergamon Press, Oxford, (1989)

170. Sawyer, L.C., and Grubb, D.T., "Polymer Microscopy", Chapman & Hall, London, 2nd edition, (1996)

171. Bretas, R.E.S., Chapter 5 "Polarized Light Optical Microscopy", in: "Polymer Characterization Techniques and Their Application to Blends", Simon, G.P., Ed., Oxford University Press, New York, (2003)

172. Hemsley, D.A., “The Light Microscopy of Synthetic Polymers”, Oxford University Press, New York, (1984)

173. Woodward, A.E., “Atlas of Polymer Morphology”, Carl Hanser Verlag, New York, (1989)

174. Hobbs, S.Y., and Watkins, V.H., Chapter 9 “Morphology Characterization by Microscopy Techniques”, in: “Polymer Blends Volume 1: Formulation”, Paul, D.R., and Bucknall, C.B., Eds., John Wiley & Sons Inc., New York, (2000)

175. Inoue, T., Chapter 8 “Morphology of Polymer Blends”, in: “Polymer Blends Handbook Volume 1”, Utracki, L.A., Ed., Kluwer Academic Publishers, Boston, (2002)

176. Lovinger, A.J., and Williams, M.L., “Tensile Properties and Morphology of Blends of Polyethylene and Polypropylene”, J. App. Polym. Sci., 25, 1703-1713, (1980)

177. Martuscelli, E., Silvestre, C., Addonizio, M.L., and Amelino, L., “Phase Structure and Compatibility Studies in Poly(ethylene oxide)/poly(methyl methacrylate) Blends”, Makromol. Chem., 187, 1577-1571, (1986)

178. Bulakh, N., and Jog, J.P., “Crystallization of Poly(phenylene sulfide)/amorphous polyamide blends: DSC and Microscopic Studies”, J. Macromol. Sci.-Phys., B38(3), 277-287, (1999)

179. Bassett, D.C., and Vaughan, A.S., Chapter 15 “Electron Microscopy of Polymer Blends”, in: “Polymer Characterization Techniques and Their Application to Blends”, Simon, G.P., Ed., Oxford University Press, New York, (2003)

180. Lee, J.K., and Han, C.D., “Evolution of Polymer Blend Morphology During Compounding in an Internal Mixer”, Polymer, 40, 6277-6296, (1999)

181. Lee, J.K., and Han, C.D., “Evolution of Polymer Blend Morphology During Compounding in a Twin-screw Extruder”, Polymer, 41, 1799-1815, (2000)

182. Pukanszky, B., and Belina, K., Chapter 9 “Tensile Properties, Creep, and Stress Relaxation”, in: “Polymer Characterization Techniques and Their Application to Blends”, Simon, G.P., Ed., Oxford University Press, New York, (2003)

183. Xavier, S.F., Chapter 12 “Properties and Performance of Polymer Blends”, in: “Polymer Blends Handbook Volume 2”, Utracki, L.A., Ed., Kluwer Academic Publishers, Boston, (2002)

184. Nielsen, L.E., and Landel, R.F., “Mechanical Properties of Polymers and Composites”, Marcel Dekker, New York, 2nd edition, (1994)

185. Paul, D.R., Locke, C.E., and Vinson, C.E., “Chlorinated Polyethylene Modification of Blends Derived from Waste Plastics Part 1: Mechanical Behaviour”, Polym. Eng. Sci., 13, 202-208, (1973)

186. Locke, C.E., and Paul, D.R., “Graft Copolymer Modification of Polyethylene-Polystyrene Blends II: Properties of Modified Blends”, J. App. Polym. Sci., 17, 2791-2800, (1973)

187. Fayt, R., Jerome, R., and Teyssie, PH., Molecular Design of Multicomponent Polymer Systems XIV: Control of the Mechanical Properties of Polyethylene-Polystyrene Blends by Block Copolymers”, J. Polym. Sci., Part B: Polym. Phys., 27, 775-793, (1989)

188. Perkins, W.G., “Polymer Toughness and Impact Resistance”, Polym. Eng. Sci., 39, 2445-2460, (1999)

189. Wu, S., “Phase Structure and Adhesion in Polymer Blends: A criterion for Rubber Toughening”, Polymer, 26, 1855-1863, (1985)

190. Wunderlich, B., “Thermal Analysis”, Academic Press, San Diego, 417-428, (1990)

191. Ray, I., and Khastgir, D., “Correlation Between Morphology with Dynamic Mechanical, Thermal, Physicomechanical Properties and Electrical Conductivity for EVA-LDPE Blends”, Polymer, 34, 2030-2037, (1993)

192. Harris, J.E., and Robeson, L.M., “Isomorphic Behavior of Poly(aryl ether ketone) Blends”, J. Polym. Sci. Polym. Phys., 25, 311-323, (1987)

193. Gupta, A.K., and Purwar, S.N., “Crystallisation of PP/SEBS Blends and Its Correlation with Tensile Properties”, J. App. Polym. Sci., 29, 1595-1609, (1984)

194. Hale, W., Keskkula, H., and Paul, D.R., “Effect of Crosslinking Reactions and Order of Mixing on Properties of Compatibilized PBT/ABS Blends”, Polymer, 40, 3665-3676, (1999)

195. Nadkarni, V.M., and Jog, J.P., Chapter 8 “Crystallization Behaviour in Polymer Blends”, in: “Two-Phase Polymer Systems”, Utracki, L.A., Ed., Hanser Publishers, Munich, (1991)

196. Aref-Azar, A., Hay, J.N., Marsden, B.J., and Walker, N., “Crystallization Characteristics of Polymer Blends: 1. Polyethylene and Polystyrene”, J. Polym. Sci. Polym. Phys. Ed., 18, 637-643, (1980)

197. Hobbs, S.Y., and Pratt, C.F., “Multiple melting in Poly(butylenes terephthalate)”, Polymer, 16, 462-464, (1975)

198. Sclavons, M., Franquinet, P., Carlier, V., Verfaillie, G., Fallais, I., Legras, R., and Laurent, M., “Quantification of the Maleic Anhydride Grafted onto Polypropylene by Chemical and Viscosimetric Titrations, and FTIR Spectroscopy”, Polymer, 41, 1989-1999, (2000)

199. Lee, H., and Neville, K, “Handbook of Epoxy Resins”, McGraw-Hill, New York, (1967)

200. Bayram, G., Yilmazer, U., and Xanthos, M., “Viscoelastic Properties of Reactive and Non-Reactive Blends of Ethylene-Methyl Acrylate Copolymers with Styrene-Maleic Anhydride Copolymer”, Polym. Eng. Sci., 41, 262-274, (2001)

201. Bayram, G., Yilmazer, U., Xanthos, M., and Patel, S.H., “Rheological Behaviour of Styrene-Maleic Anhydride/Polyol Blends Obtained Through Reactive Process”, J. App. Polym. Sci., 85, 2615-2623, (2002)

202. Koga, N., and Tanaka, H., “Kinetics and Mechanism of the Isothermal Dehydration of Zinc Dihydrate”, Thermochim. Acta, 303, 69-76, (1997)

203. Nishikida, K., and Coates, J., Chapter 7 “Infrared and Raman Analysis of Polymers”, in: “Handbook of Plastics Analysis”, Lobo, H. and Bonilla, J.V., Eds, Marcel Dekker, New York, (2003)

204. Mertzel, E., and Koenig, J.L., “Application of FT-IR and NMR to Epoxy Resins”, Adv. Polym. Sci., 75, 73-112, (1986)

205. Brezinski, D., “An Infrared Spectroscopy Atlas for the Coatings Industry, Vol. 1”, 4$^{th}$ Ed, Federation of Societies for Coatings Technology, Blue Bell, Pennsylvania, 47-48, (1991)

206. Zheng, S., Hu, Y., Guo, Q., and Wei, J., “Miscibility, Morphology and Fracture Toughness of Epoxy Resin / Poly(vinyl actetae) Blends”, Colloid Polym. Sci., 274, 410-417, (1996)

207. Nielsen, L.E., “Predicting the Properties of Mixtures: Mixture Rules in Science and Engineering”, Marcel Dekker, New York, (1978)

208. Ha, T.H., Jang, J.Y., Cho, Y.B., Jeong, H.M., and Kim, B.K., “Maleic Anhydride Grafted Polyethylene Powder Coated With Epoxy Resin: A Novel Reactive Hot Melt Adhesive”, J. App. Polym. Sci., 116, 328-332, (2010)

209. Scheirs, J., “Compositional and Failure Analysis of Polymers: A Practical Approach”, John Wiley & Sons, Chichester, (2000)

210. Bellamy, L.J., “The Infra-red Spectra of Complex Molecules”, 3rd Ed, Chapman and Hall, London, (1975)

211. Utracki, L.A., Chapter 2, “Thermodynamics of Polymer Blends”, in: “Polymer Blends Handbook Vol. 1”, Utracki, L.A. Ed., Kluwer Academic Publishers, (2002)

212. Coleman, M.M., Serman, C.J., Bhagwagar, D.E., and Painter, P.C., “Polymer Reviews: A practical Guide to Polymer Miscibility”, Polymer, 31, 1187-1203, (1990)

213. Hourston, D.J., Lane, S., and Zhang, H.X., “Toughened Thermoplastics: 3. Blends of Poly (butylenes terephthalate) with (butadiene-co-acrylonitrile) Rubbers”, Polymer, 36, 3051-3054, (1995)

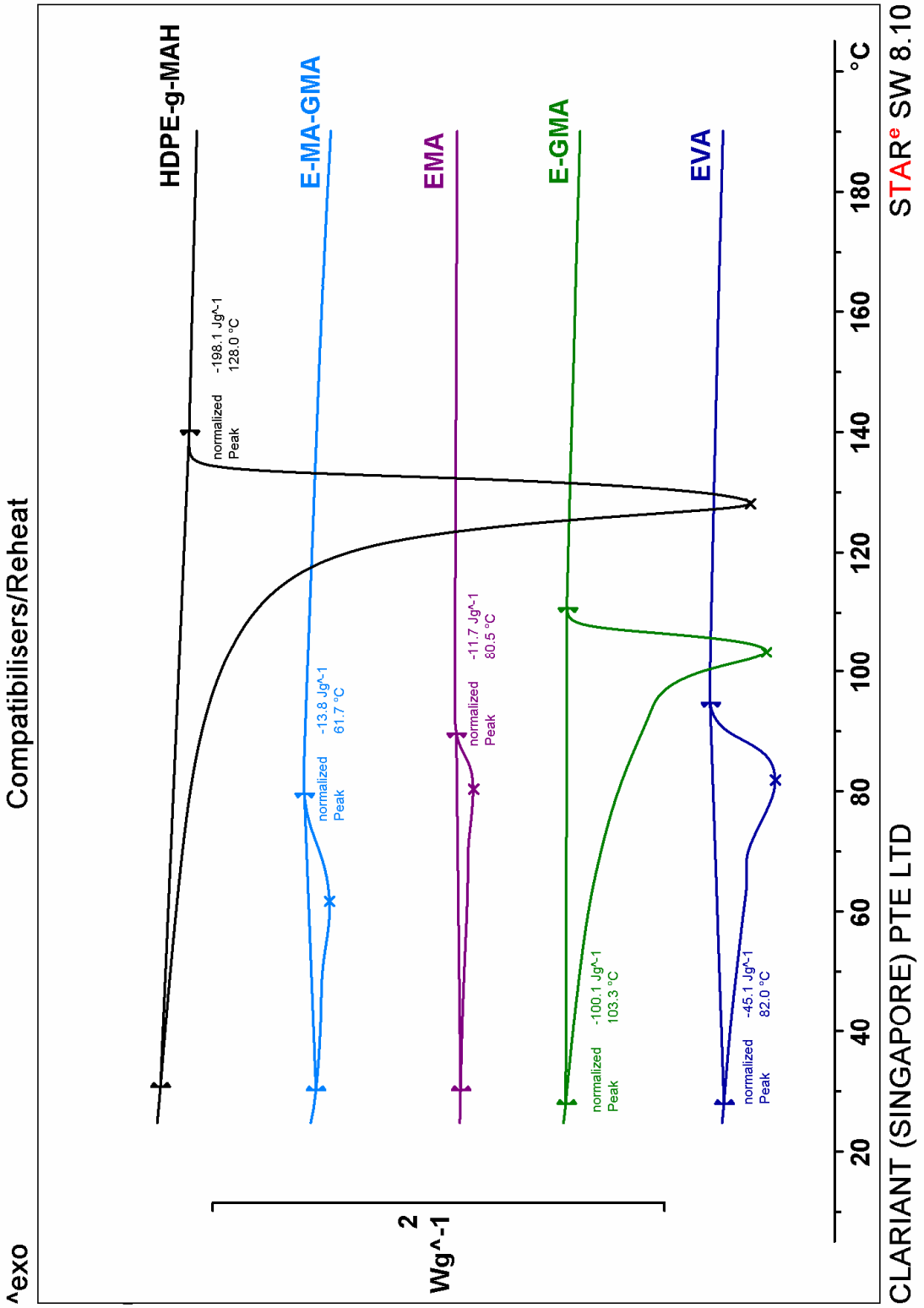
Compatibilisers/Reheat
^exo
HDPE-g-MAH
normalized
Peak
-198.1 Jg^-1
128.0 °C
E-MA-GMA
normalized
Peak
-13.8 Jg^-1
61.7 °C
EMA
normalized
Peak
-11.7 Jg^-1
80.5 °C
E-GMA
normalized
Peak
-100.1 Jg^-1
103.3 °C
EVA
normalized
Peak
-45.1 Jg^-1
82.0 °C
2
Wg^-1
20
40
60
80
100
120
140
160
180
°C
CLARIANT (SINGAPORE) PTE LTD
STARe SW 8.10

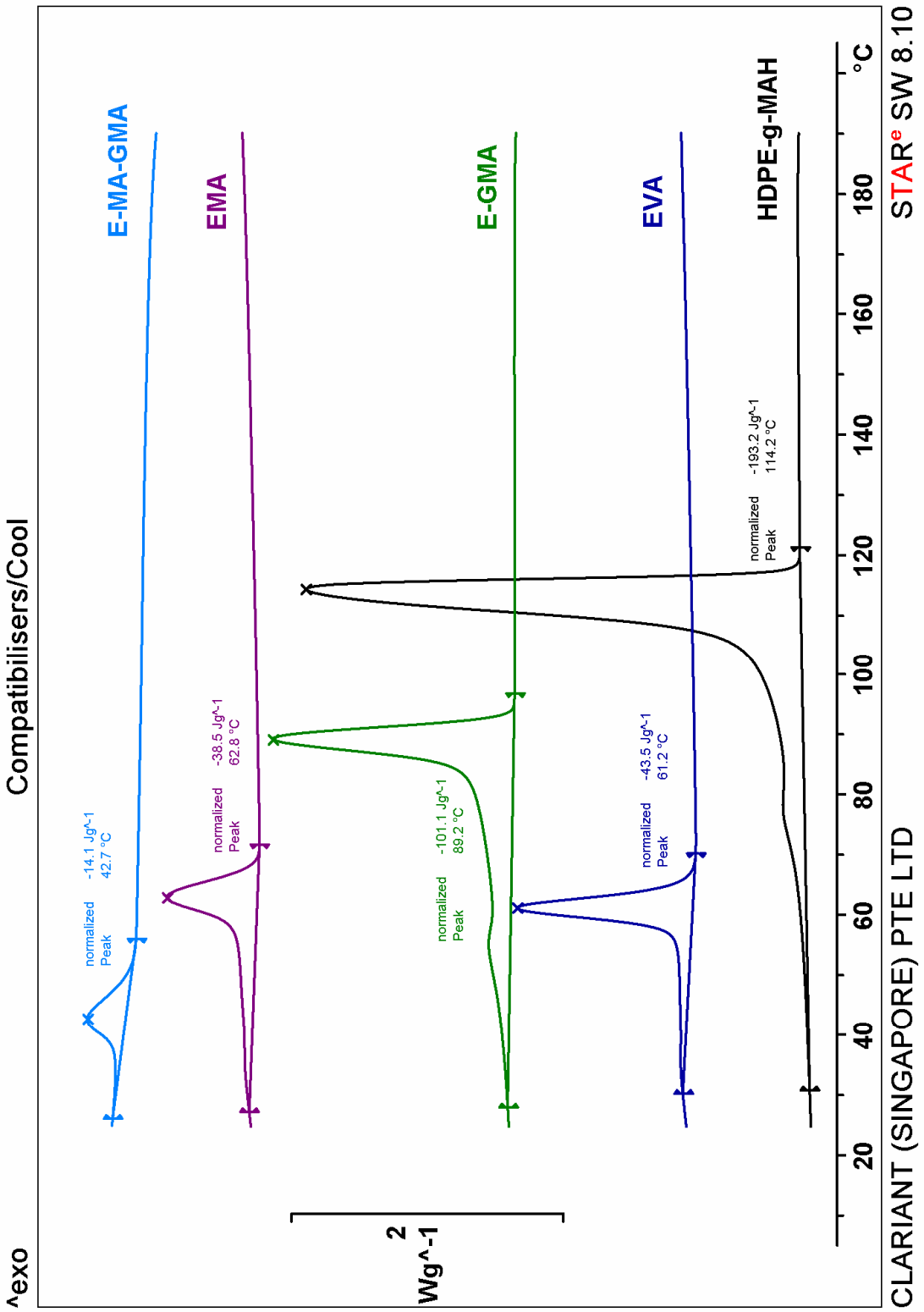
Compatibilisers/Cool
^exo
E-MA-GMA
normalized
Peak
-14.1 Jg^-1
42.7 °C
EMA
normalized
Peak
-38.5 Jg^-1
62.8 °C
E-GMA
normalized
Peak
-101.1 Jg^-1
89.2 °C
EVA
normalized
Peak
-43.5 Jg^-1
61.2 °C
HDPE-g-MAH
normalized
Peak
-193.2 Jg^-1
114.2 °C
2
Wg^-1
20
40
60
80
100
120
140
160
180
°C
CLARIANT (SINGAPORE) PTE LTD
STARe SW 8.10

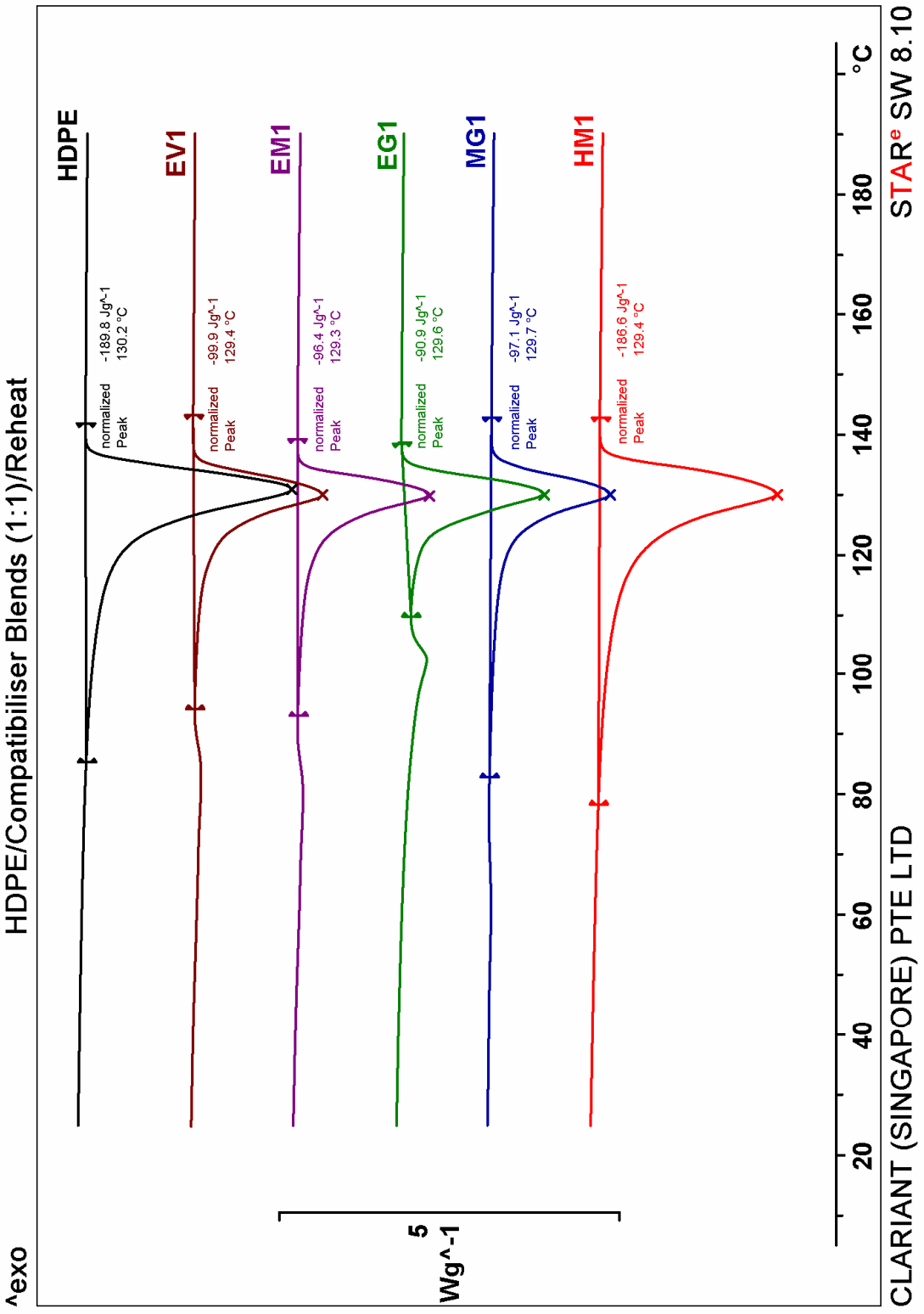
HDPE/Compatibiliser Blends (1:1)/Reheat
^exo
HDPE
EV1
EM1
EG1
MG1
HM1
normalized
Peak
-189.8 Jg^-1
130.2 °C
-99.9 Jg^-1
129.4 °C
-96.4 Jg^-1
129.3 °C
-90.9 Jg^-1
129.6 °C
-97.1 Jg^-1
129.7 °C
-186.6 Jg^-1
129.4 °C
5
Wg^-1
20
40
60
80
100
120
140
160
180
°C
CLARIANT (SINGAPORE) PTE LTD
STARe SW 8.10

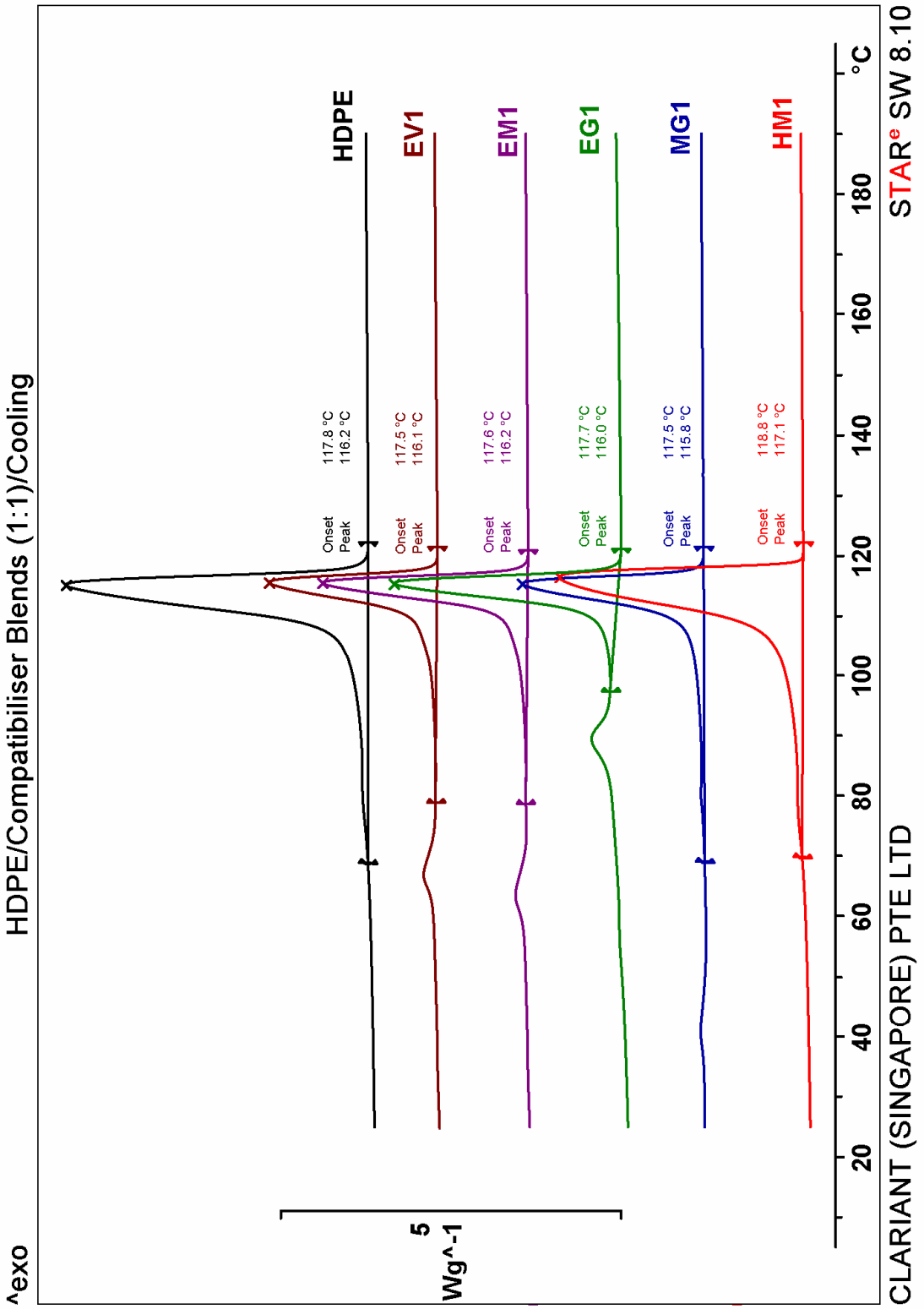
HDPE/Compatibiliser Blends (1:1)/Cooling
^exo
5
Wg^-1
HDPE
EV1
EM1
EG1
MG1
HM1
Onset 117.8 °C
Peak 116.2 °C
Onset 117.5 °C
Peak 116.1 °C
Onset 117.6 °C
Peak 116.2 °C
Onset 117.7 °C
Peak 116.0 °C
Onset 117.5 °C
Peak 115.8 °C
Onset 118.8 °C
Peak 117.1 °C
20
40
60
80
100
120
140
160
180
°C
CLARIANT (SINGAPORE) PTE LTD
STARe SW 8.10

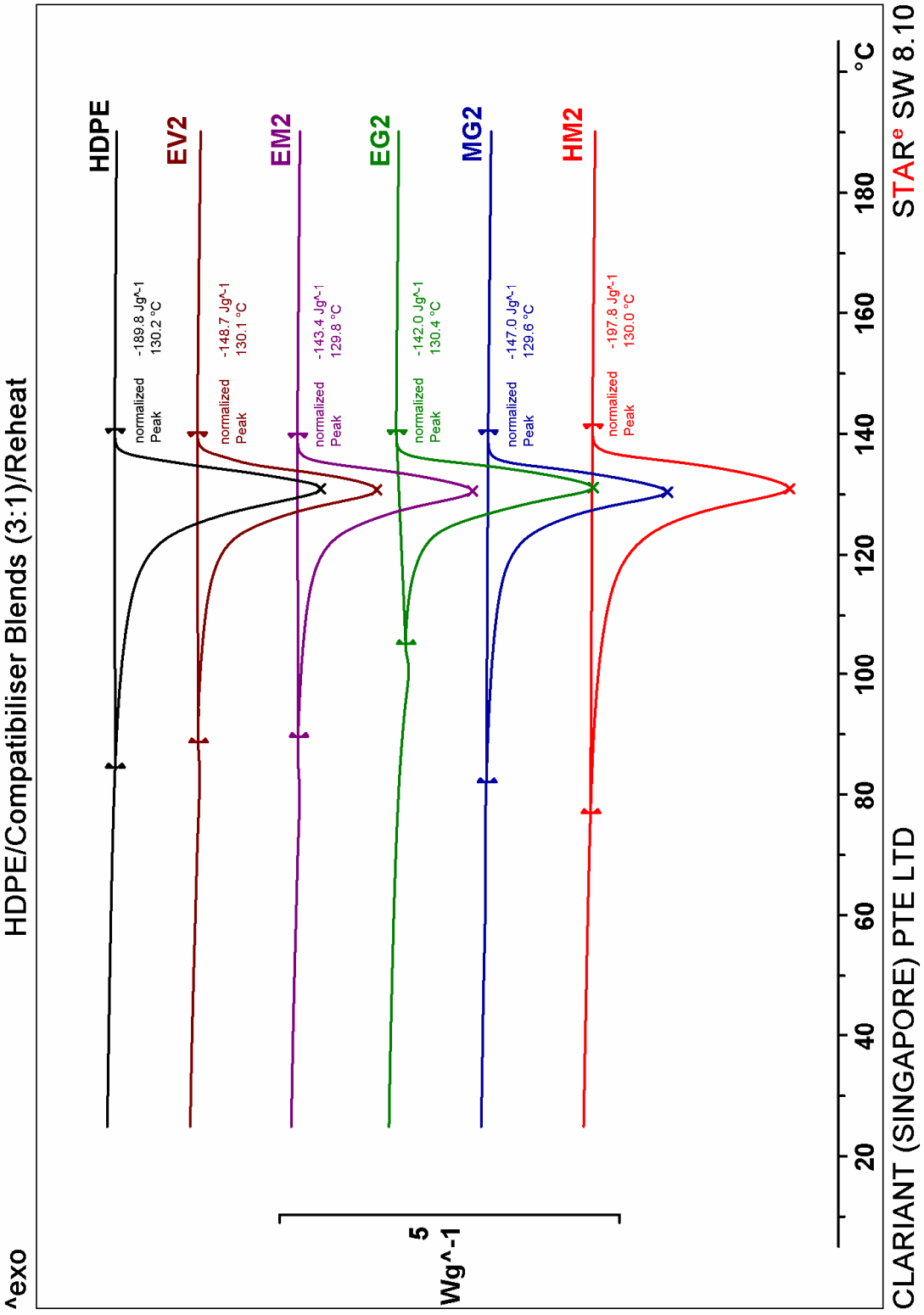
HDPE/Compatibiliser Blends (3:1)/Reheat
^exo
5
Wg^-1
HDPE
EV2
EM2
EG2
MG2
HM2
normalized
Peak
-189.8 Jg^-1
130.2 °C
-148.7 Jg^-1
130.1 °C
-143.4 Jg^-1
129.8 °C
-142.0 Jg^-1
130.4 °C
-147.0 Jg^-1
129.6 °C
-197.8 Jg^-1
130.0 °C
20
40
60
80
100
120
140
160
180
°C
CLARIANT (SINGAPORE) PTE LTD
STARe SW 8.10

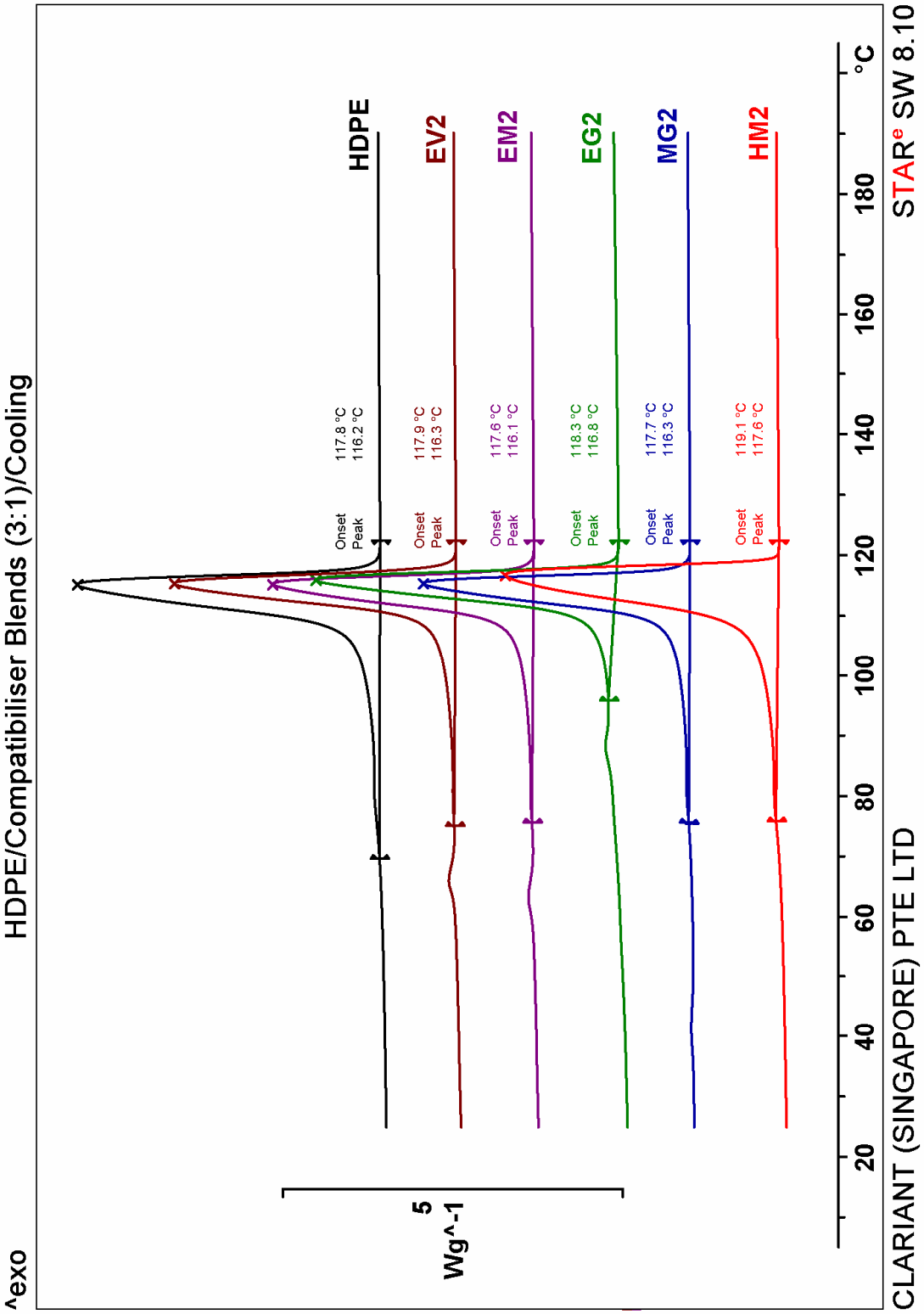
HDPE/Compatibiliser Blends (3:1)/Cooling
^exo
5
Wg^-1
HDPE
EV2
EM2
EG2
MG2
HM2
Onset 117.8 °C
Peak 116.2 °C
Onset 117.9 °C
Peak 116.3 °C
Onset 117.6 °C
Peak 116.1 °C
Onset 118.3 °C
Peak 116.8 °C
Onset 117.7 °C
Peak 116.3 °C
Onset 119.1 °C
Peak 117.6 °C
20
40
60
80
100
120
140
160
180
°C
CLARIANT (SINGAPORE) PTE LTD
STARe SW 8.10

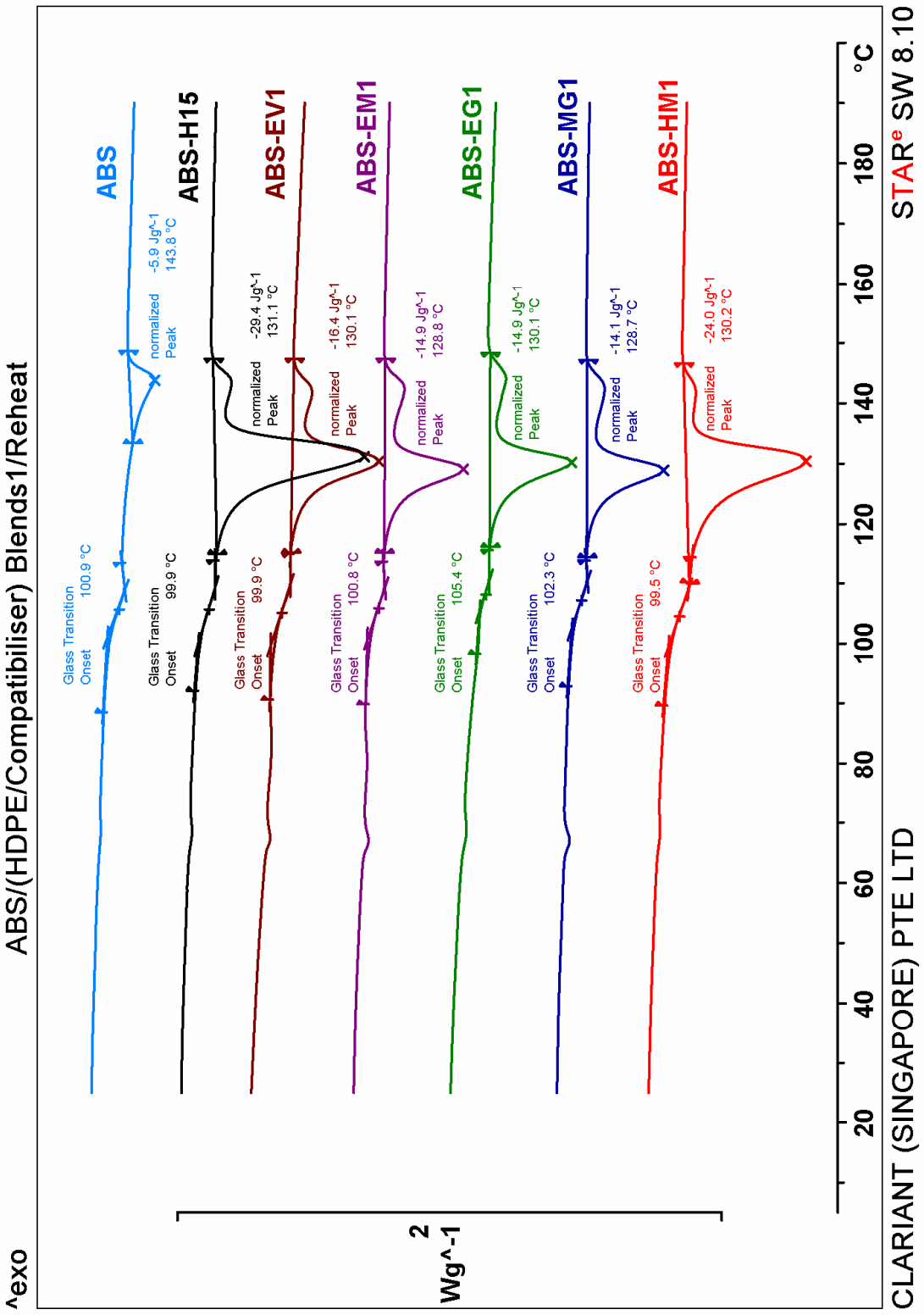
ABS/(HDPE/Compatibiliser) Blends1/Reheat
^exo
2
Wg^-1
ABS
Glass Transition
Onset 100.9 °C
normalized
Peak -5.9 Jg^-1
143.8 °C
ABS-H15
Glass Transition
Onset 99.9 °C
normalized
Peak -29.4 Jg^-1
131.1 °C
ABS-EV1
Glass Transition
Onset 99.9 °C
normalized
Peak -16.4 Jg^-1
130.1 °C
ABS-EM1
Glass Transition
Onset 100.8 °C
normalized
Peak -14.9 Jg^-1
128.8 °C
ABS-EG1
Glass Transition
Onset 105.4 °C
normalized
Peak -14.9 Jg^-1
130.1 °C
ABS-MG1
Glass Transition
Onset 102.3 °C
normalized
Peak -14.1 Jg^-1
128.7 °C
ABS-HM1
Glass Transition
Onset 99.5 °C
normalized
Peak -24.0 Jg^-1
130.2 °C
20
40
60
80
100
120
140
160
180
°C
CLARIANT (SINGAPORE) PTE LTD
STARe SW 8.10

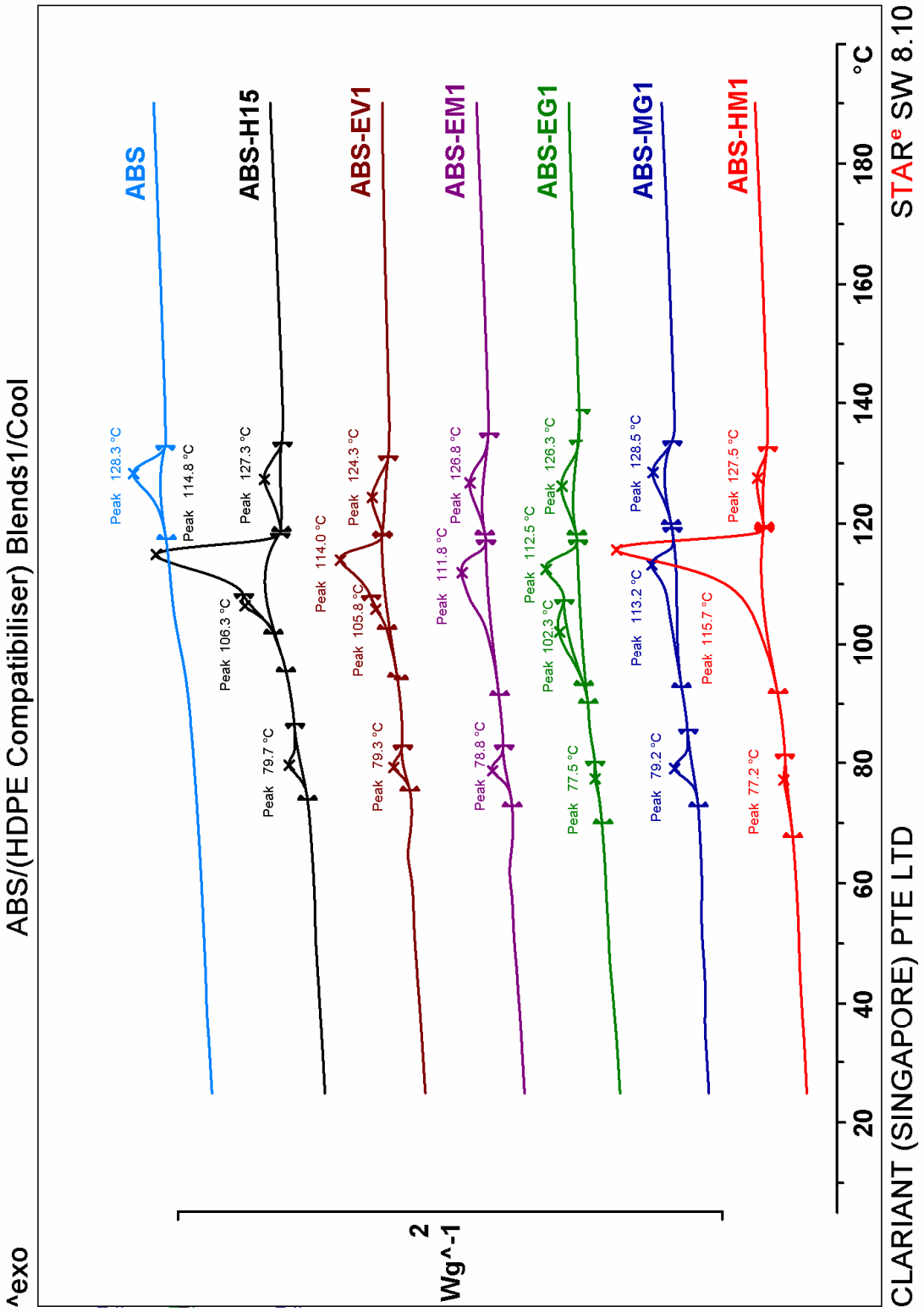
ABS/(HDPE Compatibiliser) Blends1/Cool
^exo
2
Wg^-1
ABS
ABS-H15
ABS-EV1
ABS-EM1
ABS-EG1
ABS-MG1
ABS-HM1
Peak 128.3 °C
Peak 114.8 °C
Peak 106.3 °C
Peak 127.3 °C
Peak 79.7 °C
Peak 114.0 °C
Peak 105.8 °C
Peak 124.3 °C
Peak 79.3 °C
Peak 111.8 °C
Peak 126.8 °C
Peak 78.8 °C
Peak 112.5 °C
Peak 102.3 °C
Peak 126.3 °C
Peak 77.5 °C
Peak 113.2 °C
Peak 128.5 °C
Peak 79.2 °C
Peak 115.7 °C
Peak 127.5 °C
Peak 77.2 °C
20
40
60
80
100
120
140
160
180
°C
CLARIANT (SINGAPORE) PTE LTD
STARe SW 8.10

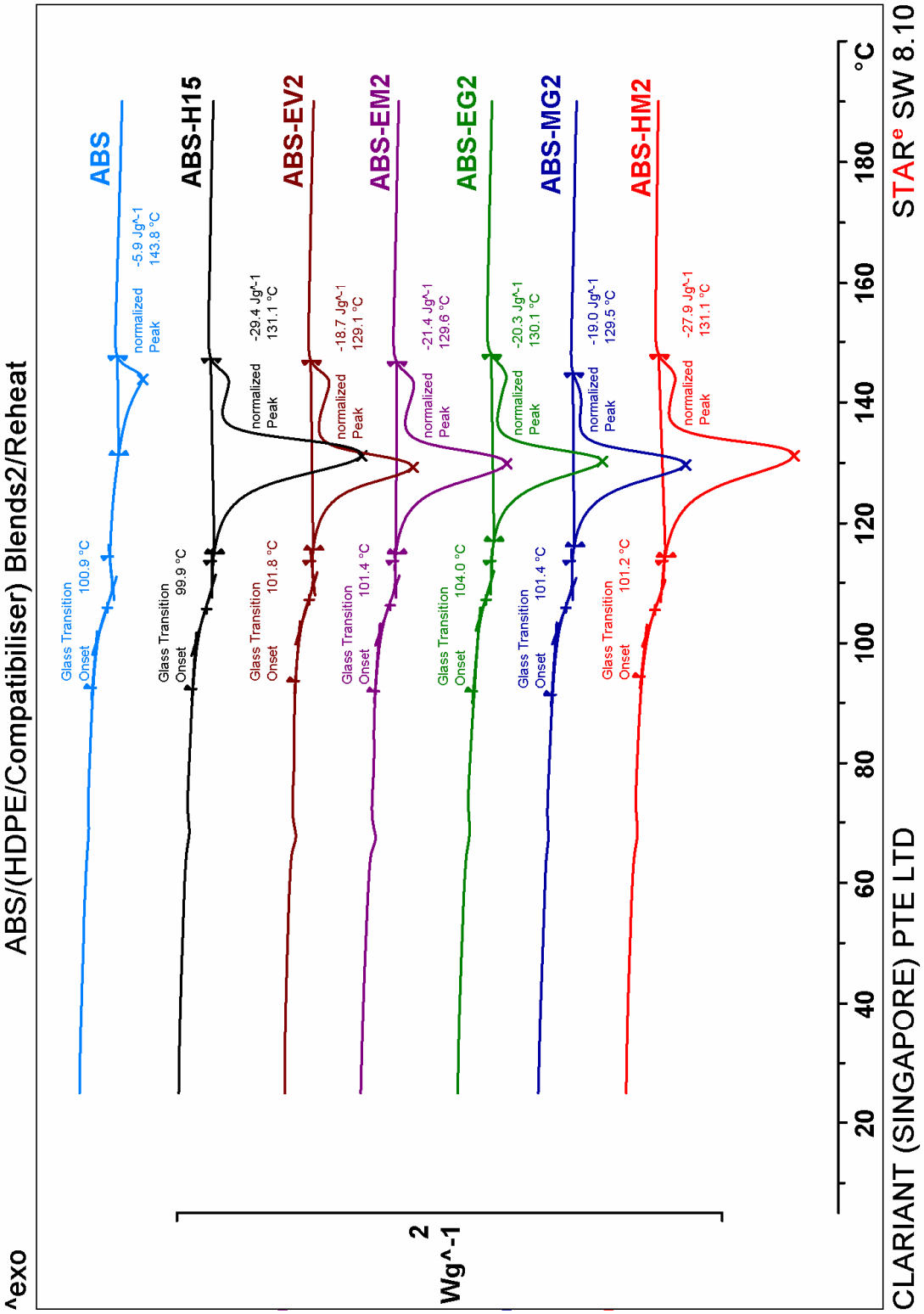
ABS/(HDPE/Compatibiliser) Blends2/Reheat
^exo
2
Wg^-1
ABS
Glass Transition
Onset 100.9 °C
normalized
Peak -5.9 Jg^-1 143.8 °C
ABS-H15
Glass Transition
Onset 99.9 °C
normalized
Peak -29.4 Jg^-1 131.1 °C
ABS-EV2
Glass Transition
Onset 101.8 °C
normalized
Peak -18.7 Jg^-1 129.1 °C
ABS-EM2
Glass Transition
Onset 101.4 °C
normalized
Peak -21.4 Jg^-1 129.6 °C
ABS-EG2
Glass Transition
Onset 104.0 °C
normalized
Peak -20.3 Jg^-1 130.1 °C
ABS-MG2
Glass Transition
Onset 101.4 °C
normalized
Peak -19.0 Jg^-1 129.5 °C
ABS-HM2
Glass Transition
Onset 101.2 °C
normalized
Peak -27.9 Jg^-1 131.1 °C
20
40
60
80
100
120
140
160
180
°C
CLARIANT (SINGAPORE) PTE LTD
STARe SW 8.10

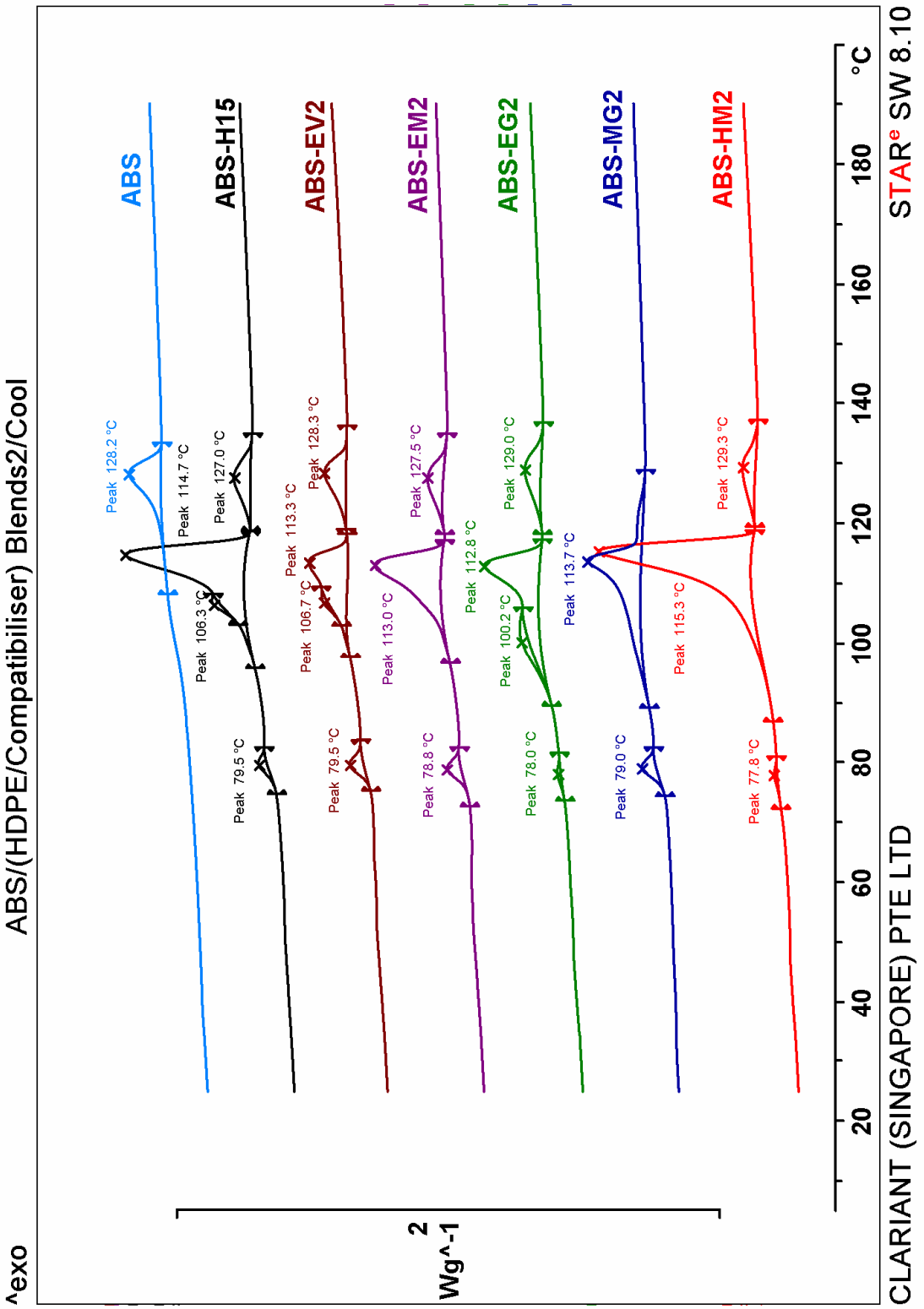
ABS/(HDPE/Compatibiliser) Blends2/Cool
^exo
Wg^-1
ABS
ABS-H15
ABS-EV2
ABS-EM2
ABS-EG2
ABS-MG2
ABS-HM2
Peak 128.2 °C
Peak 114.7 °C
Peak 127.0 °C
Peak 106.3 °C
Peak 79.5 °C
Peak 113.3 °C
Peak 128.3 °C
Peak 106.7 °C
Peak 79.5 °C
Peak 113.0 °C
Peak 127.5 °C
Peak 112.8 °C
Peak 78.8 °C
Peak 100.2 °C
Peak 129.0 °C
Peak 78.0 °C
Peak 113.7 °C
Peak 79.0 °C
Peak 115.3 °C
Peak 129.3 °C
Peak 77.8 °C
20
40
60
80
100
120
140
160
180
°C
CLARIANT (SINGAPORE) PTE LTD
STARe SW 8.10

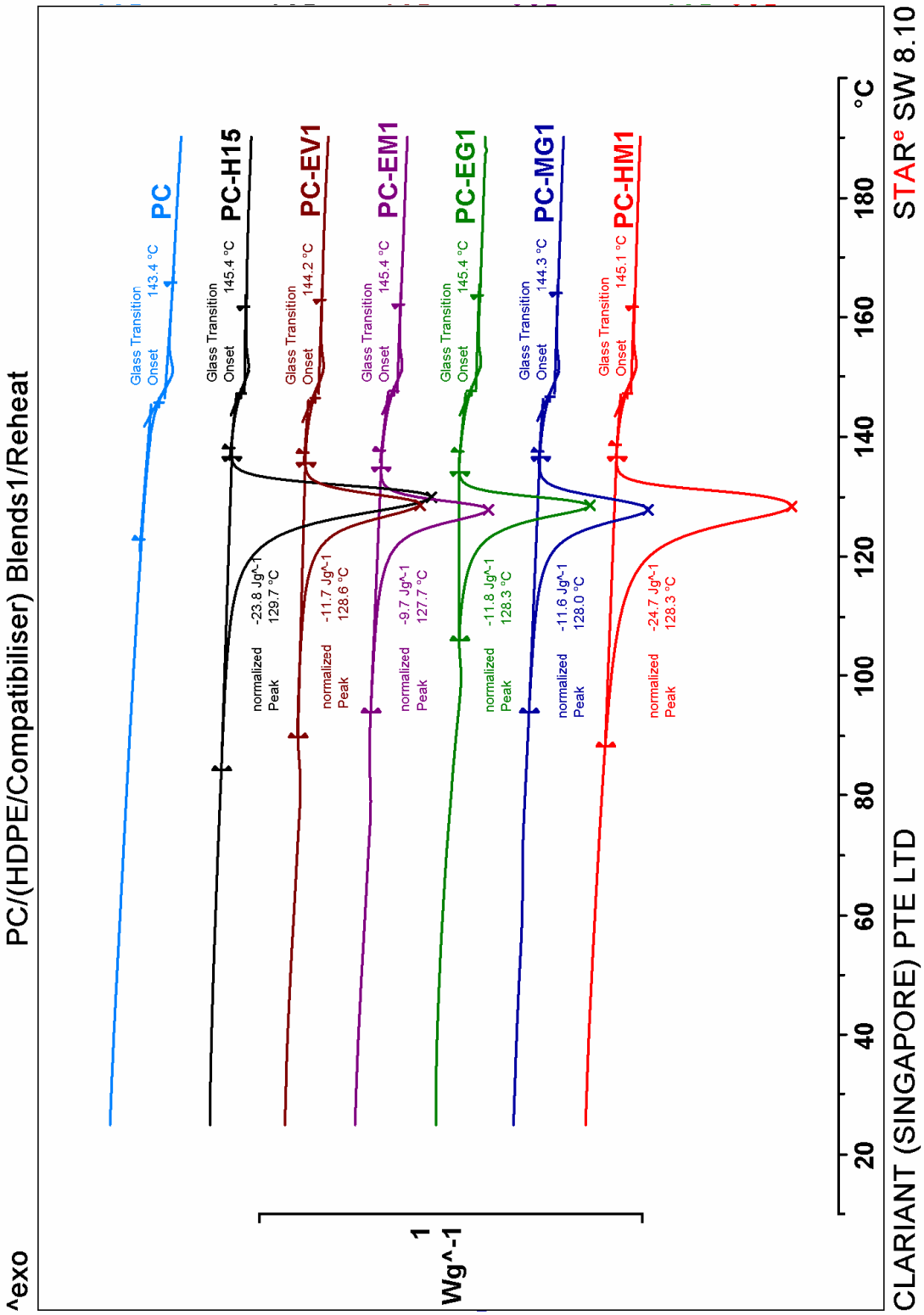
PC/(HDPE/Compatibiliser) Blends1/Reheat
^exo
1
Wg^-1
PC
Glass Transition
Onset 143.4 °C
PC-H15
Glass Transition
Onset 145.4 °C
normalized
Peak -23.8 Jg^-1
129.7 °C
PC-EV1
Glass Transition
Onset 144.2 °C
normalized
Peak -11.7 Jg^-1
128.6 °C
PC-EM1
Glass Transition
Onset 145.4 °C
normalized
Peak -9.7 Jg^-1
127.7 °C
PC-EG1
Glass Transition
Onset 145.4 °C
normalized
Peak -11.8 Jg^-1
128.3 °C
PC-MG1
Glass Transition
Onset 144.3 °C
normalized
Peak -11.6 Jg^-1
128.0 °C
PC-HM1
Glass Transition
Onset 145.1 °C
normalized
Peak -24.7 Jg^-1
128.3 °C
20
40
60
80
100
120
140
160
180
°C
CLARIANT (SINGAPORE) PTE LTD
STARe SW 8.10

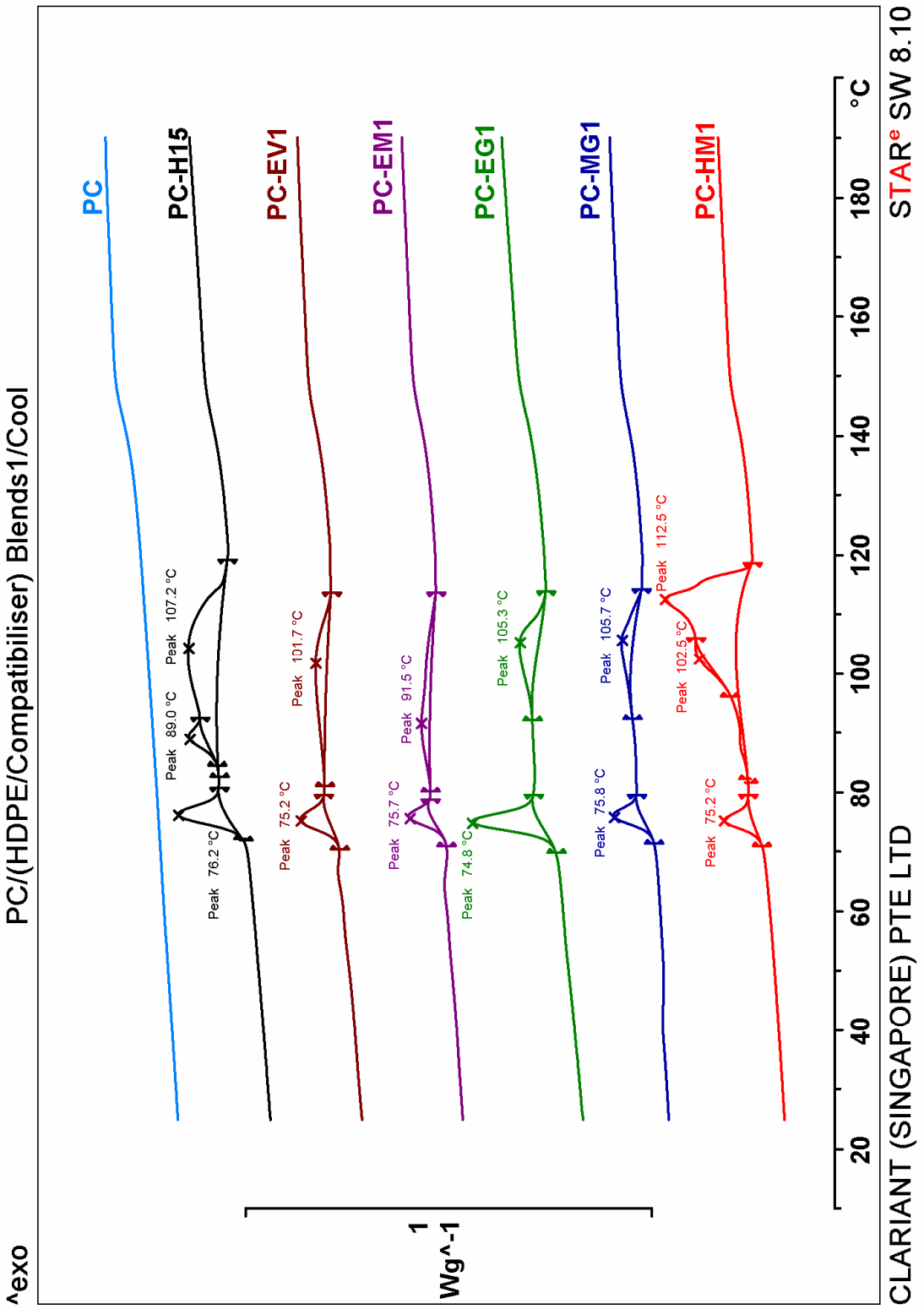
PC/(HDPE/Compatibiliser) Blends1/Cool
^exo
1
Wg^-1
PC
PC-H15
PC-EV1
PC-EM1
PC-EG1
PC-MG1
PC-HM1
Peak 76.2 °C
Peak 89.0 °C
Peak 107.2 °C
Peak 75.2 °C
Peak 101.7 °C
Peak 75.7 °C
Peak 91.5 °C
Peak 74.8 °C
Peak 105.3 °C
Peak 75.8 °C
Peak 105.7 °C
Peak 102.5 °C
Peak 112.5 °C
Peak 75.2 °C
20
40
60
80
100
120
140
160
180
°C
CLARIANT (SINGAPORE) PTE LTD
STARe SW 8.10

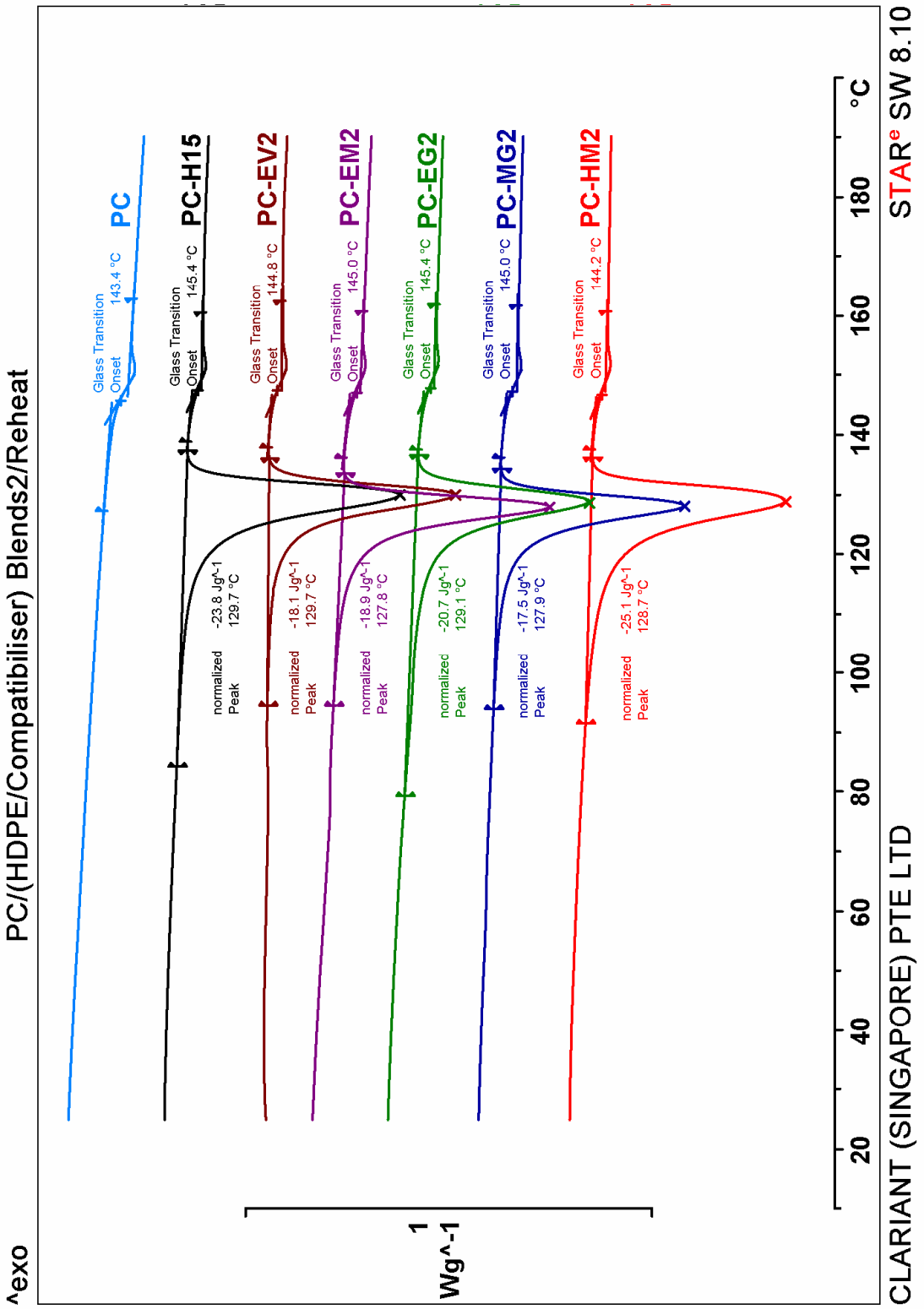
PC/(HDPE/Compatibiliser) Blends2/Reheat
^exo
1
Wg^-1
PC
Glass Transition
Onset 143.4 °C
PC-H15
Glass Transition
Onset 145.4 °C
normalized -23.8 Jg^-1
Peak 129.7 °C
PC-EV2
Glass Transition
Onset 144.8 °C
normalized -18.1 Jg^-1
Peak 129.7 °C
PC-EM2
Glass Transition
Onset 145.0 °C
normalized -18.9 Jg^-1
Peak 127.8 °C
PC-EG2
Glass Transition
Onset 145.4 °C
normalized -20.7 Jg^-1
Peak 129.1 °C
PC-MG2
Glass Transition
Onset 145.0 °C
normalized -17.5 Jg^-1
Peak 127.9 °C
PC-HM2
Glass Transition
Onset 144.2 °C
normalized -25.1 Jg^-1
Peak 128.7 °C
20
40
60
80
100
120
140
160
180
°C
CLARIANT (SINGAPORE) PTE LTD
STARe SW 8.10

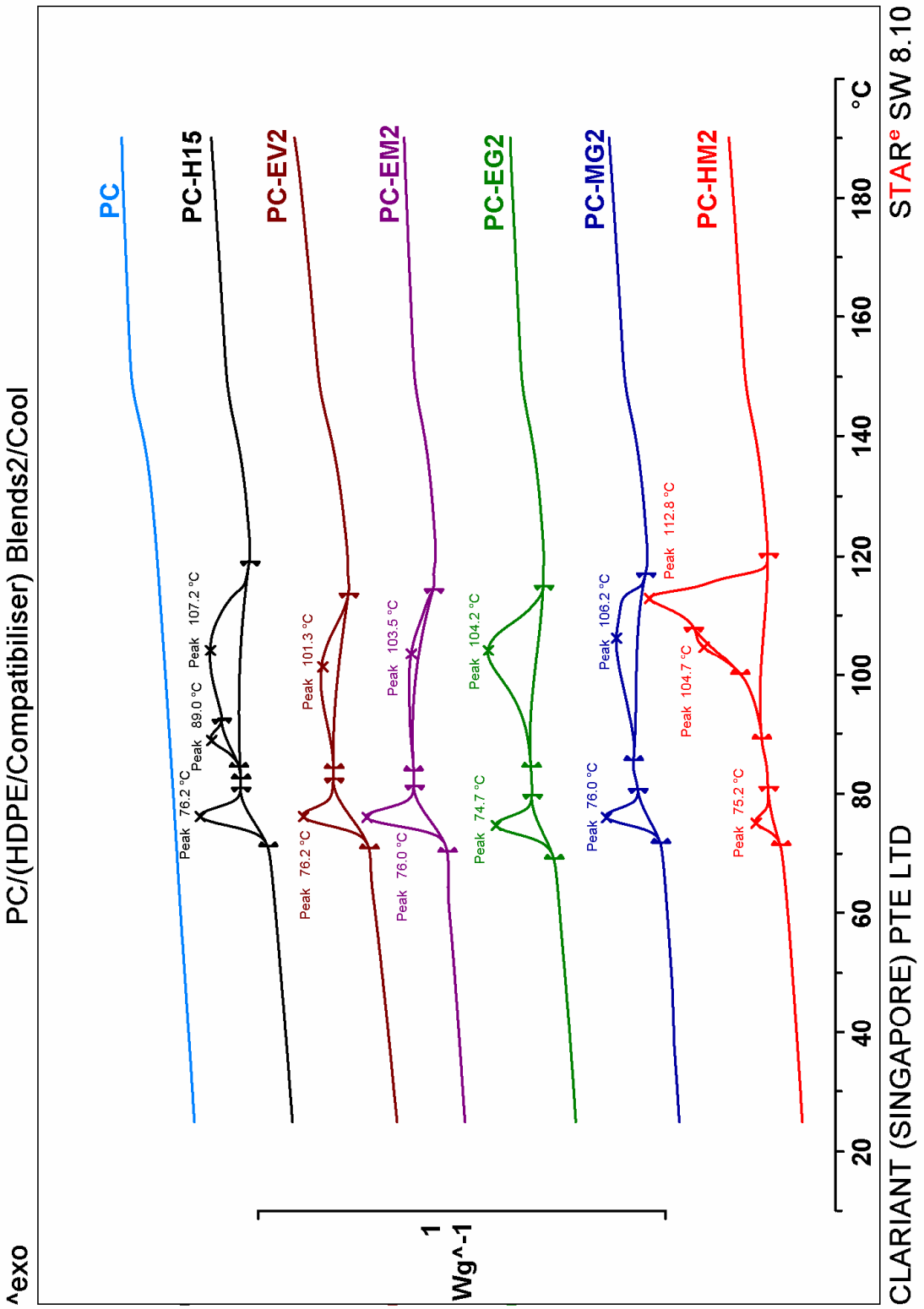
PC/(HDPE/Compatibiliser) Blends2/Cool
^exo
1
Wg^-1
PC
PC-H15
PC-EV2
PC-EM2
PC-EG2
PC-MG2
PC-HM2
Peak 76.2 °C
Peak 89.0 °C
Peak 107.2 °C
Peak 76.2 °C
Peak 101.3 °C
Peak 76.0 °C
Peak 103.5 °C
Peak 74.7 °C
Peak 104.2 °C
Peak 76.0 °C
Peak 106.2 °C
Peak 104.7 °C
Peak 112.8 °C
Peak 75.2 °C
20
40
60
80
100
120
140
160
180
°C
CLARIANT (SINGAPORE) PTE LTD
STARe SW 8.10

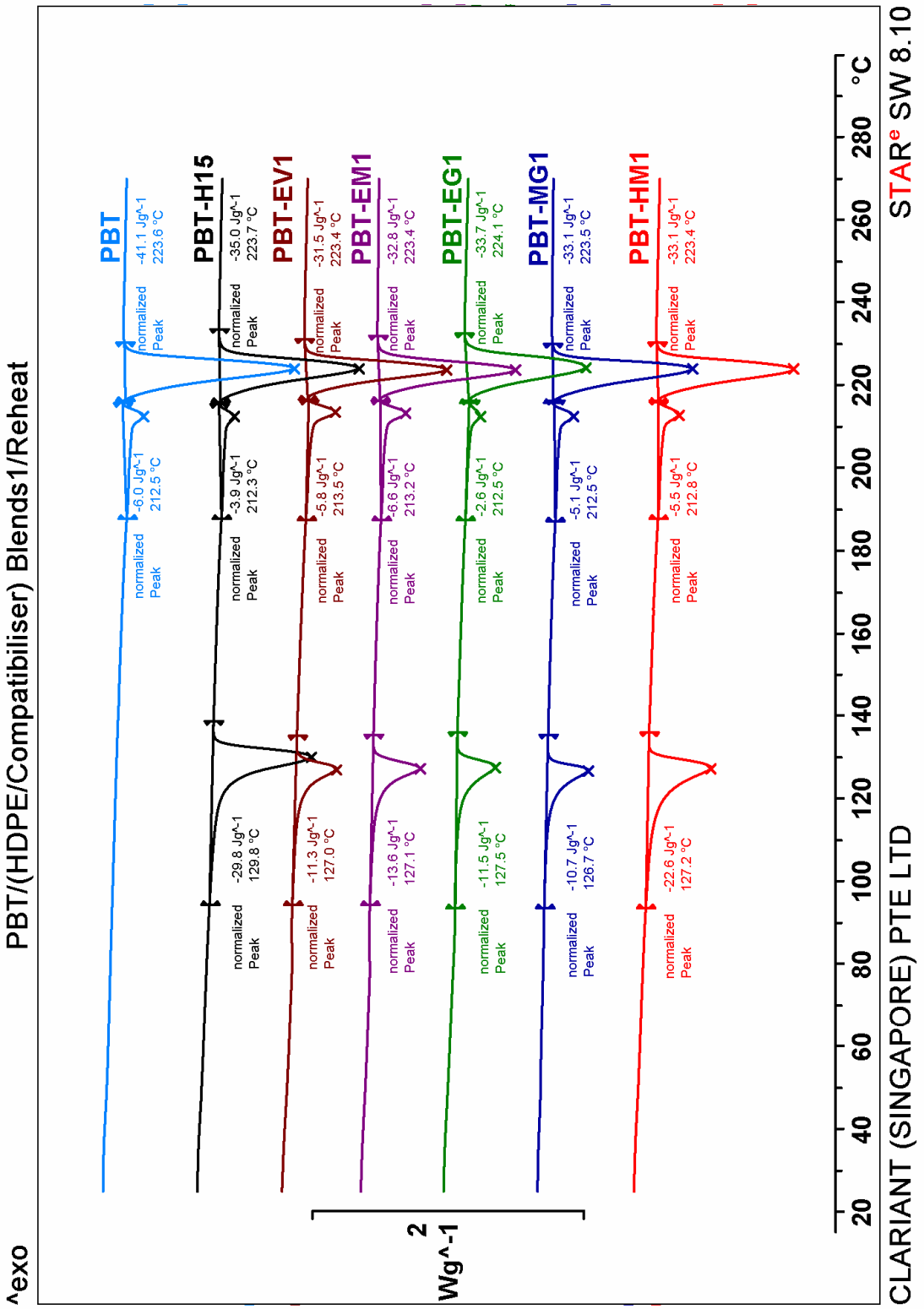
PBT/(HDPE/Compatibiliser) Blends1/Reheat
^exo
W/g
2
PBT
normalized
Peak
-41.1 J/g
223.6 °C
-6.0 J/g
212.5 °C
PBT-H15
-35.0 J/g
223.7 °C
-3.9 J/g
212.3 °C
-29.8 J/g
129.8 °C
PBT-EV1
-31.5 J/g
223.4 °C
-5.8 J/g
213.5 °C
-11.3 J/g
127.0 °C
PBT-EM1
-32.8 J/g
223.4 °C
-6.6 J/g
213.2 °C
-13.6 J/g
127.1 °C
PBT-EG1
-33.7 J/g
224.1 °C
-2.6 J/g
212.5 °C
-11.5 J/g
127.5 °C
PBT-MG1
-33.1 J/g
223.5 °C
-5.1 J/g
212.5 °C
-10.7 J/g
126.7 °C
PBT-HM1
-33.1 J/g
223.4 °C
-5.5 J/g
212.8 °C
-22.6 J/g
127.2 °C
20
40
60
80
100
120
140
160
180
200
220
240
260
280
°C
CLARIANT (SINGAPORE) PTE LTD
STARe SW 8.10

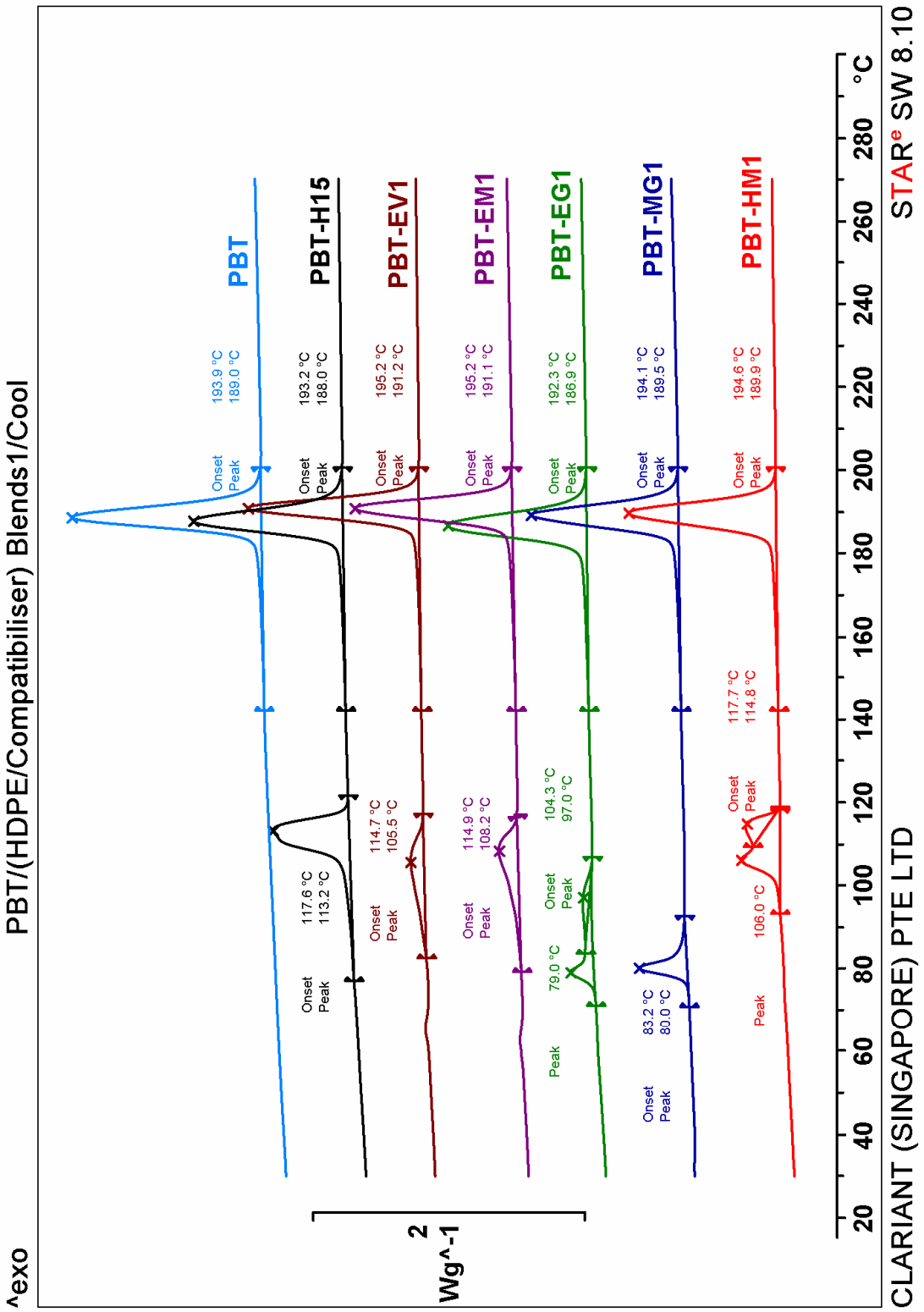
PBT/(HDPE/Compatibiliser) Blends1/Cool
^exo
2
Wg^-1
PBT
PBT-H15
PBT-EV1
PBT-EM1
PBT-EG1
PBT-MG1
PBT-HM1
Onset 193.9 °C
Peak 189.0 °C
Onset 193.2 °C
Peak 188.0 °C
Onset 117.6 °C
Peak 113.2 °C
Onset 195.2 °C
Peak 191.2 °C
Onset 114.7 °C
Peak 105.5 °C
Onset 195.2 °C
Peak 191.1 °C
Onset 114.9 °C
Peak 108.2 °C
Onset 192.3 °C
Peak 186.9 °C
Onset 104.3 °C
Peak 97.0 °C
Peak 79.0 °C
Onset 194.1 °C
Peak 189.5 °C
Onset 83.2 °C
Peak 80.0 °C
Onset 194.6 °C
Peak 189.9 °C
Onset 117.7 °C
Peak 114.8 °C
Peak 106.0 °C
20 40 60 80 100 120 140 160 180 200 220 240 260 280 °C
CLARIANT (SINGAPORE) PTE LTD
STARe SW 8.10

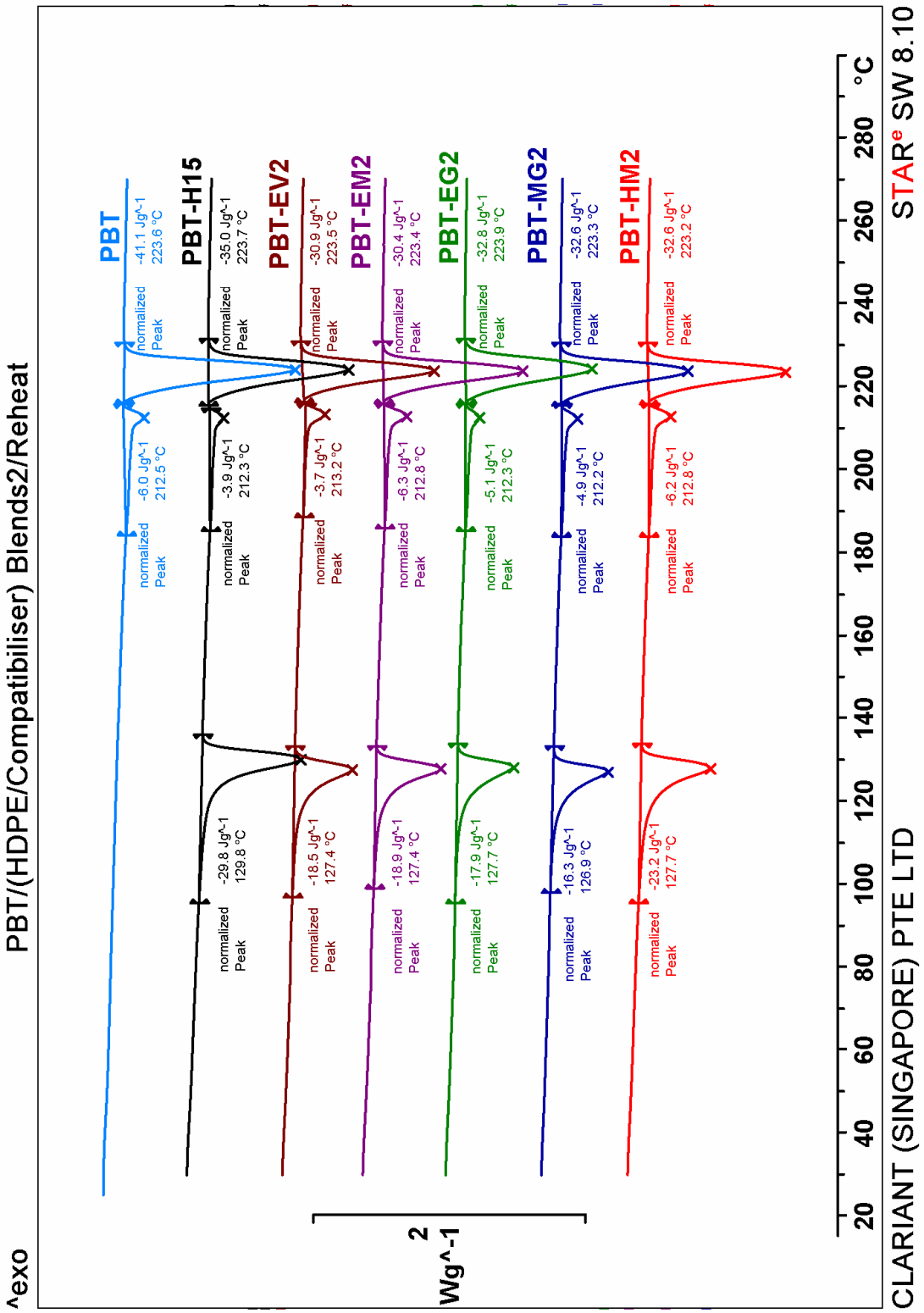
PBT/(HDPE/Compatibiliser) Blends2/Reheat
^exo
Wg^-1
2
PBT
-41.1 Jg^-1
223.6 °C
-6.0 Jg^-1
212.5 °C
-29.8 Jg^-1
129.8 °C
-18.5 Jg^-1
127.4 °C
PBT-H15
-35.0 Jg^-1
223.7 °C
-3.9 Jg^-1
212.3 °C
-18.9 Jg^-1
127.4 °C
PBT-EV2
-30.9 Jg^-1
223.5 °C
-3.7 Jg^-1
213.2 °C
-17.9 Jg^-1
127.7 °C
PBT-EM2
-30.4 Jg^-1
223.4 °C
-6.3 Jg^-1
212.8 °C
-16.3 Jg^-1
126.9 °C
PBT-EG2
-32.8 Jg^-1
223.9 °C
-5.1 Jg^-1
212.3 °C
-23.2 Jg^-1
127.7 °C
PBT-MG2
-32.6 Jg^-1
223.3 °C
-4.9 Jg^-1
212.2 °C
PBT-HM2
-32.6 Jg^-1
223.2 °C
-6.2 Jg^-1
212.8 °C
normalized
Peak
20
40
60
80
100
120
140
160
180
200
220
240
260
280
°C
CLARIANT (SINGAPORE) PTE LTD
STARe SW 8.10

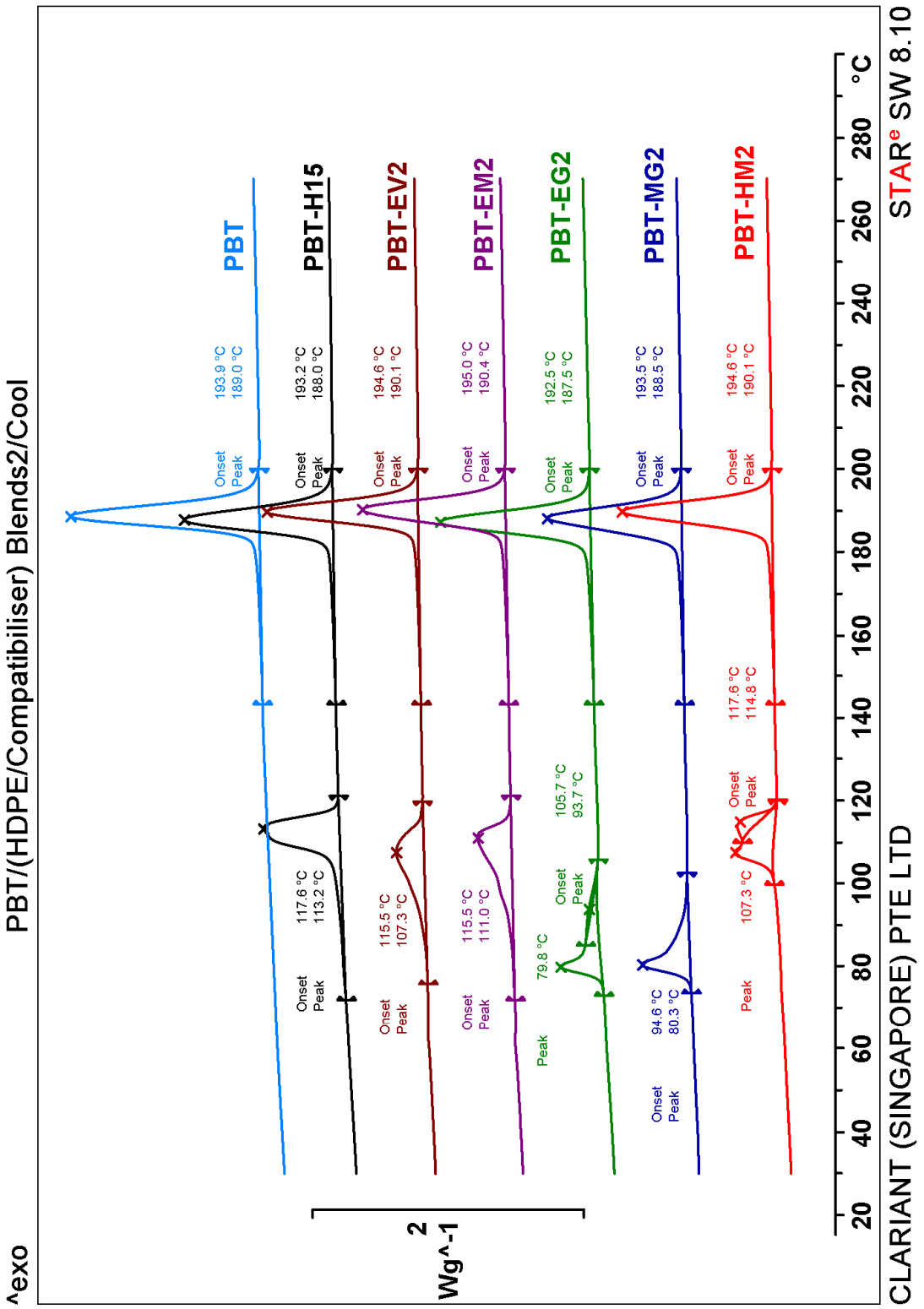
PBT/(HDPE/Compatibiliser) Blends2/Cool
^exo
2
Wg^-1
PBT
PBT-H15
PBT-EV2
PBT-EM2
PBT-EG2
PBT-MG2
PBT-HM2
Onset 193.9 °C
Peak 189.0 °C
Onset 193.2 °C
Peak 188.0 °C
Onset 117.6 °C
Peak 113.2 °C
Onset 194.6 °C
Peak 190.1 °C
Onset 115.5 °C
Peak 107.3 °C
Onset 195.0 °C
Peak 190.4 °C
Onset 115.5 °C
Peak 111.0 °C
Onset 192.5 °C
Peak 187.5 °C
Peak 79.8 °C
Onset 105.7 °C
Peak 93.7 °C
Onset 193.5 °C
Peak 188.5 °C
Onset 94.8 °C
Peak 80.3 °C
Onset 194.6 °C
Peak 190.1 °C
Onset 117.6 °C
Peak 114.8 °C
Peak 107.3 °C
20
40
60
80
100
120
140
160
180
200
220
240
260
280
°C
CLARIANT (SINGAPORE) PTE LTD
STARe SW 8.10

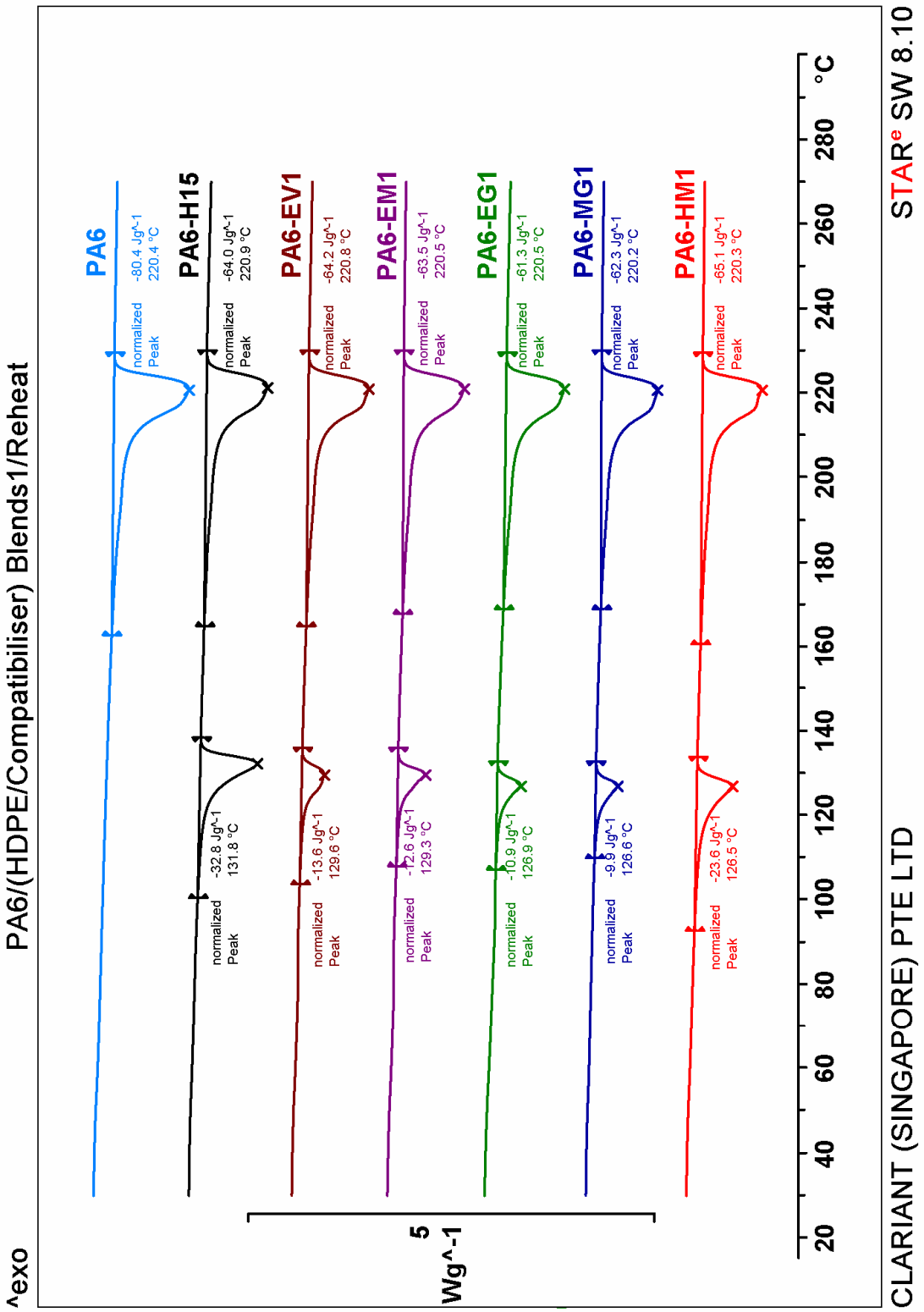
PA6/(HDPE/Compatibiliser) Blends1/Reheat
^exo
5
Wg^-1
PA6
normalized
Peak
-80.4 Jg^-1
220.4 °C
PA6-H15
normalized
Peak
-32.8 Jg^-1
131.8 °C
normalized
Peak
-64.0 Jg^-1
220.9 °C
PA6-EV1
normalized
Peak
-13.6 Jg^-1
129.6 °C
normalized
Peak
-64.2 Jg^-1
220.8 °C
PA6-EM1
normalized
Peak
-12.6 Jg^-1
129.3 °C
normalized
Peak
-63.5 Jg^-1
220.5 °C
PA6-EG1
normalized
Peak
-10.9 Jg^-1
126.9 °C
normalized
Peak
-61.3 Jg^-1
220.5 °C
PA6-MG1
normalized
Peak
-9.9 Jg^-1
126.6 °C
normalized
Peak
-62.3 Jg^-1
220.2 °C
PA6-HM1
normalized
Peak
-23.6 Jg^-1
126.5 °C
normalized
Peak
-65.1 Jg^-1
220.3 °C
20
40
60
80
100
120
140
160
180
200
220
240
260
280
°C
CLARIANT (SINGAPORE) PTE LTD
STARe SW 8.10

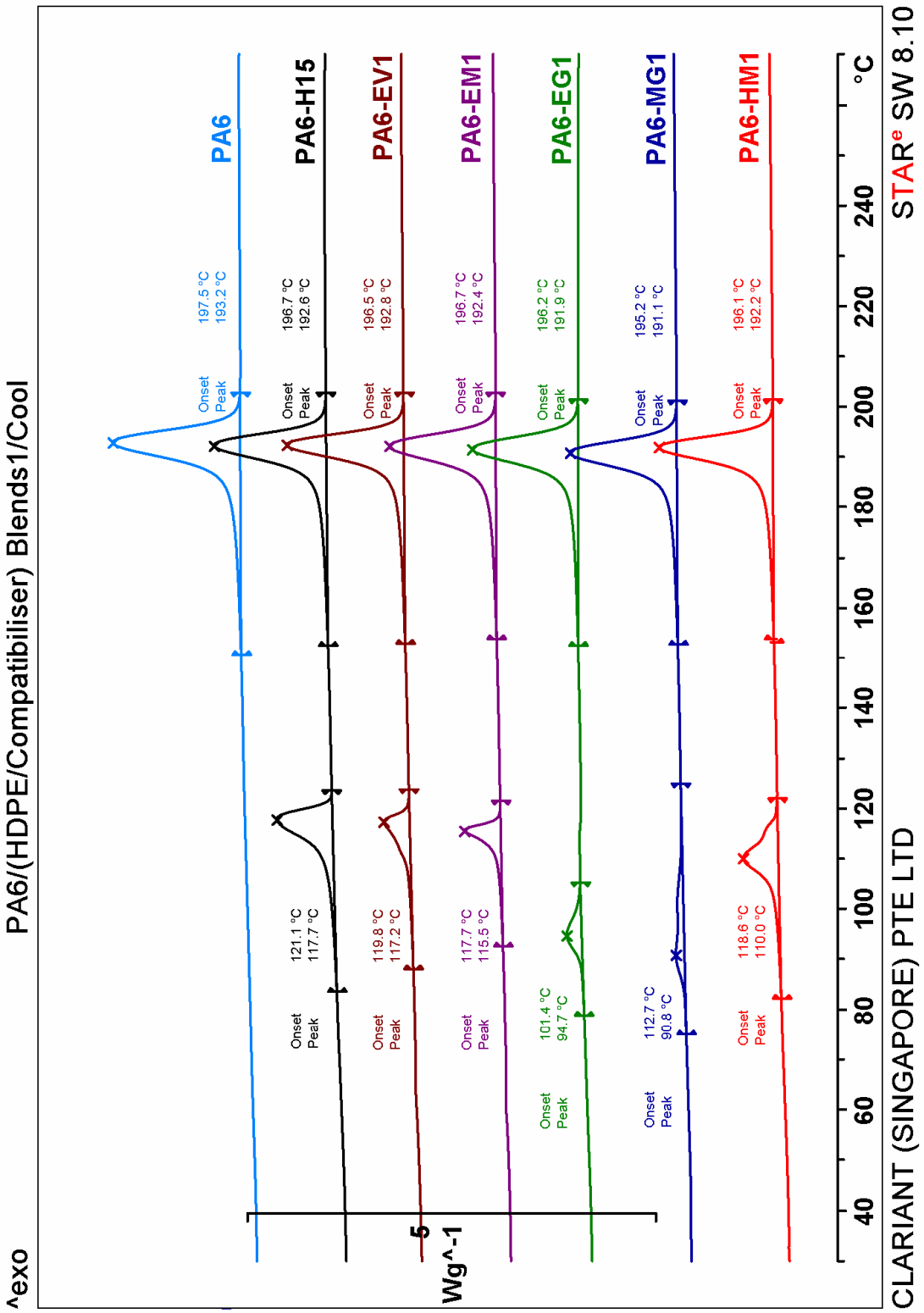
PA6/(HDPE/Compatibiliser) Blends1/Cool
^exo
Wg^-1
5
PA6
Onset 197.5 °C
Peak 193.2 °C
PA6-H15
Onset 196.7 °C
Peak 192.6 °C
Onset 121.1 °C
Peak 117.7 °C
PA6-EV1
Onset 196.5 °C
Peak 192.8 °C
Onset 119.8 °C
Peak 117.2 °C
PA6-EM1
Onset 196.7 °C
Peak 192.4 °C
Onset 117.7 °C
Peak 115.5 °C
PA6-EG1
Onset 196.2 °C
Peak 191.9 °C
Onset 101.4 °C
Peak 94.7 °C
PA6-MG1
Onset 195.2 °C
Peak 191.1 °C
Onset 112.7 °C
Peak 90.8 °C
PA6-HM1
Onset 196.1 °C
Peak 192.2 °C
Onset 118.6 °C
Peak 110.0 °C
40
60
80
100
120
140
160
180
200
220
240
°C
CLARIANT (SINGAPORE) PTE LTD
STARe SW 8.10

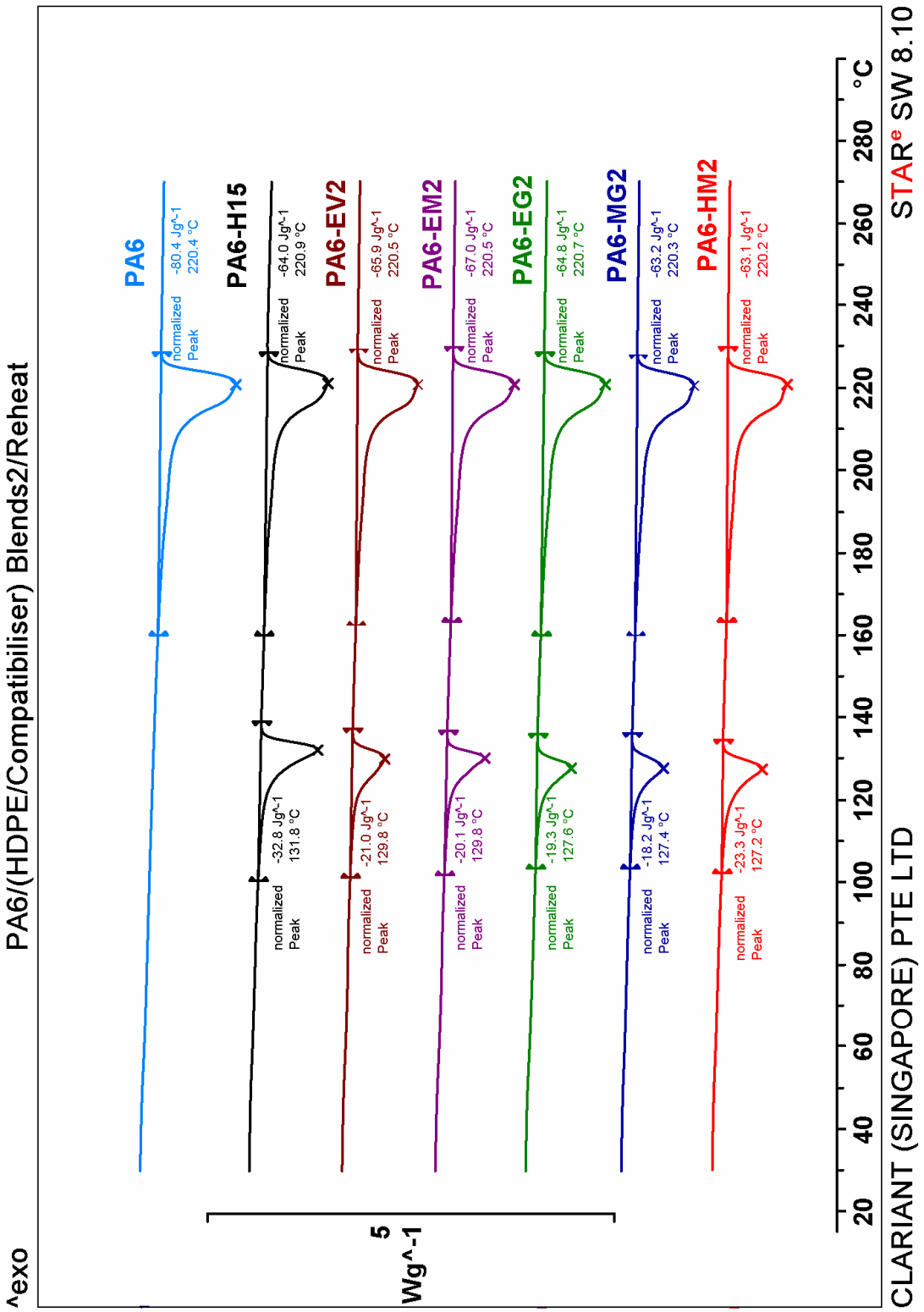
PA6/(HDPE/Compatibiliser) Blends2/Reheat
^exo
5
Wg^-1
PA6
normalized
Peak
-80.4 Jg^-1
220.4 °C
PA6-H15
normalized
Peak
-64.0 Jg^-1
220.9 °C
normalized
Peak
-32.8 Jg^-1
131.8 °C
PA6-EV2
normalized
Peak
-65.9 Jg^-1
220.5 °C
normalized
Peak
-21.0 Jg^-1
129.8 °C
PA6-EM2
normalized
Peak
-67.0 Jg^-1
220.5 °C
normalized
Peak
-20.1 Jg^-1
129.8 °C
PA6-EG2
normalized
Peak
-64.8 Jg^-1
220.7 °C
normalized
Peak
-19.3 Jg^-1
127.6 °C
PA6-MG2
normalized
Peak
-63.2 Jg^-1
220.3 °C
normalized
Peak
-18.2 Jg^-1
127.4 °C
PA6-HM2
normalized
Peak
-63.1 Jg^-1
220.2 °C
normalized
Peak
-23.3 Jg^-1
127.2 °C
20
40
60
80
100
120
140
160
180
200
220
240
260
280
°C
CLARIANT (SINGAPORE) PTE LTD
STARe SW 8.10

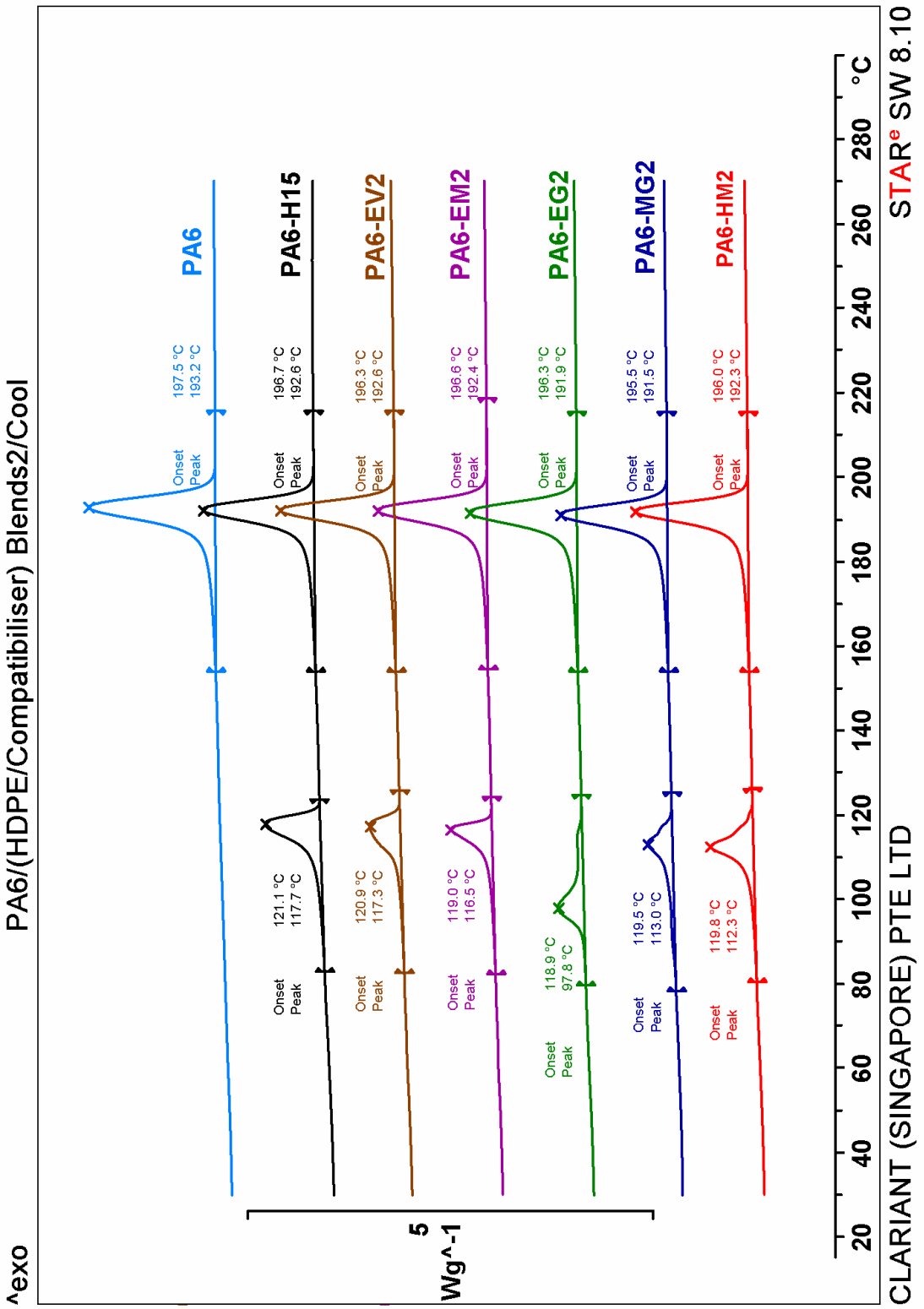
PA6/(HDPE/Compatibiliser) Blends2/Cool
^exo
5
Wg^-1
PA6
Onset 197.5 °C
Peak 193.2 °C
PA6-H15
Onset 196.7 °C
Peak 192.6 °C
Onset 121.1 °C
Peak 117.7 °C
PA6-EV2
Onset 196.3 °C
Peak 192.6 °C
Onset 120.9 °C
Peak 117.3 °C
PA6-EM2
Onset 196.6 °C
Peak 192.4 °C
Onset 119.0 °C
Peak 116.5 °C
PA6-EG2
Onset 196.3 °C
Peak 191.9 °C
Onset 118.9 °C
Peak 97.8 °C
PA6-MG2
Onset 195.5 °C
Peak 191.5 °C
Onset 119.5 °C
Peak 113.0 °C
PA6-HM2
Onset 196.0 °C
Peak 192.3 °C
Onset 119.8 °C
Peak 112.3 °C
20 40 60 80 100 120 140 160 180 200 220 240 260 280 °C
CLARIANT (SINGAPORE) PTE LTD
STARe SW 8.10

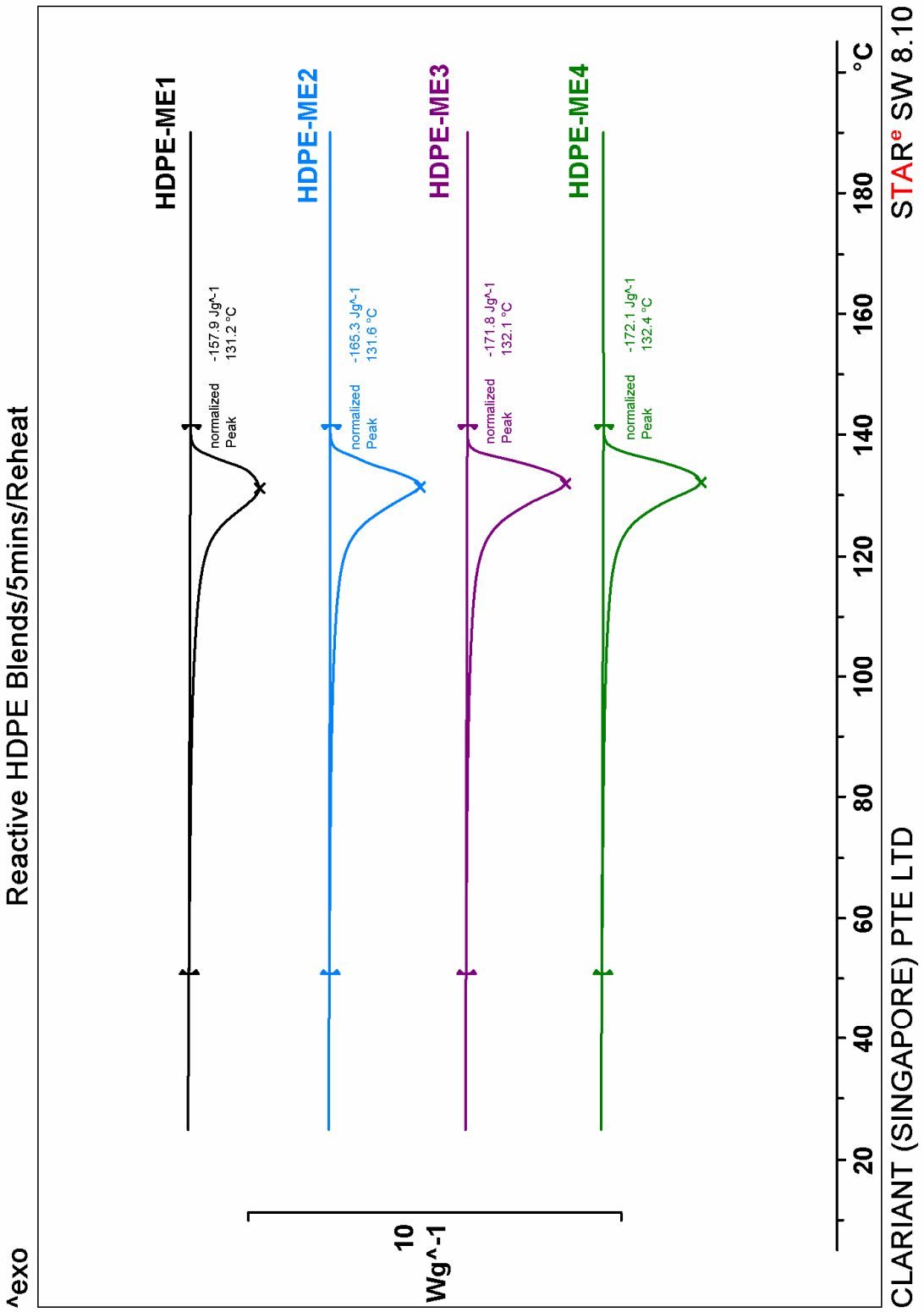
Reactive HDPE Blends/5mins/Reheat
^exo
HDPE-ME1
-157.9 Jg^-1
131.2 °C
normalized
Peak
HDPE-ME2
-165.3 Jg^-1
131.6 °C
normalized
Peak
HDPE-ME3
-171.8 Jg^-1
132.1 °C
normalized
Peak
HDPE-ME4
-172.1 Jg^-1
132.4 °C
normalized
Peak
10
Wg^-1
20
40
60
80
100
120
140
160
180
°C
CLARIANT (SINGAPORE) PTE LTD
STARe SW 8.10

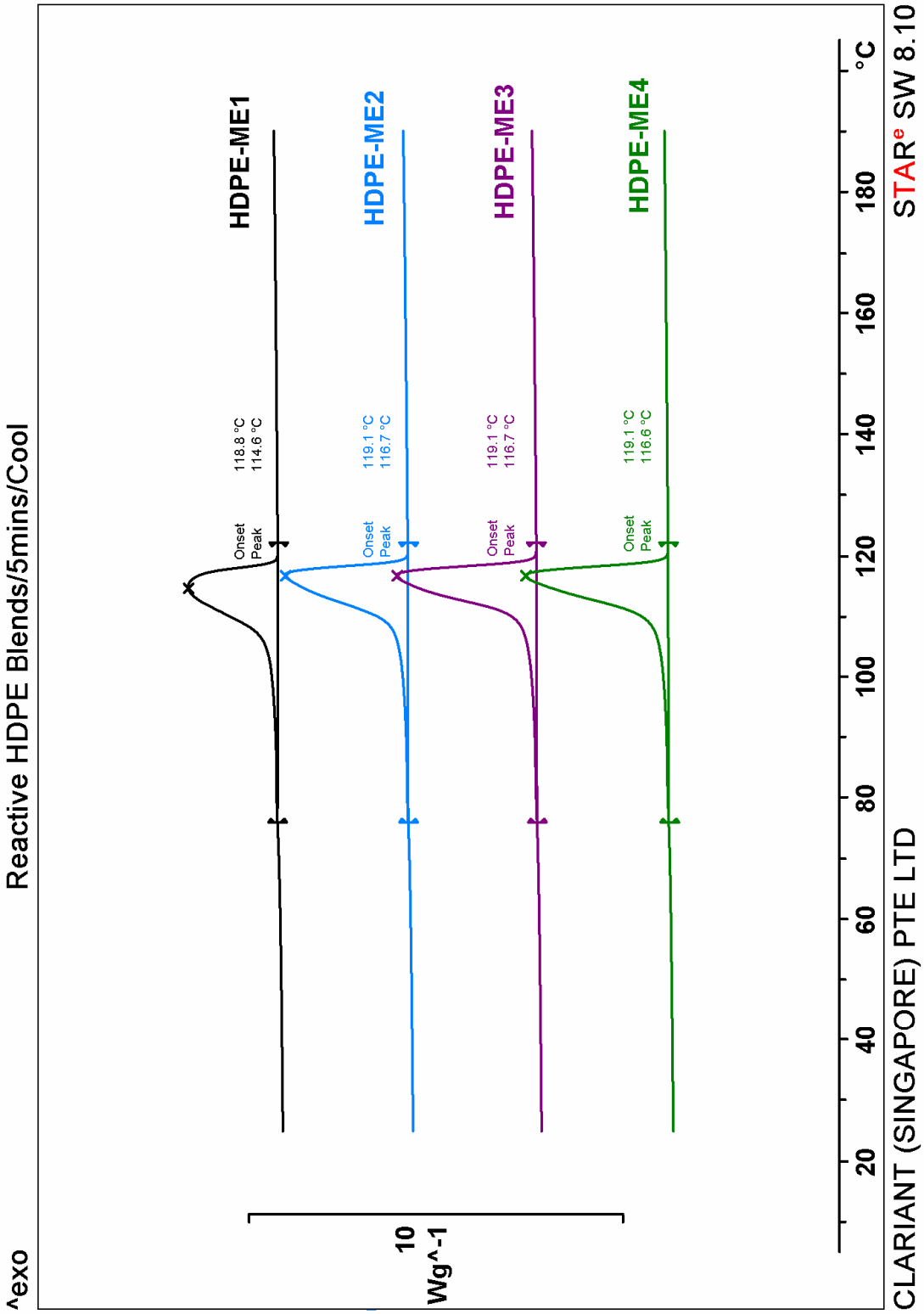
Reactive HDPE Blends/5mins/Cool
^exo
10
Wg^-1
HDPE-ME1
Onset 118.8 °C
Peak 114.6 °C
HDPE-ME2
Onset 119.1 °C
Peak 116.7 °C
HDPE-ME3
Onset 119.1 °C
Peak 116.7 °C
HDPE-ME4
Onset 119.1 °C
Peak 116.6 °C
20
40
60
80
100
120
140
160
180
°C
CLARIANT (SINGAPORE) PTE LTD
STARe SW 8.10

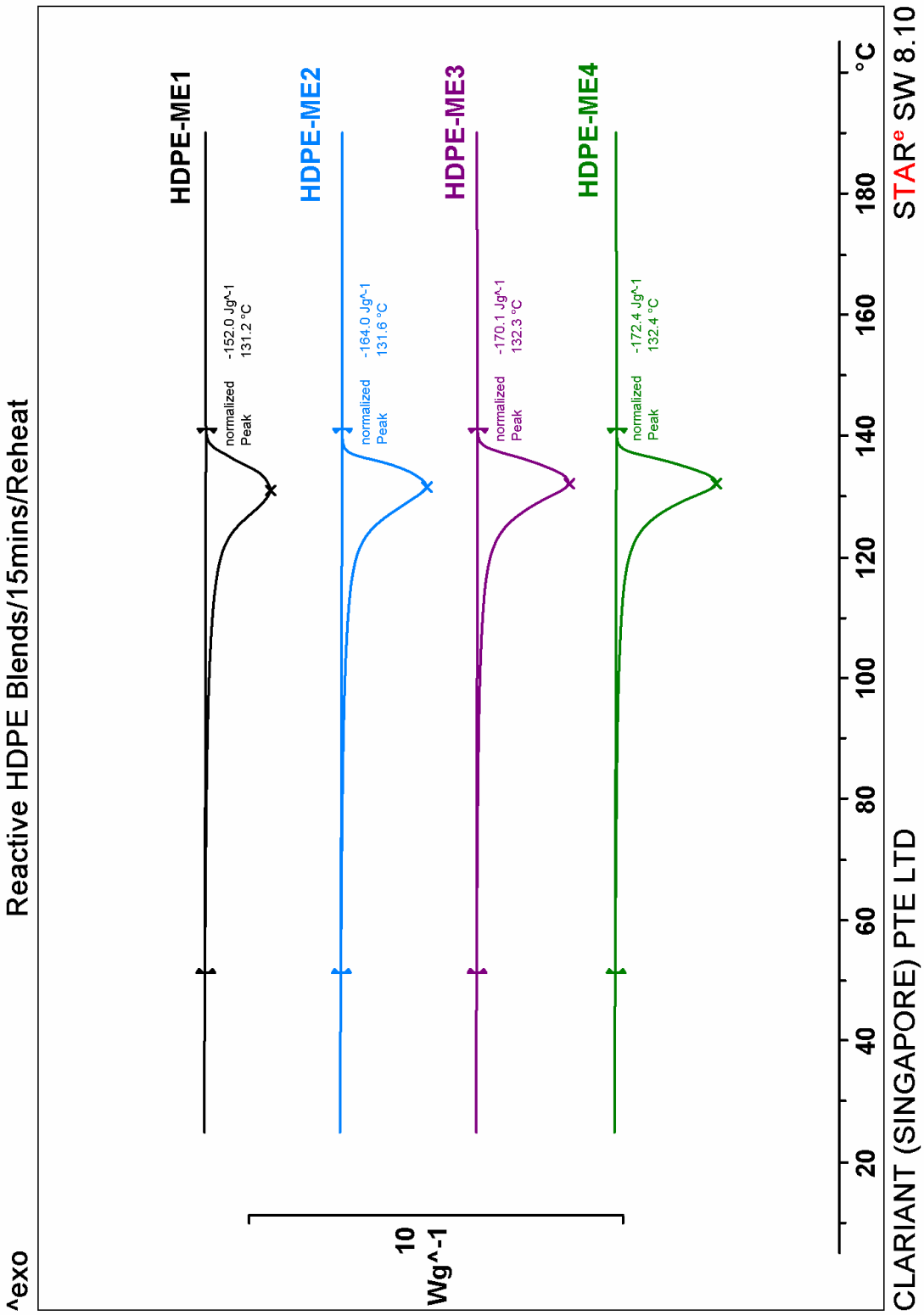
Reactive HDPE Blends/15mins/Reheat
^exo
10
Wg^-1
HDPE-ME1
-152.0 Jg^-1
131.2 °C
normalized
Peak
HDPE-ME2
-164.0 Jg^-1
131.6 °C
normalized
Peak
HDPE-ME3
-170.1 Jg^-1
132.3 °C
normalized
Peak
HDPE-ME4
-172.4 Jg^-1
132.4 °C
normalized
Peak
20
40
60
80
100
120
140
160
180
°C
CLARIANT (SINGAPORE) PTE LTD
STARe SW 8.10

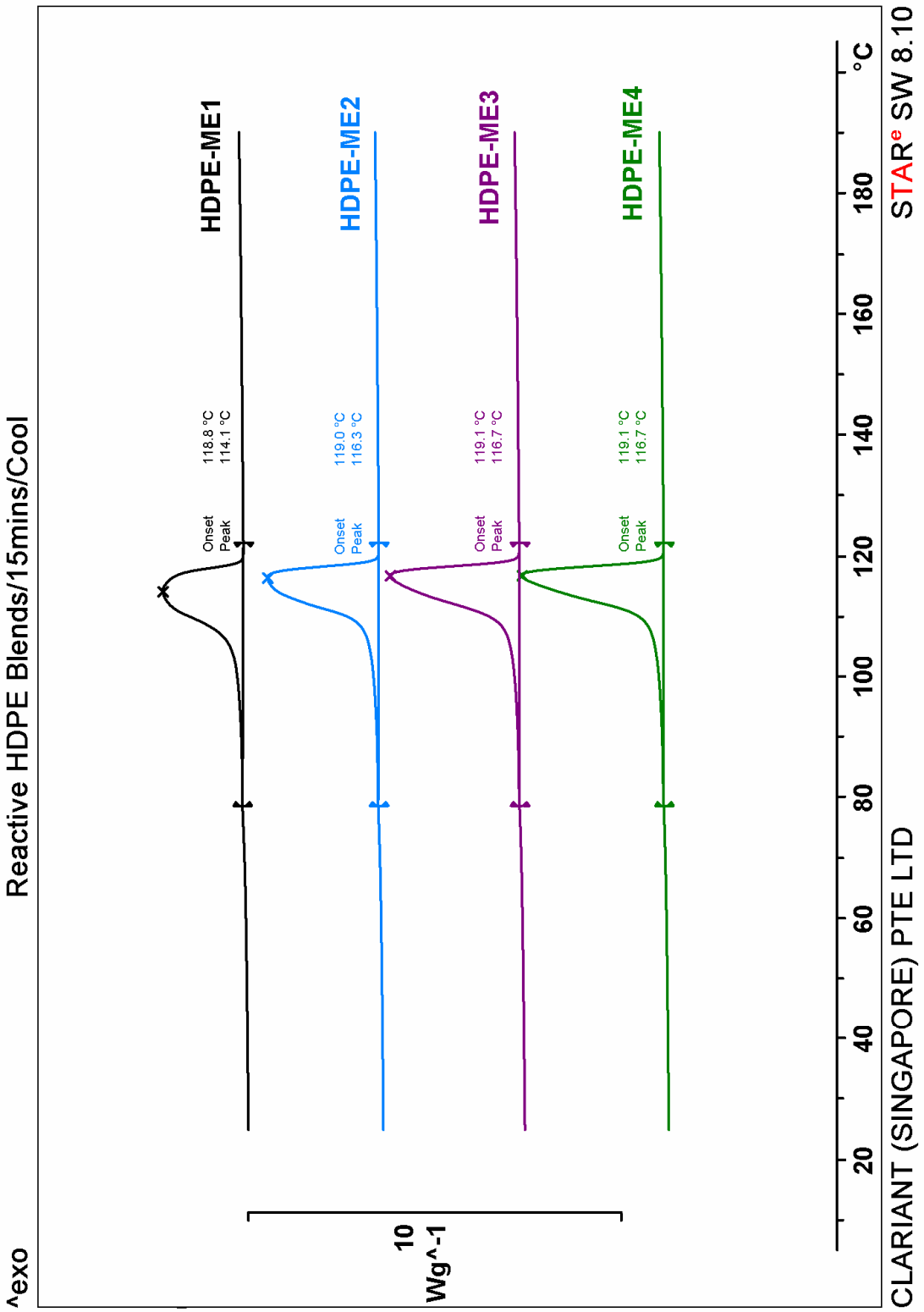
Reactive HDPE Blends/15mins/Cool
^exo
10
Wg^-1
HDPE-ME1
Onset 118.8 °C
Peak 114.1 °C
HDPE-ME2
Onset 119.0 °C
Peak 116.3 °C
HDPE-ME3
Onset 119.1 °C
Peak 116.7 °C
HDPE-ME4
Onset 119.1 °C
Peak 116.7 °C
20
40
60
80
100
120
140
160
180
°C
CLARIANT (SINGAPORE) PTE LTD
STARe SW 8.10

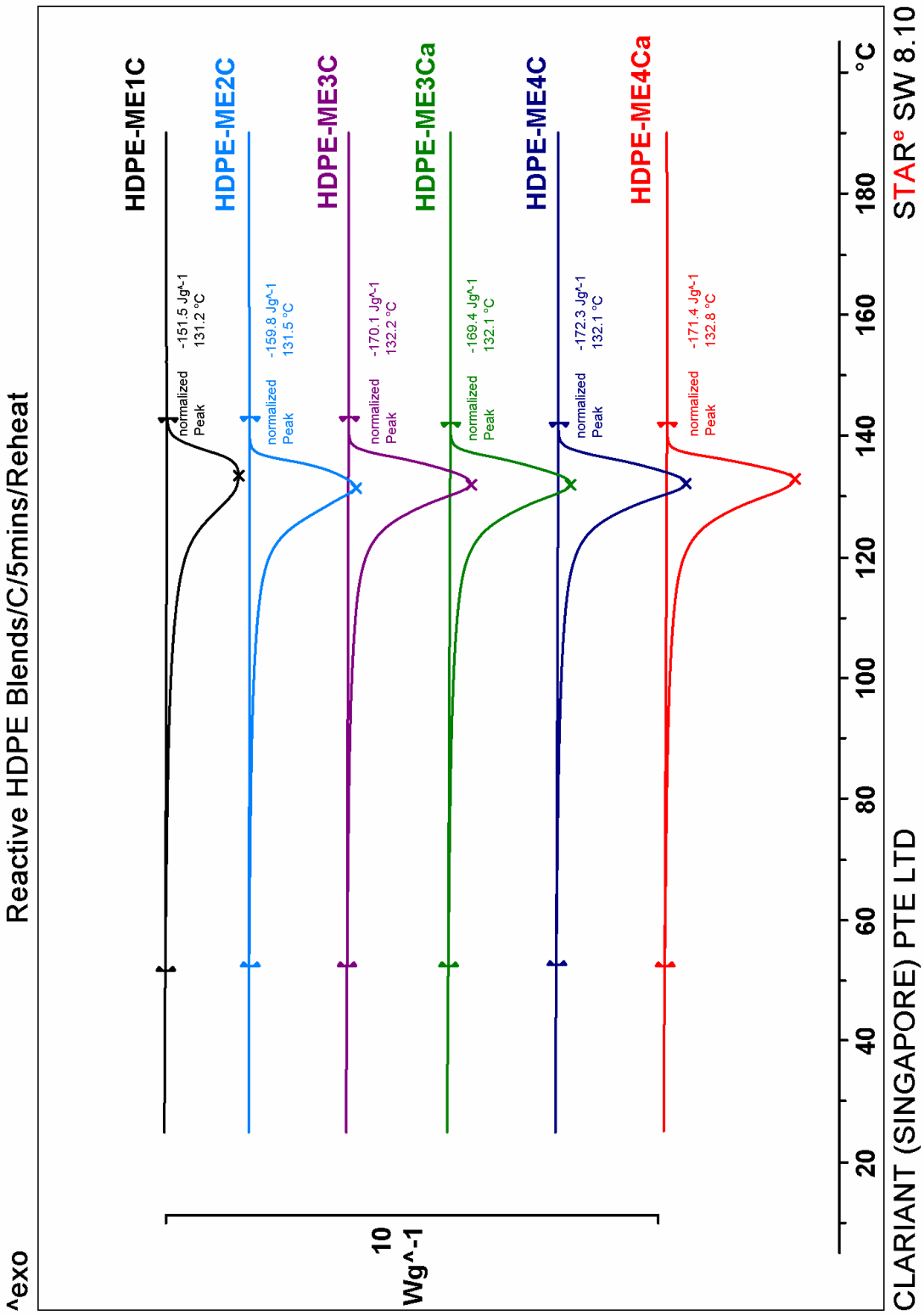
Reactive HDPE Blends/C/5mins/Reheat
^exo
10
Wg^-1
HDPE-ME1C
-151.5 Jg^-1
131.2 °C
normalized
Peak
HDPE-ME2C
-159.8 Jg^-1
131.5 °C
normalized
Peak
HDPE-ME3C
-170.1 Jg^-1
132.2 °C
normalized
Peak
HDPE-ME3Ca
-169.4 Jg^-1
132.1 °C
normalized
Peak
HDPE-ME4C
-172.3 Jg^-1
132.1 °C
normalized
Peak
HDPE-ME4Ca
-171.4 Jg^-1
132.8 °C
normalized
Peak
20
40
60
80
100
120
140
160
180
°C
CLARIANT (SINGAPORE) PTE LTD
STARe SW 8.10

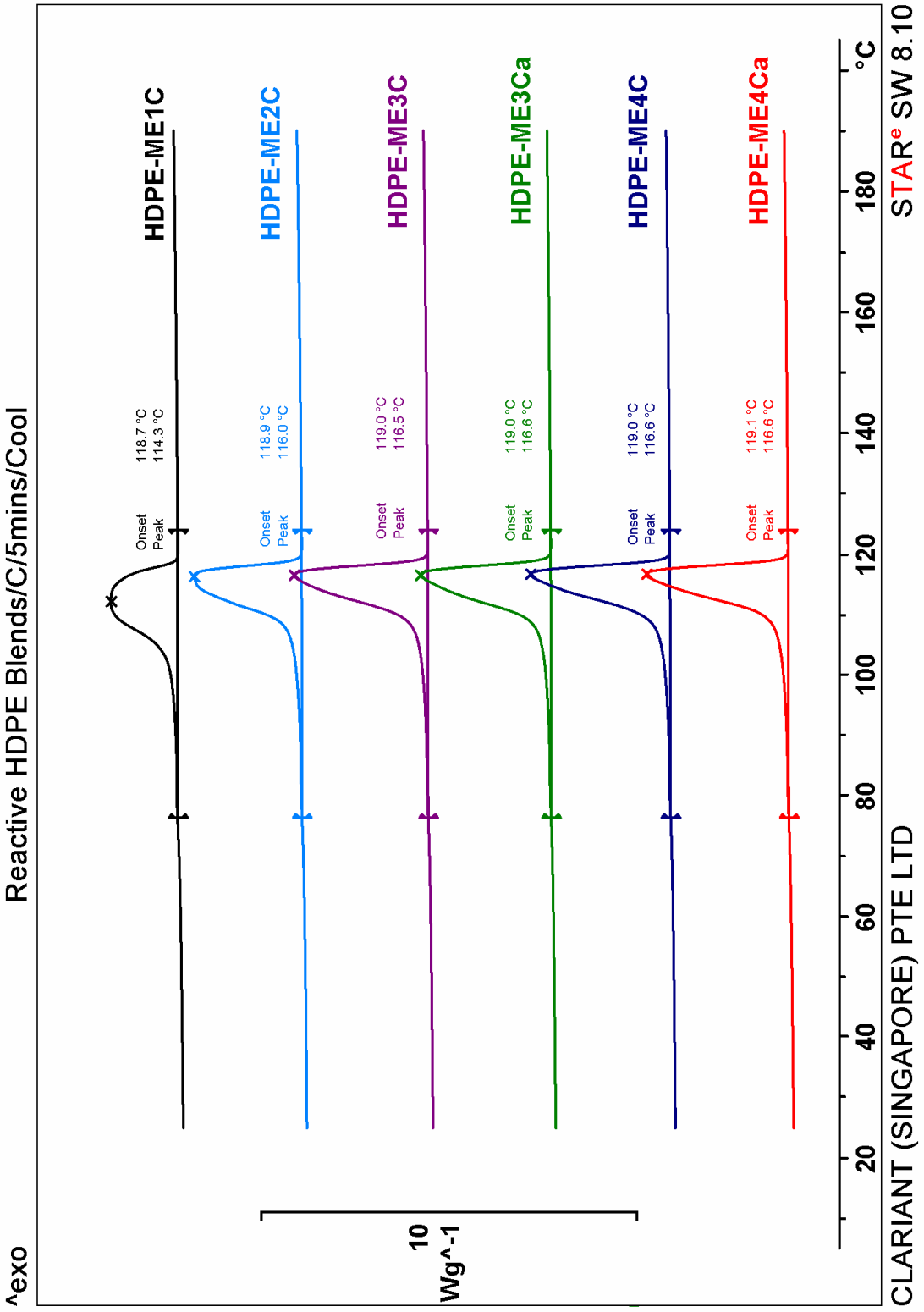
Reactive HDPE Blends/C/5mins/Cool
^exo
10
Wg^-1
HDPE-ME1C
Onset 118.7 °C
Peak 114.3 °C
HDPE-ME2C
Onset 118.9 °C
Peak 116.0 °C
HDPE-ME3C
Onset 119.0 °C
Peak 116.5 °C
HDPE-ME3Ca
Onset 119.0 °C
Peak 116.6 °C
HDPE-ME4C
Onset 119.0 °C
Peak 116.6 °C
HDPE-ME4Ca
Onset 119.1 °C
Peak 116.6 °C
20
40
60
80
100
120
140
160
180
°C
CLARIANT (SINGAPORE) PTE LTD
STARe SW 8.10

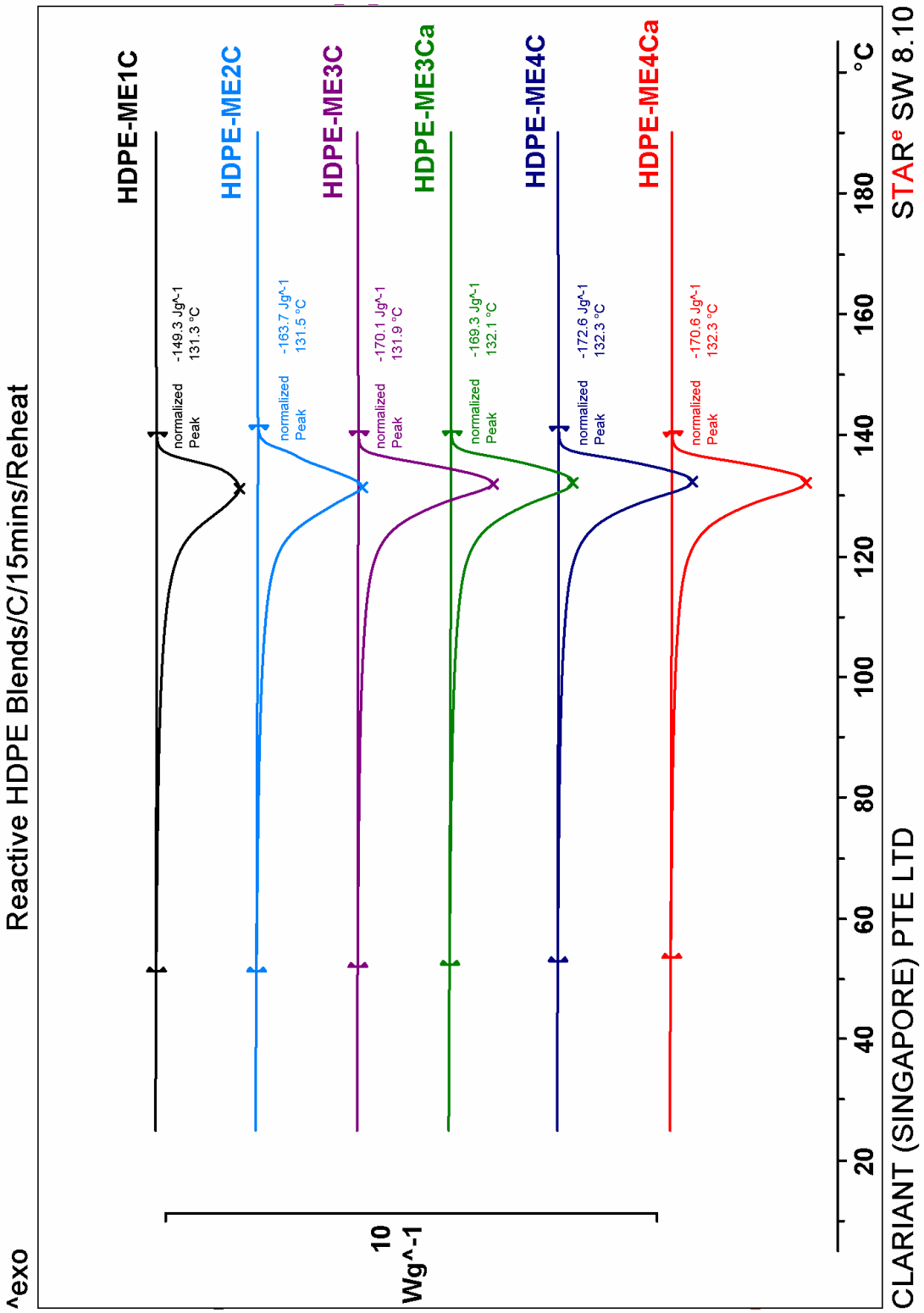
Reactive HDPE Blends/C/15mins/Reheat
^exo
10
Wg^-1
HDPE-ME1C
normalized
Peak
-149.3 Jg^-1
131.3 °C
HDPE-ME2C
normalized
Peak
-163.7 Jg^-1
131.5 °C
HDPE-ME3C
normalized
Peak
-170.1 Jg^-1
131.9 °C
HDPE-ME3Ca
normalized
Peak
-169.3 Jg^-1
132.1 °C
HDPE-ME4C
normalized
Peak
-172.6 Jg^-1
132.3 °C
HDPE-ME4Ca
normalized
Peak
-170.6 Jg^-1
132.3 °C
20
40
60
80
100
120
140
160
180
°C
CLARIANT (SINGAPORE) PTE LTD
STARe SW 8.10

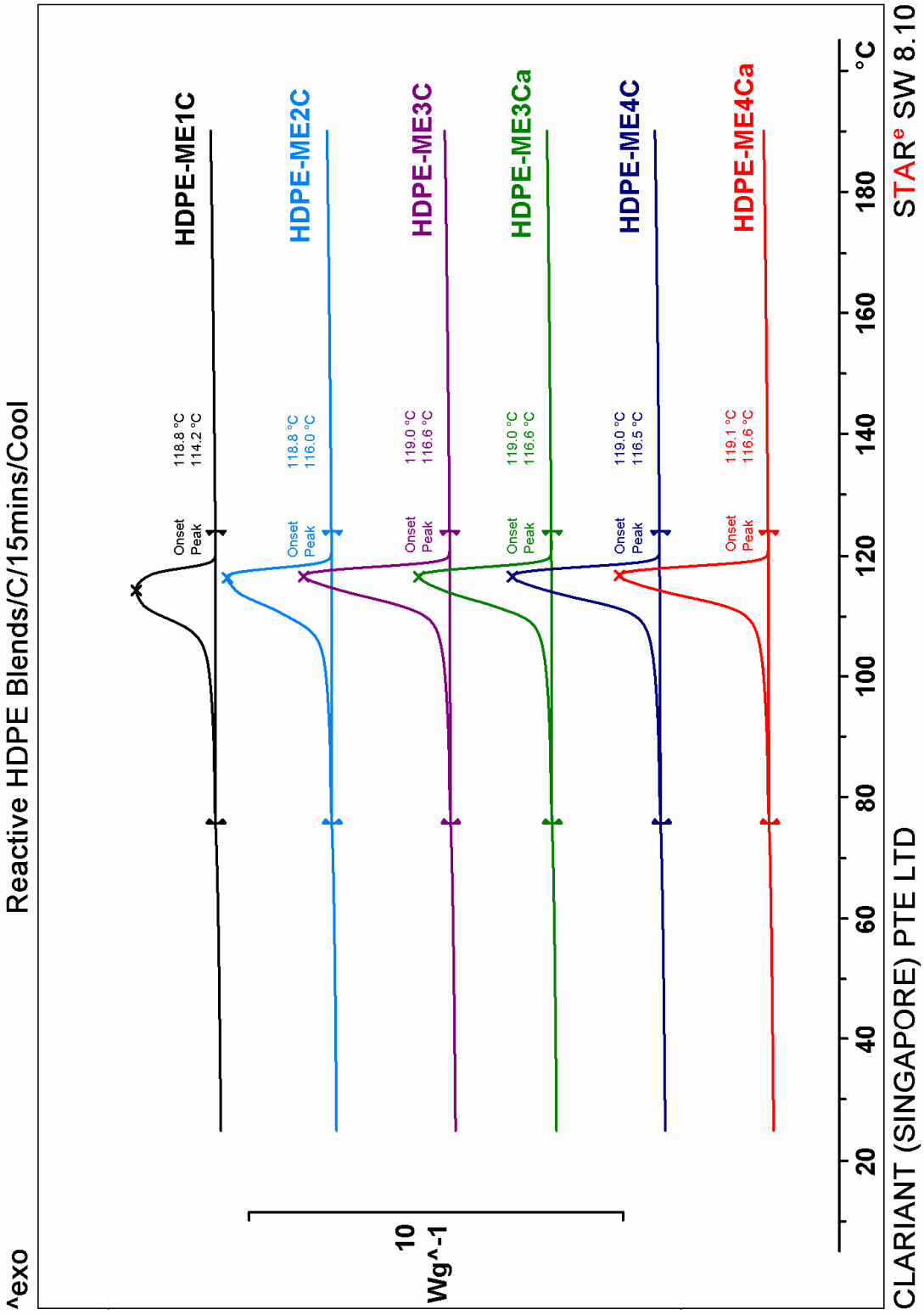
Reactive HDPE Blends/C/15mins/Cool
^exo
10
Wg^-1
HDPE-ME1C
Onset 118.8 °C
Peak 114.2 °C
HDPE-ME2C
Onset 118.8 °C
Peak 116.0 °C
HDPE-ME3C
Onset 119.0 °C
Peak 116.6 °C
HDPE-ME3Ca
Onset 119.0 °C
Peak 116.6 °C
HDPE-ME4C
Onset 119.0 °C
Peak 116.5 °C
HDPE-ME4Ca
Onset 119.1 °C
Peak 116.6 °C
20
40
60
80
100
120
140
160
180
°C
CLARIANT (SINGAPORE) PTE LTD
STARe SW 8.10

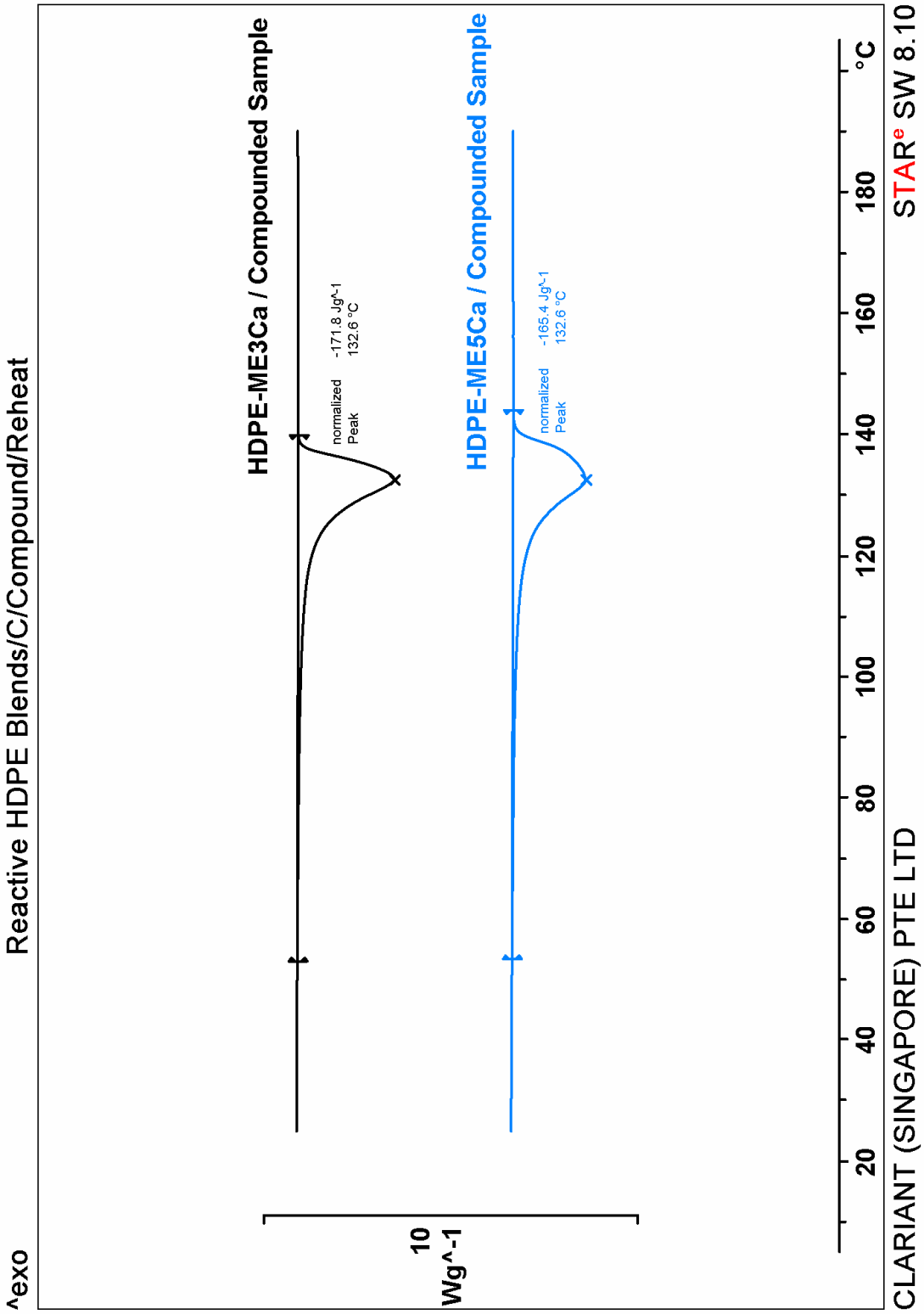
Reactive HDPE Blends/C/Compound/Reheat
^exo
HDPE-ME3Ca / Compounded Sample
normalized
Peak
-171.8 Jg^-1
132.6 °C
HDPE-ME5Ca / Compounded Sample
normalized
Peak
-165.4 Jg^-1
132.6 °C
10
Wg^-1
20
40
60
80
100
120
140
160
180
°C
CLARIANT (SINGAPORE) PTE LTD
STARe SW 8.10

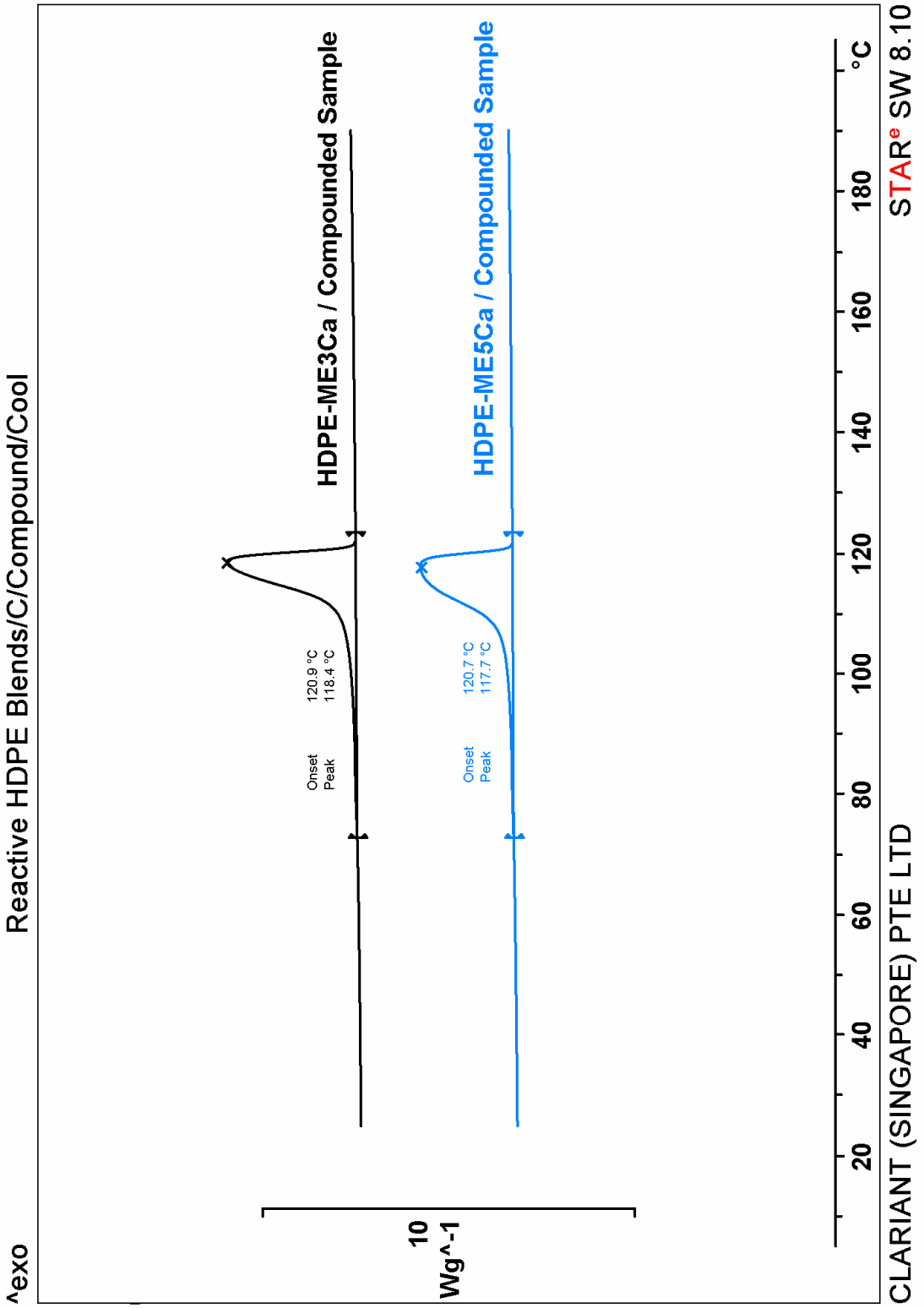
Reactive HDPE Blends/C/Compound/Cool
^exo
10
Wg^-1
HDPE-ME3Ca / Compounded Sample
Onset 120.9 °C
Peak 118.4 °C
HDPE-ME5Ca / Compounded Sample
Onset 120.7 °C
Peak 117.7 °C
20
40
60
80
100
120
140
160
180
°C
CLARIANT (SINGAPORE) PTE LTD
STARe SW 8.10

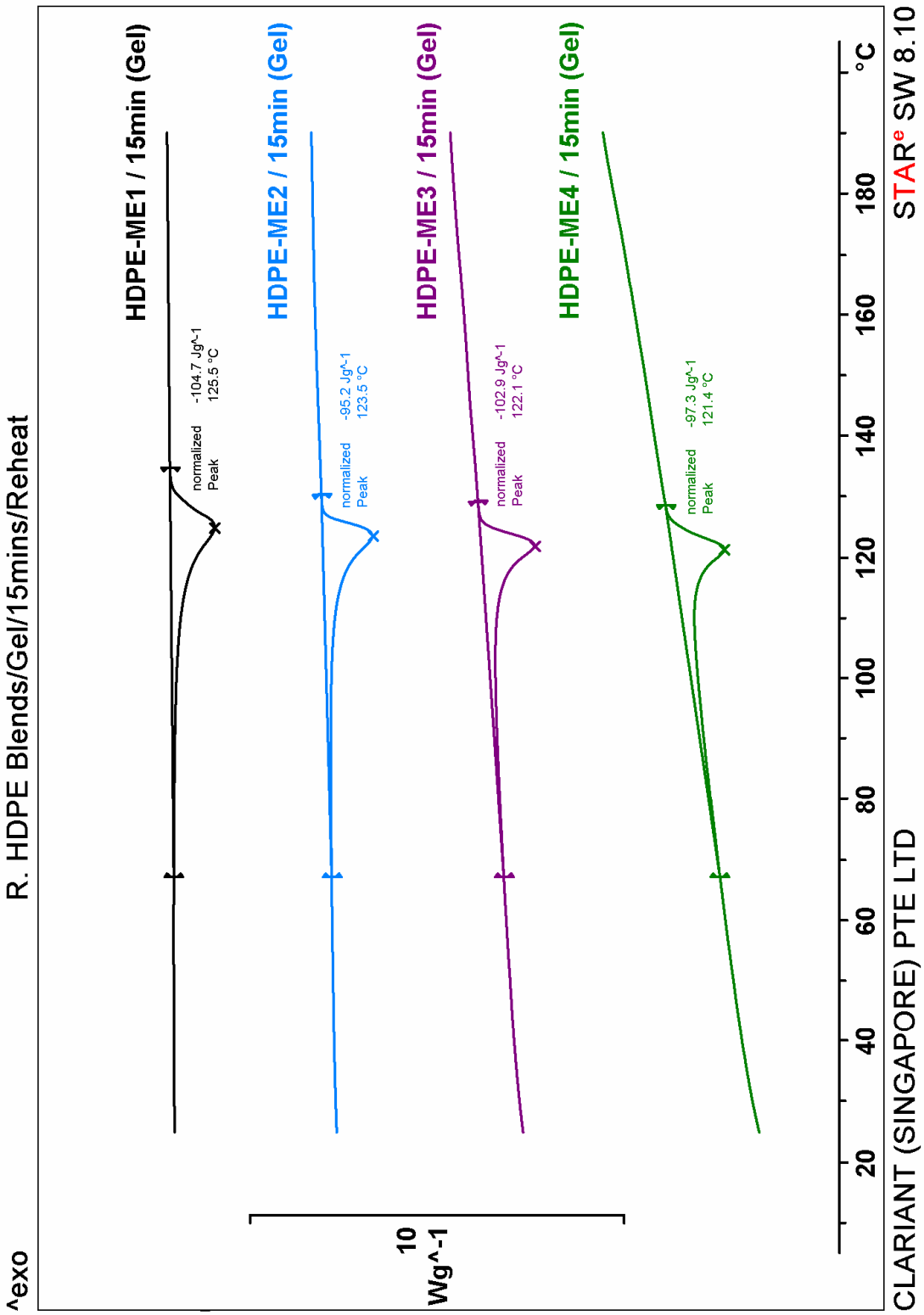
R. HDPE Blends/Gel/15mins/Reheat
^exo
HDPE-ME1 / 15min (Gel)
-104.7 Jg^-1
125.5 °C
normalized
Peak
HDPE-ME2 / 15min (Gel)
-95.2 Jg^-1
123.5 °C
normalized
Peak
HDPE-ME3 / 15min (Gel)
-102.9 Jg^-1
122.1 °C
normalized
Peak
HDPE-ME4 / 15min (Gel)
-97.3 Jg^-1
121.4 °C
normalized
Peak
10
Wg^-1
20
40
60
80
100
120
140
160
180
°C
CLARIANT (SINGAPORE) PTE LTD
STARe SW 8.10

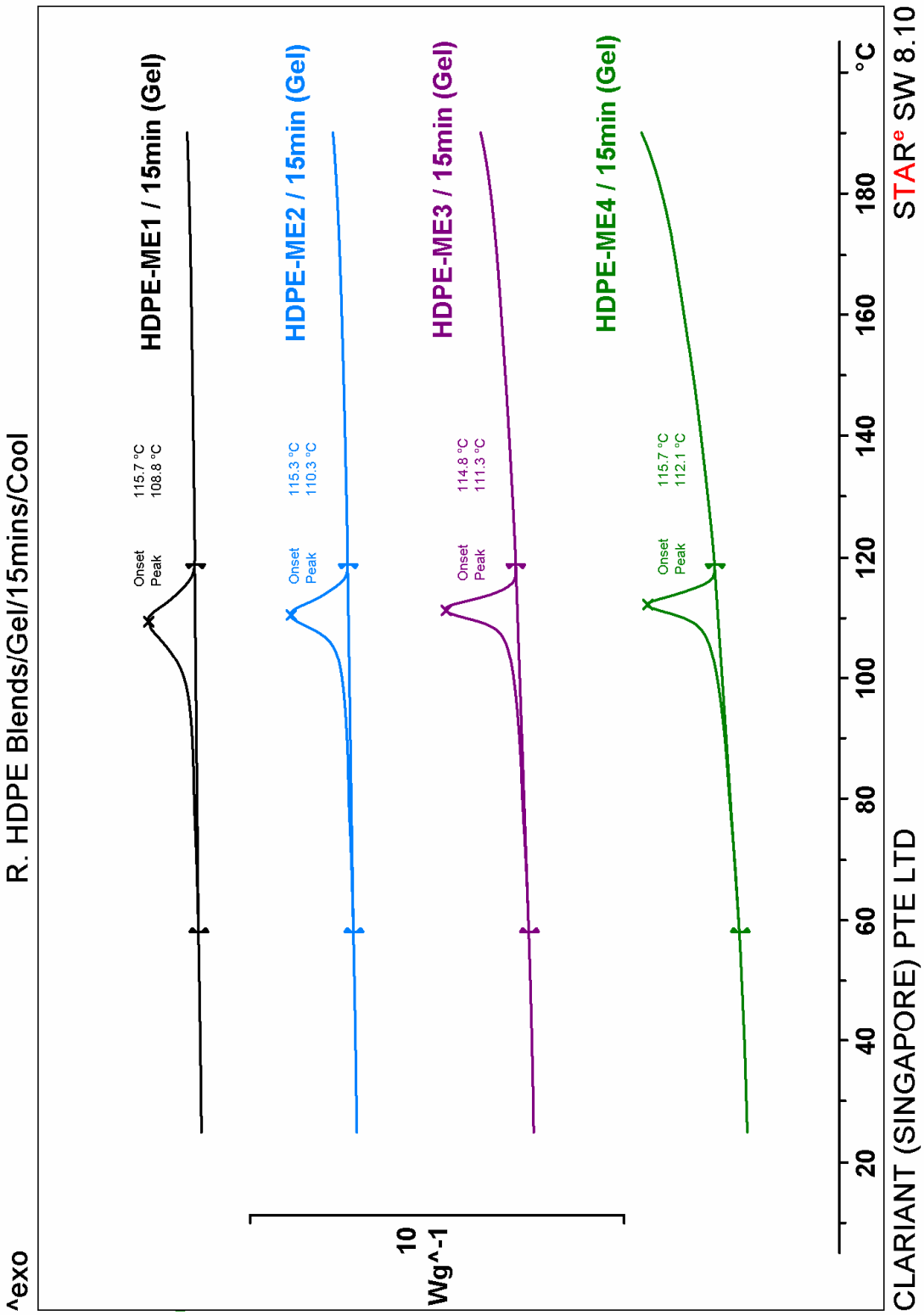
R. HDPE Blends/Gel/15mins/Cool
^exo
10
Wg^-1
HDPE-ME1 / 15min (Gel)
Onset 115.7 °C
Peak 108.8 °C
HDPE-ME2 / 15min (Gel)
Onset 115.3 °C
Peak 110.3 °C
HDPE-ME3 / 15min (Gel)
Onset 114.8 °C
Peak 111.3 °C
HDPE-ME4 / 15min (Gel)
Onset 115.7 °C
Peak 112.1 °C
20
40
60
80
100
120
140
160
180
°C
CLARIANT (SINGAPORE) PTE LTD
STARe SW 8.10

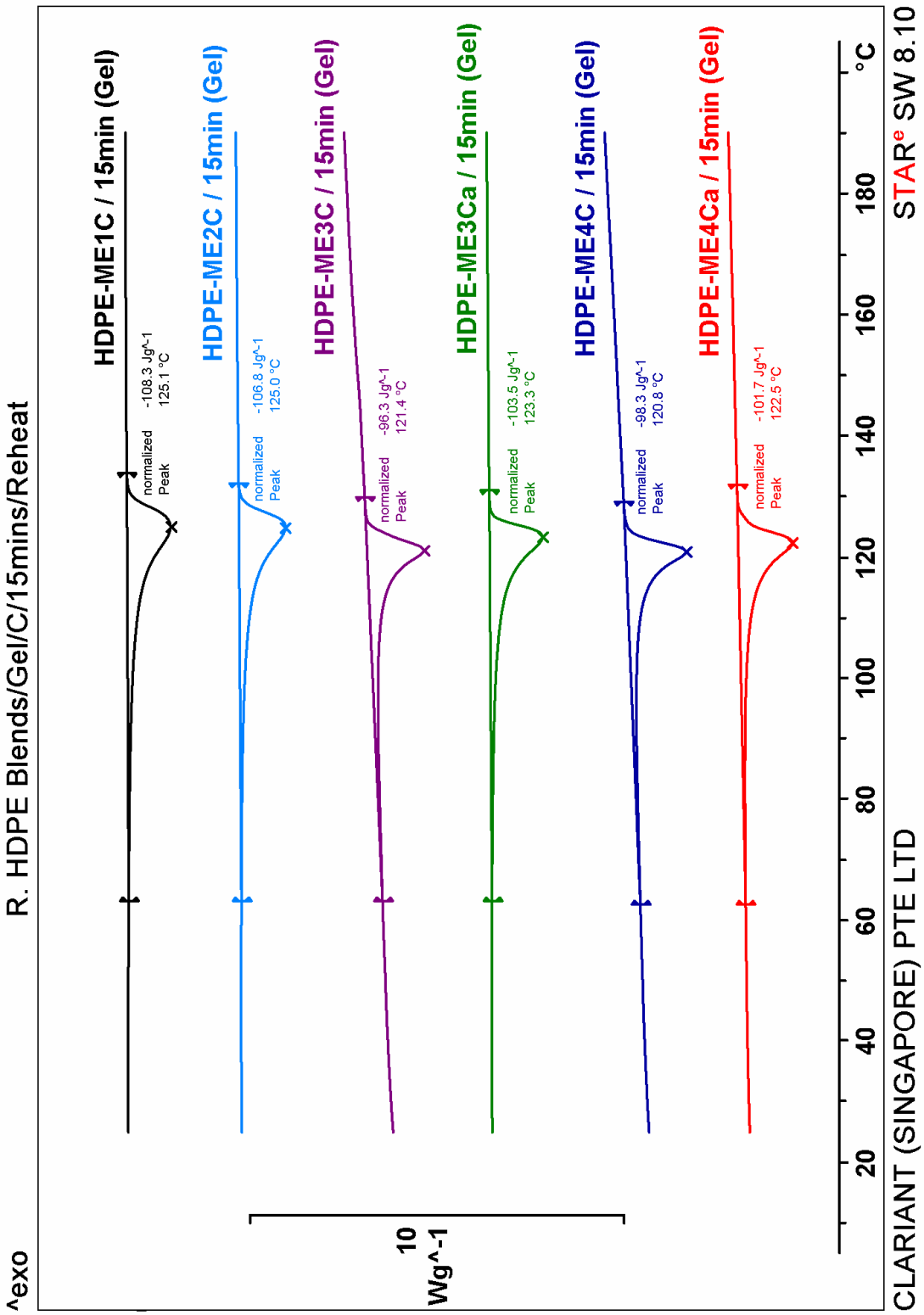
R. HDPE Blends/Gel/C/15mins/Reheat
^exo
10
Wg^-1
HDPE-ME1C / 15min (Gel)
-108.3 Jg^-1
125.1 °C
normalized
Peak
HDPE-ME2C / 15min (Gel)
-106.8 Jg^-1
125.0 °C
normalized
Peak
HDPE-ME3C / 15min (Gel)
-96.3 Jg^-1
121.4 °C
normalized
Peak
HDPE-ME3Ca / 15min (Gel)
-103.5 Jg^-1
123.3 °C
normalized
Peak
HDPE-ME4C / 15min (Gel)
-98.3 Jg^-1
120.8 °C
normalized
Peak
HDPE-ME4Ca / 15min (Gel)
-101.7 Jg^-1
122.5 °C
normalized
Peak
20
40
60
80
100
120
140
160
180
°C
CLARIANT (SINGAPORE) PTE LTD
STARe SW 8.10

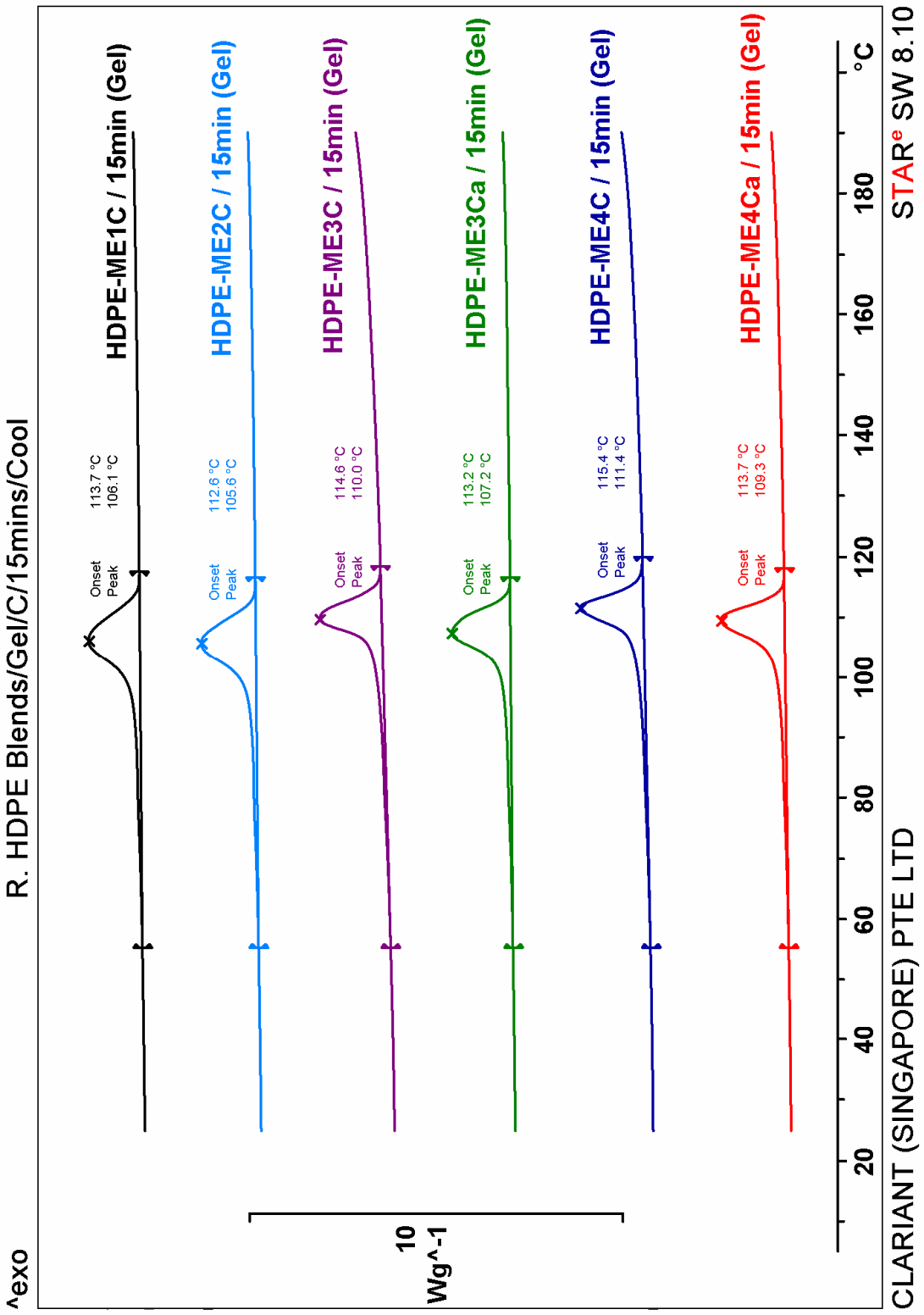
R. HDPE Blends/Gel/C/15mins/Cool
^exo
10
Wg^-1
HDPE-ME1C / 15min (Gel)
Onset 113.7 °C
Peak 106.1 °C
HDPE-ME2C / 15min (Gel)
Onset 112.6 °C
Peak 105.6 °C
HDPE-ME3C / 15min (Gel)
Onset 114.6 °C
Peak 110.0 °C
HDPE-ME3Ca / 15min (Gel)
Onset 113.2 °C
Peak 107.2 °C
HDPE-ME4C / 15min (Gel)
Onset 115.4 °C
Peak 111.4 °C
HDPE-ME4Ca / 15min (Gel)
Onset 113.7 °C
Peak 109.3 °C
20
40
60
80
100
120
140
160
180
°C
CLARIANT (SINGAPORE) PTE LTD
STARe SW 8.10

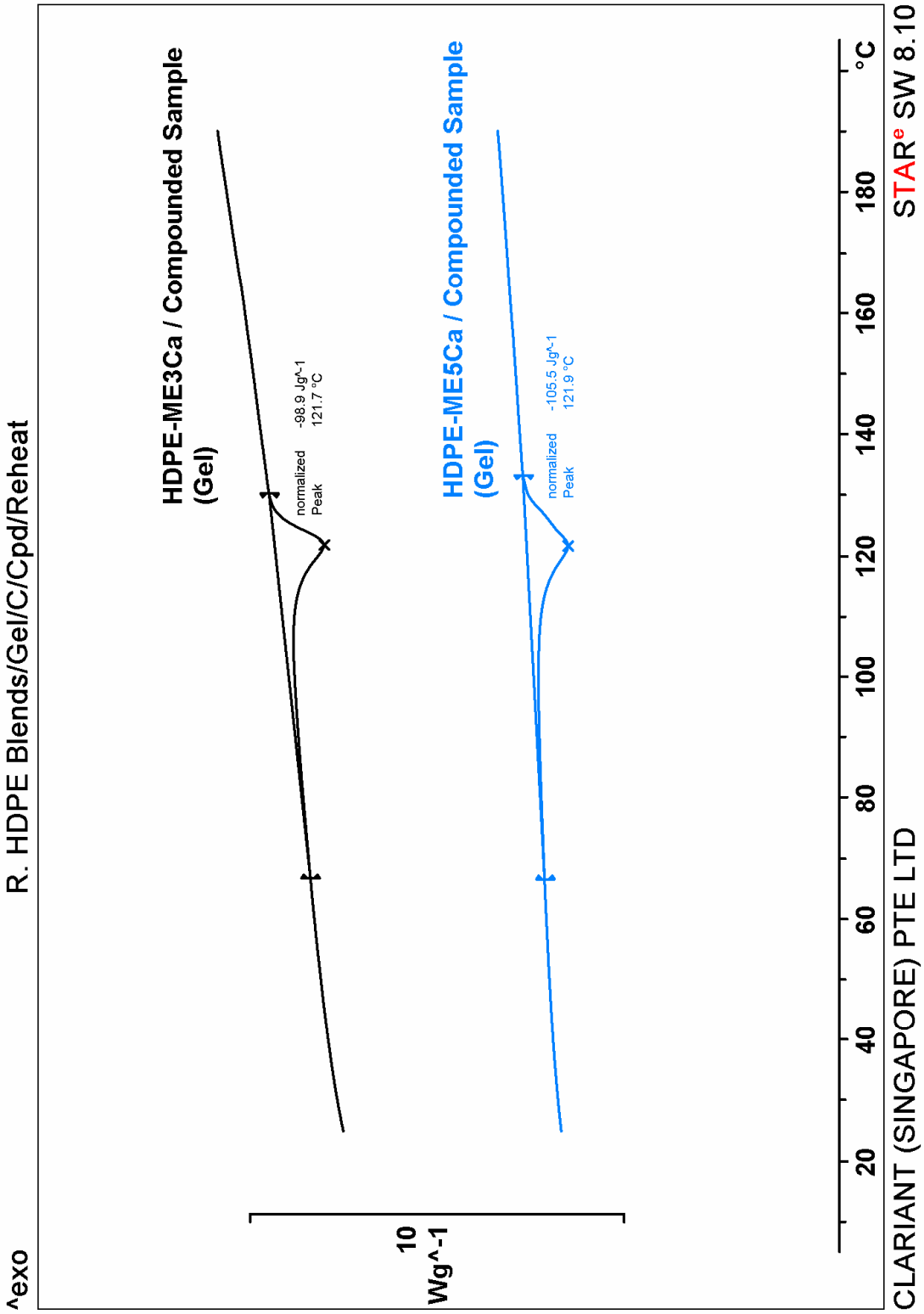
R. HDPE Blends/Gel/C/Cpd/Reheat
^exo
HDPE-ME3Ca / Compounded Sample
(Gel)
normalized
Peak
-98.9 Jg^-1
121.7 °C
HDPE-ME5Ca / Compounded Sample
(Gel)
normalized
Peak
-105.5 Jg^-1
121.9 °C
10
Wg^-1
20
40
60
80
100
120
140
160
180
°C
CLARIANT (SINGAPORE) PTE LTD
STARe SW 8.10

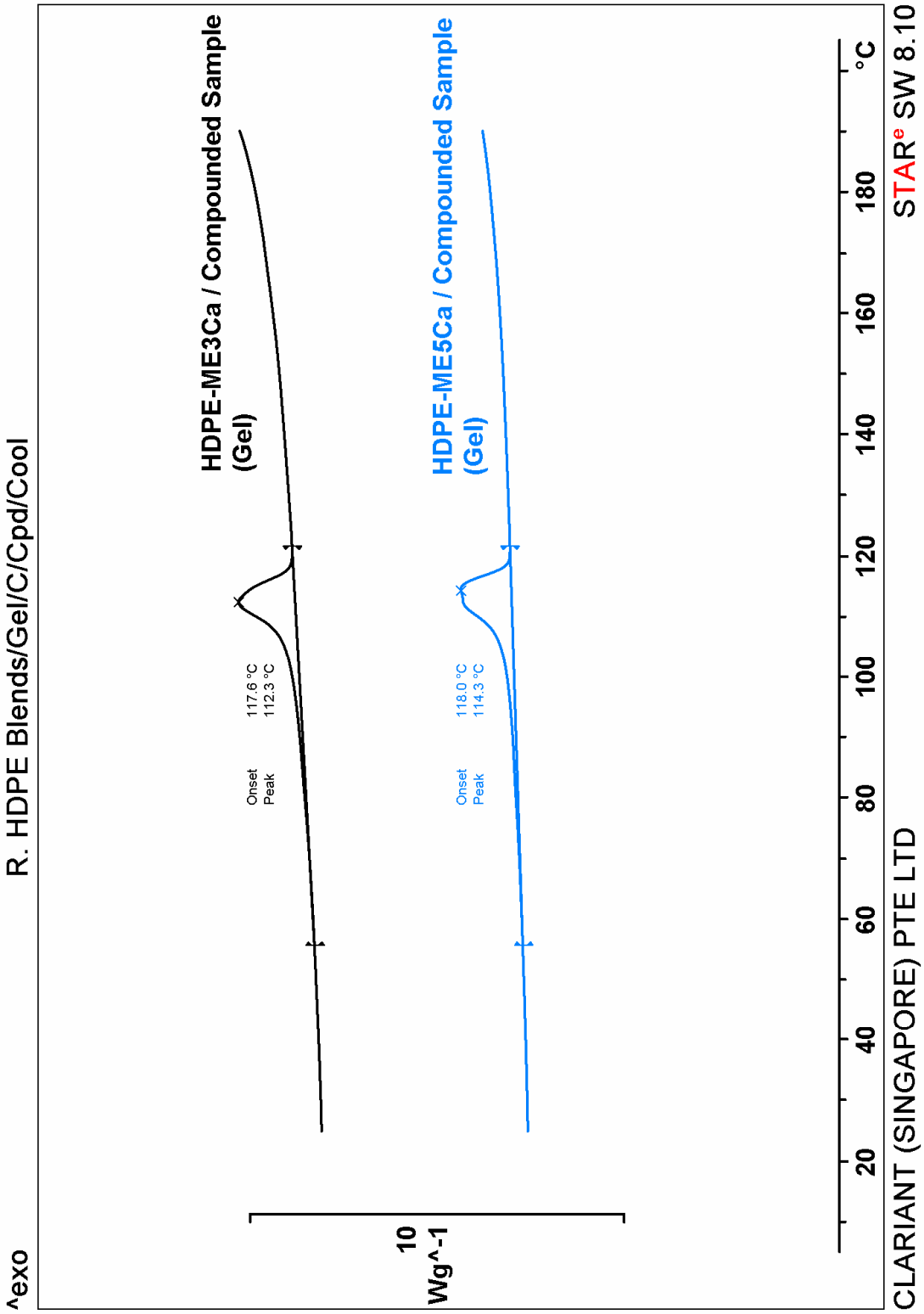
R. HDPE Blends/Gel/C/Cpd/Cool
^exo
HDPE-ME3Ca / Compounded Sample (Gel)
Onset 117.6 °C
Peak 112.3 °C
HDPE-ME5Ca / Compounded Sample (Gel)
Onset 118.0 °C
Peak 114.3 °C
10
Wg^-1
20
40
60
80
100
120
140
160
180
°C
CLARIANT (SINGAPORE) PTE LTD
STARe SW 8.10

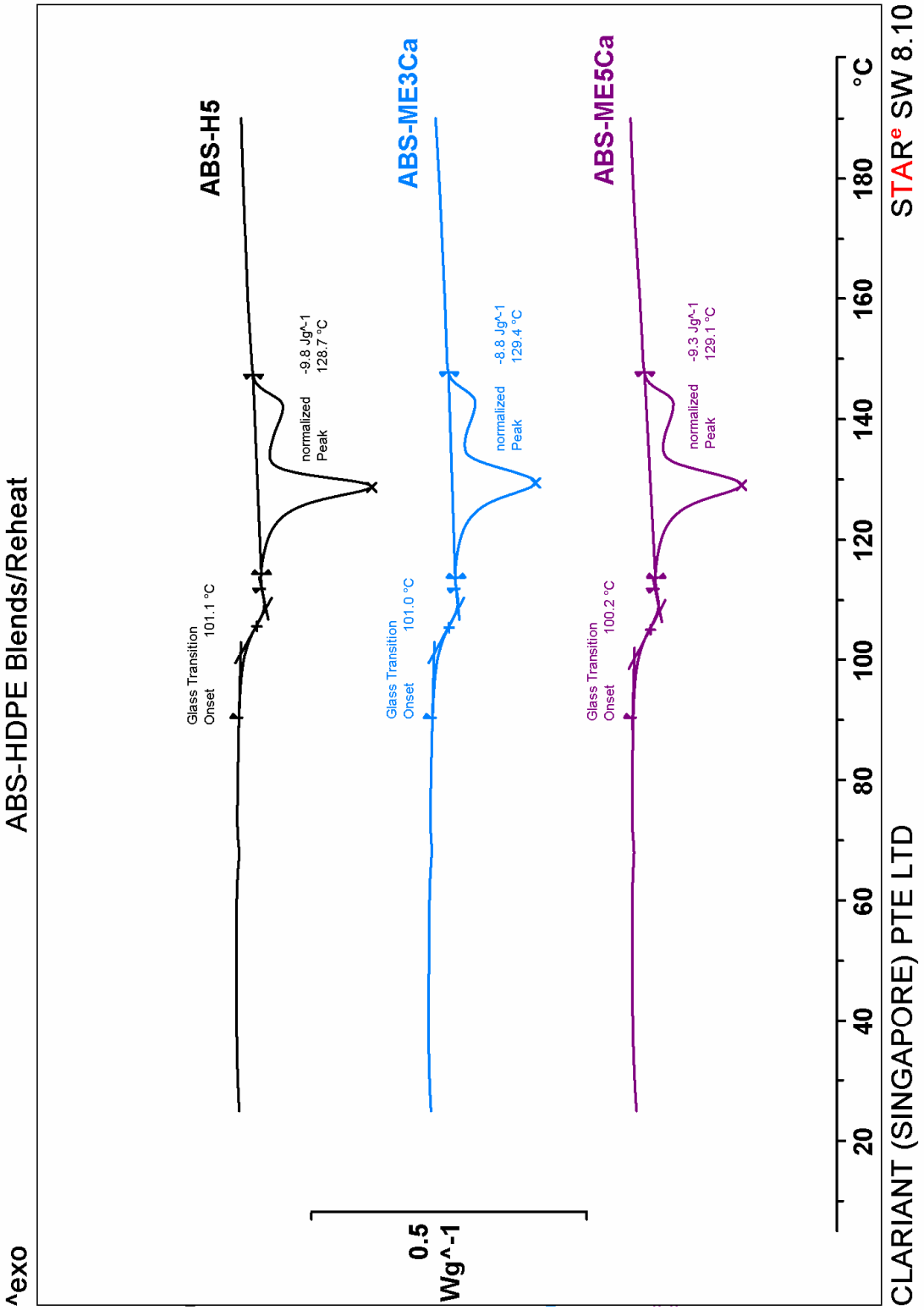
ABS-HDPE Blends/Reheat
^exo
0.5
Wg^-1
ABS-H5
Glass Transition
Onset 101.1 °C
normalized
Peak -9.8 Jg^-1
128.7 °C
ABS-ME3Ca
Glass Transition
Onset 101.0 °C
normalized
Peak -8.8 Jg^-1
129.4 °C
ABS-ME5Ca
Glass Transition
Onset 100.2 °C
normalized
Peak -9.3 Jg^-1
129.1 °C
20
40
60
80
100
120
140
160
180
°C
CLARIANT (SINGAPORE) PTE LTD
STARe SW 8.10

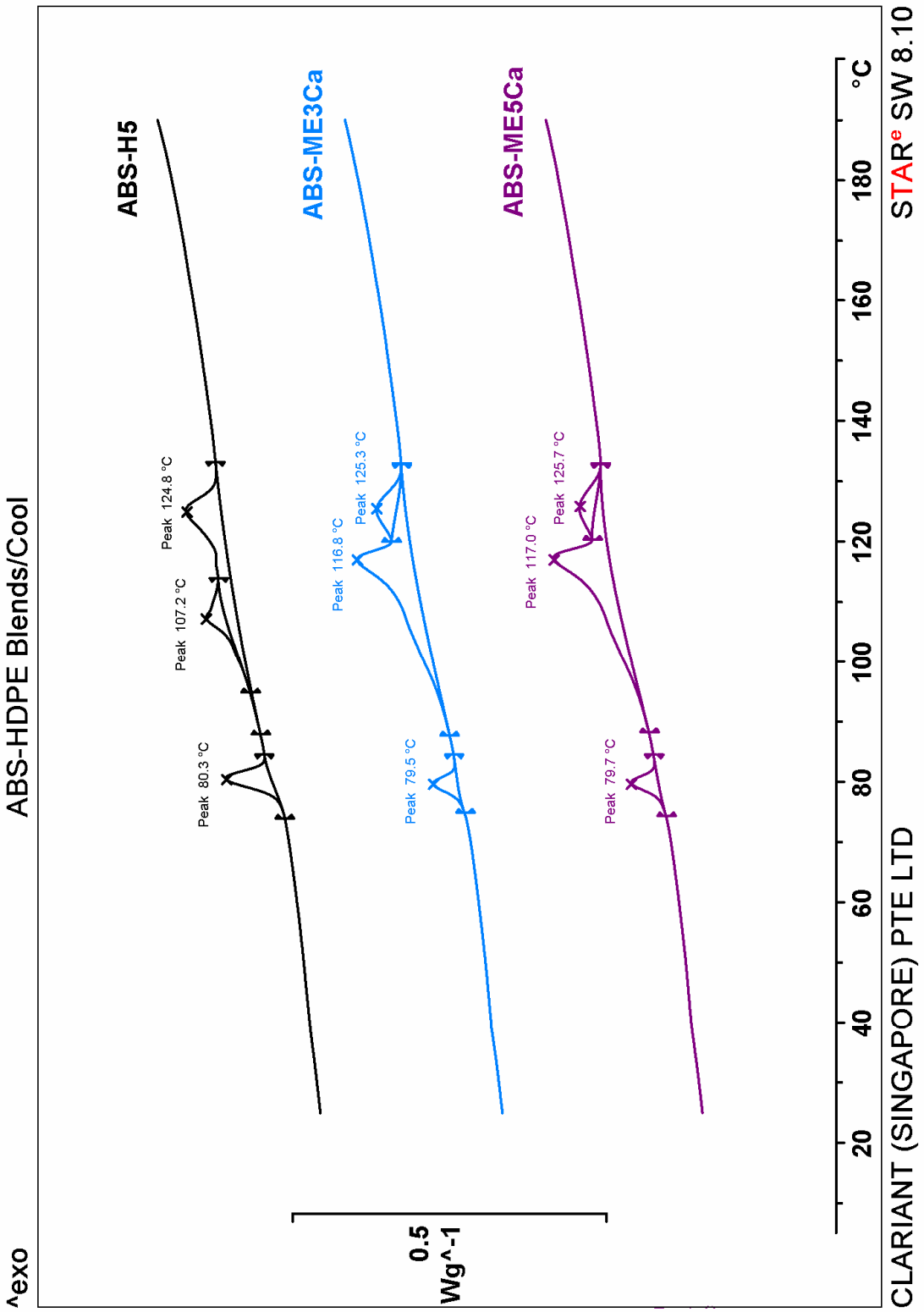
ABS-HDPE Blends/Cool
^exo
ABS-H5
Peak 124.8 °C
Peak 107.2 °C
Peak 80.3 °C
ABS-ME3Ca
Peak 125.3 °C
Peak 116.8 °C
Peak 79.5 °C
ABS-ME5Ca
Peak 125.7 °C
Peak 117.0 °C
Peak 79.7 °C
0.5
Wg^-1
20
40
60
80
100
120
140
160
180
°C
CLARIANT (SINGAPORE) PTE LTD
STARe SW 8.10

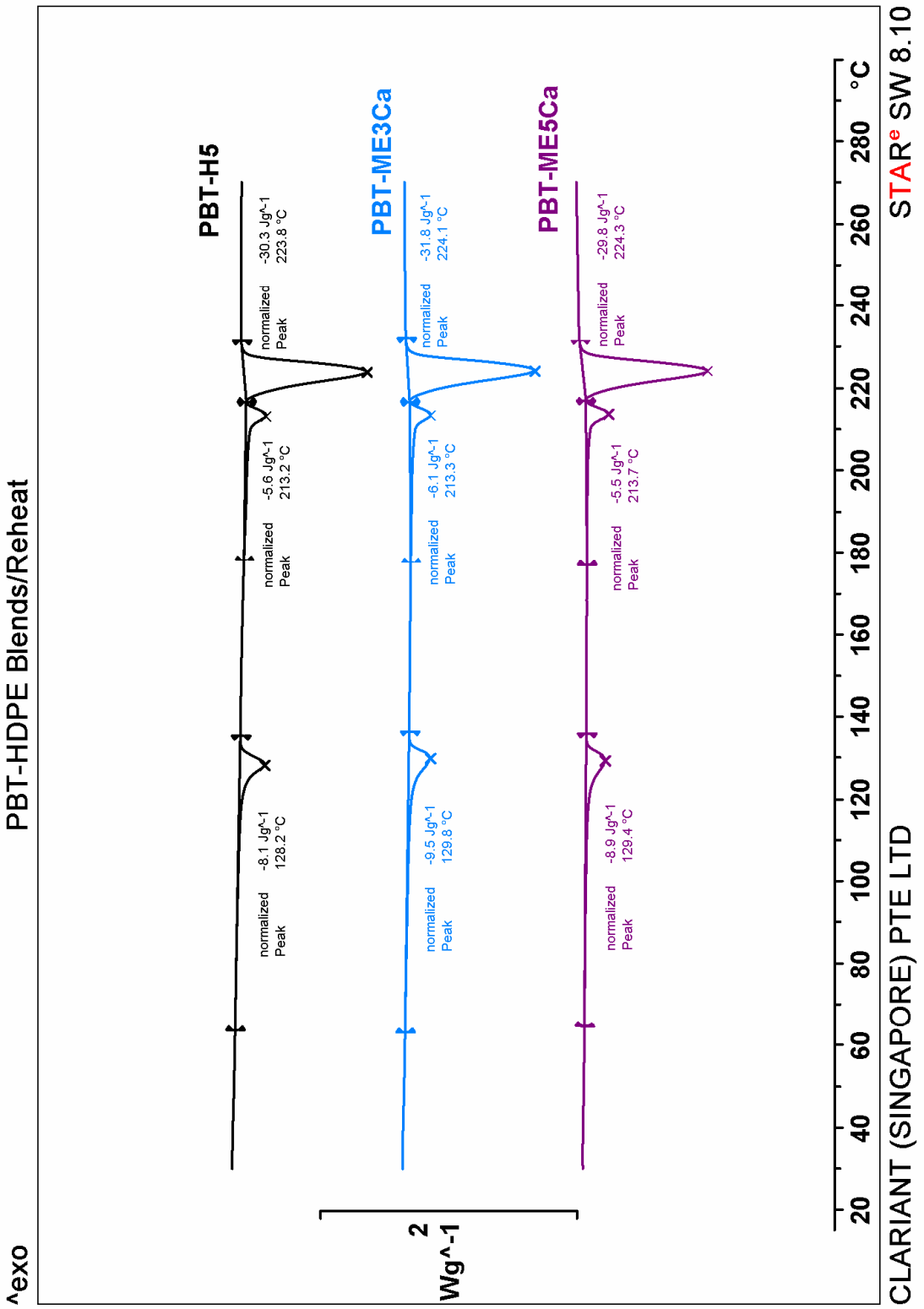
PBT-HDPE Blends/Reheat
^exo
2
Wg^-1
PBT-H5
normalized
Peak
-8.1 Jg^-1
128.2 °C
normalized
Peak
-5.6 Jg^-1
213.2 °C
normalized
Peak
-30.3 Jg^-1
223.8 °C
PBT-ME3Ca
normalized
Peak
-9.5 Jg^-1
129.8 °C
normalized
Peak
-6.1 Jg^-1
213.3 °C
normalized
Peak
-31.8 Jg^-1
224.1 °C
PBT-ME5Ca
normalized
Peak
-8.9 Jg^-1
129.4 °C
normalized
Peak
-5.5 Jg^-1
213.7 °C
normalized
Peak
-29.8 Jg^-1
224.3 °C
20
40
60
80
100
120
140
160
180
200
220
240
260
280
°C
CLARIANT (SINGAPORE) PTE LTD
STARe SW 8.10

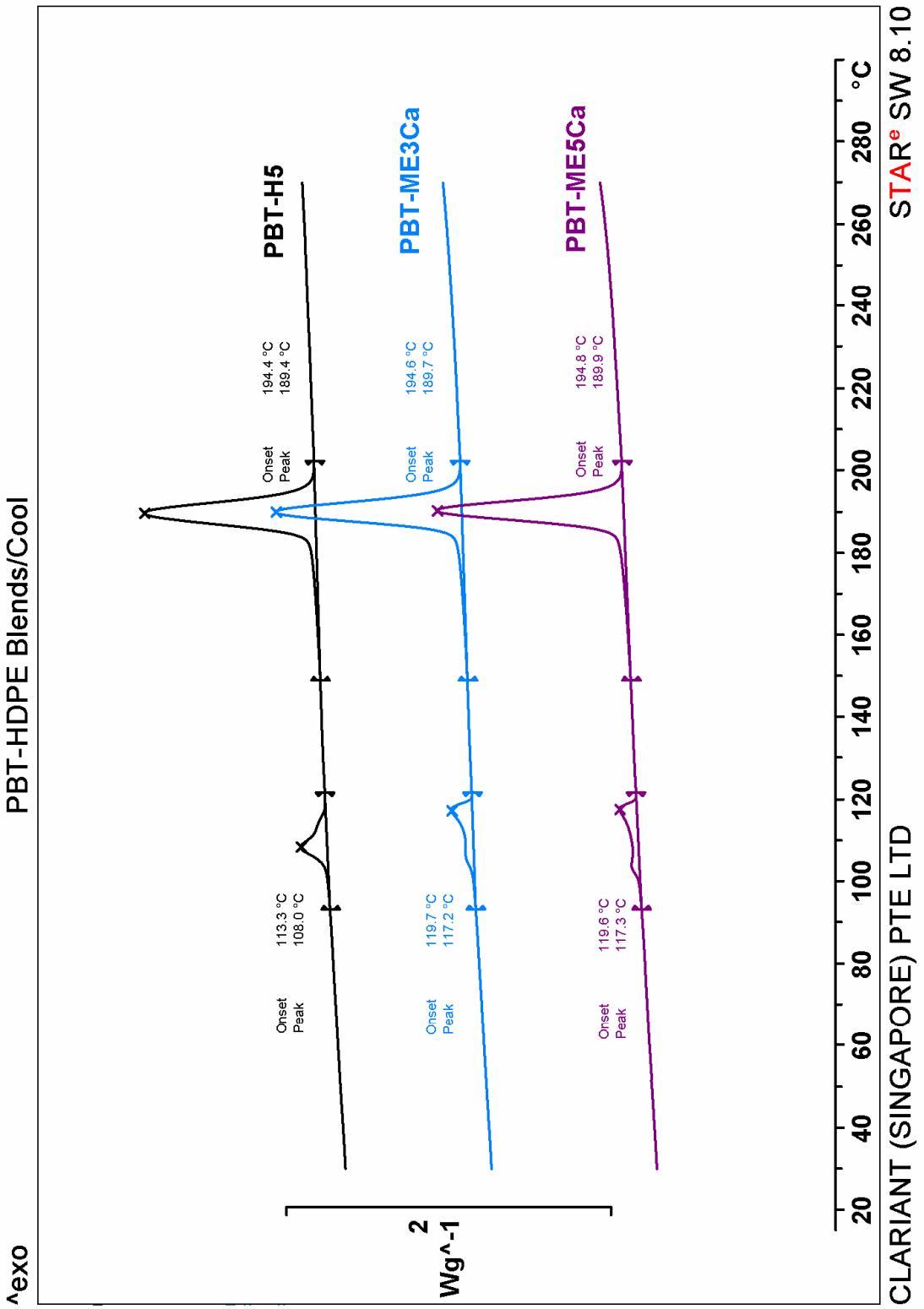
PBT-HDPE Blends/Cool
^exo
2
Wg^-1
PBT-H5
Onset 194.4 °C
Peak 189.4 °C
Onset 113.3 °C
Peak 108.0 °C
PBT-ME3Ca
Onset 194.6 °C
Peak 189.7 °C
Onset 119.7 °C
Peak 117.2 °C
PBT-ME5Ca
Onset 194.8 °C
Peak 189.9 °C
Onset 119.6 °C
Peak 117.3 °C
20 40 60 80 100 120 140 160 180 200 220 240 260 280 °C
CLARIANT (SINGAPORE) PTE LTD
STARe SW 8.10

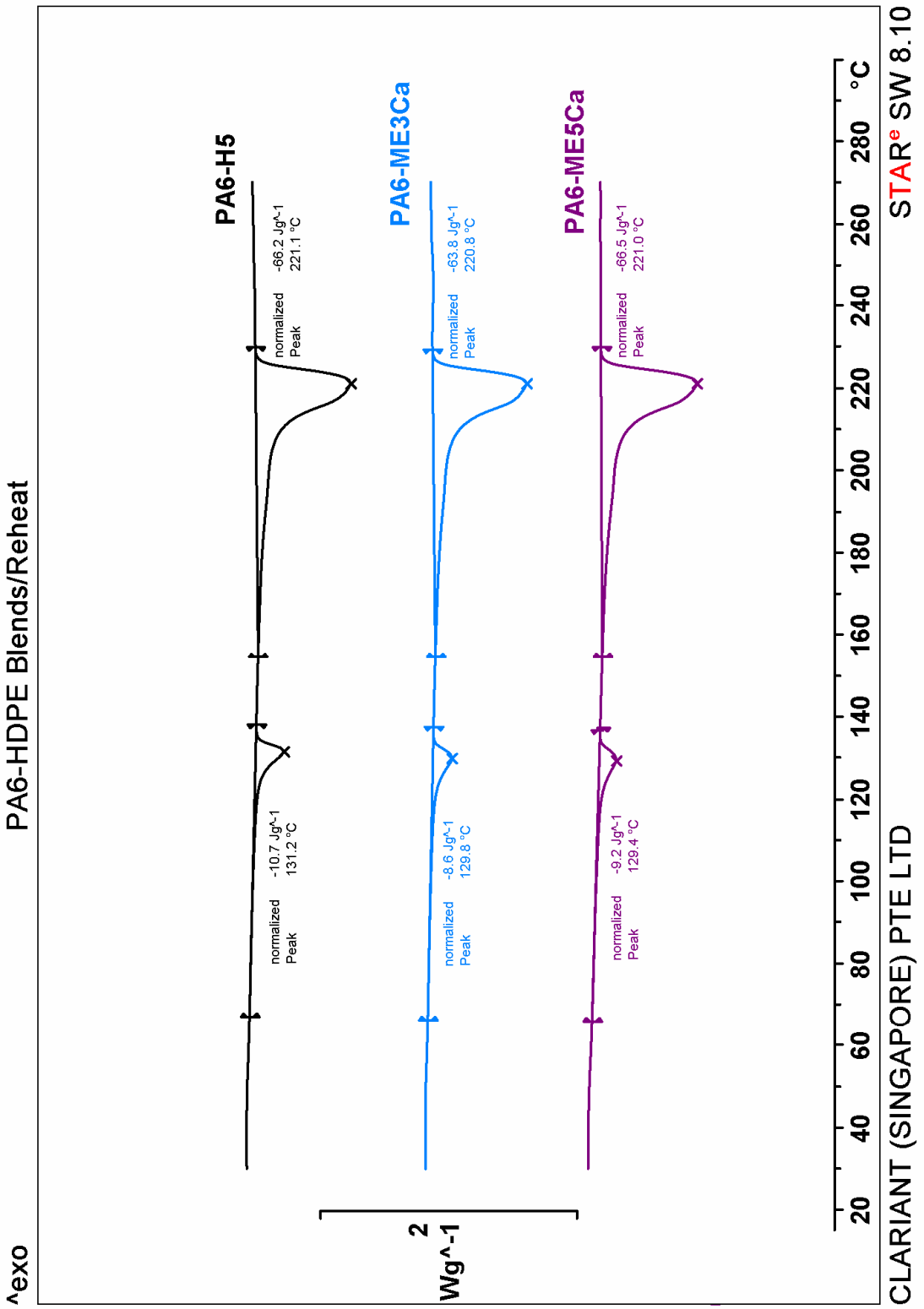
PA6-HDPE Blends/Reheat
^exo
2
Wg^-1
PA6-H5
normalized
Peak
-10.7 Jg^-1
131.2 °C
normalized
Peak
-66.2 Jg^-1
221.1 °C
PA6-ME3Ca
normalized
Peak
-8.6 Jg^-1
129.8 °C
normalized
Peak
-63.8 Jg^-1
220.8 °C
PA6-ME5Ca
normalized
Peak
-9.2 Jg^-1
129.4 °C
normalized
Peak
-66.5 Jg^-1
221.0 °C
20
40
60
80
100
120
140
160
180
200
220
240
260
280
°C
CLARIANT (SINGAPORE) PTE LTD
STARe SW 8.10

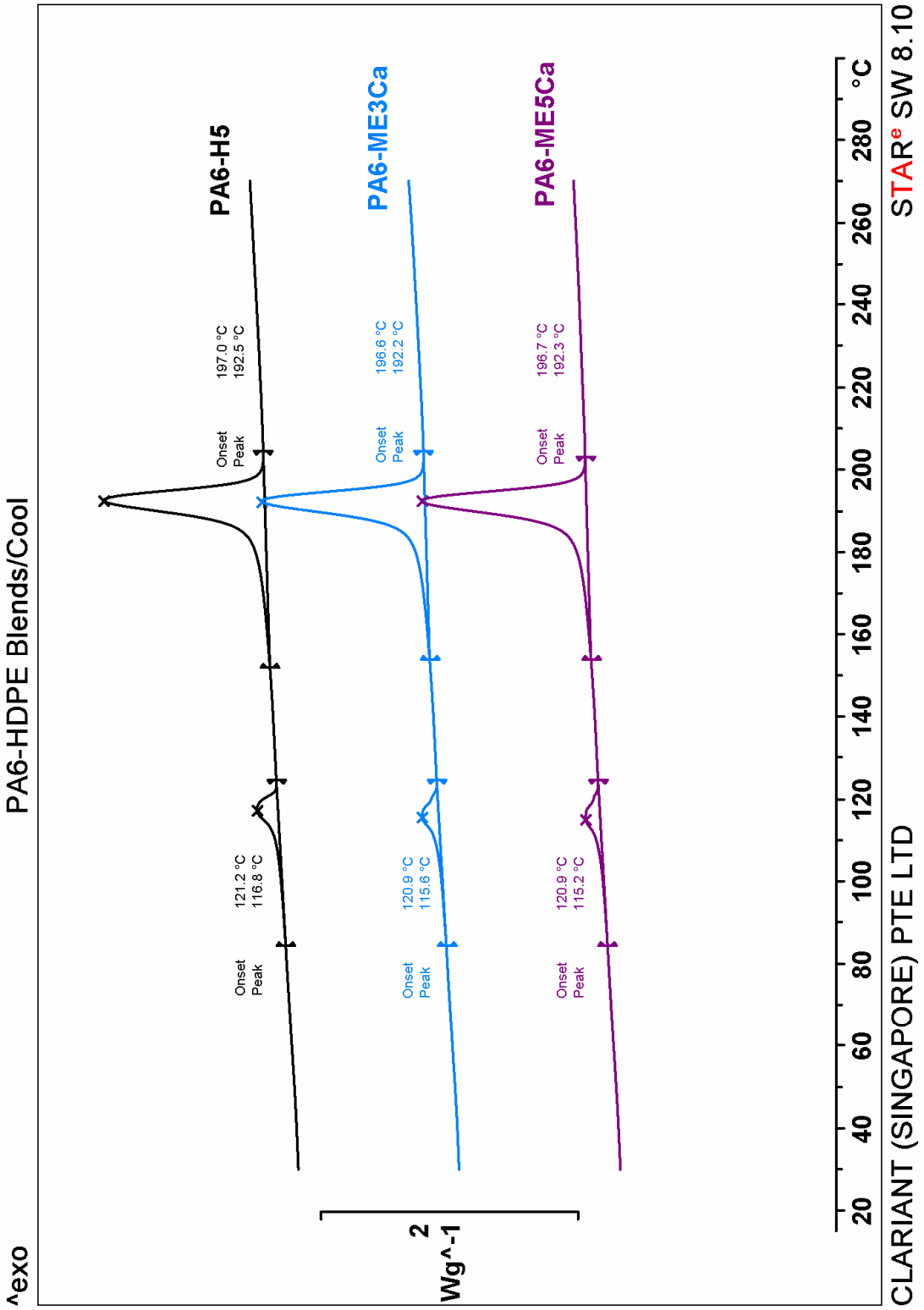
PA6-HDPE Blends/Cool
^exo
2
Wg^-1
PA6-H5
Onset 197.0 °C
Peak 192.5 °C
Onset 121.2 °C
Peak 116.8 °C
PA6-ME3Ca
Onset 196.6 °C
Peak 192.2 °C
Onset 120.9 °C
Peak 115.6 °C
PA6-ME5Ca
Onset 196.7 °C
Peak 192.3 °C
Onset 120.9 °C
Peak 115.2 °C
20 40 60 80 100 120 140 160 180 200 220 240 260 280 °C
CLARIANT (SINGAPORE) PTE LTD
STARe SW 8.10

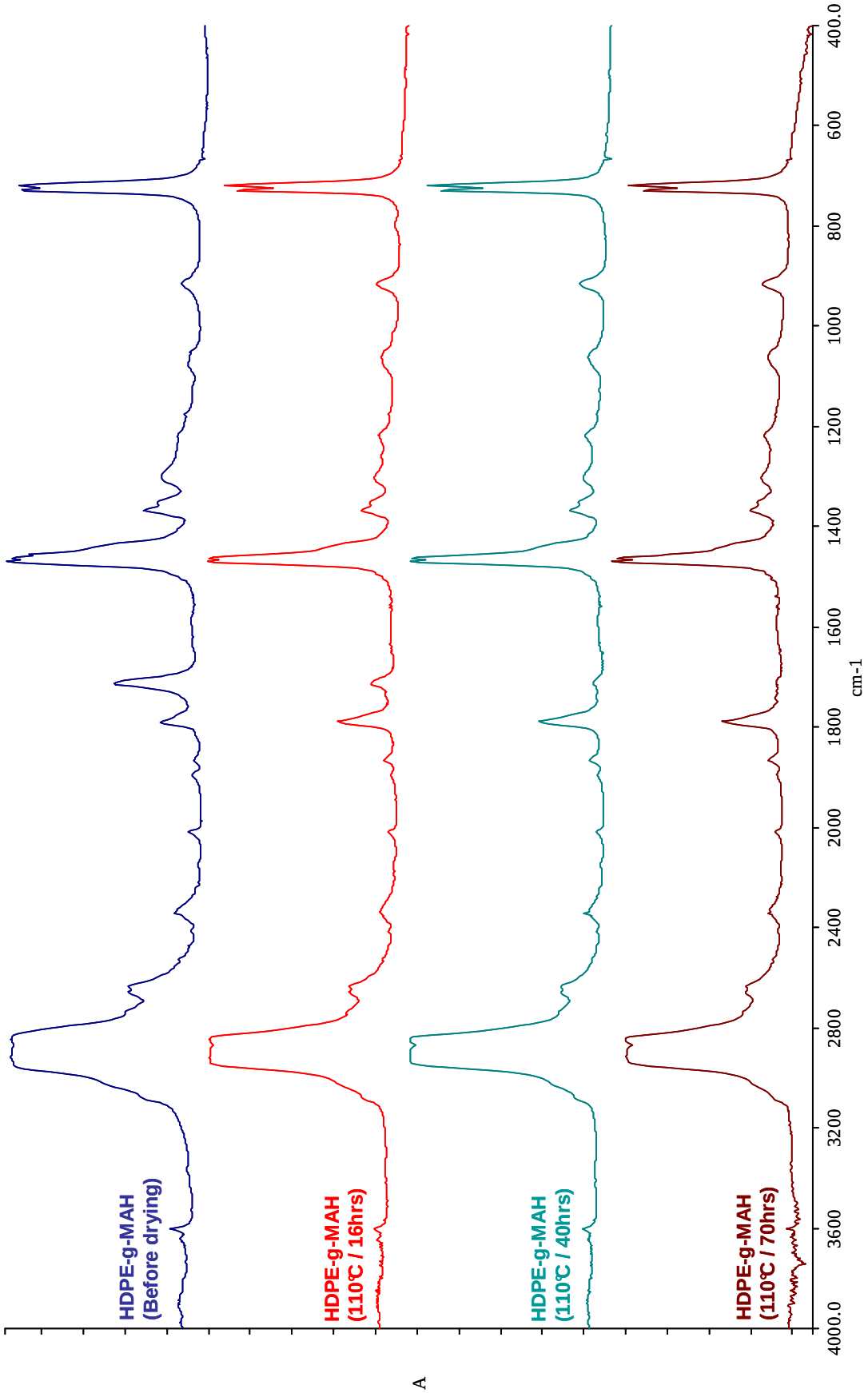
HDPE-g-MAH
(Before drying)
HDPE-g-MAH
(110℃ / 16hrs)
HDPE-g-MAH
(110℃ / 40hrs)
HDPE-g-MAH
(110℃ / 70hrs)
A
4000.0
3600
3200
2800
2400
2000
1800
1600
1400
1200
1000
800
600
400.0
cm-1

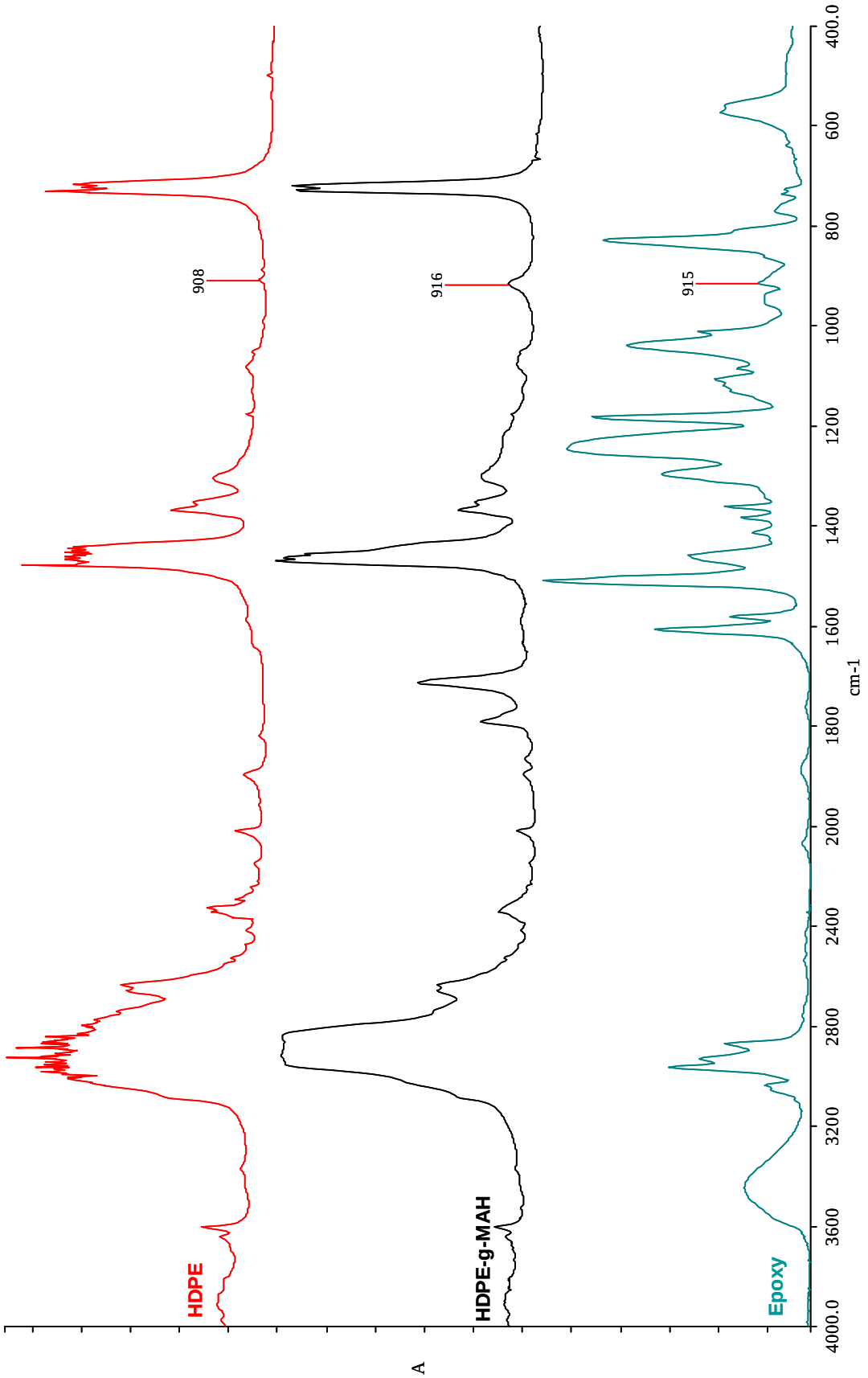
HDPE
HDPE-g-MAH
Epoxy
908
916
915
A
cm-1
4000.0
3600
3200
2800
2400
2000
1800
1600
1400
1200
1000
800
600
400.0

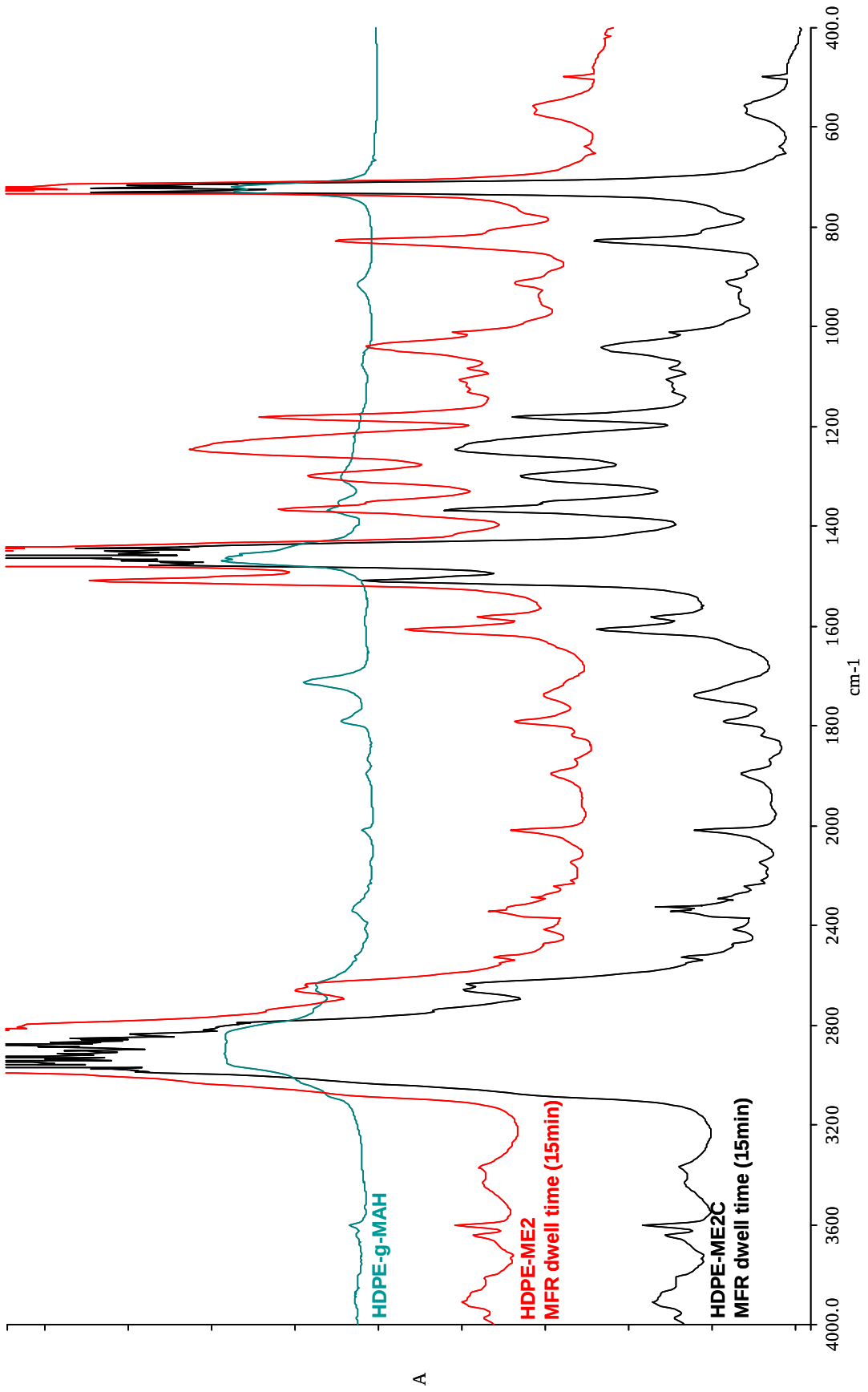
HDPE-g-MAH
HDPE-ME2
MFR dwell time (15min)
HDPE-ME2C
MFR dwell time (15min)
A
cm-1
4000.0
3600
3200
2800
2400
2000
1800
1600
1400
1200
1000
800
600
400.0

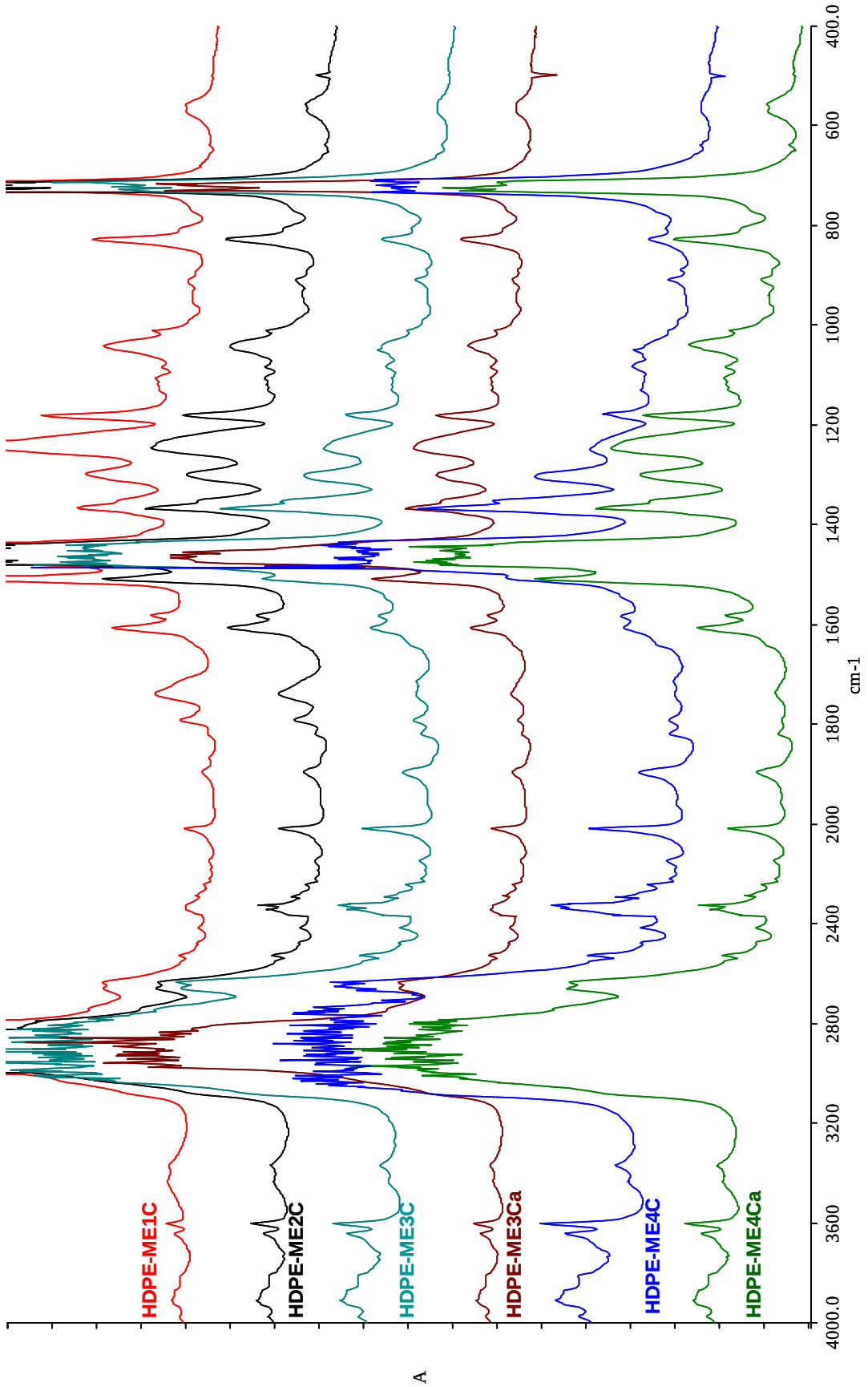
HDPE-ME1C
HDPE-ME2C
HDPE-ME3C
HDPE-ME3Ca
HDPE-ME4C
HDPE-ME4Ca
A
cm-1
4000.0
3600
3200
2800
2400
2000
1800
1600
1400
1200
1000
800
600
400.0

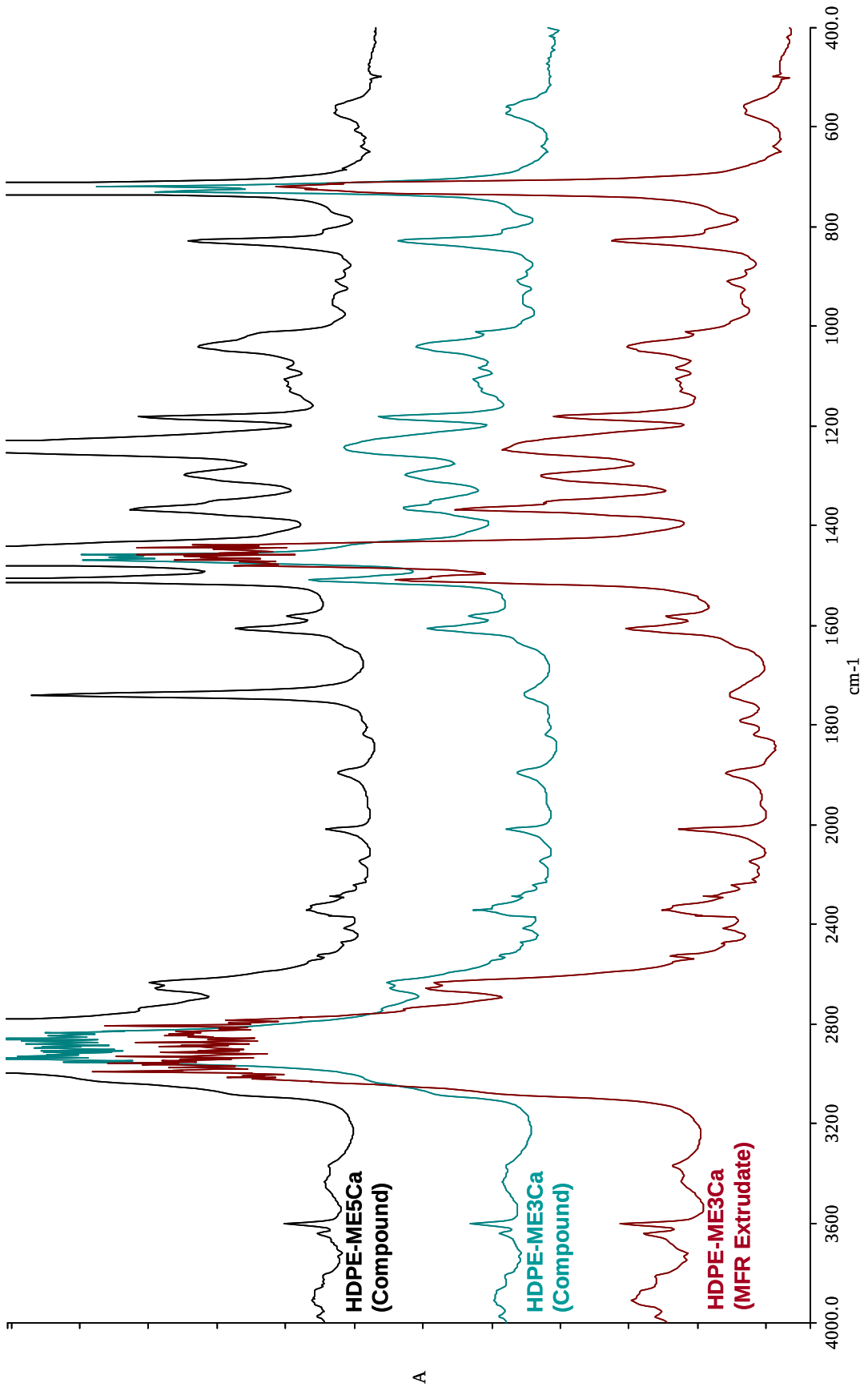
HDPE-ME5Ca
(Compound)
HDPE-ME3Ca
(Compound)
HDPE-ME3Ca
(MFR Extrudate)
A
cm-1
4000.0
3600
3200
2800
2400
2000
1800
1600
1400
1200
1000
800
600
400.0

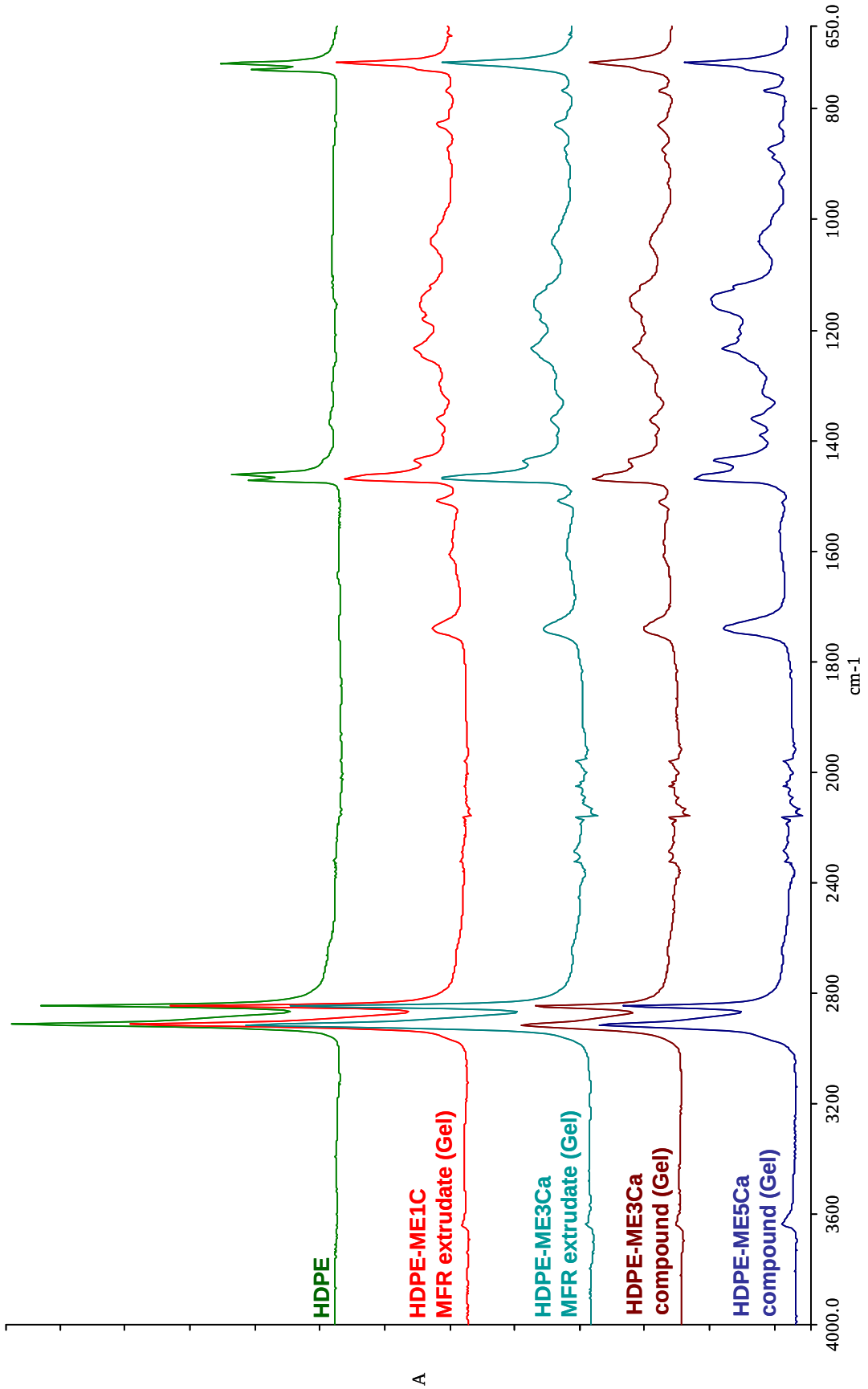
HDPE
HDPE-ME1C
MFR extrudate (Gel)
HDPE-ME3Ca
MFR extrudate (Gel)
HDPE-ME3Ca
compound (Gel)
HDPE-ME5Ca
compound (Gel)
A
4000.0
3600
3200
2800
2400
2000
1800
1600
1400
1200
1000
800
650.0
cm-1

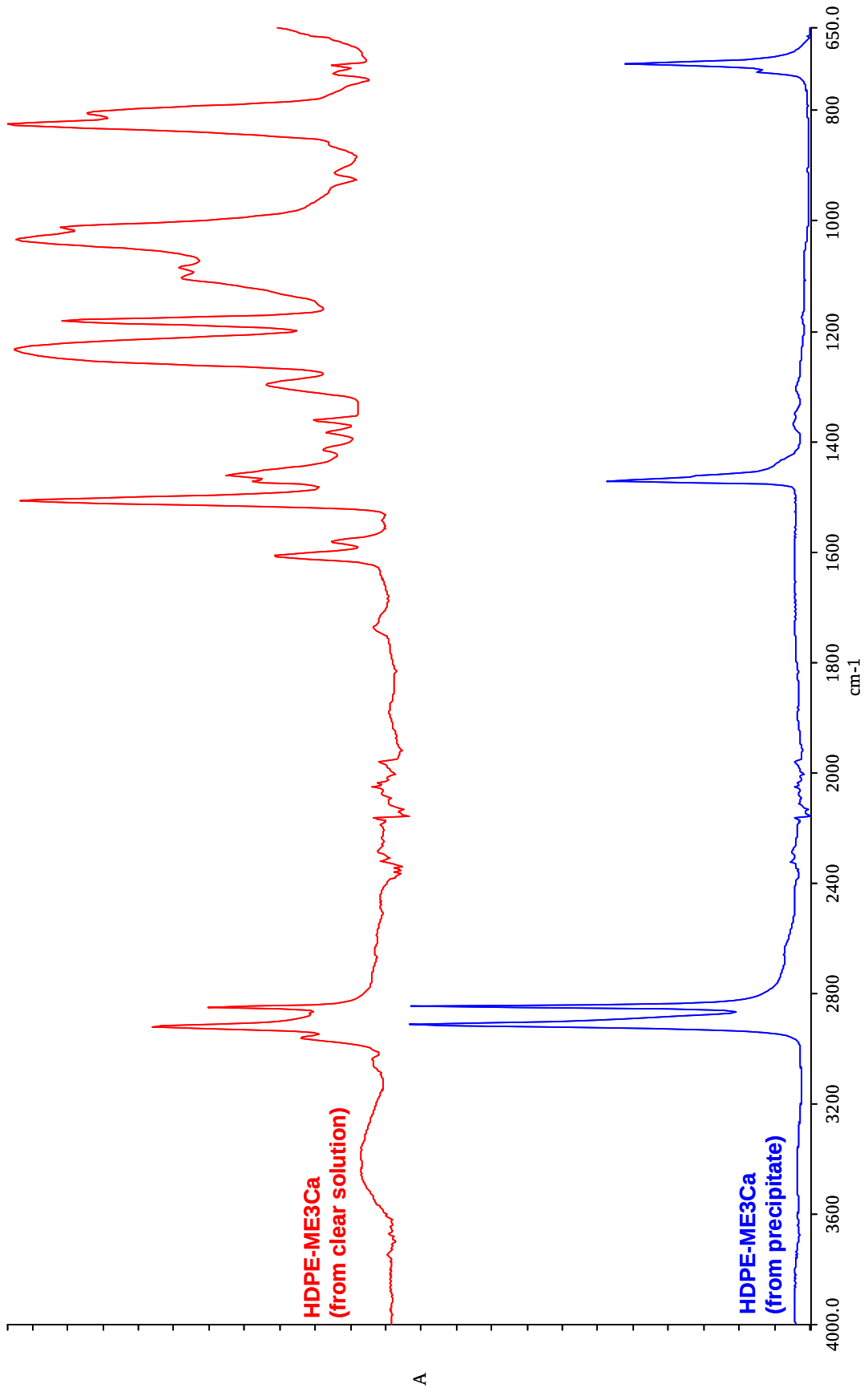
HDPE-ME3Ca
(from clear solution)
HDPE-ME3Ca
(from precipitate)
A
4000.0
3600
3200
2800
2400
2000
1800
1600
1400
1200
1000
800
650.0
cm-1

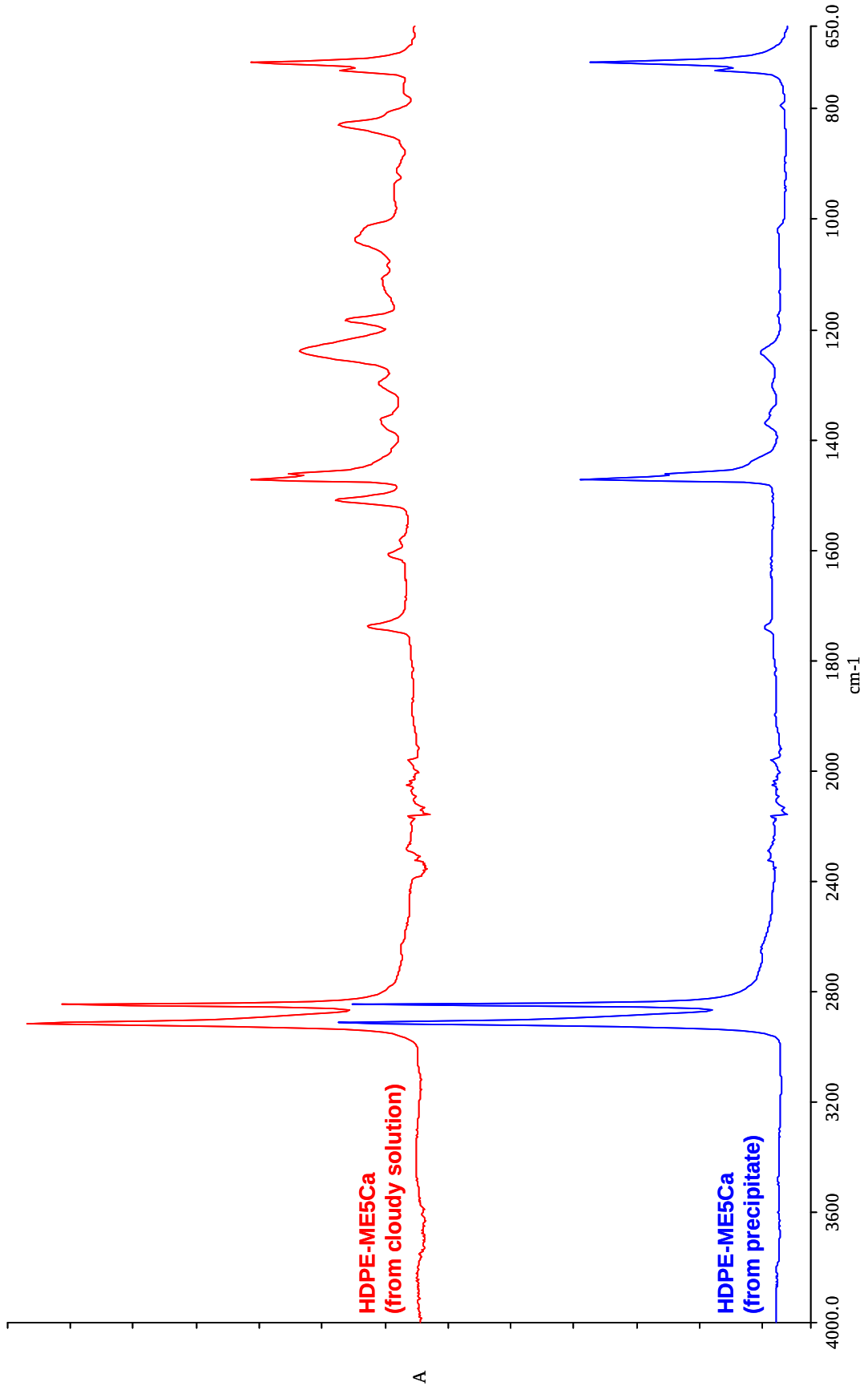
HDPE-ME5Ca
(from cloudy solution)
HDPE-ME5Ca
(from precipitate)
A
4000.0
3600
3200
2800
2400
2000
1800
1600
1400
1200
1000
800
650.0
cm-1

## *Determination of Gel Content*

| Sample ID | Weight (g) | | | | Gel Content (wt%) | Average (wt%) | Std. Dev. (wt%) |
|---|---|---|---|---|---|---|---|
| | W1 | W2 | W3 | W4 | | | |
| HDPE_S1 | 1.1327 | 1.4358 | 1.4662 | 1.1653 | **0.7** | **0.8** | **0.1** |
| HDPE_S2 | 1.0807 | 1.3832 | 1.4142 | 1.1143 | **0.9** | | |
| HDPE-ME1_S1 | 1.1853 | 1.4857 | 1.5166 | 1.2821 | **21.9** | **21.8** | **0.1** |
| HDPE-ME1_S2 | 1.1658 | 1.4664 | 1.4971 | 1.2617 | **21.7** | | |
| HDPE-ME1C_S1 | 1.0962 | 1.3975 | 1.4283 | 1.2053 | **26.0** | **26.2** | **0.2** |
| HDPE-ME1C_S2 | 1.1882 | 1.4865 | 1.5175 | 1.2978 | **26.3** | | |
| HDPE-ME2_S1 | 0.9133 | 1.2135 | 1.2444 | 0.9717 | **9.2** | **9.8** | **0.8** |
| HDPE-ME2_S2 | 1.0957 | 1.3974 | 1.4282 | 1.1575 | **10.3** | | |
| HDPE-ME2C_S1 | 0.9250 | 1.2253 | 1.2562 | 0.9948 | **13.0** | **12.9** | **0.2** |
| HDPE-ME2C_S2 | 1.0473 | 1.3470 | 1.3776 | 1.1159 | **12.7** | | |
| HDPE-ME3_S1 | 1.0161 | 1.3176 | 1.3486 | 1.0576 | **3.5** | **2.9** | **0.8** |
| HDPE-ME3_S2 | 0.9715 | 1.2744 | 1.3053 | 1.0095 | **2.3** | | |
| HDPE-ME3C_S1 | 1.1248 | 1.4238 | 1.4532 | 1.1665 | **4.1** | **4.3** | **0.3** |
| HDPE-ME3C_S2 | 1.2215 | 1.5233 | 1.5538 | 1.2657 | **4.5** | | |
| HDPE-ME3Ca_S1 | 1.6003 | 1.9007 | 1.9318 | 1.6459 | **4.8** | **5.1** | **0.4** |
| HDPE-ME3Ca_S2 | 1.4990 | 1.8003 | 1.8311 | 1.5457 | **5.3** | | |
| HDPE-ME3Ca (compounded)_S1 | 1.3782 | 1.6770 | 1.7076 | 1.4376 | **9.6** | **9.9** | **0.4** |
| HDPE-ME3Ca (compounded)_S2 | 1.2299 | 1.5286 | 1.5596 | 1.2914 | **10.2** | | |
| HDPE-ME4_S1 | 0.9252 | 1.2242 | 1.2550 | 0.9598 | **1.3** | **1.2** | **0.2** |
| HDPE-ME4_S2 | 1.0776 | 1.3790 | 1.4100 | 1.1117 | **1.0** | | |
| HDPE-ME4C_S1 | 0.9507 | 1.2505 | 1.2803 | 0.9853 | **1.6** | **1.7** | **0.1** |
| HDPE-ME4C_S2 | 0.9684 | 1.2686 | 1.2993 | 1.0041 | **1.7** | | |
| HDPE-ME4Ca_S1 | 0.9212 | 1.2232 | 1.2537 | 0.9591 | **2.5** | **2.6** | **0.1** |
| HDPE-ME4Ca_S2 | 1.4418 | 1.7424 | 1.7735 | 1.4807 | **2.6** | | |
| HDPE-ME5Ca (compounded)_S1 | 1.0231 | 1.3301 | 1.3609 | 1.0754 | **7.0** | **7.2** | **0.3** |
| HDPE-ME5Ca (compounded)_S2 | 1.1183 | 1.4167 | 1.4474 | 1.1710 | **7.4** | | |

Remarks: W1 = Weight of pouch

W2 = Weight of specimen + pouch

W3 = Weight of specimen + stapled shut cage

W4 = Weight of specimen + stapled shut cage after extraction & drying

Gel content = 100-(((W3-W4)/(W2-W1))*100)

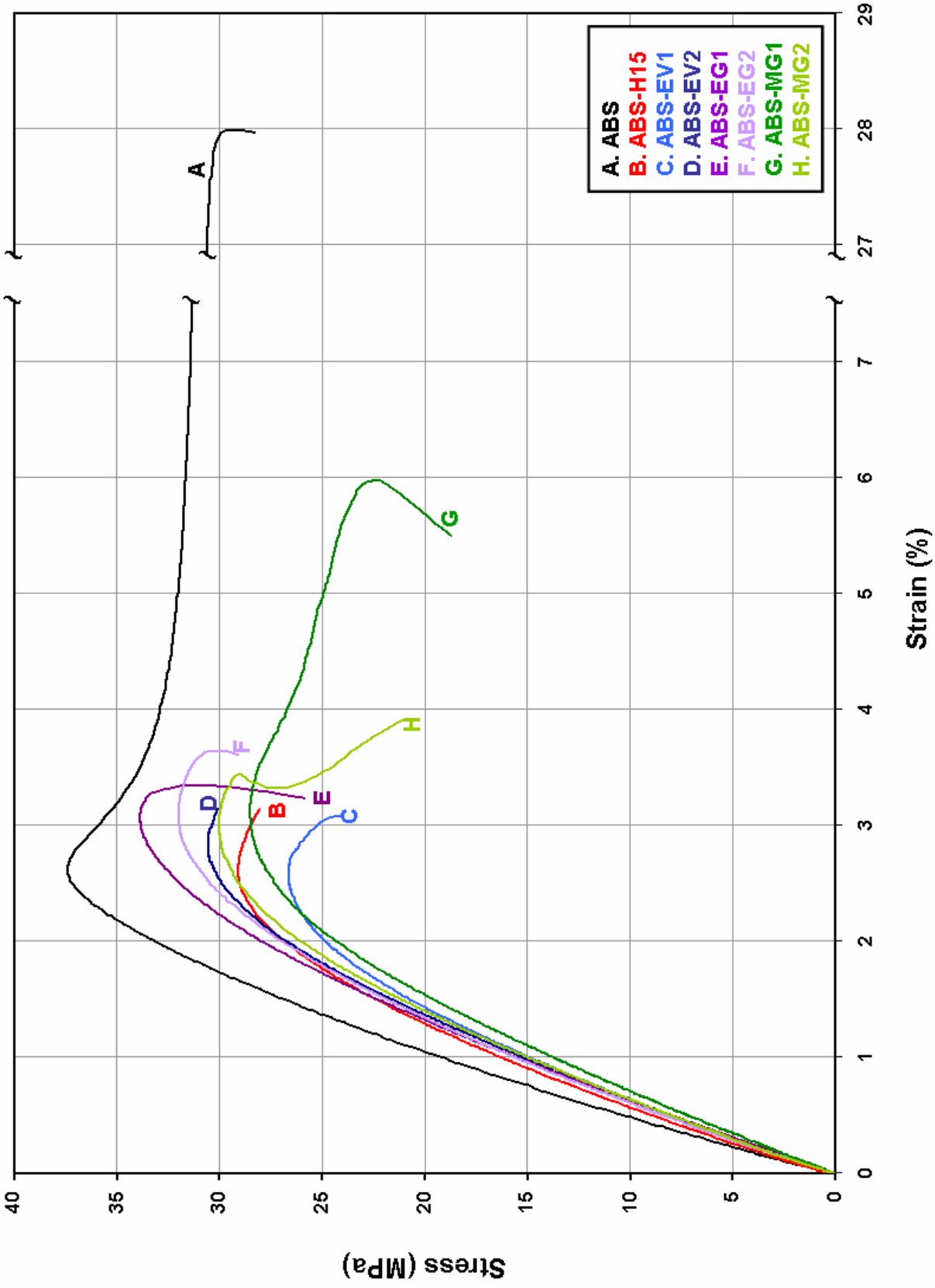
A. ABS
B. ABS-H15
C. ABS-EV1
D. ABS-EV2
E. ABS-EG1
F. ABS-EG2
G. ABS-MG1
H. ABS-MG2
Stress (MPa)
Strain (%)
0
5
10
15
20
25
30
35
40
0
1
2
3
4
5
6
7
27
28
29
A
B
C
D
E
F
G
H

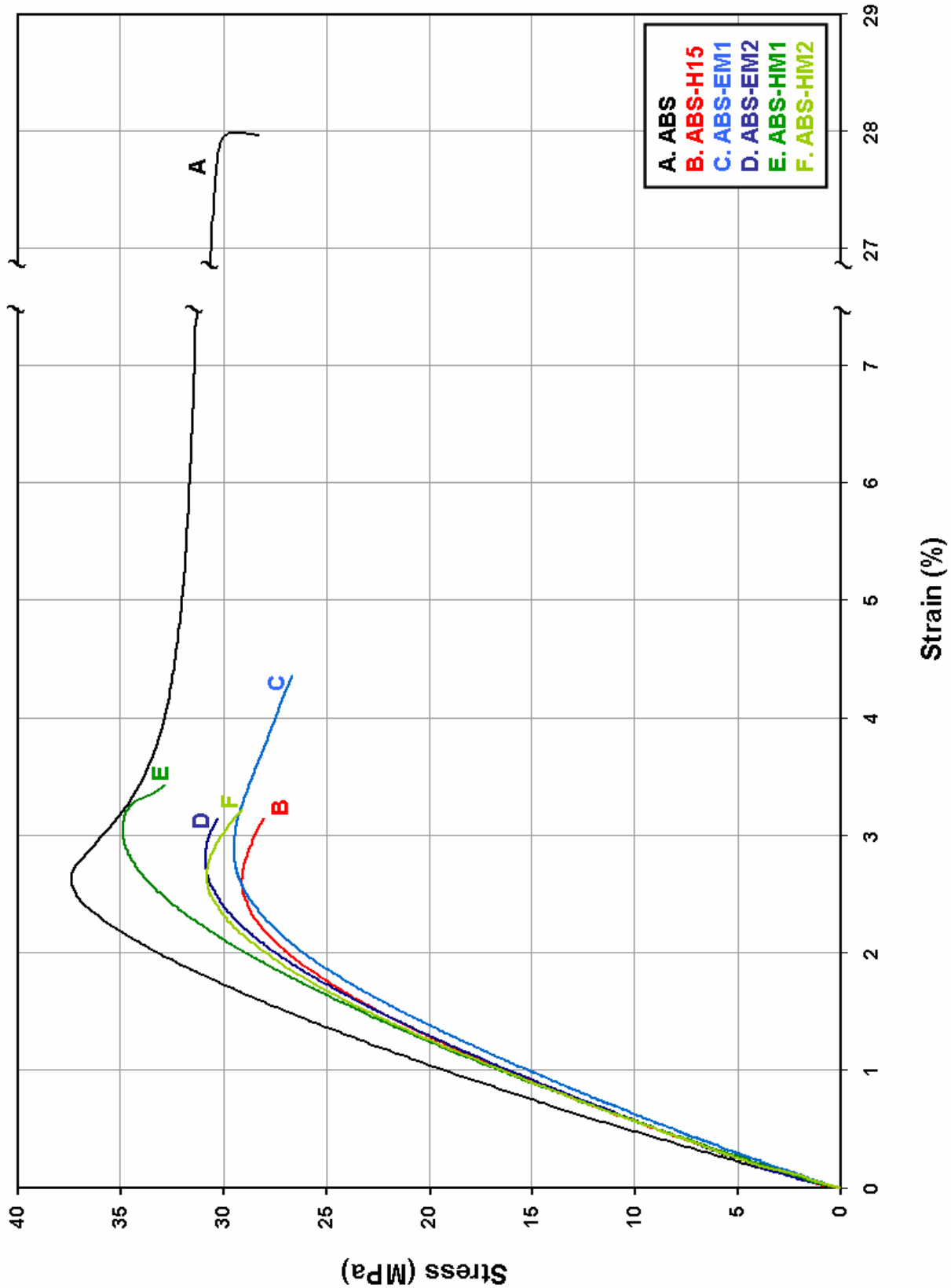
A. ABS
B. ABS-H15
C. ABS-EM1
D. ABS-EM2
E. ABS-HM1
F. ABS-HM2
A
B
C
D
E
F
Stress (MPa)
Strain (%)
0
5
10
15
20
25
30
35
40
0
1
2
3
4
5
6
7
27
28
29

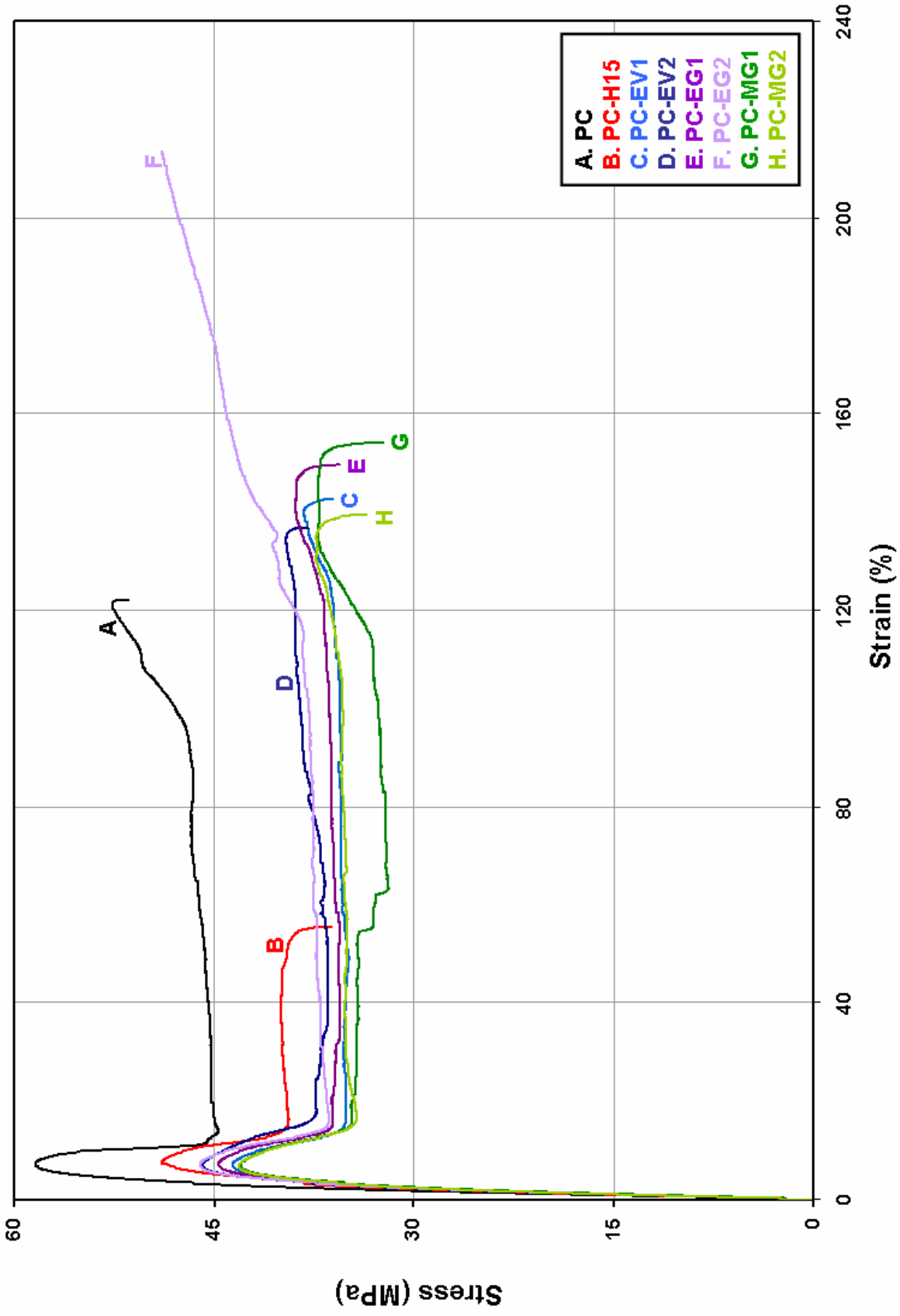
A. PC
B. PC-H15
C. PC-EV1
D. PC-EV2
E. PC-EG1
F. PC-EG2
G. PC-MG1
H. PC-MG2
Stress (MPa)
Strain (%)
0
15
30
45
60
0
40
80
120
160
200
240
A
B
C
D
E
F
G
H

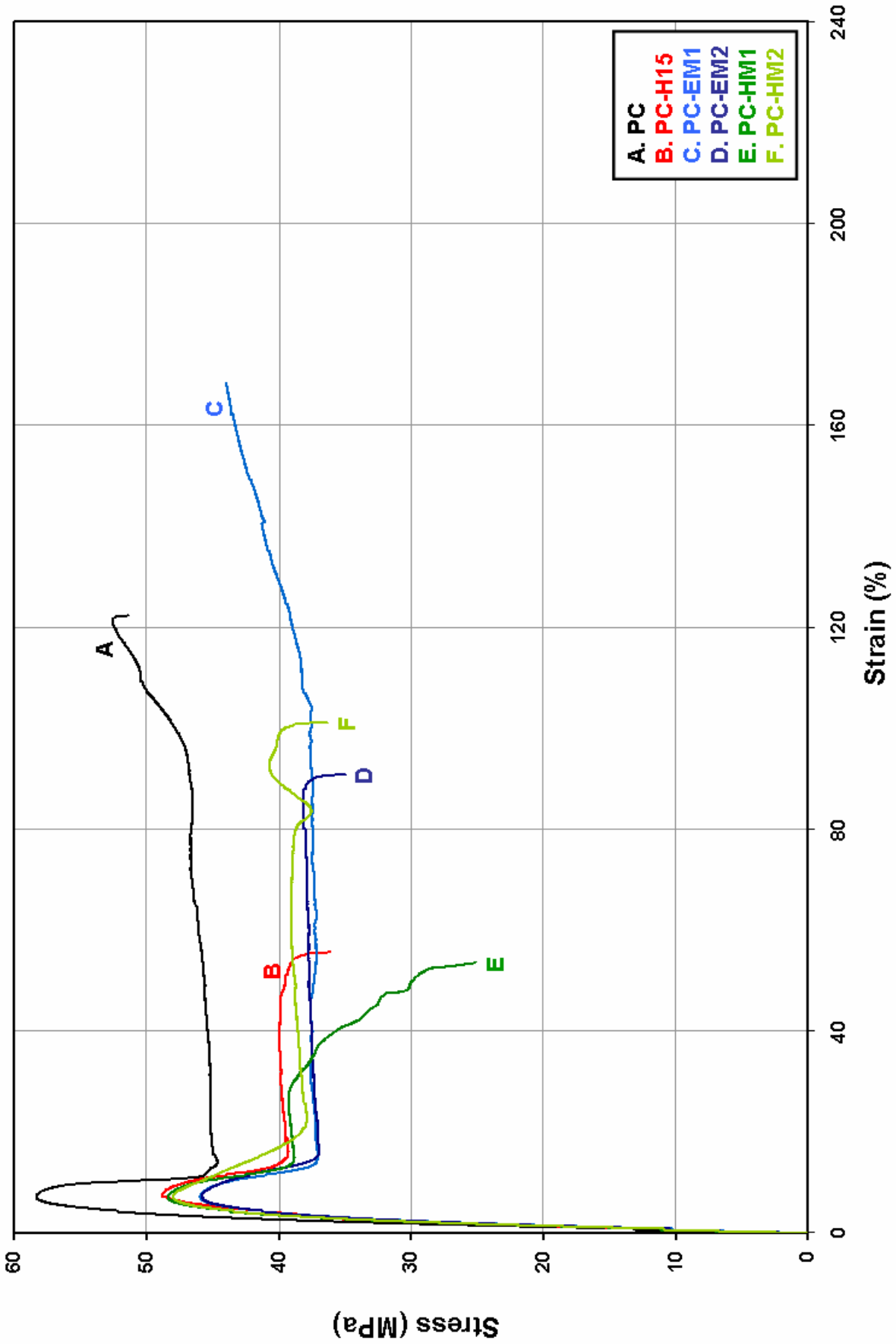
A. PC
B. PC-H15
C. PC-EM1
D. PC-EM2
E. PC-HM1
F. PC-HM2
A
B
C
D
E
F
Stress (MPa)
0
10
20
30
40
50
60
Strain (%)
0
40
80
120
160
200
240

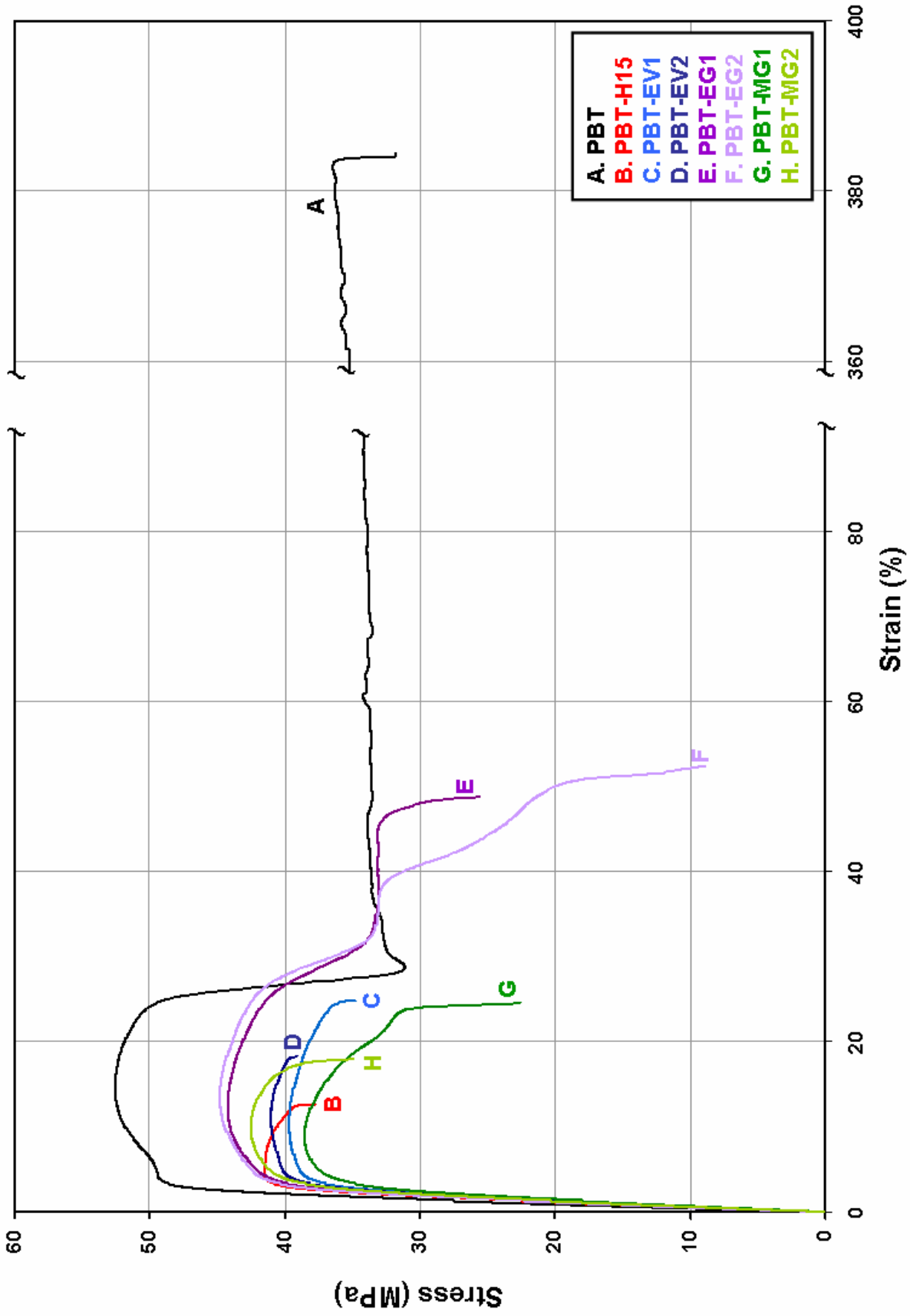
A. PBT
B. PBT-H15
C. PBT-EV1
D. PBT-EV2
E. PBT-EG1
F. PBT-EG2
G. PBT-MG1
H. PBT-MG2
A
B
C
D
E
F
G
H
Stress (MPa)
Strain (%)
0
10
20
30
40
50
60
0
20
40
60
80
360
380
400

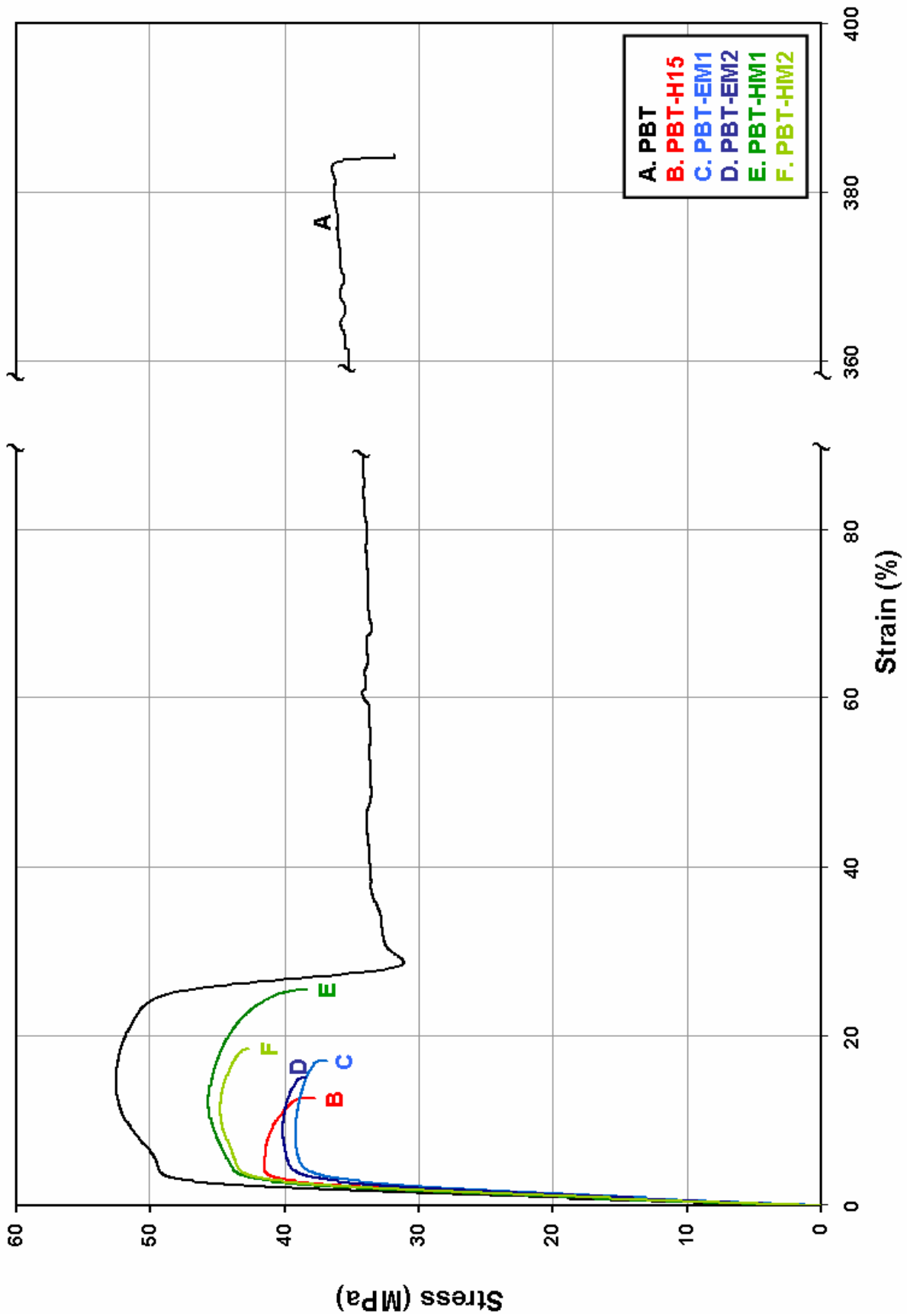
A. PBT
B. PBT-H15
C. PBT-EM1
D. PBT-EM2
E. PBT-HM1
F. PBT-HM2
A
B
C
D
E
F
Stress (MPa)
Strain (%)
0
10
20
30
40
50
60
0
20
40
60
80
360
380
400

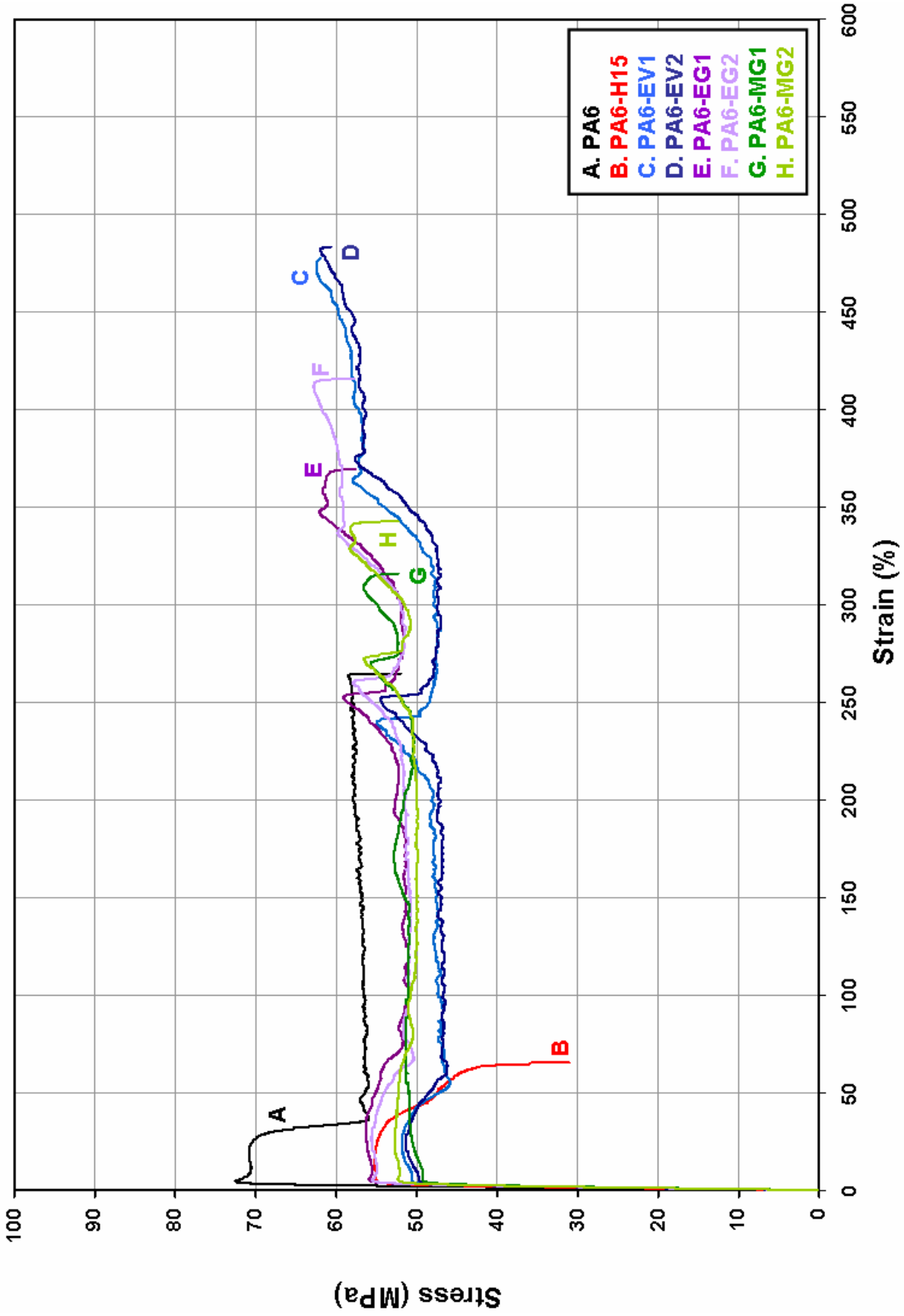
A. PA6
B. PA6-H15
C. PA6-EV1
D. PA6-EV2
E. PA6-EG1
F. PA6-EG2
G. PA6-MG1
H. PA6-MG2
A
B
C
D
E
F
G
H
Strain (%)
0
50
100
150
200
250
300
350
400
450
500
550
600
Stress (MPa)
0
10
20
30
40
50
60
70
80
90
100

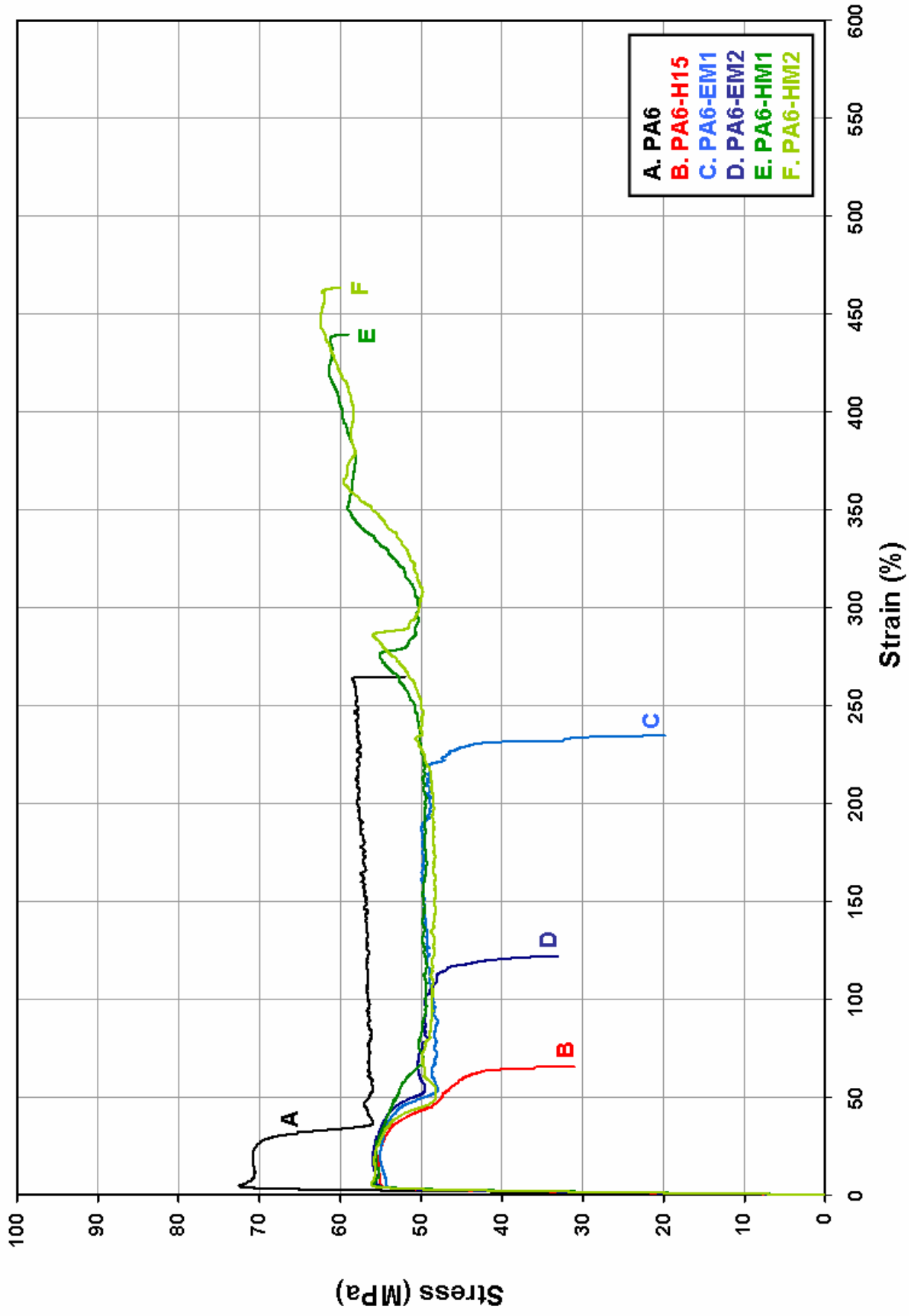
A. PA6
B. PA6-H15
C. PA6-EM1
D. PA6-EM2
E. PA6-HM1
F. PA6-HM2
A
B
C
D
E
F
Stress (MPa)
Strain (%)
0
10
20
30
40
50
60
70
80
90
100
0
50
100
150
200
250
300
350
400
450
500
550
600

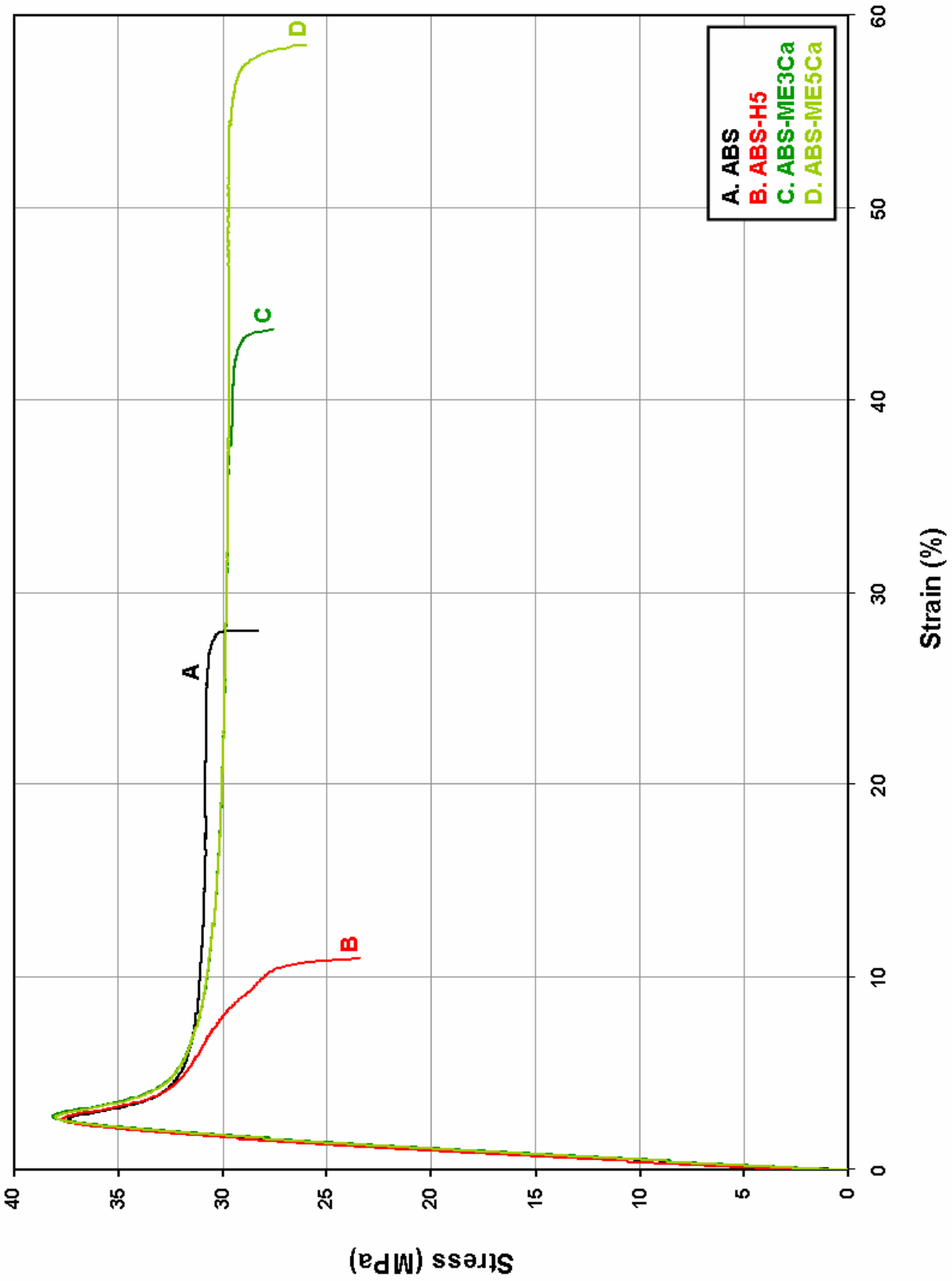
A. ABS
B. ABS-H5
C. ABS-ME3Ca
D. ABS-ME5Ca
A
B
C
D
Stress (MPa)
0
5
10
15
20
25
30
35
40
Strain (%)
0
10
20
30
40
50
60

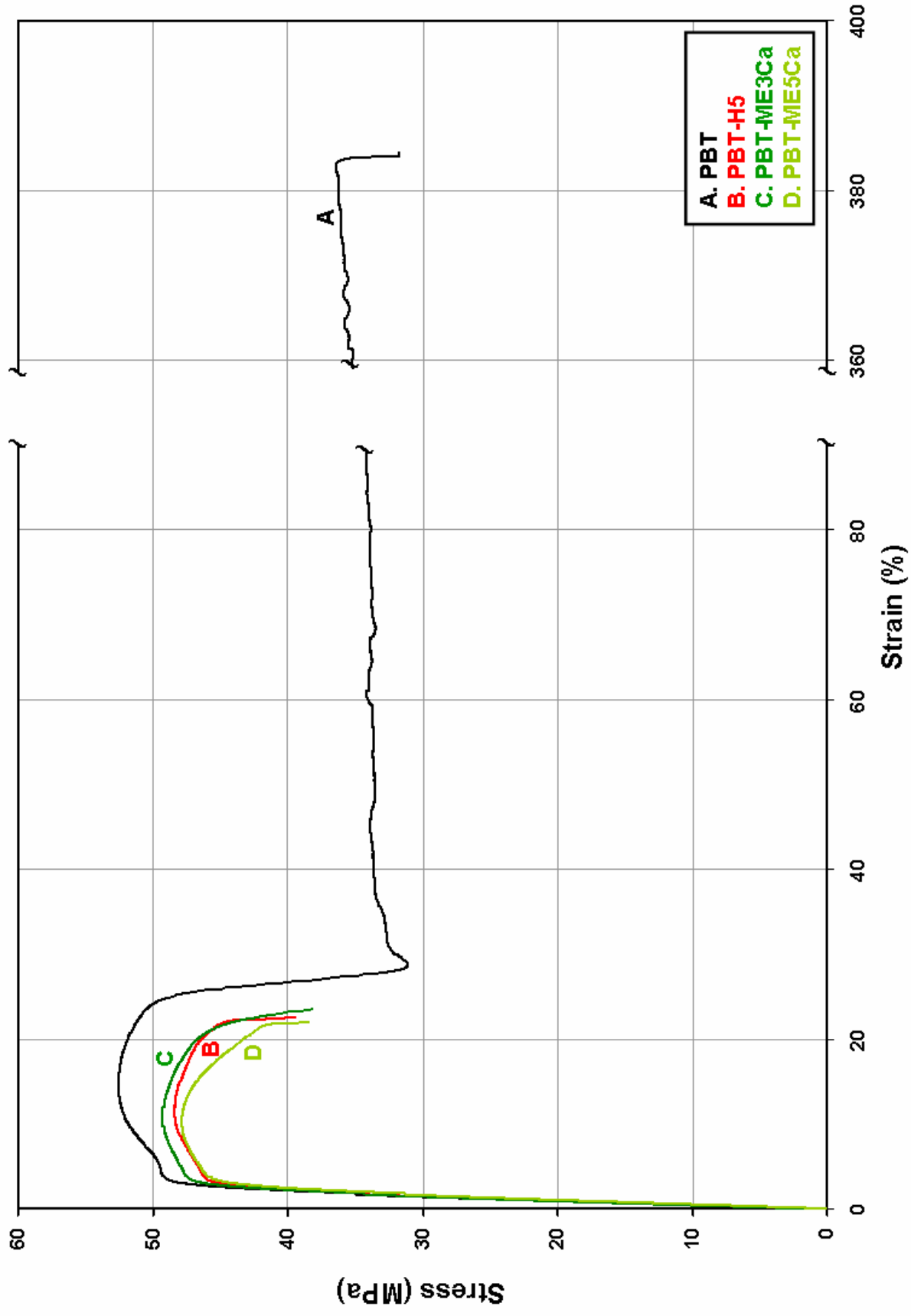
A. PBT
B. PBT-H5
C. PBT-ME3Ca
D. PBT-ME5Ca
A
B
C
D
Stress (MPa)
Strain (%)
0
10
20
30
40
50
60
0
20
40
60
80
360
380
400

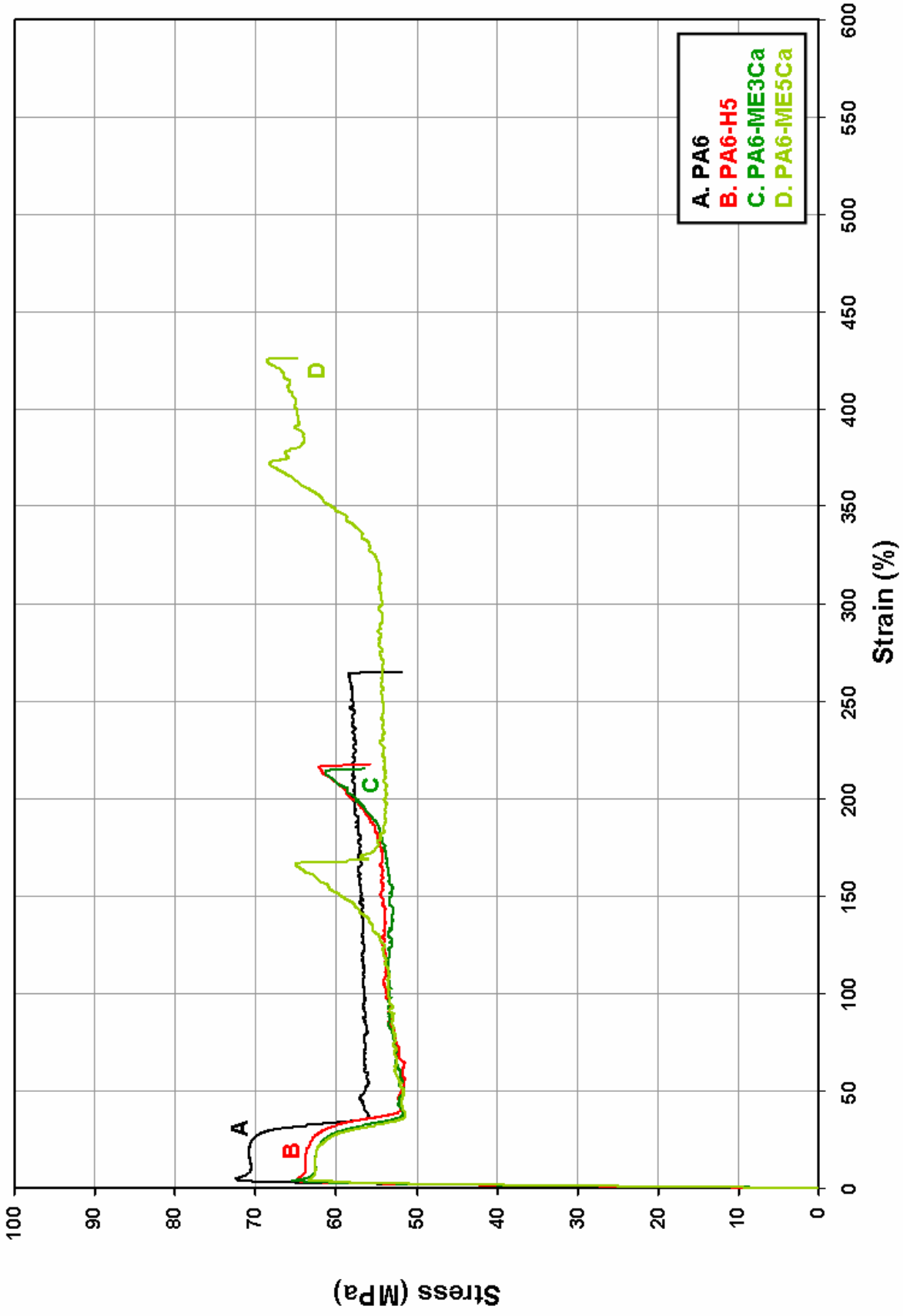
A. PA6
B. PA6-H5
C. PA6-ME3Ca
D. PA6-ME5Ca
A
B
C
D
Stress (MPa)
Strain (%)
0
10
20
30
40
50
60
70
80
90
100
0
50
100
150
200
250
300
350
400
450
500
550
600

**PBT (NOTCHED)**

| **Energy of Hammer:** 1.0 J | **Specimen Width:** 12.60 mm | **Specimen Thickness:** 3.32 mm | |
|---|---|---|---|
| **Specimen No.** | **Absorbed Energy (J)** | **Impact Strength (J/m)** | **Type of Failure*** |
| 1 | 0.089 | 27 | CB |
| 2 | 0.086 | 26 | CB |
| 3 | 0.094 | 28 | CB |
| 4 | 0.100 | 30 | CB |
| 5 | 0.094 | 28 | CB |
| 6 | 0.089 | 27 | CB |
| 7 | 0.102 | 31 | CB |
| 8 | 0.104 | 31 | CB |
| 9 | 0.099 | 30 | CB |
| 10 | 0.114 | 34 | CB |
| 11 | 0.104 | 31 | CB |
| 12 | 0.098 | 30 | CB |
| 13 | 0.088 | 27 | CB |
| 14 | 0.095 | 29 | CB |
| 15 | 0.105 | 32 | CB |
| 16 | 0.102 | 31 | CB |
| 17 | 0.103 | 31 | CB |
| 18 | 0.096 | 29 | CB |
| 19 | 0.092 | 28 | CB |
| 20 | 0.096 | 29 | CB |
| 21 | 0.084 | 25 | CB |
| **Ave** | **0.097** | **29** | **-** |
| **SD** | **0.007** | **2** | **-** |

**PBT (REVERSED NOTCH)**

| **Energy of Hammer:** 7.5 J | **Specimen Width:** 12.60 mm | **Specimen Thickness:** 3.30 mm | |
|---|---|---|---|
| **Specimen No.** | **Absorbed Energy (J)** | **Impact Strength (J/m)** | **Type of Failure*** |
| 1 | 3.277 | 993 | CB |
| 2 | 3.865 | 1171 | CB |
| 3 | 3.125 | 947 | CB |
| 4 | 3.167 | 960 | CB |
| 5 | 2.944 | 892 | CB |
| 6 | 2.864 | 868 | CB |
| 7 | 3.829 | 1160 | CB |
| 8 | 3.470 | 1052 | CB |
| 9 | 4.248 | 1287 | CB |
| 10 | 3.675 | 1114 | CB |
| 11 | 4.111 | 1246 | CB |
| 12 | 4.215 | 1277 | CB |
| 13 | 3.825 | 1159 | CB |
| 14 | 3.442 | 1043 | CB |
| 15 | 2.965 | 898 | CB |
| 16 | 3.868 | 1172 | CB |
| 17 | 3.245 | 983 | CB |
| 18 | 3.606 | 1093 | CB |
| 19 | 3.387 | 1026 | CB |
| 20 | 3.288 | 996 | CB |
| 21 | 3.009 | 912 | CB |
| **Ave** | **3.496** | **1060** | **-** |
| **SD** | **0.426** | **129** | **-** |

*The abbreviation, CB, denotes Complete Break

**PBT-H15 (NOTCHED)**

| **Energy of Hammer:** 1.0 J | **Specimen Width:** 12.53 mm | **Specimen Thickness:** 3.29 mm | |
|---|---|---|---|
| **Specimen No.** | **Absorbed Energy (J)** | **Impact Strength (J/m)** | **Type of Failure*** |
| 1 | 0.074 | 22 | CB |
| 2 | 0.082 | 25 | CB |
| 3 | 0.081 | 25 | CB |
| 4 | 0.077 | 23 | CB |
| 5 | 0.078 | 24 | CB |
| 6 | 0.077 | 23 | CB |
| 7 | 0.081 | 25 | CB |
| 8 | 0.082 | 25 | CB |
| 9 | 0.084 | 26 | CB |
| 10 | 0.079 | 24 | CB |
| 11 | 0.085 | 26 | CB |
| 12 | 0.086 | 26 | CB |
| 13 | 0.082 | 25 | CB |
| 14 | 0.087 | 26 | CB |
| 15 | 0.080 | 24 | CB |
| 16 | 0.090 | 27 | CB |
| 17 | 0.083 | 25 | CB |
| 18 | 0.072 | 22 | CB |
| 19 | 0.092 | 28 | CB |
| 20 | 0.083 | 25 | CB |
| 21 | 0.094 | 29 | CB |
| **Ave** | **0.082** | **25** | **-** |
| **SD** | **0.006** | **2** | **-** |

**PBT-H15 (REVERSED NOTCH)**

| **Energy of Hammer:** 2.0 J | **Specimen Width:** 12.50 mm | **Specimen Thickness:** 3.30 mm | |
|---|---|---|---|
| **Specimen No.** | **Absorbed Energy (J)** | **Impact Strength (J/m)** | **Type of Failure*** |
| 1 | 1.321 | 400 | CB |
| 2 | 1.353 | 410 | CB |
| 3 | 1.209 | 366 | CB |
| 4 | 1.549 | 469 | CB |
| 5 | 1.328 | 402 | CB |
| 6 | 1.271 | 385 | CB |
| 7 | 1.165 | 353 | CB |
| 8 | 1.259 | 382 | CB |
| 9 | 1.355 | 411 | CB |
| 10 | 1.241 | 376 | CB |
| 11 | 1.341 | 406 | CB |
| 12 | 1.244 | 377 | CB |
| 13 | 1.253 | 380 | CB |
| 14 | 1.259 | 382 | CB |
| 15 | 1.377 | 417 | CB |
| 16 | 1.353 | 410 | CB |
| 17 | 1.360 | 412 | CB |
| 18 | 1.322 | 401 | CB |
| 19 | 1.291 | 391 | CB |
| 20 | 1.275 | 386 | CB |
| 21 | 1.340 | 406 | CB |
| **Ave** | **1.308** | **396** | **-** |
| **SD** | **0.079** | **24** | **-** |

*The abbreviation, CB, denotes Complete Break

**PBT-EV1 (NOTCHED)**

| **Energy of Hammer:** 1.0 J | **Specimen Width:** 12.52 mm | **Specimen Thickness:** 3.26 mm | |
|---|---|---|---|
| **Specimen No.** | **Absorbed Energy (J)** | **Impact Strength (J/m)** | **Type of Failure*** |
| 1 | 0.124 | 38 | CB |
| 2 | 0.133 | 41 | CB |
| 3 | 0.156 | 48 | CB |
| 4 | 0.110 | 34 | CB |
| 5 | 0.129 | 40 | CB |
| 6 | 0.120 | 37 | CB |
| 7 | 0.134 | 41 | CB |
| 8 | 0.131 | 40 | CB |
| 9 | 0.122 | 37 | CB |
| 10 | 0.125 | 38 | CB |
| 11 | 0.116 | 36 | CB |
| 12 | 0.149 | 46 | CB |
| 13 | 0.130 | 40 | CB |
| 14 | 0.129 | 40 | CB |
| 15 | 0.133 | 41 | CB |
| 16 | 0.134 | 41 | CB |
| 17 | 0.129 | 40 | CB |
| 18 | 0.127 | 39 | CB |
| 19 | 0.126 | 39 | CB |
| 20 | 0.119 | 37 | CB |
| 21 | 0.118 | 36 | CB |
| **Ave** | **0.128** | **39** | **-** |
| **SD** | **0.010** | **3** | **-** |

**PBT-EV1 (REVERSED NOTCH)**

| **Energy of Hammer:** 4.0 J | **Specimen Width:** 12.52 mm | **Specimen Thickness:** 3.28 mm | |
|---|---|---|---|
| **Specimen No.** | **Absorbed Energy (J)** | **Impact Strength (J/m)** | **Type of Failure*** |
| 1 | 2.471 | 753 | CB |
| 2 | 2.430 | 741 | CB |
| 3 | 2.483 | 757 | CB |
| 4 | 2.374 | 724 | CB |
| 5 | 2.512 | 766 | CB |
| 6 | 2.583 | 788 | CB |
| 7 | 2.510 | 765 | CB |
| 8 | 2.415 | 736 | CB |
| 9 | 2.366 | 721 | CB |
| 10 | 2.581 | 787 | CB |
| 11 | 2.539 | 774 | CB |
| 12 | 2.496 | 761 | CB |
| 13 | 2.471 | 753 | CB |
| 14 | 2.521 | 769 | CB |
| 15 | 2.502 | 763 | CB |
| 16 | 2.498 | 762 | CB |
| 17 | 2.521 | 769 | CB |
| 18 | 2.544 | 776 | CB |
| 19 | 2.539 | 774 | CB |
| 20 | 2.624 | 800 | CB |
| 21 | 2.469 | 753 | CB |
| **Ave** | **2.498** | **761** | **-** |
| **SD** | **0.065** | **20** | **-** |

*The abbreviation, CB, denotes Complete Break

**PBT-EM1 (NOTCHED)**

| **Energy of Hammer:** 1.0 J | **Specimen Width:** 12.53 mm | **Specimen Thickness:** 3.28 mm | |
|---|---|---|---|
| **Specimen No.** | **Absorbed Energy (J)** | **Impact Strength (J/m)** | **Type of Failure*** |
| 1 | 0.098 | 30 | CB |
| 2 | 0.094 | 29 | CB |
| 3 | 0.104 | 32 | CB |
| 4 | 0.102 | 31 | CB |
| 5 | 0.105 | 32 | CB |
| 6 | 0.096 | 29 | CB |
| 7 | 0.101 | 31 | CB |
| 8 | 0.104 | 32 | CB |
| 9 | 0.096 | 29 | CB |
| 10 | 0.110 | 34 | CB |
| 11 | 0.101 | 31 | CB |
| 12 | 0.105 | 32 | CB |
| 13 | 0.115 | 35 | CB |
| 14 | 0.104 | 32 | CB |
| 15 | 0.101 | 31 | CB |
| 16 | 0.094 | 29 | CB |
| 17 | 0.098 | 30 | CB |
| 18 | 0.109 | 33 | CB |
| 19 | 0.106 | 32 | CB |
| 20 | 0.104 | 32 | CB |
| 21 | 0.114 | 35 | CB |
| **Ave** | **0.103** | **31** | **-** |
| **SD** | **0.006** | **2** | **-** |

**PBT-EM1 (REVERSED NOTCH)**

| **Energy of Hammer:** 4.0 J | **Specimen Width:** 12.50 mm | **Specimen Thickness:** 3.28 mm | |
|---|---|---|---|
| **Specimen No.** | **Absorbed Energy (J)** | **Impact Strength (J/m)** | **Type of Failure*** |
| 1 | 2.222 | 677 | CB |
| 2 | 2.315 | 706 | CB |
| 3 | 2.022 | 616 | CB |
| 4 | 2.355 | 718 | CB |
| 5 | 2.534 | 773 | CB |
| 6 | 2.585 | 788 | CB |
| 7 | 2.366 | 721 | CB |
| 8 | 2.465 | 752 | CB |
| 9 | 2.295 | 700 | CB |
| 10 | 2.481 | 756 | CB |
| 11 | 2.532 | 772 | CB |
| 12 | 2.482 | 757 | CB |
| 13 | 2.543 | 775 | CB |
| 14 | 2.286 | 697 | CB |
| 15 | 2.465 | 752 | CB |
| 16 | 2.455 | 748 | CB |
| 17 | 2.267 | 691 | CB |
| 18 | 2.305 | 703 | CB |
| 19 | 2.436 | 743 | CB |
| 20 | 2.423 | 739 | CB |
| 21 | 2.330 | 710 | CB |
| **Ave** | **2.389** | **728** | **-** |
| **SD** | **0.133** | **41** | **-** |

*The abbreviation, CB, denotes Complete Break

**PBT-EG1 (NOTCHED)**

| **Energy of Hammer:** 1.0 J | **Specimen Width:** 12.52 mm | **Specimen Thickness:** 3.30 mm | |
|---|---|---|---|
| **Specimen No.** | **Absorbed Energy (J)** | **Impact Strength (J/m)** | **Type of Failure*** |
| 1 | 0.207 | 63 | CB |
| 2 | 0.210 | 64 | CB |
| 3 | 0.197 | 60 | CB |
| 4 | 0.203 | 62 | CB |
| 5 | 0.211 | 64 | CB |
| 6 | 0.210 | 64 | CB |
| 7 | 0.182 | 55 | CB |
| 8 | 0.193 | 58 | CB |
| 9 | 0.190 | 58 | CB |
| 10 | 0.211 | 64 | CB |
| 11 | 0.210 | 64 | CB |
| 12 | 0.206 | 62 | CB |
| 13 | 0.205 | 62 | CB |
| 14 | 0.210 | 64 | CB |
| 15 | 0.210 | 64 | CB |
| 16 | 0.215 | 65 | CB |
| 17 | 0.199 | 60 | CB |
| 18 | 0.210 | 64 | CB |
| 19 | 0.208 | 63 | CB |
| 20 | 0.195 | 59 | CB |
| 21 | 0.197 | 60 | CB |
| **Ave** | **0.204** | **62** | **-** |
| **SD** | **0.009** | **3** | **-** |

**PBT-EG1 (REVERSED NOTCH)**

| **Energy of Hammer:** 5.5 J | **Specimen Width:** 12.52 mm | **Specimen Thickness:** 3.28 mm | |
|---|---|---|---|
| **Specimen No.** | **Absorbed Energy (J)** | **Impact Strength (J/m)** | **Type of Failure*** |
| 1 | 4.522 | 1379 | CB |
| 2 | 4.453 | 1358 | CB |
| 3 | 4.258 | 1298 | CB |
| 4 | 4.401 | 1342 | CB |
| 5 | 4.507 | 1374 | CB |
| 6 | 4.295 | 1309 | CB |
| 7 | 4.410 | 1345 | CB |
| 8 | 4.520 | 1378 | CB |
| 9 | 4.425 | 1349 | CB |
| 10 | 4.341 | 1323 | CB |
| 11 | 4.345 | 1325 | CB |
| 12 | 4.385 | 1337 | CB |
| 13 | 4.417 | 1347 | CB |
| 14 | 4.405 | 1343 | CB |
| 15 | 4.324 | 1318 | CB |
| 16 | 4.452 | 1357 | CB |
| 17 | 4.324 | 1318 | CB |
| 18 | 4.229 | 1289 | CB |
| 19 | 4.414 | 1346 | CB |
| 20 | 4.417 | 1347 | CB |
| 21 | 4.396 | 1340 | CB |
| **Ave** | **4.392** | **1339** | **-** |
| **SD** | **0.079** | **24** | **-** |

*The abbreviation, CB, denotes Complete Break

**PBT-MG1 (NOTCHED)**

| **Energy of Hammer:** 1.0 J | **Specimen Width:** 12.52 mm | **Specimen Thickness:** 3.25 mm |
|---|---|---|

| Specimen No. | Absorbed Energy (J) | Impact Strength (J/m) | Type of Failure* |
|---|---|---|---|
| 1 | 0.245 | 75 | CB |
| 2 | 0.255 | 78 | CB |
| 3 | 0.261 | 80 | CB |
| 4 | 0.241 | 74 | CB |
| 5 | 0.272 | 84 | CB |
| 6 | 0.256 | 79 | CB |
| 7 | 0.261 | 80 | CB |
| 8 | 0.240 | 74 | CB |
| 9 | 0.244 | 75 | CB |
| 10 | 0.238 | 73 | CB |
| 11 | 0.240 | 74 | CB |
| 12 | 0.252 | 78 | CB |
| 13 | 0.270 | 83 | CB |
| 14 | 0.261 | 80 | CB |
| 15 | 0.277 | 85 | CB |
| 16 | 0.247 | 76 | CB |
| 17 | 0.265 | 82 | CB |
| 18 | 0.252 | 78 | CB |
| 19 | 0.263 | 81 | CB |
| 20 | 0.267 | 82 | CB |
| 21 | 0.276 | 85 | CB |
| **Ave** | **0.256** | **79** | **-** |
| **SD** | **0.012** | **4** | **-** |

**PBT-MG1 (REVERSED NOTCH)**

| **Energy of Hammer:** 5.5 J | **Specimen Width:** 12.51 mm | **Specimen Thickness:** 3.26 mm |
|---|---|---|

| Specimen No. | Absorbed Energy (J) | Impact Strength (J/m) | Type of Failure* |
|---|---|---|---|
| 1 | 4.044 | 1240 | CB |
| 2 | 4.165 | 1278 | CB |
| 3 | 4.124 | 1265 | CB |
| 4 | 4.462 | 1369 | CB |
| 5 | 4.480 | 1374 | CB |
| 6 | 4.500 | 1380 | CB |
| 7 | 4.385 | 1345 | CB |
| 8 | 4.484 | 1375 | CB |
| 9 | 4.625 | 1419 | CB |
| 10 | 4.500 | 1380 | CB |
| 11 | 4.623 | 1418 | CB |
| 12 | 4.081 | 1252 | CB |
| 13 | 4.420 | 1356 | CB |
| 14 | 4.272 | 1310 | CB |
| 15 | 4.522 | 1387 | CB |
| 16 | 4.470 | 1371 | CB |
| 17 | 4.270 | 1310 | CB |
| 18 | 4.454 | 1366 | CB |
| 19 | 4.334 | 1329 | CB |
| 20 | 4.522 | 1387 | CB |
| 21 | 4.322 | 1326 | CB |
| **Ave** | **4.384** | **1345** | **-** |
| **SD** | **0.169** | **52** | **-** |

*The abbreviation, CB, denotes Complete Break

**PBT-HM1 (NOTCHED)**

| **Energy of Hammer:** 1.0 J | **Specimen Width:** 12.52 mm | **Specimen Thickness:** 3.31 mm | |
|---|---|---|---|
| **Specimen No.** | **Absorbed Energy (J)** | **Impact Strength (J/m)** | **Type of Failure*** |
| 1 | 0.095 | 29 | CB |
| 2 | 0.104 | 31 | CB |
| 3 | 0.115 | 35 | CB |
| 4 | 0.110 | 33 | CB |
| 5 | 0.105 | 32 | CB |
| 6 | 0.111 | 34 | CB |
| 7 | 0.109 | 33 | CB |
| 8 | 0.104 | 31 | CB |
| 9 | 0.104 | 31 | CB |
| 10 | 0.108 | 33 | CB |
| 11 | 0.102 | 31 | CB |
| 12 | 0.110 | 33 | CB |
| 13 | 0.108 | 33 | CB |
| 14 | 0.108 | 33 | CB |
| 15 | 0.101 | 31 | CB |
| 16 | 0.104 | 31 | CB |
| 17 | 0.107 | 32 | CB |
| 18 | 0.108 | 33 | CB |
| 19 | 0.108 | 33 | CB |
| 20 | 0.112 | 34 | CB |
| 21 | 0.117 | 35 | CB |
| **Ave** | **0.107** | **32** | **-** |
| **SD** | **0.005** | **1** | **-** |

**PBT-HM1 (REVERSED NOTCH)**

| **Energy of Hammer:** 1.0 J | **Specimen Width:** 12.52 mm | **Specimen Thickness:** 3.31 mm | |
|---|---|---|---|
| **Specimen No.** | **Absorbed Energy (J)** | **Impact Strength (J/m)** | **Type of Failure*** |
| 1 | 3.050 | 921 | CB |
| 2 | 2.961 | 895 | CB |
| 3 | 2.874 | 868 | CB |
| 4 | 2.889 | 873 | CB |
| 5 | 2.991 | 904 | CB |
| 6 | 2.990 | 903 | CB |
| 7 | 2.917 | 881 | CB |
| 8 | 2.777 | 839 | CB |
| 9 | 3.021 | 913 | CB |
| 10 | 2.778 | 839 | CB |
| 11 | 3.004 | 908 | CB |
| 12 | 2.838 | 857 | CB |
| 13 | 2.666 | 805 | CB |
| 14 | 2.811 | 849 | CB |
| 15 | 2.814 | 850 | CB |
| 16 | 2.834 | 856 | CB |
| 17 | 2.794 | 844 | CB |
| 18 | 2.864 | 865 | CB |
| 19 | 2.857 | 863 | CB |
| 20 | 2.807 | 848 | CB |
| 21 | 2.747 | 830 | CB |
| **Ave** | **2.871** | **867** | **-** |
| **SD** | **0.101** | **31** | **-** |

*The abbreviation, CB, denotes Complete Break

**HDPE-ME1**

| Test No. | 5 mins Dwell Time (190℃ / 2.16kg) | | | 15 mins Dwell Time (190℃ / 2.16kg) | | |
|---|---|---|---|---|---|---|
| | Weight of Extrudate (g) | Cut-off Time-interval (s) | MFR (g/10min) | Weight of Extrudate (g) | Cut-off Time-interval (s) | MFR (g/10min) |
| 1 | - | - | No Flow | - | - | No Flow |
| 2 | - | - | No Flow | - | - | No Flow |
| 3 | - | - | No Flow | - | - | No Flow |
| **Ave** | - | - | **No Flow** | - | - | **No Flow** |
| **SD** | - | - | **No Flow** | - | - | **No Flow** |

**HDPE-ME1C**

| Test No. | 5 mins Dwell Time (190℃ / 2.16kg) | | | 15 mins Dwell Time (190℃ / 2.16kg) | | |
|---|---|---|---|---|---|---|
| | Weight of Extrudate (g) | Cut-off Time-interval (s) | MFR (g/10min) | Weight of Extrudate (g) | Cut-off Time-interval (s) | MFR (g/10min) |
| 1 | - | - | No Flow | - | - | No Flow |
| 2 | - | - | No Flow | - | - | No Flow |
| 3 | - | - | No Flow | - | - | No Flow |
| **Ave** | - | - | **No Flow** | - | - | **No Flow** |
| **SD** | - | - | **No Flow** | - | - | **No Flow** |

**HDPE-ME2**

| Test No. | 5 mins Dwell Time (190℃ / 2.16kg) | | | 15 mins Dwell Time (190℃ / 2.16kg) | | |
|---|---|---|---|---|---|---|
| | Weight of Extrudate (g) | Cut-off Time-interval (s) | MFR (g/10min) | Weight of Extrudate (g) | Cut-off Time-interval (s) | MFR (g/10min) |
| 1 | 0.911 | 180 | 3.0 | 0.851 | 180 | 2.8 |
| 2 | 0.985 | 180 | 3.3 | 0.951 | 180 | 3.2 |
| 3 | 0.984 | 180 | 3.3 | 0.902 | 180 | 3.0 |
| **Ave** | - | - | **3.2** | - | - | **3.0** |
| **SD** | - | - | **0.1** | - | - | **0.2** |

**HDPE-ME2C**

| Test No. | 5 mins Dwell Time (190℃/2.16kg) | | | 15 mins Dwell Time (190℃/2.16kg) | | |
|---|---|---|---|---|---|---|
| | Weight of Extrudate (g) | Cut-off Time-interval (s) | MFR (g/10min) | Weight of Extrudate (g) | Cut-off Time-interval (s) | MFR (g/10min) |
| 1 | 0.988 | 180 | 3.3 | 1.091 | 180 | 3.6 |
| 2 | 1.094 | 180 | 3.6 | 0.949 | 180 | 3.2 |
| 3 | 1.144 | 180 | 3.8 | 0.875 | 180 | 2.9 |
| **Ave** | - | - | **3.6** | - | - | **3.2** |
| **SD** | - | - | **0.3** | - | - | **0.4** |

**HDPE-ME3**

| Test No. | 5 mins Dwell Time (190℃ / 2.16kg) | | | 15 mins Dwell Time (190℃ / 2.16kg) | | |
|---|---|---|---|---|---|---|
| | Weight of Extrudate (g) | Cut-off Time-interval (s) | MFR (g/10min) | Weight of Extrudate (g) | Cut-off Time-interval (s) | MFR (g/10min) |
| 1 | 1.188 | 60 | 11.9 | 0.948 | 60 | 9.5 |
| 2 | 1.108 | 60 | 11.1 | 0.940 | 60 | 9.4 |
| 3 | 1.115 | 60 | 11.2 | 0.966 | 60 | 9.7 |
| **Ave** | - | - | **11.4** | - | - | **9.5** |
| **SD** | - | - | **0.4** | - | - | **0.1** |

**HDPE-ME3C**

| Test No. | 5 mins Dwell Time (190℃ / 2.16kg) | | | 15 mins Dwell Time (190℃ / 2.16kg) | | |
|---|---|---|---|---|---|---|
| | Weight of Extrudate (g) | Cut-off Time-interval (s) | MFR (g/10min) | Weight of Extrudate (g) | Cut-off Time-interval (s) | MFR (g/10min) |
| 1 | 1.013 | 60 | 10.1 | 1.007 | 60 | 10.1 |
| 2 | 1.022 | 60 | 10.2 | 1.029 | 60 | 10.3 |
| 3 | 1.074 | 60 | 10.7 | 1.067 | 60 | 10.7 |
| **Ave** | - | - | **10.4** | - | - | **10.3** |
| **SD** | - | - | **0.3** | - | - | **0.3** |

**HDPE-ME3Ca**

| Test No. | 5 mins Dwell Time (190℃ / 2.16kg) | | | 15 mins Dwell Time (190℃ / 2.16kg) | | |
|---|---|---|---|---|---|---|
| | Weight of Extrudate (g) | Cut-off Time-interval (s) | MFR (g/10min) | Weight of Extrudate (g) | Cut-off Time-interval (s) | MFR (g/10min) |
| 1 | 1.109 | 60 | 11.1 | 1.079 | 60 | 10.8 |
| 2 | 1.057 | 60 | 10.6 | 1.059 | 60 | 10.6 |
| 3 | 1.085 | 60 | 10.9 | 1.056 | 60 | 10.6 |
| **Ave** | - | - | **10.8** | - | - | **10.6** |
| **SD** | - | - | **0.3** | - | - | **0.1** |

**HDPE-ME3Ca[C]**

| Test No. | 5 mins Dwell Time (190℃/2.16kg) | | | 15 mins Dwell Time (190℃/2.16kg) | | |
|---|---|---|---|---|---|---|
| | Weight of Extrudate (g) | Cut-off Time-interval (s) | MFR (g/10min) | Weight of Extrudate (g) | Cut-off Time-interval (s) | MFR (g/10min) |
| 1 | 0.832 | 60 | 8.3 | 0.801 | 60 | 8.0 |
| 2 | 0.789 | 60 | 7.9 | 0.808 | 60 | 8.1 |
| 3 | 0.806 | 60 | 8.1 | 0.817 | 60 | 8.2 |
| **Ave** | - | - | **8.1** | - | - | **8.1** |
| **SD** | - | - | **0.2** | - | - | **0.1** |

**HDPE-ME4**

| Test No. | 5 mins Dwell Time (190℃ / 2.16kg) | | | 15 mins Dwell Time (190℃ / 2.16kg) | | |
|---|---|---|---|---|---|---|
| | Weight of Extrudate (g) | Cut-off Time-interval (s) | MFR (g/10min) | Weight of Extrudate (g) | Cut-off Time-interval (s) | MFR (g/10min) |
| 1 | 1.461 | 60 | 14.6 | 1.423 | 60 | 14.2 |
| 2 | 1.531 | 60 | 15.3 | 1.418 | 60 | 14.2 |
| 3 | 1.530 | 60 | 15.3 | 1.442 | 60 | 14.4 |
| **Ave** | - | - | **15.1** | - | - | **14.3** |
| **SD** | - | - | **0.4** | - | - | **0.1** |

**HDPE-ME4C**

| Test No. | 5 mins Dwell Time (190℃ / 2.16kg) | | | 15 mins Dwell Time (190℃ / 2.16kg) | | |
|---|---|---|---|---|---|---|
| | Weight of Extrudate (g) | Cut-off Time-interval (s) | MFR (g/10min) | Weight of Extrudate (g) | Cut-off Time-interval (s) | MFR (g/10min) |
| 1 | 1.491 | 60 | 14.9 | 1.444 | 60 | 14.4 |
| 2 | 1.517 | 60 | 15.2 | 1.391 | 60 | 13.9 |
| 3 | 1.533 | 60 | 15.3 | 1.424 | 60 | 14.2 |
| **Ave** | - | - | **15.1** | - | - | **14.2** |
| **SD** | - | - | **0.2** | - | - | **0.3** |

**HDPE-ME4Ca**

| Test No. | 5 mins Dwell Time (190℃ / 2.16kg) | | | 15 mins Dwell Time (190℃ / 2.16kg) | | |
|---|---|---|---|---|---|---|
| | Weight of Extrudate (g) | Cut-off Time-interval (s) | MFR (g/10min) | Weight of Extrudate (g) | Cut-off Time-interval (s) | MFR (g/10min) |
| 1 | 1.507 | 60 | 15.1 | 1.507 | 60 | 15.1 |
| 2 | 1.478 | 60 | 14.8 | 1.475 | 60 | 14.8 |
| 3 | 1.474 | 60 | 14.7 | 1.438 | 60 | 14.4 |
| **Ave** | - | - | **14.9** | - | - | **14.7** |
| **SD** | - | - | **0.2** | - | - | **0.3** |

**HDPE-ME5Ca[C]**

| Test No. | 5 mins Dwell Time (190℃/2.16kg) | | | 15 mins Dwell Time (190℃/2.16kg) | | |
|---|---|---|---|---|---|---|
| | Weight of Extrudate (g) | Cut-off Time-interval (s) | MFR (g/10min) | Weight of Extrudate (g) | Cut-off Time-interval (s) | MFR (g/10min) |
| 1 | 0.742 | 60 | 7.4 | 0.702 | 60 | 7.0 |
| 2 | 0.722 | 60 | 7.2 | 0.700 | 60 | 7.0 |
| 3 | 0.742 | 60 | 7.4 | 0.689 | 60 | 6.9 |
| **Ave** | - | - | **7.4** | - | - | **7.0** |
| **SD** | - | - | **0.1** | - | - | **0.1** |

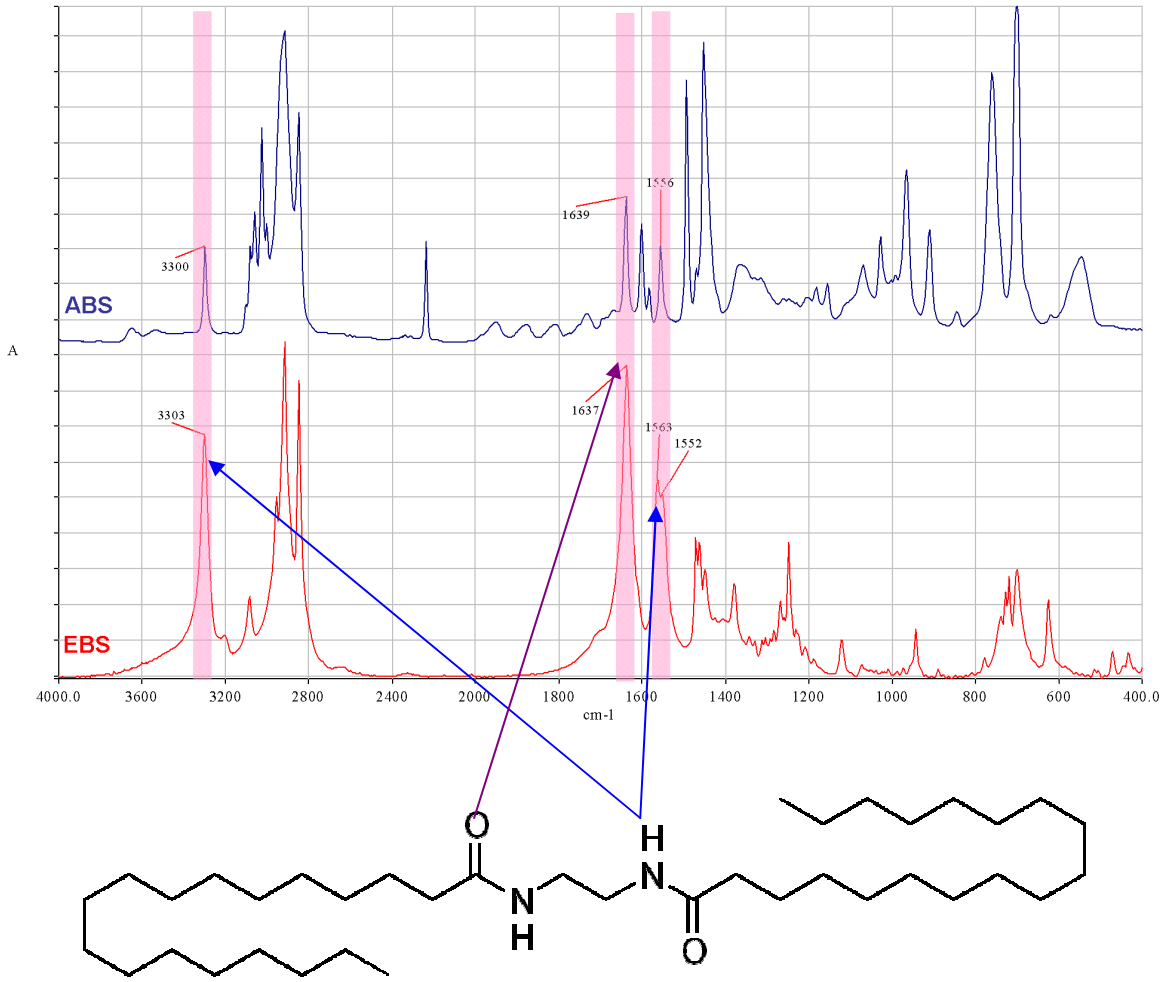


**FTIR spectrum of ABS [Terluran GP-35 from BASF] and a reference ethylene bis-stearamide (EBS) wax [Alflow H-50 F from Nippon Oil & Fats Co., Ltd.]**

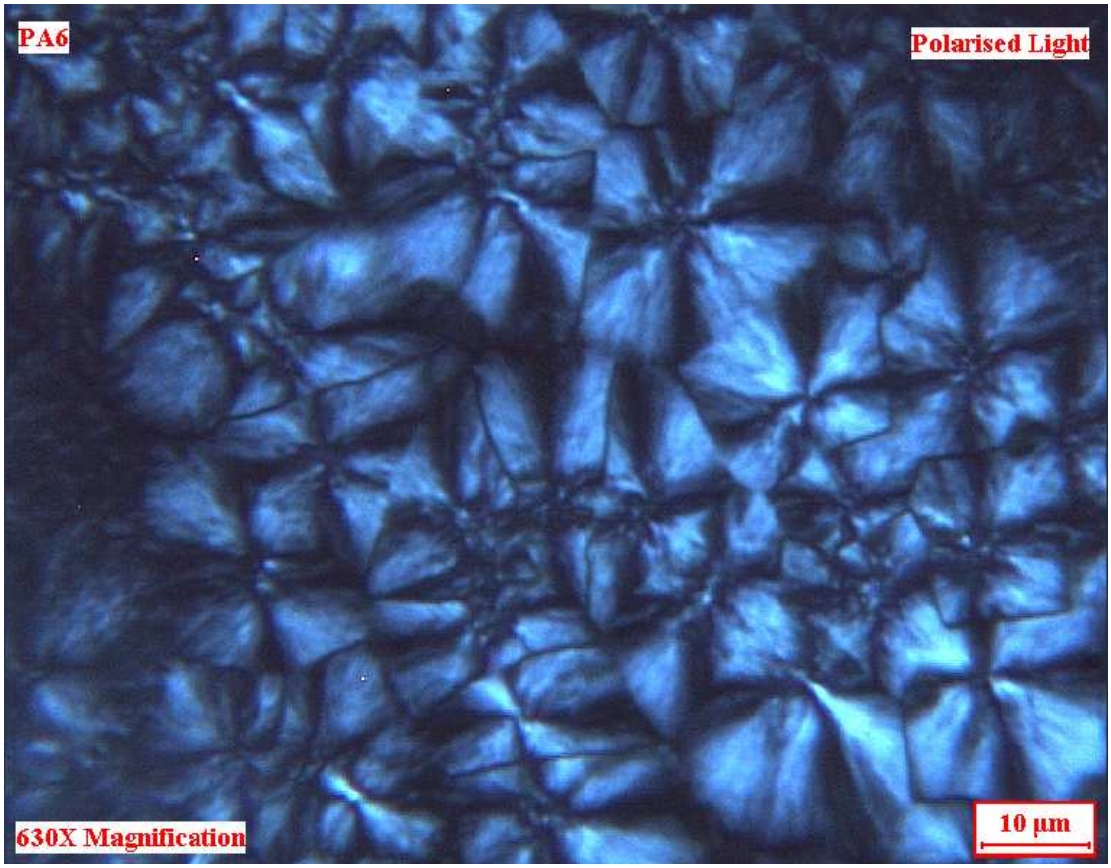


**Optical micrograph of a non-nucleated PA6 [Zisamaide HP-3403 from Zig Sheng Industrial Co., Ltd]**